

Developments in Geotechnical Engineering, 76

Waste Disposal in Rock

R. Pusch

Clay Technology AB, IDEON Research Center, S-223 70 Lund, Sweden

Department of Geotechnology, Lund University of Technology, S-221 00 Lund, Sweden



ELSEVIER

Amsterdam — London — New York — Tokyo 1994

Further titles in this series:

Volumes 2, 3, 5-7, 9, 10, 12, 13, 15, 16A, 22 and 26 are out of print

1. G. SANGLERAT – THE PENETROMETER AND SOIL EXPLORATION
4. R. SILVESTER – COASTAL ENGINEERING. 1 AND 2
8. L.N. PERSEN – ROCK DYNAMICS AND GEOPHYSICAL EXPLORATION
Introduction to Stress Waves in Rocks
11. H.K. GUPTA AND B.K. RASTOGI – DAMS AND EARTHQUAKES
14. B. VOIGHT (Editor) – ROCKSLIDES AND AVALANCHES. 1 and 2
17. A.P.S. SELVADURAI – ELASTIC ANALYSIS OF SOIL-FOUNDATION INTERACTION
18. J. FEDA – STRESS IN SUBSOIL AND METHODS OF FINAL SETTLEMENT CALCULATION
19. Á. KÉZDI – STABILIZED EARTH ROADS
20. E.W. BRAND AND R.P. BRENNER (Editors) – SOFT-CLAY ENGINEERING
21. A. MYSLIVE AND Z. KYSELA – THE BEARING CAPACITY OF BUILDING FOUNDATIONS
23. P. BRUUN – STABILITY OF TIDAL INLETS – Theory and Engineering
24. Z. BAŽANT – METHODS OF FOUNDATION ENGINEERING
25. Á. KÉZDI – SOIL PHYSICS - Selected Topics
27. D. STEPHENSON – ROCKFILL IN HYDRAULIC ENGINEERING
28. P.E. FRIVIK, N. JANBU, R. SAETERSDAL AND L.I. FINBORUD (Editors) – GROUND FREEZING 1980
29. P. PETER – CANAL AND RIVER LEVÉES
30. J. FEDA – MECHANICS OF PARTICULATE MATERIALS - The Principles
31. Q. ZÁRUBA AND V. MENCL – LANDSLIDES AND THEIR CONTROL
Second completely revised edition
32. I.W. FARMER (Editor) – STRATA MECHANICS
33. L. HOBST AND J. ZAJÍC – ANCHORING IN ROCK AND SOIL
Second completely revised edition
34. G. SANGLERAT, G. OLIVARI AND B. CAMBOU – PRACTICAL PROBLEMS IN SOIL MECHANICS AND
FOUNDATION ENGINEERING, 1 and 2
35. L. RÉTHÁTI – GROUNDWATER IN CIVIL ENGINEERING
36. S.S. VYALOV – RHEOLOGICAL FUNDAMENTALS OF SOIL MECHANICS
37. P. BRUUN (Editor) – DESIGN AND CONSTRUCTION OF MOUNDS FOR BREAKWATER AND
COASTAL PROTECTION
38. W.F. CHEN AND G.Y. BALADI – SOIL PLASTICITY - Theory and Implementation
39. E.T. HANRAHAN – THE GEOTECTONICS OF REAL MATERIALS: THE $\varepsilon_g \varepsilon_k$ METHOD
40. J. ALDORF AND K. EXNER – MINE OPENINGS - Stability and Support
41. J.E. GILLOT – CLAY IN ENGINEERING GEOLOGY
42. A.S. CAKMAK (Editor) – SOIL DYNAMICS AND LIQUEFACTION
43. A.S. CAKMAK (Editor) – SOIL-STRUCTURE INTERACTION
44. A.S. CAKMAK (Editor) – GROUND MOTION AND ENGINEERING SEISMOLOGY
45. A.S. CAKMAK (Editor) – STRUCTURES, UNDERGROUND STRUCTURES, DAMS, AND
STOCHASTIC METHODS
46. L. RÉTHÁTI – PROBABILISTIC SOLUTIONS IN GEOTECTONICS
47. B.M. DAS – THEORETICAL FOUNDATION ENGINEERING
48. W. DERSKI, R. IZBICKI, I. KISIEL AND Z. MROZ – ROCK AND SOIL MECHANICS
49. T. ARIMAN, M. HAMADA, A.C. SINGHAL, M.A. HAROUN AND A.S. CAKMAK (Editors) – RECENT
ADVANCES IN LIFELINE EARTHQUAKE ENGINEERING
50. B.M. DAS – EARTH ANCHORS
51. K. THIEL – ROCK MECHANICS IN HYDROENGINEERING
52. W.F. CHEN AND X.L. LIU – LIMIT ANALYSIS IN SOIL MECHANICS
53. W.F. CHEN AND E. MIZUNO – NONLINEAR ANALYSIS IN SOIL MECHANICS
54. F.H. CHEN – FOUNDATIONS ON EXPANSIVE SOILS
55. J. VERFEL – ROCK GROUTING AND DIAPHRAGM WALL CONSTRUCTION
56. B.N. WHITTAKER AND D.J. REDDISH – SUBSIDENCE – Occurrence, Prediction and Control
57. E. NONVEILLER – GROUTING, THEORY AND PRACTICE
58. V. KOLÁŘ AND I. NĚMEC – MODELLING OF SOIL STRUCTURE INTERACTION
- 59A. R.S. SINHA (Editor) – UNDERGROUND STRUCTURES – Design and Instrumentation
- 59B. R.S. SINHA (Editor) – UNDERGROUND STRUCTURES – Design and Construction
60. R.L. HARLAN, K.E. KOLM AND E.D. GUTENTAG – WATER-WELL DESIGN AND CONSTRUCTION
61. I. KASDA – FINITE ELEMENT TECHNIQUES IN GROUNDWATER FLOW STUDIES
62. L. FIALOVŠZKY (Editor) – SURVEYING INSTRUMENTS AND THEIR OPERATIONAL PRINCIPLES

63. H. GIL – THE THEORY OF STRATA MECHANICS
64. H.K. GUPTA – RESERVOIR-INDUCED EARTHQUAKES
65. V.J. LUNARDINI – HEAT TRANSFER WITH FREEZING AND THAWING
66. T.S. NAGARAI – PRINCIPLES OF TESTING SOILS, ROCKS AND CONCRETE
67. E. JUHÁSOVÁ – SEISMIC EFFECTS ON STRUCTURES
68. J. FEDA – CREEP OF SOILS – And Related Phenomena
69. E. DULÁCSKA – SOIL SETTLEMENT EFFECTS ON BUILDINGS
70. D. MILOVIĆ – STRESSES AND DISPLACEMENTS FOR SHALLOW FOUNDATIONS
71. B.N. WHITTAKER, R.N. SINGH AND G. SUN – ROCK FRACTURE MECHANICS – Principles, Design and Applications
72. M.A. MAHTAB AND P. GRASSO – GEOMECHANICS PRINCIPLES IN THE DESIGN OF TUNNELS AND CAVERNS IN ROCK
73. R.N. YONG, A.M.O. MOHAMED AND B.P. WARKENTIN – PRINCIPLES OF CONTAMINANT TRANSPORT IN SOILS
74. H. BURGER (Editor) – OPTIONS FOR TUNNELING 1993
75. S. HANSBO – FOUNDATION ENGINEERING

ELSEVIER SCIENCE B.V.
Sara Burgerhartstraat 25
P.O. Box 211, 1000 AE Amsterdam, The Netherlands

Library of Congress Cataloging-in-Publication Data

Pusch, Roland.

Waste disposal in rock / R. Pusch.

p. cm. -- (Developments in geotechnical engineering ; 76)

Includes bibliographical references and index.

ISBN 0-444-89449-7

1. Radioactive waste disposal in the ground. 2. Environmental geotechnology. 3. Rock mechanics. I. Title. II. Series.

TD898.2.P87 1994

628.4'4566--dc20

93-48194

CIP

ISBN: 0-444-89449-7

© 1994 Elsevier Science B.V. All rights reserved.

No part of this publication may be reproduced, stored in a retrieval system or transmitted in any form or by any means, electronic, mechanical, photocopying, recording or otherwise, without the prior written permission of the publisher, Elsevier Science B.V., Copyright & Permissions Department, P.O. Box 521, 1000 AM Amsterdam, The Netherlands.

Special regulations for readers in the USA - This publication has been registered with the Copyright Clearance Center Inc. (CCC), Salem, Massachusetts. Information can be obtained from the CCC about conditions under which photocopies of parts of this publication may be made in the USA. All other copyright questions, including photocopying outside of the USA, should be referred to the publisher.

No responsibility is assumed by the publisher for any injury and/or damage to persons or property as a matter of products liability, negligence or otherwise, or from any use or operation of any methods, products, instructions or ideas contained in the material herein.

This book is printed on acid-free paper.

Printed in The Netherlands

Foreword

Early 1978 the author - at that time professor in soil mechanics at the University of Luleå with a background in rock mechanics, geology and structural design of industrial plants - became engaged in the work that had just been initiated by the Swedish Nuclear Fuel and Waste Management Co (SKB), Stockholm, for development of a technical solution of the problem of safe disposal of radioactive waste from the Swedish nuclear reactors. This engagement has continued through the years and the combined efforts of SKB and its consultants, catalyzed by governmental authorities, has resulted in a successively improved understanding of the long-term performance of repositories for radioactive waste with metal waste containers and clay seals as major engineered barriers to radionuclide escape to the biosphere. Several candidate concepts for disposal of highly radioactive burnt-out fuel from the Swedish nuclear reactors have evolved from this work and a repository for disposal of low- and medium level radioactive waste constructed at Forsmark in Sweden with the author being responsible for the clay-based barriers.

Around 1980 the international Stripa Project - an autonomous OECD activity for developing and testing techniques for isolating highly radioactive waste - was started with Canada, Finland, France, Great Britain, Japan, Sweden and USA as member nations. The project, which was headed by SKB, comprised geophysical, geochemical and geohydrological studies and a number of field experiments with clay materials for shielding simulated highly radioactive waste. The latter experiments, for which the author was responsible as principal investigator, also included rock sealing and plug construction and testing.

The experience from the comprehensive SKB research and the Stripa Project work on clay-based engineered barriers and rock performance is huge but reporting has mainly been in internal technical reports to which access is limited. Since information from the two activities is expected to be of interest to a wide group of organizations and authorities that deal with disposal of hazardous and particularly radioactive waste, as well as to consultants and construction companies and also university students interested in environmental protection, the reason for writing this book has been to present both fundamental principles of the behavior of repository barriers as they have evolved in the SKB research work, and practically useful information from the Stripa tests. The title of the book indicates that disposal of all sorts of hazardous waste will be treated but the reader will find that most of the examples refer to radioactive waste, which is explained both by the fact that the author's work has been focused

on such waste and by the belief of the author and a number of his colleagues that the same techniques can be used for isolation of radioactive and other hazardous waste, like toxic chemical waste although they have not yet been utilized.

The aim has been to put together a sort of scientific will comprising a synthesis and presentation of major current ideas and of the most important results and findings evolved in the work in which the author and his collaborators at the company Clay Technology AB, Lund, Sweden, have been involved, rather than to give a complete state-of-art overview of waste disposal in general. The reader will therefore find that most references carry the author's and his near colleagues' names.

The author has refrained from loading the text with mathematics and the reader will not even find any deductions of the few equations that show up since the purpose has been to give the reader an idea of what techniques, design and construction principles that can be used in the establishment of deeply located waste repositories rather than to use up the space with the theoretical background that is accessible through the references referred to.

The author wants to underline that the statements given are the author's, which are not necessarily in line with the opinion of any organization involved in the matter in Sweden or elsewhere. Also, the book should be considered as an interim document since much work is going on internationally and future research may change the views.

Legend and abbreviations

The book contains a number of notations, symbols, and constants as well as abbreviations, which are compiled in this chapter.

LEGEND

Latin letters

a, b, c, distances, dimensions, μm , mm, cm, dm, m, km

A, cross section area

c, cohesion, MPa; concentration, ppm, g/l

C, heat capacity, Ws/kg.K

CEC, cation exchange capacity, mE/100 g solid material

d, grain and particle size; fracture aperture, μm , mm; days

D, diffusion coefficient, m^2/s , m^2/a (square meters per annum, i.e. year)

D_a , apparent diffusion coefficient, m^2/s

D_e , effective diffusion coefficient, m^2/s

D_w , coefficient of diffusive water transport, m^2/s

e, base of natural logarithms; void ratio (ratio of volume of voids and volume of solid mass)

E, (Young's) modulus of elasticity, MPa, GPa

g, earth acceleration, m/s^2

G, shear modulus, MPa, GPa

Gy, Gray, adsorbed radiation energy, J/kg

i, hydraulic gradient

JCOH, joint cohesion, kPa, MPa

JDIL, joint dilation angle, degrees

JFRIC, joint friction coefficient

JKN, joint normal stiffness, MPa/m, GPa/m

JKS, joint shear stiffness, MPa/m, GPa/m

JTEN, joint tensile strength, kPa, MPa

K, hydraulic conductivity, m/s

m, grout viscosity parameter, Pas

M, magnitude of earthquakes on the Richter scale

n, porosity (ratio of volume of voids and total volume); constant

N, migration rate, m/s

p, total pressure, bar, kPa, MPa

p_s , swelling pressure, kPa, MPa

q, flux, water flow, l/m^2 , ml/s, m^3/s ; deviator stress, kPa, MPa

r, radius

S, Sievert, radiation dose,

t, time, s (seconds), min (minutes), h (hours), d (days), a (annum), y (years)

t_0 , t_r , constants in creep equations

T, temperature, $^{\circ}\text{C}$, K; time

u , porewater pressure, kPa, MPa; flow rate m/s

v , Q , velocity, flow rate, m/s

w , water content (ratio of mass of water and solid mass), %

w/c , water/cement (mass) ratio for cement

w_L , liquid limit (ratio of mass of water and solid mass at certain defined consistency) %

W , fracture aperture

x , y , coordinates

\AA , Ångström unit, 10^{-8} cm

Greek symbols

α , angle; radiation; creep parameter

β , angle

δ , settlement, mm, cm

ϕ , friction angle, degrees

γ , angle, angular strain

γ , creep rate, s^{-1}

λ , heat conductivity, W/m,K

ρ , bulk density, (ratio of mass and total volume), g/cm^3 , t/m^3

ρ_d , dry density (ratio of solid mass and total volume), g/cm^3 , t/m^3

ρ_s , density at complete water saturation (ratio of mass of water + solid mass and total volume), g/cm^3 , t/m^3

ρ_w , density of water, g/cm^3 , t/m^3

η , viscosity, Ns/m^2

ν , Poisson's ratio

σ , σ_n , normal stress, Pa, kPa, MPa

σ_1 , major principal stress, kPa, MPa

σ_3 , minor principal stress, kPa, MPa

σ_h , σ_H , minimum and maximum (primary) horizontal total stress, kPa, MPa

σ_v , vertical total stress, kPa, MPa

σ' , effective stress ("grain pressure"), kPa, MPa

τ , shear stress, Pa, kPa, MPa

ABBREVIATIONS:

Organizations:

AECL, Atomic Energy Company of Canada Ltd

CEA, Commissariat à l'Energie Atomique, France

ENRESA, Empresa Nacional de Residuos Radioactivos S.A., Spain

IAEA, International Atomic Energy Agency

ICRP, International Committee for Radiation Protection

NAGRA, Nationale Genossenschaft für die Lagerung Radioaktiver Abfälle, Switzerland

NEDRA, Scientific Industrial Company on Superdeep Drilling and Comprehensive Investigation of the Earth's Interior, Russia

OECD, Organisation for Economic Cooperation and Development

SKB, Swedish Nuclear Fuel & Waste Management Co, Sweden

TVO, Teollisuuden Voima Oy, Finland

VTT, Technical Research Center of Finland

Others:

1st - 7th order discontinuities, fracture zones, fractures, fissures, and weaknesses

2D, two-dimensional

3D, three-dimensional

ABAQUS, finite element code

BAT, piezometer Bq, radioactivity, Bequerel

BMT, Buffer Mass Test (Stripa Project)

CB, careful blasting

FEM, finite element method, numerical code

FLAC, fast Lagrangian Analysis of Continua, numerical code

GMM, general microstructural model

hcb, HCB, highly compacted bentonite

HLW, high-level radioactive waste

ic, injection chamber

ILW, intermediate-level radioactive waste

KBS3, current Swedish repository for high-level radioactive water

LID, Large borehole Injection Device

LLW, low-level radioactive waste

MLW, medium-level radioactive waste

NB, normal blasting

R&D, research and development

SEK, Swedish currency, crowns

SFR, Swedish repository for low-level and medium-level radioactive waste

SVC, drift in the Stripa mine

TBM, tunnel boring machine

3DEC, 3-dimensional Distinct Element Code, numerical code

UDEC, Universal Distinct Element Code, 2-dimensional numerical code

VCB, very careful blasting

VDH, Swedish repository concept for high-level radioactive waste (“very deep holes”)

VLH, Swedish repository concept for high-level radioactive waste (“very long holes”)

XRD, X-ray diffraction

Chapter

1 *Introduction*

1-1 Scope and approach

The scope of this book is to give an overview of concepts and technical means of isolating hazardous waste at depth in crystalline rock, applying the multiple barrier philosophy and focusing on groundwater percolation and migration of dissolved toxic species in the nearfield of waste containers. Focus will be on the function, design and construction of engineered barriers for isolating hazardous waste, considering also the performance of rock, which are all items that make up an essential part of the basis for safety assessment. Such assessment is a huge subject per se and will not be a major issue in this book. A large number of new aspects and a significantly improved understanding of the function of waste repositories have evolved in the last decade, particularly through the intense international work in the field of disposal of radioactive waste products, to which reference will be made throughout the book.

1-2 Advantages in storing waste products at depth in rock

Some people may think that disposal of hazardous waste at depth in rock is to apply ostrich philosophy, i.e. to believe that once the stuff is out of sight everything is OK and that one does not have to bother. In fact, there are several significant advantages in disposing waste at a large depth, a major one of course being that the passages for contaminated water will be very long and tortuous. A further point is that dangerous species can be located in an environment with which they fit chemically. Mines offer this advantage as exemplified by storing batteries where mercury-rich ore was once extracted and where the surrounding rock therefore has some mercury content that reduces the dissolution of mercury from the waste. Looking closer at the possibility of finding a proper environment for hazardous waste one finds that there are plenty of possibilities to identify old mines in which the rock offers very good chemical buf-

fering capacity like marble and limestone mines and quarries with high pH groundwater. However, the major advantage in locating dangerous waste deep down is that the transport paths to the biosphere are very long and that groundwater flow can be insignificant if the hydraulic gradients are small and the hydraulic conductivity low. Still, in recent time, research in the field of radioactive waste disposal in Sweden tends to show that although rock - or more generally the "geosphere" - may offer very effective isolation, its most important property is to serve as a mechanical protection of the "chemical apparatus", i.e. engineered barriers in the form of clay or cement embedment of the waste containers [1]. It is obvious from such investigations that the rock structural features that are or can become passages for migrating species, i.e. the system of conductive discontinuities, control the isolating potential of a rock mass, and that shaping and orienting rock caverns properly with respect to the structural features can greatly improve the isolating power of a repository.

In addition to the advantage of creating long transport paths from the repository to the biosphere for retarding the migration of hazardous species as offered by locating repositories at large depths, the rock is also generally tighter at depth, i.e. the average hydraulic conductivity decreases as indicated in Figure 1. Still, recently reported results from the comprehensive research carried out in the former Soviet Union demonstrate that hydraulically active zones extend to several kilometers depth and are components of regional conductive systems consisting of interconnected flatlying and steep zones.

While location of repositories at large depths is advantageous because it yields low flow rates and long passages for water flow to the ground surface, the high stresses that prevail deep down may also cause problems by overstressing the rock in the construction phase, and the fracturing of the nearfield rock may raise the conductivity of the rock next to the waste packages and generate increased flow along holes and tunnels containing the waste. These matters, which involve rock mechanics and excavation technique, will be treated in detail in this book.

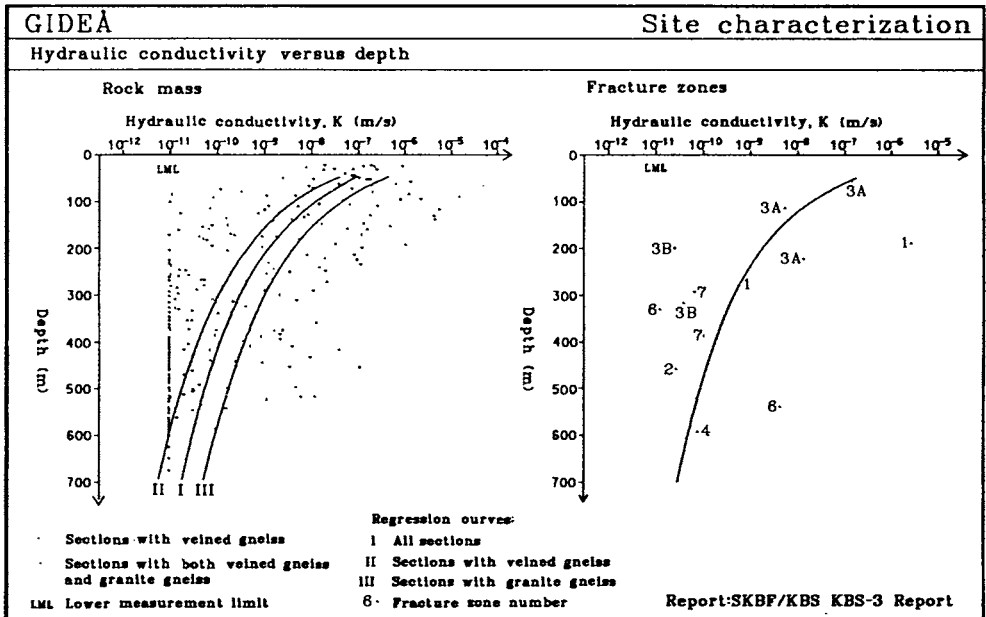


Figure 1 Recorded hydraulic conductivity data in crystalline rock at Gideå, Sweden. The left graph shows the evaluated conductivity of the bulk rock and the right data for fracture zones (SKB)

1-3 General principles of waste disposal

1-3.1 The multibarrier philosophy

A common philosophy is to apply the multiple barrier concept, which means that more than one medium or mechanism, physical or chemical, prevent or retard release and migration of hazardous elements emanating from the waste. For deeply located repositories the rock naturally forms one barrier by having a low hydraulic conductivity and a sorbing capacity, and waste embedment by suitable backfilling forms a second barrier with an even lower conductivity. Waste containers of metal make up a third barrier and the waste itself can in fact be considered as a fourth barrier if it is in solid form since the dissolution process is a hampering factor.

One realizes that although the barriers appear to operate independently, they in fact depend on each other. Hence, clay materials embedding waste containers may undergo chemical changes by interaction with the waste or waste containers, and if the rock degrades by shearing and tension induced by tectonics, the waste containers an embedment may break or soften and offer less protection to the waste. A basic principle, which is particularly important for safe disposal of highly radioactive waste, is therefore to locate the repository in rock so that large water-bearing fracture zones, which may undergo shearing, are avoided.

The main function of a repository, which naturally is to confine the waste so effectively that only acceptable concentrations of the hazardous species appear in dissolved form in the groundwater, needs to be preserved for a sufficient period of time and here is where we find the major difference between storage of chemical and radioactive waste. Thus, while radioactive waste undergoes decay, hazardous industrial waste commonly maintains its toxicity, which implies that repositories for radioactive waste are allowed to deteriorate while a storage of chemical waste should remain intact “forever” or degrade at a rate that yields a constant release of the hazardous elements. We will see later that areas where future glaciation is expected may offer the best opportunities of safe disposal of toxic waste.

1-3.2 What are the criteria of required waste isolation?

The basic principle of proper location and design of terrestrial repositories, with which we will be concerned, is to isolate the waste from the biosphere such that the concentration of toxic substances in the groundwater or in lakes and estuaries does not exceed the maximum values stipulated by national authorities. According to the European communities, dangerous waste materials fall into the categories: very toxic, toxic, oxydizing, and explosive substances. A general recommendation of the communities is to apply recycling for minimizing the volume of waste but this instead tends to yield smaller amounts of more dangerous species, for which the communities have specified the lists I and II below. The latter refers to substances that can have a harmful effect on groundwater.

LIST I OF FAMILIES AND GROUPS OF SUBSTANCES

- 1. Organohalogen compounds and substances which may form such compounds in aquatic environment**
- 2. Organophosphorous compounds**

3. Organotin compounds**4. Substances which possess carcinogenic mutagenic or teratogenic properties****5. Mercury and its compounds****6. Cadmium and its compounds****7. Mineral oils and hydrocarbons****8. Cyanides****LIST II OF FAMILIES AND GROUPS OF SUBSTANCES****1. The following metalloids and metals and their compounds:**

Zink, copper, nickel, chrome, lead, selenium, arsenic, antimony, molybdenum, titanium, tin, barium, beryllium, boron, uranium, vanadium, cobalt, thallium, tellurium, silver

2. Biocides and their derivatives not appearing in List I**3. Substances which have a deleterious effect on the taste and/or odour of groundwater****4. Toxic or persistent organic compounds of silicon****5. Inorganic compounds of phosphorous and elemental phosphorous****6. Fluorides****7. Ammonia and nitrites**

A guiding principle for selecting a proper place for a repository is to locate it so that percolated water is discharged into a large recipient in which the concentration of dangerous substances will hence be low. However, the European communities specify the same maximum tolerable concentrations for many toxic substances in estuary and territorial waters as for inland surface waters, which hence means that effective isolation of certain substances is still required. The degree of isolation effort that is required is judged on the basis of hydrological calculations for predicting the concentration of particularly dangerous substances that emanate from the repository and appear in drinking water, which is the key question. The maximum tolerable concentration of such substances is indicated in Table 1 for ordinary climatic

and geographic conditions and simple treatment (filtration and disinfection) of the water pumped up from the groundwater aquifer or lake.

The possible advantage of locating toxic chemical waste in shallow repositories in areas where future glaciation is expected is also due to the dispersion that will take place when a large ice sheet scrapes off the earth surface and distributes the debris over a very large area, leading to an extremely low concentration of the hazardous elements. The difficulties in applying this principle are obvious, however, as we will see later.

Table 1 Maximum tolerable concentration of major dangerous substances in drinking water

Substance	Concentration ppm
Nitrate	50
Fluoride	1.5
Copper	0.05
Zink	3
Arsenic	0.05
Cadmium	0.005
Chromium	0.05
Lead	0.05
Selenium	0.01
Mercury	0.001
Barium	0.1
Cyanid	0.05
Sulphate	250
Phenol	0.001
Polycyclic aromatic hydrocarbons	0.0002
Pesticides (BHC)	0.001

For radioactive waste the International Atomic Energy Agency (IAEA) has defined five categories with respect to final disposal as given by Table 2. The international committee for radiation protection (ICRP), which launched the ALARA principle that all radiation doses shall be kept as “low as reasonably achievable” with respect to economic considerations and to society, has defined a number of criteria that have to do with the exposure of the whole body or part of it to radiation, and to the definition of groups of people that are particularly exposed to radiation, i.e. radiologists and “critical” groups. For the latter, the maximum allowable yearly radiation dose is 1 mSv for the full body (occasionally 5 mSv), and 50 mSv for individual organs.

Table 2 Definition of radioactive waste for final disposal

Category	Major properties
I High-level, long-lived (HLW)	High beta/gamma-activity, considerable alpha activity, high radio-toxicity, high heat production
II Medium-level, long-lived (MLW)	Intermediate beta/gamma activity, considerable alpha-activity, Intermediate radio-toxicity, low heat production
III Low-level, long-lived (LLW)	Low beta/gamma-activity, considerable alpha-activity, low- to intermediate radio-toxicity, insignificant heat production
IV Medium-level, short-lived (MLW-S)	Intermediate beta/gamma-activity, insignificant alpha-activity, intermediate radio-toxicity, low heat production
V Low-level, short-lived (LLW-S)	Insignificant beta/gamma-activity, insignificant alpha-activity, low radio-toxicity, Insignificant heat production.

1-3.3 What is risk?

The reason for isolating toxic waste is naturally to minimize the risk of exposing the “biosphere” to dangerous species emanating from the waste. The risk can be defined as the product of the probability of such exposure and the health consequence. Assessment of the former, which depends on the performance of the repository with special respect to exogenic processes, is a major issue for designers and licensing authorities and requires deep insight in the physico/chemical function of rock and waste containers and embedments, while the latter

is naturally a medical matter. It has undergone change and will continue to be redefined in future, which means that “risk” will also be defined differently from what it is today. In this book we will refer to commonly accepted maximum concentrations of major toxic species and to current maximum radiation doses for illustrating the function of the various repositories that will be discussed, without introducing explicitly any health aspects. Instead, we will focus on the technical function of repositories in order to give a basis of risk estimation.

1-3.4 Main principles of location of repositories

Two major principles can be considered for location of repositories, i.e. “dry” conditions with the repository above the groundwater surface and designed so that it is not infiltrated and percolated by water, and “wet” conditions with the repository located so that the amount of percolating groundwater is at minimum and becomes discharged into large recipients, where the concentrations will be small.

The first principle, which implies that the dissolution of the waste and contamination of the groundwater are negligible, requires very shallow location of the repository in most areas, except for deserts, but problems can be identified: Climatic alterations must be foreseen, such as change from arid to humid conditions, and glaciation. Location in rock above the present groundwater level may represent an additional risk if the repository is planned to host highly radioactive waste because the heat associated with the radioactive decay will cause expansion of the groundwater below the repository and may drive up water causing convective flow through and around the repository. The thermal pulse will also induce rock strain that may cause permanent increase in fracture apertures and hence an increased hydraulic conductivity. Furthermore, shallow location of repositories means that accidental human intrusion is much more probable than in repositories at large depth.

The second principle is expected to be of general use and there are numerous examples of accordingly planned but not yet constructed repositories, primarily for radioactive waste. For “wet” repositories, changes in hydrological conditions in the rock caused by tectonic and thermal processes may become critical. Future glaciations, which are expected in no more than 5000-10 000 years in Scandinavia, will also affect the rock mechanically and change both the hydraulic conductivity and the magnitude and direction of the hydraulic gradients that drive water through the repository.

Both principles imply that the stability of the rock is of fundamental importance for the function of repositories, which requires that rock mechanics and stress conditions in the earth

crust are considered in localizing and designing rock repositories. This is a major subject of this book.

1-3.5 Design principles

The most simple design principle is to apply the waste in caverns without backfilling them, but sealing adits and ramps by casting concrete plugs. This principle was used in designing the large repository for low-level (LLW), short-lived radioactive waste in Sweden about ten years ago and can be used when degradation and collapse of the surrounding rock is of negligible importance in a long-term perspective.

More effective isolation of the waste is obtained by surrounding it with a low-permeable substance like concrete or clay which also offer a suitable chemical environment and, for clay, also rheological properties like ductility and ability to undergo stress relaxation for maintaining homogeneity and uniform embedment. This principle, which is frequently applied in shallow disposal of industrial waste using liners as sealing components, has been used also in underground repositories, like those for medium-level radioactive waste in Sweden and Finland. The one in Sweden, the Forsmark repository, will be used here as an example of how the entire planning, design and construction work can be made and also how safety assessment can be made.

The most effective isolation of waste is obtained by encapsulating it in long-lived containers, "canisters", which are embedded in concrete or clay and emplaced in rock caverns located in low-permeable rock and excavated so as to minimize mechanical disturbance. Employing also strategic sealing by plugging and grouting makes such a multibarrier repository very suitable for long-term isolation of particularly hazardous material, like highly radioactive waste (HLW) from the nuclear industry.

The difficulty in predicting and assessing long-term stability and tightness of waste containers in a chemical environment that may undergo substantial change with time makes it necessary to accept that perfect confinement over extremely long periods of time cannot be achieved and that a concept should instead be worked out that employs barrier components which degrade sufficiently slowly to release hazardous elements at an acceptable rate.

1-4 Long-term function

1-4.1 Rock stability

A basic requirement for long-term performance of a repository is that the rock strain that is inevitable because of the “massage” of the earth crust caused by tidal phenomena and tectonic impact, and the superimposed heat effects in HLW radioactive repositories, will not jeopardize the isolation of the waste. Tectonics, commonly but not always associated with seismicity, yields momentaneous slip along major faults generating secondary displacements along smaller discontinuities and causing accumulated strain through creep. This may widen the aperture of major fractures and increase the hydraulic conductivity, which may also be enhanced by strain induced by the thermal pulse that is associated with the radioactive decay in radwaste repositories (Figure 2). These processes may also alter the passage-ways and the entire flow pattern so that groundwater will be forced through the waste instead of passing it. Naturally, topographic reshaping due to weathering or glaciation may cause very considerable changes in orientation and magnitude of the regional hydraulic gradients. A matter of particular importance for HLW repositories is tectonically induced deformation of canisters. Thus, shearing of large fracture zones may generate displacement along small-scale discontinuities that intersect deposition holes and tunnels and this may lead to critically large deformation of waste canisters and their embedment (Figure 3), which has to be soft enough to sustain some rock strain without generating too high stresses in the waste containers, and at the same time to be stiff enough to prevent significant settlement of the containers.

All these matters are of fundamental importance for the long-term function of rock repositories and have to be considered in the safety or risk analysis that has to be made for any repository holding hazardous waste. We will consider them in detail in this book.

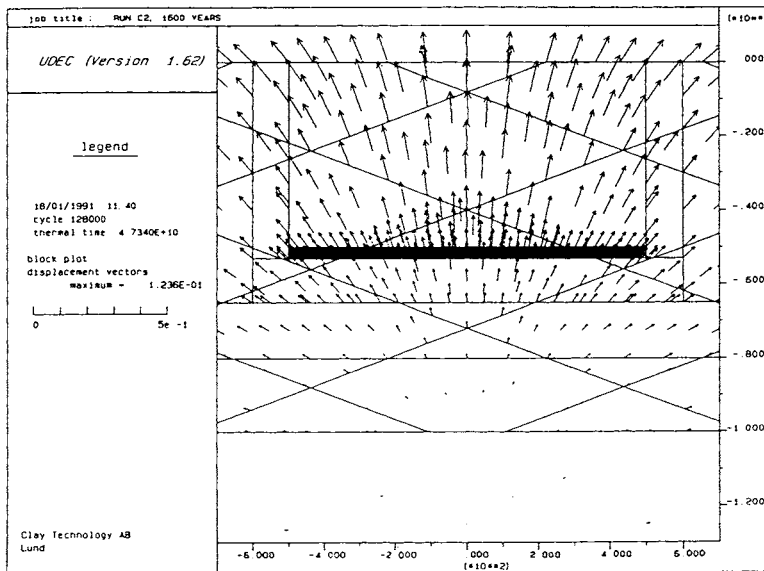
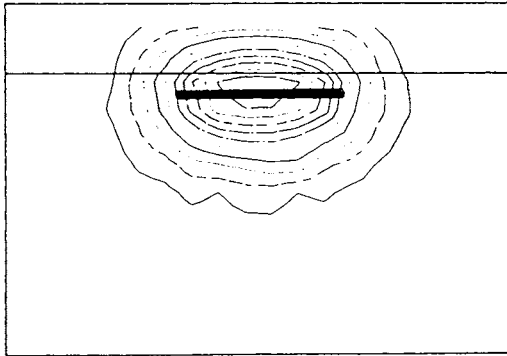


Figure 2 Temperature fields (upper) and displacements in host rock of a HLW repository (marked black) according to a 2D numerical calculation. The iso-line interval in the upper picture is 2°C , the horizontal line representing a major fracture zone. The strain accumulates to a couple of decimeters of the ground surface over the repository in 1600 years [2]

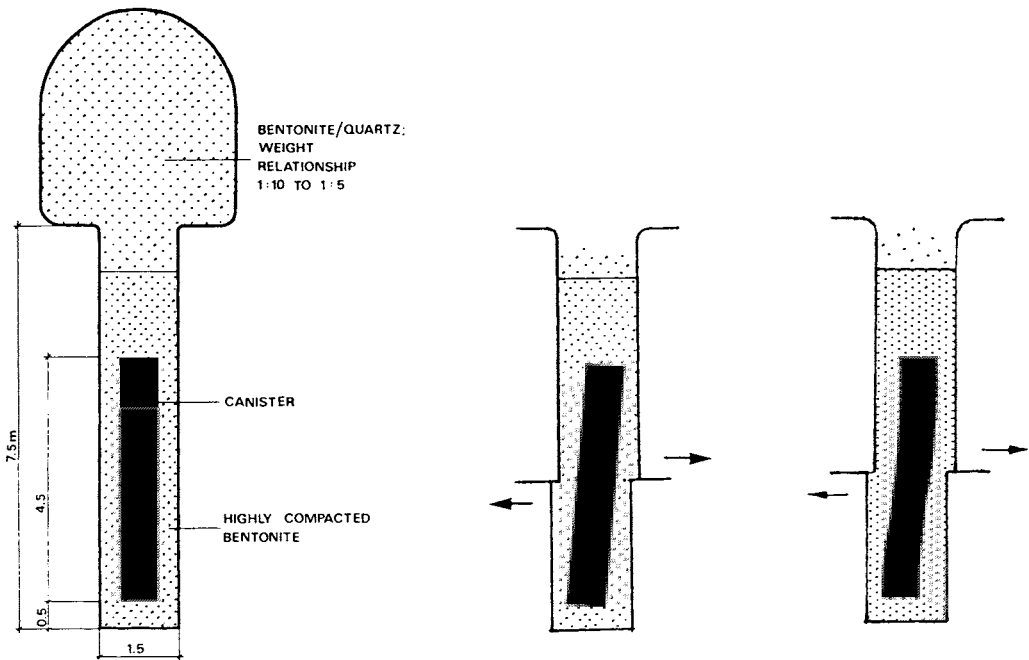


Figure 3 Shearing of canister along major fracture passing through a deposition hole in a Swedish KBS3 repository

1-4.2 Longevity of barrier components

The required operative lifetime of barriers other than rock, such as concrete in plugs, cement for sealing rock fractures, and clay for embedding waste containers, needs to be defined and assured. This is one of the most difficult issues for the synthetic materials cement and concrete since no evidence of their longevity is offered by natural analogs. While both cement and clay materials are thermodynamically unstable in repository environment, there are

numerous examples of geologically well-defined clay materials that have undergone heating and loading without losing much of their sealing ability, which demonstrates that there are clay minerals that can be largely preserved for hundreds of millions of years under repository-like conditions.

Metal canisters also degrade with time at a rate that strongly depends on the chemical environment offered by the canister embedment. Hence, it is clear that copper, which is perfectly thermodynamically stable in pure water and suggested as canister material for Swedish HLW repositories, is attacked by oxygen and sulphur which are present in groundwater and in clay embedment. Titanium and acid-proof stainless steel may be heavily attacked by corrosion depending on the chemical environment provided by the repository.

We will consider all these barriers in this book but emphasis will be put on clay and cementitious components, which play a central rôle in all sorts of repositories.

1-5 Example of planning and design of a repository - the Forsmark case

1-5.1 General

A major aim of this book is to examine the principles of location and design of repositories and give examples of practical applications. Repositories for radioactive waste products will be considered in particular, partly because more work has been performed in this field than in any other discipline of toxic waste disposal, and partly because a number of technical solutions and components intended for such repositories can be used also for isolating other hazardous waste products.

A recently finished repository for low- and medium-level radioactive waste of categories IV and V in Table 2 at Forsmark in Sweden serves as a good example of proper planning and suitable design of rock caverns for hosting dangerous waste and we will examine and comment on it in order to show the major phases of its evolution. In subsequent chapters we will deal more deeply with disposal of radwaste and we will also come back to the Forsmark repository as a reference case for identifying the structural features of a large rock mass. In this

chapter we will give a general overview of the planning and design work as an introduction to the more detailed treatment of these subjects later in the book.

1-5.2 Location of the Forsmark repository

The approximate location of the Forsmark repository, the size of which had been estimated on the basis of the predicted total amount of low- and medium-level waste over the time that nuclear power will be used in Sweden, was given from start: it had to be close to the harbor of a coastal nuclear power plant some 150 km north of Stockholm. The major questions that had to be answered at the planning stage were:

1. Where exactly should the various storage rooms be located?
2. Which is the best design with respect to the orientation and cross section of the rooms, and what seals should be used for blocking flow passages like tunnels and fracture zones?
3. What instrumentation and monitoring is required and how long should it be operable?

1-5.3 Site conditions

The most important criterion for locating the repository was that it should not interfere with any major fracture zone of which several were known to be present in the area. This required geological investigations in the form of comprehensive core drilling and geophysical testing for characterization of the rock structure. Figure 4 shows the thereby identified, major fracture zones. Their hydraulic conductivity was determined by conventional packer tests in which sections of boreholes were pressurized and the outflow measured over a relatively short time. As in the hydraulic characterization of the underground for any sort of subsurface construction, the conductivity was evaluated by assuming the rock to behave as a homogeneous porous medium but we will see later that this is not suitable for all purposes. An often used measure of the permeability of fracture zones is the so-called transmissivity (m^2/s), which is the product of the hydraulic conductivity (m/s) and the width of the zone (m). In this book we will refer only to the hydraulic conductivity as a characteristic measure of the permeability of rock and soil units of defined size.

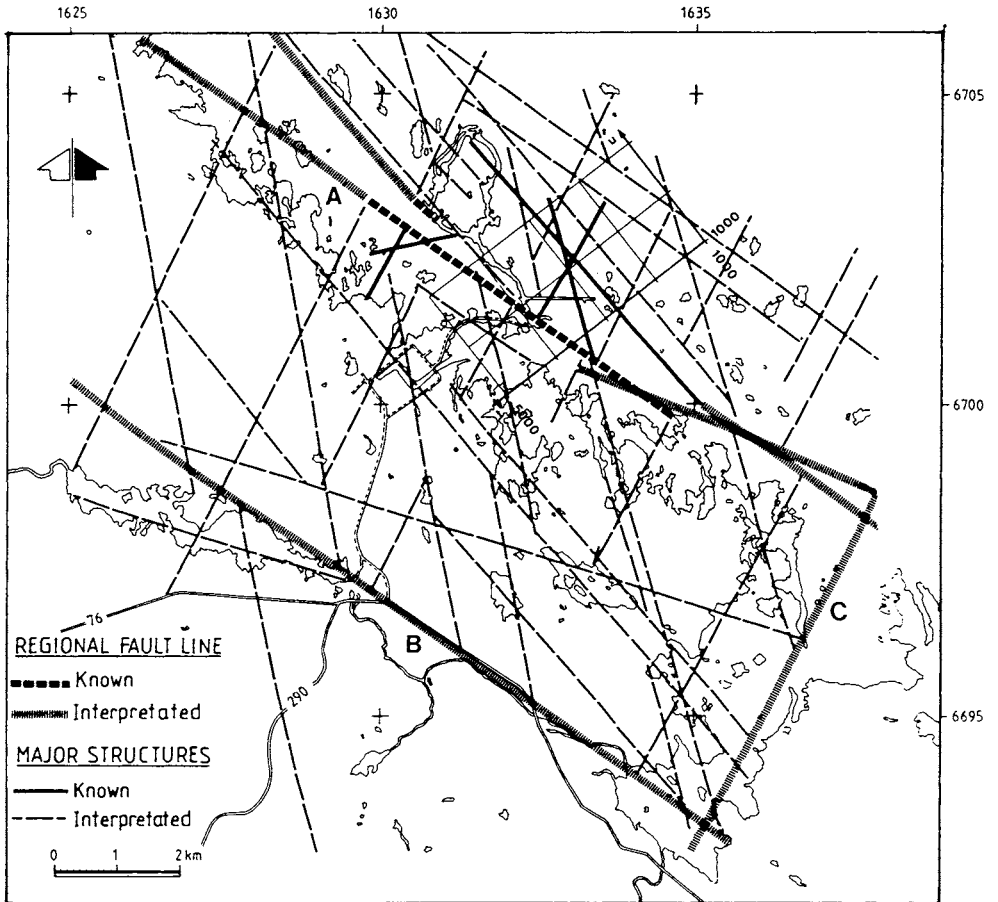


Figure 4 Major fracture zones in the Forsmark area. Notice the obvious rhomboidal or nearly orthogonal pattern that they form. A, B and C are dominant features

A more detailed picture of the identified, steeply oriented fracture zones and the finally decided location of the repository area is given in Figure 5. It illustrates that the repository, consisting of a silo and a number of vaults, is located in a rock block bounded by four major, steep fracture zones. The core drillings and geophysical investigations showed that there is

also a major flatlying zones (H2) located a few tens of meters below the silo. It gave off 160 liters of groundwater per hour to the cavern before the silo was constructed.

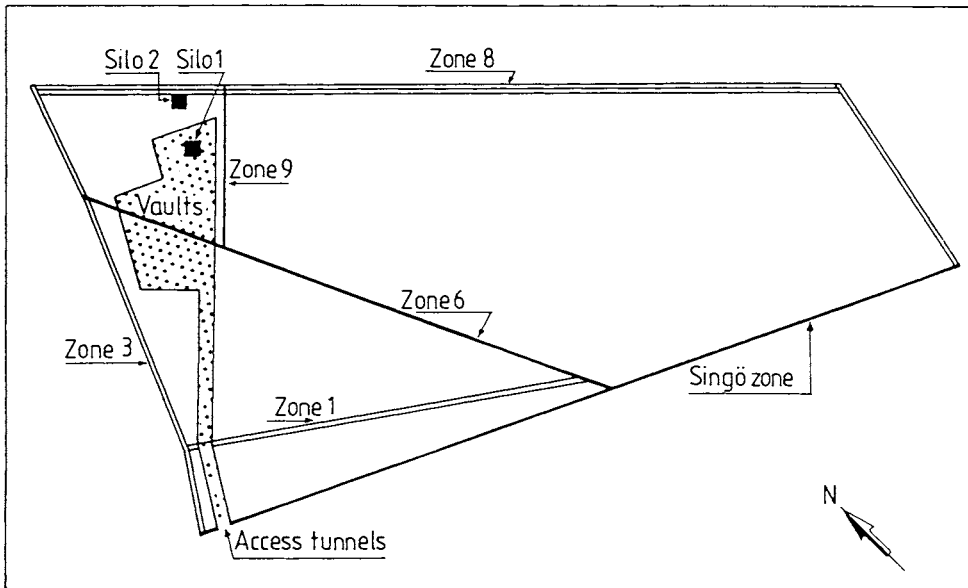


Figure 5 Area studied with respect to groundwater flow and suitable location of the repository. The length of Zone 8 shown in the plan drawing is 1600 m

At the planning stage, which comprised preliminary design, it became obvious that the rock structure and quality allowed excavation of the required number of big tunnels for the waste from construction points of view, and it was concluded that most of the waste could be stored in vaults with a width of about 15 m and a spacing of 20 m. However, the large amount of hazardous medium-level waste was concluded to require special isolation in a closed concrete silo. This silo, which should have a storing capacity of at least 40 000 m³, needed to be very rigid and embedded in low-permeable bentonite clay in order to minimize groundwater percolation, which also required location of the silo such that no major water-bearing fractured zone in the rock would be intersected by the rock cavern hosting the silo. The finally decided repository plan is shown in Figure 6. The much less hazardous low-level waste in the vaults did not require very effective isolation, which made it possible to use unlined rooms

with no sealing between or around the packages, paying only little attention to the presence of intersecting fracture zones.

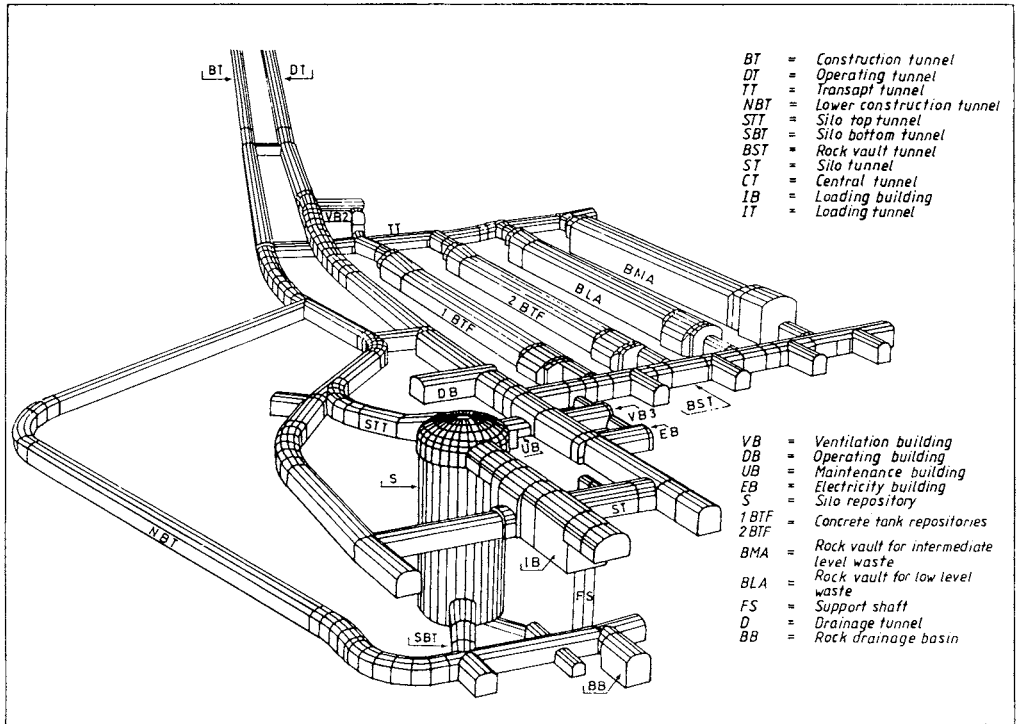


Figure 6 Layout of the SFR repository with the big silo and the four big storage vaults. Two adits reach from the repository level to the ground surface

1-5.4 Design

REQUIREMENTS

A major criterion was that the isolating ability of the embedded silo should be maintained for at least 300 years. Still, a degradation scenario of the silo over a 5000 year period had to be worked out.

We will confine ourselves here to examine the silo with medium-level waste, for which the multibarrier principle was applied. Thus, the waste contained in steel drums and concrete boxes formed a first barrier because of the low or moderately high solubility of the waste and the retardation of the migration of radionuclides caused by the containers, while the concrete silo represented an effective second barrier, the clay-based embedment of the silo a third barrier, and the surrounding rock a fourth barrier.

The following major problems had to be solved in the design work, which was preceded by comprehensive geophysical and geological surveys for determining the hydraulic properties of the identified zones and for locating the silo in an optimum fashion with respect to the groundwater flow pattern induced by the zones:

1. What is the optimum shape of a blast-excavated rock cavern that can accommodate a 50 000 m³ silo? The top of the silo should be 50 m below the ground surface, which is the sea bottom. The water depth is about 5 m in the area.
2. What is the best silo construction method?
3. Can the silo be embedded by a clay-based medium with a hydraulic conductivity that is not higher than that of the surrounding rock?
4. Can the silo be so designed that the pressure from the embedding clay and the rock pressure exerted by slipping wedges of the type shown in Figure 7 do not cause tilting or failure?
5. Can the gas pressure produced by degradation of organic waste and corrosion of steel components, like the reinforcement of the silo, be released without yielding gas pressures high enough to break the silo or to increase its hydraulic conductivity to more than that of the surrounding rock?
6. Can the system of confining rock, silo and embedment be composed so that the contact and interaction between them is maintained for at least 500 years?

THE SHAPE OF THE SILO CAVERN

A silo with the requested storing capacity and stability occupies a space of about $50\,000\text{ m}^3$, and since rock mechanical stability criteria imply that the diameter of the cavern should not exceed 25-30 m its height must be around 50 m. The finally selected theoretical diameter was 29 m and the height 50 m at the walls and 65 m at the center of the cavern, the cross section of the roof being semi-elliptical. The cavern was excavated by blasting, applying ordinary technique and thus causing some disturbance of the “nearfield” rock.

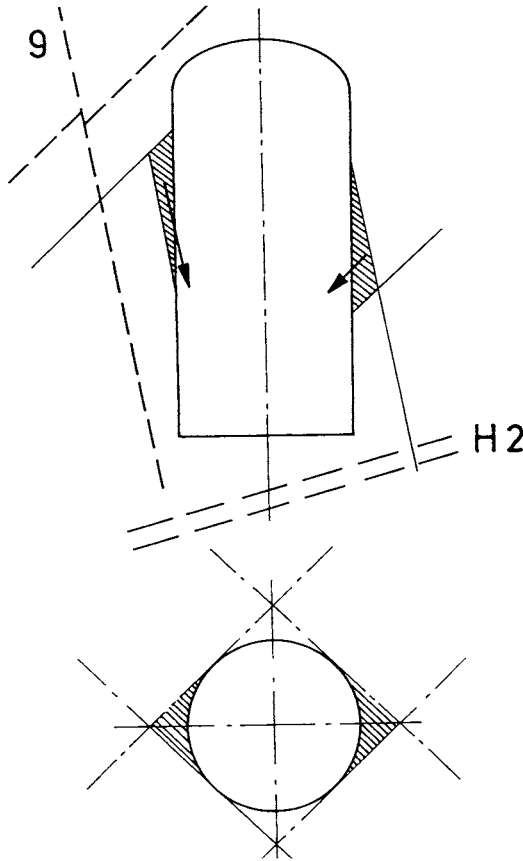


Figure 7 Schematic section of the rock with identified potentially slipping rock wedges. Two major fracture zones 9 and H2 are indicated (cf. Figure 5)

The stability of the cavern and the time-dependent displacements of the roof and walls with associated changes in hydraulic conductivity of the rock were predicted on the basis of rock mechanical analyses, which required determination of the primary (in-situ) rock stresses. These matters, which are of great practical importance for any rock construction project, are described in rock mechanical textbooks to which the interested reader is referred [3].

DESIGN AND CONSTRUCTION OF THE SILO AND EMBEDMENT

The monolithic cell structure of the silo and the way of preparing it, i.e. by applying slipform construction, were estimated to give the silo sufficient strength and stability. The choice of wall thickness and reinforcement was based on finite element calculations considering different possible load constellations in a five hundred year perspective, the most critical ones being maximum external groundwater pressure before water has yet entered the interior, and non-uniform external swelling pressure exerted by the surrounding bentonite embedment. The latter matter is of fundamental importance for most repository design and we will return to it in several chapters of this book.

The base of the silo consists of a 1 m thick concrete slab that rests on a 1.5 m thick bed consisting of a mixture of 90 % sand and 10 % bentonite, applied and compacted layerwise by heavy vibrating rollers. The top of the silo has not yet been constructed but the preliminary design implies that it will be similar to the base but equipped with filter-type outlets that permit gas to escape while offering significant flow resistance to water.

The required embedment of the silo was obtained by constructing a low-permeable bottom bed of sand mixed with bentonite clay, and by surrounding the silo by filling the 1-2 m wide slot between the silo and rock with granulated, air-dry Na bentonite. This fill has several purposes:

- * It serves as a low-permeable isolation with a lower hydraulic conductivity than that of the host rock
- * It helps to redistribute non-uniform rock pressure on the silo that may arise from tectonic activities. Through this the structural integrity and tightness of the silo will be largely preserved
- * It establishes and maintains an intimate contact with both the rock and the silo, preventing water from flowing along these boundaries

* Like the bottom bed and the forthcoming top bed of similar design, it offers “backvalve”-type escape of gas from the silo without undergoing significant permanent microstructural damage.

The problem of finding a simple and rational way for applying the slot fill so that it becomes uniform and not very dense, which would yield a too high swelling pressure, required comprehensive full-scale testing. The finally selected technique of applying the bentonite granulate was to let it flow down through 0.15 to 0.20 m diameter tubes from a hopper that was moved along the periphery of the silo top. Due to successive compaction of the fill by its own weight, its density varied almost linearly as shown by the diagram in Figure 8. For the obtained density interval the ultimate swelling pressure was predicted to become about 0.5 MPa, while the hydraulic conductivity was estimated to be less than 1 % of that of the surrounding rock, thus yielding the diverting effect of groundwater that is illustrated by Figure 9. Figure 10 shows a generalized vertical section of the silo.

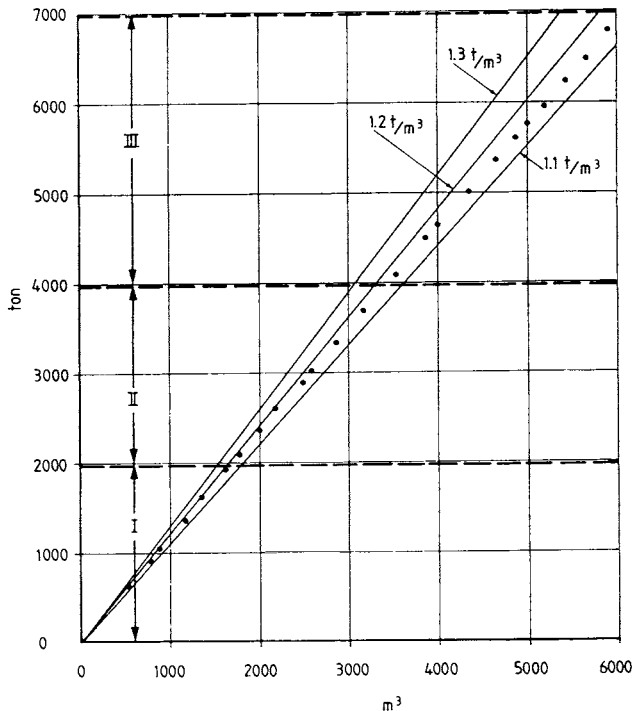


Figure 8 Net average bulk density evaluated in the course of the filling operation. The dry density (ratio of solid mineral substance and total volume including voids): Zone I: 0.98-1.02 t/m³, Zone II 0.98-1.01 t/m³, Zone III 0.98-1.00 t/m³

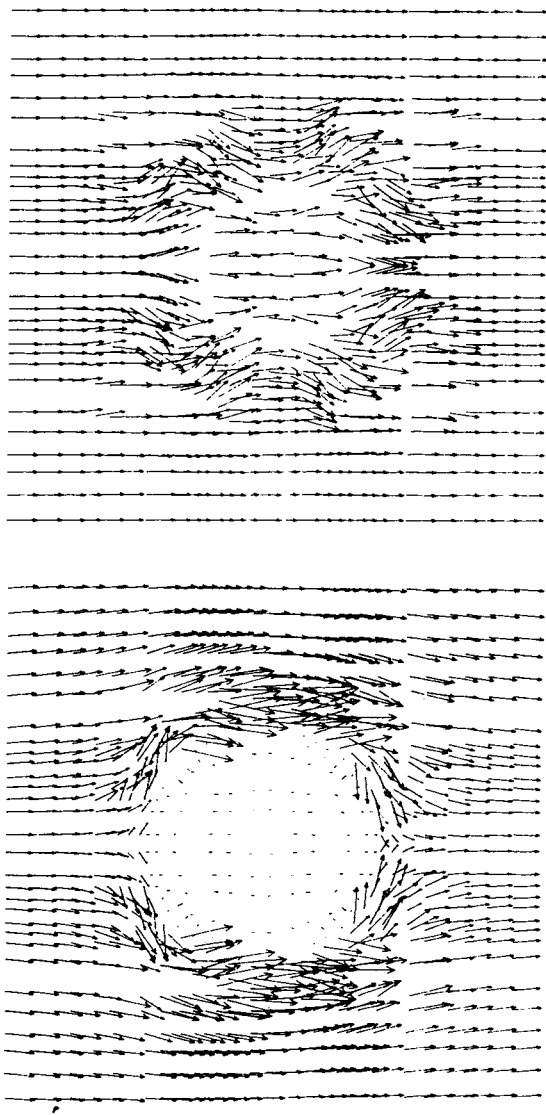


Figure 9 FEM-calculated change in horizontal groundwater flux through the Forsmark silo by introducing a bentonite-filled slot around the concrete silo. Upper: Unfilled slot. Lower: Slot filled with bentonite. The hydraulic conductivity of the rock and bentonite backfill 10^{-8} and 10^{-10} m/s, respectively

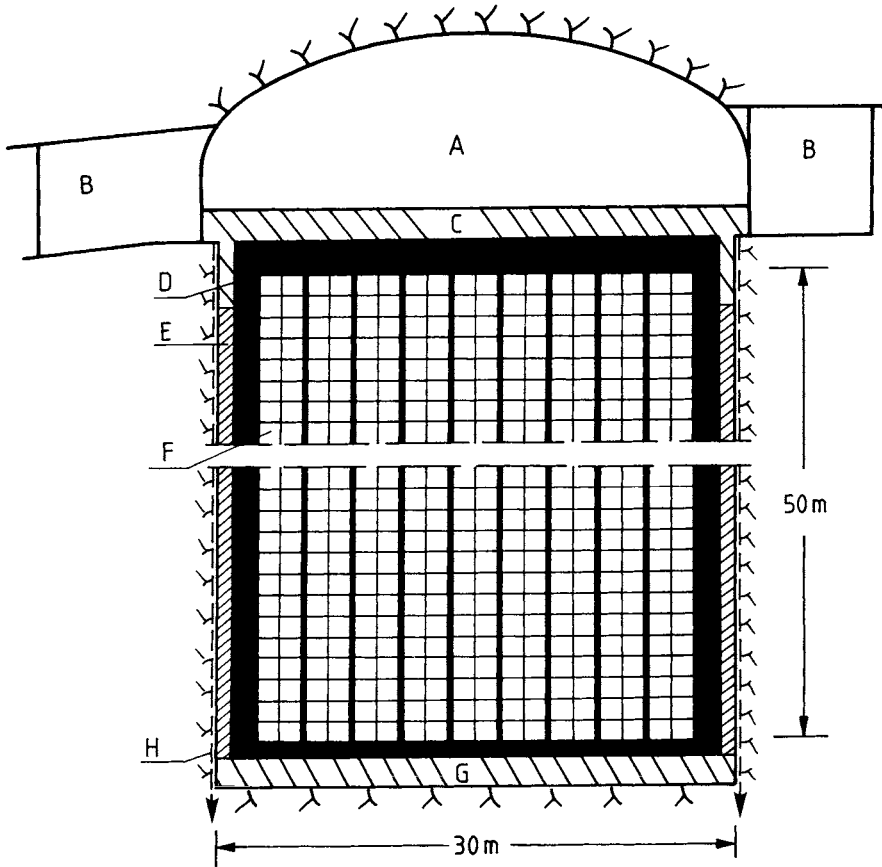


Figure 10 Schematic cross section of the silo cavern. A) Cement-stabilized sand-fill, B) Concrete plugs, C) Bentonite/sand top bed, D) Concrete silo, E) Bentonite backfill, F) Waste packs, G) Bentonite/sand bottom bed, H) Drains connected to tunnel system [4]

After completing the design, the next step would be to conduct a performance analysis, or in practice a safety analysis, for predicting the release of the hazardous elements, i.e. radionuclides, from the waste. This work needs quantification of the “source” term and modelling of the geosphere as well as the biosphere, which involves a number of scientific fields. We will only give an indication here of the outcome of this work.

1-5.5 Safety assessment

FLOW CALCULATIONS

The safety assessment comprised several studies of radiation protection in handling and transport of the waste as well as of the mechanisms involved in release and migration of radionuclides within and from the vaults and the silo, but we will confine ourselves here to describe the performance and results of groundwater flow calculations required for estimating the contamination of the biosphere in a long term perspective.

Calculations of the groundwater flow through the large rock block with the silo and vaults located in the framework of fracture zones in Figures 4,5 and 7, were made by numerical calculations using a finite element code named GWHRT. The relevance of the numerical model and the validity of the calculations could be checked by recording the piezometric pressures in a large number of deep boreholes and the inflow of water into the finally constructed repository. Figure 11 shows the pressure distribution in a vertical section through the repository before the silo construction started, from which one finds that the lower, flatlying zone H2 served as a major drain and that the hydraulic gradients were locally very high in the construction period. After closure sometimes in the next century, they are expected to be evened out and, ultimately, the regional gradient 10^{-3} to 10^{-2} will prevail.

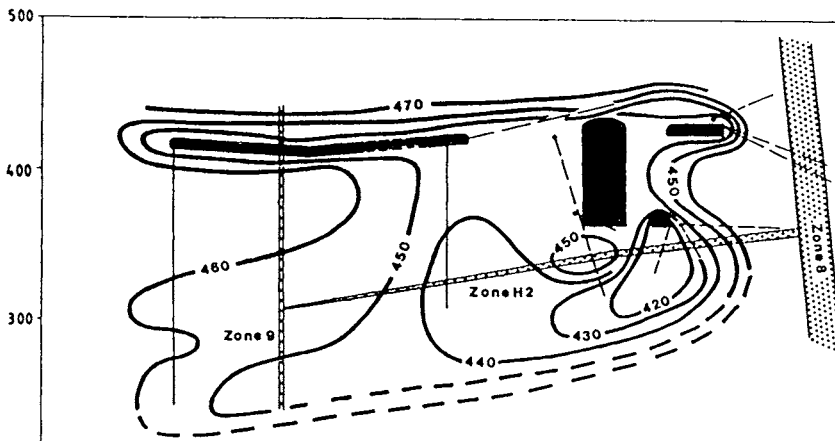


Figure 11 Groundwater pressure distribution in the repository in the construction period. Black areas indicate excavated tunnels from which boreholes extend.

The flow calculations in the safety assessment were made by assuming that the driving force for groundwater flow will be the regional hydraulic gradient resulting from the ongoing land rise in the area [5]. The present rate of annual upheaval is about 6 mm. No percolation of the silo was concluded to take place at all as long as the silo and its embedment are intact, but applying relevant but conservative processes it was found that the barriers will begin to leak after 1000 years.

The calculations were mostly made by assuming plane flow, i.e. two-dimensional conditions (2D), focussing on the groundwater movement in the large Zone 3 oriented NNE/SSW. The flux through the repository was found to be $5 \text{ l/m}^2\text{,y}$ after 1000 years and $15 \text{ l/m}^2\text{,y}$ after 2500 years. Figure 13 illustrates the flow pattern.

RADIONUCLIDES APPEARING IN DRINKING WATER

The design criterion had been set at $100 \mu\text{Sv/y}$ as maximum permitted individual dose for members of the most strongly exposed group of people in the area, based on the total activity of the silo and the decay rate (Figure 12). The diagram demonstrates that the activity is on the same order as the background value after a few hundred years and that an increased percolation of the silo does not really matter after 500 years.

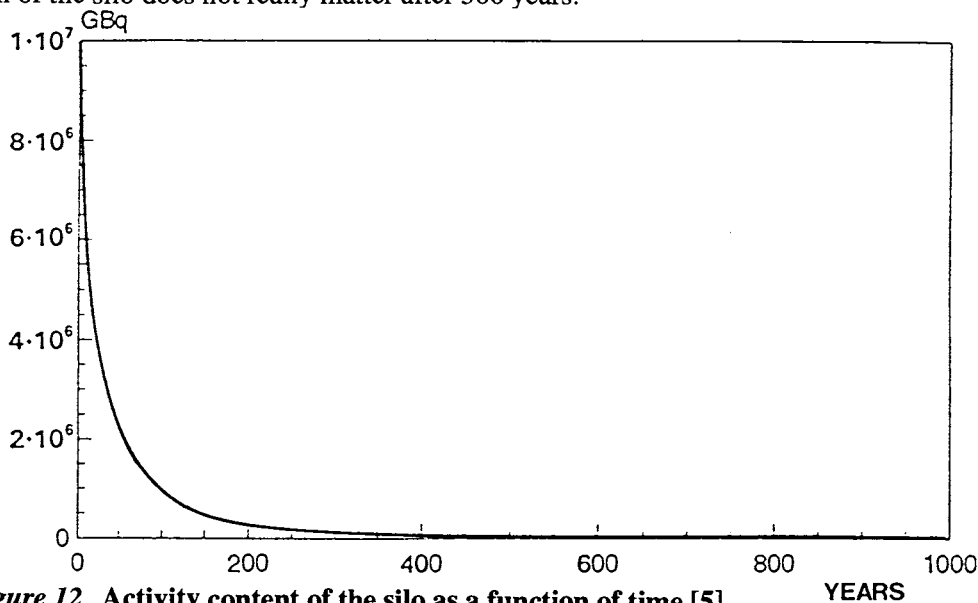


Figure 12 Activity content of the silo as a function of time [5]

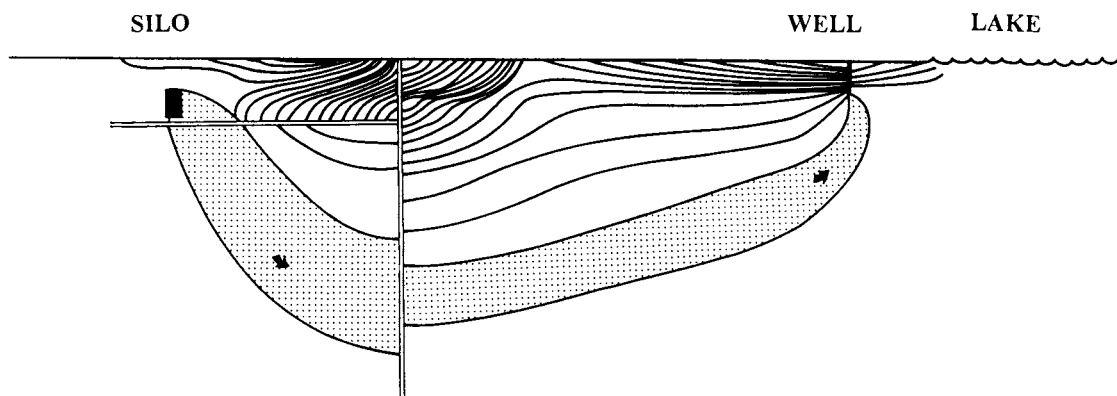


Figure 13 Stream-tubes from inland to a well according to flow calculation concerning the conditions after 2500 years when land upheaval has moved the shoreline eastwards (“Lake”) and made farming possible [5]

The very strong dilution in the huge bay that serves as recipient, means that the individual dose will be less than $1 \mu\text{Sv/y}$ in the first 1000 years, when the land rise is expected to have turned the bay to dry land. Before this happens, i.e. when the sea still covers the area, the release of radionuclides from the silo takes place only by diffusion through the barriers and by expulsion of radioactive water from the interior of the silo driven by gas formed i.a. by corrosion of steel drums and reinforcement bars. At this stage the risk will be even lower.

Calculation of the concentration of radionuclides in a hypothetical well for a medium-sized farm on the newly formed land was found to yield a dose of up to $30 \mu\text{Sv/y}$ after 2500 years, which is, however, very much lower than the present value for many wells in Sweden and also one third of the design criterion (cf. Chapter 1-3.2). The major radionuclides in the waste are cesium-137 and cobalt-60 at the time of closure of the repository in year 2010, while carbon-14 and plutonium are the major long-lived species.

1-5.6 Instrumentation and monitoring

Recording of piezometric pressures and sampling in boreholes for chemical analysis of the groundwater were made throughout the construction period and they will be pursued until the closure of the repository for checking the groundwater flow model. The chemical analyses are particularly revealing since the initial groundwater composition is characterized by stratification with the uppermost part of the aquifer being freshwater below which there are two horizons of strongly brackish water, the upper one consisting of relic salt water.

The physical function of the clay and concrete barriers is also being investigated using a test program which comprises measurement of the settlement of the silo, and the development of swelling pressures in the bentonite backfill, as well as the piezometric pressure at the interface of the backfill and the rock wall. The settlement of the silo is being recorded for validation of a prediction that forms the basis of a future decision of how the backfilling on the top of the silo shall be made in order to maintain contact between the bottom bed, the silo with top filling and the overlying rock. It is expected to increase from the present value 6 mm after 6 years (Figure 14), with only a small amount of waste, to about 30 mm when the silo is

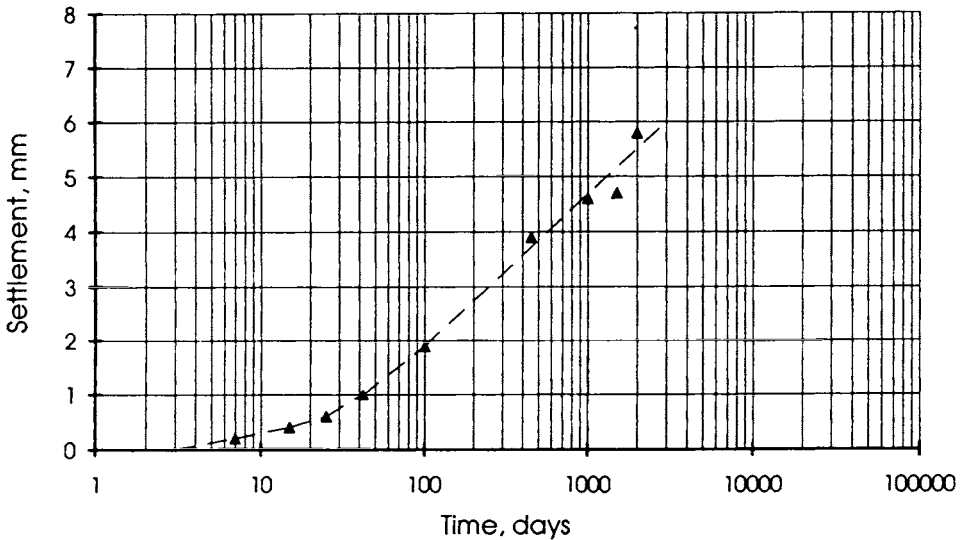


Figure 14 Recording of settlement Δ caused by compression of the bottom bed consisting of a heavily compacted mixture of 10 % bentonite and 90 % properly graded ballast. T is time in days after construction

finally filled with waste containers. It will, however, turn into a slight heave due to buoyancy when the piezometric conditions have finally be restored after closure of the repository. The silo and the top bed will undergo slow compression due to their own weights, and the rock roof will move downwards by creep as illustrated in Figure 15, meaning that the interaction of all the components becomes very complex. Both soil and rock mechanics have to be applied for making an optimum choice of the composition of the top filling so as to eliminate formation of gaps and short-circuiting passages for radioactive water.

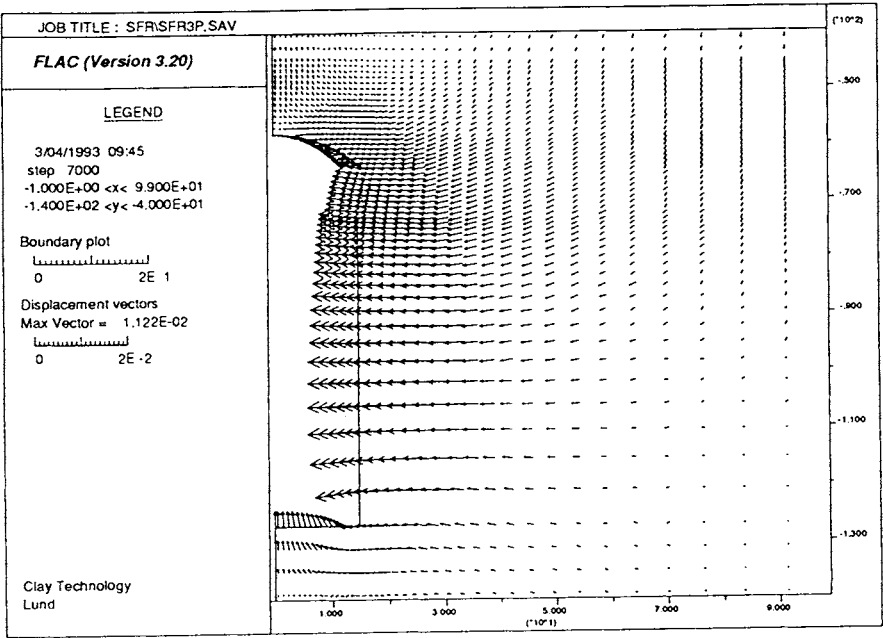


Figure 15 Displacements of the rock cavern as predicted by numerical calculations. Maximum strain vector is 11.2 mm [6]

1-5.7 Cost

The total cost for the design, construction and installations in SFR was about 740 MSEK referring to the price level in Sweden in 1987 but excluding costs for the geophysical and geological investigations. The distribution of the cost of major activities was as follows:

1. Rock excavation and stabilization ($430\,000\text{ m}^3$): 133 MSEK
2. Construction of silo and rock caverns: 148 MSEK
3. Design, administration, staff on site: 230 MSEK
4. Mechanical equipment: 100 MSEK
5. Electrical and communication installations: 60 MSEK

1-6 References

- 1 Swedish Nuclear Fuel and Waste Management Co (SKB). SKB 91 Final disposal of spent nuclear fuel. Importance of the bedrock for safety. SKB Technical Report TR 92-20, SKB, Stockholm, 1992
- 2 Hökmark, H. Thermomechanical study of jointed rock around a KBS3-type nuclear waste repository. SKB Internal Report AR 92-75, 1992
- 3 Pusch, R. Rock mechanics on a geological base. Elsevier Publ. Co. (In press)
- 4 Pusch, R. and Cederström, M. Clay isolation of a large underground storage for nuclear wastes. Proc. 12th Int. Conf. Soil Mech. a. Found. Engng., Rio de Janeiro, Vol.3, pp.1903-1906
- 5 SKB. SFR-1 Fördjupad säkerhetsanalys. SKB Arbetsrapport SFR 91-10. SKB, Stockholm, 1991

6 Hökmark, H. Numerical analysis of time-dependent deformations in the rock surrounding the SFR repository. SKB Internal report, SKB, Stockholm, Feb. 1993

Chapter

2 *Location of Repositories*

2-1 Major factors

A number of factors affect the location of waste repositories; the major ones are:

- * Toxicity of the waste
- * Risk of contamination of the groundwater
- * Compatibility of the host rock and the waste
- * Presence of valuable mineral resources
- * Cost

TOXICITY

Naturally, less toxic waste does not need as effective isolation from the biosphere as strongly hazardous waste, as is illustrated by the fact that low- and medium-level radioactive waste is deposited in shallow or on-ground repositories while highly radioactive waste has to be disposed of at much larger depth. Certain geological and climatic conditions make it possible to obtain sufficiently safe conditions for shallow repositories, which of course causes appreciably lower cost than what deep-sited repositories require, and both low-level radioactive waste and moderately toxic chemical waste may be disposed of in relatively simple repositories at shallow depth. However, it is necessary to realize that while radioactive waste undergoes decay and becomes less dangerous with time, heavy metals and other toxic waste products maintain their toxicity forever. As for highly radioactive waste, very hazardous chemical waste should therefore be disposed of in repositories that give off toxic elements in a control-

led fashion, i.e. so that the contamination of the biosphere remains acceptable for any period of time. Disposal at large depth is hence preferable of hazardous chemical waste but cost aspects make it necessary to consider other solutions than constructing repositories deep down in the rock. Mines seem to offer a good, economic alternative.

CONTAMINATION OF GROUNDWATER

The risk of groundwater contamination is of importance only when pollution implies danger for living species, i.e. when the concentration of toxic elements has reached a critical level. It depends on two factors: the solubility of the waste and the dispersion, which is - in turn - controlled by the transport mechanisms and paths. The solubility is strongly dependent on the pH conditions, and the dispersion on the hydraulic conductivity and gradient as well as on diffusion and sorption. Strong and quick dispersion of toxic elements released from waste material is effected by high hydraulic gradients and a high hydraulic conductivity and lack of sorption in the host rock. Very toxic waste, for which disposal in deep repositories may be required, should naturally be located in rock where groundwater movements are at minimum, which implies that the waste is isolated from water-bearing zones and that the hydraulic gradients are low.

COMPATIBILITY OF ROCK AND WASTE

An example of excellent compatibility of rock and waste, i.e. a condition in which chemical degradation of the host rock is not induced by the introduction of the waste, or vice versa, is that of disposal of industrial waste products rich in arsenic and mercury in a deep mine with As- and Hg-bearing ore. Similar examples are offered by cadmium-bearing waste, like batteries, when disposed of in mines where Cd-rich ore has been exploited, and plumbum dumped in mines with Pb-bearing ore. Disposal of radioactive waste in uranium mines is naturally very suitable for the same reason. There is also a number of possibilities for minimizing release of hazardous elements, like adjusting pH by using Na-saturated smectite clay (bentonite), concrete with cement of Portland type or Portland cement mortar for waste embedment, or mixing the waste with carbonate rock. Such measures increase the pH and thereby reduce the solubility of heavy metal waste. In fact, disposal of such waste in thick limestone deposits of sedimentary origin or formed at depth in crystalline rock, could also be a good solution from this point of view, as may also disposal in thick deposits of zeolites and smectitic clay, since they serve as very good cation exchangers and absorb released dissolved metals, and in addition, clays have a very low hydraulic conductivity. However, carbonate rock and zeolite

and clay deposits are mechanically weak and cause substantial difficulties like creep in the excavation and waste application phases, which may last for many decades. The excellent stability and tightness of igneous or metamorphic, crystalline rock make them primary candidates for hosting repositories at depth, which is the reason for dealing only with such rock in the present book.

VALUABLE MINERAL RESOURCES

Naturally, regions with mineral resources like valuable ore or oil and gas are not suitable for hosting waste repositories. The matter is a bit complicated, however, since abandoned mines or mines in operation with incompletely exploited ore bodies may be excellent for disposal of hazardous chemical waste akin but not identical to the ore. In practice, it calls for considering each individual case separately and carefully and it requires assessment of the economic potential of not yet mined ore as well as assessment of environmental impact and safety.

COST

In practice, the cost aspect is the most important issue. As illustrated by the Forsmark example in Chapter 1 rock excavation by applying moderately careful blasting costs around 3000 SEK (about 400 US\$) per cubic meter excavated rock (1987 price level), and waste embedment may amount to the same figure using concrete and bentonite clay. Hence, only the most toxic waste can be disposed of in deeply located, well isolated repositories that are constructed for the purpose of waste disposal and one realizes that mines may represent ideal sites for disposal of toxic waste. An example of how such a mine can be utilized is the Stripa mine in Sweden where an OECD research project was conducted in the period 1978-1992 for developing methods for large- and small-scale hydraulic characterization and for effective isolation of radioactive waste. This project and relevant results emanating from it will be referred to throughout this book.

2-2 Rock structure

2-2.1 What is important?

The major factors influencing the selection of a suitable location of a repository for toxic waste are the hydraulic conductivity and the flow paths of the rock mass hosting the repository. Both are determined by the rock structure, particularly the large-scale features, for which we will use a practical classification scheme [1].

2-2.2 Basis of characterization

Structural features of different types appear more or less regularly in rock of various sorts, a matter that is considered in several rock classification systems like the wellknown mode of characterizing rock proposed by Barton, Lien and Lunde [2]. Such systems are primarily intended for relating specified degrees of fracturing and fracture properties as well as hydraulic conditions to stability conditions in tunnels and slopes and for estimating the need of reinforcement, but they are of limited value for describing the hydraulic and mechanical behavior of a rock mass with differently organized structural components on a large as well as small scale. For this purpose other ways of characterizing rock are required, particularly for definition of the various discontinuities which control the physical behavior of any rock mass. The 7 order discontinuity scheme is of practical use and will be applied in this book [1,3].

2-2.3 The 7 order discontinuity scheme

The basis of structural modelling is the hierarchy of practically important discontinuities. Before going deeper into defining them and their properties we need to make a distinction between “fractures”, “joints”, and “fissures”, which are often used interchangeably for any rock break. According to geological practice one should apply the term joint for tensile breaks only while fractures are commonly associated with shear failure and fissures referred to as discrete breaks of unknown origin. We will devoid from such specification and use the term fracture for all sorts of breaks. Since it has become common to apply the term joint rather than fracture in numerical rock mechanics, we will do so in dealing with stress/strain calculations. We will use the term “fissures” to describe very fine fractures.

The structure scheme, which is generic and agrees, in principle, with Figure 16, gives a common basis for rock structure modelling and rock mechanical and hydrological calculations. It is of great help in identifying and defining proper sites of repositories and of sealing components in them by ascribing typical hydraulic conductivity and rheological properties to the seven categories of discontinuities.

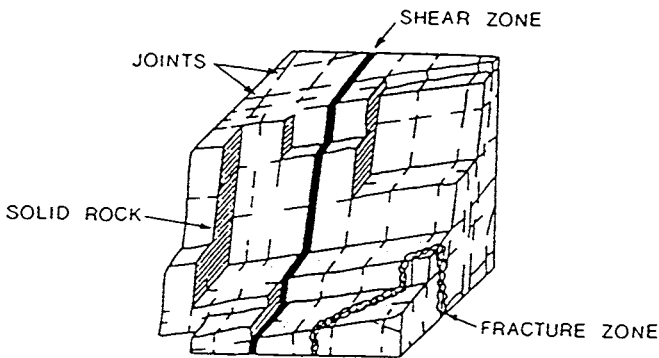


Figure 16 Generalized picture of granitic rock (After Witherspoon and Gale)

1ST ORDER DISCONTINUITIES

Regional fracture zones with a few km spacing and an extension of several tens of kilometers. The width of the central, most hydraulically active core, which is usually characterized by clay and iron compounds, ranges from meters to tens of meters and the zones contain closely spaced and interconnected breaks, yielding an average hydraulic conductivity of around 10^{-6} m/s. The conductivity may range between 10^{-7} to 10^{-5} m/s, but it may locally be much lower.

2ND ORDER DISCONTINUITIES

Local fracture zones with a spacing of several hundred meters and an extension of several kilometers. The character is similar to that of 1st order discontinuities although with less width, fracture frequency and clay content. The average hydraulic conductivity is on the order of 10^{-7} m/s, the actual span being 10^{-8} to 10^{-6} m/s except for local much tighter parts.

3RD ORDER DISCONTINUITIES

Local fracture zones with a spacing of a few tens to a few hundred meters and a width of a few decimeters up to a couple of meters. A cross section shows no clay but several, not always interacting fractures yielding an average hydraulic conductivity of such zones of 10^{-8} m/s. The actual span is 10^{-9} to 10^{-7} m/s and locally lower than that.

4TH ORDER DISCONTINUITIES

The 4th order discontinuities are the major hydraulically active small-scale members of rock located between low-order discontinuities. They occur - or can be generalized - as discrete fractures with a common spacing of 2-10 m and an extension in their own planes on the same order of magnitude but occasionally much more than that. A common average spacing is 5 m. The pervious part of the fractures are channels distributed over the fracture plane but more commonly at the intersection of fracture planes. Rock with discontinuities of 4th and higher orders usually has an average hydraulic conductivity of 10^{-11} to 10^{-9} m/s.

5TH ORDER DISCONTINUITIES

5th order discontinuities represent the rest, i.e. about 90 %, of the visible discrete fractures of the rock between low-order discontinuities. They do not contribute significantly to the bulk hydraulic conductivity either because they do not interact, or because they are healed by pressure solution or precipitation. Their average spacing is about one tenth of that of 4th order discontinuities, and their interaction is poor. However, they represent potential weaknesses so that mechanically or thermally induced strain can activate or - with a modern term - stimulate them hydraulically by shearing or tension.

6TH ORDER DISCONTINUITIES

6th order discontinuities can be seen with the unaided eye but require microscopy for characterization. They represent weaknesses in the form of zonal enrichment or orientation of certain minerals, or of fine fissures, and they commonly form subsystems that conform more or less to the 5th and 4th order discontinuities.

7TH ORDER DISCONTINUITIES

7th order discontinuities represent inter- and intracrystalline voids and incomplete crystal contacts, all serving as embryonic breaks, i.e. "Griffith cracks".

2-2.4 Examples

Following the reverse order, i.e. starting with the smallest structural features, some typical examples will be illustrated here as a basis of the structural modelling that is required for numerical calculation of groundwater flow and rock stability in repository design and performance assessment. Naturally, there are no clear boundaries between the various types of discontinuities but the defined different physical properties makes it possible and suitable to assign any discernible discontinuity to the respective category. Scale effects may cause uncertainties and there are naturally difficulties in deciding from examining a fracture-rich drill core whether it represents the central part of a 3rd order zone or if it originates from the rim zone of a 1st or 2nd order zone. However, any rock sample - be it a drill core or the rock exposed in a tunnel wall - should be characterized on the basis of what can be observed and tested, while the task to model the rock mass is another, namely to put together and assess the information from individual observations for making a synthesis from which the model evolves.

HIGH-ORDER DISCONTINUITIES

Before entering this subject we need to give some general comments on the nature of rock structure. Thus, by definition, the high-order discontinuities represent discrete features.

However, a close look at those representing 4th, 5th and 6th orders commonly reveals that in addition to a major, not always continuous major break that controls the physical behavior of the discontinuity, they also consist of several interacting fissures. For practical reasons one has to disregard from their actual complex nature and generalize high-order components to represent discrete, plane discontinuities that operate as individual structural components.

Starting the discussion by considering 7th order discontinuities, one finds the actual nature of the 7th order discontinuities to be as illustrated in Figure 17. They are important from a rock mechanical point of view because they are embryotic breaks from which fractures develop under critical stress conditions, and their importance for the migration of toxic species like radionuclides is considerable: they form tortuous pathways for diffusing species and their interconnectivity controls the diffusion rate, which is strongly affected by sorption effects (Figure 18). It is estimated, by considering the aperture, tortuosity and incomplete interconnectivity of 7th order discontinuities, which are usually randomly oriented, that they yield a bulk hydraulic conductivity on the order of 10^{-13} m/s as concluded also from various laboratory tests. The existence of these submicroscopic defects is visually manifested by the capillary suction that even the most dense piece of rock exhibits.

Proceeding to the 6th order discontinuities, they are represented by a large number of more or less parallel features for which classical structural petrology (“Gefügekunde”) uses the generic term “s-planes” [4]. They are hardly visible in undisturbed rock but are clearly seen by “etching” through erosion as demonstrated by Figure 19.

Depending on their nature and origin - crystal orientation, local enrichment of minerals of easy cleavage, fissures etc - these features have a spacing and extension in their own planes of centimeters to decimeters. The rock matrix containing only 7th and 6th order discontinuities has a high strength as manifested by the high shear resistance of core samples. Naturally, the presence of the larger 6th order discontinuities means that the hydraulic conductivity is higher than when there are only submicroscopic features of 7th order, but it is still as low as 10^{-12} to 10^{-10} m/s as concluded from laboratory tests and theoretical estimates.

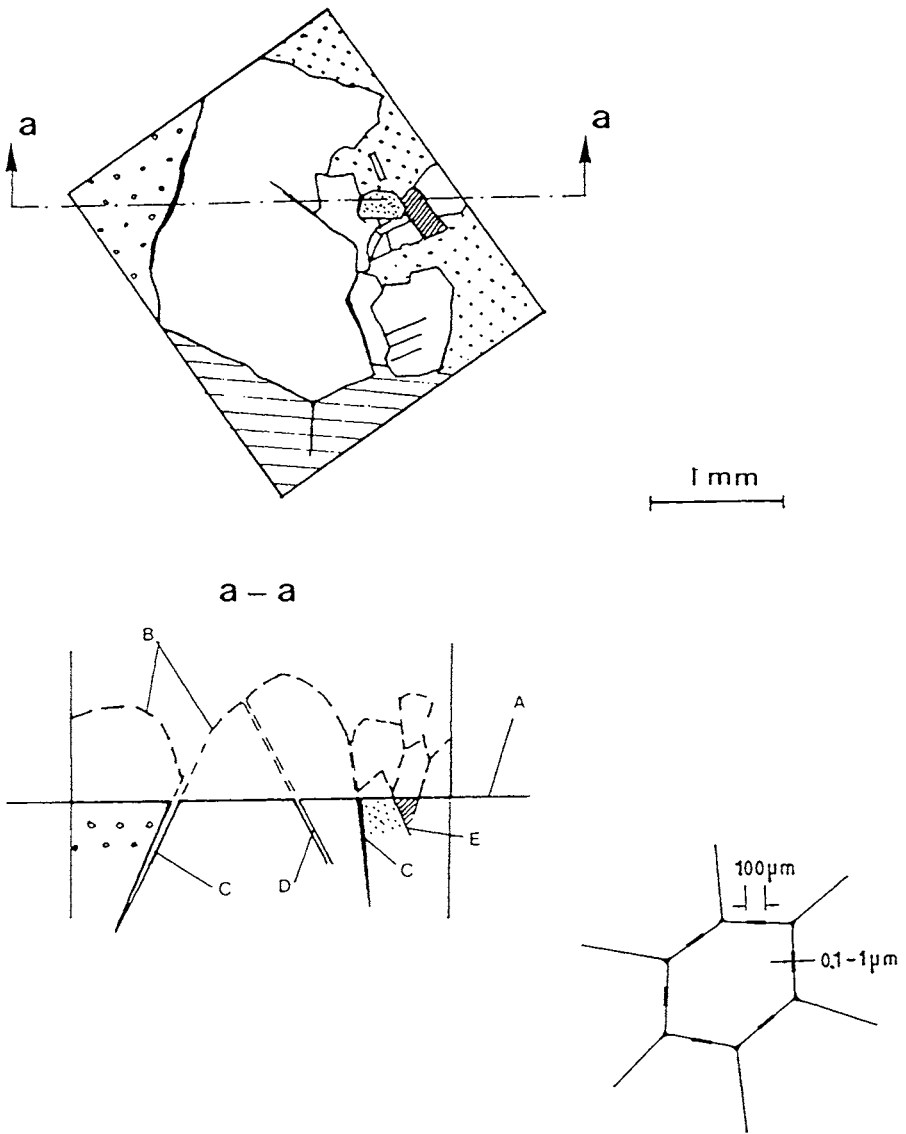


Figure 17 7th order discontinuities in crystalline rock. a-a represents cross section of crystal matrix. A) Polished surface of thin section, B) Actual irregular surface of a joint, C) Incomplete intergrain contacts, D) Fissure, E) Tightly contacting crystals. Lowest picture shows generalized 7th order discontinuities

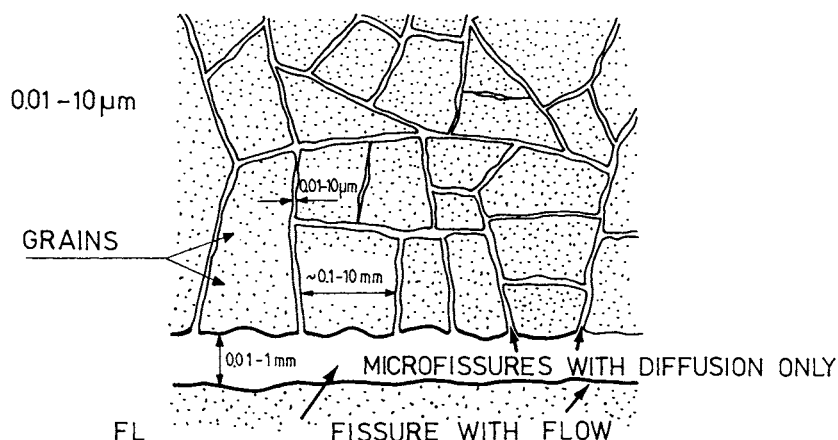


Figure 18 Two-dimensional view of the microstructure of granite used for illustrating the numerous paths in matrix diffusion, which strongly retards the migration of dissolved species [5]

Turning over to the 5th order discontinuities, which represent the large majority of clearly visible and easily characterized mineral zonations and more or less sealed fractures, their larger size yields a lower bulk strength than of rock that holds only 6th and 7th order breaks. As to porosity and hydraulic conductivity, on the other hand, the introduction of 5th order discontinuities in rock with only higher order discontinuities is estimated to have a rather small effect due to the large difference in frequency of the 5th and 6th order breaks. Hence, mechanically undisturbed rock with 5th and higher order discontinuities has approximately the same bulk hydraulic conductivity as rock with only 6th and 7th order breaks, i.e. 10^{-12} to 10^{-10} m/s.

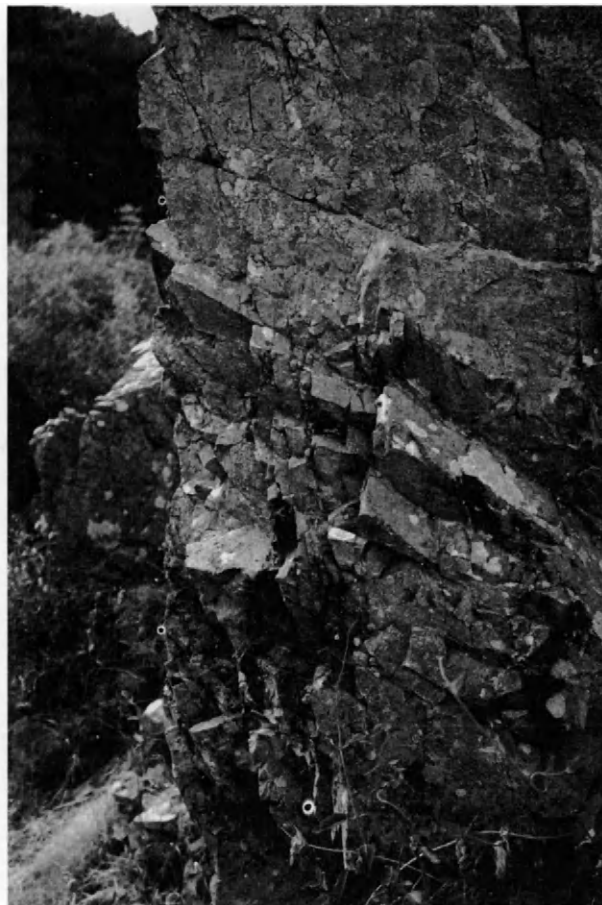


Figure 19 Appearance of 6th order discontinuities in rhombohedral or nearly orthogonal pattern made visible through erosion and frost action in granite close to the shore at Arild, northern Skåne, Sweden

5th order discontinuities, which are commonly more or less sealed fractures, form about 90 % of all macroscopic fractures and do not contribute much to the bulk hydraulic conductivity except close to blasted tunnels where they have been activated by the blasting and altered stress conditions. We will return to this issue several times later in the book.

The 4th order discontinuities, to which the 5th order discontinuities usually conform rather well, are hydraulically interacting, long-extending fractures that are responsible for the major

urity of the water percolation in virgin granite between fracture zones. The frequency of water-bearing channels in them has been estimated by counting the number of major water-bearing spots over exposed rock surfaces in tunnels and the reported figures are in the interval 1 per 25-100 m² cross section area. Assuming that the spots are located where 4th order discontinuities intersect, orthogonal systems of such features would be characterized by spacings of 5-10 m, i.e. yielding an average hydraulic conductivity of rock with only 4th and higher-order discontinuities of 10^{-11} to 10^{-9} m/s. While those of 5th and higher orders are largely sealed in undisturbed rock, 4th order discontinuities are partly open and considerably weaker. One reason for the weakness is that the most common natural filling of 4th order discontinuities is chlorite, which has a low friction angle.

The schematic drawing in Figure 20 illustrates a simplified pattern of hydraulically interacting 4th order discontinuities with an integrated subsystem of 5th order discontinuities with less hydraulic interaction and numerous "dead ends". In principle, the drawing also applies to the interaction of 5th and 6th order discontinuities if those of 4th order are replaced by 5th order features, and those of 5th order are taken to represent discontinuities of 6th order. Figure 21 shows granite with typical sets of 4th order discontinuities.

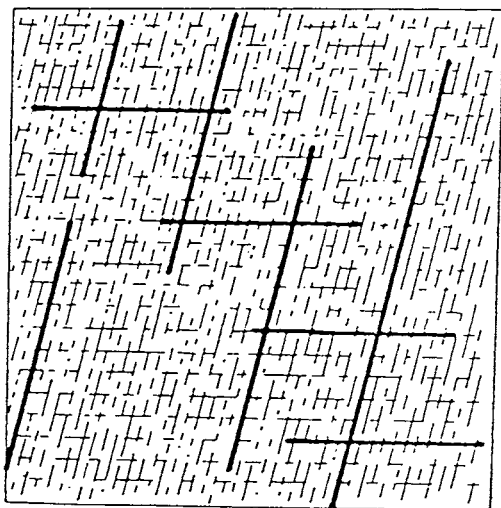


Figure 20 Rhombohedral or nearly orthogonal pattern of interconnected 4th order discontinuities with an integrated subsystem of 5th order discontinuities

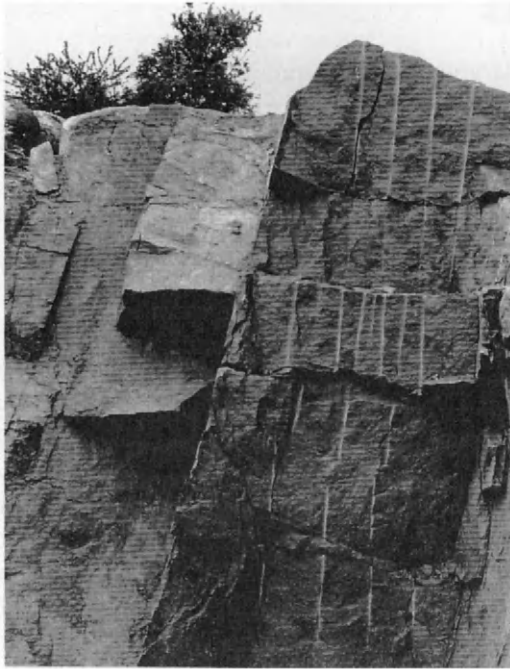


Figure 21 Upper: Typical block structure in granite on the island Bornholm (Denmark), characterized by steep, sheared 4th order discontinuities (plane and long-extending), and flatlying 4th and 5th order breaks that are tension fractures. Lower: Set of 4th order fractures (towards the sea) in granite with integrated 5th order breaks (Skåne, Sweden)

LOW-ORDER DISCONTINUITIES

The actual nature of deeply located, large-scale discontinuities of low order are best illustrated where big underground construction work has been performed. Characterization of typical low-order discontinuities has been made of those identified and investigated in the underground repository for low- and medium-level radioactive wastes at Forsmark, and in the Stripa mine [6,7].

Examples of major, regional fracture zones were given back in Figures 4 and 5 in Chapter 1, i.e. the steeply oriented structures A, B and C forming a more or less orthogonal or rhombohedral pattern. They represent 1st order discontinuities while the rest can be taken to be of 2nd order. The so-called Singö zone (A), of which the central most hydraulically active part is about 30 m wide, is the dominant structure in the area. The large concrete silo that was mentioned in Chapter 1 is located in a polygon-shaped group of steeply oriented discontinuities, i.e. Zones 3,6,8, and 9 (Figure 5). The 7 m wide Zone 3 and Zone 8 with 15 m wide core, can be ranked as 2nd order discontinuities, while Zone 6 and Zone 9, with cores of significantly less width, represent 3rd order discontinuities or possibly discontinuities of 2nd order. The core of the Singö zone as well as the cores of Zones 3 and 8, have a hydraulic conductivity of slightly more than 10^{-6} m/s, while Zones 6 and 9 have a conductivity of around 10^{-8} to 10^{-7} m/s. The 1st and 2nd order zones have undergone considerable disintegration and contain rather much clay gouge.

Turning back also to Figure 7 in Chapter 1, we recognize the close-by Zone 9 and the remote Zone 8, as well as a subhorizontal, major 2nd order discontinuity termed Zone H2. Its core has a width of about 5 m and a hydraulic conductivity of about 10^{-6} m/s.

Typical 3rd order zones, i.e. multiple fracture zones with a small width and no clay gouge, are represented by the structures termed J, K in the granitic Stripa rock (cf. Figure 22). They are members of a set of four NW/SE-striking narrow fracture zones, J,K,M and RP, all dipping about 65 to 85° NE and having an average spacing of 50-100 m [7]. The J-zone was investigated in detail in conjunction with a grouting experiment which showed that its average conductivity in virgin state was on the order of 10^{-8} m/s. Its internal structure, as evaluated from comprehensive core drilling and hydraulic measurements, can be generalized as a regular pattern of orthogonal fine fractures with rhombohedral water-conducting channels formed at the intersection of the fractures (Figure 23). Figure 22 also shows two additional, steeply dipping zones H and C, of which H is a weathered and slightly clay-bearing structure of 2nd order with an average hydraulic conductivity of 10^{-8} to 10^{-7} m/s, while C is a typical 3rd order discontinuity with a hydraulic conductivity of 10^{-9} to 10^{-8} m/s.

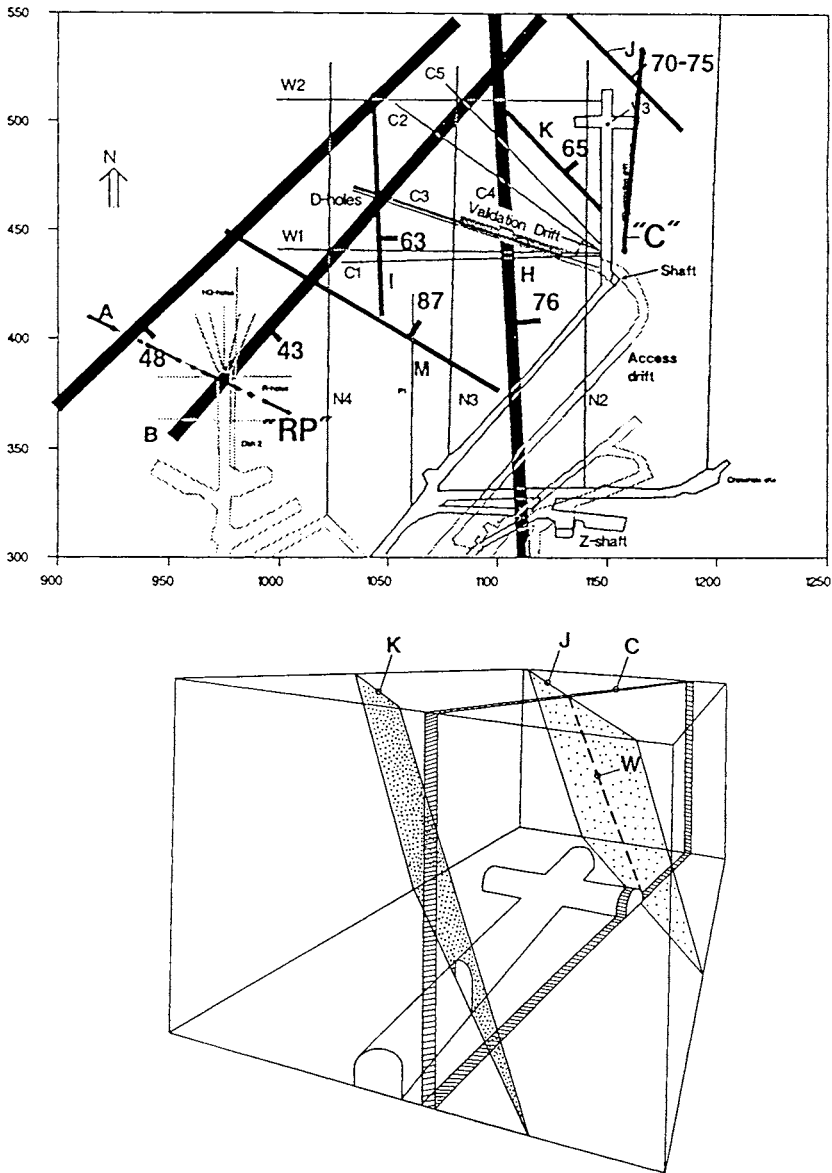


Figure 22 Upper: Plan view of major discontinuities at the 385 m level at Stripa. Lower: Perspective view of the 3rd order discontinuities [7]

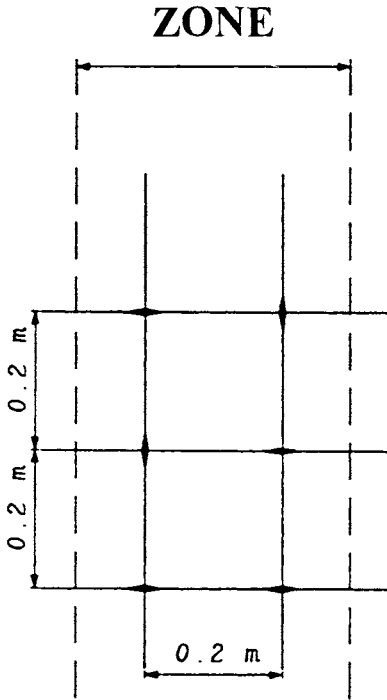


Figure 23 Schematic channel pattern in the J zone. The orthogonal set of lines represent generalized fractures [7]

The largest low-order zones often appear in relatively irregular patterns, partly because of the inhomogeneous stress fields and varying composition of the earth crust where they were formed and partly because they often represent different generations of large-scale structures that were formed under different regional stress conditions. Still, NW/SE-striking low-order discontinuities representing shear-zones usually appear as regular sets in Scandinavia both with respect to spacing and orientation (cf. Figure 24).



Figure 24 Aerial photo of granitic rock areas in Sweden. Notice the regular spacing and orientation of the large zones and the integrated “3rd order” zones. The width of the photo is about 700 m

Table 3 specifies typical average geometrical and hydraulic data of the 7 orders of discontinuities [1]. It should be noted that the respective data are considered to be typical but that there are exceptions. Experience tells that hydraulic testing in boreholes gives a large variation in conductivity and that the number of boreholes must be large for complete characterization, as is also indicated by Figure 25, which shows the recorded flow rate in l/min by hydraulic packer testing of 6 boreholes intersecting the H-zone at Stripa. The average hydraulic conductivity evaluated as the geometric mean of the individual conductivity values was 10^{-8} to 10^{-7} , which is within the interval for 2nd order discontinuities. The scheme represents commonly recorded geometrical and hydraulic data and can be referred to in any rock project. Further generalization may be made for special purposes.

Table 3 General Rock Structure scheme [1] (Common mean given in brackets)

GEOMETRY				CHARACTERISTICS		
Discontinuity	Length, m	Spacing, m	Width, m	Transmissivity, m^2/s	Hydr. conduct. m/s	Gouge seam thickn., m
Low-order discontinuities (conductivity of resp. discontinuity, which are fracture zones)						
1st order	$>10^4$	$>10^3$	$>10^2$	$10^{-5}-10^{-2}$	$10^{-7}-10^{-5}$ (10^{-6})	10^0
2nd order	10^3-10^4	10^2-10^3	10^1-10^2	$10^{-7}-10^{-4}$	$10^{-8}-10^{-6}$ (10^{-7})	10^{-1}
3rd order	10^2-10^3	10^1-10^2	10^0-10^1	$10^{-9}-10^{-6}$	$10^{-9}-10^{-7}$ (10^{-8})	$\leq 10^{-2}$
High-order discontinuities (conductivity figures refer to rock with no breaks of lower order)						
4th order	10^1-10^2	10^0-10^1	-	-	$10^{-11}-10^{-9}$ (10^{-10})	-
5th order	10^0-10^1	$10^{-1}-10^0$	-	-	$10^{-12}-10^{-10}$ (10^{-11})	-
6th order	$10^{-1}-10^0$	$10^{-2}-10^{-1}$	-	-	$10^{-13}-10^{-11}$ (10^{-11})	-
7th order	$<10^{-1}$	$<10^{-2}$	-	-	$<10^{-13}$	-

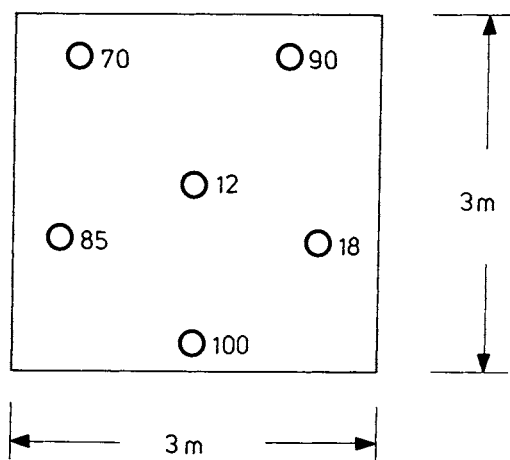


Figure 25 Example of evaluated hydraulic conductivity from packer tests in 6 holes drilled through the 2nd order discontinuity (H) in Figure 22 [8]. The figures denote the flow rate in percent of that of the most permeable part (100 %)

2-2.5 Rock structure modelling

The need for generalized rock structure models has become very strong in later years in the field of applied rock mechanics, i.a. for proper planning of blasting and location and design of supporting structures and for analyzing the performance of competing designs of rock repository concepts.

It appears that many rocks exhibit self-repeating patterns of discontinuities of which the largest ones are major multifracture groundwater conductors and potential tectonic yield zones, the intermediate ones are discrete, more or less water-bearing fractures, and the smallest ones mechanical weaknesses which affect the bulk strength of the rock but not significantly its hydraulic conductivity. The hierarchy of discontinuities of different frequency and properties, expressed in terms of different orders, needs to be considered in all sorts of rock construction and a major aim of all rock investigations is in fact to identify practically important structural features and to create a rock structure model.

Self-similarity or repeatability on different scales of structural patterns will be referred to

here as “fractal”-like although it is not a matter of true fractal structures, which have strictly defined dimensions. Self-repeating systems are common features and if they exist and can be identified they are naturally of great help in structural modelling although we will see that while geometrical patterns may be repeated on different scales, the physical properties are usually very scale-dependent. We will go somewhat deeper into this and also give some further examples of the nature and scale-related grouping of low- and high-order discontinuities. We will start with the latter.

HIGH-ORDER DISCONTINUITIES

As illustrated by Figure 26, the finest 6th order discontinuities, which often has the character of zonal enrichment of certain minerals in the phase of magma cooling [9], may form more or less regular orthogonal or rhombohedral patterns although they are usually more stochastically oriented and distributed than those of lower order. Figure 27 illustrates the rather common case with similarly oriented 3rd to 6th order discontinuities appearing in fractal-like patterns.

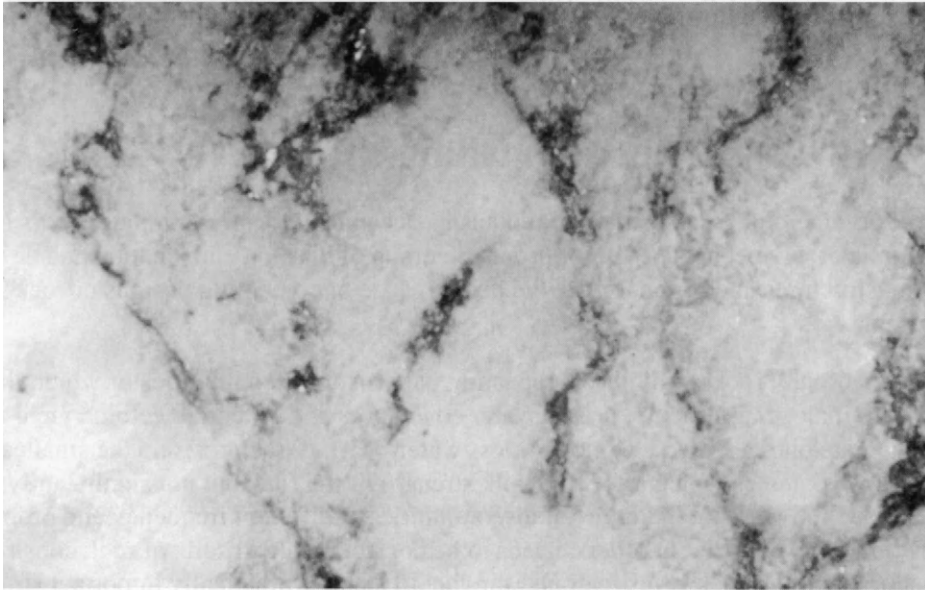


Figure 26 Swiss granite (Grimsel) with orthogonal patterns of zonal enrichment of biotite (20x)

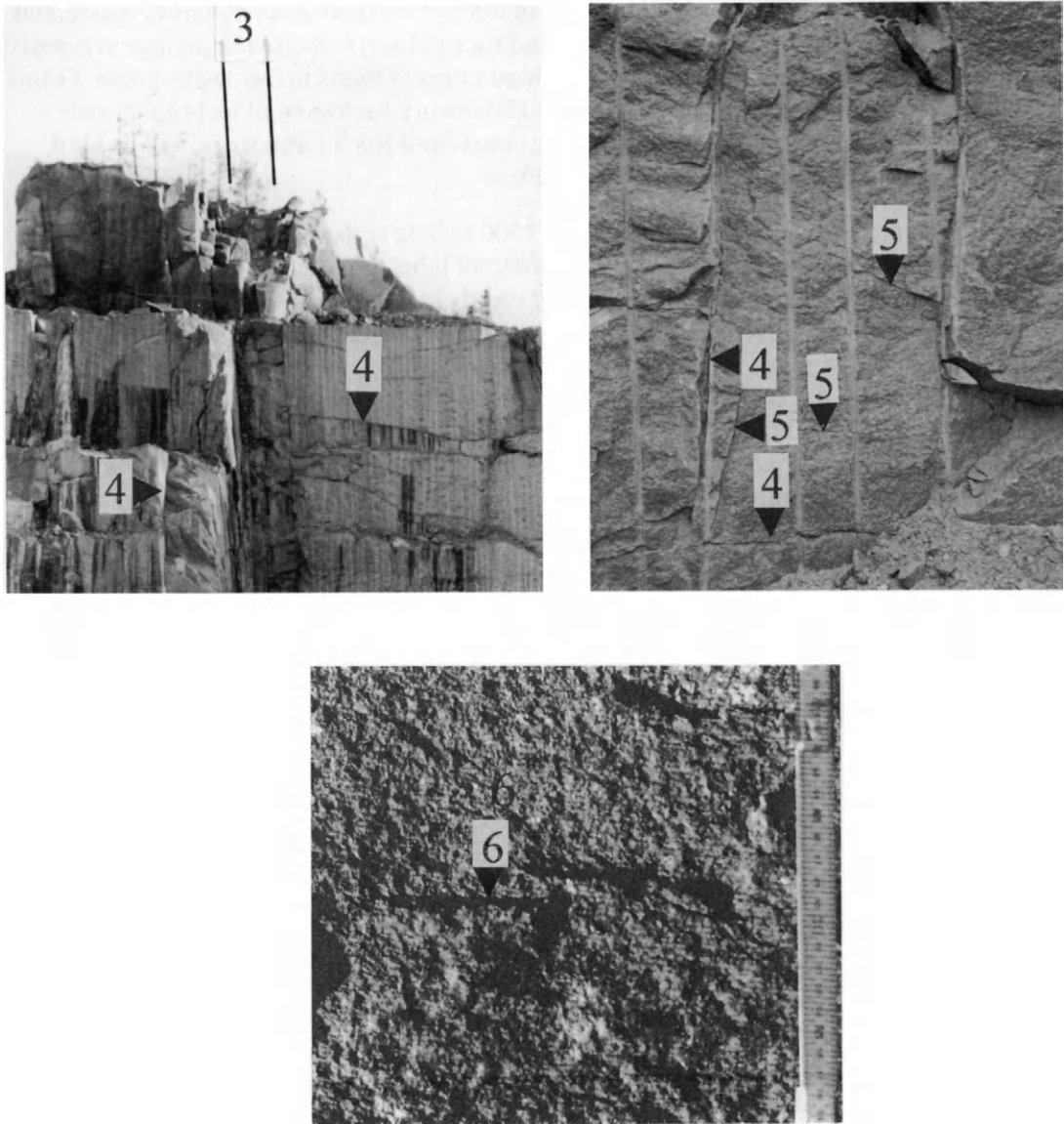


Figure 27 Example of organization of orthogonal patterns of discontinuities of 3rd to 6th orders in a granite quarry.

The actual degree of regularity and correlation of 4th and 5th order discontinuities is essential for proper orientation of tunnels and cavities and for location of plugs and sealings in repositories as well as for selection of an optimum shape of excavations in the design phase. Detailed examination of a new Swedish underground laboratory for testing of techniques and materials for isolation of radioactive waste, the Äspö Hard Rock Laboratory, will be used here to illustrate how generalizations can be made.

The access ramp consists of an approximately 1500 m long straight part that runs NNW/SSE through Småland granite and minor zones of different lithologies, has been carefully mapped with respect to the orientation and extension of clearly visible discontinuities and to their water-bearing capacity. Five 30 m long sections representing different, typical structural patterns were mapped with recording of discontinuities of 4th order type, defined as water-bearing fractures with a trace length of at least 5 m, and with comparison of the orientation of 4th and 5th order discontinuities. The five sections yielded obvious patterns with somewhat but not entirely different frequencies and groupings of the 4th order sets, a natural and typical observation being that flatlying ones were under-represented. Despite the variations, it was possible to define a generalized rock structure for the entire ramp described as superimposed, more or less orthogonal sets of somewhat different orientation. The variation in orientation, which is typical of most granitic rocks, can be described as undulation and twisting of the basic rock structure.

The spacing of the individual members of the sets of 4th order discontinuities is summarized in Table 4. One finds that the average spacing of discontinuities belonging to the respective sets varies from 4 to 10 meters, which is typical of 4th order discontinuities.

Table 4 Average spacing in meters of 4th order discontinuities of the sets

Set	Section 0/445-0/475 m	Section 0/485-0/515 m	Section 0/660-0/690 m	Section 1/100-1/130 m	Section 1/430-1/460 m
Red	9 and higher	8-9	6 and higher	5-10	4 and higher
Blue	10	(zone)	(zone)	10	7
Green	5 and higher	10	-	-	-

Taking the average strike and dip of the various sets of discontinuities one can define the hydraulically and mechanically active rock structure to be composed of three major sets of 4th order discontinuities:

Red: N75W/80N, N10E/80W and N25E/10W

Blue: N100W/90 and N/90

Green: N100W/40N and N90W/40S

It was found that over about 1 km tunnel length the long-extending discontinuities of 4th order make up one dominating “orthogonal”-type system (red) with the discontinuities oriented more or less WNW and NNE as well as subhorizontally, one system (blue) with WSW- and N-striking discontinuities, and a third system (green) striking like the blue system but dipping 40° to the north and south. Figure 28 shows a generalized picture with these three systems marked in parallel perspective form. The blue set lacks a (not identified) subhorizontal component but it can be provided by the red set. Similarly, the green set lacks a steep N-oriented component, which may be provided by the blue set. Further simplification is possible, such as defining a compromise of the red and blue sets, which would reduce the structure to consist of two major almost orthogonal sets of 4th order discontinuities:

I: N85W/85N, N5E/85W and N25/10W (average spacing 7 m)

II: N95W/45N and N95/45S (average spacing 7 m)

The issue of whether and to what extent 4th and 5th order discontinuities are interrelated was investigated by comparing the orientation of these discontinuities as they appeared in randomly selected wall and roof areas. The results are illustrated in histogram form in Figure 29 in which the frequency of 5th order discontinuities (black columns) is plotted as a function of their orientation expressed as the measured angle α between a base line (lower edge of the tunnel) and their projection on the wall and roof, respectively. The orientation of 4th order discontinuities in the same areas is indicated by the unfilled columns marked “4”.

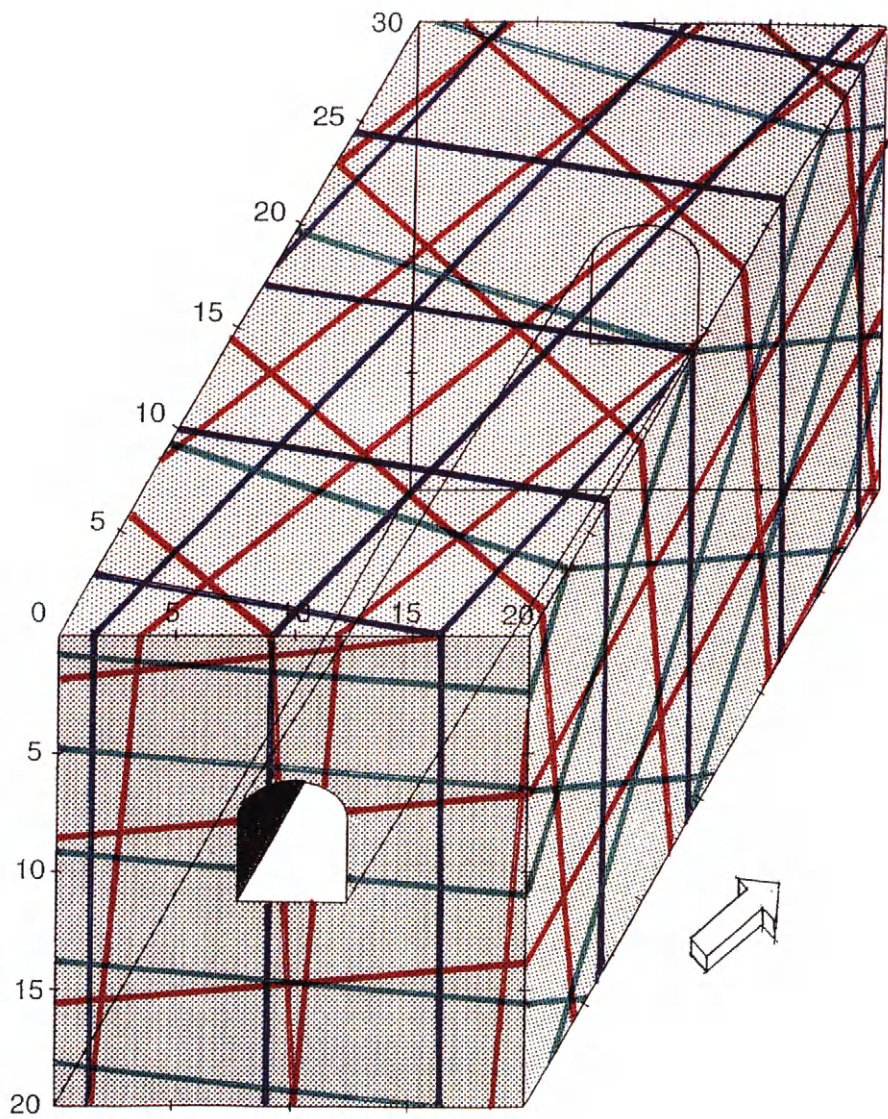


Figure 28 Parallel perspective of generalized systems of 4th order discontinuities in the nearfield of the Äspö ramp. The spacings are generalized at 7 m while the true measure ranges between 4 and more than 10 m

0/450 - 0/470

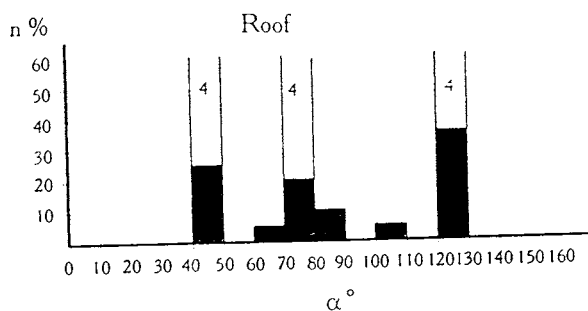
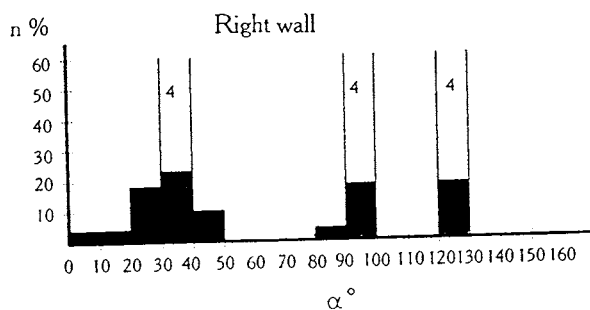
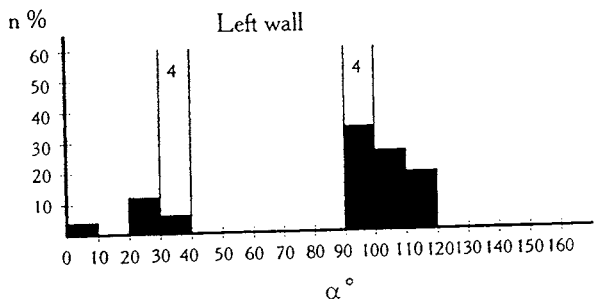


Figure 29 Histograms showing the orientation of 5th order discontinuities compared to that of identified 4th order discontinuities (unfilled columns marked “4”). The agreement between the orientation of the two categories of discontinuities is obvious

Figure 29 demonstrates that there are two or three major 4th order sets in each investigated area and that the large majority of the 5th order discontinuities are grouped around them or even coincide. Still, as documented by the histograms, “erratic” features exist as well.

LOW-ORDER DISCONTINUITIES

The mode of formation and nature of low-order discontinuities as well as their properties vary very much. The basis of classification was given in the early fifties by E.M. Anderson [1] applying Mohr/Coulomb failure modes (Figure 30) and his views still apply in principle as illustrated by Figure 31.

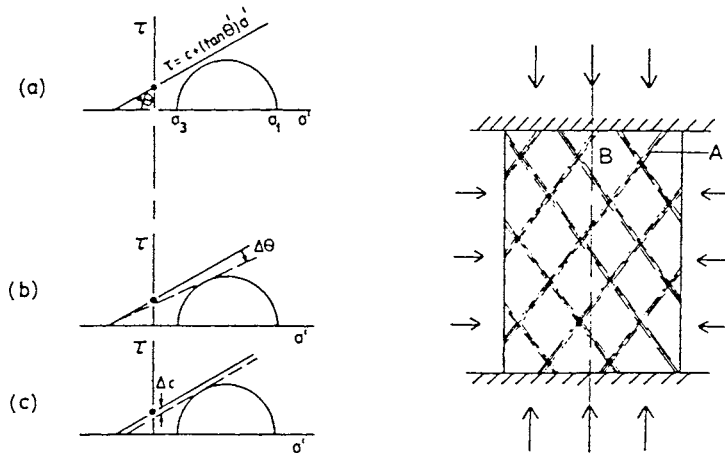


Figure 30 Left: Mohr stress circles with failure envelope corresponding to Mohr/Coulomb failure for: a) stable conditions, b) failure due to strain-induced drop in internal friction, c) failure due to strain-induced drop in cohesion. Right: Mohr/Coulomb failure mode at large strain in slip zones (A) leaving zones with embryonic failure in between (B)

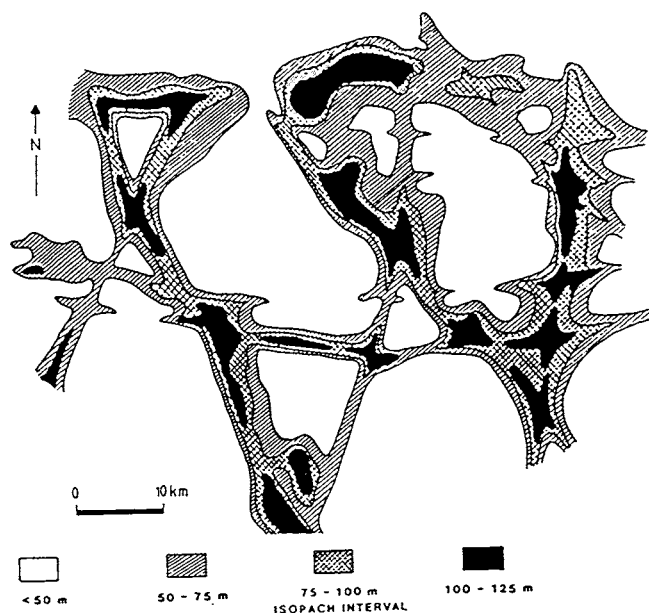


Figure 31 Mohr/Coulomb-type deformation pattern revealed by the anomalous thickness of upper Silurian carbonate deposits in cavities, the depth of which indicate the location of major fracture zones (After Sanford & Thompson)

Figure 31 shows a very regular Mohr-Coulomb type pattern with the fault zones representing 1st order discontinuities, but low-order structures are usually not so regular as indicated by Figures 32 and 33, of which the firstmentioned illustrates the influence of shear strain on the structure and the complexity of large zones, and the lastmentioned the wide rim or transition zones of enhanced hydraulic conductivity of 1st and 2nd order fracture zones. Naturally, this is an important issue for the location and orientation of repositories: there should be a sufficient margin left between the caverns or tunnels where waste is deposited and the nearest zone of enhanced hydraulic conductivity.

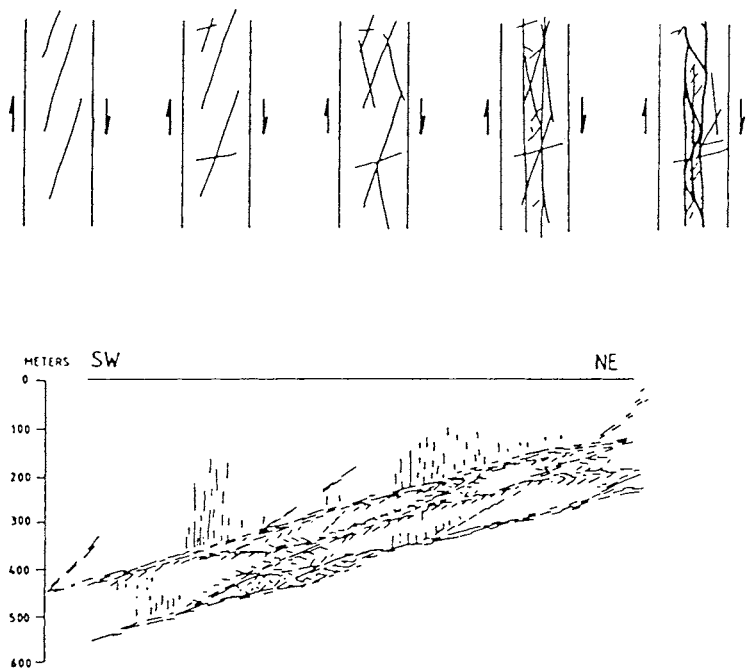


Figure 32 Example of the nature of fracture zones. Upper: Increased shear (left to right) yields higher fracture frequency and ultimately a central core of strongly disintegrated rock [6]. Lower: The nature of the large subhorizontal zone H2 below the silo at Forsmark [6] (cf. Ch. 1-5.4)

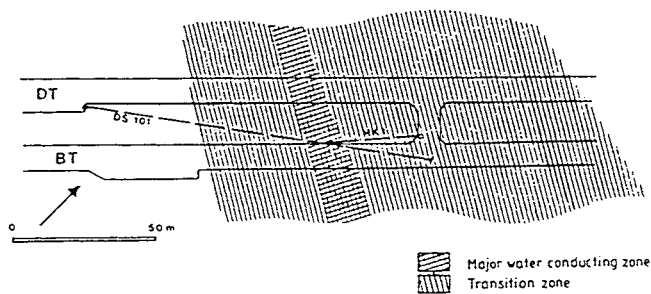


Figure 33 Extension of rim (transition) zones of a 1st order discontinuity (Singö)

There are several reasons for the complexity and irregular nature of low-order zones, like inhomogeneous or rotating stress fields in the course of their propagation, interchanging brittle and ductile rock mass units through which they propagated, and presence of old weaknesses that controlled their location and orientation [11].

All these factors combined to yield considerable variations in strain and therefore also in structure. The amount of strain that the discontinuities have undergone is naturally largest for the 1st order discontinuities than for that of 2nd order breaks, which is in turn larger than for 3rd order breaks. Usually, the most intense displacement took place within a relatively narrow core zone with rim zones of less disturbance. For 1st order zones the core may be a few tens of meters while for the 3rd order zones it is commonly a few decimeters. The major structure-forming processes were the following:

- 1. Small strain generated on single occasions by overloading produced brittle failure in the form of discrete fracture planes, which were initially oriented in the direction of the major principal stress. If the strain was very small and the breaks isolated, they may have retained their chemical constitution and become partly or wholly closed by creep effects or by “pressure solution” depending on the stress history. Such breaks represent 5th or higher order discontinuities**
- 2. Larger but still moderate strain generated on single occasions caused propagation of the weakest of the initially formed breaks, yielding systems of interconnected fractures. Part of them underwent shearing while the rest were exposed to tension. The resulting discontinuities are of 4th order, and they may or may not have been exposed to penetration of hydrothermal solutions from which chlorite, epidote or calcite precipitated. Large strain resulted in 3rd order discontinuities, i.e. development of sets of closely located and partly interconnected fractures**
- 3. Repeated large strain taking place in the multifracture networks of 3rd order zones caused further fracturing and formation of fine fissures by which the rock material disintegrated and clay minerals were neoformed. Depending on the amount of strain, 2nd or 1st order discontinuities were formed, and they may have undergone such intense mechanical agitation and chemical alteration that they were transformed to soil**

The described mode of formation of discontinuities of different orders suggests a fractal-type appearance, which has been exemplified by Tchalenko [11], cf. Figure 34, and which is in agreement with Figures 21, 24, 27 and 29. Figure 24 illustrates the common case of integra-

ted systems of steeply oriented major and minor, i.e. 2nd and 3rd order fracture zones of rather regular spacing. Various studies in Sweden, Finland and Russia have yielded data that are in agreement with the typical spacings and extensions ascribed to low-order discontinuities in Table 3 and they have also demonstrated that slip and tension breaks in rock located between major zones were often developed parallel and perpendicular to these zones, yielding more or less orthogonal or rhombohedral patterns (Figure 35).

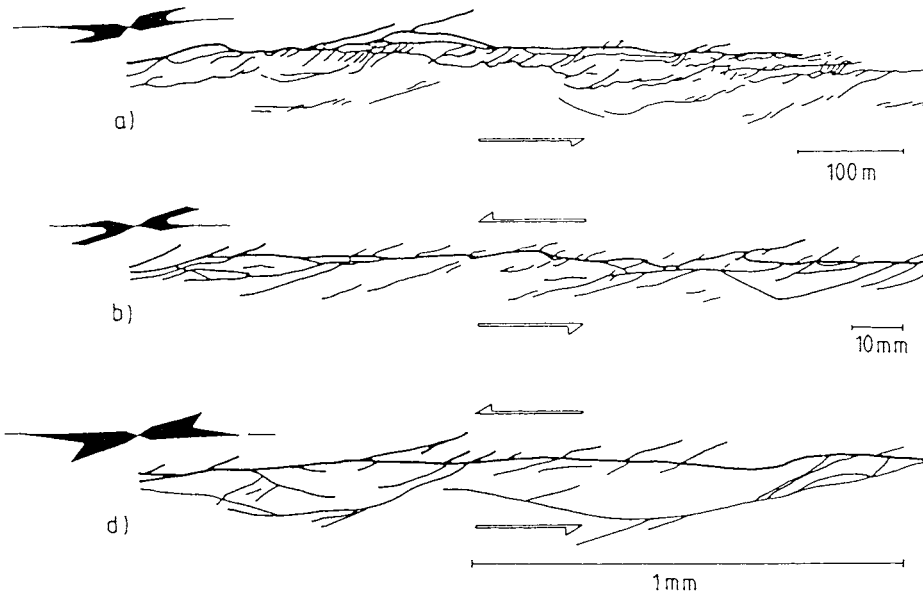


Figure 34 Similar fracture patterns on different scales, i.e. repeatable patterns [11]. The upper diagram shows shear-induced surface fractures mapped in eastern Iran, the lower ones are from reproduction on a small scale by laboratory shear tests. Rosette diagrams to the left

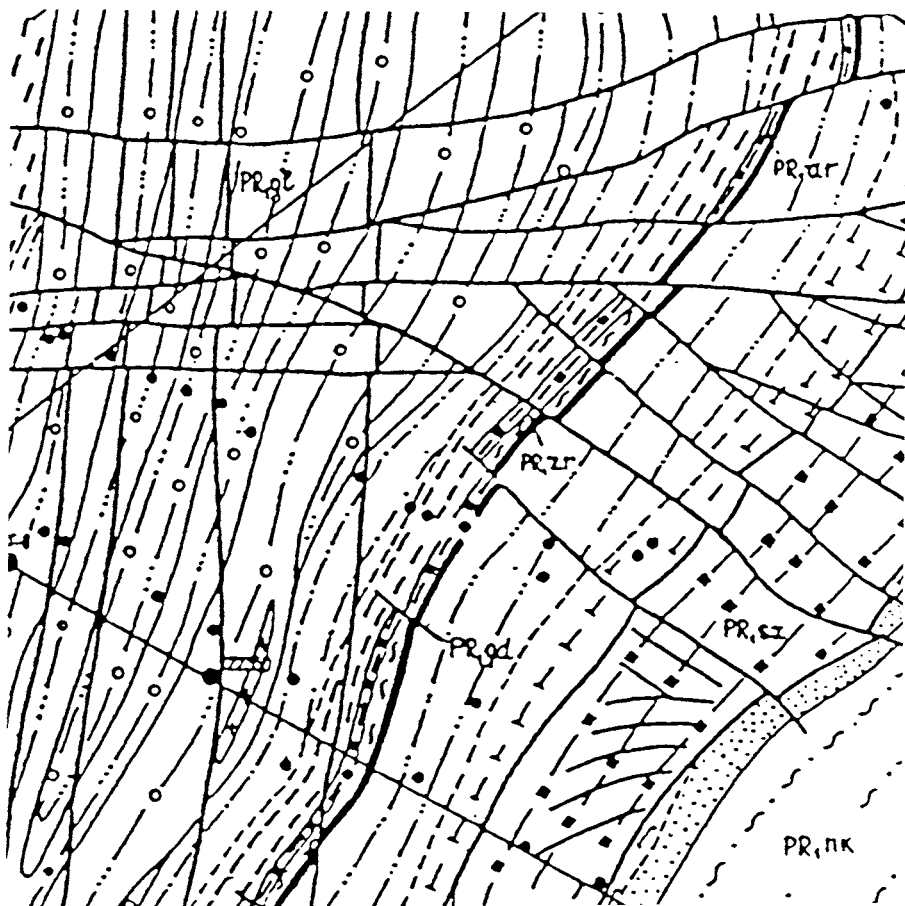


Figure 35 Central part of the Krivoy area, Russia [NEDRA]. Notice the orthogonal-type organization of the major zones (1st and 2nd order). The width of the map is about 5 km

The extensive investigations of the earth crust in Russia, employing deep drilling to 12 km depth and comprehensive geophysical measurements, have revealed that flatlying discontinuities of all orders are present to large depths as illustrated by Figure 36. These studies showed that deeply located zones are hydraulically active to at least 4 km depth, which naturally is of fundamental importance for the design and function of deep-sited repositories. Again, rim zones are expected also of the flatlying major zones, to which due respect should be paid, both for practical reasons in the construction phase and for proper long-term performance.

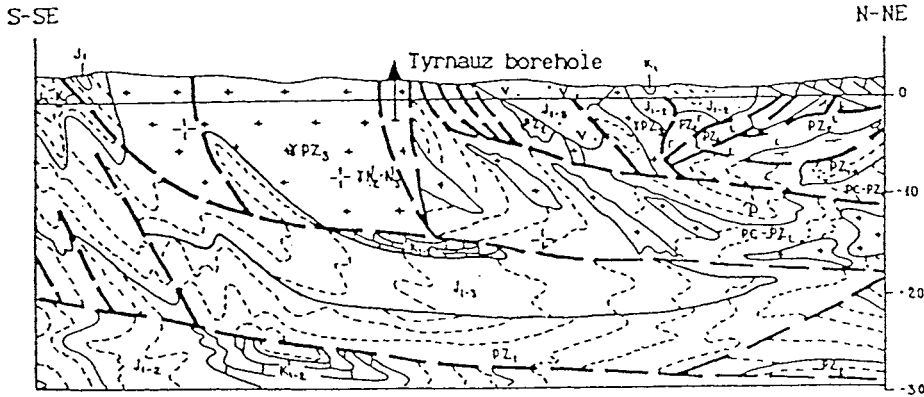


Figure 36 Vertical section of the upper part of the earth crust in Caucasus [NEDRA], showing major steep and subhorizontal discontinuities (broken, thick lines). The scale is in kilometers

2-2.6 Synthesis

DISCONTINUITIES

The 7 order rock structural scheme is sufficiently detailed for characterizing individual discontinuities in designing and constructing repositories. Naturally, there are variations in character and properties over the length of each individual discontinuity, particularly of the ones of low order, which means that single borehole inspections do not allow for safe identification and that several methods for characterization have to be applied for classifying such features. Except for the 1st and 2nd order discontinuities, which represent different scales but imply similar but not identical properties and compositions, all other members of the scheme have different functions in the rock and are different by definition. The stress/strain properties may vary along the discontinuities for the same reason, but average rheological properties can be ascribed to them for use in numerical calculations as will be shown in Chapter 3, which deals with design of repositories. This makes it possible to get at least a rough indication of the expected future displacements induced by tectonics and glaciations, which both need to be considered in the design of repositories and in performance analyses.

STRUCTURE MODELLING

The common condition of several generations of large-scale structures induced by differently oriented regional stress fields in the course of the evolution of the earth crust explains that the regularity of low-order discontinuities is often obscured, although the examples in Figures 24 and 31 show that they may be arranged in remarkably regular sequences. There are indications that there is a correlation between other earth crust properties, like the thickness, and the spacings of 1st and 2nd order discontinuities, and that the intervals specified in Table 3 are in agreement with this.

As to the higher-order discontinuities that are of major practical importance in the present context, i.e. those of 4th order, they often form rather regular patterns which can be generalized as orthogonal or rhombohedral. Regular changes in orientation can be modelled as undulation.

The common similarity in orientation of 2nd, 3rd and 4th, and even 5th order discontinuities and the fractal-like appearance of such structural features, makes it possible to visualize a crystalline rock mass - in its basic, most simple form - in the fashion shown in Figure 37. Combination of two or more structural patterns yields the actual rock constitution model that can be taken as a basis for preliminary planning and design of repositories as well for general estimation of groundwater flow and of the influence of changes in regional stress fields that are associated with tectonics and glaciation.

2-3 Factors influencing the location of repositories

2-3.1 Importance of rock structure on the location and orientation of excavations - the “disturbed zone”

One of the most important issues since the start of developing technical concepts for the disposal of highly radioactive waste products has been to find out whether excavation generates a “disturbed zone” with mechanical disturbance and an increased hydraulic conductivity along the excavation. The existence of such a zone, which may control the amount and paths of groundwater flow through a repository, can be illustrated by calculating the radial strain associated with excavating a cylindrical room, using a relevant relationship between strain and hydraulic conductivity, and isotropic primary rock stress conditions [12].

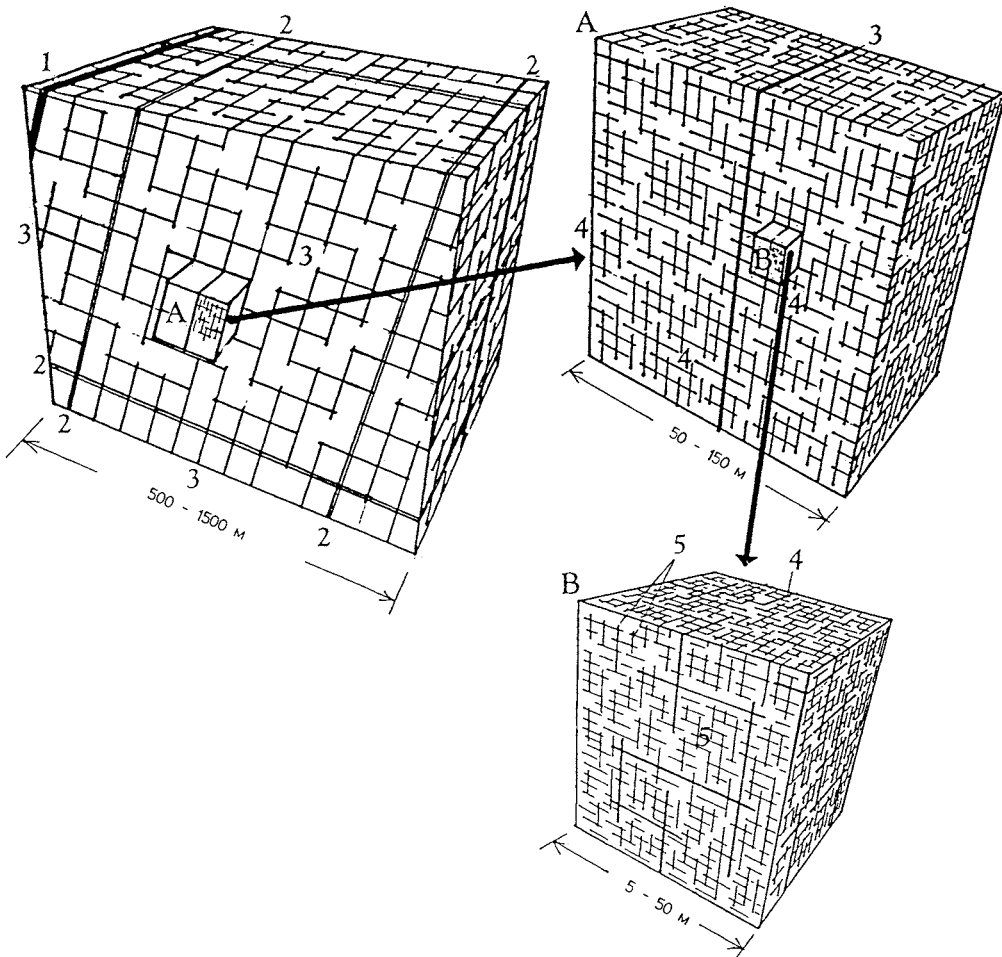


Figure 37 Schematic picture of rock structure of crystalline, primarily granitic rock, showing the presence of major faults and regional fracture zones (1st and 2nd order discontinuities), and minor fracture zones (3rd order). 4th order discontinuities are discrete water-bearing fractures of long extension, while 5th order discontinuities are hydraulically less active fractures. 6th and 7th order discontinuities are not shown

Figure 38 illustrates the resulting change in hydraulic conductivity from K_0 for virgin rock to $K_{z\theta}$ axially in “onion”-type fractures, and to K_r and K_{zr} in radial fractures. The stress-induced compression of radially oriented fractures is the basis of the “skin” zone concept, implying that the inflow into the opening should be reduced, while the axial flow should be enhanced about ten times according to the diagram.

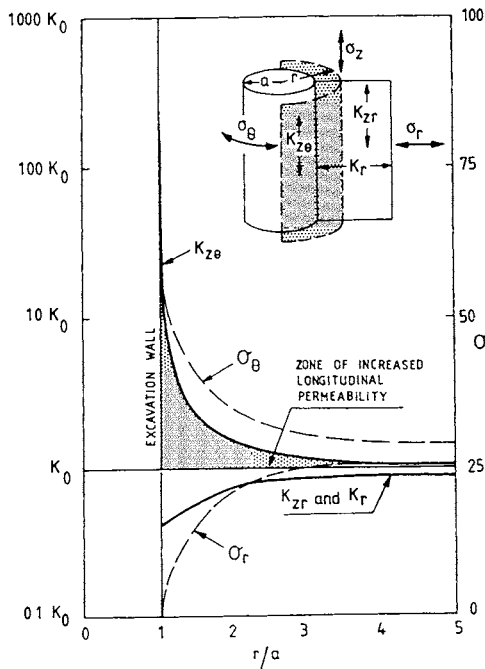


Figure 38 Predicted change in hydraulic conductivity due to excavation-induced stress changes [12]

In practice there are of course no onion-type fractures and stress-induced changes in axial hydraulic conductivity are in fact more related to shearing-associated widening of plane fractures of 4th order and activation of 5th order breaks as can be demonstrated by applying numerical methods like the distinct element codes UDEC for 2D and 3DEC for 3D calculations. We will consider this issue in detail in Chapters 3 and 5, which deal with the design and function of rock repositories, and confine ourselves here to underline a basic principle of proper orientation of repository tunnels, namely to let them form a sufficiently large angle with the strike of major discontinuities. Thus, Figure 39, which refers to the condition of aligned major fracture sets and tunnel, gives evidence of the strong increase in axial conductivity that

results from unsuitable orientation. The matter is complicated by the fact that the stress conditions affect the degree of disturbance, and by the desire of orienting the tunnels oblique to the regional hydraulic gradient and these factors also need to be considered as discussed in these later chapters.

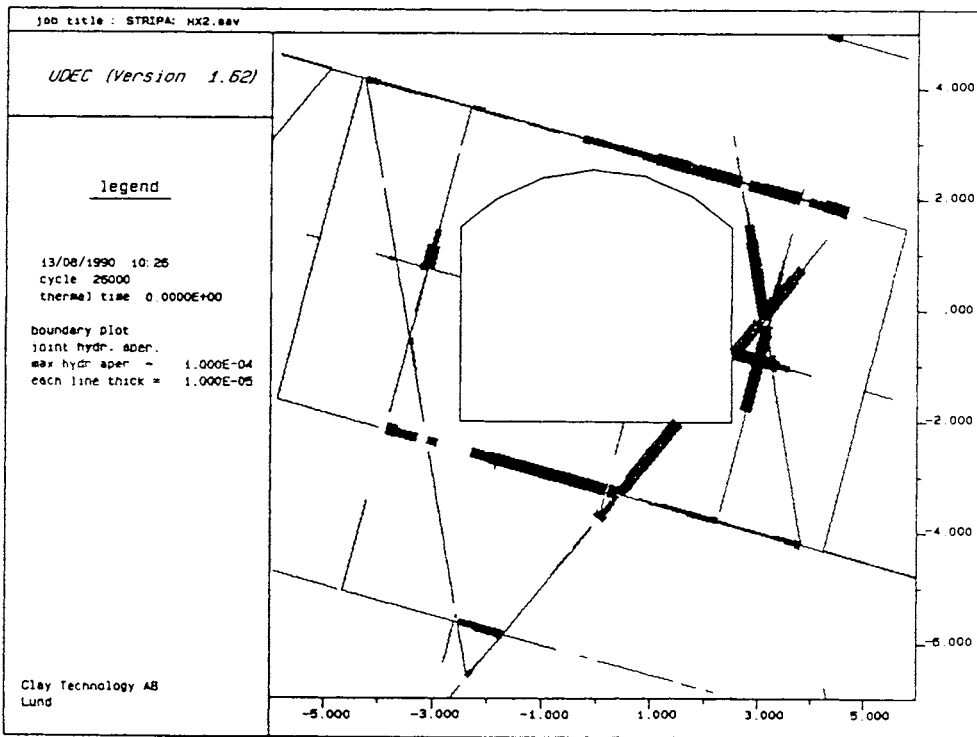


Figure 39 Example of change in aperture in rock with discontinuities of 4th and 5th orders after excavation (The BMT drift at 360 m depth in the Stripa mine). The initial aperture set at $10\ \mu\text{m}$ is increased to at least $100\ \mu\text{m}$, implying an increase in conductivity by 1000 times

2-3.2 Influence of tectonics on repository rock

STRENGTH OF DISCONTINUITIES

Design of all types of underground excavations requires that due respect is paid to the variation in bearing capacity of the rock mass, i.e. in practice to the mechanical strength of the various weaknesses. For proper location of repositories there is also another important strength-related issue, namely the distribution of tectonically induced strain. This is because large displacements along low-order discontinuities may generate activation also of the higher-order discontinuities that intersect tunnels with mechanically sensitive waste containers. We will consider this risk, for which we need strength parameter values of the 7 orders of discontinuities.

The strength and stress/strain properties of 1st and 2nd order discontinuities are primarily determined by the degree of disintegration, and by the microstructure and content of soil-type constituents, while those of 3rd order discontinuities are controlled by the degree of interaction of the relatively few fractures and by the fracture fillings, as well as by the fracture topography. For high-order discontinuities the fracture minerals and topography of the discontinuities determine the mechanical properties. Applying the Mohr/Coulomb failure theory we will consider them as discrete weaknesses with a strength characterized only by friction, while the crystal matrix, in which they are distributed, has a high strength with both cohesion and friction [1]. The following general strength properties can be assumed for the various types of discontinuities:

1st order discontinuities

Shear displacements have been large enough to yield the residual strength [1]. A significant fraction of the core material is clayey with smectites, hydrous mica and chlorite as major minerals, and it is expected to behave as moraine clay, for which the friction angle is in the interval 15-25°. The dilatancy is very small.

2nd order discontinuities

The character of these discontinuities is similar to that of the 1st order discontinuities but the degree of disintegration and the clay content are lower; the friction angle is in the interval 20-25°.

3rd order discontinuities

3rd order zones may be taken to behave as heavily compacted rock fill. Since large strain has led to a state where the residual strength is reached and since chlorite is a common fracture mineral, the peak friction angle is not higher than about 25-30°. The dilatancy is very small due to the large strain that such zones have undergone.

4th order discontinuities

Despite the plane nature of most discontinuities of this order, their ruggedness suggests a peak friction angle of 30-40°. Plane, very smooth chlorite-coated fractures that have undergone significant shear strain may have a friction angle of down to 20-25°. The dilatancy is small to moderate.

5th order discontinuities

Discontinuities of 5th order have a rough topography, which suggests a peak friction angle in the interval 35-45°. The dilatancy may be significant.

6th order discontinuities

6th order discontinuities consisting of very small, sealed fractures or zones of enriched minerals, have an even higher peak friction angle than those of 5th order; the value is expected to be in the interval 40-55° and the dilatancy may be very significant.

7th order discontinuities

Griffith cracks can hardly be characterized by any specific shear strength. However, rock material with only 7th order discontinuities is estimated to have a very high friction angle (45-60°) and a high cohesion (>10 MPa).

Table 5 gives averaged values that can be used for practical application [1].

Table 5 Approximate values of the strength parameters (friction angle) of discontinuities of crystalline rock

Discontinuity	Friction angle (°)	
	Peak	Residual
1st order	15-25	15-20
2nd order	20-25	15-20
3rd order	25-30	20-25
4th order	30-40	25-30
5th order	35-45	30-35
6th order	40-55	35-40
7th order	-	-

SHEAR DISPLACEMENTS OF REPOSITORY ROCK INDUCED BY TECTONICS

A major problem in finding a proper site for a repository is to foresee where and to what extent future displacements will take place in the rock. In later years it has been documented that earthquake-related movements have the character of stick-slip sliding, triggered at asperities of faults where stress concentrations have been accumulated in the course of creep motion of non-seismic type. Such creep may amount to several millimeters per year along 1st order discontinuities as indicated by Russian estimates. Experience from a few kilometers deep mines in South Africa indicates that earthquakes of magnitude 2-3 (M 2 to M 3) are associated with quick shear displacements of 1st and 2nd order discontinuities of 50-100 mm, but much larger motions have been reported for stronger earthquakes, i.e. 0.2 m for M 4.5 and 1.4 m for M 8.3 [1]. The shearing caused by earthquakes of magnitudes 5-6 is concluded to be both displacement in a narrow part of the fracture zone, activation and propagation of previously healed fractures, and creation of new breaks in and adjacent to the zone. One concludes from this that repositories should not be intersected by 1st and 2nd order discontinuities.

Numerical calculations using basic structure models of the type shown in Figure 37 with 2nd, 3rd, and 4th order discontinuities and strength properties indicated in Table 5, and assuming common stress/strain data and typical rock stress conditions, have indicated the distribution of shear strain in the system [13]. Hence, a regional stress change yielding 200 mm instantaneous shearing of the 2nd order discontinuities - corresponding roughly to M 5 earthquakes - generates maximum 50 mm shear strain of the 3rd order zones while the 4th order discontinuities are sheared by somewhat less than 1 mm. Since 4th order discontinuities will be rather frequently represented in repositories and since earthquakes of this magnitude may take place in almost any area, it is clear that one needs to take such strain into consideration. Single events cause no problems but since repeated shearing must be expected, the accumulated strain may become critically large in a long-term perspective. The matter will be discussed in Chapters 3 and 5, dealing with the design and performance of repositories.

2-3.3 Favorable and unfavorable location of repositories

Naturally, any rock mass can be used for hosting a repository, including rock rich in open fractures, provided that the waste is sufficiently well encapsulated and the rock effectively sealed by plugging and grouting of fractures. Hence, for any given repository site, the design can be adapted to fit the rock conditions for fulfilling the criteria that have been set respecting the rate of release of toxic species. Still, if more than one site is offered scoring can be made on the grounds described below; in practice the cost aspect will rule out a number of options.

FACTORS OF MAJOR IMPORTANCE:

1. Areas with frequent, closely spaced low-order discontinuities should be avoided
2. Nearness to major low-order discontinuities should be avoided
3. Very permeable rock matrix with numerous open fractures is not suitable
4. Seismically active areas are not suitable
5. Low regional hydraulic gradients are preferable
6. Cost for construction and transport facilities should be reasonable

FACTORS OF MINOR IMPORTANCE:

1. The space between low-order discontinuities that is available for hosting repository caverns and vaults should be large enough to allow suitable orientation and shaping of the rooms
2. Regions with groundwater that is known to speed up deterioration of the waste embedment and dissolution of the waste are not suitable
3. Areas with very high rock stresses that endanger rock stability or generates rock strain that increases the hydraulic conductivity should be avoided

2-3.4 Identification and characterization of structural features and rock stresses

STRUCTURAL PARAMETERS

The means of identifying the most important structural features, i.e. major discontinuities of 1st and 2nd orders, and the rock stress conditions are wellknown in engineering geology and applied rock mechanics. The interested reader is referred to the vast literature on these subjects.

Geology supplies us with suitable parameters for describing the orientation in space of the various structural discontinuities. The matter is dealt with in any textbook on applied structural geology and we will confine ourselves to refer only to the following classical concepts (Figure 40):

Strike: The orientation in the horizontal plane of the line of intersection of a structural plane and the horizontal plane. It is given by the angle between this line and the direction of Geographic or Magnetic North. Several ways of expressing it are in use, such as N45W or 315, both referring to a northwest/southeast striking feature.

Dip: The inclination of a structural plane expressed as the angle between this plane and the horizontal plane. The figure is associated with an indication of the direction, i.e. southeast (SE), northwest (NW) etc. Hence, a plane described as N45W/60NE dips 60 degrees towards northeast and strikes in northwestern/southeastern direction. The simplest way to express the strike and dip for such a plane is 315/60/45.

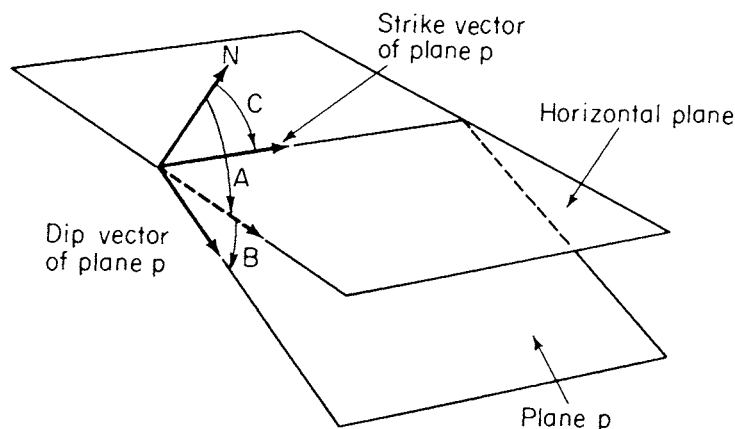


Figure 40 Definition of strike and dip

A very useful way of visualizing orientation of planar structures in space is offered by stereographic projection using stereo nets. The object is imagined to be placed in the center of the semi-hemisphere net and its orientation is given by the horizontal projection of the point of intersection of the normal to the plane and the lower hemisphere (Figure 41). For statistical analysis of orientations one nowadays often uses a modification of the "equal angle" stereographic projection that produces "equal areas" and can be developed from the simple projection by applying basic trigonometry. Hence, the distance from the center to the projection point is $r \tan(\alpha/2)$ in the equal angle representation and $1.41 r \tan(\alpha/2)$ in the equal area representation, α being the angle between the planar structure and the vertical through the center, and r being the radius of the hemisphere. Figures 42 and 43 illustrate typical plottings of 2nd, and 4th + 5th order discontinuities in granite. The application of stereographic projection in statistical analyses is treated in textbooks on structural geology to which the interested reader is referred.

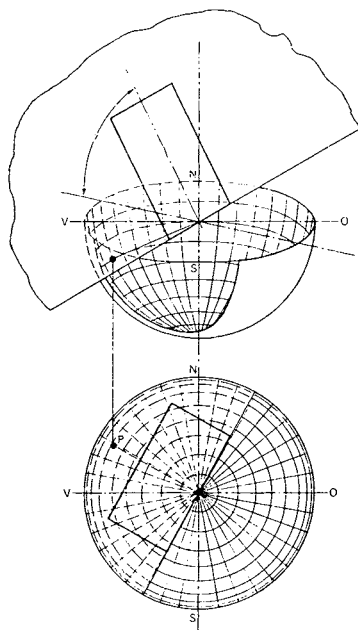


Figure 41 Plotting of orientation of a single planar structure using the lower hemisphere of an equal angle stereographic net

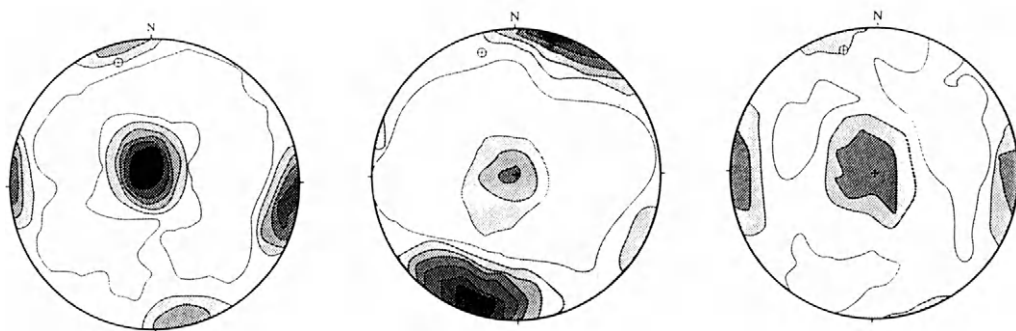


Figure 42 Orthogonal-type organization of discontinuities in granite (Munier). Left: Oxidized, Central: Calcite-filled, Right: Clay-filled

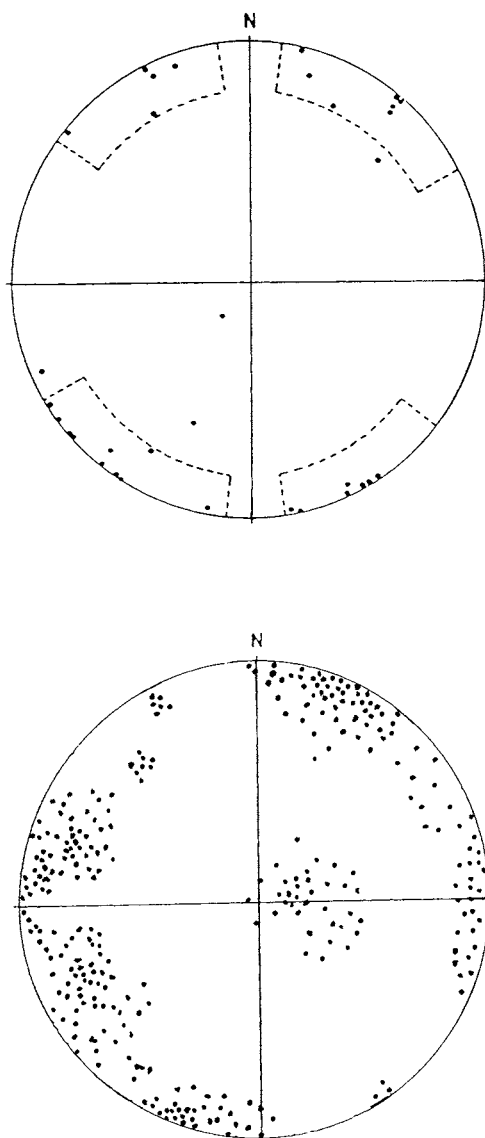


Figure 43 Examples of stereographic projections of low- and high-order discontinuities in granite. Upper: 4th (dots) and lower order discontinuities (areas within dotted boundaries) indicating alignment of the two categories (Ahlbom et al.). Lower: Strong variation in orientation of fractures in blasted rock with orthogonally arranged discontinuities in virgin state

ROCK STRESS PARAMETERS

The rock stresses that prevail in the earth crust reflect its evolution. The stress state in any element can be expressed in terms of principal stresses, which, by definition, are normal to (principal) planes in which no shear stresses operate. This concept is fundamental for the solution of strain- and stability-related problems in rock mechanics and hence also for the design of repositories [1].

The stress ellipsoid, which illustrates the relative magnitude of the three principal stresses $\sigma_1 > \sigma_2 > \sigma_3$ (Figure 44), is often oriented with the major principal stress more or less in the horizontal plane in virgin rock and with the minor component in the vertical direction, corresponding to the load of the overburden. However, as illustrated by Figure 45, there are large variations both regionally and locally. The use of these stresses, which are often termed “primary” for natural conditions, and “secondary” for those generated by excavation, will be exemplified in Chapter 3 dealing with the design of repositories. We will confine ourselves here to state that regions with very anisotropic stress states and the major principal stress being on the order of the compressive strength of the rock matrix, are unsuitable for repositories because of the risk of unstable conditions.

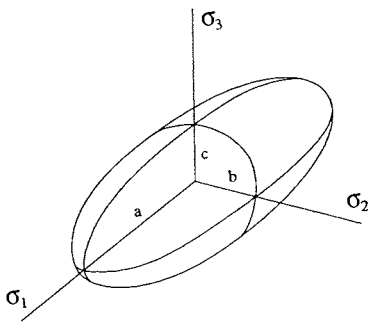


Figure 44 The stress ellipsoid

FIELD INVESTIGATIONS

The presence of discontinuities of 1st and 2nd order can be identified by the usual procedures applied in engineering geology, i.e. interpretation of topographical, geological, and aerial maps, as well as by air-borne geophysics. Detailed characterization of such zones and of 3rd

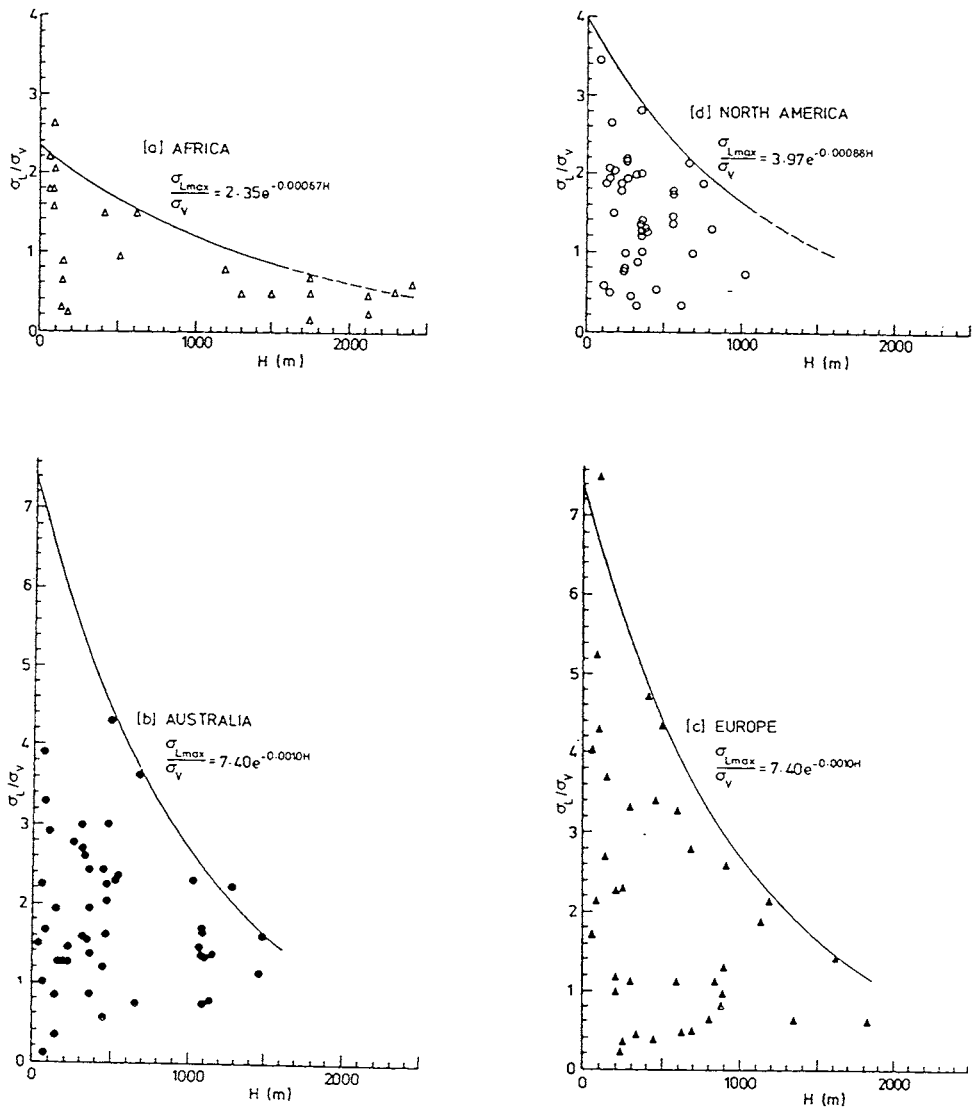


Figure 45 Compilation of the ratio of the maximum horizontal stress and the vertical stress (After Stephansson)

order discontinuities requires on-ground geophysics of higher resolution and core drilling for sampling and in-hole measurements, as well as cross-hole geophysics and hydraulic measurements. In recent years radar measurements in long boreholes have turned out to be of great help in field surveying (Figure 46). Still, not all low-order discontinuities can be identified and characterized by measurements conducted from the ground surface and the rock characterization therefore has to be continued in the course of the excavation work. This is made by strategic core drilling of pilot holes for visualizing the character of the rock and for hydraulic and radar measurements as well as for rock stress measurements.

More detailed structural surveys for characterization of 3rd order zones and for identifying 4th and higher order discontinuities are usually superfluous except for optimum location of mechanically sensitive waste containers and for predicting the groutability as will be discussed in Chapter 5. Such high-resolution investigations are very time-consuming and expensive but rather economic surveys can be made by partial replacement of core drilling by percussion drilling and replacing some of the common hydraulic packer testing by simple inflow tests and borehole inspection using optical or TV instruments.

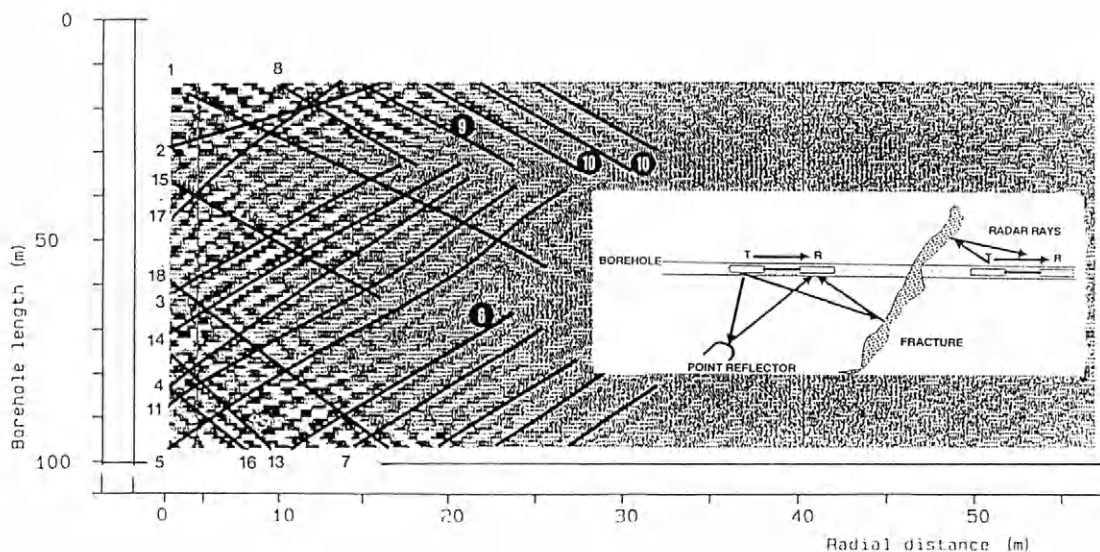


Figure 46 Radar survey in 100 m borehole [14]. Water-bearing discontinuities are identified to 30 m distance. Legend: T=transmitter, R=receiver

Rock stress measurements can be made in boreholes extending from the ground surface to large depth but the local variation of the stress tensor that is caused by the varying degree of interaction of adjacent rock blocks (Figure 47) makes the evaluation questionable unless many boreholes are investigated at each local site [1]. This leads to very high costs and still some confusion and it is therefore preferable to conduct more extensive investigations in conjunction with the construction work.

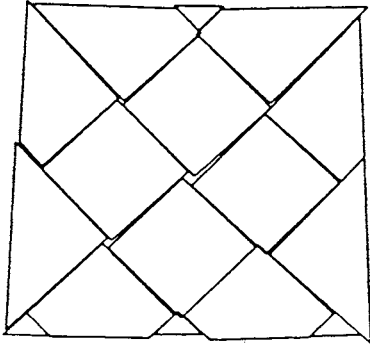


Figure 47 Schematic block structure in which no reliable stress measurements can be made

2-3.5 Adaption to the prevailing rock structure

Once the major structural features have been recognized in the region where the repository shall be located the first coarse design principles have to be decided, i.e. what the concept should be: big caverns, system of tunnels or a few very long tunnels, or systems of deep boreholes. This matter, which will be discussed rather extensively later in the book, strongly depends on the rock structure and on the possibility of adapting the repository to the rock structure in an optimum fashion, i.e. to bring in as much waste as possible per unit volume of excavated rock and to isolate it as effectively as possible from the biosphere.

We will consider as an example a practical case represented by ongoing work in Sweden to locate a HLW repository of the KBS3 type, i.e. with waste canisters in densely spaced holes drilled from the floor of tunnels with a spacing of 25 m, in crystalline rock of granitic type (Figure 3). With SKB terminology the term tunnel is used for vault.

Figure 48 shows a generalized structural pattern of steep discontinuities of 1st and second order at the actual site. Applying the basic features of the structural model in Figure 37, it is

assumed that 3rd and 4th order discontinuities are parallel to the sets of NW/SE-oriented 2nd order zones. The issue is to find an optimum pattern for placing the deposition tunnels, the governing parameters being the orientation and frequency of major sets of discontinuities, the required distance to these discontinuities, and the prevailing rock stresses.

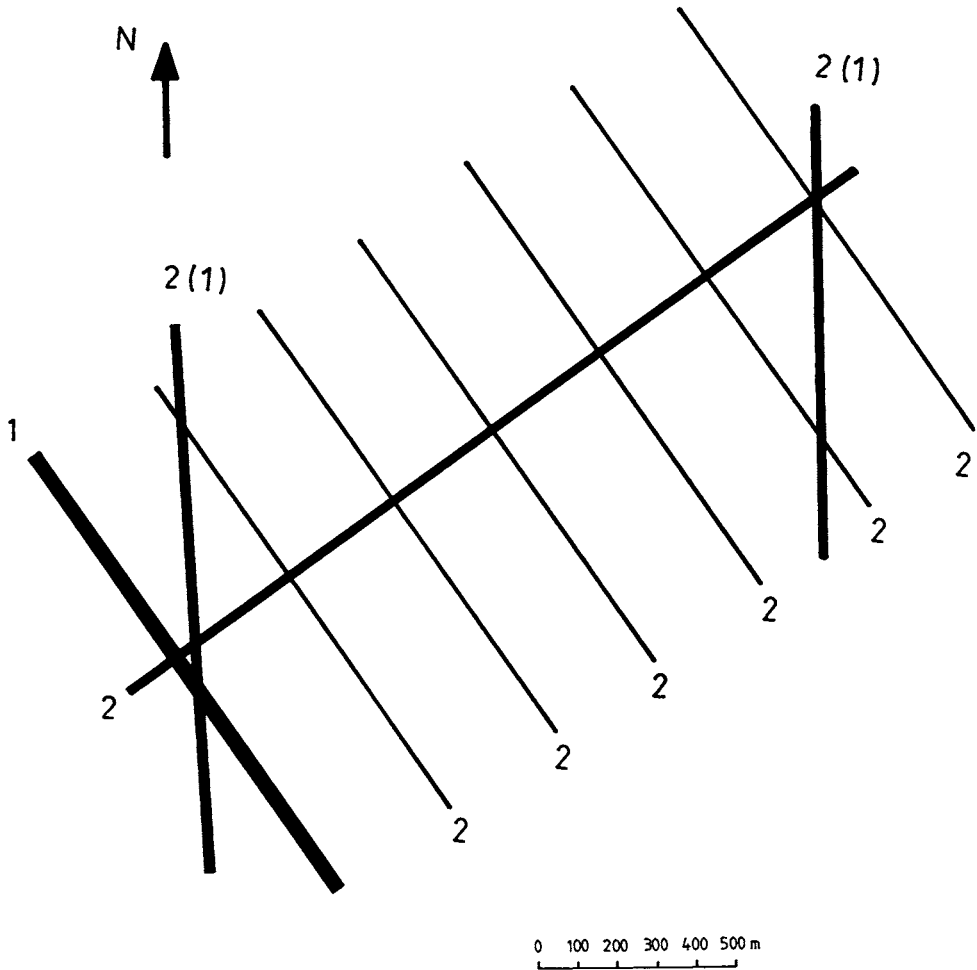


Figure 48 Generalized structural pattern of site for HLW repository. The figure 2 denotes 2nd order zones; 2(1) indicates zones that may possibly be of 1st order

As to the first issue, which will be discussed in detail later, the criterion for minimizing the development of very conductive axial “disturbed zones” is that the orientation of the tunnels should deviate from that of the dominant discontinuities by at least 15° .

The second issue, i.e. the required distance from the deposition tunnels to low-order discontinuities can be debated, but it is reasonable to apply the criterion that the tunnels should not be located closer to the core of 1st and 2nd order discontinuities than 50 m keeping in mind that the rim zones extend a few tens of meters from the core. Naturally, it has to be accepted that the tunnels become intersected by 3rd order zones but it is essential to orient the tunnels such that the interference is at minimum. Flattening zones are of particular importance for avoiding interaction with the deposition holes.

The third issue, the primary stress conditions, can be critical if the ratio of the maximum and minimum principal stresses in a plane perpendicular to the tunnel axis exceeds 3, since tension is then produced, and if the maximum principal stress is on the same order of magnitude as the compression strength, spalling and rock burst may take place. In Scandinavia, the dominant orientation of the maximum principal stress is NNW/SSE to NW/SE, i.e. approximately the same as the orientation of major discontinuities. Thus, while this is not a favorable direction for minimizing the “disturbed zone” around the tunnels, it is the most suitable orientation for the tunnels from the point of stress conditions, which is naturally a dilemma. However, the common variation in orientation of the stress ellipsoid and the relatively low accuracy in determining the stress level by use of the commonly used techniques [1] makes the stress factor less important, except when it is unanimously indicated that critical conditions must be expected as in the AECL rock laboratory in Manitoba, Canada, where tunnel excavation also logically yielded comprehensive spalling and rock burst [15]. However, in most cases, including the one investigated by SKB, the primary stresses do not yield critical conditions and the rock structure is therefore taken to be of major importance. Hence, a preferable orientation of the deposition tunnels is W/E or NS.

Referring to the various criteria, one finds that the arrangement of vaults, or deposition tunnels that we will call them, shown in Figure 49 may be at optimum.

2-3.6 Are there particularly good sites for repositories?

ROCK TYPE

A rock mass with few and widely spaced low-order discontinuities is naturally preferable for

hosting repositories. As to the type of rock material, gneiss may be more suitable than granite because of less common long-extending straight 3rd and 4th order discontinuities, the more

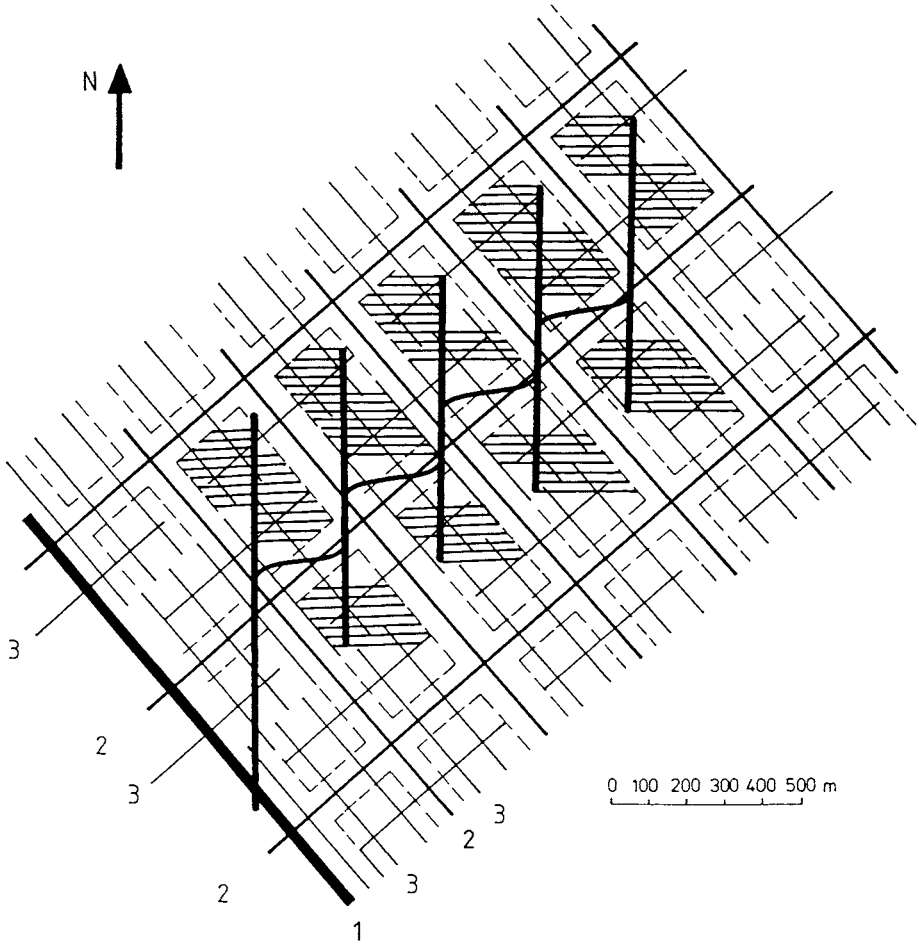


Figure 49 Plan view of KBS3 repository adapted to the generalized structure pattern in Figure 48, fitting the whole repository between N/S-oriented major 1st or 2nd order discontinuities (not shown). The broken lines represent 50 m distance from the center of 2nd and 3rd order discontinuities, i.e. a suitable distance to the nearest deposition tunnel. Black vertical lines are main tunnels

ductile and less brittle behavior, and the higher content of phyllosilicates that gives a higher potential of self-sealing under the hydrothermal period. Gabbro and basalt seem to offer advantages from a chemical point of view. However, of much greater importance is the location with respect to large-scale groundwater-directing features: if the repository can be excavated in crystalline rock that is covered by thick clayey sediments the latter will serve as a tight lid. Furthermore, if the area forms the base of a not too large island at sea or in an estuary, the absence of significant hydraulic gradients is a significant advantage. Such a case will be described here without proposing that it should be used for hosting a HLW repository.

REGION

Among the most important factors that affect the transport capacity of toxic elements like radionuclides and their release from the nearfield, are the regional hydraulic gradient and the risk of seismic events. The lowest gradients prevail under the sea and below shallow isles, like the Swedish island Gotland, which is located in the Baltic Sea at a distance from the nearest coast of 90 km (Figure 50). Several other sites of similar type are available along the coasts of the Baltic Sea.

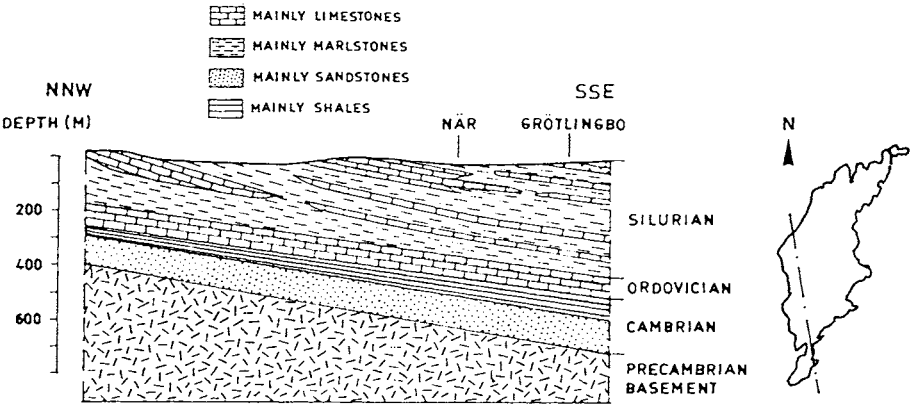


Figure 50 NW/SE section through central Gotland

The island is less than 85 m high and serves as an example of a region with a number of suitable physical properties for hosting a high-risk waste repository:

1. It is made up of 300-500 m clay-bearing Ordovician and Silurian sedimentary rocks that cover crystalline rock. For a repository excavated in the crystalline rock, which is safer and more economic than constructing it in sedimentary rock, the overlying sediments with their frequent low-permeable bentonite clay horizons and long lateral extension, serve as a practically impervious lid. This means that the hydraulic gradient in the host rock is practically zero, and that there is no driving force for water flow. These conditions will prevail for tens of thousands of years also considering the ongoing slow and slight upheaval.
2. Insignificant tectonic movements have taken place in this part of the Baltic Sea in the last 400 million years and the area is not seismically active. Hence, both the crystalline rock and the sediment rocks are expected to maintain their tightness, which means that radionuclides would only move by diffusion and not appear at the ground surface until after many millions of years.

The fault line that is conformous to the eastern shoreline of Gotland and coincides with it in Figure 51, may have represented a large-scale weakness of “zeroth” order that controlled the shape of the land mass that remained after the latest glacier attack. Assuming that this NW/SE oriented set is associated with a similar set of faults oriented NE/SW the island would have obtained rhombohedral shape, which is in fact also the case.

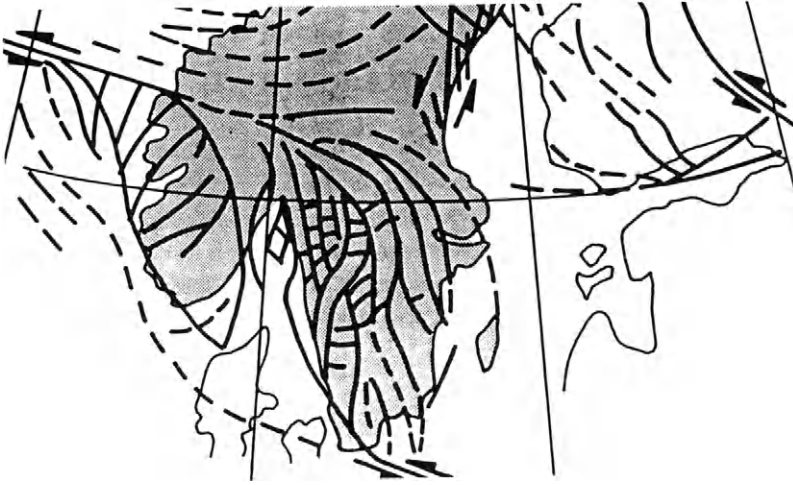


Figure 51 Fault patterns in southern Sweden according to Talbot and Slunga [16]

The island's steep discontinuities, which mirror those in the underlying crystalline rock, indeed illustrate the regular, fractal-like rock structure that one can find in many crystalline rock masses although it is often complexed by superposition of several generations of fracture systems. Thus, Figure 52, which shows all the water-bearing major zones identified by the Swedish Geological Survey, illustrates that the somewhat more than 150 zones with very few exceptions are oriented almost parallel to the major faults. Their average extension is 5–20 km and the average spacing about 3.5 km (NW/SE) and 4.3 km (NE/SW), which makes them rank as 1st order discontinuities. No recording of smaller zones have been made but 4th order discontinuities are well exposed in sandstone in the southern part of the island. They form very regular, nearly orthogonal systems of steep, plane breaks with a spacing of 3–7 m and an extension of 10 m and occasionally much more. Integrated in these systems are conformous subsystems of smaller, closed and less interconnected fractures of 5th order. Recent core-drilling to 80 m depth in clayey marl clearly demonstrated orthogonal-type fine fractures along which the marl broke up on drying (Figure 53).

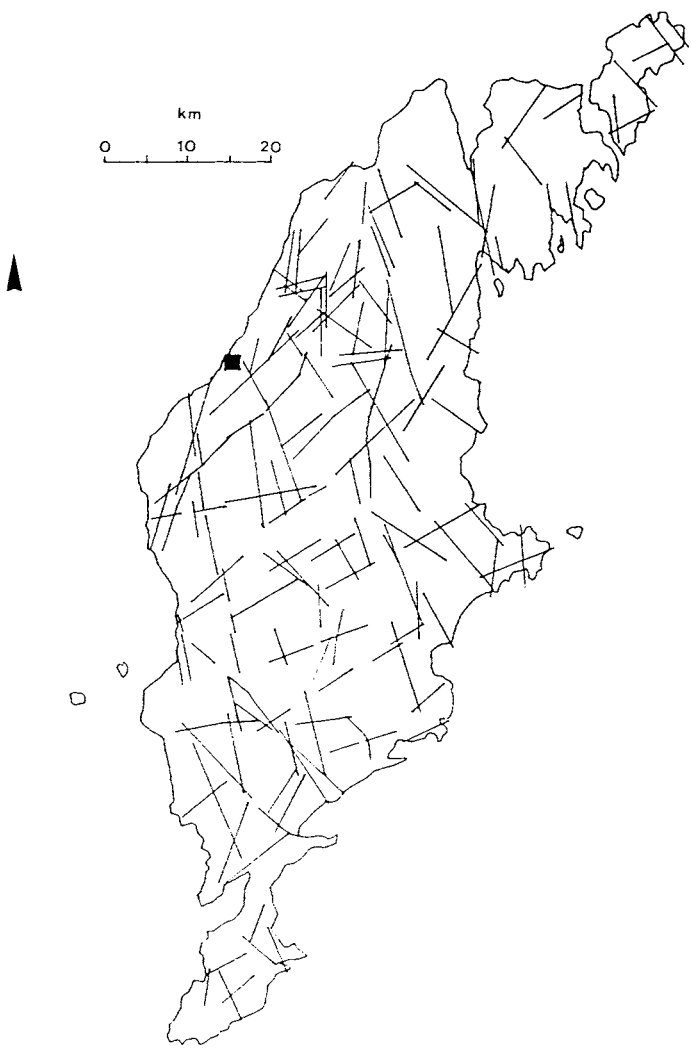


Figure 52 Major water-bearing zones of Gotland. North is up (17)

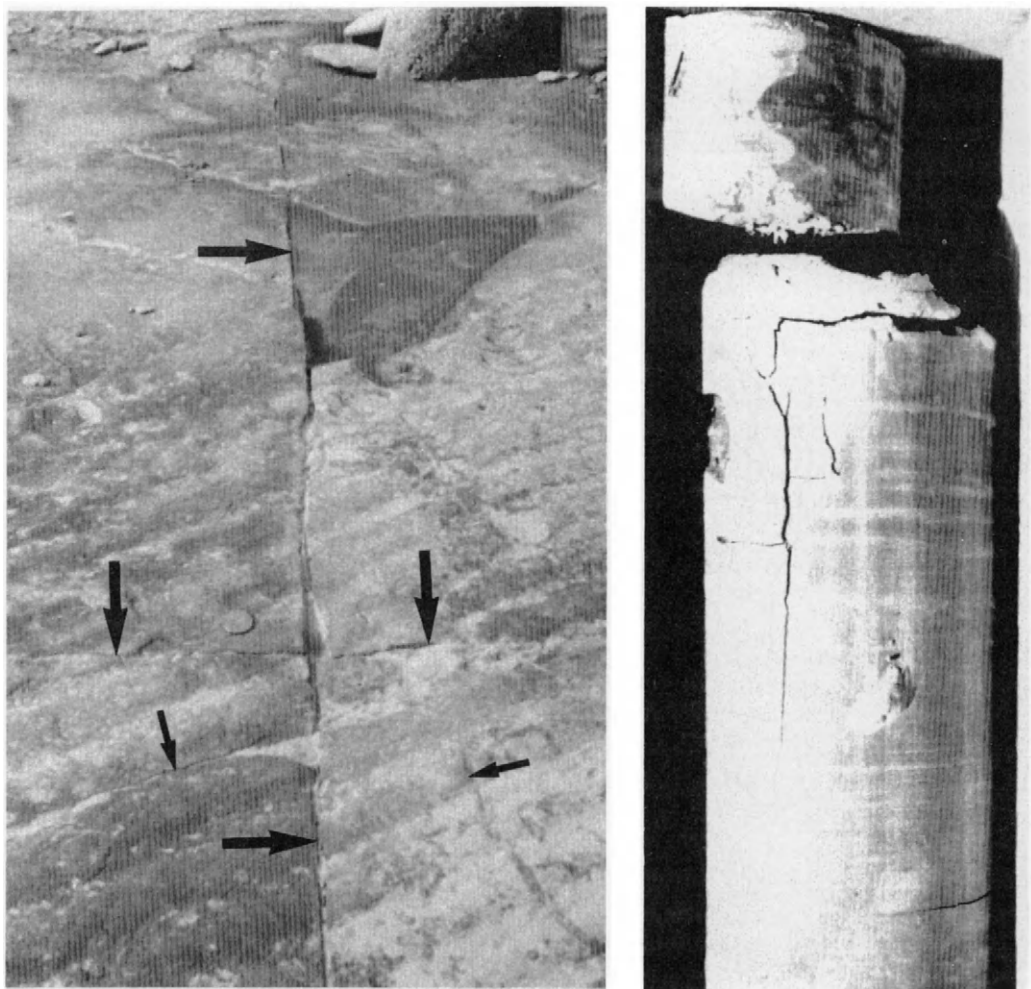


Figure 53 Left: Typical 4th (big arrows) and 5th (small arrows) order discontinuities at the shoreline on southwestern Gotland. Right: Drill core from 20 m depth in clay marl exhibiting orthogonal-type fracturing

2-4 References

- 1 Pusch,R. Rock mechanics on a geological base. Elsevier Publ. Co. (In press)
- 2 Barton,N., Lien,R. and Lunde,J. Engineering classification of rock masses for the design of tunnel support. *Rock Mech.*, Vol.6, No.4, pp.189-236, 1974
- 3 Pusch,R. and Svemar,C. Influence of rock properties on selection of design for spent fuel repository. *Tunnelling and Underground Space Technology*, Vol.8, No.3, 1993
- 4 Müller,L. Der Felsbau. I Band. Theoretischer Teil. Felsbau über Tag. Ferdinand Enke Verlag, 1963
- 5 Birgersson,L. & Neretnieks,I. Diffusion in the matrix of granitic rock. Field test in the Stripa mine. Final Report. SKB Technical Report TR 88-08, SKB, Stockholm, 1988
- 6 Carlsson,L., Winberg,A. and Grundfelt,B. Hydraulic modelling of the final repository for reactor waste (SFR). SKB Progress Report SFR 86-07, SKB, Stockholm, 1986
- 7 Pusch,R. Final report on Test 4 - Sealing of natural fine-fracture zone. Stripa Project Technical Report TR 91-26, SKB, Stockholm, 1991
- 8 Olsson,O., Andersson,P. & Gustafsson,E. Site characterization and validation - Monitoring of saline tracer transport by borehole radar measurements, Final Report. Stripa Project, Technical Report TR 91-18, SKB, Stockholm, 1991
- 9 Wollenberg,H., Flexser,S. and Andersson,L. Petrology and radiology of the Stripa pluton. Swed-Amer. Coop. Program on Radioactive waste storage in mined caverns in crystalline rock. LBL,-11654, UC-70 (SAC-36), University of California at Berkeley, 1980
- 10 Andersson,E.M. The dynamics of faulting. Hafner, N.Y., 1951
- 9 Tchalenko,J. Similarities between shear zones of different magnitudes. *Bull. Geol. Soc. Amer.* Vol.81, pp.1625-1640, 1970
- 12 Kelsall,P.C., Case,J.B. and Chabannes,C. Evaluation of excavation-induced changes in rock permeability. *Int. J. Rock Mech. Min. Sci. Geomech. Abstr.* Vol.21, pp. 123-135, 1984
- 13 Pusch,R. and Börgesson,L. Performance assessment of bentonite clay barrier and nearfield

rock assuming intact canisters. A PASS-project on alternative systems, SKB Technical Report TR 92-12, SKB, Stockholm, 1992

14 Olsson,O. and Palmqvist,K. Radar investigations at the Saltsjötunnel - predictions and validation. SKB Technical Report TR 89-18, SKB, Stockholm, 1989

15 Martin,C.D. and Simmons,G.R. The underground research laboratory. An opportunity for basic rock mechanics. News Journal, Int. Soc. Rock Mech., Vol.1, No.1, 1992

16 Talbot,C.J. and Slunga,R. Patterns of active shear in Fennoscandia. Kluwer Academic Publ., pp.441-466) 1989

17 Karlqvist,L., Fogdestam,B. and Engqvist,P. Description and appendices to the hydrogeological map of Gotland county. Swedish Geological Survey, Serie Ah, Nr.3, 1982

Chapter

3 *Design of Repositories*

3-1 Introduction

Naturally, the rather recently appearing need for repositories particularly intended for hosting hazardous waste means that no specifications or recommendations concerning the arrangement and dimensions of caverns and vaults have yet been proposed or required and it is not even clear what general features a repository should have. The basis of repository design is therefore the experience from mining and construction of deep underground rooms constructed for the hydropower industry, and also from the comprehensive research and technical development for the nuclear industry. A study of great importance related to the disposal of radioactive waste is the OCDE/NEA Stripa project that will be referred to throughout this book.

Several countries have more than one option for “geological” disposal, namely crystalline rock, salt beds or domes, and thick clay beds, but salt and clay are much less available than crystalline rock, which hence gives more possibilities for finding suitable sites of repositories of all kinds. For this reason and also because of the vast experience from excavating crystalline bedrock and of the mechanical and chemical stability of such rock, it is the type of host rock considered in this book [1].

In principle, there are two major ways of preparing repositories at depth for hazardous waste, i.e. by utilizing mines, and by constructing suitable disposal rooms at depth in rock. Both require that the rooms are located in rock with a limited number of low-order discontinuities and moderate primary stresses, and that the waste is embedded in a suitable medium offering sufficient mechanical and chemical buffering capacity, and also that ramps, adits and shafts connecting the repository to the ground surface can be effectively sealed. Since much of the recent R&D work has concerned excavation of rooms in virgin rock the book will deal with this way of preparing repositories but the possibility of utilizing mines will be illustrated as well.

Since the same principles can be applied for isolating high-risk waste of any kind and much international work has concerned radioactive waste, the text refers primarily to the disposal of this particularly hazardous waste type.

3-2 Major components to be considered in the design

The major point in selecting an optimum repository design is to apply the ALARA principle with the safety assessment yielding acceptable contamination for relevant scenarios as exemplified by the Forsmark repository described in Chapter 1. The most important factors are the **waste** and **waste containment**, the **embedment of the waste containment**, and the **transport conditions** for corrodants and released radionuclides, as well as the **mechanical properties of the host rock**. The waste, waste containment and its embedment are primary components of the “near-field” engineered barriers.

WASTE AND WASTE CONTAINMENT

Elements released from any waste as well as from the containment will interact chemically with the surroundings. Radioactive waste has two additional effects: the radioactive decay is associated with heat production, and the radiation given off requires remote handling in the emplacement phase and it also causes radiolysis, i.e. dissociation of water into oxygen and hydrogen and a number of other compounds when gamma radiation emanating from the waste hits water surrounding the waste containers and when dissolved radionuclides migrate from leaking containers.

The mechanical strength and corrosion resistance of the containment naturally determine its isolation power. Low-level radioactive waste (LLW) does not need to be very effectively contained and releases radionuclides early after emplacement but the nearfield, consisting of concrete, clay and the host rock, delay their migration effectively as exemplified by the Forsmark case in Chapter 1. HLW requires very tight containment.

WASTE EMBEDMENT

The waste containment, i.e. containers and canisters, has to be protected from rock strain by a ductile embedding medium. Bentonite clay was proposed for this purpose early in the Swedish research work and since it also has a number of very valuable isolating properties, it has become a major engineered barrier in most technical concepts in the world. Thus, it is practically impermeable and sorbs released radionuclide cations, and its swelling potential makes it fill up the space between the canisters and the rock excavation and yield homogeneous embedment.

TRANSPORT CONDITIONS AND MECHANICAL PROPERTIES OF THE HOST ROCK

Proper location of repositories implies that the storage rooms like deposition tunnels are separated from major low-order zones and that they are suitably oriented with respect to the rock structure, stress field and regional gradients. Also, the shape of the storage rooms and the methods to excavate them have to be selected so as to minimize the enhancement of the hydraulic conductivity in the “disturbed” zone. Still, special means for minimizing ground-water flow through the nearfield rock may be required both in the construction phase and for providing acceptable long-term performance. This can be made by applying engineered barriers in the nearfield and at distance from the waste, i.e. in the “farfield”, both in the form of plugging and grouting, i.e. injection of clay-based or cementitious materials.

We will consider all these components in this chapter, paying particular attention to the shape of the disposal rooms and to the design of the engineered barriers.

3-3 Design concepts

Several concepts have been proposed for disposal of radioactive waste, the example from Forsmark for MLW representing a large-room version that may - in less ambitious form - be applied for toxic industrial waste. The examples in Figures 54 and 55 illustrate concepts that are being investigated in various countries for final disposal of HLW. Some or all of them can also give an input to the design of repositories for high-risk industrial waste.

The KBS3 concept, described in condensed form in Chapter 1 (cf. Figure 3), has the advantage that the location of the canister holes - 1.5 m in diameter and 8-13 m deep depending on whether each hole host 1 or two canisters - can be decided individually with respect to the local rock structure, and that rather simple technique can be applied for application of the canisters and their bentonite embedment, as well as of the tunnel backfilling. The concepts with several canisters in each hole give slightly less good opportunity for locating the individual canisters ideally with respect to the rock structure and require use of a somewhat more sophisticated technique for application of canisters and embedment but they may be more rational than KBS3. In fact, a VLH repository consisting of a few, very long tunnels with large spacing is expected to yield minimum release of radionuclides to the biosphere. The VDH concept represents a different philosophy: the rather small and weak canisters are contained in the lower 2 km part of the 4 km deep holes with rather poorly isolating clay embed-

ment, while the upper 2 km are effectively plugged with dense bentonite clay. This concept may give excellent isolation of the waste but the stability of the deep holes may be insufficient and critical in the canister application phase and the required techniques for safe application of canisters and “deployment” mud are not yet at hand.

The VLH concept is very rational but makes it difficult to adapt to the rock structure and major low-order discontinuities will be crossed. Hence, the utilization factor is expected to be lower than that of the KBS3 concept and strong water inflow in the course of the tunnel boring and in the waste application phase may give considerable difficulties, particularly at lengths exceeding 500 m. The VDH concept represents a different philosophy: the rather small and weak waste canisters are contained in the lower 2 km part with rather poorly isolating clay embedment, while the upper 2 km are effectively plugged with dense bentonite clay. This concept may give acceptable isolation of the waste but the stability of the deep holes may be insufficient and critical in the canister application phase and the required technique for safe application of canisters and “deployment” mud is not yet at hand. We will discuss these matters in some more detail later in this chapter.

From an economical point of view the spacing of the canisters and hence of the holes and tunnels is the key factor in all the concepts. It is strongly dependent on what temperature and temperature gradients that can be accepted from the viewpoint of rock behavior and clay longevity as will be discussed in detail.

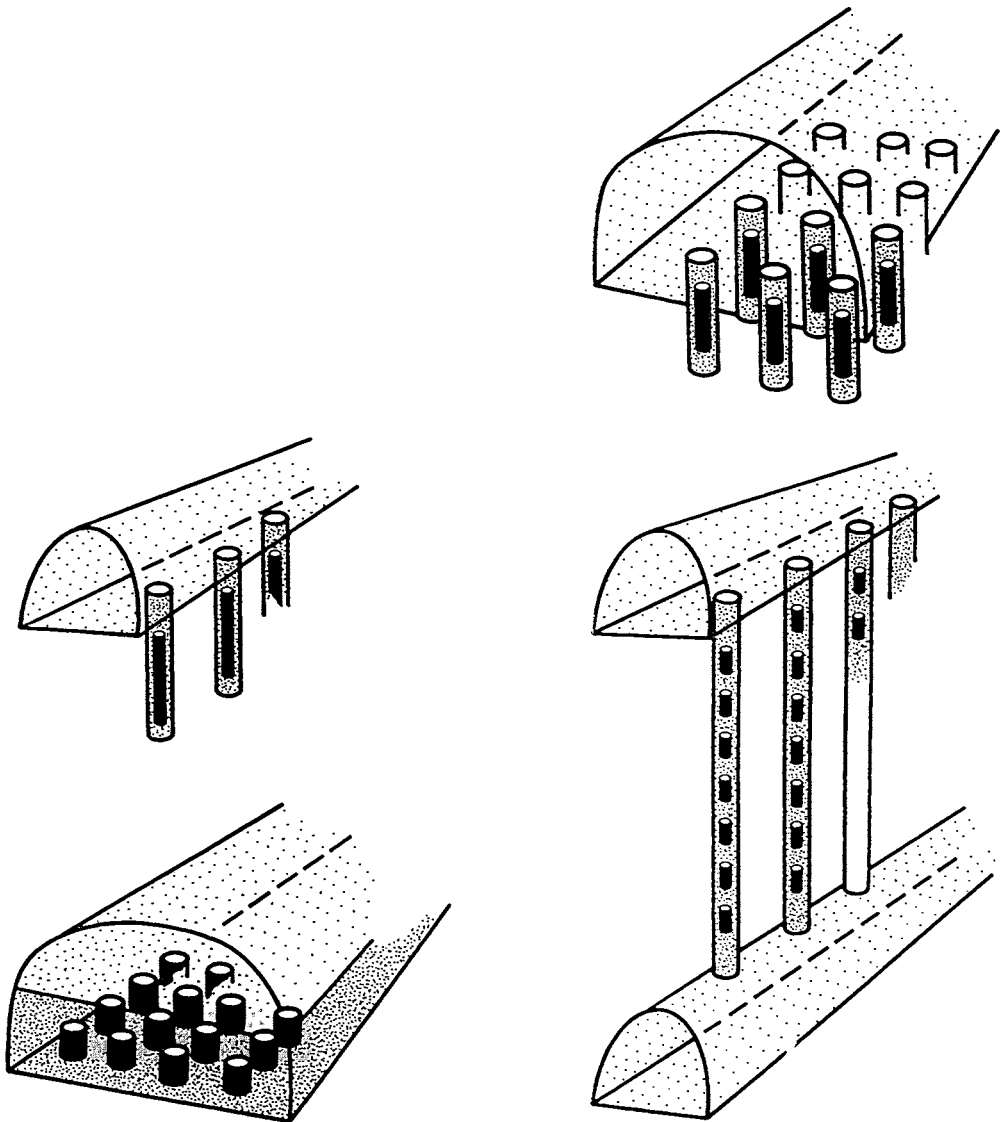


Figure 54 Repository concepts. Upper left: KBS3 (major Swedish concept). Upper right: Multiple deposition holes in large vault. Lower left: Containers embedded in large tunnel. Lower right: Several canisters in medium-long holes connecting horizontal tunnels

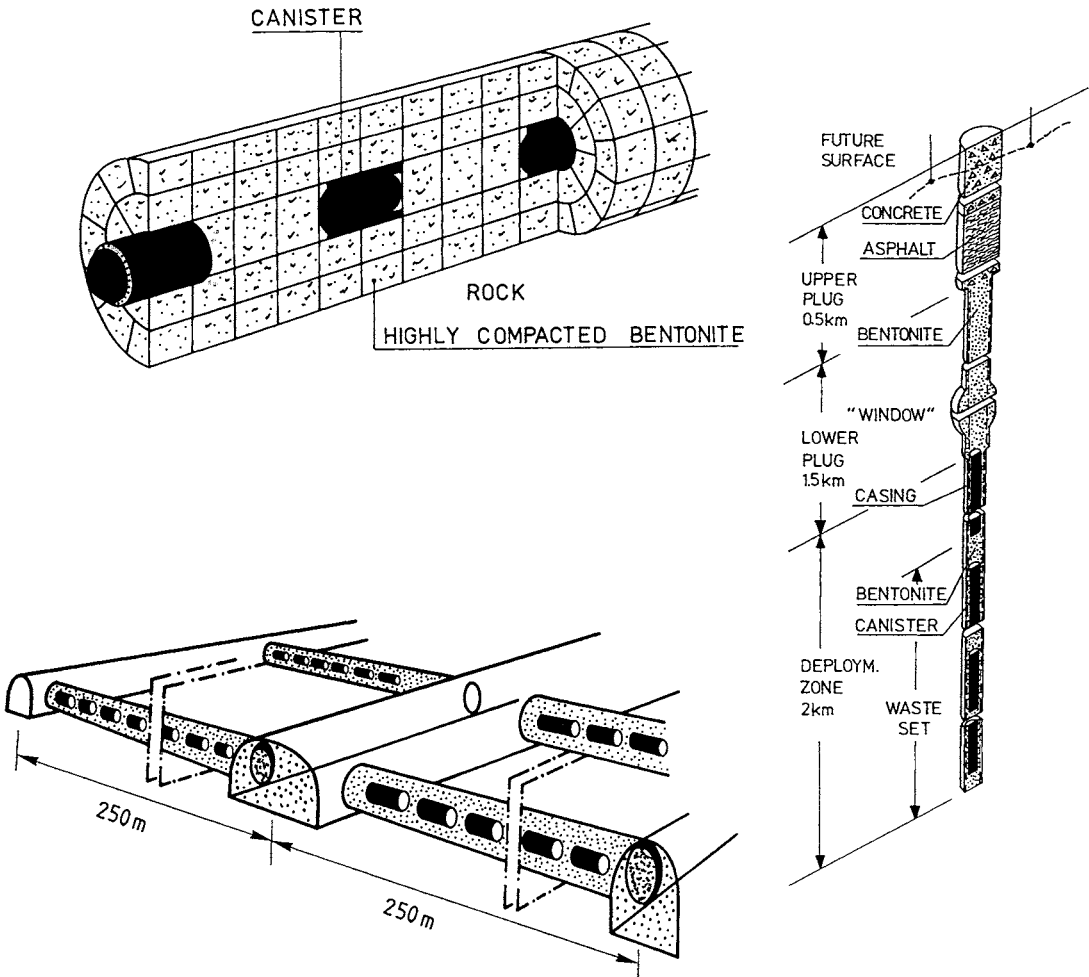


Figure 55 Long-hole concepts. Upper left: Very long holes (VLH) drilled by TBM technique. Lower left: Horizontal deposition holes drilled from blasted tunnels (ENRESA). Right: Very deep holes, VDH (SKB)

3-4 Waste containers

Low-level but long-lived radioactive waste, LLW and MLW, which are comparable to toxic industrial waste, is commonly cast in concrete boxes if it is in solid form, or filled in thin steel drums that are sealed with asphalt if it is in liquid form. The weak and short-lived containers that can be accepted for less dangerous waste naturally let toxic elements or radionuclides through soon after emplacement, which, depending on their concentration, may require very effectively isolating embedment of the containers. For the most dangerous waste, the corrosion rate of the canisters is naturally of fundamental importance but it is also essential to consider canister defects that appear in the encapsulation process and that yield early release of radionuclides, i.e. as soon as water has penetrated the clay embedment. HLW can be reprocessed nuclear fuel that is vitrified and cast in relatively thin steel canisters with the low solubility of the glass matrix as a main barrier (at the high pH provided by the clay embedment), or unprocessed, burnt-out fuel encapsulated in steel, titanium, copper or copper/steel composite canisters (Figures 56 and 57).

The resistance to imposed strain and to corrosion of the weak containers for LLW and MLW is small and the embedment and farfield barriers have to be relied on. This is also the case for high-risk industrial waste contained in simple steel barrels or cast in concrete containers, particularly if gas is produced. Poorly embedded containers can only be relied on if they are virtually tight and sufficiently resistant to expected strain and chemical attack.

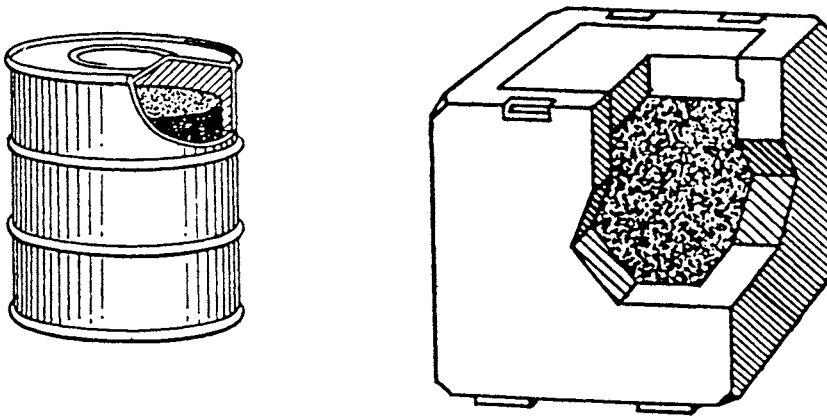


Figure 56 Containment of LLW (steel drums) and MLW (concrete containers)

In Chapter 2 it was specified that tectonically induced rock displacements must be expected to take place along 4th and lower order discontinuities and that they may be significant in a few thousand years, and in Chapter 1 an example was given of thermal effects in HLW repositories that will also generate rock displacements. It was stated that, due to such effects and to the difficulty in assessing the behavior of the rock, the major burden of supplying effective isolation of the waste should be taken by the engineered barriers, which must therefore not degrade at a higher rate than what is required to maintain the concentration of escaped toxic elements below the critical level. For HLW the canisters should be largely intact in a 100 000 year perspective, which requires that they have a sufficient mechanical strength and corrosion resistance. Naturally, this implies that the degrading processes, i.e. mechanical strain and chemical attack are understood, quantified and counteracted. Theoretically, the canisters can be designed to maintain the required tightness for extreme periods of time - gold would be a perfect material - but in practice defects in the manufacturing are unavoidable and they will, in practice, control contamination of the groundwater from the moment the canisters are emplaced.

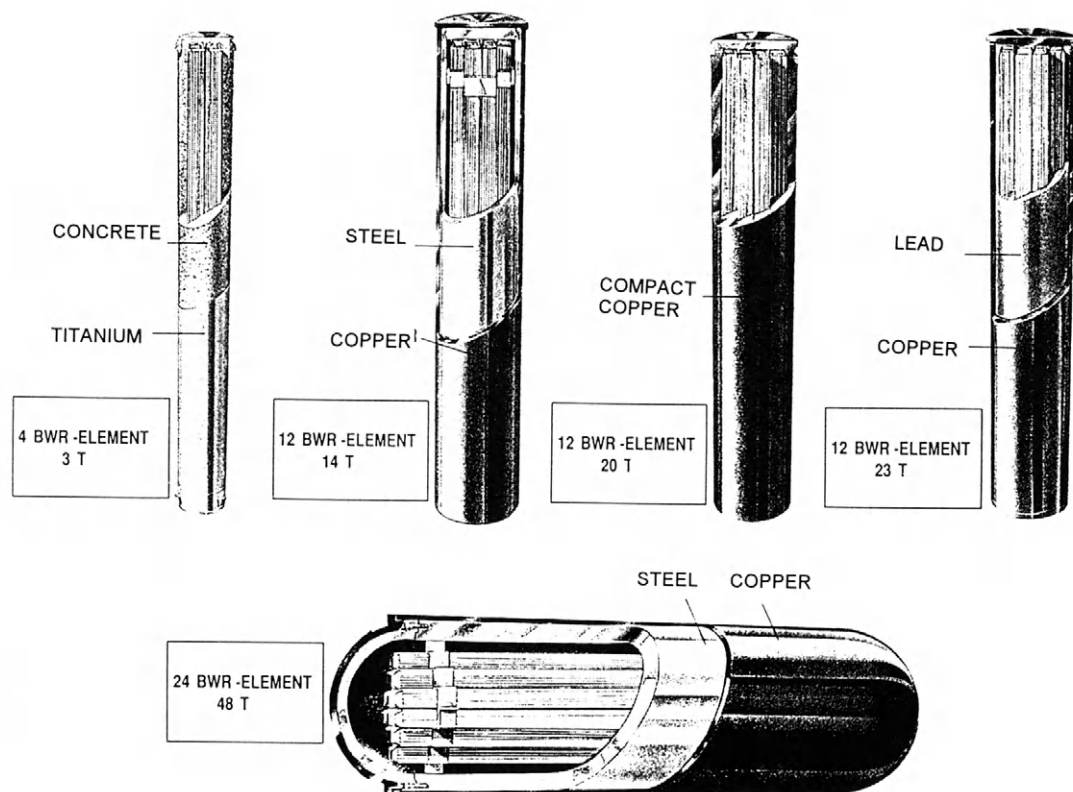


Figure 57 Examples of HLW canisters [2]. Upper row, from left: 1) Titanium /concrete canister (3 t) for VDH. 2) Copper/steel composite canister for KBS3 with empty space between the steel and the waste (14 t). 3) Compact copper prepared by hot isostatic compression of copper powder in copper cylinder, for KBS3; the waste is "impregnated" with copper with a very low porosity (20 t). 4) Copper/lead canister for KBS3 (23 t). Lower: Copper/steel canister for VLH with empty space between steel and waste (48 t)

3-5 Embedment of containment

3-5.1 Bentonite

Bentonite is a geological term for expansive clay formed from volcanic ash deposited in the sea or in estuaries. The main clay mineral belongs to the smectite group of which montmorillonite is a common species. In later years it has become customary to use the term bentonite also for smectite clay formed as a reaction product from in-situ weathering of rock like rhyolite. Such weathered material forms large masses in countries like Japan, while bentonites emanating from volcanic ash usually appear as centimeter- to decimeter-thick layers or occasionally a few meters thick beds. Bentonites are common all over the world and are exploited for a number of industrial purposes, like pelletization, and for use as drilling mud. This latter application is because of the strong thixotropy of smectites, i.e. a dramatic loss in mechanical resistance on shearing of soft smectite clay and a very quick gelation and strength regain at rest, which also makes it work well as grout for sealing of rock fractures.

The main application in repositories is for tight embedding of waste containers and for sealing boreholes, shafts and tunnels. The cost of good commercial bentonites, i.e. with at least 70 % smectite, in granulated form and delivered in bulk is about 1000 SEK (150 US\$), referring to the 1993 price level.

SMECTITE CLAY MATERIAL

Montmorillonite is not the most stable smectite mineral but it is very common and most commercially available bentonites have montmorillonite as major clay mineral. The lattice constitution is similar to that of the micas but without potassium ions as ligands, and the individual lamellae are therefore easily separated in conjunction with uptake of water molecules in interlamellar positions (Figure 58). The common concept is that lattice substitutions give the lamellae a negative charge, which is compensated by exchangeable cations that hold the lamellae together. The interlamellar space has a strong potential for water uptake because of the hydration power of the cations or possibly - for sodium and lithium in interlamellar positions - because of direct establishment of a water lattice directly on hydroxyls exposed on the internal surfaces [3]. If a stack of montmorillonite lamellae, or flakes, is free to absorb water it is concluded to have 3 interlamellar hydrate layers established if sodium or lithium are adsorbed cations, while only 2 are formed if calcium and most other cations replace sodium.

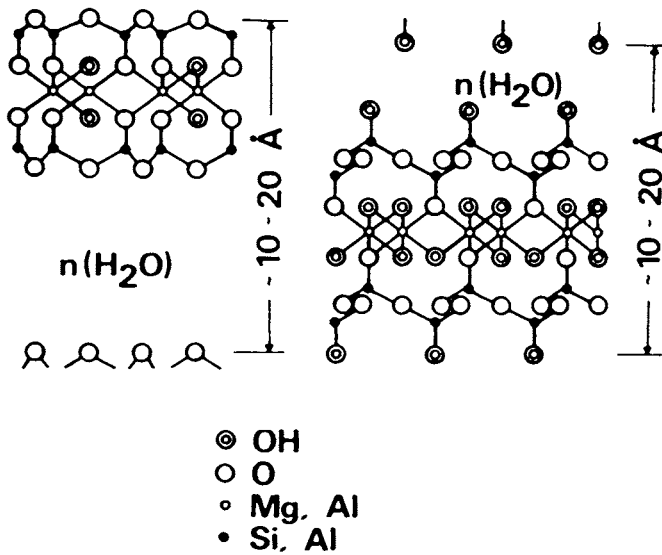


Figure 58 The montmorillonite lattice. Left: Common condition (Hofmann/Endell & Wilm). Right: Possible condition for Na or Li as adsorbed interlamellar cation and temperatures below about 150°C (Edelman/Favejee) [3]

The interlamellar or “internal” water is largely immobile under ordinary hydraulic gradients and since it forms a larger part of the total water content in Na and Li montmorillonite clay than when Ca is the adsorbed cation, the swelling power and thereby the sealing ability are higher of Na and Li montmorillonites than of Ca montmorillonite (Figure 59). Since Ca is the most common adsorbed cation in natural bentonites and Na bentonite is commonly asked for, conversion from Ca to Na is a standard industrial process. For this purpose the ground bentonite from the quarries is mixed with sodium carbonate, which reacts with the clay material by exchanging most of the initially adsorbed calcium ions to sodium and by forming calcium carbonate. In the relatively few natural Na bentonites, like the ones in Wyoming and South Dakota, USA, a fraction of the exchange sites are always occupied by calcium, and calcium carbonate is also present as an accessory mineral.

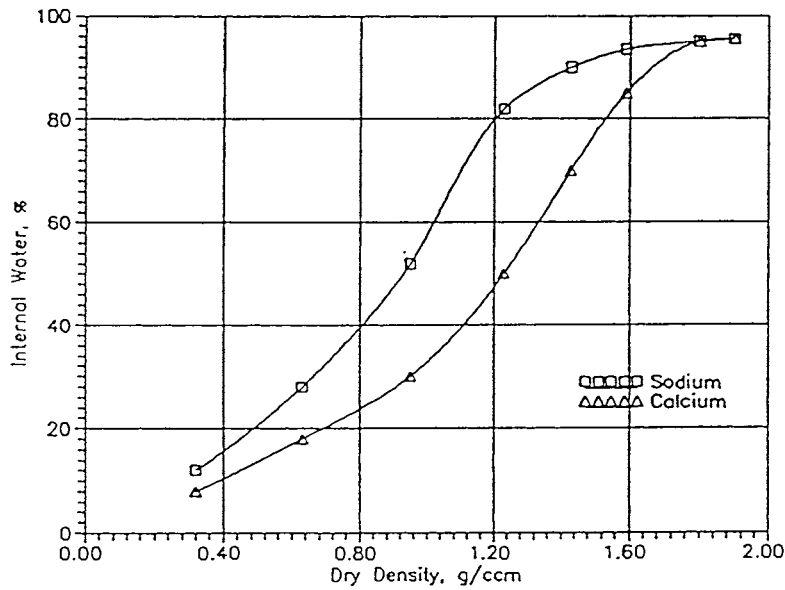


Figure 59 Amount of internal water in percent of the total water content for Na and Ca montmorillonite. The curves were derived from theoretical models of stack arrangements (5)

Naturally, the interlamellar space does not represent all voids in smectite clays. Thus, the narrow variable space between adjacent stacks of flakes is where electrical double-layers interact mutually and with the mineral lattices [4], and there are also more or less interconnected larger voids which let water through [5]. Such water is termed “external” and represents the difference between 100 % and the percentages given in Figure 59 for the “internal” (interlamellar) water. Figure 60 illustrates a fully expanded stack of flakes in montmorillonite clay, and Figure 61 shows general pictures of the microstructure of dense and very soft smectite clay.

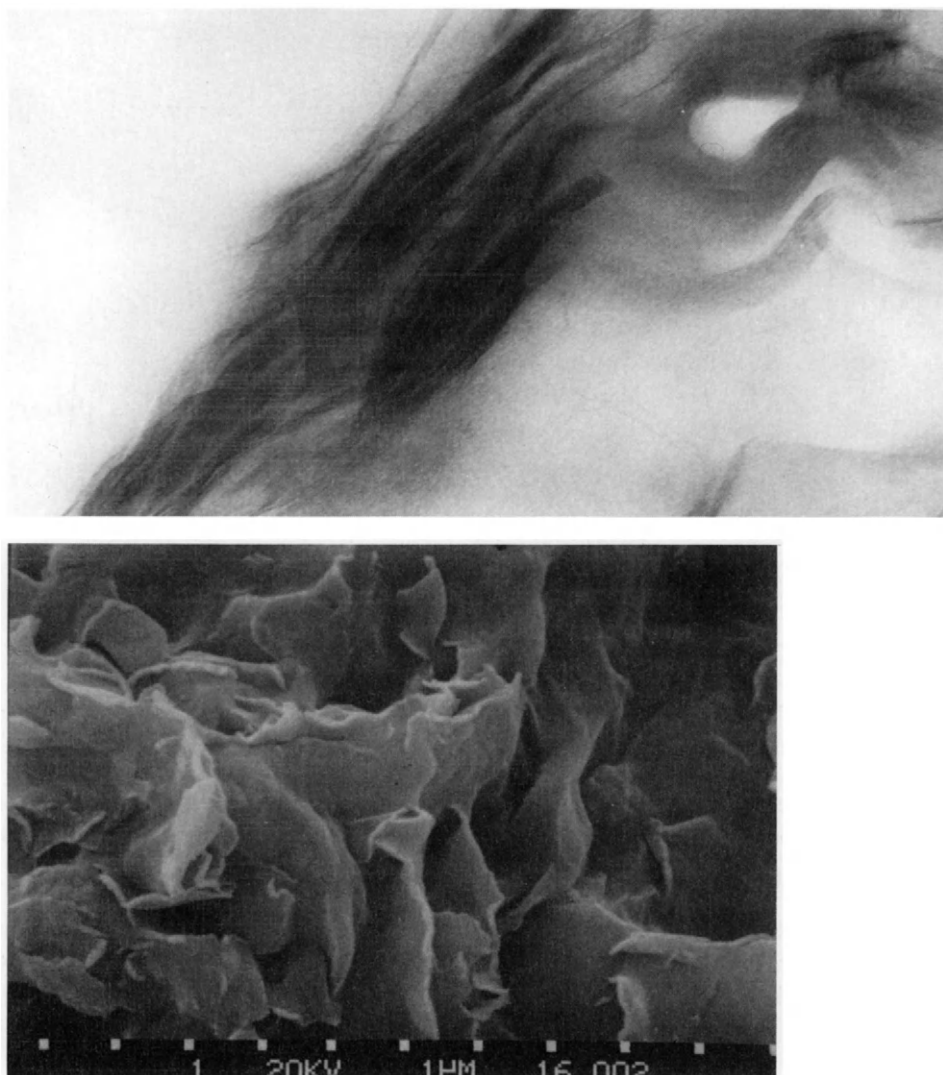


Figure 60 Electron images of expanded montmorillonite clay. Upper: Transmission micrograph of a few hundred Å thick section of polymer-embedded material showing curly interwoven stacks of flakes (100 000 x). Lower: Scanning micrograph of freeze-dried montmorillonite clay (10 000 x). The much lower resolution power of the scanning micrograph means that the flakes cannot be identified

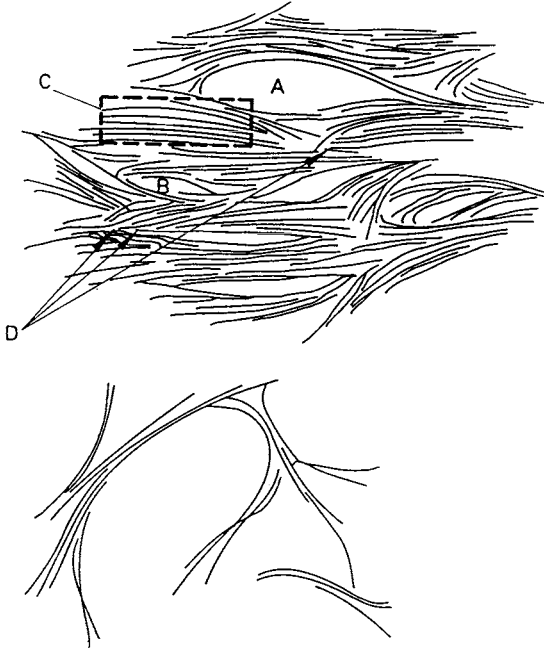


Figure 61 Schematic picture of the microstructure of smectite. A) Large more or less continuous void. B) Small isolated void C) Interlamellar space , D) Contact region of interacting stacks with electrical double-layers

In practice, the microstructural constitution evolves according to the conditions under which the clay matures: unconfined dry smectite powder that is wetted absorbs water, expands and turns into slurry, while confined powder wetted through a filter forms a water-saturated clay with a density that is uniquely determined by the volume that it occupies and the solid clay mineral mass (Figure 62).

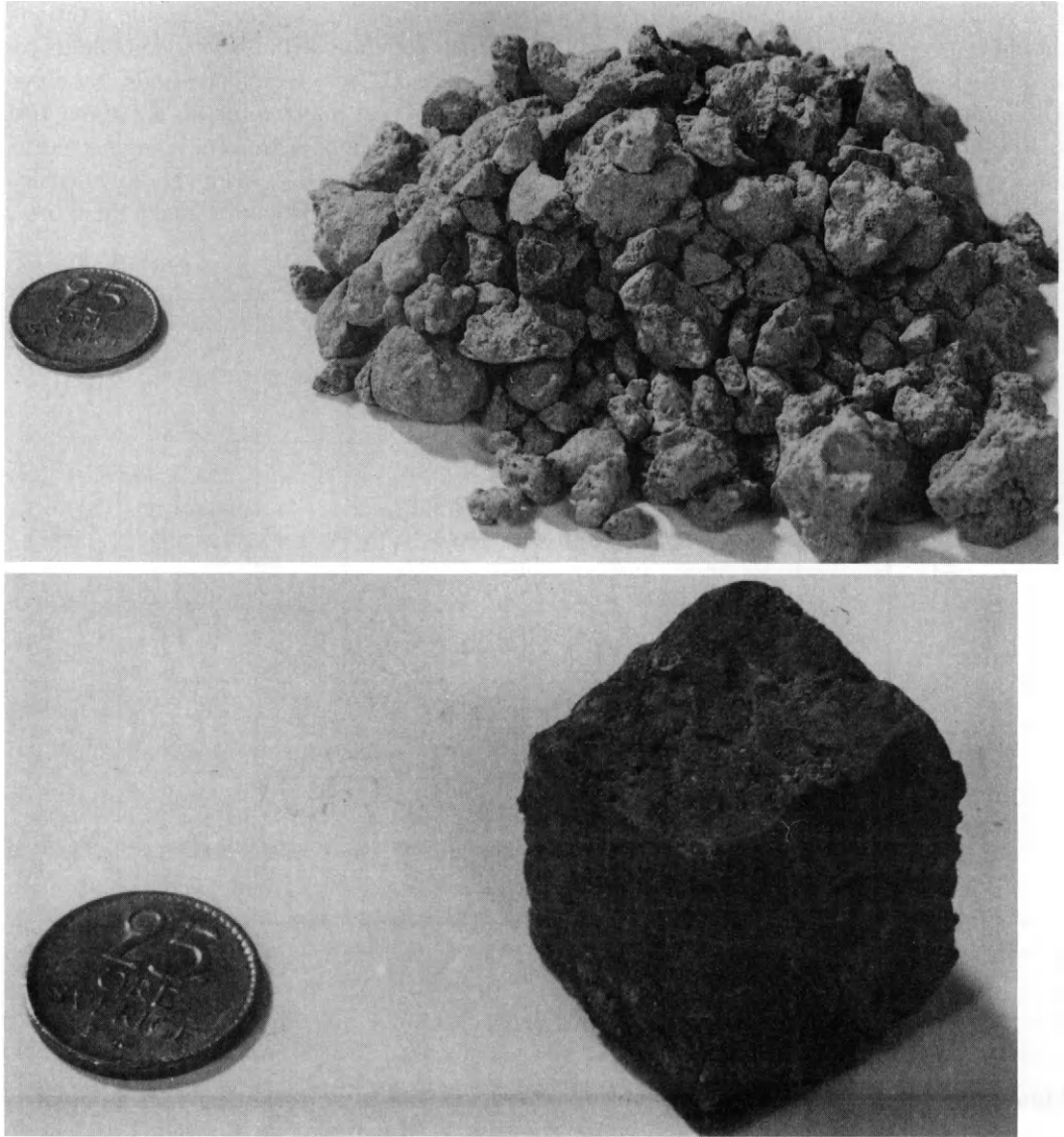


Figure 62 Transformation of dry bentonite powder to dense, homogeneous clay by taking up water under confined conditions

The property of adsorbing much of the porewater in interlamellar, largely immobile positions should imply a much lower hydraulic conductivity than for clays with non-expandable minerals, which is also demonstrated by the diagram in Figure 63, from which one finds that clays with hydrous mica (“illite”) and kandites (kaolinite, dickite) as major minerals are about 100 to 10 000 times more conductive at any void ratio. This is a major reason for using smectitic clays as seals in repositories. The amazing thing is that smectite gels of even very low density are remarkably tight, which, in combination with their thixotropic behavior, make them useful as grouts for sealing rock fractures.

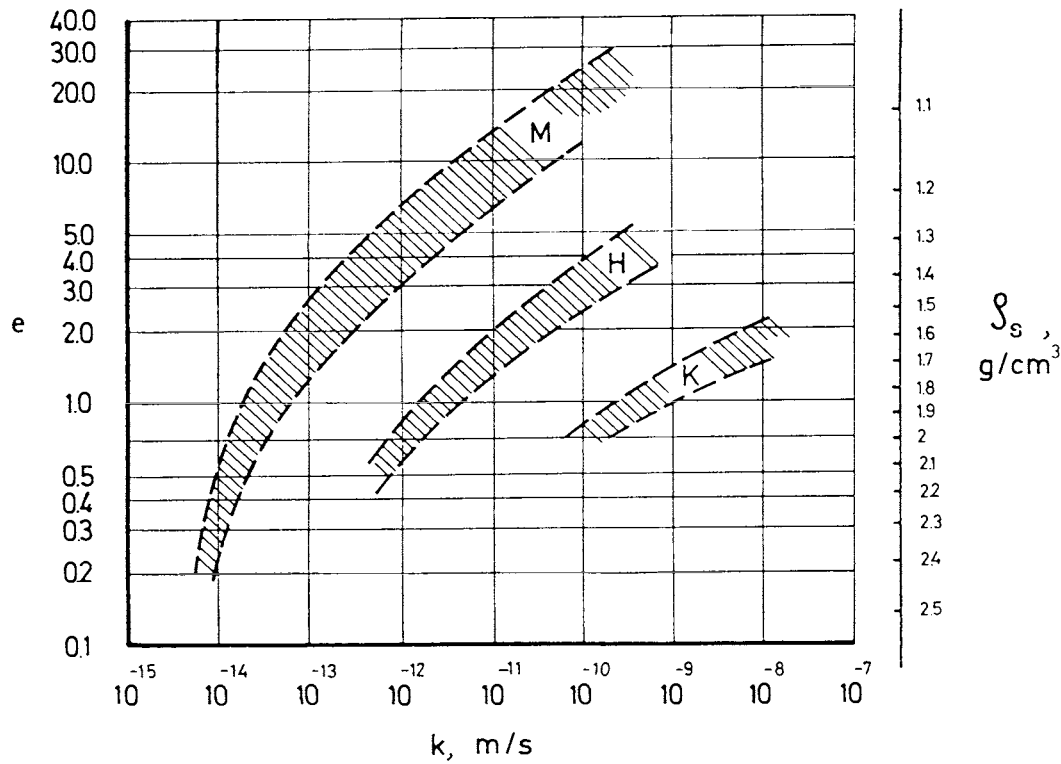


Figure 63 Hydraulic conductivity of pure clays, the bands representing variations in hydraulic gradients and water chemistry. M is montmorillonite, H hydrous mica and K kandites (e is void ratio, ρ_s is density at complete water saturation)

The microstructural constitution of smectite clays, especially when montmorillonite is the major clay mineral, has a significant impact on the diffusion transport capacity of dissolved ions, expressed as the product of the diffusion coefficient and the porosity, which is naturally of fundamental importance for the seals in repositories for high-risk waste. It is clear that the charge conditions imply that the interlamellar space can only hold cations ("Donnan exclusion"), which means that although the anion diffusion **rate** as evaluated by applying Fick's law may be as high as that of cations, the anion diffusion **capacity** is very low at high bulk densities and high at low densities. The cation diffusion capacity would hence be expected to be higher than that of anions, which is actually also the case at least for certain ions. Still it is lower than for pure water because the diffusion rate is retarded by the place exchange involved in the surface diffusion process that is the predominant mechanism at high densities.

If fully water saturated bentonite clay is confined in a rigid cell and contacted with water through a stiff filter, the clay will tend to take up more water and expand, yielding a swelling pressure that is very high for high clay densities and very low but measurable even at very low densities and complete hydration of the interlamellar space. The fact that a swelling pressure can be recorded even in low-density smectite is because one component of this pressure is the repulsion of electrical double-layers formed at the boundaries of the stacks, which are concluded to consist of 3-5 flakes in Na montmorillonite and about 10 in Ca montmorillonite. Figures 64 illustrate schematical relationships between density and swelling pressure for Na and Ca montmorillonite clays.

One of the important functions of the embedment of waste containment is to protect it from being exposed to very high stresses or large strain induced by tectonics or thermomechanical effects. This requires ductile behavior and a relatively low shear modulus, as well as ability to undergo stress relaxation. However, the softness must not imply that the heavy containers or canisters sink in the embedment and slip out of it, and a suitable density interval yielding sufficient softness and bearing capacity must hence be found for each application. Despite the very special microstructural constitution with quasi-crystalline interlamellar water as one component, smectites do not deviate significantly from other clays, i.e. the effective stress concept applies except possibly at very high densities, and the general relationships between effective stress and shear strength and void ratio apply, in principle at least [6].

One realizes that the exceptionally low hydraulic conductivity of dense Na clay, and the swelling and homogenization potential of this sort of smectite clay make it very useful for embedment of waste containers. Adding to this the significant cation exchange (and adsorption) ability, it is clear that smectite clay, especially in Na form, serves well as embedment of waste containment from a physical point of view. A question that we will come back to is how and to what extent the physical properties are changed in a long-term perspective.

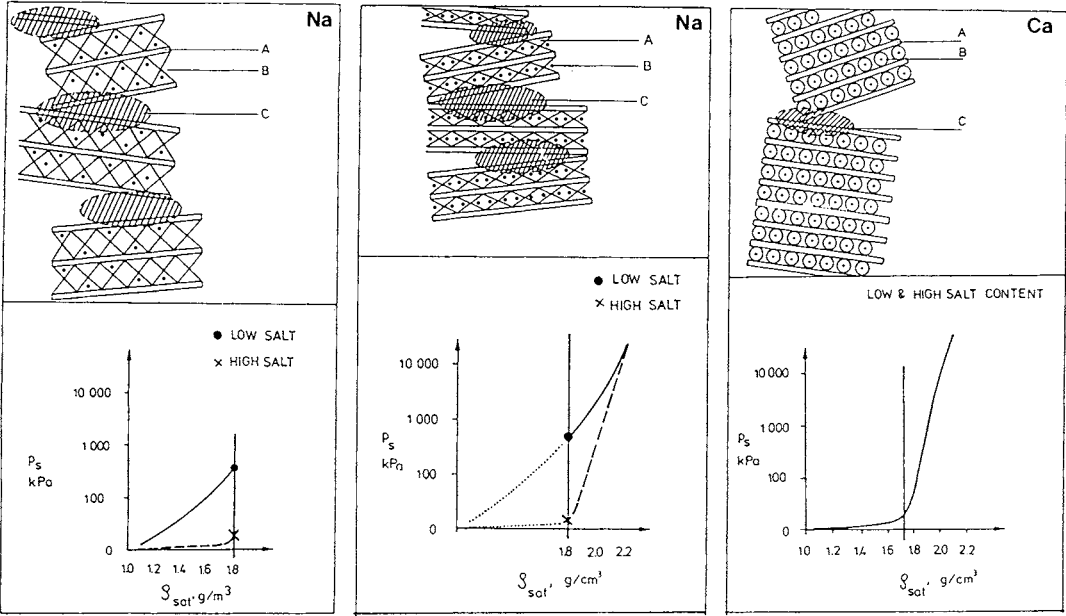


Figure 64 Schematic pictures of stack assemblages and influence of density (at water saturation) and salinity for Na and Ca montmorillonite clay. A) Flake, B) interlamellar space, C) Stack contact region with interacting electrical double-layers. Left and central: Na clay, Right; Ca clay [5]

3-5.2 Physical properties of commercial bentonites

The most important physical properties of clay as waste embedment are:

1. Hydraulic conductivity
2. Ion diffusion capacity
3. Swelling potential (expressed in terms of swelling pressure)
4. Rheological properties
5. Thermal properties

Hydraulic conductivity

Determination of the hydraulic conductivity of smectitic clays is made in the same fashion as for other types of soils, i.e the sample is confined in an oedometer or triaxial cell and percolated by exposing it to water pressure gradient (Figure 65). The scale-dependence of the conductivity and other physical properties of dense smectite clay is insignificant because of the ability of evening out local differences in density through the eminent swelling potential.

The hydraulic conductivity of commercial bentonites is naturally higher than that of pure smectite clay but still on the same order of magnitude. Figure 65 gives the relationship between density and conductivity of Na and Ca bentonites, illustrating the importance of the more homogeneous microstructure when Na is the adsorbed cation. The apparatus used for recording the hydraulic conductivity is also used for determining the swelling pressure. The larger, less expandable stacks and fewer stack contacts in Ca than in Na smectite clay yields larger voids and a much higher conductivity of Ca bentonite and explain the dramatic increase in conductivity that this type of bentonite exhibits when the density drops below about $1.5\text{--}1.6\text{ g/cm}^3$. A very important fact is that Na bentonite clay with such low density, matured by taking up low-electrolyte water with sodium as major cation, undergoes significant microstructural alteration in the form of syneresis-type contraction with formation of large voids if it is percolated by Ca-rich water.

A major question is if the conductivity depends on the hydraulic gradient and if it is temperature-dependent. The answer is that the gradient-dependence is insignificant but the very high gradients that are commonly applied in laboratory experiments in order to get water through in measurable quantities in reasonable time can produce compression and increased tightness of the clay. As to the influence of heating it turns out that the clay actually becomes less permeable by moderate heat treatment. The reason for this is that the microstructure becomes more homogeneous but this may only be valid for bentonite prepared by compacting granula-

ted powder to blocks samples because the granules break up by the heating, by which the number of individual thin stacks of flakes increases and become distributed in the voids between the granules (cf. Figure 62).

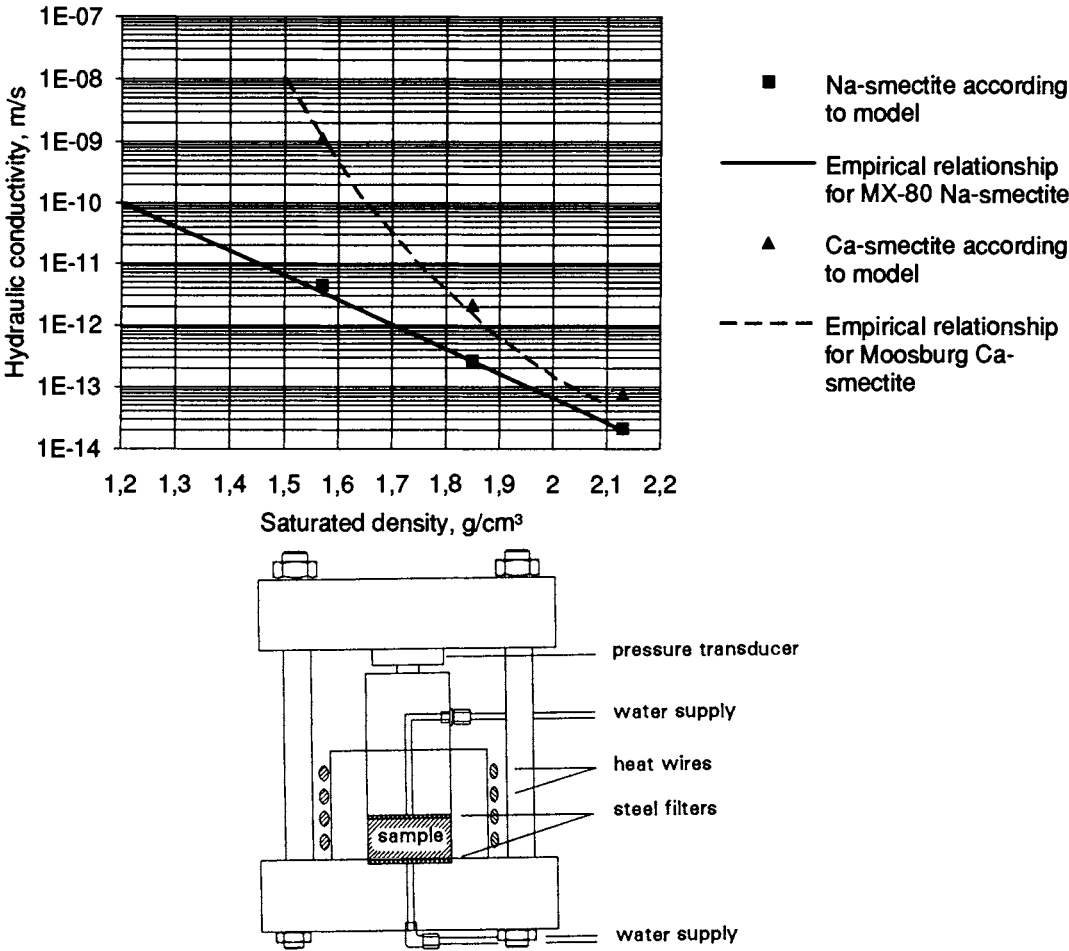


Figure 65 Hydraulic conductivity of Na and Ca bentonite percolated by electrolyte-poor water. Curves represent empirical relationships, triangles and squares represent data calculated by applying microstructural models [5]. The lower picture is a schematic section of oedometers used for determining the hydraulic conductivity and the swelling pressure at normal and enhanced temperature

Microstructural models have been developed for smectite clay and they yield values in good agreement with actually recorded conductivities as illustrated by the diagram in Figure 65 [5]. Homogenization of the microstructure by heating is actually manifested by the time-dependent change in swelling pressure at increased temperature (Figure 68). Thus, freshly compacted, air-dry bentonite powder exhibits a peak swelling pressure caused by the expandability of the “prestressed” dense granules but the pressure drops initially because they deform and disintegrate into thinner stacks that slide into more stable positions. This phenomenon is seen also at room temperature but it is enhanced at higher temperature.

Ion diffusion capacity

Diffusive ion transport takes place due to gradients in concentration of dissolved species. In repositories with low-permeable clay embedment of the canisters and low hydraulic gradients, diffusive migration of dissolved toxic elements is the major transport mechanism. The diffusion rate is determined by the tortuosity of the void system in the clay and of sorbing processes, which strongly depend on the charge distribution of the crystal lattice and of the stacks of thin crystallites, which we call flakes or lamellae. It can be evaluated from recording the concentration profile of samples exposed to concentration gradients using test equipments of the sort illustrated in Figure 66, and be expressed in terms of the “apparent” diffusion coefficient D_a , which commonly varies in the interval 10^{-12} to 10^{-9} m²/s. The evaluation of D_a is simply made by curve fitting adapting the recorded curve as closely as possible to theoretically derived curves applying Fick’s law [7]. The nice curve shape exemplified in the diagram in Figure 66 is not always obtained in diffusion experiments because of chemical processes, like carbonate formation due to carbon dioxide dissolved in the porewater or change in valency of certain radionuclides in the course of the diffusion process, and D_a is often hard to evaluate with a high degree of accuracy.

The “apparent” diffusivity does not give any information on the various mechanisms involved in diffusive transport or of the diffusion transport capacity. The latter is expressed by the “effective” diffusion coefficient, which refers to the actual “effective” porosity and is of great practical use. It also gives some information on the ion transport on the microstructural level in contrast to the “apparent” diffusion coefficient. Thus, the importance of referring to the porosity is realized by the fact that cation diffusion takes place in several ways, i.e. in continuous water-filled voids, along exposed stack surfaces with electrical double-layers, and through the interlamellar space. The latter two mechanisms involve ion-exchange mechanisms for which a sorption parameter, K_d , is introduced [8]. In practice, the ion transport capacity can be evaluated by applying Fick’s law and relevant values of the coefficient of “effective”

diffusion, D_e , for any density. Table 6 gives typical literature-derived data on this parameter for smectite-rich bentonite with a density of 2 t/m^3 , which represents the density of canister-embedding clay. For bentonite/ballast mixtures the diffusion coefficient is up to 100 times higher.

Table 6 Effective diffusion coefficient for elements migrating in bentonite [7]

Species	$D_e \text{ m}^2/\text{a}$
C-14	3.2e-03
I-129	7.9e-05
Sr-90	7.9e-01
Na-22	5.2e-02
Cs-137	7.9e-01
Pu-238	3.2e-03
Am-243	3.2e-03

Swelling pressure

As indicated in Figure 64 the swelling pressure is strongly dependent on the density and the salinity and major type of adsorbed cation are of great importance at low densities. However, at densities higher than around $1.6\text{-}1.7 \text{ g/cm}^3$ the swelling pressure is less affected by the porewater chemistry and this means that dense bentonite saturated with electrolyte-poor water has its tightness and swelling potential largely preserved even if the porewater is replaced by ocean water (Figure 67). In fact, the swelling pressure of Na and Ca percolated by 10 % NaCl and CaCl_2 solutions does not drop very significantly when the density is higher than around 1.8 g/cm^3 [5].

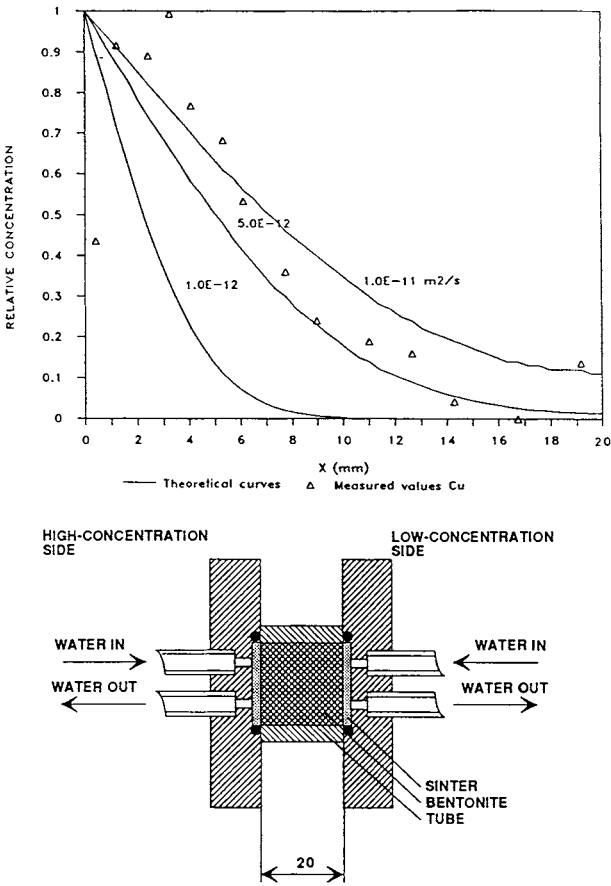


Figure 66 Example of recorded concentration profile of copper in ionic form in bentonite and three theoretical curves indicating that D_a is around $10^{-11} \text{ m}^2/\text{s}$ [7]. The lower picture shows the test equipment used for recording the concentration profile in clay sample. The concentration at both ends are maintained constant by circulating the respective solutions

Heating changes the swelling pressure. Thus, if the temperature is raised of a sample of water saturated bentonite and the porewater overpressure that is generated by the heating is allowed to dissipate, the swelling pressure is found to increase for Na bentonite while it decreases for Ca bentonite (Figure 68). The reason is that the net effect of two mechanisms i.e. lattice contraction due to dehydration of the interlamellar space and increase of the osmotic pressure at the stack contacts, is different in the two types of clay [5]. The lattice contraction dominates

for Ca bentonite while the increase in osmotic pressure dominates for Na bentonite because of the much higher frequency of stack contacts in Na bentonite. Heating is of negligible importance for very high bulk densities, while it is rather significant at low bulk densities as demonstrated by the diagrams in Figure 68.

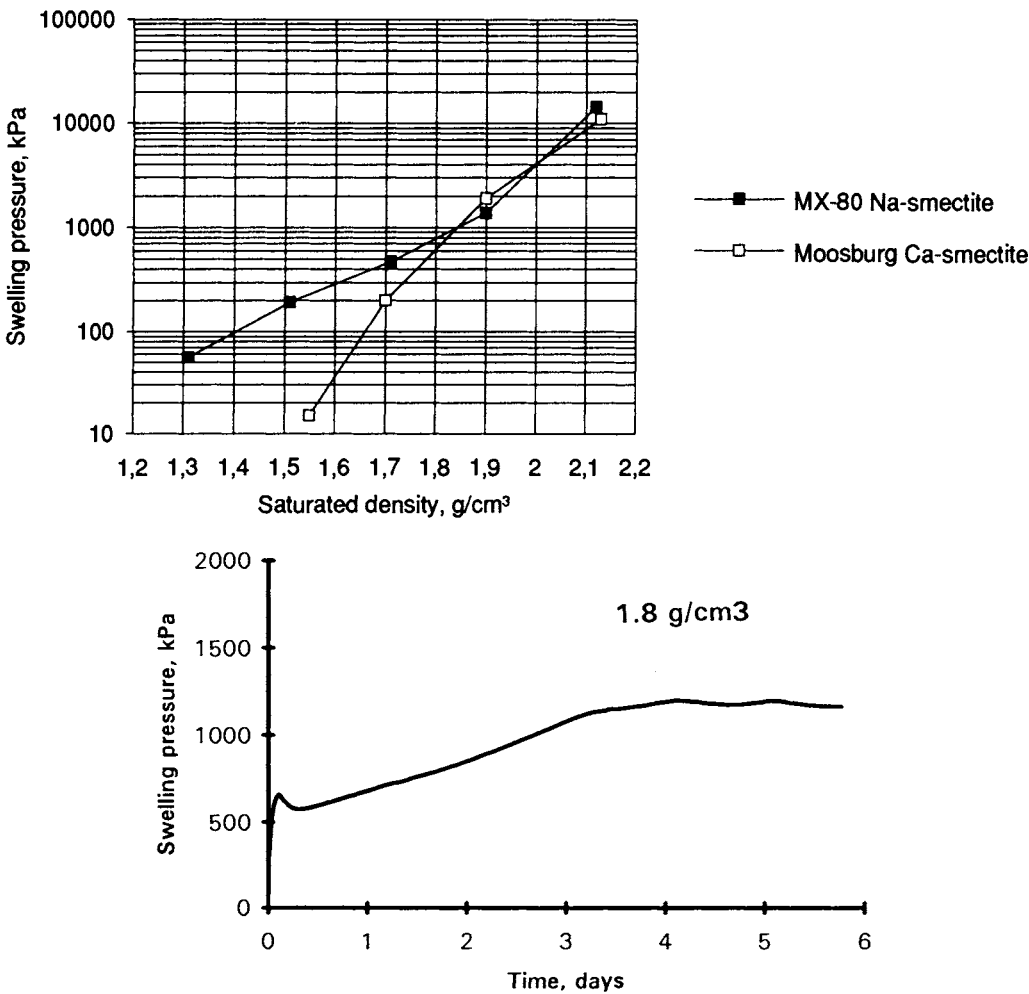


Figure 67 Swelling pressure of bentonite. Upper: Recorded pressure of Na and Ca bentonites saturated with distilled water [5]. Lower: Typical time-dependent evolution of swelling pressure on wetting of compacted bentonite powder

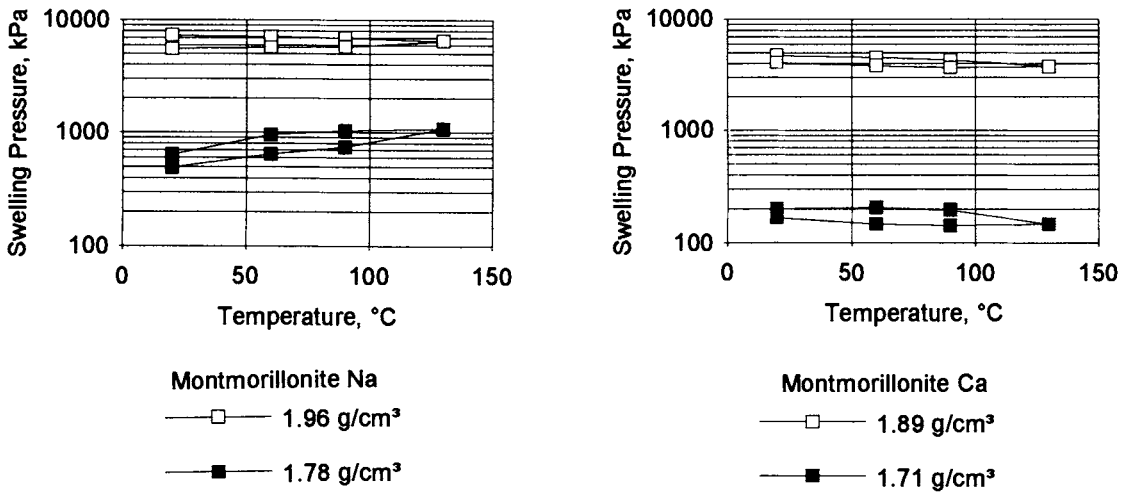


Figure 68 Change in swelling pressure of Na (left) and Ca bentonite on heating [5]

Rheological properties

The rheological properties are of importance in two contexts: they determine the stress conditions in waste containers and canisters at rock shearing, and they control the settlement rate of containers and canisters as illustrated by the Forsmark silo described in Chapter 1. The first-mentioned case implies quick shearing with no change in water content, i.e. deformation under undrained conditions, while the other takes place so slowly that the porewater pressure can dissipate. Recently developed general material models can be used for solving such problems and they will be summarized here [6].

Non-linear plastic strain can be expressed either by the classical Drucker-Prager and Cam-clay models, while non-linear elastic behavior can be described by a porous-elastic model. The difference between the two plastic models is indicated in Figure 69. In the Cam-clay

model an elliptic yield curve separates the elastic from the plastic region of the q/p plane and failure is reached either when the stress path reaches the critical state line or the yield curve where it is located above the critical state line. The yield curve of the Drucker-Prager model is a straight line or rather a cone in the principal stress space, and the failure curve is parallel to it. The elastic zone has no end at increasing p .

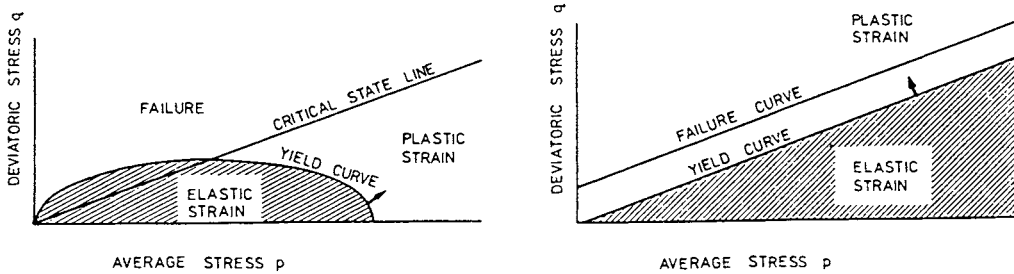


Figure 69 Stress/strain models. Left: Cam-clay. Right: Drucker-Prager

The influence of time on strain can be expressed in several ways. From a practical point of view, creep under undrained conditions, i.e. quick shearing with no change in water content, is most important since it represents the case of shearing of canisters caused by tectonic movements. A general material model of wide use is the one given in Eq.1 [6]. It is based on the empirical creep law proposed by Singh and Mitchell [9]. Figure 70 illustrates a typical creep curve and a schematic cross section of a triaxial compression cell for determining the stress/strain behavior and the shear strength.

$$\dot{\gamma} = \dot{\gamma}_0 e^{\alpha \frac{(\sigma_1 - \sigma_3)}{(\sigma_1 - \sigma_3)_f} (-\alpha) \frac{(\sigma_1 - \sigma_3)_0}{(\sigma_1 - \sigma_3)_f} \left(\frac{t}{t_r}\right)^n} \quad (1)$$

where:

t_r = reference time (10^5 s)

$(\sigma_1 - \sigma_3)_o$ = reference deviator stress $[0.5(\sigma_1 - \sigma_3)_f]$

$(\sigma_1 - \sigma_3)_f$ = deviator stress at failure

γ_o = creep rate at time t_r

n and α = parameters derived from laboratory tests

Thermal properties

The canister-embedding clay should be able to transfer heat to the surrounding rock so that it does not become exposed to temperatures higher than 100-130°C, partly because it means that the degradation of the clay will be moderate, and partly because the rheological properties of the canister material and its corrosion resistance will not deteriorate substantially.

The heat conductivity depends on the amount of water in the clay. Commercially available bentonite is delivered with a water content (ratio of water and solid matter) of 10-15 %, which corresponds to 1 to 2 interlamellar hydrite layers, and compaction to very high bulk densities can give a heat conductivity of up to 0.7 W/m,K. At complete water saturation the conductivity of such dense smectite clays will increase to about 1.5 W/m,K, which is sufficient for yielding a maximum temperature of about 70°C for repository concepts like KBS3, while it may be significantly more than 100°C for VLH. Since it will take several years and even decades for unsaturated canister-embedment to become fully saturated, several ways of increasing the initial heat conductivity have been proposed, like adding water to the bentonite powder to be compressed to blocks, mixing the bentonite powder with quartz, and adding graphite to the bentonite. The results are very promising but chemical effects like cementation need to be considered. We will return to this issue later.

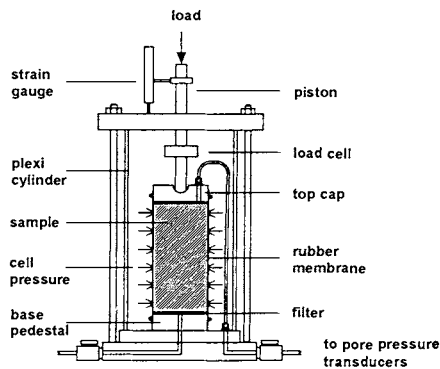
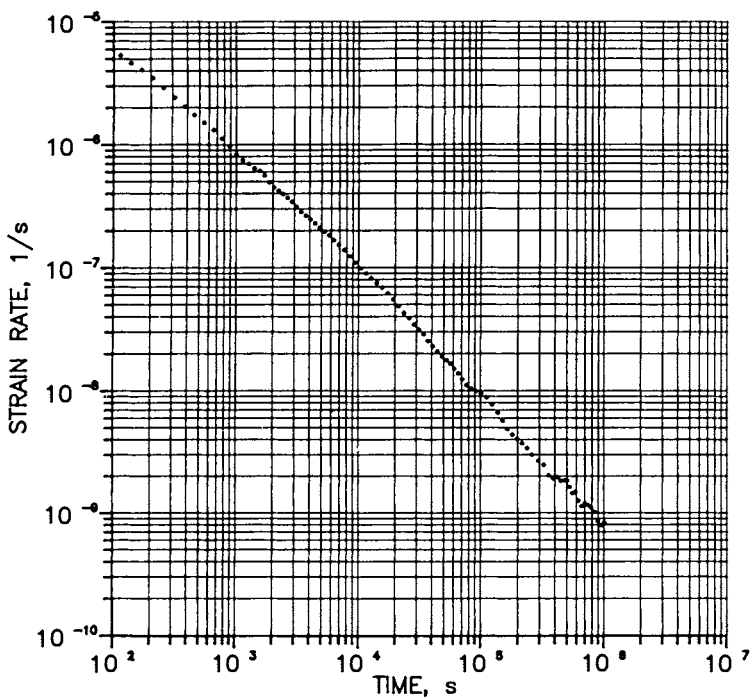


Figure 70 Typical creep curve of Na bentonite showing almost perfect log time behaviour ($n=-1$ in Eq.1). The lower picture illustrates a triaxial cell used for rheological tests and determination of the shear strength

Figure 71 illustrates the test arrangement for recording the thermal properties of clay materials. A test probe containing a wire heater and a thermocouple is inserted in borehole in the sample, which is shown as a compacted block of clay [10]. Constant power increases the temperature of the probe and the sample as a function of the heat conductivity of the clay, which is evaluated by applying simple physical laws for transient heat flow from a linear source.

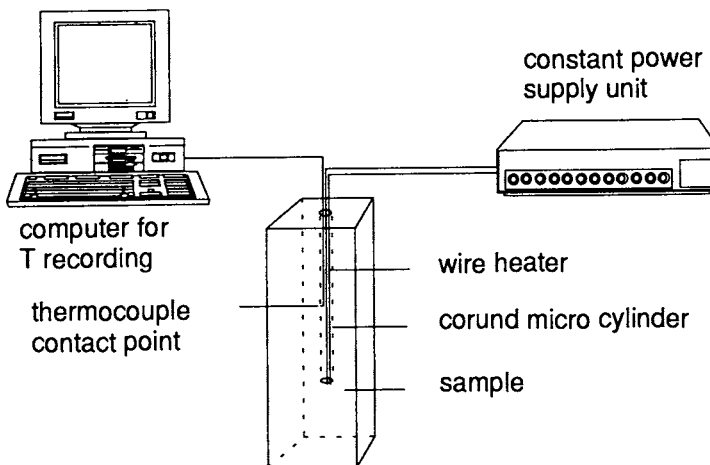


Figure 71 Arrangement for measuring the thermal properties of clays

3-5.3 Physical properties of bentonite mixtures

For certain purposes some of the physical properties of pure bentonite are not at optimum and mixtures of bentonite as a sealing component and properly graded “ballast” (aggregate) material is preferred. This is the case when constructing a bed for a heavy object like the big concrete silo at Forsmark (cf. Chapter 1), for which very small compressibility and hydraulic conductivity values were major requirements. A pure bentonite bed would have caused large vertical movements up and down of the silo in the water saturation phase when only little waste had been applied, and when the waste application is finally completed and the top backfilling is on site. Other examples is backfilling of repository tunnels and shafts where

only very small movements are acceptable. Mixtures of bentonite and other components have not been investigated as extensively as bentonites but the physical properties of a number of bentonite/ballast materials are sufficiently wellknown to make them useful as low-permeable mixtures of low compressibility.

Microstructure

A bentonite-based mixture has a low compressibility if the dominant constituent consists of a dense network of incompressible grains with clay between. This can only be achieved by using a low bentonite content and a size distribution of the grains - the ballast - that makes smaller grains fit in the voids between larger ones (Figure 72).

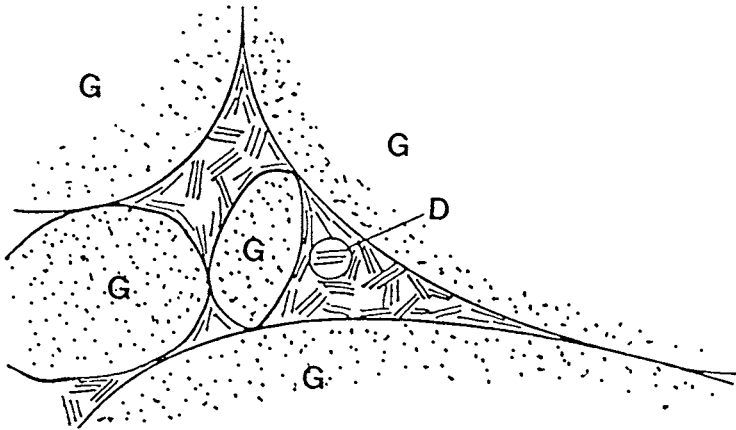


Figure 72 Schematic picture of the microstructure of bentonite-poor mixtures. G=Ballast grain, D=clay component

The issue of finding an ideal gradation for effective filling of voids between larger ballast grains with smaller ones, has led to a number of practical rules. A commonly applied principle is to compose the ballast according to Fuller's curve, which has the shape of a parabola in an ordinary grain size diagram, as approximated by the three curves a,b,and c in Figure 73. Figure 74 shows the dry bulk density for laboratory-compacted mixtures of these ballast materials and very fine-grained bentonite.

Naturally, the extent to which the clay fills the voids and the density of the clay filling determine the hydraulic conductivity, while the porosity of the ballast network is the major factor that influences the compressibility.

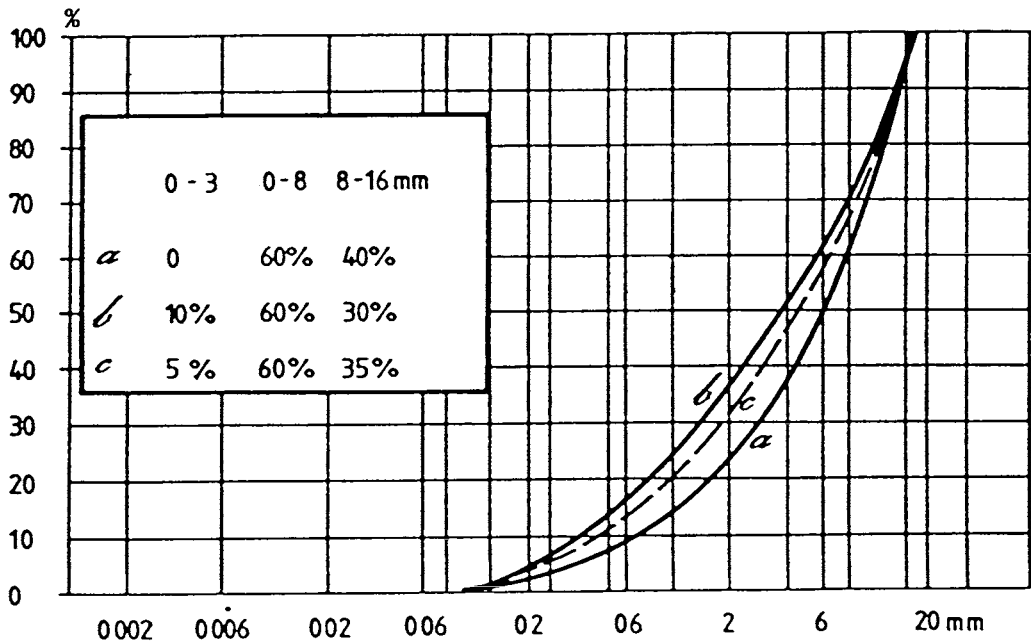


Figure 73 Granulometry of three suitable ballast compositions. The vertical axis shows the percentage of material finer than the respective grain size, which is given by the horizontal scale

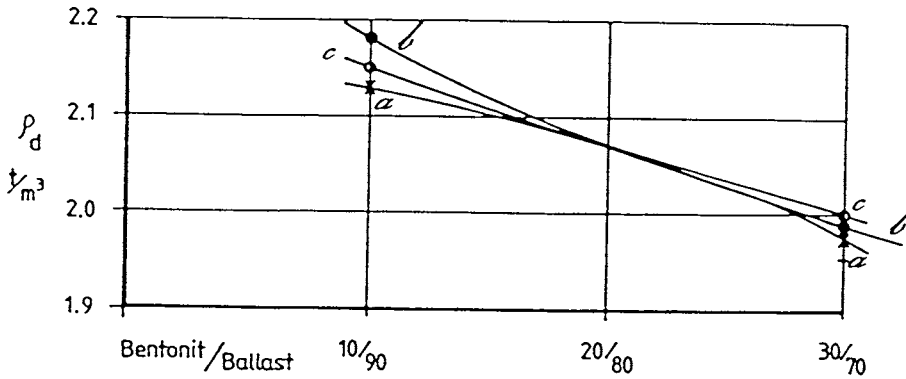


Figure 74 Dry density of compacted mixtures of bentonite and ballasts a, b and c

Homogeneity

The distribution of clay in the mixture is of course of great importance for the tightness. If it is not uniform, which can be caused by improper mixing and application, heterogeneity with pervious passages may be formed that yield a scale-dependent high average hydraulic conductivity. This can be avoided by using high bentonite contents, but this causes problems when low compressibility is required and the cost may also be very high. The matter will be discussed in the subsequent chapter dealing with construction of repositories.

Hydraulic conductivity

The hydraulic conductivity of a very dense network of ballast grains can be low, i.e. down to about 10^{-5} m/s, also with no clay in the voids if the size distribution is suitable. With clay in the voids the conductivity can be reduced by as much as a million times. Very effective filling either requires that both the ballast and the clay are very dry and that the clay component is very fine-grained, or that water is added to what is known as the optimum water content. The density of the clay component can hardly become higher than about 1.5 g/cm^3 at saturation, which means that the conductivity of the clay can be as low as 10^{-11} m/s if the percolate is

very poor in electrolytes. However, coagulation that raises the conductivity of such soft bentonite clay by orders of magnitude takes place if the percolate is electrolyte-rich, particularly when Ca is the dominant cation. Bentonite-poor mixtures are therefore very sensitive to changes in groundwater chemistry. Hence, while a bentonite content of around 5 weight percent may theoretically be sufficient for effective sealing the voids of a very dense ballast when percolating the mixture by saline water, 10 % by weight may be a practical minimum for obtaining a net conductivity of less than 10^{-9} m/s, which was required for the bottom and top beds of the Forsmark silo (Chapter 1). We will see later that unless great care is taken in the mixing operation, even this bentonite content may be too low to yield a sufficiently uniform distribution of the clay component and a low bulk conductivity.

If the bentonite content is increased to slightly more than 20 %, the ballast grains will be surrounded and embedded by a clay matrix which significantly reduces the conductivity but also makes the mixture compressible to a practically important extent.

Swelling pressure

The low density of the clay component means that the swelling pressure of bentonite-poor mixtures is low. For mixtures with 10 weight percent Na bentonite saturated with distilled water, it can be as high as a few hundred kilopascals, while percolation by electrolyte-rich water - particularly with Ca as dominant cation - makes it drop to a few tens of kilopascals.

CHARACTERISTIC PHYSICAL DATA OF BENTONITE-BASED MATERIALS

Table 7 gives characteristic data of the hydraulic conductivity (K) and swelling pressure (p_s), as well as of the thermal properties heat conductivity (λ), and heat capacity (C) of bentonite-based materials with common bulk densities at complete saturation (ρ_s).

Table 7 Typical physical data of bentonite-based materials saturated with low-electrolyte (L) and high-electrolyte (H) porewater, L/H

Material	ρ_s , g/cm ³	K, m/s	p_s , kPa	λ , W/m,K	C,Ws/kg,K
Na benton.	1,4	$10^{-11}/10^{-9}$	100/0	0.9	1800
Na benton.	1.8	$10^{-12}/10^{-11}$	800/300	1.1	1700
Na benton.	2.1	$10^{-14}/10^{-14}$	$10^4/10^4$	1.4	1600
Ca benton.	1.4	— / —	— / —	0.9	1800
Ca benton.	1.8	$10^{-11}/10^{-10}$	500/50	1.1	1700
Ca benton.	2.1	$10^{-13}/10^{-13}$	$10^4/10^4$	2.1	1600
10/90 Na-bentonite/ ballast	2.1	$10^{-8}/10^{-7}$	100/20	1.4/2.4	1600
30/70 Na-bentonite/ ballast	2.1	$10^{-10}/10^{-9}$	500/200	1.4/2.2	1600
50/50 Na-bentonite/ ballast	2.1	$10^{-12}/10^{-10}$	2000/1000	1.4/2.0	1600

3-6 The nearfield rock

3-6.1 Transport conditions

The matter of orienting excavations properly for minimizing the disturbance of the nearfield rock has been touched on in Chapter 2 and we will now turn back to this issue for quantifying the change in hydraulic conductivity that may result from the change in aperture by the excavation-induced disturbance. Major factors are the blast-disturbance, with which we will deal

both in this chapter and later in the construction chapter, and the stress-induced disturbance, which depends on the rock stress situation and on the shape of the cross section of the excavation. The disturbance is naturally different for bored and blasted excavations. We will consider this issue in detail because of its significance for groundwater flow in repositories [11].

BLAST-DISTURBANCE

Processes

Blasting affects the rock in a number of ways:

- * Creation of radial fractures along the larger part of the “contour” holes at the periphery
- * Expansion and propagation of natural discontinuities
- * Crushing of the rock within a few millimeters distance from the holes
- * Intense fracturing to one or a few decimeters from the tip of the holes

The gas pressure can be several hundred MPa and cause tension fractures that extend from preexisting weaknesses in the rock, like 5th and 6th order discontinuities intersected by the blast-holes. If natural fractures are blocked by gouge, gas will not penetrate effectively but otherwise it will enter deeply, and make them propagate and undergo expansion that will be partly permanent. Assuming an instantly produced gas pressure of 500 MPa and a bulk compression modulus of the rock of 10^5 MPa, the estimated width of a blast-induced fracture is on the order of 20–200 μm . If 50 % of this width remains after dissipation of the gas pressure, debris preventing the fractures from closing, the net axial hydraulic conductivity of a blast-disturbed zone of a few decimeters depth is in the interval 10^{-9} to 10^{-6} m/s at an average spacing of the blast-holes of 0.5 m.

Modelling

Applying the experience from recent investigations that normal blasting generates one major, radially oriented fracture and a few shorter radial fractures along the larger part of the blast-holes, superposition of this fracture pattern on the basic rock structure with 4th, 5th and 6th order discontinuities yields the structural pattern in Figure 75 [12]. A number of the natural

“latent” discontinuities become activated by the stress waves and penetrating gas, which reduces the average cohesion and friction angle of the rock within a few decimeters to somewhat more than 1 m from the periphery. For common primary stress conditions at depth one can imagine such activation to be of the kind shown in Figure 76.

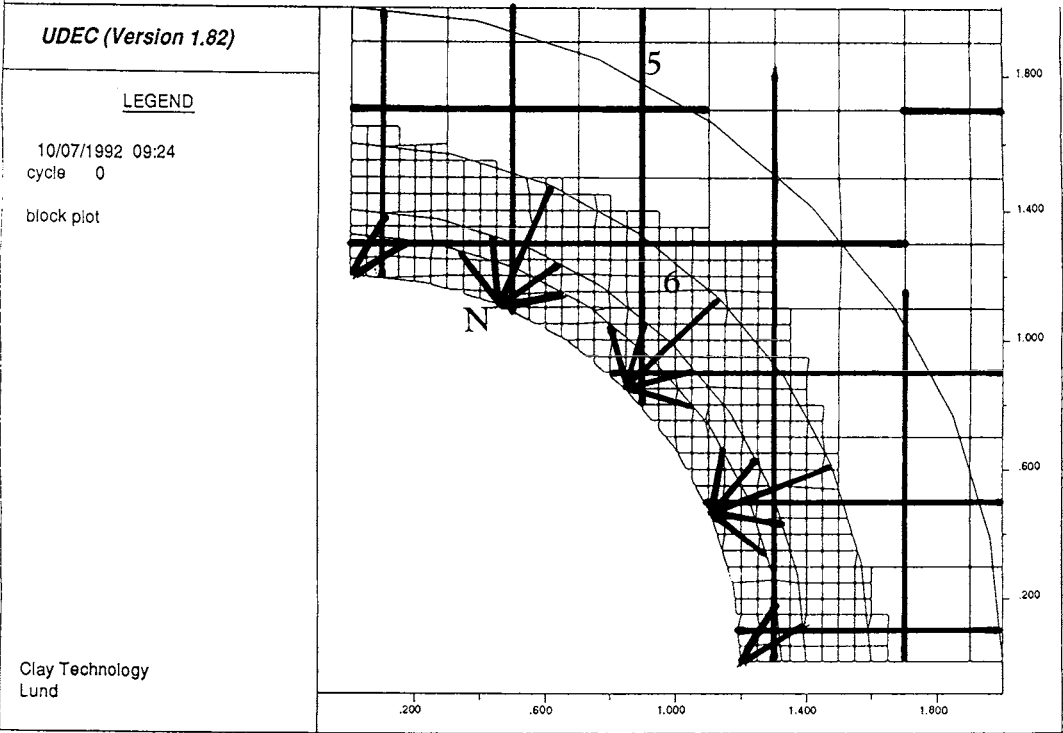


Figure 75 Model of blast-induced disturbance of the nearfield rock of a tunnel. N are new fractures, 5 and 6 represent discontinuities of respective orders

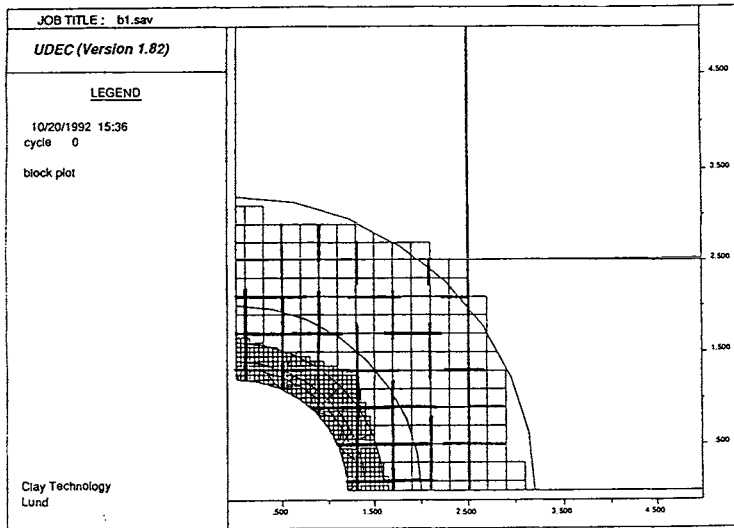


Figure 76 Blast-induced activation of 5th order discontinuities (dark lines in the coarse grid of unactivated ones) and of 6th order breaks (fine-hatched area)

The formation of new fractures and activation of latent breaks cause a reduction in strength that is illustrated by the theoretical example in Figure 77, and it also yields an increased porosity and thereby also a significant increase in hydraulic conductivity of the nearfield rock. The drop in strength is associated with a reduced modulus of deformation and, in turn, with a substantial stress reduction at the periphery and with stress concentration at some distance from it. This matter, which is illustrated in Figure 77, affects the stability of the rock as will be discussed below.

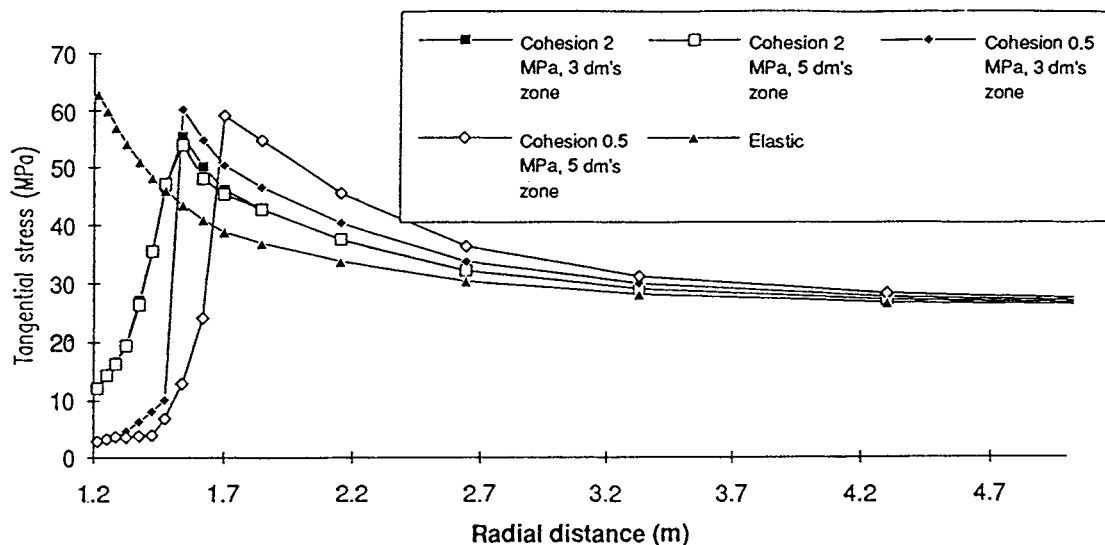


Figure 77 Example of change in stress conditions around a blasted tunnel. Drop in tangential (hoop) stress as a function of reduced cohesion, which is assumed to be 10 MPa in the undisturbed rock (“elastic”)

MECHANICAL DISTURBANCE BY DRILLING

Core drilling produces practically no mechanical disturbance while full-face or tunnel-boring (TBM) causes damage that is concluded to yield some increase in hydraulic conductivity close to the periphery. Inspection of granite cores taken perpendicularly to the walls of TBM-drilled tunnels has indicated that microscopic fissures are formed and that natural 6th and 7th order discontinuities become widened and propagate to an extent that indicates an average bulk conductivity of one to three orders of magnitude higher than that of the virgin rock matrix within 10-30 mm from the openings. Somewhat less disturbance is concluded to take place within the next 50-100 mm radial distance from the periphery, and a rough estimate is that the average conductivity of the most shallow 100 mm can be taken to be one order of magnitude higher than that of the virgin rock matrix for short, straight canister-deposition holes drilled by use of full-face techniques. For curved, long holes, like those intended for the Swedish VLH concept, disturbance is expected to extend to about 0.3 m from the periphery. The reason for the different degrees of damaging will be considered in the chapter on construction techniques.

STRESS DISTURBANCE

Stress changes induced by excavation cause shearing of natural discontinuities - termed joints by most investigators using rock mechanical codes - and altered aperture of certain critically oriented discontinuities, which may enhance the hydraulic conductivity along tunnels and holes. The change in conductivity depends very much on their orientation with respect to the direction of major fracture sets and several investigations have been made for quantification. One of them was conducted in conjunction with a performance analysis of candidate HLW concepts in Sweden and it will be used here to illustrate the use of numerical codes for stress/strain analyses and the different impact on stress-induced aperture changes of different repository concepts [13].

CONSIDERED CASES

We will consider a tunnel of KBS3 type, a canister deposition hole of KBS3-type, and a combination of them. The size and cross section shape of the tunnels and the structural features of the rock refer to a full scale field test in the Stripa mine to which we will return later. The tunnel height is about 4.5 m and the width 5 m, while the diameter and depth of the hole is 0.8 m and 3m, respectively. Since rock mechanics is basis to the calculation and prediction of excavation-induced disturbance we will go through the procedure in numerical calculation in some detail for making the reader familiar with the procedure and parameters. The interested reader is referred to rock mechanical textbooks for further information [1].

Joint pattern

Fracture mapping showed that the rock was characterized by four major fracture sets of 4th order, of which three were approximated to strike parallel to the tunnel, as shown in Figures 78 and 79. They will be termed joints with properties defined as [14]:

- JKN, Joint normal stiffness, which describes the stress/strain behavior normal to the plane
- JTEN, Joint tensile strength, i.e. the ability to take tensile stresses normal to the plane

- JKS, Joint shear stiffness, which describes the stress/strain behaviour on shearing
- JFRIC, Joint friction coefficient, which describes the friction resistance on shearing
- JDIL, Joint dilation angle, which describes the widening on shearing
- JCOH, Joint cohesion, which describes the shear strength at zero normal stress

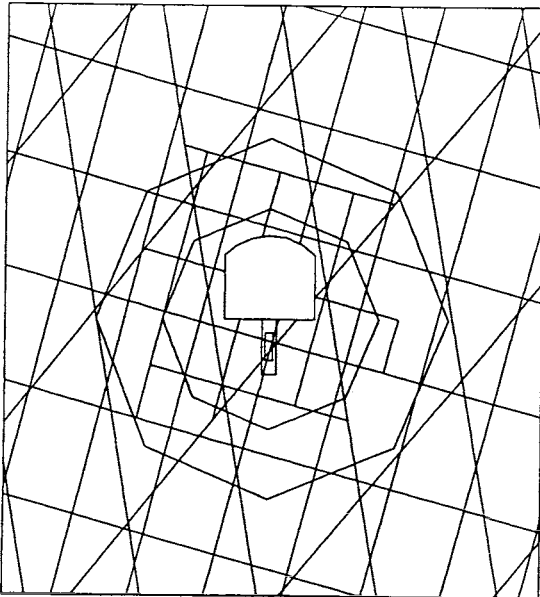


Figure 78 Joint geometry of tunnel cross section. The octahedrons are auxiliary elements with no influence on the stress/strain behavior of the system. The interaction of the tunnel and the three 4th order fracture sets yields 8 fractures extending from the periphery. Four of them are steep and two flatlying

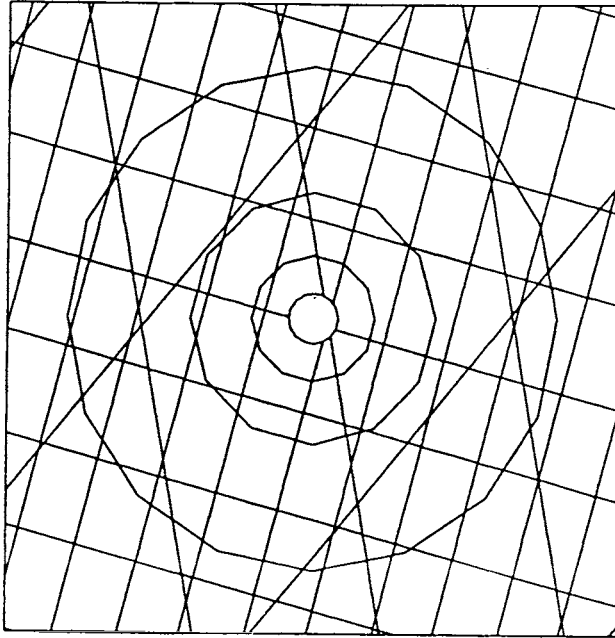


Figure 79 Joint geometry of deposition hole (horizontal section). The interaction of the hole and the three 4th order fracture sets yields 6 steep fractures extending from the periphery of the 0.8 m diameter hole

Two of the most important mechanical properties of the joints are illustrated by the diagram in Figure 80. The shear stress/strain diagram demonstrates the influence of the normal stress on the maximum shear stress and the fact that a peak value is reached at a few cm strain and stays almost constant at further deformation. The dilatancy diagram shows that even a very high normal stress cannot prevent expansion and that it is not at maximum even at 20 mm shear strain.

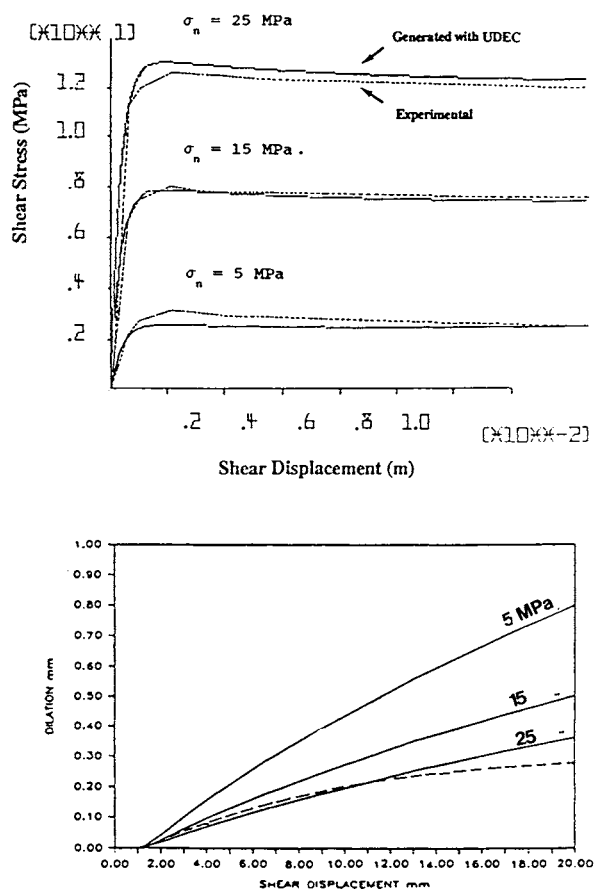


Figure 80 Stress/strain behavior of joints. Upper: Shear stress versus shear displacement. Lower: Dilation versus shear displacement

Calculations - 2D

The procedure requires use of computers and access to a number of rock data as described in textbooks on rock mechanics and engineering geology [1].

The primary stress condition needs to be known and for the present case the horizontal stress was measured and found to be 15 MPa, while the vertical was 6 MPa. Common values were adopted for the bulk compression modulus and the shear modulus, i.e. 39 and 17 GPa, respec-

tively [14]. The excavation of the tunnel was simulated by applying the 2D code UDEC for calculating rock block movements in vector form and shear displacements along the joints, as well as changes in aperture. Typical results are shown in Figures 81 and 82 from which one concludes that practically all displacements take place within a distance of about 2/3 of the diameter of the tunnel. The maximum displacement takes place in the right wall where a rock block moves into the tunnel by about 4.7 mm. A block in the floor moves upwards and both these movements are associated with about 3 mm shear displacement along the same fracture, one downwards and the other upwards.

Figure 82 demonstrates the most important effect on water and ion transport conditions in the nearfield rock, namely the expansion of flatlying fractures in the floor and roof and of two steep fractures in the right wall. The largest widening is about 1.5 mm of the assumed original 0.01 mm aperture, which naturally results in a dramatic increase in axial conductivity. Applying the cube law (Eq.2), to which reference was made in the analytical derivation of such increase in Chapter 2, one can calculate the axial conductivity K of the nearfield of the tunnel case that we are presently considering.

$$K = \frac{d^3 g \rho_w}{12 e \eta} \quad (2)$$

where:

d =aperture of fracture, ρ_w =density of water, e =spacing of parallel fracture, and η viscosity of water (10^{-3} Ns/m² at 18°C).

The result of such calculations is given in generalized form for five zones in Figure 83, from which it is obvious that the strongest increase is expected where the largest aperture increase takes place, i.e. close to right wall and in the floor. Here, the average conductivity is increased by about 200 to 2500 times, while the increase is practically none at larger distance than 2/3 of the diameter. The fundamental importance of the rock structure is obvious from this example but it must be kept in mind that it refers to a very conservative and unsuitable case, i.e. the one with the tunnel oriented parallel to major fracture sets.

A matter of interest in this context is naturally if the excavation-induced stress changes activates discontinuities of higher orders and thereby further increases the conductivity. We will look into this later in this chapter.

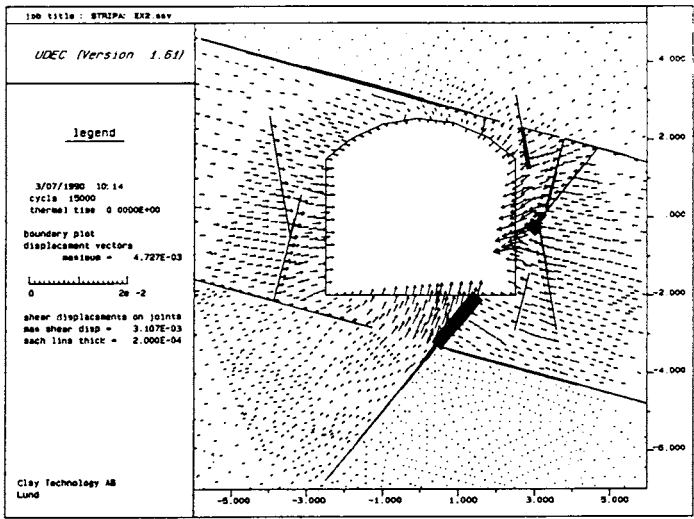


Figure 81 Rock displacement vectors (arrows) and shear displacements (black lines, scale indicated in the legend)

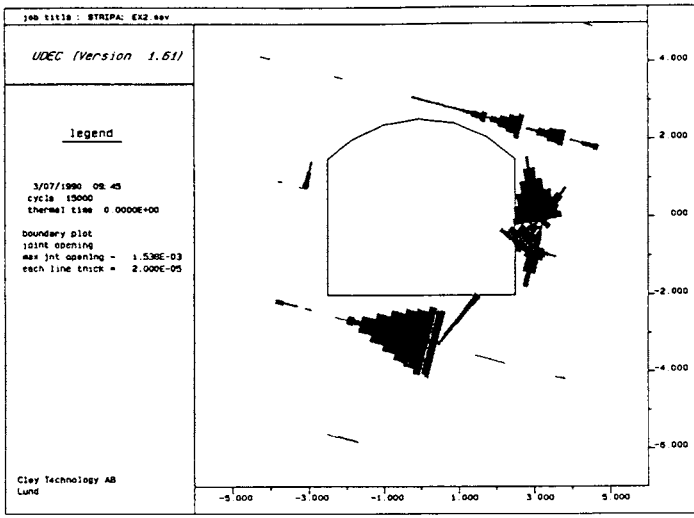


Figure 82 Joint widening or separation due to excavation. Maximum increase in aperture is about 1.5 mm

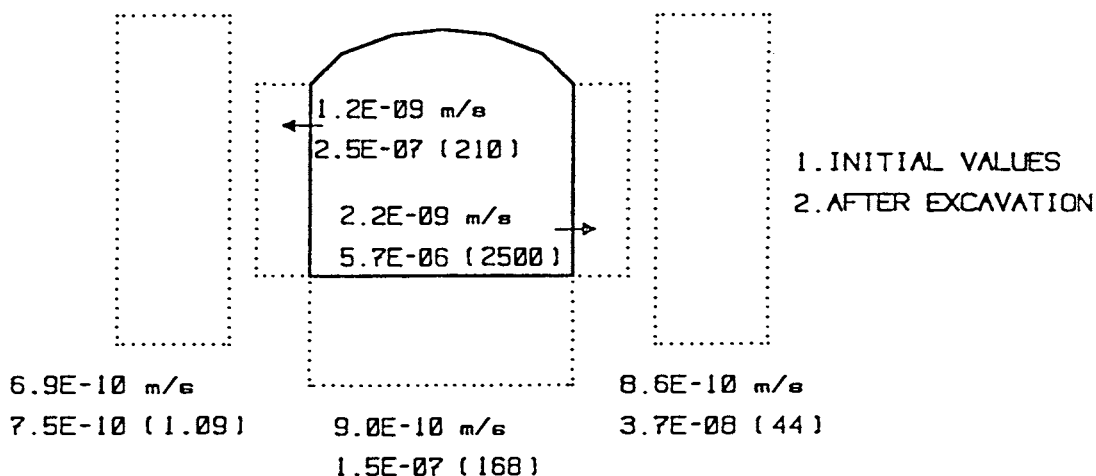


Figure 83 Axial conductivity in tunnel direction of five regions (dotted) around the tunnel. The initial conductivity of each zone, controlled by the natural fracture systems, is represented by the upper figure, while the lower shows the conductivity after excavation. Bracketed values show the ratio

As to the deposition holes, the same procedure of calculation using the primary rock stresses $\sigma_x=20$ MPa and $\sigma_y=10$ MPa which are slightly different from the ones used for the tunnel analyses because of the influence of the nearness of the tunnel, yielded the strain patterns in Figures 84 and 85. They show that the maximum inward movement is about 0.25 mm while the maximum shear displacement along fracture planes is about 0.15 mm and the maximum fracture expansion somewhat less than 1 μm . This demonstrates that the nearfield of the hole undergoes insignificant change in hydraulic conductivity, which is primarily explained by its small size. The maximum tangential (hoop) stress is increased to about 60 MPa but this is much less than the compressive strength of unweathered granite and causes no stability problems. We will see later that this may be a problem for some repository concepts.

Combining the tunnel and borehole cases in a 2D model, which greatly exaggerates some displacements for large spacings of the holes but is relatively correct for small spacings, one arrives at the diagrams in Figures 86 and 87. Quite logically the presence of the holes causes less stress concentration in both the right wall and the floor, but induces expansion of fractures in the left wall because the rock below the tunnel becomes free to move.

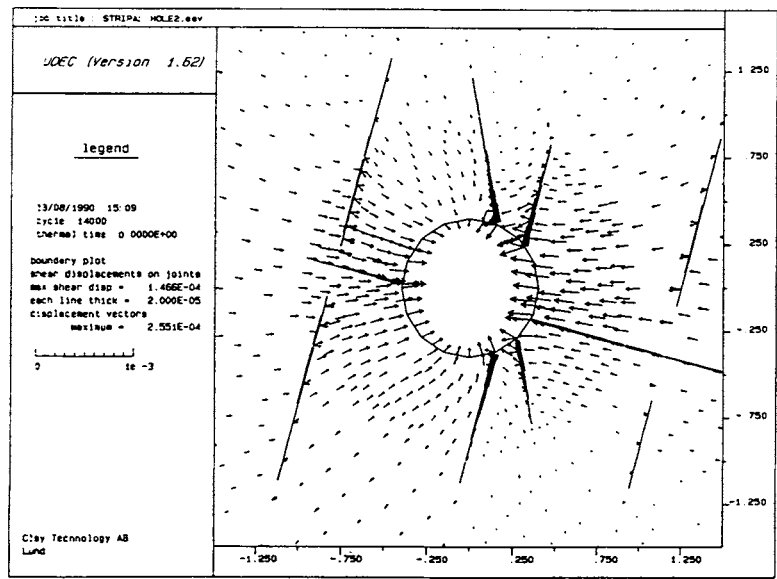


Figure 84 Rock displacements and joint shear displacements induced by drilling the hole

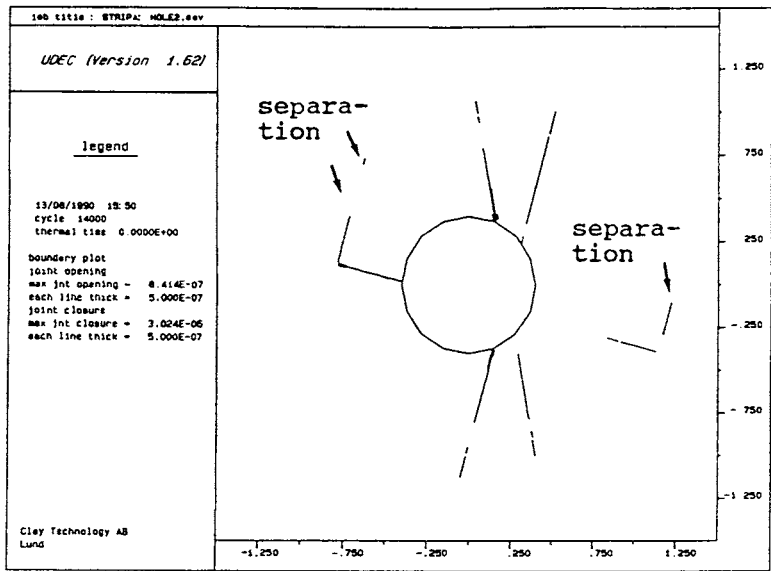


Figure 85 Closure and expansion of joints induced by drilling the hole

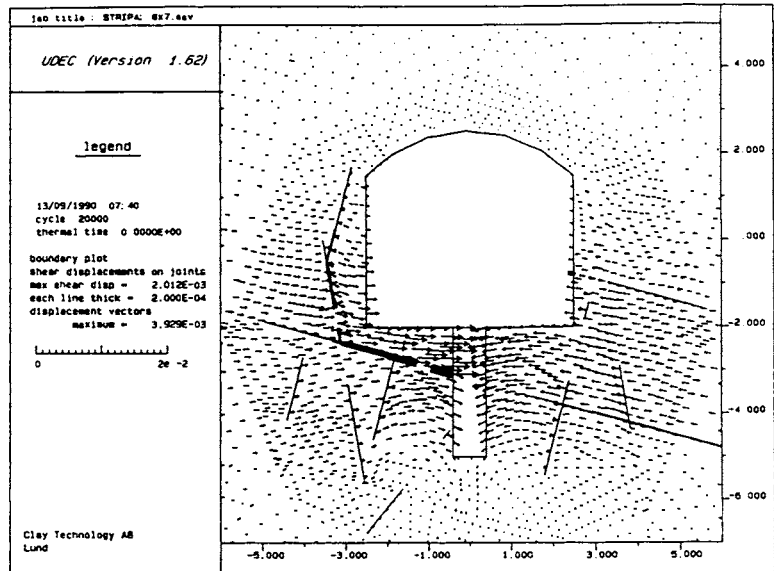


Figure 86 Rock movements and joint shear displacements by introducing tightly spaced holes, i.e. a wide slot, in the tunnel floor

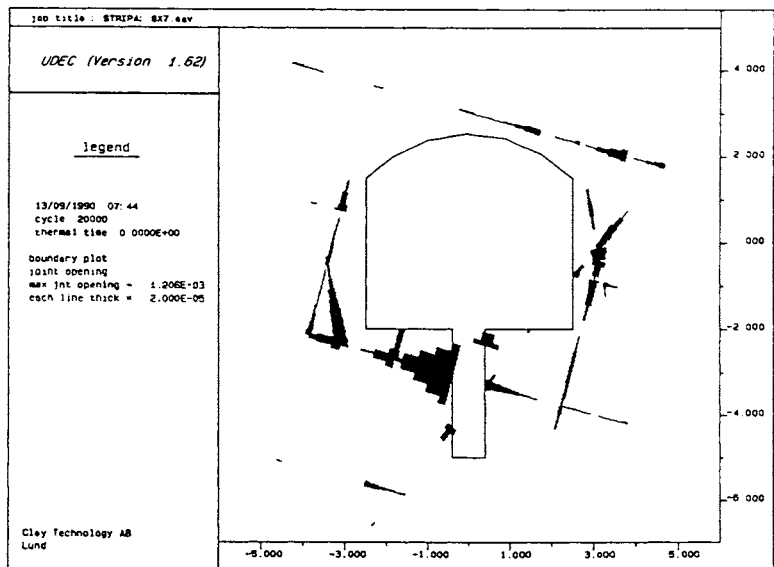


Figure 87 Closure and expansion of joints in the combined case

A most important thing is of course the influence of thermal loads caused by the radioactive decay and this can be investigated by use of the same code using relevant thermal data of the rock and a correct decay rate. The heating rate, which is controlled by the power and the heat conductivity, determines the temperature gradient which affects the rock structure, primarily through uneven expansion of the blocks from the hole periphery and outwards in the transient heat evolution. Experience from field tests shows that while the temperature distribution can be well predicted, the heat-induced strain cannot and the reason for this is that the heat-induced strain is concentrated to the joints as exemplified by the diagrams in Figures 88 and 89. They represent the conditions after a few thousand years in a KBS3 repository where the maximum temperature does not exceed about 70°C and show that certain major fractures have become somewhat closed while others have expanded. The heave of the floor is up to about 3 mm. The most important thing is of course what the net change will be after cooling and an extension of the study to cover a complete heating/cooling cycle has shown that the permanent strain is rather insignificant. However, creep effects are expected to cause significantly larger strain, which will be considered in conjunction with the discussion of rock stability. An effect that has not been recognized or assessed is self-healing of fractures under the hydrothermal conditions that prevail in HLW repositories.

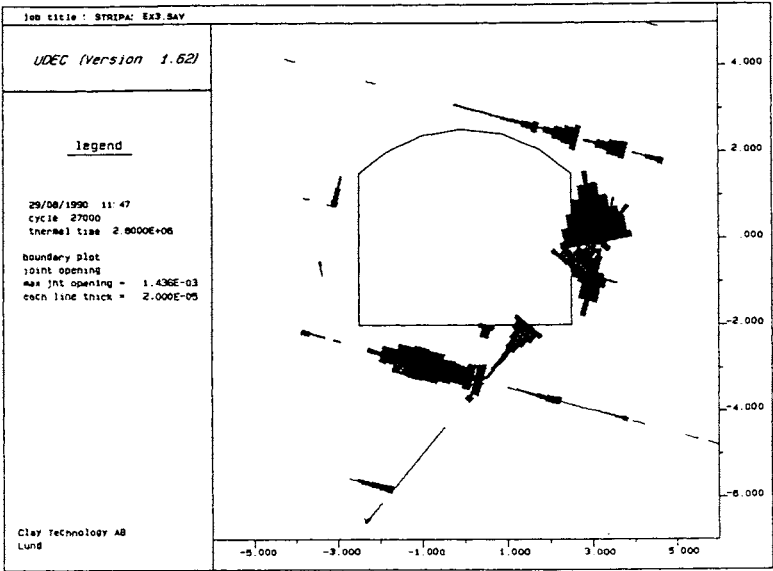


Figure 88 Change in joint aperture by excavation and heating of KBS3-type tunnel

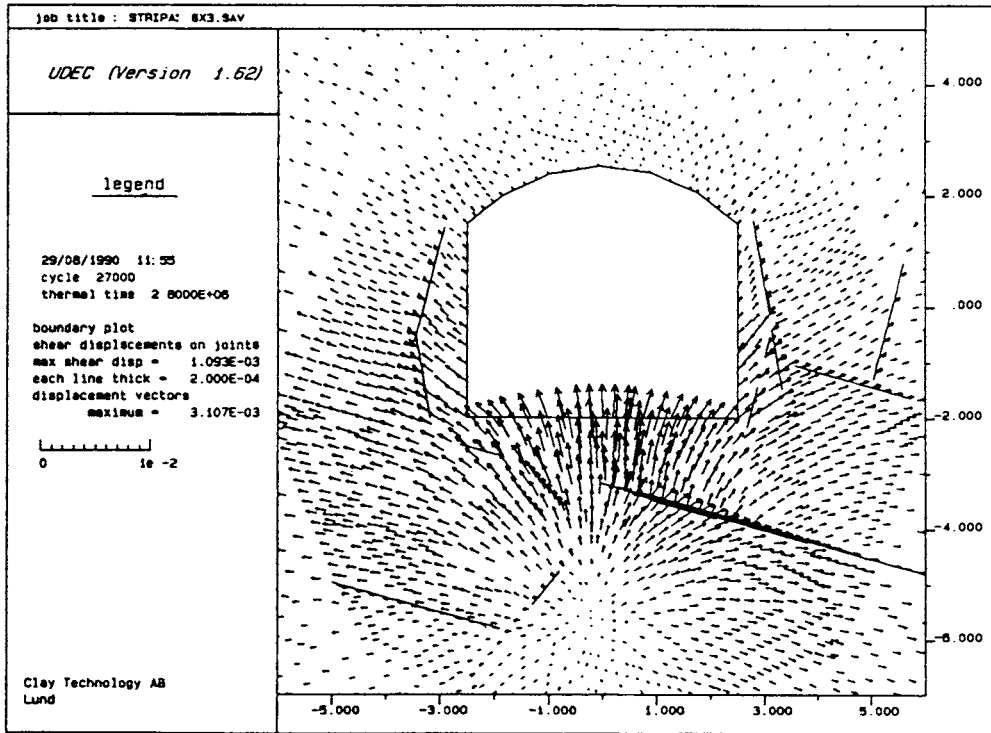


Figure 89 Rock block movements and joint shear displacements induced by heat generation of radioactive waste in deposition holes of KBS3-type in the floor

Calculations - 3D

Having now some feeling of the influence on the excavation-induced stress changes on the joint pattern of the tunnel case in the 2D study, we will return to the matter of proper location of tunnels and holes with respect to the local rock structure that was touched on in Chapter 2. Figure 90 gives a hint of what the effect on the axial conductivity will be of reorientation of the tunnel such that its axis deviates from the strike of major discontinuities. It is estimated from application of such simple geometrical patterns that deviation by 15° should be sufficient for significant reduction of the stress-induced expansion of natural fractures. Such deviation would also minimize activation and growth of latent 5th and embryonic 6th order

discontinuities as we will see later. Quantification of the influence on the axial conductivity by such deviation can be offered by 3D numerical calculations although there are difficulties in selecting relevant rock parameters. There is certainly need for special codes like 3DEC for determination of the influence of three-dimensional features and we will consider an example here that is directly related to the tunnel case just described [15].

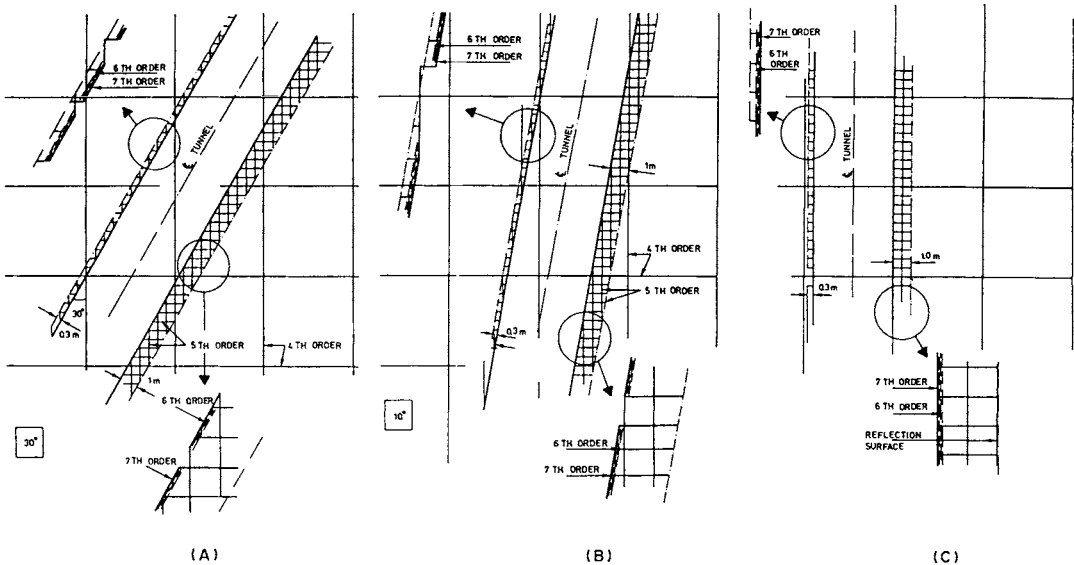


Figure 90 Schematic example of the effect on the nearfield of redirecting a tunnel A) basic system of continuous 4th order fractures of large spacing and activated 5th and 6th order breaks in 0.3 or 1.0 m deep disturbed zone at the periphery of tunnel turned 30° from the strike of one major set of breaks; B) tunnel turned through 10°; and C) tunnel oriented parallel to the strike of one major set of fractures

The effect of turning a tunnel away from the direction of major fracture sets is exemplified by comparison of the two upper cases in Figure 91, where all fractures are parallel to the the tunnel in the upper 2D case, which has already been treated in this chapter, and where one set is turned by 15 or 30° in the central 3D case. The calculation of the 3D case was based on the same assumptions with respect to primary rock stresses and properties as those made in the 2D case. The lowest diagram represents an intermediate case and a way of simulating 3D cases using 2D codes and restricting the extension of some of fracture sets.

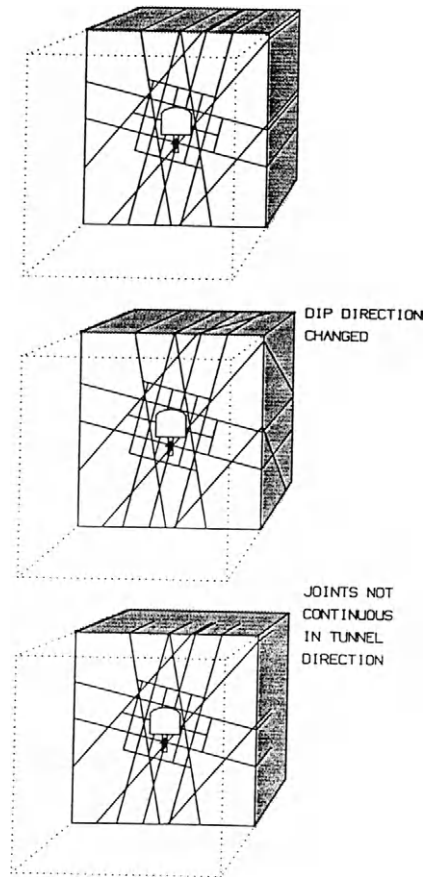


Figure 91 Image of the 2D and 3D versions. The discontinuities - of 4th order - that dip to the left and have the smallest dip angle in the upper model are turned in the central model. The case with restricted fracture length is the lowest one

The results are summarized in Figure 92, showing the maximum expansion of fractures by turning one of the most critical fracture sets away from the direction of the tunnel axis and, in Figure 93, the maximum block movements towards the tunnel. Both diagrams demonstrate the important effect of reorienting the tunnel. Thus, the excavation-induced increase in aperture of fractures in the right wall that was 1.4 mm in the 2D case drops to around 0.5 mm by turning the fracture set by 15°, and to slightly less than 0.4 mm by turning it by 30°. Similar reduction takes place also in the floor region.

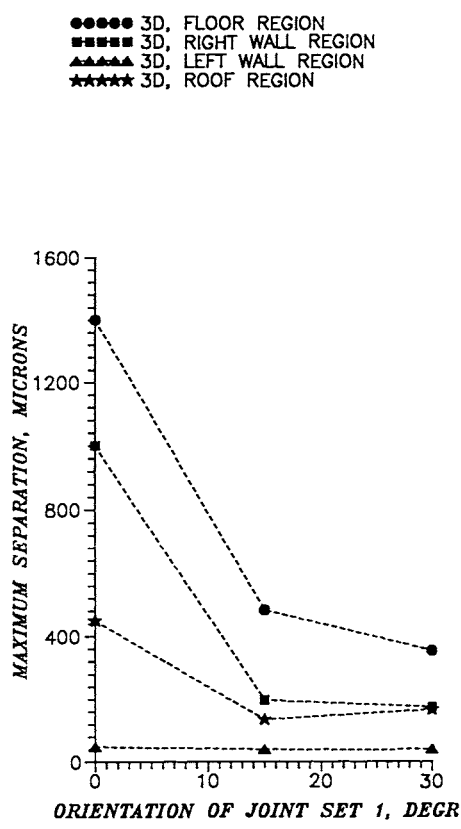


Figure 92 Maximum aperture of joints in the 2D case (0°), and when turning one set (1) by 15 and 30°, respectively

The diagram in Figure 93 shows that the block movements towards the tunnel drop most strongly in the floor region and relatively little in the other regions, including the right wall.

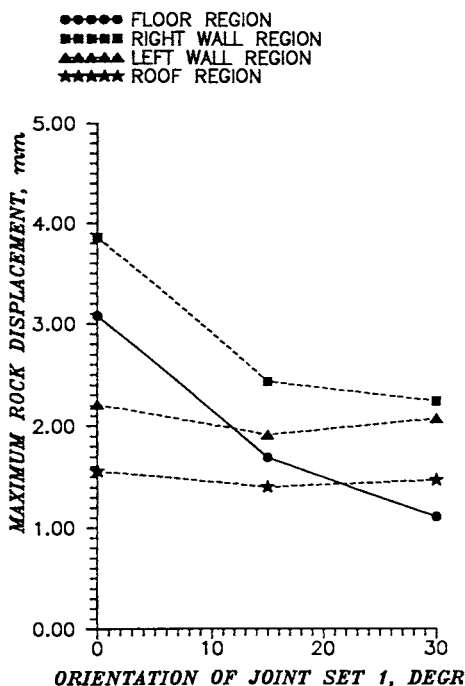


Figure 93 Maximum rock displacement of the tunnel periphery in the 2D case (0°), and when turning one set by 15 and 30°, respectively

EXPERIMENTAL EVIDENCE

Naturally, decisions concerning repository design cannot be taken solely on the basis of numerical calculations and a first requirement is of course to validate the models for which several large-scale projects have been performed. The most comprehensive one is the Stripa Project, which gave several examples of the applicability of a number of models referred to in the preceding text. Two tests, corresponding to the tunnel and hole cases used for numerical

calculation will be referred to, and a few additional examples of the disturbance of the near-field rock around tunnels will also be presented.

The Stripa BMT test area

Figure 94 shows a plan view of the Stripa mine, where a number of geophysical and geochemical as well as hydraulic and rock mechanical experiments were conducted during a 15 year long period, and where also several sealing tests of fundamental importance were carried out.

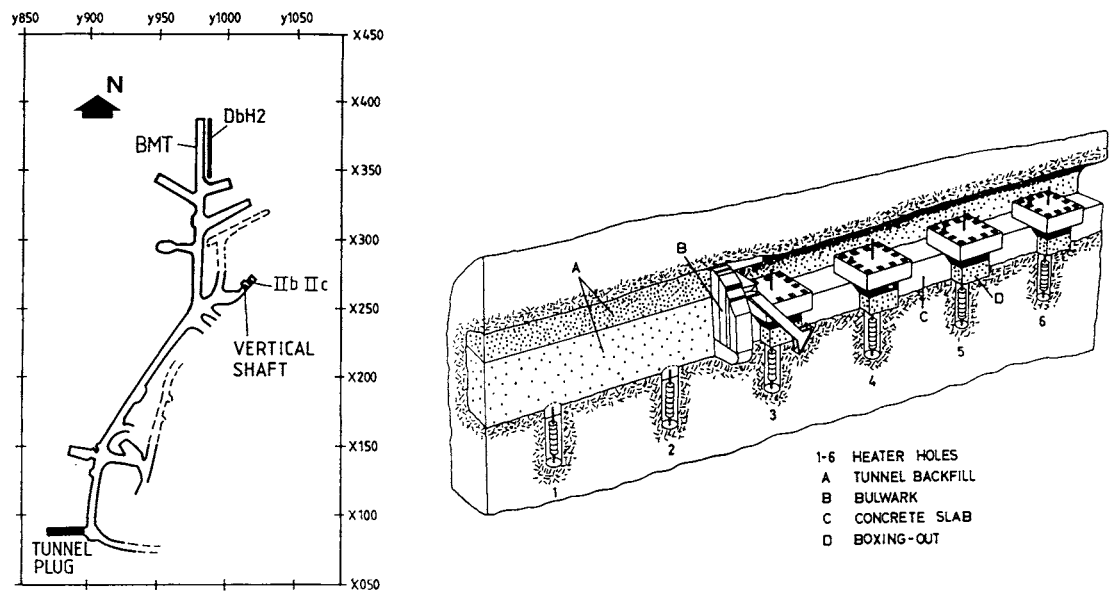


Figure 94 The Stripa mine. Left: experimental area at 330-400 m depth. Right: The BMT drift with 6 holes with heaters embedded in bentonite for simulating HLW canisters in KBS3 repository

The mine, which is located in a granite intrusive in leptite, was abandoned in 1976 after 500 years exploitation of iron ore, and the granitic used for a number of large-scale experiments. The rock mass is characterized by typical 2nd and 3rd order discontinuities as illustrated in Chapter 2, and by rather regular sets of 4th order breaks as described in conjunction with the presentation of the numerical calculations in this chapter. The actual orientation of the so-called BMT (Buffer Mass Test) drift, which is equivalent to the tunnel considered in these calculations, was such that the major fracture sets formed about 30° angle with the axis of the drift, i.e. resembling the case depicted in Figure 90 A, but the fracture pattern was somewhat more complex as demonstrated by Figures 78 and 79. Generalizing the major water-bearing fractures - most of them of 4th order type - to appear as thin ellipsoids, the rock structure can be visualized as in Figure 95. The BMT drift and most other rooms in the Stripa mine were excavated by applying careful blasting, a matter that will be further considered in the chapter dealing with construction of repositories, i.e. Chapter 4.

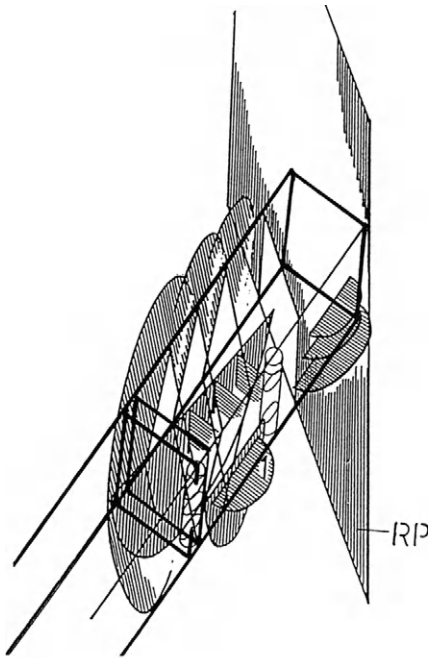


Figure 95 Major water-bearing fractures of 4th order identified in the BMT drift at Stripa

Careful scanning of the profile of blasted rooms for determination of the orientation of long-extending discontinuities gives a good picture of the presence of long-extending, discrete fractures of 4th order, but the excavation-induced activation of latent 5th and 6th order discontinuities and the creation of new blast-generated fractures obscure the 4th order patterns. Figure 96 shows a typical scanning profile from which the basic pattern of 4th order discontinuities can be discerned.

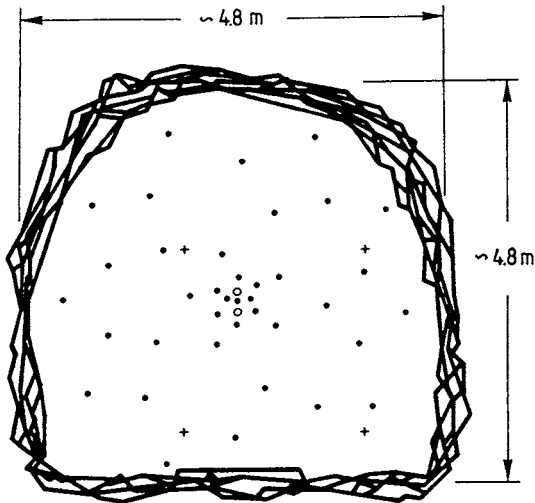


Figure 96 Superimposed scanned profiles of the BMT drift with the blast-holes marked except for the contour holes

The BMT experiment of interest in the present context is one in which the axial hydraulic conductivity of the nearfield rock was determined [15]. The principle was simply to cut slots by radial drilling of closely spaced boreholes at the inner and outer ends of the drift and to conduct flow tests by pressurizing the inner slot and recording the flow from it. Each borehole gallery consisted of 76 radial holes with 6.25 m length and 50 mm diameter percussion-drilled with 0.2 m spacing from the bottom of a 0.75 m deep continuous slot extending from the periphery. Figure 97 shows a longitudinal section of the drift.

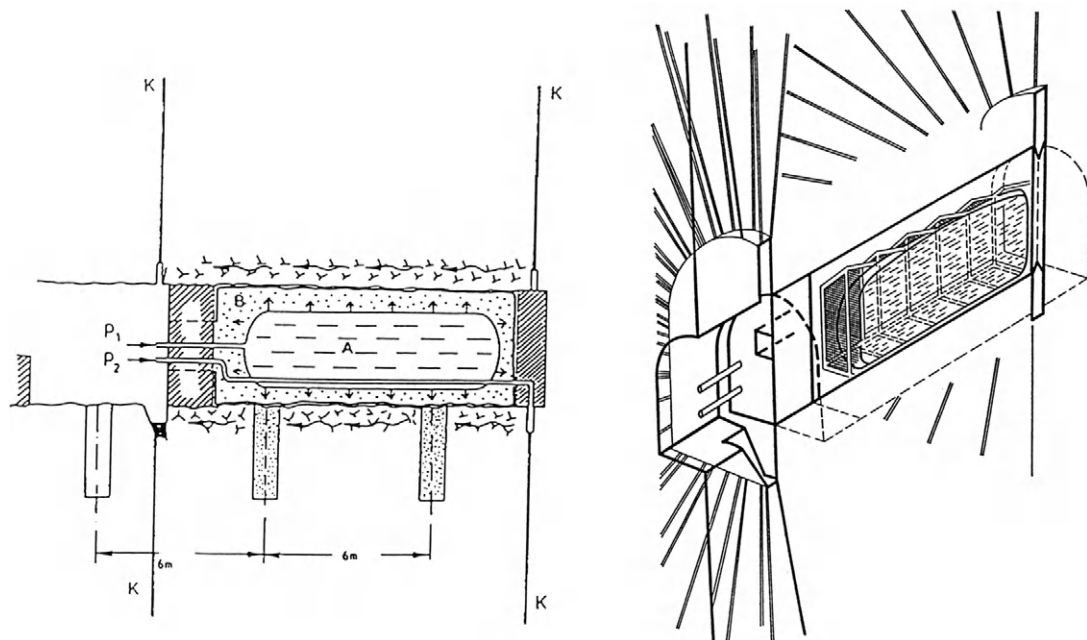


Figure 97 Test set-up for determination of the hydraulic conductivity of the nearfield rock. A large rubber bladder (A) pressurized the bentonite slurry (B) for preventing water from flowing into and through the drift [15]

The major problem in preparing relevant test sites for this kind of experiment is to prevent water from flowing from the pressurized slot into the excavation, for which one can use rubber bladders expanded to form a tight contact with the rock. This works in bored tunnels if special steps are taken to prevent flow along the bladder/rock contact but it is not suitable for the irregular topography of blasted rooms since rubber bladders cannot sustain the locally very large strain. A further problem is that cables and tubings from gauges like piezometric cells located in the rock and extending into the room, may cause bladder failure and flow

short-circuits. Hence, a preferable arrangement, that was used in the Stripa test, is to apply bentonite slurry in the room in order to give space for the instrumentation and to prevent flow along the rock surface. This requires that the slurry is pressurized somewhat more than the water in the inner slot, which was a principle applied in the Stripa test series. The 220 m³ large room contained 100 m³ slurry. For identifying possible differences in flow in the roof, floor and walls, the slots were divided into 4 separate zones for which the in- and outflows were recorded individually. All the zones were equally pressurized.

The experiment had the form of stepwise pressurizing the inner slot and recording the inflow or outflow from the inner and outer zones, while recording also the water pressure exerted on gauges located at different distances from the inner slot and at different distance from the periphery. Proper evaluation of tests of this sort requires that the initial piezometric conditions are known and considered in the course of the experiment. Theoretical considerations show that the time to reach equilibrium after each pressure change should be a few days for the estimated relatively high porosity of blast-disturbed rock and this was confirmed by recording the flow as exemplified by Figure 98. The proof of the validity of the assumed flow process taking place in the narrow, disturbed zone is the recorded pressure gradient along the drift (Figure 99).

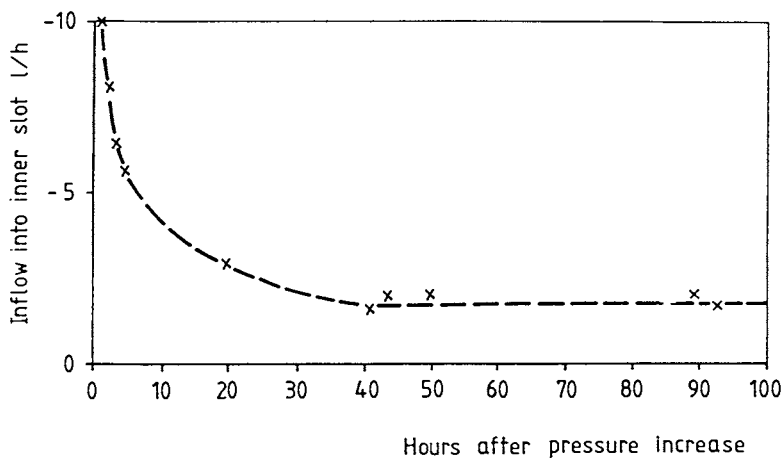


Figure 98 Recorded outflow (negative inflow) from the inner slot after pressurizing it with 700 kPa

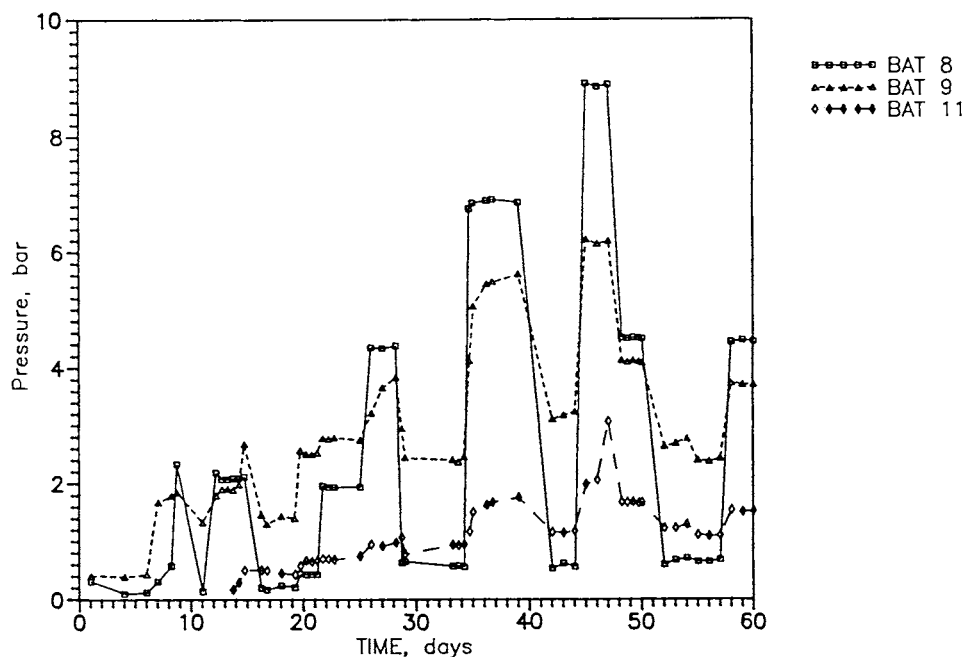


Figure 99 Example of recorded water pressure along the test drift. The squares represent gauges located close to the inner, pressurized end of the drift; the rhombs show the pressure at the outer end, and the triangles the pressure in between

Quantification of the hydraulic conductivity of the rock requires application of flow models for simulating the water transport and there are various possibilities to do so. Naturally, a “porous medium” finite element model would be preferable since it offers a simple, straightforward way of determining the flow vectors and the flux, as well as the piezometric pattern. However, it is required to be compatible also with the true system of water-bearing structural features, which presents difficulties at a first sight. Thus, the small number of channels, estimated to be one per 25-100 m² in undisturbed rock, would suggest very heterogeneous flow

and water transfer along a few channels that is more in line with discrete fracture modelling. However, in the nearfield rock of blasted tunnels, i.e. within about 2/3 of the diameter, the amount of activated latent 5th and 6th order discontinuities is large enough to represent a porous medium. In order to account also for the surrounding undisturbed rock, which is also involved in the flow process, a relevant flow model would be a combination of a porous medium, representing the nearfield, and a surrounding system of discrete flow passages. It turns out, however, that simplifying the entire system to consist of zones with average hydraulic conductivities gives sufficiently accurate flux data to be applied in practice.

The applied finite element model had the form shown in Figure 100. Preceding large-scale field tests had indicated that the bulk hydraulic conductivity of the virgin rock at Stripa is in the interval 10^{-11} to 10^{-10} m/s, which formed a starting point of the modelling. Thus, defining two zones of disturbance - a blast-disturbed zone extending 0.75 m from the periphery, and a

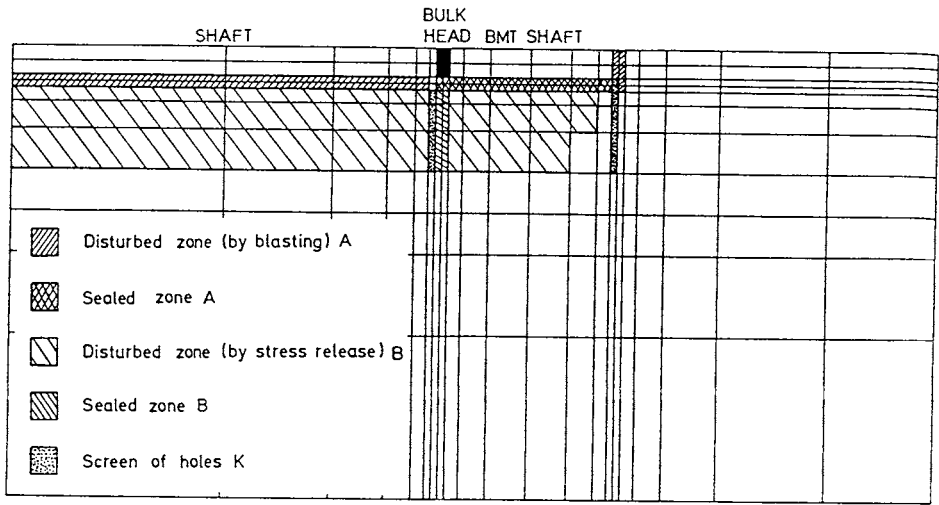


Figure 100 Axisymmetric mesh of elements with different hydraulic properties. The upper boundary represents the axis of symmetry

stress-disturbed zone extending 6.25 m from the outer boundary of the blast-induced zone - the flow recording gave the following conductivity data:

- Blast-disturbed zone with isotropic conductivity: $K=1.2 \times 10^{-8}$ m/s
- Stress-disturbed zone with axial conductivity $K_a=10^{-9}$ m/s axially and $K_r=10^{-11}$ m/s radially
- The virgin rock has an isotropic conductivity of 3×10^{-11} m/s except for the inner half of the drift where a 3rd-order zone gives an average conductivity of 10^{-10} m/s.

The hydraulic conductivity of the nearfield of the blasted BMT drift is further illustrated by a subsequent series of tests of the rock around two 0.76 m diameter core- drilled boreholes extending from the floor of the BMT drift to about 3 m depth. The hydraulic properties were evaluated from flow tests with section-wise pressurizing the hole by use of the “megapacker” equipment illustrated in Figure 101 [16]. This equipment had been developed also for grouting of large-diameter holes, a technique that will be described later . The conductivity was found to vary from very high values near the floor to that of virgin rock, i.e. on the order of 10^{-11} to 10^{-10} at 3 m depth as indicated by Figure 102. The fact that the average conductivity exceeded 10^{-7} down to about 1 m depth from the floor demonstrates that the blast-disturbance was much stronger in the floor than in the walls and roof since the average conductivity evaluated from the BMT drift flow test was only slightly higher than 10^{-8} m/s.

The mapping of water-bearing fractures in the holes in Figure 103, which does not show the actual large number of fine, hydraulically active fractures down to about 1 meter from the floor, demonstrates that below this level only a couple of fractures are responsible for the large majority of the inflow. While they represent 4th order discontinuities and some activated 5th order breaks, those higher up are mechanically activated 5th and 6th order discontinuities.

A common and important question is whether blasting causes local disturbance only or if continuous conductive zones are created. We will return to this matter in the chapter on construction of repositories but the hydraulic data just described show that one must expect that a continuous zone with an average conductivity of 10^{-8} to 10^{-7} m/s is formed in the central part of the floor, and that the conductivity may locally be as high as 10^{-6} m/s.

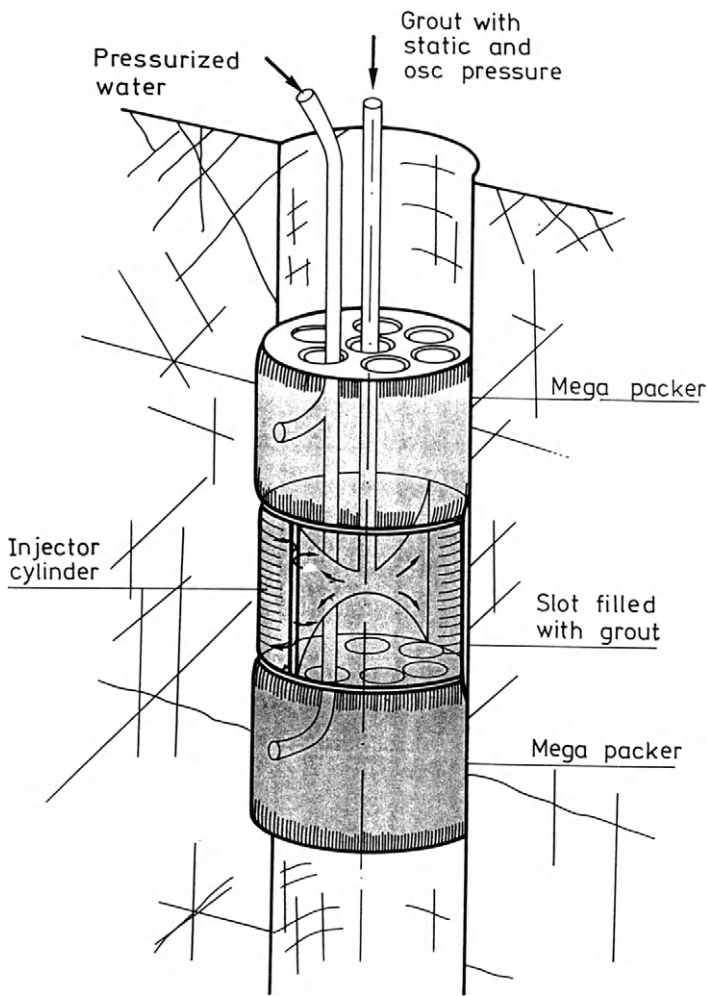


Figure 101 Megapacker for section-wise determination of the conductivity and for grouting of the rock around drilled holes and tunnels [17]

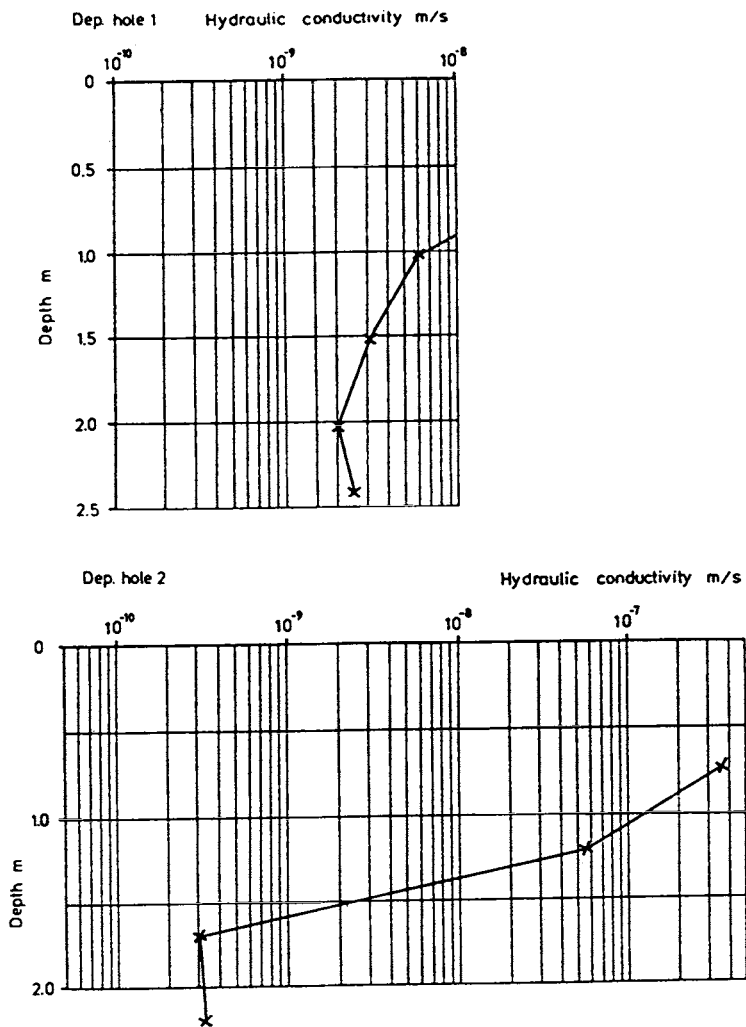


Figure 102 Evaluated hydraulic conductivity from the megapacker testing of the two holes [17]

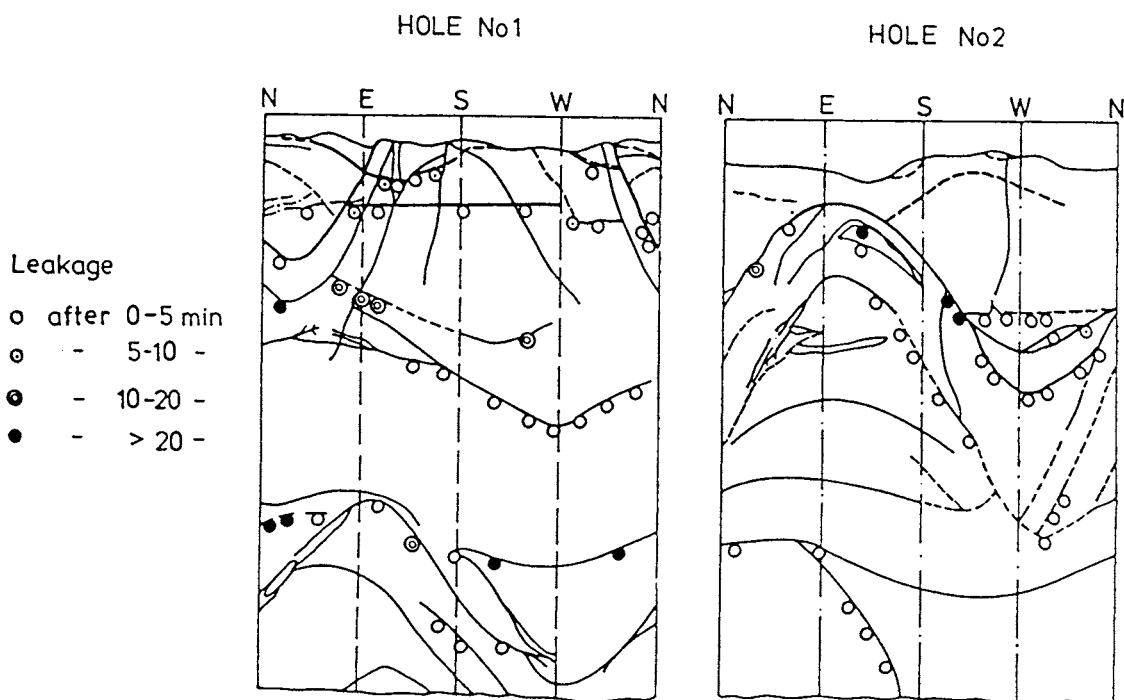


Figure 103 Mapping of water-bearing fractures in the two 3 m deep holes [17]. The rings indicate where water appeared after drying the holes by use of mobile air-driers

There are several techniques other than hydraulic testing for identifying the depth and nature of the disturbed zone, like geological characterization, acoustic logging, vibration testing and geophysical logging. The first and last techniques are very useful for characterization of the disturbance [18]. Geological investigations comprise mapping of cores drilled through the disturbed zone as illustrated by Figures 104 and 105. Both represent cores drilled from the walls of tunnels and drifts that deviate 20-30° from the orientation of major fracture sets and

they demonstrate that the average spacing of blast- and stress-induced fractures is 10-30 cm within a distance of 1 meter from the periphery.

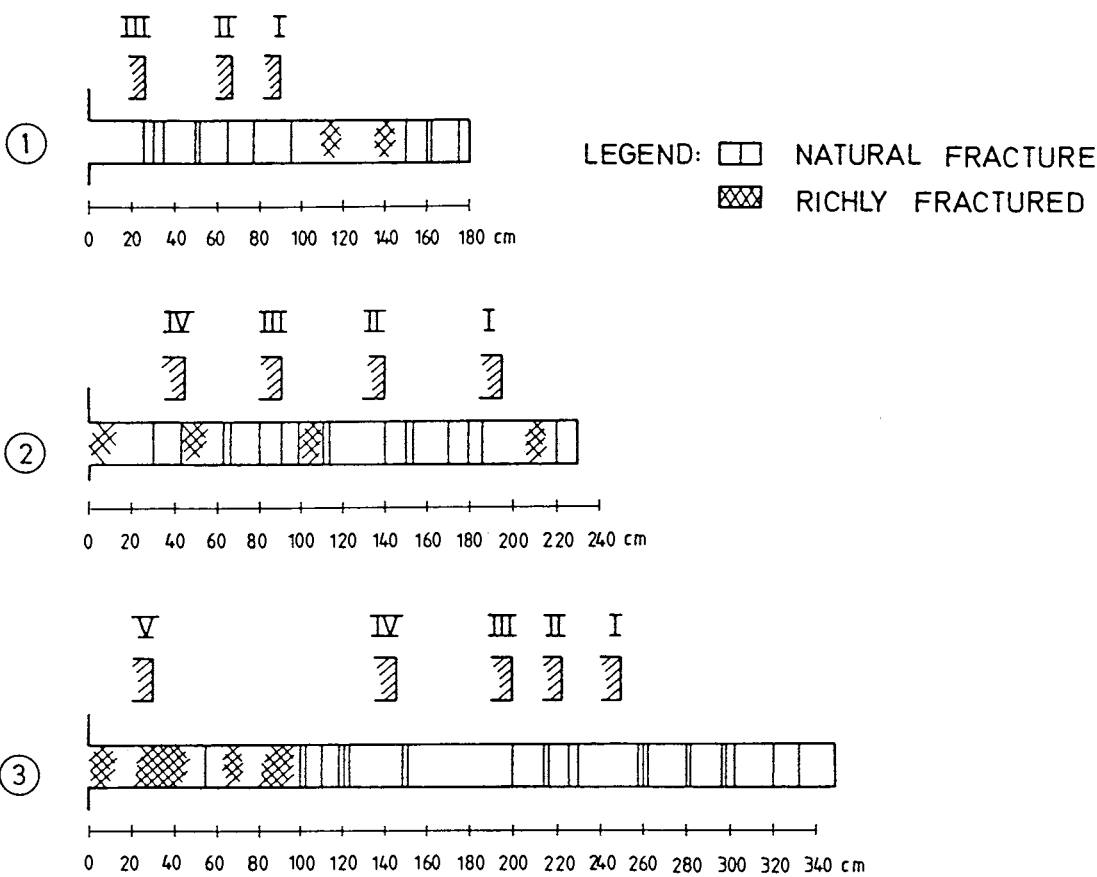


Figure 104 Schematic picture of core mappings of drill-cores from tunnel walls in granite [11]

Figure 105 indicates that the frequency of blast- and stress-induced fractures including activated latent 5th order discontinuities is enhanced to within at least 2 meters distance from the walls, which is in agreement with the results of the BMT tests.

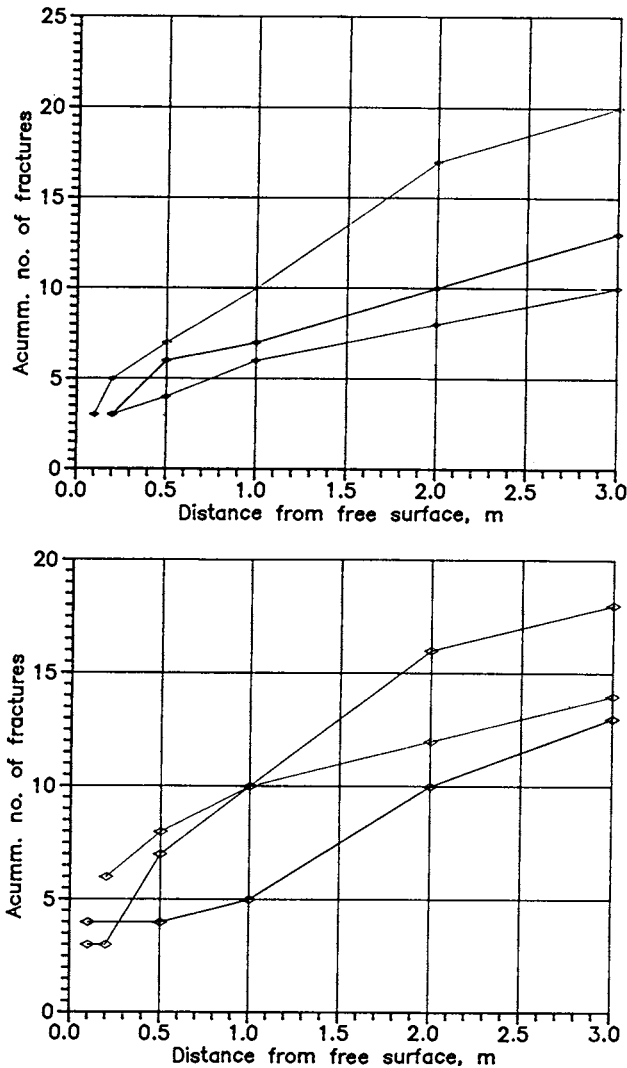


Figure 105 Recorded number of open fractures in drill-cores as a function of the distance from the periphery of blasted drifts at Stripa. Notice the high fracture frequency close to the periphery [13]

Geophysical testing using ultrasonic and seismic methods give a good picture of the softening of the disturbed zone. This is demonstrated by the diagrams in Figure 106, which also shows the results of cyclic plate load tests for evaluating the E-modulus of the shallow rock. The diagrams demonstrate a significant disintegration and drop in wave propagation rate

from about 5500 m/s of the undisturbed rock to less than 3000 m/s to 0.5-1.0 m distance from the tunnel walls where the E-modulus was found to be around 2×10^4 to 4×10^4 MPa, i.e. about one tenth of the value for undisturbed rock [1]. As in all cyclic load tests on strongly fractured rock, the ones referred to in Figure 106 gave permanent “plastic” strain through successively improved fitting of fractured blocks. A rough estimate of the porosity of the blast-disturbed rock in this particular experiment is 1-5 %.

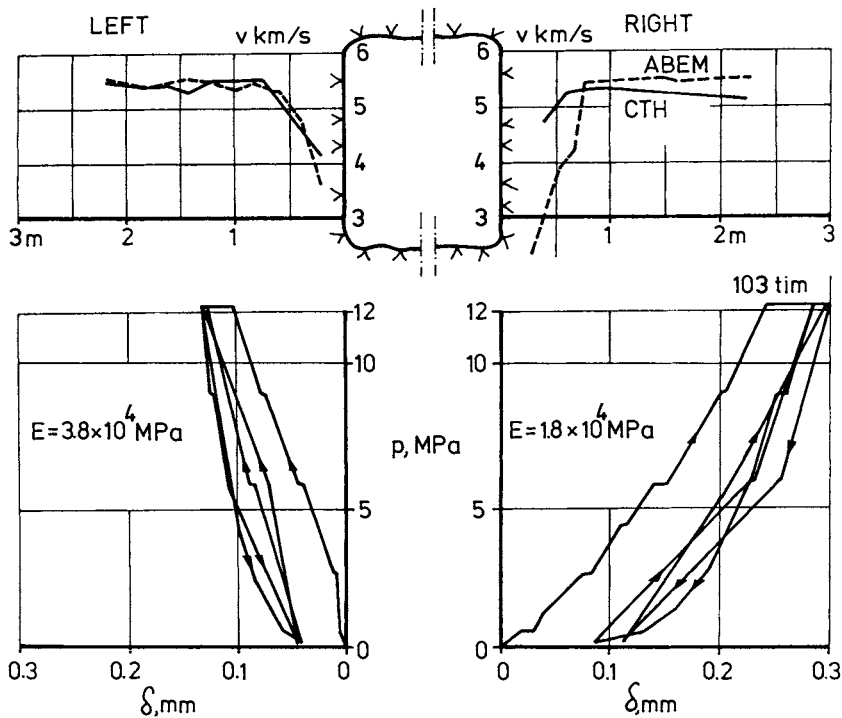


Figure 106 Example of ways of identifying the depth and nature of the disturbed zone by geophysical methods and loading tests [1]

BASIS OF CALCULATING WATER FLOW ALONG DEPOSITION TUNNELS AND HOLES

Both the theoretical derivation and experimental determinations of the hydraulic conductivity of the nearfield rock of blasted tunnels under common primary rock stress conditions, show that it may increase by 100 to 10 000 times within a few decimeters depth - up to 1 meter in the floor - by blasting, and that the stress-induced increase in axial conductivity within a distance corresponding to $2/3$ of the diameter may be about 10 times, and also that the stress-induced decrease in radial conductivity within this zone may be about 5 times. The theoretical derivation of stress-induced changes in nearfield rock conductivity around large drilled holes indicates that only insignificant changes can be expected, which is supported by the reported field tests. A schematic picture of the distribution of the conductivity around a blasted tunnel is illustrated in Figure 107.

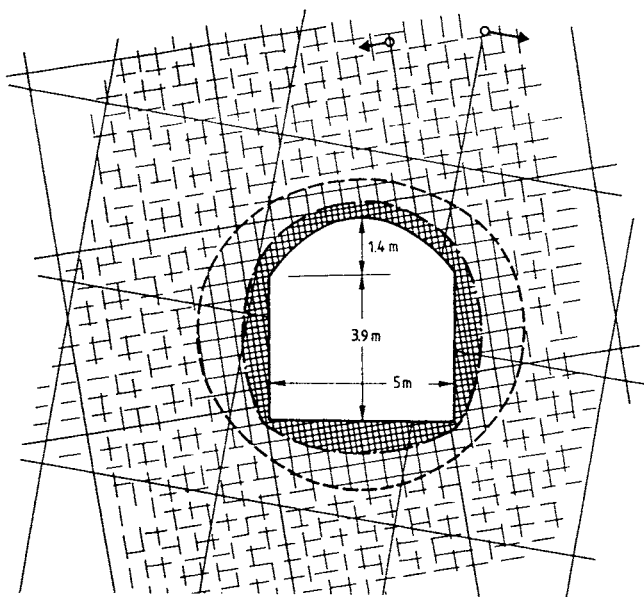


Figure 107 Schematic model of rock disturbance associated with enhanced axial conductivity. Continuous straight lines form two orthogonal 4th order fracture sets while the broken lines represent “latent” 5th order breaks that become activated and water-bearing within 3-5 m from the periphery. Adjacent to the periphery increased fracturing takes place as indicated by the hatching

The continuous straight lines in Figure 107 represent two orthogonal 4th order fracture sets, while the broken lines represent discontinuous “latent” 5th order fractures that become activated and water-bearing within up to $2/3$ diameter distance from the periphery. Adjacent to the periphery there is a zone of blast-induced fine-fracturing indicated by the fine-crossed hatching

Naturally, the system of hydraulically activated 5th and 6th order discontinuities and the neo-formed blast-induced fractures is far from regular. Generalizing the flow pattern in a KBS3 repository to be represented by channels formed at intersection of fractures, which is a commonly observed phenomenon as illustrated by Figure 108, the system of permeable paths can be as indicated in Figure 109, and the average axial conductivity as given in Table 8. For comparison, the corresponding generalized flow patterns are given also for the VDH and VLH repository concepts in Figure 110 and in Table 8.



Figure 108 Photograph of the wall of one of the 0.78 m diameter core-drilled holes in the BMT experiment. Black blots are water flowing from fractures appearing white

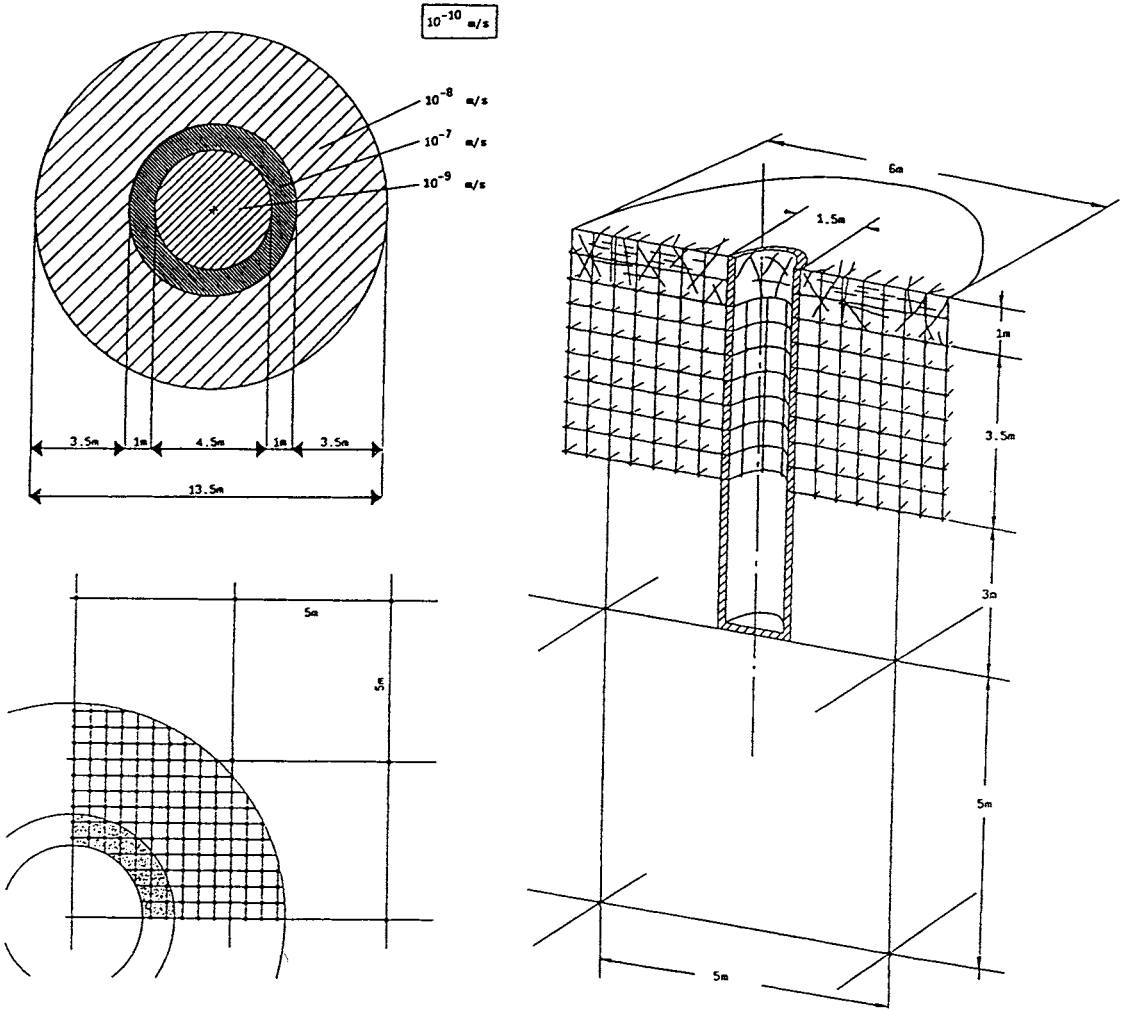


Figure 109 Schematic cross sections of 5 m diameter KBS3 tunnel and 1.6 m deposition holes located in rock matrix with an average conductivity of 10^{-10} m/s. Left: Generalized picture of tunnel with 1 m blast-induced inner zone with $k=10^{-8}$ m/s and a 3.5 m stress-disturbed zone with an axial conductivity with $k=10^{-9}$ m/s; the virgin rock is characterized by orthogonal 4th order discontinuities with 5 m spacing. Crosses represent intersections of fractures. Right: Deposition hole in blast-disturbed hole to 1 m depth and in stress-disturbed rock to 4.5 m depth. The lowest part is located in virtually undisturbed rock except for the 10 cm mechanically disturbed zone with $k=10^{-9}$ m/s [13]

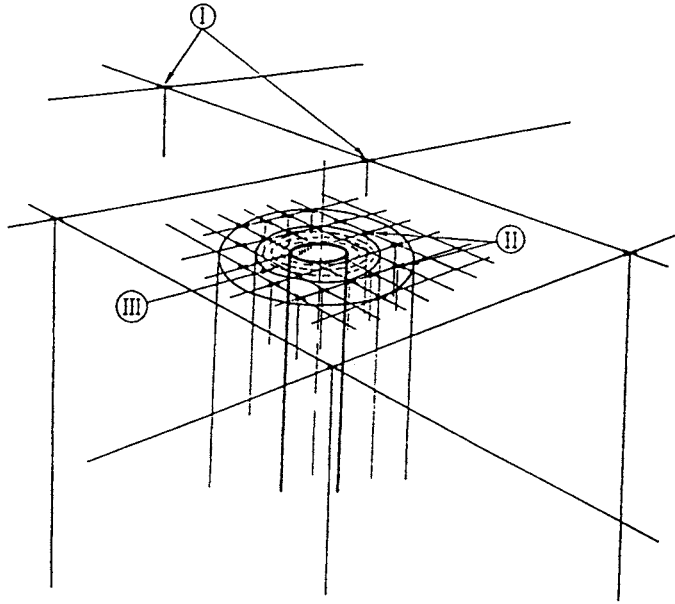


Figure 110 Schematic cross section of 0.6 m VDH and 2.4 m VLH. VDH: Zone I with channels at the intersection of fractures of 4th order representing virgin rock matrix with $k=10^{-11}$ m/s. Zone II is stress-disturbed zone with 1 m width with channels at the intersection of activated 5th order breaks ($k=10^{-10}$ m/s). III is 10 cm mechanically disturbed zone with $k=10^{-8}$ m/s. VLH: Zone I with channels at the intersection of fractures of 4th order representing virgin rock (5m fracture spacing, $k=10$ m/s). II is stress-disturbed zone with 1.5 m width with channels at the intersection of activated 5th order breaks (10^{-9} m/s). III is 10 cm mechanically disturbed zone with $k=10^{-8}$ m/s [13]

Table 8 Groundwater flux (q) through the nearfield of canisters (gradient=1). A = cross section, K= hydraulic conductivity [13]

Concept	A, m ²	k, m/s	q, m ³ /s	Remark
VDH	0.2	10 ⁻⁸	2x10 ⁻⁹	Axial
VDH	5	10 ⁻¹⁰	5x10 ⁻⁹	Axial
KBS3 (upper)	5	10 ⁻⁸	5x10 ⁻⁸	Tangential
KBS3 (upper)	15	10 ⁻⁸	2x10 ⁻⁷	Axial
KBS3 (central)	15	10 ⁻⁹	2x10 ⁻⁸	Tangential
KBS3 (central)	15	10 ⁻⁹	2x10 ⁻⁸	Axial
KBS3 (lower)	0.6	10 ⁻⁹	6x10 ⁻¹⁰	Tangential
KBS3 (lower)	0.3	10 ⁻⁹	3x10 ⁻¹⁰	Axial
VLH	2.5	10 ⁻⁸	3x10 ⁻⁸	Axial
VLH	20	10 ⁻⁹	2x10 ⁻⁸	Axial

Total axial flux of VDH = 7x10⁻⁹ m³/s

Total axial flux of VLH = 5x10⁻⁸ m³/s

The data in Table 8 show that the flux through the nearfield rock along the canister holes is in the interval 10⁻⁹ to 5x10⁻⁸ m³/s at a hydraulic gradient equal to unity, disregarding from the upper part of the KBS3 holes since this strongly fractured part can be avoided by extending the holes by a few meters. In the first decades the gradient may be much higher than unity and it is expected to range between 10⁻¹ to 10⁰, yielding a flux along the canister holes of as much as a few thousands of liters per year. After a few hundred years the gradient is expected to be on the order of 10⁻², which means that the flux will then be a few deciliters to a few tens of liters per year depending on the concept.

One realizes from this that if effective sealing of the disturbed zone around deposition holes can be made, isolated hydraulic regimes with much lower hydraulic gradients can be created, and that percolation of the nearfield can then be reduced to virtually none at all. The transport

of toxic elements would thereby take place only by diffusion through the rock, which is an extremely slow process. It is in fact even slower than in highly compacted smectitic clay because of the very low porosity of the rock.

The simplest way of estimating the transport of toxic elements is to multiply the flux by the amount of released species per time unit, the release rate being determined by the solubility of the respective species and by the rate with which they are brought in contact with the flowing water. This latter parameter is controlled by the diffusion rate within the system of canisters and canister-embedding clay. The matter has been dealt with in various studies and a simple way of getting a practical measure of the transport rate is to introduce the equivalent flowrate Q_{eq} , which is a fictitious water flux along the canister holes that carries with it a concentration equal to that at the rock/clay interface [19].

The model is illustrated by Figure 111, which shows a porous rock element contacting the canister-embedding clay and being percolated by a flux q . On approaching the contaminated clay the water is clean but while it flows along the clay, toxic elements diffuse into the water and contaminates it. If the concentration at the contact between clay and the rock is c_w , the migration rate N of the elements from the clay to the water is:

$$N = qW\eta c_w \quad (3)$$

where

W = width of the contact area clay/rock

η = mean penetration depth

η can be obtained by integrating the solution of the diffusion equation for the residence time t_w , i.e. the time during which the water is in contact with the bentonite, yielding the expression:

$$N = qWc_w \sqrt{\frac{4D_w t_w}{\pi}} \quad (4)$$

and the equivalent flow rate:

$$Q_{eq} = qW \sqrt{\frac{4D_w t_w}{\pi}} \quad (5)$$

where D_w is the diffusion coefficient and t_w the residence time

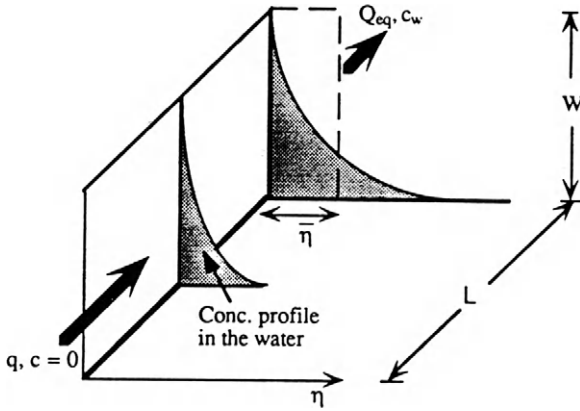


Figure 111 Schematic picture of flow through rock along canister-embedding clay [17]

Using this model one can calculate the release of radionuclides into the nearfield as exemplified by Figure 112, which refers to the case of defect canisters that give off radionuclides from the very start [19]. As for diffusive migration of cations in bentonite, sorption by ion exchange causes considerable delay in transport also in rock, in which it is primarily due to the huge amount of interconnected fine discontinuities of 7th order that are exposed in fractures (cf. Figure 18) causing effective retardation of many species. This has been documented in several reports [19].

Figure 112 implies that Cs-137 does not represent any risk in the case of deep-sited repositories of VLH- or KBS3-type because of the extremely low concentration and the quick fading out of the release pulse. It also implies that plutonium appears in totally negligible concentrations and at a very late stage. Iodine, on the other hand, appears in the water very early although the concentration in the water is low. One realizes from this that the dilution in groundwater that flows quickly along the canister holes will be very strong, but the risk of accumulation of long-lived species in a concentrated area at the ground surface is still there. Hence, following the policy defined in Chapter 1, maximum retardation of nearfield flow should be aimed at, which can be obtained by locating the repository properly with respect to

the rock structure and to the hydraulic properties, as well as by designing it in an optimum fashion with respect to the application of seals, and by applying construction techniques that yield minimum rock disturbance.

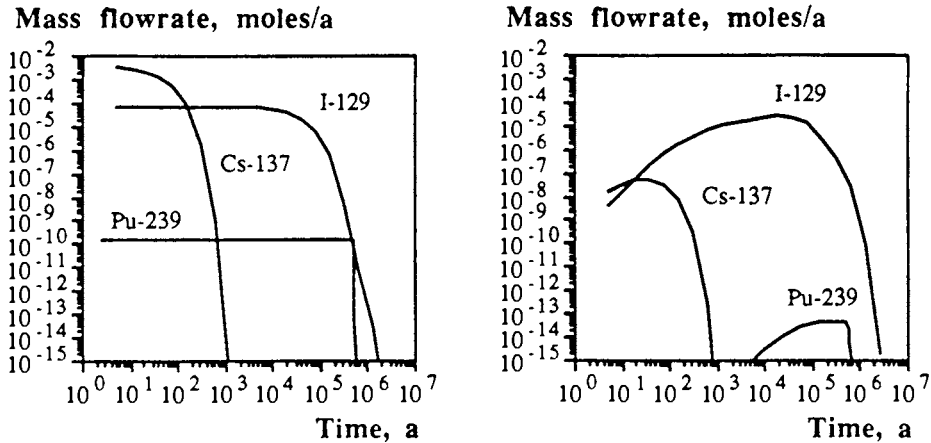


Figure 112 Predicted radionuclide release from canister holes in KBS3 repositories [19]. The left diagram shows the release from the canisters and the right one the release into water in the disturbed zone

3-6.2 Mechanical properties, stability

OVERSTRESSING OF NEARFIELD ROCK

A matter of fundamental importance is naturally the stability of the various excavations in a repository. Thus, rock failure in the construction phase or at the stage of canister transport or application, may create very critical conditions, and large momentaneous or time-dependent

strain may yield continuous passages which totally change the hydraulic behavior of the host rock. For radioactive waste repositories there is an additional major factor of psychological art: any mishap, injury or casualty in the construction phase will be taken as an example of the risk of utilizing nuclear energy.

Starting with the problem of rock failure by overstressing the rock, there are simple ways of foreseeing the risk, primarily by determining the primary stresses and designing the rooms with respect to these stresses, as well as by selecting a suitable construction technique. The risk of rock failure is determined by the stress conditions that develop in the nearfield of excavations as a function of the prevailing primary stresses [1]. The rock around large holes and tunnels drilled by tunnel boring or raise-boring techniques is not much disturbed and retains its strength, which means that it carries the high tangential (hoop) stresses induced by high primary stresses (cf. Figure 77). When blasting is applied, the shallow rock is softened and high stresses will instead be transferred away from the peripheral parts. Such destressing can be enhanced by drilling and blasting so that the blast-disturbed zone is extended, a method that is naturally not suitable in repositories for disposal of very hazardous waste since the disturbance causes a dramatic increase in hydraulic conductivity.

The schematic picture in Figure 113 illustrates the phenomenon of rock spalling due to overstressing the rock by tunnel boring. Breakage in the form of propagation of critically oriented

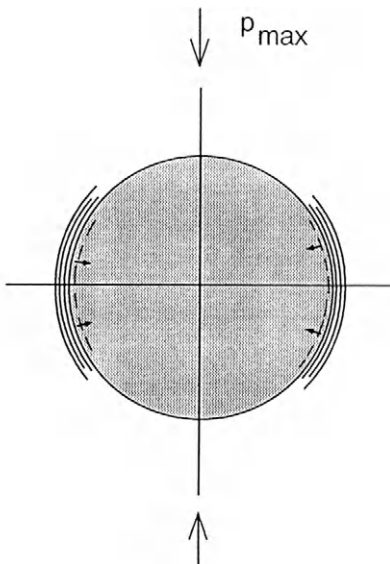


Figure 113 “Spalling” in boreholes and drilled tunnels

6th and 7th order discontinuities takes place in the direction of the major principal stress in the nearfield, which is the tangential (hoop) stress, and thin rock slabs may be released like projectiles. Breakage takes place by formation of sets of parallel, more or less long-extending fractures, giving the most shallow rock a schistose character. This means that the fracturing also causes an increased hydraulic conductivity of the shallow rock.

The key parameter is naturally the ability of the rock material to sustain high stresses, which, for this particular case, is manifested by the unconfined compressive strength. It is commonly in the interval 150-300 MPa for good granite, which is hence also the critical hoop stress. For stable conditions the hoop stress must be less than the critical value, and one can easily estimate its value by determining or estimating the primary stress field. Excepting the Caledonian ridge, where very high pressures prevail, the primary rock stress conditions in Scandinavia down to about 500 m depth are characterized by a maximum horizontal stress of 20-35 MPa and a minimum horizontal stress of 10-25 MPa. The vertical stress, which is proportional to the depth, is about 13 MPa at 500 m depth. Simple rock mechanical estimates show that the maximum hoop stress down to about 500 m depth does hardly exceed about 100 MPa of drilled holes or tunnels in most areas in Scandinavia, which means that one can expect stable conditions at excavation to this depth and a bit further. Still, a good example of the difficulties in maintaining stability at larger depths is offered by drillings to about 7 km depth in Sweden and to about 12 km at Kola in Russia. At both sites, problems with wall stability appeared in the interval 500 to 1000 m depth as illustrated by Figure 114, which shows the maximum diameter of the Russian borehole that had a theoretical diameter of 214 mm [20].

Heat-producing waste like HLW, changes the conditions to an extent that depends on the initial stress state and on the absolute temperature. Hence, when the temperature rises significantly, which happens within a few months after emplacement of the waste canisters according to the concepts VDH, KBS3 and VLH as discussed in a subsequent chapter, the heat-induced expansion increases the hoop stress but stable conditions still prevail for the primary stress conditions mentioned above if the absolute temperature is less than about 100-150°C. However, at higher temperatures 7th order discontinuities start to propagate even at moderate deviator stresses [1].

The selection of a suitable excavation technique in the construction of repositories where very hazardous waste will be disposed of, is a demanding task. The advantage of applying tunnel boring in the construction of repositories at a moderate depth when, i.e. in practice not deeper than 500 m, is obvious in light of the discussion of the stability of the nearfield rock. However, for repositories constructed at large depths, more than 1000 m, it seems advisable to apply blasting of tunnels, although the significant increase in axial conductivity of their

nearfield is estimated to require sealing. Tunnel boring at moderate depth induces only little damage as inferred from the text earlier in this chapter and sealing is only required where major water-bearing discontinuities are intersected.

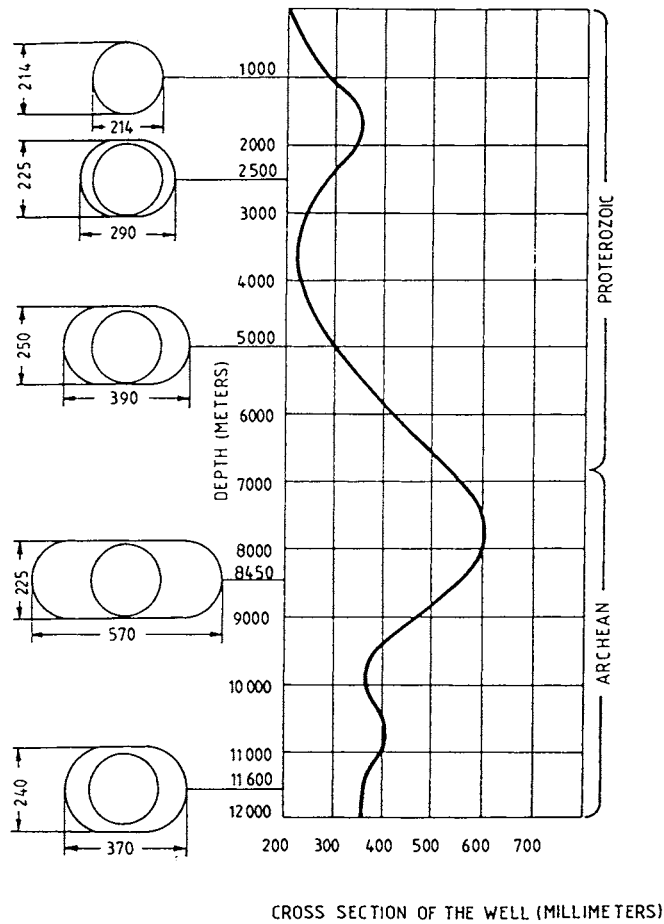


Figure 114 Maximum diameter of the 12 km deep Kola hole as a function of depth [20]

SLABBING AND DISCING

A phenomenon related to spalling is the foliation-type fracturing that may take place at the periphery of blasted tunnels at larger depths. Here, sets of aligned breaks are formed parallel to the walls and roof, especially if the tunnels are oriented more or less parallel to dominant fracture sets. The reason for this sort of excavation-induced structural change is the combined effect of high hoop stresses and high gas pressure at the moment of blasting, in combination also with the vibratory conditions. The phenomenon contributes to the increased axial conductivity of the disturbed zone as indicated earlier in the chapter. The matter is further discussed in the chapter on construction of repositories.

A common phenomenon at diamond drilling of holes perpendicularly to the plane in which high rock stresses operate is breakage of the core in the form of sets of fractures parallel to this plane. It is called “core discing” because it breaks up a drill core into millimeter- to centimeter-thick slices by growth of 6th and 7th order discontinuities in the direction of the major principal stress when the rock pressure parallel to the hole is very low. Such conditions may appear in the rock around large-diameter holes close to the floor of tunnels from which they are drilled as in KBS3-type repositories. Thus, in rock with the horizontal primary stresses 35 and 15 MPa, which represent “exceptional” but possible conditions at 500 m depth [13], tension will nearly be caused in the walls of repository tunnels at 500 m depth, while there is risk of spalling in the roof, and “discing” in the upper part of the deposition holes (Figure 115). The risk is minimized by avoiding areas with very high primary stresses and by giving the cross section of the tunnels a more or less elliptical shape with the long axis parallel to the major primary stress.

In this context it is necessary to consider also the lifting power of the highly compacted bentonite in deposition holes as indicated schematically in Figure 115, since the fractures induced by the discing will be entered and expanded by bentonite penetrating into them. Actually, they will be further expanded by the lifting forces due to the friction exerted on the walls by the upward expansion of the dense bentonite, which suggests that the upper few meters of deposition holes should not be used for hosting canisters. Both the influence of discing and the fracture-expanding effect of dense bentonite in the holes imply that the floor region of blasted and bored KBS3-tunnels may behave as a very effective hydraulic conductor.

The behavior of bentonite in deposition holes will be discussed in more detail in the chapter on the performance of repositories.

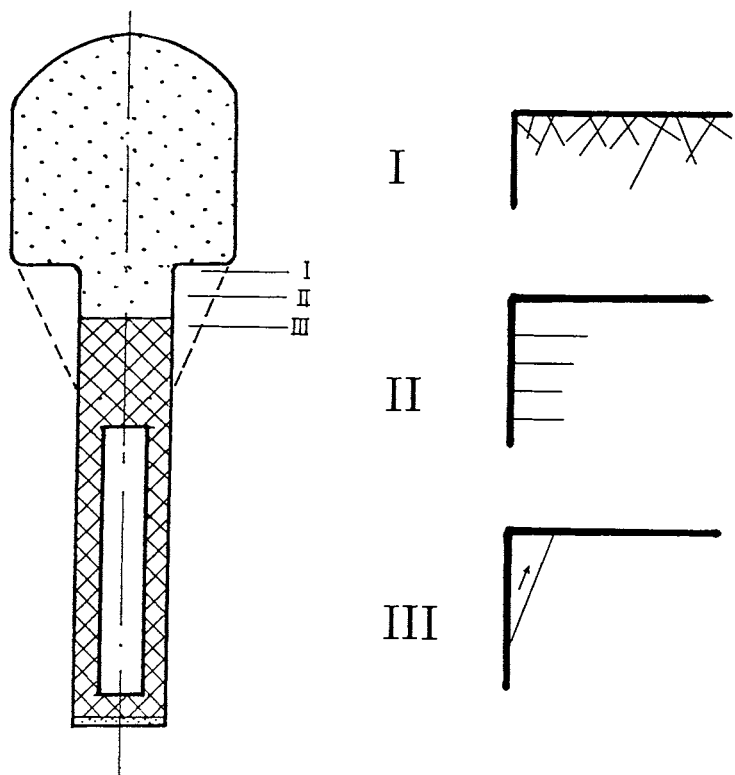


Figure 115 Schematic cross section through deposition hole with potentially unstable rock zones at the upper end of the hole. The three subzones I, II, and III represent blasting-induced fracturing, “discing”, and wedge displacements, respectively

WEDGES

Wedges formed by steeply oriented 4th order fractures intersecting close to deposition holes and tunnels may create permeable, more or less axially oriented passages that can be of practical importance if they become interconnected as illustrated in Figure 116. The lower picture shows the change in aperture along a deposition hole that is located near a crossing of two such discontinuities forming a wedge which is unstable at its tip. The upper picture shows, schematically, how consecutive sets of wedges in the roof of a bored tunnel may form continuous passages for axial water flow. The net increase in axial conductivity due to wedge formation depends very much on the orientation of the excavation with respect to the discontinuities, and one again concludes that if the two are more or less aligned, wedges will appear rather frequently in long bored tunnels and holes.

CREEP-INDUCED ROCK STRAIN

Creep effects may yield inadequate long-term stability associated with very significant time-dependent increase in axial hydraulic conductivity. The matter has been dealt with in several studies of HLW repositories located at 500 m depth, using creep models based on empirical creep laws and referring to fracture-free rock matrix [1, 21], or on rate-process theory and considering the structural nature of rock [22,23]. The first type of approach, implying micro-crack-driven creep, is applicable to the aforementioned problem of very high hoop stresses at the periphery of drilled holes of fairly small diameter, and has led to the conclusion that radial closure of KBS3-tunnels and 1.6 m diameter deposition holes may be as large as 10 mm but that this amount of creep requires thousands to millions of years to be developed. The second type of approach, implying a critical strain of about 5×10^{-3} for yielding plasticity and assuming log time creep along mechanically activated 5th order discontinuities and fractures generated by blasting, has led to the conclusion that stable conditions with very little strain will prevail in deposition holes of the KBS3 type even over hundreds of thousands of years, while critical strain will appear in the roof of blasted KBS3 tunnels in a few hundred years under normally prevailing primary stress conditions.

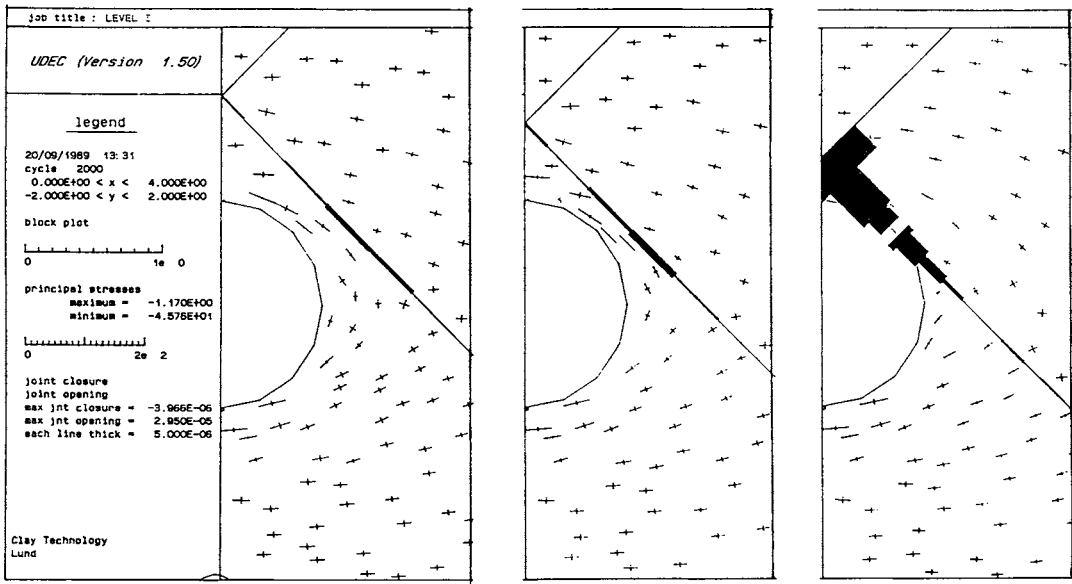
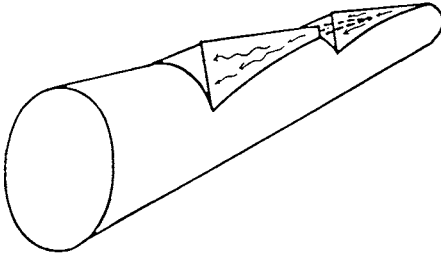


Figure 116 Wedges. Upper: Series of rock wedges in the roof of long bored tunnel. Lower: Aperture changes along a deposition hole located close to steeply dipping 4th order discontinuities (only half of the symmetric system is shown). The black parts of the discontinuities represent the increase in aperture, i.e. 2 μm for the largest distance, 27 μm for the intermediate distance, and more than 400 μm for the smallest distance, i.e. close to the tip of the wedge

Assuming that the support of the tunnel roof by the backfill is not sufficient to eliminate the creep-induced strain and associated strength reduction, which would require at least a few MPa swelling pressure and the use of highly compacted bentonite, the rock in the roof region will expand downwards and its porosity will increase, which can be interpreted as an increased aperture of more or less flatlying discontinuities of 4th and 5th orders in the roof [23]. Figure 117 illustrates the outcome of a numerical calculation of this case using the FLAC code, which yielded a downward movement of the flat roof of about 2.4 mm and a net axial hydraulic conductivity of the roof region on the order of 10^{-6} to 10^{-3} m/s. We will return to this problem in the chapter dealing with the function of repositories and confine ourselves here to point out the importance of applying a suitable cross section shape - more or less elliptic - for minimizing critical stress/strain conditions at the periphery [1].

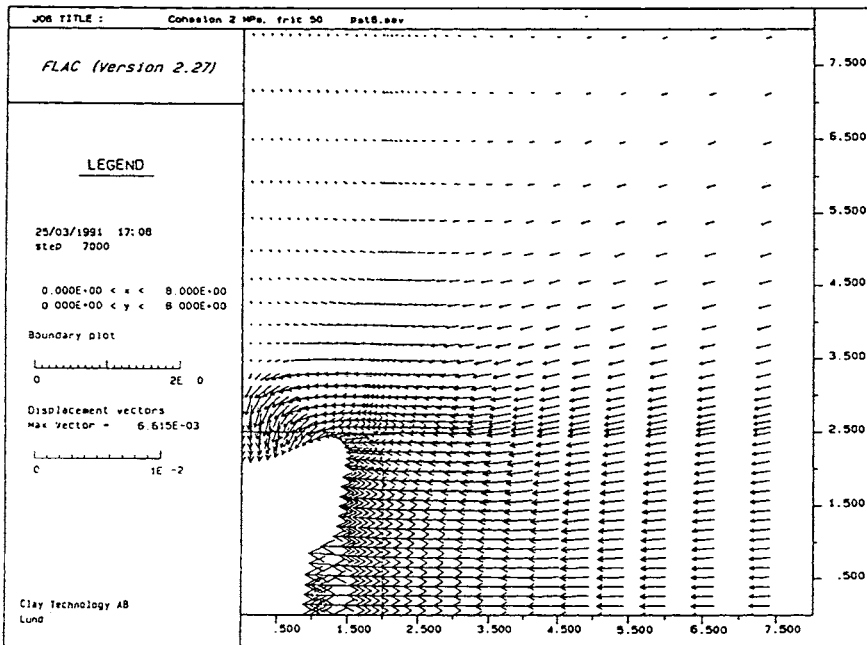


Figure 117 Possible displacements in tunnel with flat roof and steep walls

Naturally, recording of creep in rock has not been made long enough to validate any of the models used for predicting time-dependent strain and associated change in hydraulic properties but it is believed that both effects may be significant and it is also clear that heating will accelerate and magnify the processes. This is one of the degrading mechanisms in rock that makes it difficult to believe that hydraulic flow models and calculations accurately depict the flow pattern and yield reliable figures of the amounts of percolate over long periods of time. We will come back to this question in conjunction with discussing sealing techniques.

3-7 Repository sealing

3-7.1 Needs and means

There are three major types of seals in a repository:

- * Seals for making access to closed repositories difficult
- * Seals serving as confinement and mechanical support of clay-based tunnel backfills
- * Seals for blocking flow passages and redirecting water flow in nearfield and farfield rock
- * Borehole plugging. This particular sealing activity is described and discussed in Chapter 4, dealing construction of repositories

All seals must have an operative lifetime and tightness that are sufficient for effective isolation of the respective type of waste. Naturally, shallow seals will be exposed to climate-related temperature variations and mechanical and chemical attack, and where glaciation is expected to take place, strong denudation to significant depth is expected if the topography is unsuitable. Such seals therefore need to extend deep into the openings at least in repositories where very hazardous waste is deposited. Seals for confining clay-based backfills that exert a swelling pressure must be designed so as to resist the pressure for a sufficiently long time without causing chemical degradation of the backfills. Seals for blocking flow passages and redirecting water flow must operate for a sufficiently long time under the prevailing chemical and thermal conditions, implying block displacements and change in fracture apertures. It is clear from this that the choice of suitable sealing materials is an important and demanding task.

SHALLOW SEALS

Concrete plugs extending into recesses cut in the rock walls for mechanical anchoring and for obtaining tightness, can be used for shallow sealing of adits and of elevator and ventilation shafts. If the plugs are located well below the groundwater level for certifying that hydration ultimately becomes complete, and if they are covered by a few tens of meters of well compacted and graded rockfill as mechanical protection, they may serve well for many thousands of years depending on the chemical stability of the cement paste and on the groundwater chemistry, a matter to which we will return. Steel reinforcement will operate only for a limited period of time that can be estimated by assuming corrosion to take place by 1-10 μm per year, i.e. up to 15 mm in 1500-15 000 years [24]. The steel may in fact cause degradation of the concrete by the formation of hydrogen gas, a matter that has not been fully investigated but may turn out to imply that no reinforcement shall be used.

Asphalt has been considered as a material of potential use and asphalt plugs have been suggested for sealing purposes because of their excellent tightness and viscous properties that make them fill up the space and eliminate flow along the rock/plug contact [25]. Their chemical stability is estimated to be sufficient to make them operable for several tens of thousands of years if they are protected from oxygen, which is suitably achieved by covering them with concrete. A most suitable shallow plug construction may therefore be of composite type consisting of a few tens of meters of well compacted, suitably graded rockfill over a 50 m long concrete plug that is in turn overlying an equally long asphalt plug.

DEEPLY LOCATED SEALS

The major reason for sealing repositories with hazardous waste is naturally to slow down groundwater flow through or along the waste and thereby to minimize the pick-up of dissolved toxic species. An effective way of achieving this is to enclose the waste material in containments that are sufficiently stable - physically and chemically - as the thick metal canisters used for highly radioactive waste and naturally less sophisticated containment for less hazardous waste. Still, leakage of such canisters may take place sooner or later by which toxic elements become released into the groundwater and it is hence required to retard groundwater flow through the nearfield, i.e. the system composed of waste, canister embedment and surrounding nearfield rock. It can be made by using low-permeable, dense smectite clay as canister embedment, described earlier in the chapter, and by diverting the groundwater flow from the canister nearfield. The technical means for achieving the latter are effective plugging of tunnels and shafts, and fracture sealing by grouting.

The overall, beneficial effect of redirecting groundwater flow to take place around and not through a repository was illustrated by the altered flow pattern through the rock cavern hosting the bentonite-embedded concrete silo with low- and medium-level radioactive waste at Forsmark in Figure 9 (Chapter 1). In the present chapter we will consider, in a general fashion, how seals can be designed and grouting performed, and we will give an example of suitable location and required number of such seals in a repository.

3-7.2 Structural implications

The complexity in rock structure that usually prevails, requires an appropriate rather detailed structure model as a basis of selection of suitable sites for seals and for determining their overall sealing power. As an illustration we will apply the 7 order general rock structure scheme and use the schematic structural pattern that we considered already back in Chapter 2, i.e. the one shown in Figure 48, as a practical example.

PERMEABLE ZONES

It follows from the rock structure scheme that natural fracture zones of 1st and 2nd order may have a very high hydraulic conductivity, i.e. up to 10^{-5} m/s and locally more than that. Depending on the access to water that is provided by aquifers, directly or via associated water-bearing structures, inflow into ramps and tunnels may be very high in the construction phase where such discontinuities have to be crossed. Normally, conventional grouting using cement can be applied for reducing the inflow to an acceptable level but very severe conditions may require freezing or sector-wise grouting [26]. 2nd order zones are usually effectively groutable since their permeable passages have the form of well interacting fractures. 3rd order zones, which hardly cause problems by discharging unacceptable amounts of water into excavations in the construction phase but which may conduct too much water in the closed repository, are groutable but special technique is required because of the relatively low hydraulic conductivity (10^{-9} - 10^{-7} m/s). 4th order discontinuities have their permeable passages distributed in the form of channels, primarily where such discontinuities intersect, and grouting is neither effective or required, except, possibly, for very special cases as for reducing the inflow in deposition holes in the phase of application of canisters and clay embedment.

EXCAVATION-DISTURBED ZONES

As demonstrated earlier in this chapter, blasting by use of conventional techniques produces new fractures and activation and permanent expansion of preexisting ones of 4th and 5th order. The net effect of tunnel excavation is an increase in average axial hydraulic conductivity by 100 to 10 000 times within a few decimeters from the walls and roof, and within about 1.5 m from the floor. The central part of the floor in KBS3 tunnels actually becomes a continuous, highly conductive passage for axial groundwater flow. At least for very hazardous waste, effective cut-off and sealing of this passage-type is required.

3-7.3 Sealing principles

The selection of materials for sealing rock repositories has to be made with respect to the required operative lifetime. For the least dangerous radioactive waste forms LLW and MLW relatively simple sealing arrangements are sufficient, as illustrated by the design of the Forsmark repository in Chapter 1. Long-lasting seals are suitably made of materials that are chemically compatible with the rock, which is the case for smectite mineral seals in granitic rock with pH in the interval 6-8 in the groundwater. Under these circumstances bentonite is therefore very suitable provided that the temperature is not too high, a matter to which we will return later. Cement may be used as well, while epoxy compounds and other organic substances cannot be recommended for long-term service since there is not sufficient proof of their long-term stability [27].

Sealing of rock in repositories with the aim of redirecting groundwater flow can be made by plugging, i.e. construction of tight seals in tunnels, drifts and shafts. Fracture sealing can be made by injecting grout using conventional, constant pressure technique for very pervious fracture zones and special techniques for less conductive rock that requires sealing. The seals are effective over a time period that depends on the longevity of the seals and on their interaction with the rock.

PLUGGING

Plugs, which are in fact very low-permeable backfill zones, can be made in the following basic forms, which can be combined:

1. Concrete bulwarks as simple mechanical plugs for shallow application

2. Concrete bulkheads with “O-ring”-type bentonite block sealings, suitably but not necessarily combined with grouting (Figure 118)
3. Masonries of bentonite block sealings extending into slots cut in the rock, suitably but not necessarily in combination with grouting (Figure 118)

The latter two types of clay- and cement based plugs have been investigated on a full scale and found to work very well as described later in this chapter. Still, a major question that has not yet been fully answered is whether they are chemically compatible when brought together in plug constructions of type 2. The present opinion is that they are not and ongoing research is expected to indicate at what rate they interact and what the reaction products are. Since the matters of chemical compatibility and long-term stability of cement has not yet been settled it is recommended to use concrete plugs for temporary seals only, except for shallow plugs in ramps and shafts where the temperature is lower than down in HLW repositories and where their chemical and physical buffering capacity can be high by using large plug volumes.

A possible and probably optimum type of plugging is to construct concrete bulkheads in such a fashion that large parts of them can be easily removed and replaced by bentonite masonries just before completing the backfilling and closing the repository. This increases the buffering capacity of the clay plugs and reduces the amount of cementitious material by which the effect on the clay will be very small.

A practical problem with masonries of bentonite blocks is that water flowing from the rock will be taken up by the blocks, which will soon undergo shallow softening and give off a soft and very slippery slurry. It is therefore necessary to shield block masonries with simple removable “megapackers”, or possibly cement shotcrete, if backfilling of the adjacent tunnel space is not made in a few weeks and sooner than that if much water flows into the tunnels.

As indicated in the introductory remark on the design of shallow plugs contacting backfill in ramps and shafts, it is naturally important to maintain a tight contact between plugs and backfills. This requires that displacement and deformation of plugs must not take place, which, in turn, requires that also the adjacent backfills must remain in place and not undergo consolidation or shrinkage.

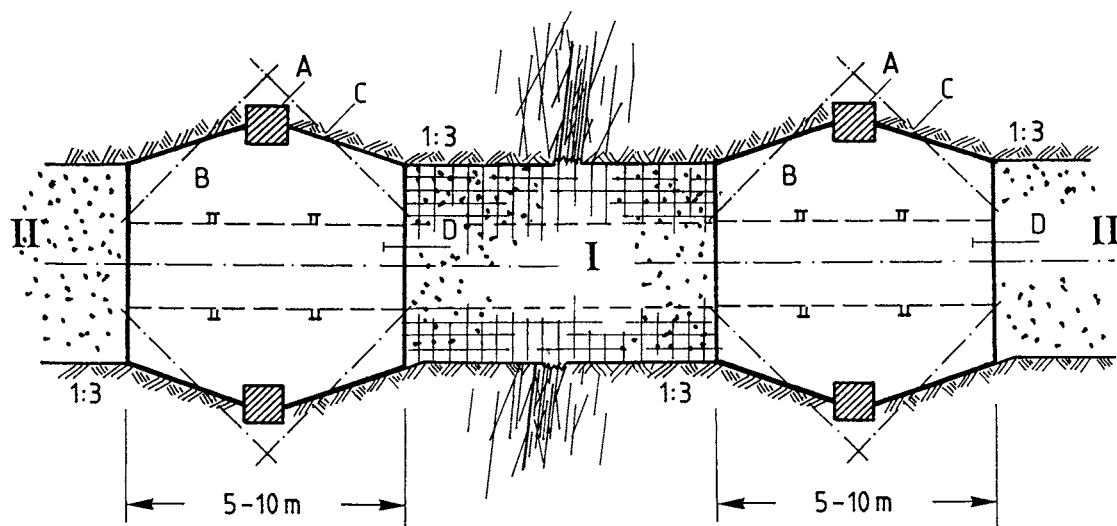


Figure 118 Concrete plugs cast in recesses and equipped with “O-ring”-type bentonite sealings (A) and grouting holes (C) for isolating a water-bearing fracture zone. I) is bentonite block masonry, II) is dense on-site compacted backfill

Physical function of plugs - the need for an effective sealing component

Numerous experiments have demonstrated that concrete plugs do not form a tight contact with surrounding rock and the need for an effective sealing component that is integrated in the concrete is obvious for eliminating leakage. The function of bentonite “O-ring” seals is to establish a perfect contact with the rock for preventing flow along the rock/clay contact. The processes leading to such a contact are illustrated in Figure 119.

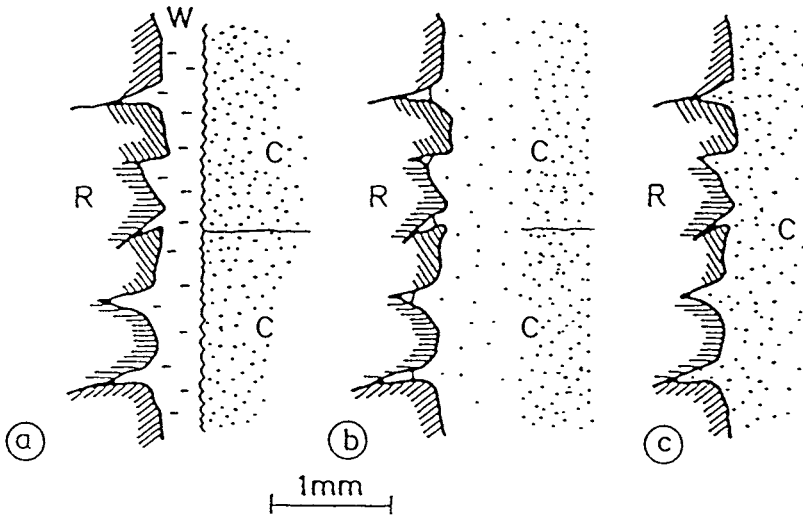


Figure 119 Schematic picture of clay penetration into the rock matrix and formation of a tight clay/rock contact. a) Clay blocks in position after application. b) Early stage of expansion. c) Final stage with integrated clay and crystal matrix. W represents water, C bentonite clay, and R rock

GROUTING

General

As demonstrated later in this chapter, the Stripa Project for testing repository sealing techniques gave a very good overview of available techniques and materials. At a rather early stage

of this project, i.e. when it had been shown that the sealing potential of highly compacted bentonite as canister embedment and plug material is very significant and practically useful, the matter of sealing fractures by grouting was proposed as a subject for field testing, and a literature study was initiated for identifying suitable grouts for use in repositories, primarily for sealing fine fractures. This study showed that longevity aspects limited the number of potentially useful grout materials to smectitic clay and cement [27]. Both were used in a series of laboratory-scaled and field experiments for testing the usefulness in grouting relatively fine-fractured rock and comprehensive studies were performed for estimating their survival potential under repository conditions.

Three major types of application

One can distinguish between three major applications of grouting in repositories:

1. Sealing of water-bearing discontinuities anywhere in the construction phase for keeping the construction site sufficiently dry and for minimizing changes in the chemistry of the inflowing water in the construction and waste application phases by reducing water inflow as much as possible
2. Sealing of fractures intersecting deposition holes and tunnels for minimizing inflow in the canister application phase and for retarding transport of radionuclides into the rock
3. Sealing of fracture zones and hydraulically important discrete fractures for redirecting groundwater flow from tunnels and depositions holes. The aim is to retard uptake of elements in the canister-embedding clay that cause degradation of the clay and corrosion of canisters

The first function is illustrated by the ongoing process of altered salinity in the Forsmark repository, where the potassium content in the water in the silo area, as recorded in borehole HK10, has increased from 15 ppm to 27 ppm from January to June 1992 (cf. Chapter 1).

The second function is illustrated in Figure 120, which shows a deposition tunnel with “disturbed” zones of high axial conductivity, connected to discrete 4th order fractures and activated 5th order fractures intersecting or interfering with deposition holes. Grouting of such discontinuities creates largely immobile groundwater regimes and extends the length of the distance that radionuclides have to migrate before they reach the pervious disturbed zone. Thus, it has been estimated that sealing of fractures to 0.1 m distance from the periphery of

KBS3 deposition holes with a grout that has a diffusion coefficient for radionuclide diffusion that is 2 orders of magnitude lower than that of water, increases the diffusion resistance by one order of magnitude, and that sealing to 1 m distance increases this resistance by two orders of magnitude. Such a grout is estimated to be represented by smectite clay with an average density of around 1.3 g/cm^3 and cement grout with $w/c < 1.0$. A field experiment of this sort was conducted at Stripa and it will be presented and discussed later in this chapter.

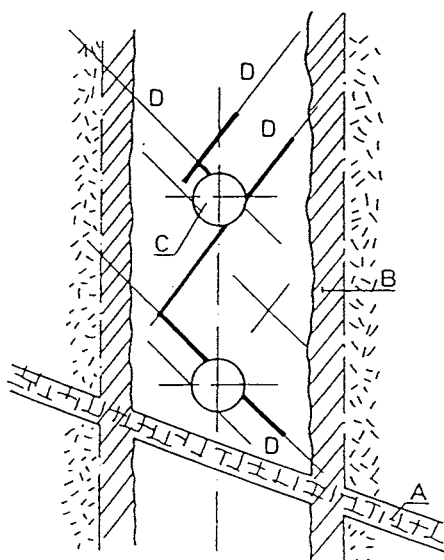


Figure 120 Shunting off groundwater flow through rock with deposition holes (C). Fractures D serve as short circuits before grouting. A is a major water-bearing zone and B is the disturbed zone with enhanced hydraulic conductivity

The third function is illustrated by an experiment at Stripa where reduction of the average hydraulic conductivity of a 3rd order zone was reduced from initially 10^{-8} to around 10^{-9} m/s ,

leading to redirection of the groundwater flow [26]. This experiment, which will be described later in this chapter, is of particular interest because it gave an insight in the nature of such zones that indicates the difficulties in successful grouting of other fractures and fractures zones than the significantly water-bearing ones.

Physical function of clay and cement grouts

Three major issues determine the physical function of grouts and thereby their sealing ability, namely the consistency required for making the grout penetrate into fractures, the evolution of shear resistance to withstand piping and erosion, and the flexibility and self-sealing potential, i.e. the property of maintaining contact with the fracture surfaces after the grouting.

Grout penetration depth

The density and type of adsorbed cation control the shear resistance of clay grout in the injection phase and thereby the penetration depth, while the water/cement ratio w/c and the grain size distribution are major parameters controlling the penetration depth of cement grouts, for which also fluidity-enhancing additives like superplasticizers are used. The shear resistance, especially of smectitic grouts, can be greatly reduced by superimposing oscillatory vibrations on the static pump pressure as illustrated by Figure 121, [28]. Eq.3 expresses the flow properties of cement and clay grouts and forms the basis for calculation of the grout penetration depth.

$$\tau = m \left(\frac{\dot{\gamma}}{\dot{\gamma}_0} \right)^n \quad (6)$$

where

τ = shear stress

$\dot{\gamma}$ = shear rate = du/dy ($\dot{\gamma}_0$ = normalized shear rate 1.0 s^{-1})

u = flow velocity

y = coordinate perpendicular to the flow plane

m = parameter related to viscosity (Pas)

n = parameter

The optimum density of smectitic clay grouts with respect to penetrability and sealing power - expressed in terms of hydraulic conductivity, piping resistance and self-sealing potential - is in the interval 1.08-1.3 g/cm³, which makes it penetrate to a depth given by Figure 122 for viscosities represented by the m-values 0.1, 0.5 and 1.0 Pas. The firstmentioned value is representative of the lowest densities and the last one of the highest density [29]. The conclusion is that the equipment used for grouting rock fractures at Stripa would give a penetration depth of up to 2 meters in a 100 μm fracture with the softest grout, while the most dense grout would only enter such a fracture to about 0.25 m depth. Further development of the dynamic technique is under way and is expected to improve the net sealing effect significantly.

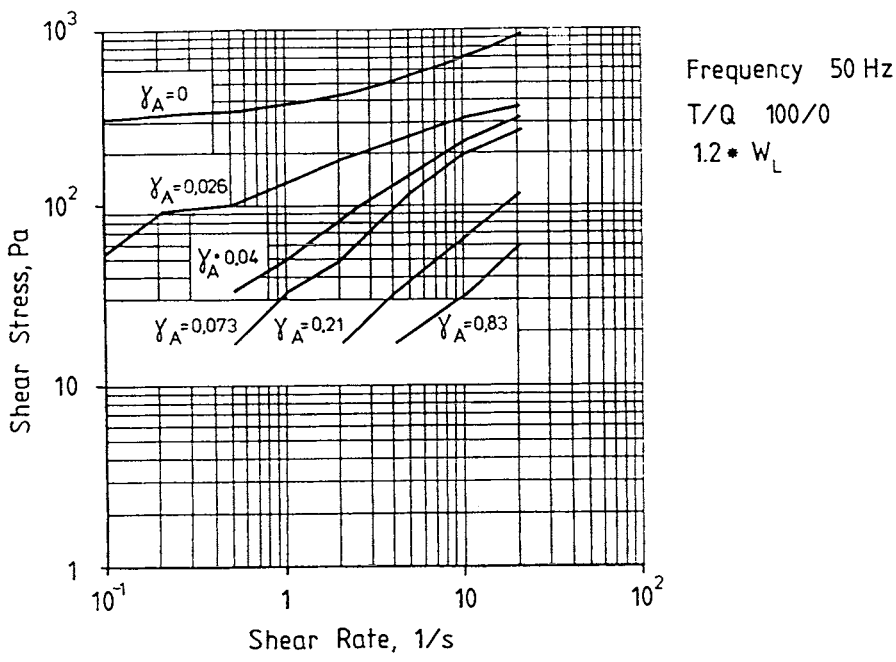


Figure 121 Shear resistance at static ($\gamma_A=0$) and dynamic injection for different shear strain amplitudes (Na bentonite with a water content equal to $1.2xw_L$), [17]

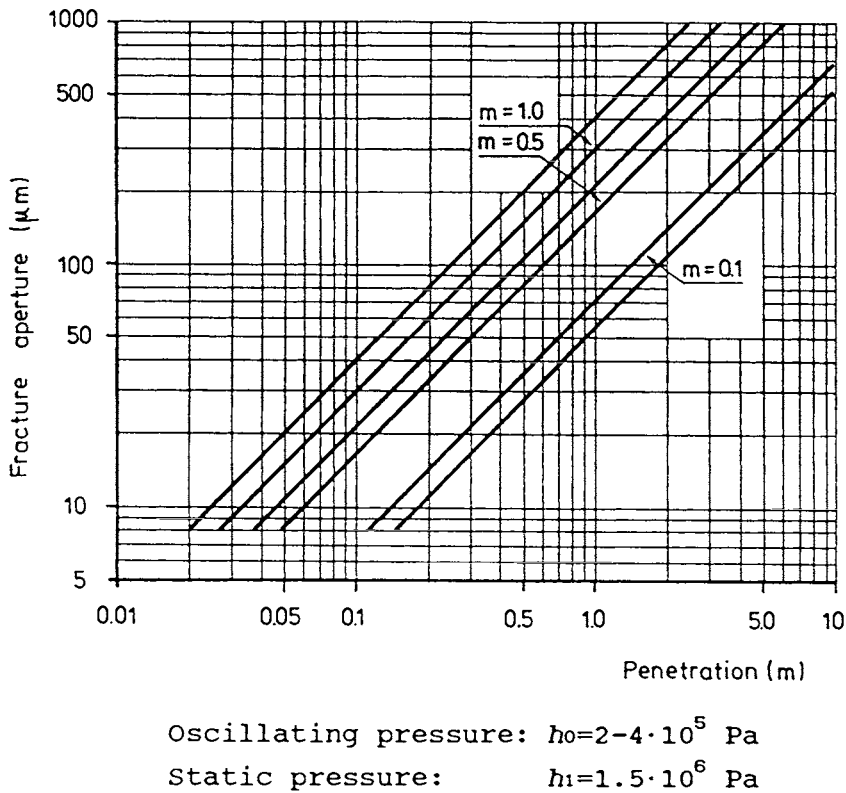


Figure 122 Predicted penetration as a function of fracture aperture for three m -values.
 The data refer to the megapacker equipment used at Stripa [17]

Cement grouts can be given a significant fluidity even at high densities by adding suitable superplasticizers. Thus, using very fine-grained cement (Alofix, $d < 15 \mu\text{m}$), 1.6 % superplasticizer (sodium naphthalene formaldehyde condensate) and adding water to $w/c=0.6$, the m -value 0.05 Pa and the penetration depth hence considerably larger than 2 m in a $100 \mu\text{m}$ fracture [28].

The influence of the degree of fracture-filling on the bulk hydraulic conductivity

The issue of how effectively a fracture can be filled with grout is naturally of fundamental importance. Thus, the limited penetration depth that results from the high friction resistance in narrow fractures also implies that grout cannot enter the most narrow parts of fracture channels (Figure 123). This was investigated in the Stripa rock sealing project, from which it was concluded that grouting of a 3rd order fracture zone with moderate injection pressures gave the typical degree of cement grout filling shown in the picture [26].

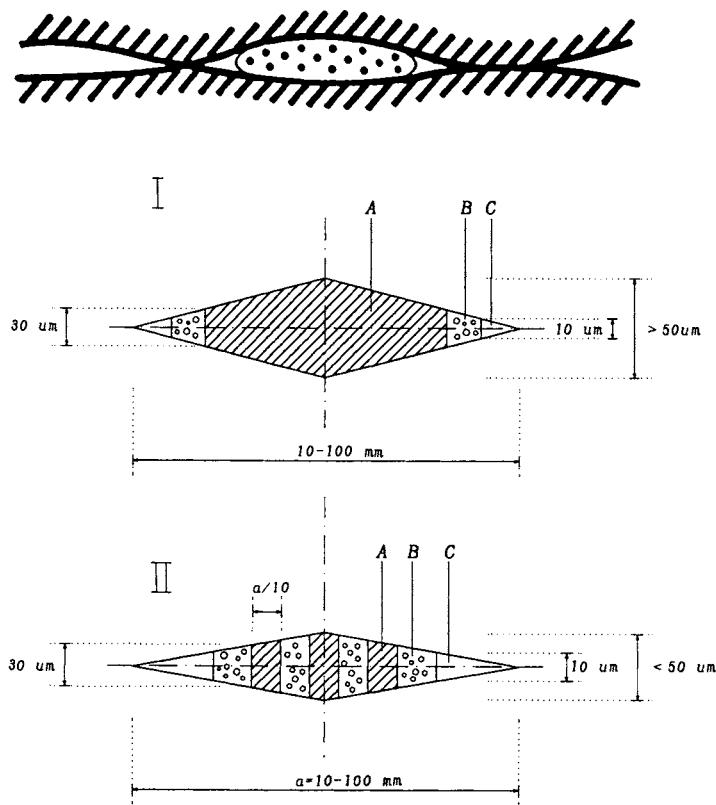


Figure 123 Upper: Schematic picture of channel with incomplete grout filling. Lower: Generalized sections of fracture channels with cement grout. A is dense cement matrix and B porous, heterogeneous cement, while C is open space

Taking these structural patterns as a basis for estimating the theoretical net hydraulic conductivity of sealed rock the data given in Table 9 are obtained. It demonstrates a practically important and wellknown fact, namely that it is difficult to reduce the average hydraulic con-

Table 9 Bulk hydraulic conductivity K of ungrouted and grouted discontinuities assuming standardized channel geometries. d =spacing of parallel channels with maximum aperture a

d, m	$a, \mu m$	Ungrouted, $K \text{ m/s}$	Grouted, $K \text{ m/s}$	Rock type
0.1	50	1.3×10^{-8}	1.7×10^{-9}	3rd order
0.1	100	1.0×10^{-7}	8.3×10^{-10}	2nd order
0.1	200	8.2×10^{-7}	4.1×10^{-10}	1st order
0.2	50	3.2×10^{-9}	4.1×10^{-10}	3rd order
0.2	100	2.6×10^{-8}	2.1×10^{-10}	3rd order
0.2	200	2.0×10^{-7}	1.0×10^{-10}	2nd order
0.5	50	5.1×10^{-10}	6.6×10^{-11}	5th order
0.5	100	4.1×10^{-9}	3.3×10^{-11}	3rd order
0.5	200	3.3×10^{-8}	1.7×10^{-11}	3rd order

ductivity of relatively low-permeable rock, represented by 3rd order discontinuities, i.e. fracture zones with an average hydraulic conductivity of $\sim 10^{-8} \text{ m/s}$, while pervious rock can be very effectively sealed.

Effect of high injection pressure on the rock

Very high injection pressures, i.e. several MPa in excess of the piezometric pressure, can increase the penetration depth and degree of channel filling but there is a risk of uncontrolled propagation of the injected fracture and of expansion of fractures that are indirectly affected by the pressurizing. Moderate injection pressures should naturally be applied when grouting shallow rock, while high injection pressures may well be used when grouting well confined rock, as in pregrouting before tunnel excavation. A preliminary theoretical study based on the FLAC code and assuming a grout pressure of 1 MPa, illustrates the possibilities and risks as exemplified by the case in which grout has entered a fracture, forming a circular disc with

0.25-0.75 m radius as illustrated in Figure 124 [26]. For a confining pressure of 0.25 MPa and the fracture located at 1.2 m depth and being parallel to the free surface (upper curve), one finds that the maximum fracture expansion at the center of a grout filling with 0.75 m radius is nearly 40 μm and that the widening extends to about 1.5 m from the center. At the periphery of the filling the expansion is about 15 μm , which is too little to let the grout penetrate further into the fracture but which leads to an open space that may interact with other fractures and thereby largely reduce the overall sealing effect. This case (5C) illustrates the need of limiting the injection pressure to very low values when grouting shallow rock, while the other cases, referring to a grout radius of 0.25 m and external pressures in the interval 1-4 MPa, show very limited expansion of the ungrouted part of the fracture. For the smaller radii of initial grout filling, the expansion of the fracture (1A, 4A and 5A) is less than 10 μm .

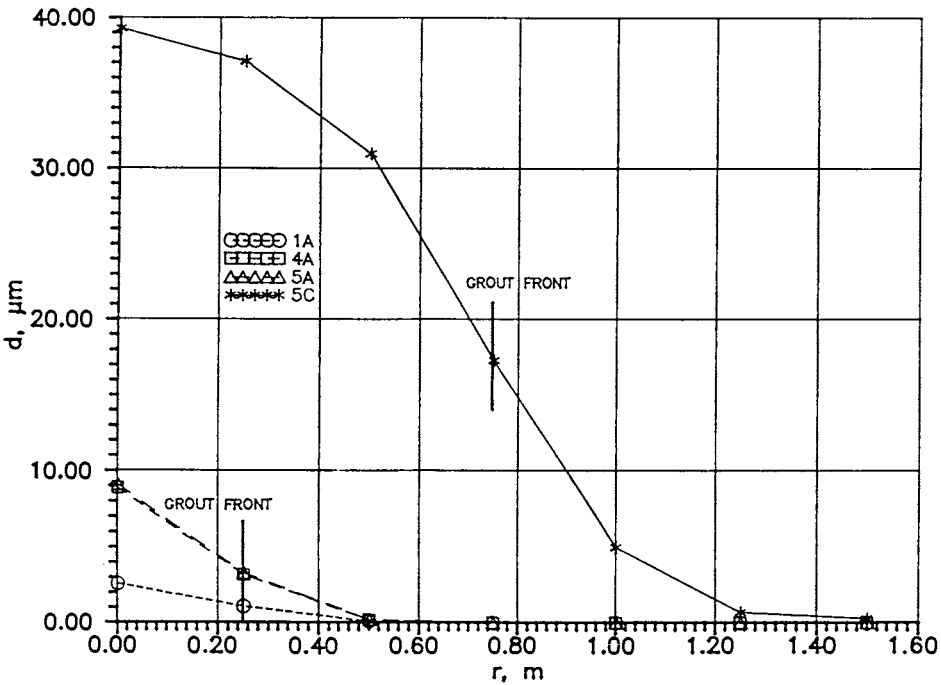


Figure 124 Expansion of fracture partly filled with grout. Vertical scale is axis of symmetry

Provided that the injection pressure is not high enough to create new fractures and cause propagation and permanent expansion of existing ones, a large part of the rock strain is elastic, which means that the fracture tends to become closed when the injection pressure drops. This causes the grout to move outwards and become consolidated under the pressure that the relaxing rock exerts. Where the grouted zone is effectively supported by the surrounding rock mass or by a bulkhead or buttress, the injection pressure can be very high and the sealing effect good. The latter conditions were at hand in a successful grouting operation made in conjunction with one of the subsequently described Stripa plug tests, where good support of the rock was offered by the plug construction. The sealing effect of the grouting corresponded to a drop in average axial hydraulic conductivity by 1 to 2 orders of magnitude.

Insignificant rock support is provided when grouting shallow rock, for which it is necessary to apply very low injection pressures. As demonstrated by an unsuccessful attempt to seal the blast-disturbed zone of the BMT drift at Stripa by use of closely spaced, short holes, the most shallow rock cannot be sealed because the packers need to be placed 10-20 cm from the rock surface. Further reasons for the poor results was concluded to be the presence of blast-induced, relatively pervious debris that leaked water but prevented grout from entering the fractures, and also fracture widening of the sort mentioned above. This test will be discussed in some detail later in this chapter since it revealed a number of important features of the blast-disturbed zone.

Physical stability - piping and erosion

Smectite clay grouts undergo very quick thixotropic strength regain after completing the injection and further increase takes place for days and weeks thereafter. Thus, the risk of piping and erosion, which both depend on the shear strength of the clay, is highest immediately after the injection. A practical measure of the piping resistance is that the maximum hydraulic gradient that the grout can sustain is about 30, meaning that a channel filled with grout of length L will be in a critical state when the water pressure at the pressurized end is around $30 L$. Hence, a 3 m long clay-filled channel will be unstable at a water pressure of slightly less than 1 MPa immediately after injection. A day later the shear strength increases by 25-50 % and after a week it may be twice the strength immediately after the injection, which would make the clay-filled channel resist about 2 MPa water head. This was actually confirmed by the combined plugging/grouting experiment described since it showed that while the grout resisted 1 MPa pressure shortly after the injection and manifested that the sealing effect was good, exposure to 2 MPa water pressure led to expulsion of clay in conjunction with piping and an increase in flux back to what was recorded prior to the grouting [26].

While smectite grouts undergo significant thixotropic stiffening almost instantaneously when the mechanical agitation caused by the injection stops, freshly injected cement slurry with 1-1.5 % superplasticizer does not experience substantial hardening until after 10 hours at room temperature and 20 hours at 10°C rock temperature. Piping tests of freshly injected cement grout using microscope technique have demonstrated that such gels are more sensitive to erosion and piping in the first 10-20 minutes than clay grouts [29]. A general rule is that the opposite condition is reached after a few hours.

Physico/chemical processes

Smectite grouts are preferably in sodium form and should be prepared with low-electrolyte water since the sealing power and groutability are then at optimum [29]. However, if such a grout is exposed to calcium-rich groundwater of higher ionic strength, coagulation takes place by which larger voids will be formed and its hydraulic conductivity increases. The contact with the fracture surfaces may be lost if the grout has a very low density and this may make the sealing effect vanish completely.

For cement it is estimated that salt water environment creates successive clogging of voids by precipitation of calcium and magnesium compounds.

Chemical stability

The ultimate reaction product of smectite under normal repository conditions is hydrous mica (illite), and grouts that become completely converted to this mineral form are much less effective as seals than the virgin grout [29]. There are several processes that can cause such conversion, but the reaction rate is determined by only two factors: the temperature and the access to dissolved potassium. At temperatures below about 60°C the conversion is concluded to be so slow **under stagnant groundwater conditions** that the smectite minerals will be preserved over tens to hundreds of thousands of years, irrespective of the K^+ conditions, while access to potassium controls the conversion rate at any temperature when groundwater percolates. At temperatures exceeding 130°C, lattice degradation yielding cementation by precipitated silica appears to take place. At ordinary ambient rock temperature, smectite grouts may be chemically stable for many hundreds of thousands of years even when salt water with a considerable content of potassium percolates. The important thing is what the net sealing effect of smectite clay will be like if and when complete conversion takes place to hydrous mica, a matter that can be investigated by assuming a relevant initial grout density

and a defined rock structure like the part of a generalized 3rd order zone shown in Figure 125. Thus, taking the width and height of the channel to be 1 cm and 100 μm , respectively, and assuming the density of the grout to be 1.1 g/cm^3 , which corresponds to an average hydraulic conductivity of 10^{-9} m/s for smectite and 10^{-5} m/s for hydrous mica, one finds that the net conductivity of the rock before grouting is $7 \times 10^{-9} \text{ m/s}$, while it is 10^{-11} m/s immediately after grouting and not more than $7 \times 10^{-11} \text{ m/s}$ after complete conversion to hydrous mica. One concludes from this that also soft clay grouts have a substantial sealing effect even after conversion to non-expanding mineral forms. The example can also be taken to represent a conservative version of the case of microstructural change induced by cation exchange from sodium to calcium or by saturation by water with high ionic strength.

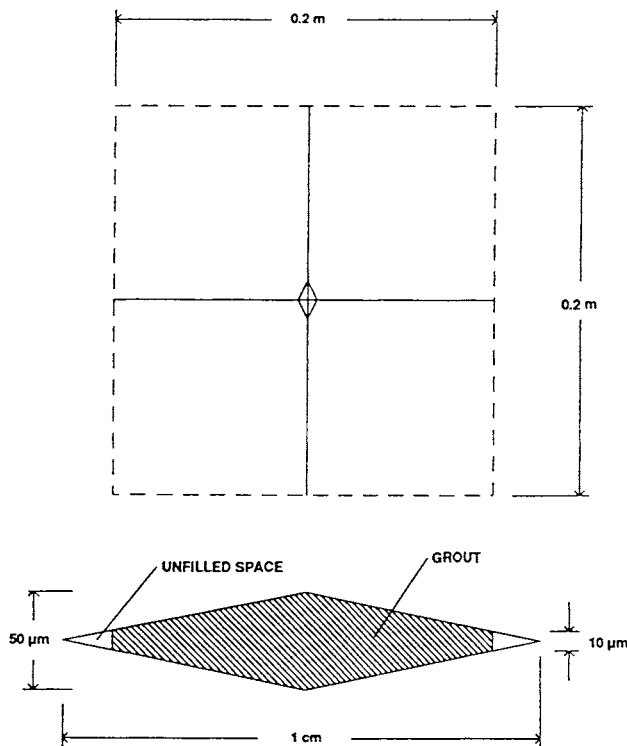


Figure 125 Unit of fracture rock with rhombohedral channel section, partly filled with clay grout

Cement exhibits similar properties, i.e. **under stagnant groundwater conditions** it will maintain a large part of its sealing power for more than a hundred thousand years, while it may lose practically all its sealing power in a few hundred years at high groundwater flow through heterogeneous grout in narrow fractures.

A fundamental difference between the two grout types is that smectites are flexible and - at least when the grout density is higher than 1.1 g/cm^3 - have some expansion potential and an ability to self-seal at fracture expansion by as much as 30 %, while the brittle cement does not exhibit these properties. Thus, fracture expansion of this order creates a gap between cement and rock where groundwater will flow and this may result in quick degradation. One way of counteracting this is to prepare the cement grouts with a very low w/c ratio, i.e. lower than what is required for complete hydration according to stoichiometry, i.e. lower than about 0.35, because this provides a “reserv” hydration and swelling potential. Since this increases the viscosity very significantly and does not allow for penetration of very narrow fractures it is necessary to mix the grout with a few percent of superplasticizer of suitable type [30]. Such additives are organic, which has been expected to limit the long-term stability and to cause a risk of migration of organic colloids serving as carriers of radionuclides, but such risks seem to be exaggerated [31].

General aspects on sealing by grouting

A number of conclusions of importance for strategic planning and performance of grouting can be drawn from the literature and, in particular, from the Stripa rock sealing activities:

1. The penetration depth is very limited, i.e. a few decimeters, when the fracture channels have an aperture of less than about $100 \mu\text{m}$ but some penetration takes place also at apertures down to $20\text{--}30 \mu\text{m}$, provided that dynamic (oscillatory) injection is applied. For channel apertures smaller than $50\text{--}100 \mu\text{m}$ the degree of filling is low and the homogeneity of the low-density grouts that have to be used becomes less good, especially when cement is used. Channel apertures exceeding $200 \mu\text{m}$ give penetration depths of at least a couple of meters at moderate injection pressures
2. Substantial improvement of the penetration power and degree of filling of channels is obtained when the conditions allow for high injection pressures. This is the case when the rock is self-supporting as in pregrouting ahead of tunnel excavation, or when excavated rock is effectively supported by concrete buttresses

3. Low density grouts (1.1 g/cm^3) have a low piping and erosion resistance and they are much more sensitive to changes in groundwater chemistry than denser grouts, which also have a much higher potential for self-sealing if disturbance by fracture displacements occurs

4. At rock temperatures up to 30-50°C, clay and cement grouts are expected to maintain a large part of their sealing ability for tens to hundreds of thousands of years irrespective of the groundwater chemistry and flow. At higher temperatures the degradation rate of both types of grout may be considerable, especially since their chemical buffering capacity is very small because of the small mass. None of the grout types is expected to serve well where significant rock displacements take place, which implies that they perform acceptably for long periods of time in 3rd and 4th order discontinuities but are less effective as seals in zones of lower order. The limited piping and erosion resistance of clay grouts and the lack of expandability of cement grouts are restrictions

5. The sensitivity of cement grouts even to insignificant rock displacements makes them unsuitable as seals that are required to serve over very long periods of time except if they are prepared with very low w/c ratios. If not, cement grouts can hardly offer reliable performance beyond the construction period. However, in this period they are indispensable for sealing water-bearing rock structures, primarily low-order zones that have to be intersected

6. A most important issue appears to be sealing of the uppermost part of deposition holes in blasted KBS3 tunnels for limiting the inflow of water in the period when application of bentonite and canisters takes place. A suitable technique has been developed for this operation, as described later, but an ideal grout is not yet at hand; it should have the sealing power and thixotropic strength regain of dense clay, and the solidification potential of cement. In fact cement grouts will perform reasonably well but they cannot be relied on in a long-term perspective.

3-7.4 Experience from large-scale sealing tests - The Stripa Rock Sealing Project

The sealing power of plugs with “O-ring”-type bentonite seals combined with grouting, and the general effects of grouting that was described in the preceding text will be further exemplified here to form a basis of the subsequent discussion of how strategic sealing can be made with special respect to what can be achieved, for what purpose it can be applied, and at what cost. These issues are naturally of great importance for future successful design and construction of repositories.

EXAMPLES OF CONCRETE PLUGS

Concrete bulwarks with “O-ring”-type bentonite sealings

Figure 126 shows a longitudinal section through a test arrangement at Stripa that was used for investigating how a strongly water-bearing zone can be intersected by a tight casing without inflow of water at its ends [32]. The casing connects two concrete bulkheads with built-in sealings of blocks of highly compacted Na bentonite. The water-bearing zone was simulated by a sand fill around the casing and perforated tubes in the fill made it possible to apply a water pressure of up to 3 MPa. Figure 127 shows a general perspective view of the arrangement and an illustration of the application of the cubical blocks with 200 mm edge length. The blocks, which were prepared by applying production methods that will be described and discussed in detail in the chapter on repository construction, were not fit together with great precision but in a fashion that can be expected from ordinary construction teams. The resulting joints and the possibility of the bentonite to expand laterally by compressing the sand gave a net dry density of about 1.6 g/cm^3 (2.0 g/cm^3 and a water content of around 26 % at complete saturation). The swelling pressure at complete saturation was found to be 5 MPa, and the hydraulic conductivity about 10^{-13} m/s . The initial degree of water saturation of the blocks was about 50 %.

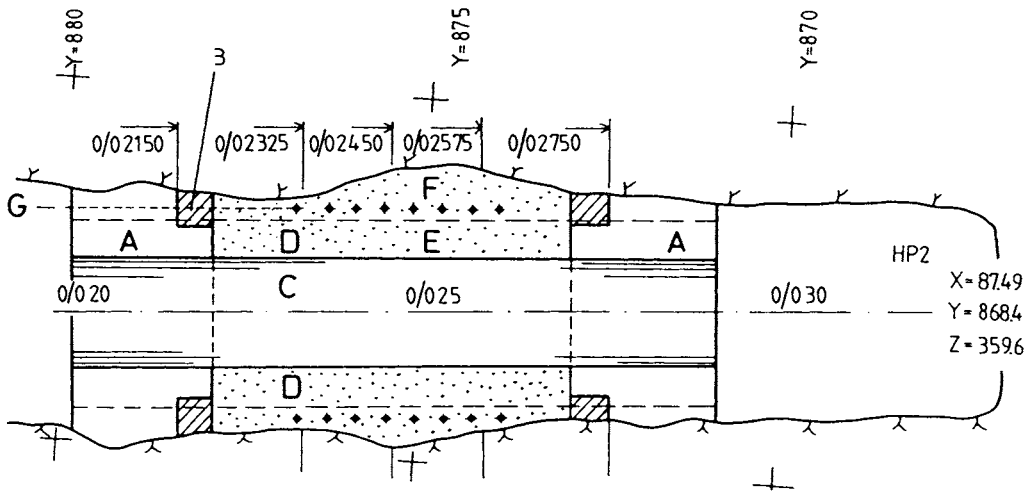


Figure 126 Longitudinal section of the plug construction at Stripa. A) concrete bulwarks, B) bentonite blocks placed in recesses, S) steel casing, D) tie-rods, E) 5 m long sand-filled injection chamber, F) pipe gallery, G) water injected by pumps

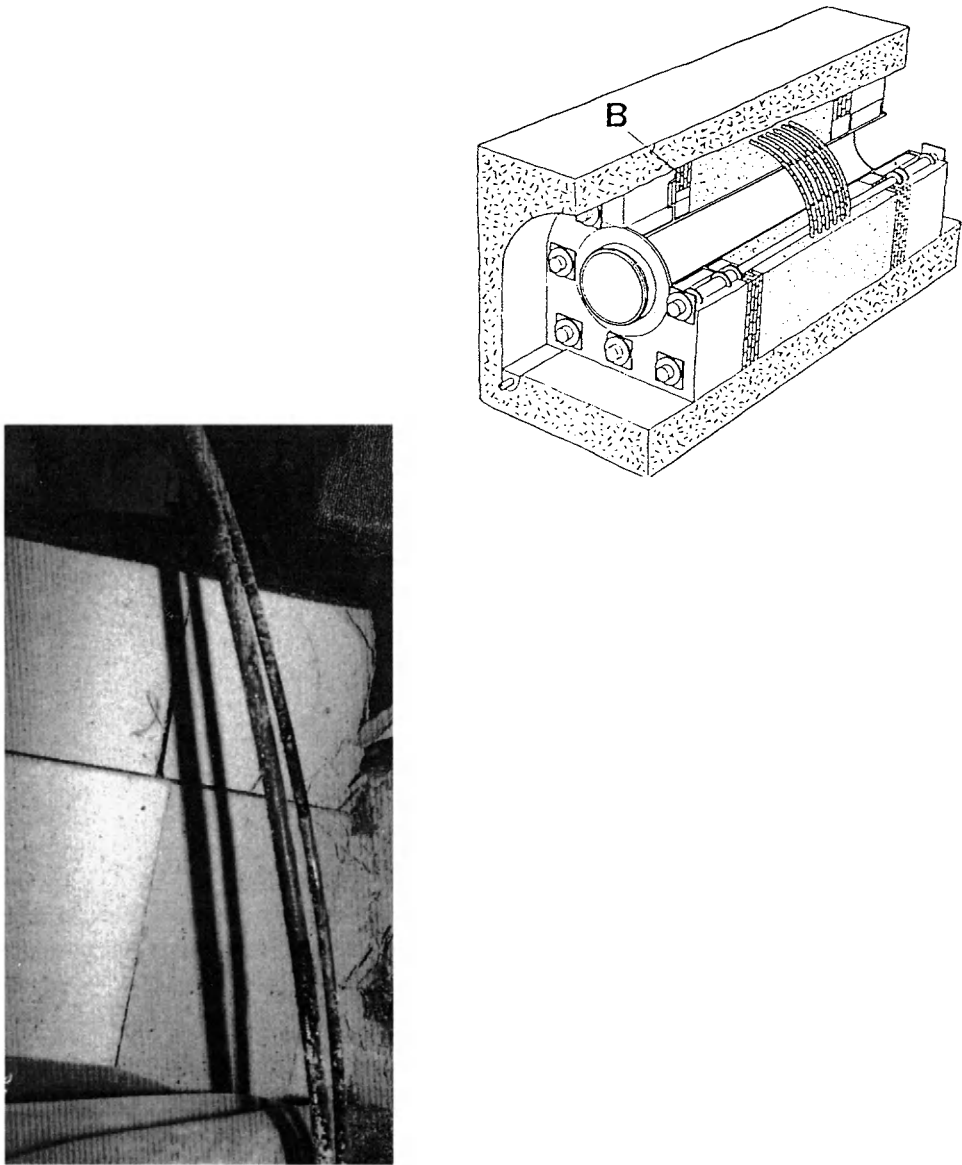


Figure 127 Upper: Schematic view of the test arrangements. B is the “O-ring”-type seals of highly compacted bentonite. Lower: Typical joints between bentonite blocks

The experiment had the form of stepwise pressurizing the sand-filled chamber and recording the resulting outflow (leakage) from the chamber, the swelling pressure developed at the concrete/bentonite and rock/bentonite contacts, and the displacement of the bulwarks. The flux of water passing along the contact between the bulwarks and the rock and through the adjacent rock was measured by collecting the water that accumulated immediately outside the two bulwarks and it turned out to be almost exactly the same as the recorded outflow. Hence, practically all the leakage took place along this contact and through the adjacent rock. Figure 128 shows the total outflow as a function of time at the various pressure steps. The outflow beyond the outer bulwark stabilized at about 20 l/h at 1 MPa, about 40 l/h at 2 MPa, and at about 75 l/h at 3 MPa pressure. The latter figure was reached after somewhat less than two years, the irregular curve shape being due to intended and accidental pressure drops.

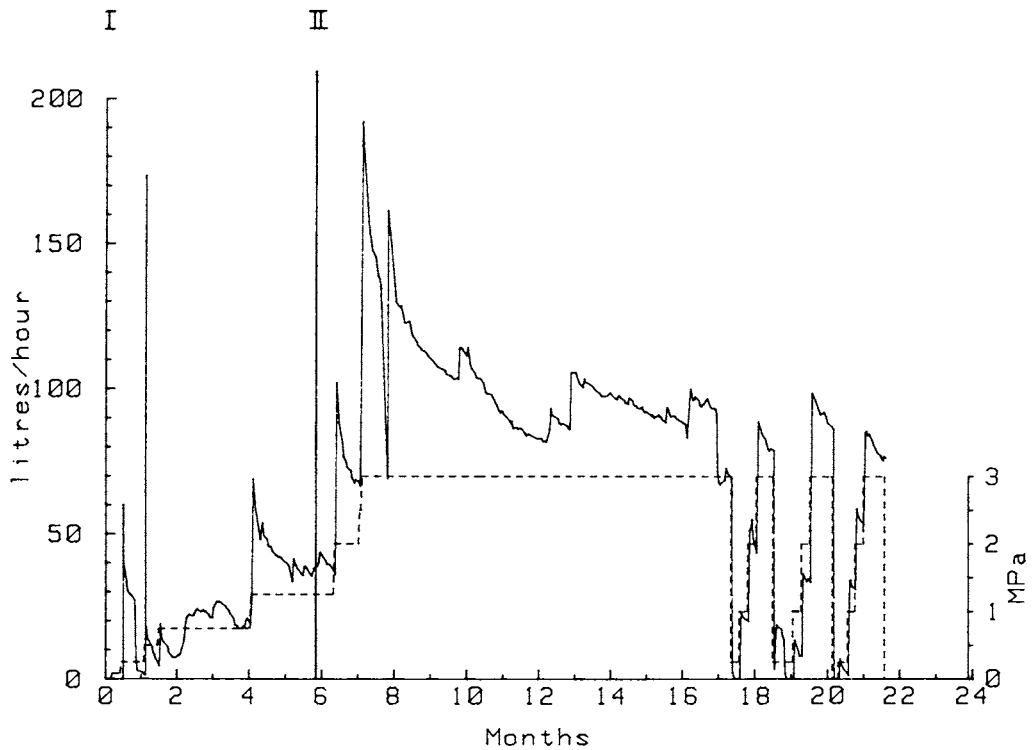


Figure 128 Outflow of water from the sand-filled chamber to the outer end of the outer bulwark. I and II denote tie-rod prestressings

At the termination of the entire experiment, which included a grouting experiment that will be described later, it turned out that the bentonite clay had become perfectly homogeneous to several centimeters distance from the rock and concrete and that it formed a completely tight contact with them (Figures 129). This observation and the fact that there was no visible leakage along the contact between rock and clay after a couple of months led to the conclusion that practically all the outflow took place through the rock after this period of time and since the rock structure had been characterized there were opportunities both to investigate the character of flow through the rock and to test whether the rock could be effectively sealed by grouting.

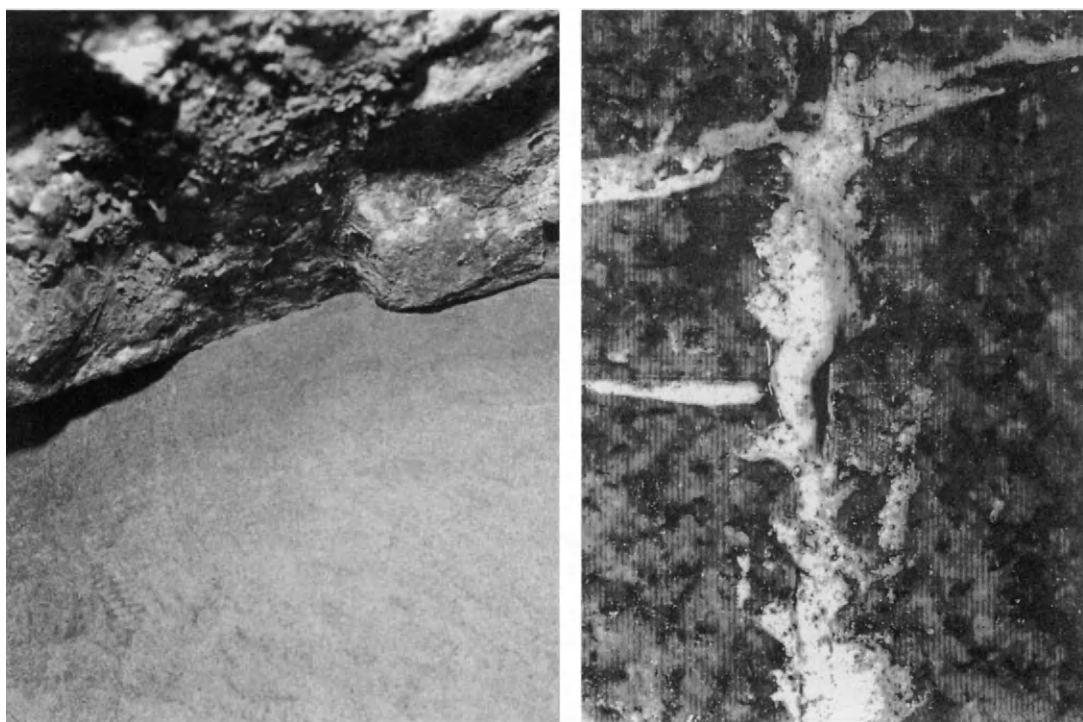


Figure 129 Contact between bentonite and rock. Left: Homogeneous clay with perfectly tight contact with the rock caused by wetting and expansion of the bentonite blocks. Right: Clay that moved into fractures was washed out after removal of the solid bentonite (about 10 times magnification)

The evaluation of the sealing effect was made by comparing the recorded flow data with those obtained from calculations which were made in two ways, i.e. by assuming that the rock behaves as a porous medium with typical average bulk conductivities of its various components, and by assuming the flow to take place through identified, discrete fractures. The firstmentioned analysis was made by applying FEM with the axi-symmetric element net and flow parameters shown in Figure 130, which also gives the pressure contours for 1 MPa water pressure in the sand-filled chamber (I). The choice of rock conductivity data was based on the conclusions from the comprehensive testing of the excavation-disturbed zone at the BMT site at Stripa, which showed that the conductivity of the blast-disturbed zone (II) in conventionally blasted granite can be taken to be isotropic and equal to 10^{-8} m/s and that of the surrounding stress-disturbed zone to be 10^{-9} m/s axially and 10^{-11} m/s radially [16]. The virgin rock was assumed to have an isotropic conductivity of 10^{-10} m/s. Figure 131 shows the flow pattern.

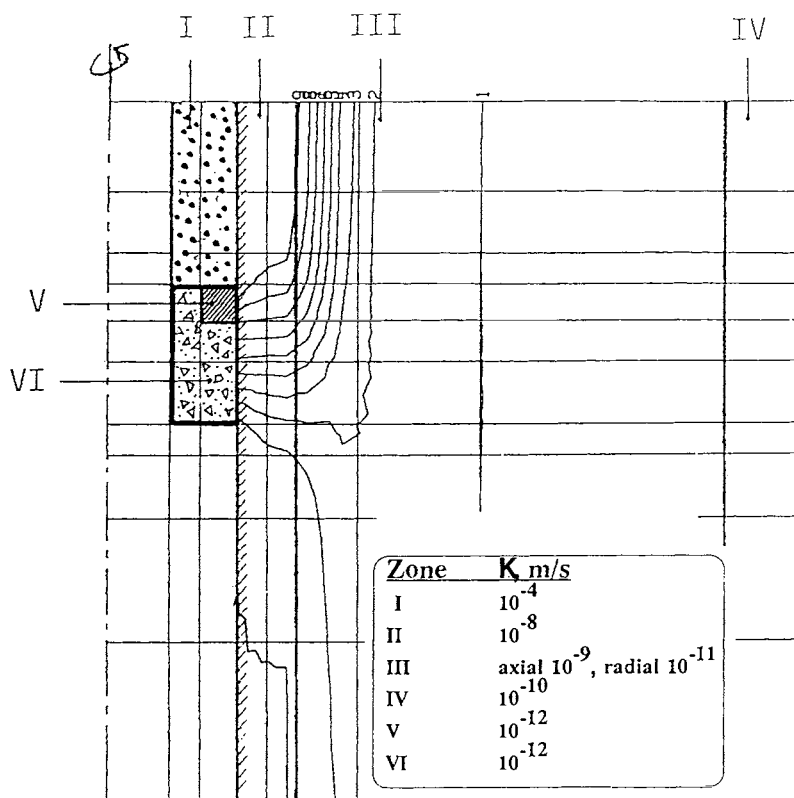


Figure 130 Element net for flow calculation. Pressure contours for porous medium case

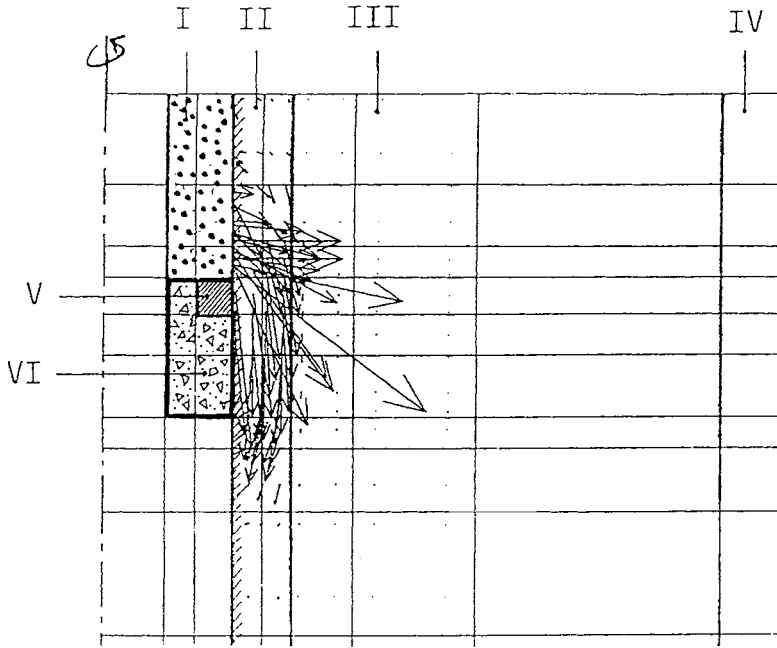


Figure 131 Flow pattern for porous medium case

The second approach, i.e. assuming the flow to take place through discrete discontinuities, was based on the identification of 8 major fractures (I-VIII) oriented N70W/90 and N40E/90, respectively (Figure 132).

The fractures termed I, IV and VIII (with the “twin” VII) represent one set of water-bearing fractures representing 4th order discontinuities, while those termed III and V belong to another set of 4th order discontinuities, which, together with the first one and a similar flat-lying set, forms a roughly orthogonal structure. The fracture termed II is taken to be a 5th order discontinuity that became hydraulically activated by the blasting, while the “erratic” one termed VI can be taken as a member of a separate set of 4th order discontinuities. The flow calculation was based on the assumption that the eight fractures contributed equally

much to the discharge from the rock and that they have the same effective hydraulic aperture. Taking the aperture of their hydraulically active parts to be equivalent to slots with 100 μm openings, which is reasonable because four out of five of them turned out to be groutable, the outflow at 1 MPa pressure was found to be 20 liters per hour, which also agrees very well with the actually recorded value.

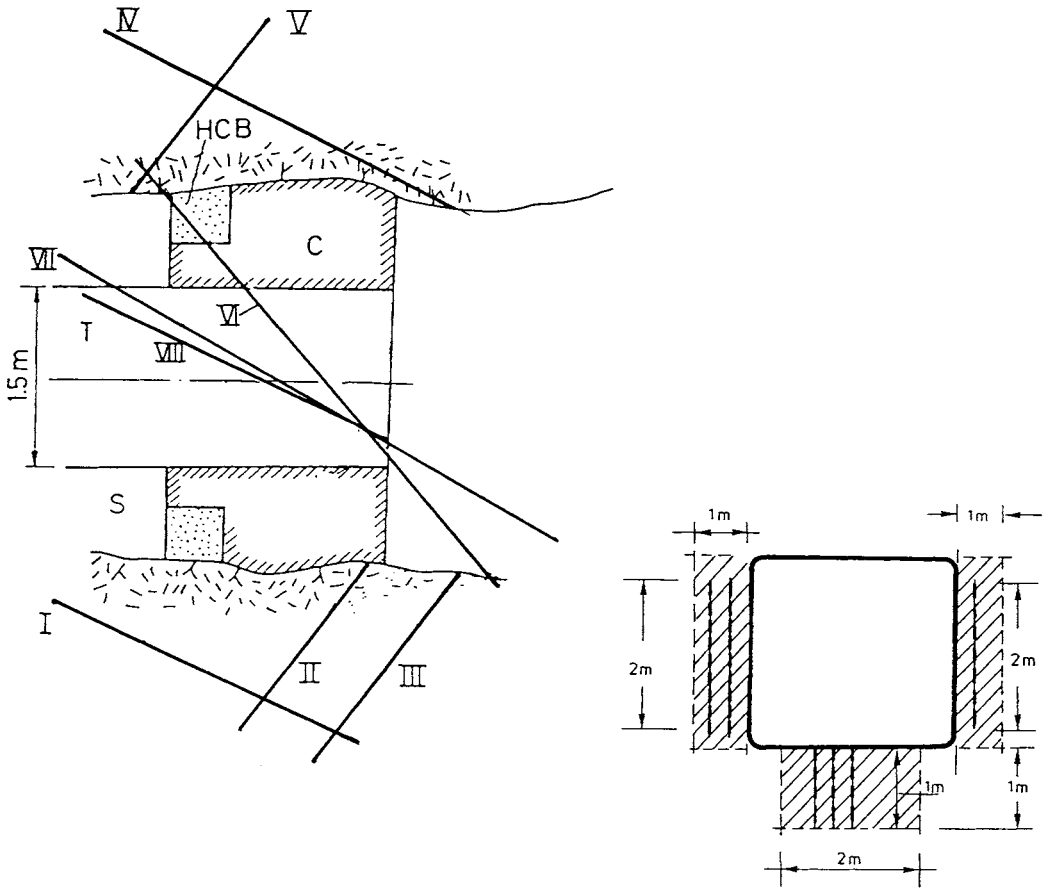


Figure 132 Schematic pictures of the eight discrete discontinuities. Upper: Plan view. Lower: Front view showing the the six fractures that discharged water

A sealing operation in which bentonite grout was injected in the six fractures I, II, III, VI, VII and VIII, reduced the outflow at 1 MPa to 40 % of that before grouting, while it should have been about 25 % if the eight fractures had contributed equally much to the outflow and if they had been completely sealed. The grouting was made by drilling and injecting five subhorizontally oriented 56 mm grouting holes through the fractures termed I, II, III, VI, VII and VIII in the figure, and injecting them, one by one, with Li-bentonite grout with a water content of about 500 %, which was only slightly higher than the liquid limit (26). Dynamic injection with peak pressures of 4 MPa was applied.

This example shows that both the porous medium model and the deterministic discrete fracture model work and yield outflows of the right order of magnitude and it is clear from this study and from later experiments at Stripa, which will be referred to extensively in the book, that the porous medium approach can be used for rock volumes of 50 m³ and larger, despite the fact that the actual flow passages have the form of a limited number of discrete discontinuities.

It is concluded that concrete plugs with highly compacted bentonite emplaced in recesses, combined with grouting of a few discrete, critically located fractures, rather effectively block groundwater flow through the plugs and the adjacent rock. In the Stripa case, the average hydraulic conductivity of the “disturbed zone” was reduced by 1 to 2 orders of magnitude and this is expected to be a commonly achievable effect. The long-term performance of plugs consisting of both concrete and and smectite clay is not yet known.

Masonries of bentonite block sealings extending into slots in the adjacent rock

Figure 133 shows the test arrangement at Stripa where the sealing ability of a shaft plug of highly compacted bentonite was investigated. The experiment comprised a first “reference” test with two concrete plugs cast by use of expansive cement for getting a perfectly tight rock/plug contact and separated by a sand-filled pressure chamber for testing the tightness of the plugs, and subsequently a “main” test with highly compacted bentonite as plug material both in the shaft and in a 25 cm deep and high slot (Figures 133), [32]. The net dry density of the bentonite masonry at complete saturation, which was not achieved because of the short duration of the experiment and of the low groundwater pressure in the test area, should become 2.05 g/cm³, if vertical expansion could be prevented, which required end plates of steel beams and tie rods to resist the more than 200 tons high separating force caused by the swelling pressure. The rate of maturation of the bentonite was illustrated by the recorded swelling pressure using Gloetzel pressure cells and by determination of the water content dist-

tribution at the end of the test (Figure 134). This figure also shows the predicted distribution of water in one part of the bentonite masonry using a simple theoretical model which we will examine in Chapter 5.

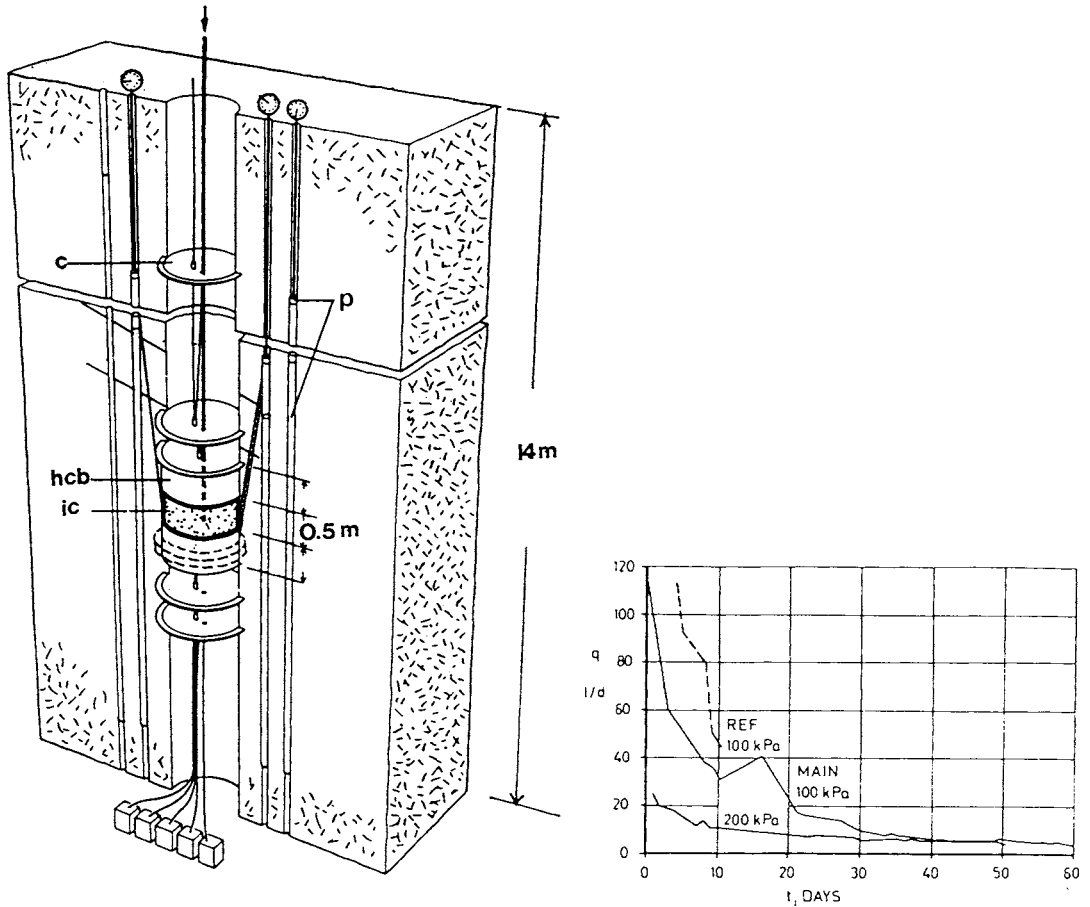


Figure 133 The shaft plugging experiment at Stripa. Upper: Test arrangement; c) water collector, hcb) bentonite in main test, ic) injection chamber, p) packer-equipped inspection holes. Lower: Flow curves

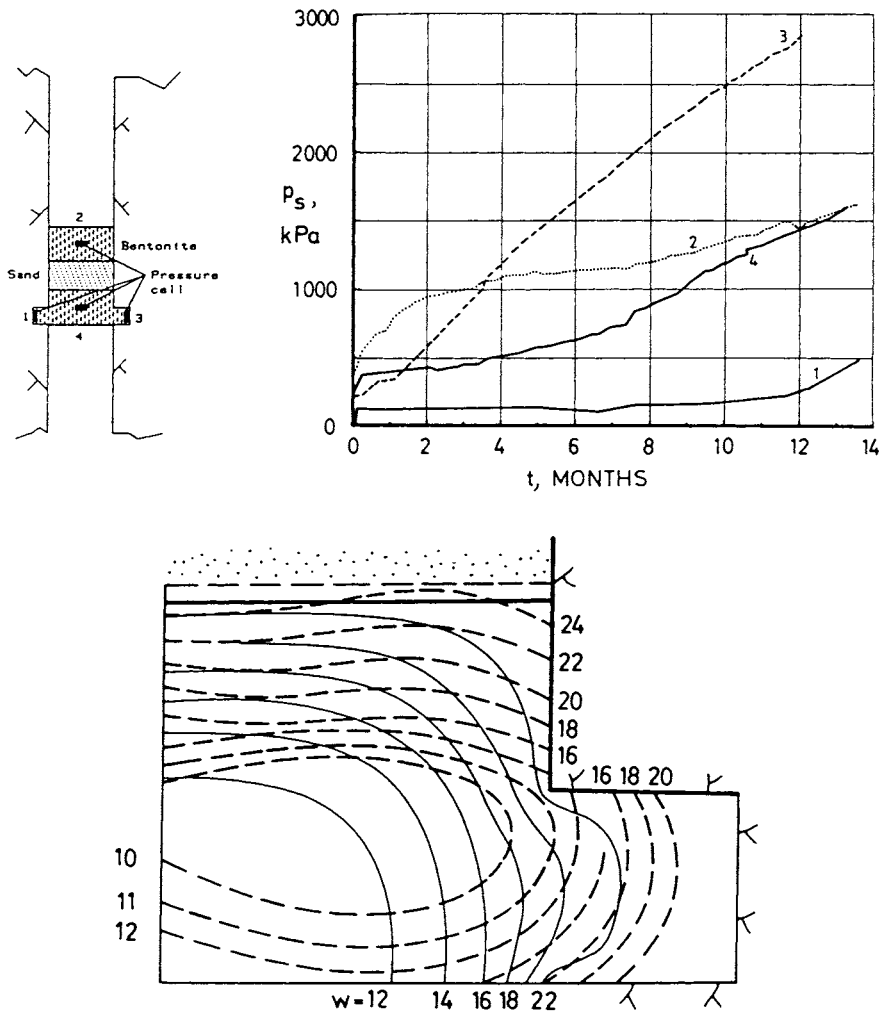


Figure 134 Maturation of plug of bentonite block masonry. Upper: Evolution of swelling pressure due to water uptake in the bentonite. The incongruent build-up was caused by inhomogeneous moistening due to the low groundwater pressure. Lower: Water content distribution in the lower part showing predicted (full lines) and actual (broken lines) “isomoistures”

The following major conclusions were drawn from the shaft plugging experiment with respect to the sealing power of highly compacted bentonite as evaluated from the recording of the outflow and from tracer testing:

1. The major rock structure component that led water from the injection chamber beyond the plugs in the reference (concrete plug) test was a steeply oriented fracture extending to a few decimeters depth into the adjacent rock. It was cut off by the bentonite-filled slot and was hence largely eliminated as a source of leakage
2. Significant leakage occurred along the rock/concrete contact in the reference test. It stopped completely when the concrete was replaced by highly compacted bentonite in the main test, primarily because of the effectively sealed contact and secondarily because of bentonite entering fractures and thirdly, and probably least significantly, through fracture compression by the swelling pressure.

Despite the obvious reduction in axial flow from the chamber when replacing the concrete by highly compacted bentonite, the reduction in net hydraulic conductivity of the “disturbed zone” was still not very significant. Thus, applying the “porous medium” model and assuming all the axial flow to take place in the 0.25 m deep and 0.5 m long zone adjacent to each plug, its axial conductivity was found to be about 10^{-8} m/s in the latest phase of the main test when the total outflow was of about 5 l/h at 200 kPa pressure, while it was about 20 to 50 times higher in the reference test, where probably 50 % of the leakage took place along the rock/plug contact. Since the hydraulic conductivity of compacted bentonite with a bulk density at complete water saturation of about 2 g/cm^3 is around 10^{-14} m/s and practically no leakage can have taken place along the rock/plug contact, it is clear that significant flow must have taken place in the rock outside the bentonite-filled slot, i.e. in the stress-disturbed zone.

General aspects

Beyond doubt, plugs of highly compacted bentonite extending into slots cut in the adjacent rock form very effective seals primarily because they are virtually watertight and establish an intimate contact with the surrounding medium and also since they self-heal because of the

significant swelling potential: any difference in void ratio and hence swelling pressure of adjacent elements is evened out. The net sealing power depends very much on the depth of the slots and the character of the water-bearing structures of the nearfield rock. Thus, extension of the bentonite plugs to reach at least 0.5-1 m into the rock is expected to increase their sealing ability considerably. Naturally, the expansion potential in axial direction of masonries of highly compacted bentonite means that they need to be supported by densely compacted low-compressible backfills or other effective long-lived buttresses.

SEALING OF DEPOSITION HOLES WITH CLAY GROUT

The 0.76 m diameter heater holes with a depth of about 3 m in the BMT drift were grouted by use of the LID megapacker shown in Figure 101 using 100 % Na bentonite and 50/50 Na bentonite/quartz powder grouts [17]. The device was a prototype which caused rather substantial loss in energy at the dynamic grouting that was applied and future refinement is expected to improve it considerably. The grouts had low densities, i.e. 1.08 and 1.2 g/cm³ of the pure bentonite and the mixture, respectively.

The rock structure exhibited in the two holes, which were 6 m apart, can be described as follows (cf. Figure 103):

From the tunnel floor down to 0.75 m

The number of potentially injectable fractures was 15-25, four of which were clearly water-bearing. The latter can be taken to represent blast-activated 5th order discontinuities except for one or two that may represent 4th order breaks

From 0.75 m to 3 m depth

The number of possibly injectable fractures was 8-10 fractures, of which 2-4 were clearly water-bearing. The latter may represent 4th order breaks

One of the holes, i.e. No 1, was intersected in its uppermost part by a 3rd order fracture zone (RP) as indicated in Figure 95, which gave a higher fracture frequency in this hole than in hole No 2. The average hydraulic conductivity, which was measured by use of the megapacker, manifested the existence of a "disturbed zone" extending down to about 1.5 m depth.

The upper 0.75 m, representing the most strongly blast-induced disturbance with new fractures generated, had an average conductivity exceeding 5×10^{-7} m/s in both holes. The rest of hole No 1 had a conductivity of 2×10^{-9} to 6×10^{-9} m/s, which is representative of 3rd order discontinuities. The interval 0.75-1.5 m depth in hole No 2 had a conductivity of about 5×10^{-8} m/s, while it was 3×10^{-10} m/s in the rest of the hole, which is representative of rock with only 4th and higher order discontinuities [17].

Using the conductivity values and the recorded number of channels in the fractures that discharged water, the aperture of the channels could be estimated, which made it possible to predict the penetration depth of the grout and the net hydraulic conductivity after grouting. The expected penetration depth was up to 0.6 m in the uppermost part of the holes and 0.1-0.35 m in the larger part of the holes and the net hydraulic conductivity after grouting was predicted to become 2×10^{-10} to 8×10^{-11} m/s, which turned out to be in very good agreement with the actually recorded conductivities. Although the grouting operations can certainly be regarded as successful one finds that it is not possible to reduce the bulk conductivity to less than about 10^{-10} m/s.

The grouting operation was followed by heating the walls of the closed holes to somewhat less than 100°C for about 3 months after which the conductivity measurements were repeated. The results, which are shown in Figure 135, illustrate that although the conductivity was generally lower than before grouting, it had increased by 2 to 50 times from the conditions after grouting. The reason for this was the block movements caused by the heat pulse. They took place over the entire length of the holes and the fact that the conductivity was even somewhat higher after heating than before grouting in the lower part of hole No 2 shows that it was not the grout that had degraded by the heating.

It is concluded from the heater hole experiment that grouting by use of dynamic technique yields penetration of the grout and reduction in hydraulic conductivity that are in good agreement with predictions. A major finding is that heating has a substantial effect on the rock and yields movements that significantly reduce the sealing effect of preceding grouting. This latter experience is of fundamental importance for strategic sealing of repositories for heat-producing waste.

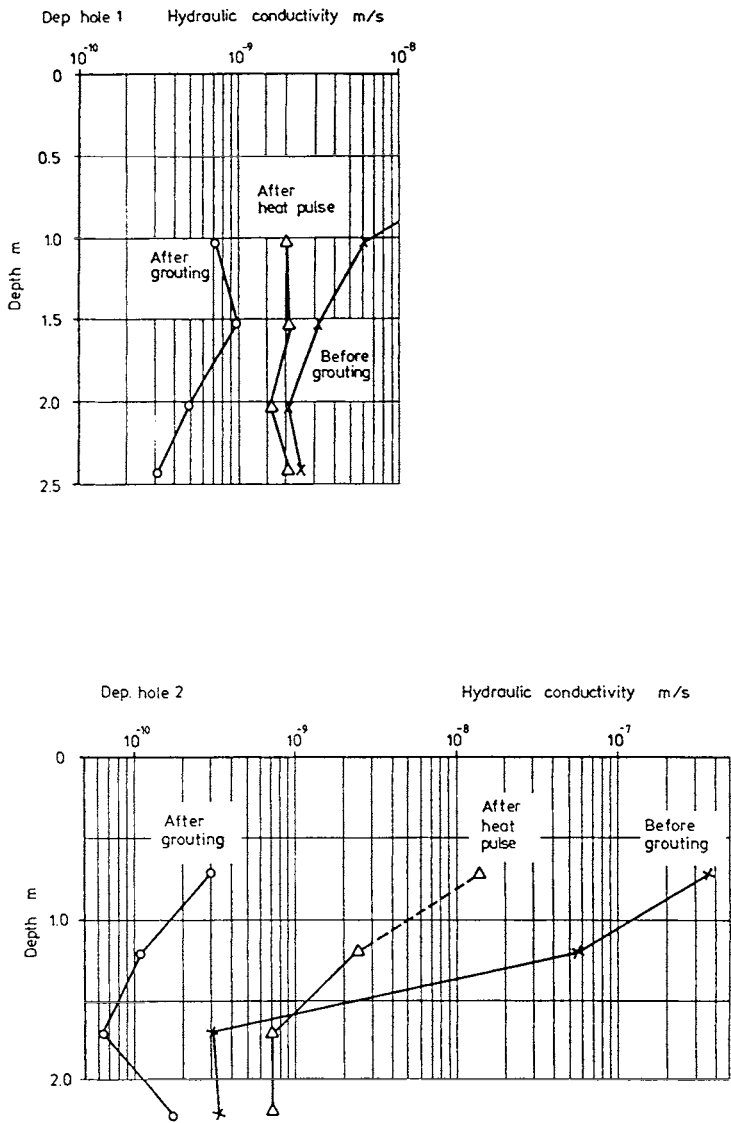


Figure 135 Evaluated hydraulic conductivities in hole No 1 (upper) and No 2 (lower)

SEALING OF “DISTURBED ZONE” WITH CEMENT

The investigation at Stripa which confirmed that the enhanced axial hydraulic conductivity of the “disturbed zone” adjacent to the periphery of blasted tunnels is predictable was followed up by an attempt to seal this zone by grouting [33]. For this purpose a sealing principle termed “hedgehog” grouting was applied, implying drilling of a large number of closely located short holes over the entire periphery of the 12 m long inner part of the BMT drift. The study comprised three phases, a reference test for determining the axial conductivity of the blast- and stress-disturbed zones, a second experiment with “hedgehog” grouting, and a third phase applying “curtain grouting” (Figure 136).

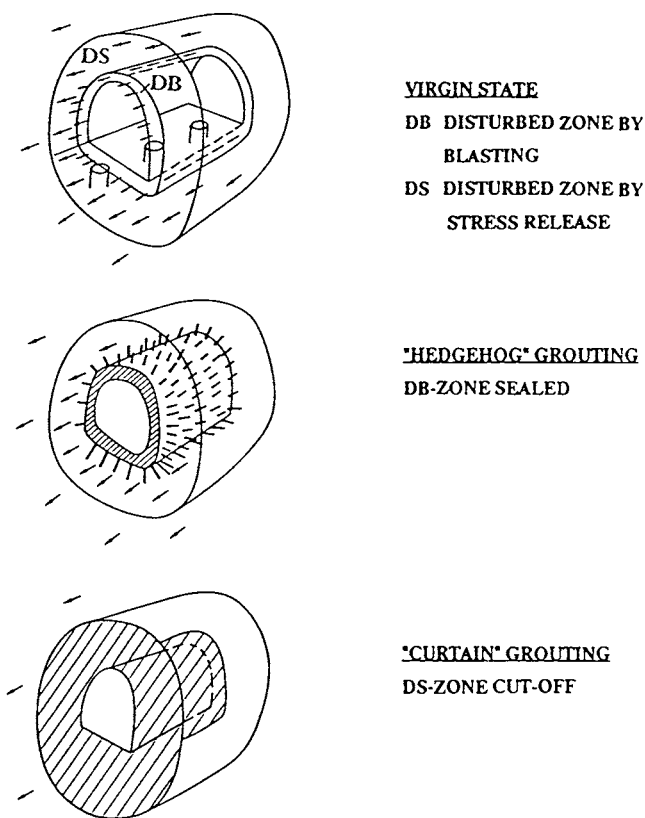


Figure 136 Schematic picture of the three test phases for investigating how the excavation-disturbed zone around blasted tunnels can be sealed

The “hedgehog” grouting was made by applying both static and dynamic injection techniques, using Alofix cement, 1.4-3 % superplasticizer and w/c in the interval 0.5-0.7. The number of percussion-drilled holes, which had a spacing of 0.4-1.15 m and a length of 1-1.2 m, was 350, and 80 of them were characterized individually with respect to the hydraulic conductivity, which formed the basis of a prediction of the grout penetration and the sealing effect as in all other Stripa sealing tests [33]. Dynamic injection was tried first and gave some heave and static injection was applied in order to minimize the block movements, which naturally gave some reduction in grout penetration and hence in sealing effect.

The effect of the “hedgehog” sealing attempt was evaluated by repeating the large-scale “Macro Flow Test” used for recording the hydraulic conductivity of the “disturbed zone” (Figure 97). The outcome of the measurements was that the disturbed zone had maintained its hydraulic conductivity and hence that the “hedgehog” grouting had no noticeable sealing effect. The major reasons for this were concluded to be debris from disintegrated fracture fillings and crushed rock prevented grout from entering fractures, but block movements probably contributed to the lack of sealing effect.

The third phase, i.e. the curtain grouting, could not be accomplished because of budget reasons. However, its expected effectiveness can be estimated by considering the rock structure as evaluated from inspection of the holes of curtains drilled around blasted drifts at Stripa (Figures 137, 138 and 139) and applying the outcome of the grouting of discrete fractures at the outer end of the tunnel plug described above.

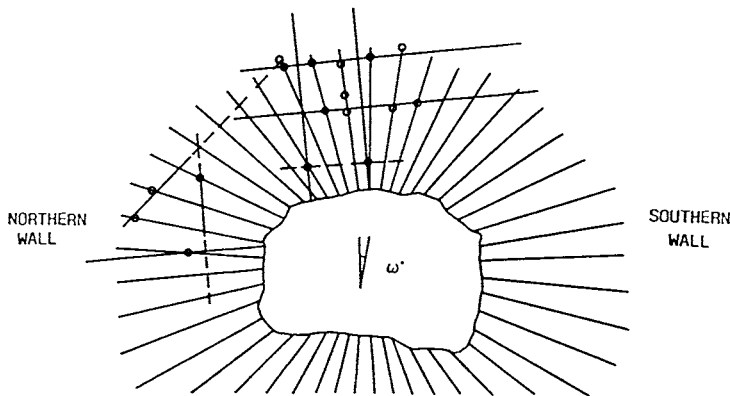


Figure 137 Water-bearing fractures identified in radially drilled borehole curtain in the walls and roof of a 4 m high drift

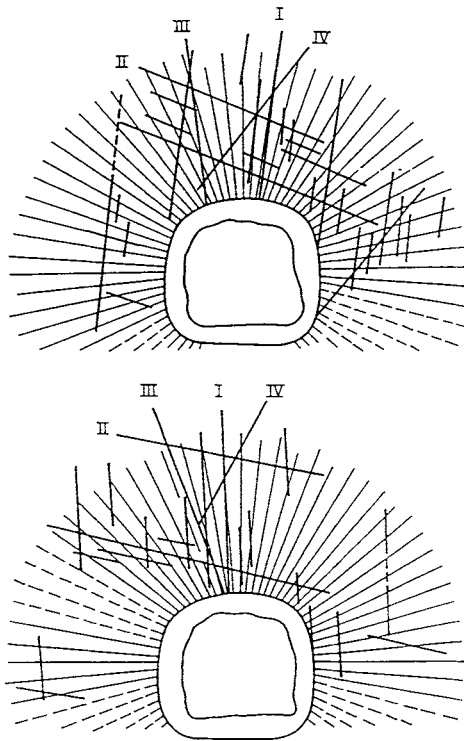


Figure 138 Positions and orientations of all water-bearing fractures in two parallel bore-hole curtains drilled radially from the BMT drift. The distance between the curtains is 12 m. One can identify three major fracture sets I, II, III and IV forming two rhombohedral structures (one by I and II, the other by III and IV). The outer solid contour of the 4.5 m high drift represents the base of a slot from which the holes were drilled

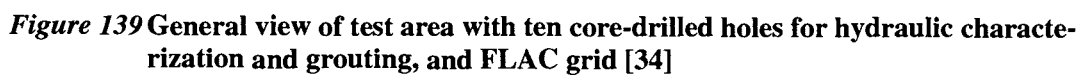
The patterns of water-bearing and hence groutable fractures could thus be regarded as characteristic of 4th order discontinuities with some integrated 5th order fractures activated by blasting and stress release. One finds that the possibility of hitting channels that can be grouted is fairly good when the spacing of the curtain holes is as small as in the examples in Figures 138 and 139, while it is estimated that the chance is small if the number of holes is reduced to about 25 holes per curtain. This could partly be compensated by applying high injection pressures, but the fact that the grout needs to flow over considerable distances through the tortuous system of interconnected channels requires that the channel aperture is several hundreds of micrometers to yield a significant sealing effect.

If the third grouting phase had been performed in the planned manner, i.e. with all the holes in Figure 139 injected, and using injection pressures of several MPa, which would have been possible because of the support of the rock offered by the big concrete bulwark, the average hydraulic conductivity of the blast- and stress-disturbed zone would probably had been reduced by at least 2 orders of magnitude, i.e. to about 10^{-10} m/s.

A general conclusion is that there is no or little use in grouting the most shallow part of the “disturbed zone” of unsupported tunnels and shafts. The only effective way of sealing this zone by grouting is to inject closely spaced holes in curtains around the periphery where effective support of the rock can be arranged in the form of bulwarks.

SEALING OF FRACTURE ZONE WITH CEMENT

Figure 139 shows the test area with the about 20 m² large grouted part of a fracture zone, which was a few decimeters wide, and the element net used for predicting the change in inflow into the drift and the associated pressure change. The computation gave the change in pressure indicated in Figure 140, which is particularly important because it demonstrates the typical effect of successful grouting, namely a pressure increase that limits the reduction in inflow in the testing period but causes a significant redirection of flowing groundwater away from the drift once the tunnels or shafts have been backfilled.



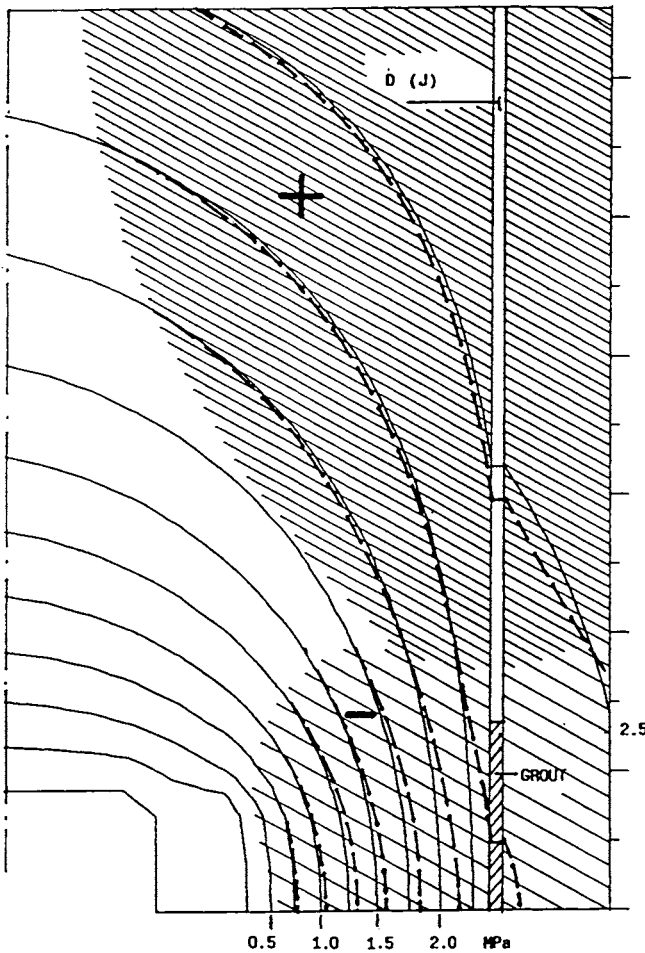


Figure 140 Regimes of piezometric increase (+) and decrease (-) by reducing the hydraulic conductivity of the D-zone by grouting [34]

A small part of a steeply oriented natural fracture zone of 3rd order type, i.e. with a width of 0.75 m and a hydraulic conductivity on the order of 10^{-8} m/s (J in Figure 22), was successfully grouted to yield the evaluated average figure 10^{-9} m/s [34]. The spacing of the ten core-drilled holes for hydraulic characterization and grouting was about 0.7 m and their length 7 m. Individual pressurizing with simultaneous inflow measurements in the other holes gave the pattern of hydraulic interaction in Figure 141, which shows that only two of the holes had hit dominant channels. The sealing effect was measured in several ways but the most directly

observable indication of the sealing effect was the redistribution of moisture given off from the walls and roof as indicated in Figure 142. Other recorded changes were the pressure build-up caused by the decreased hydraulic conductivity (Figure 140) and the redirection of flow as recorded by tracer tests.

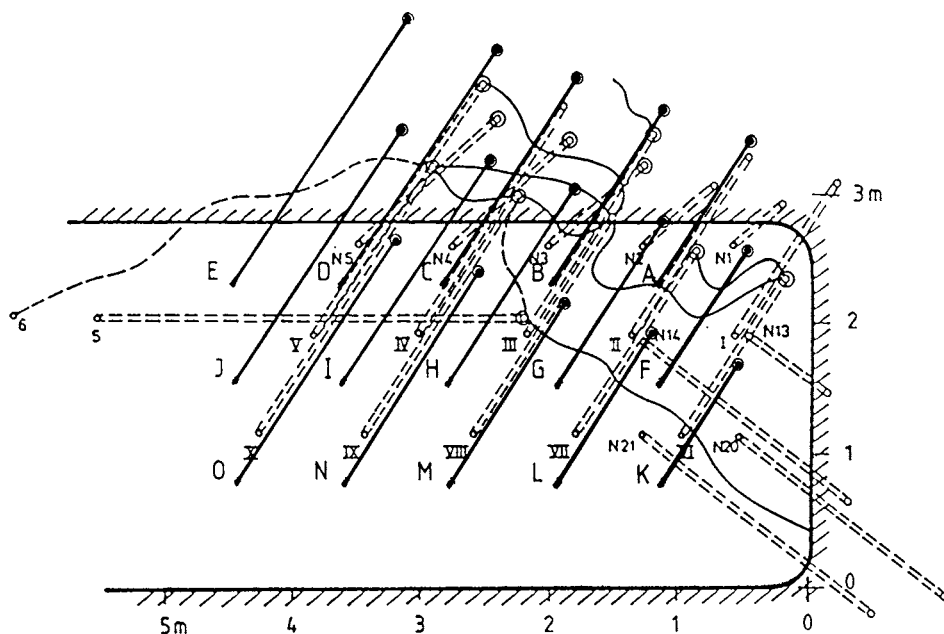


Figure 141 Hydraulic interaction of ten parallel drillholes penetrating the fracture zone. View of the tunnel wall (cf. Figure 139). Full lines show schematic channels and broken ones possible hydraulic connection through channels

The reduction in hydraulic conductivity of the local part of the zone from initially about 10^{-8} to around 10^{-9} m/s is estimated to be less than what could have been achieved by changing two parameters: the injection pressure and the hardening rate of the grout. Thus, it is estimated that with the support of the grouted zone that would be offered by the surrounding rock if grouting had taken place prior to the excavation, the injection pressure could have been increased from about 3-4 MPa (average of peak pressures and constant "backpressure" of 1 MPa)

to 5-6 MPa, which should have caused slight largely elastic channel widening and more effective penetration of the grout. The slow hardening of the cement caused piping as demonstrated by outflow of cement through fractures along the packers and after removal of the packers the day after injection. It is estimated that these two changes would have decreased the average hydraulic conductivity of the grouted part of the J-zone from initially about 10^{-8} to no more than 10^{-10} m/s, i.e. by two orders of magnitude. In fact, using clay instead of cement could have resulted in a reduction down to around 10^{-11} m/s in agreement with the theoretical analysis given earlier in this chapter.

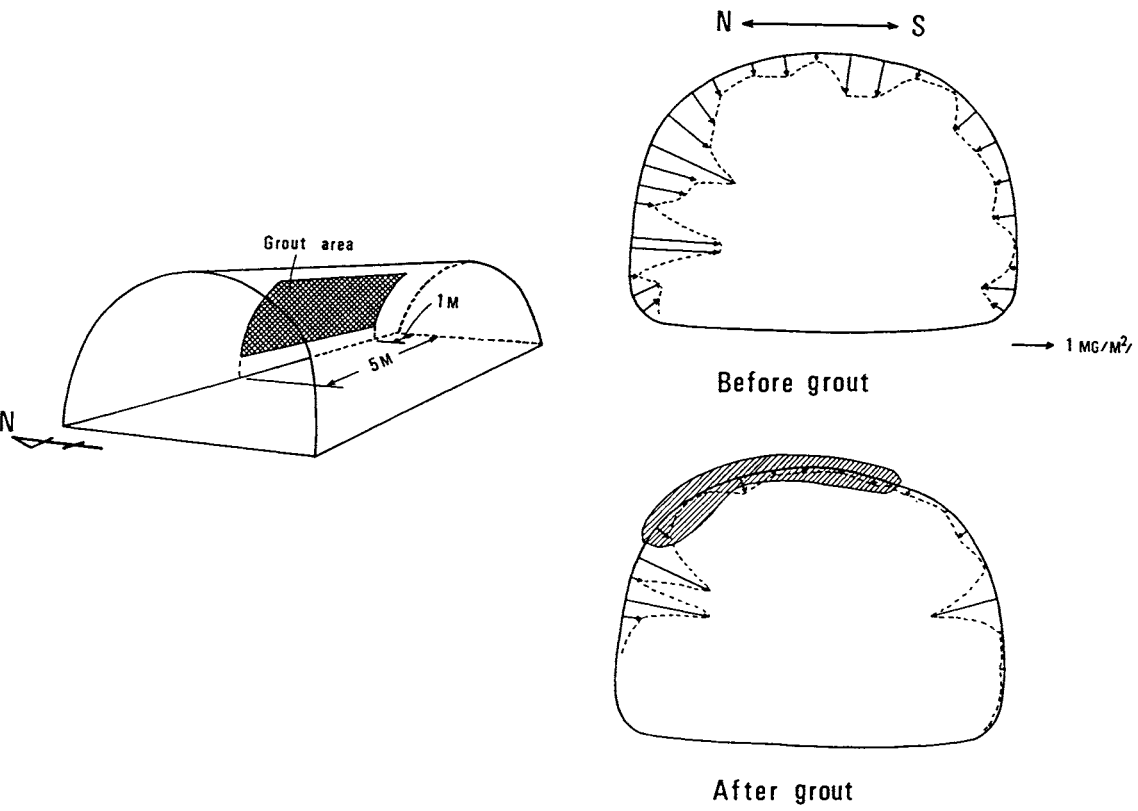


Figure 142 Reduction in evaporation from the rock surface caused by the grouting [26].
Hatched area shows maximum drying

The experience from grouting the 3rd order zone at Stripa and from a number of other attempts to seal moderately water-bearing structures is that the spacing of the boreholes must be small (0.5-1 m), the injection pressure as high as possible with respect the rock support (pregrouting is best), and the grout strength regain rapid.

GENERAL ASPECTS

The conclusions from large-scale application of grouting for sealing fine-fracture rock agrees well with those from theoretical considerations and modelling of grout penetration and of the net sealing effect. The major criteria are:

1. Effective sealing by grouting requires small spacing of the holes, high injection pressures and good support of the injected rock
2. The optimum grout must have high fluidity and regain strength quickly after injection, and also maintain a certain ductility and expandability
3. Grouting is not worth while where rock block movements by heating or tectonics are expected since channels that are not filled with grout will be activated and reduce the sealing effect
4. Long-term performance requires temperatures that do not significantly exceed about 60°C

These criteria imply that clay-based curtain grouting of the “disturbed zone” around temporary plugs of concrete and possibly also around permanent plugs in deposition tunnels may work over long periods of time, and that cement-based pre-grouting of low-order zones that will be crossed by deposition tunnels may work over a considerable period of time, i.e. thousands of years, provided that the zones will undergo only insignificant strain. Grouting of deposition holes is not expected to be effective over long periods of time because of heat-induced block movements. Still, sealing of their uppermost parts (cement) for limiting inflow from the floor is practical and probably necessary.

3-7.5 Strategic sealing

GENERAL

Considering the conclusions from the preceding chapters and confining ourselves to the two issues: sealing of the **disturbed zone** and sealing **natural fracture zones**, the interest should be focused on three types of sealing: 1) Plugs of concrete with “O-ring”-type seals of highly compacted bentonite combined with bentonite-filled slots in the surrounding rock, possibly also combined with strategic grouting (few discrete fractures) or curtain grouting, 2) pre-grouting of natural fracture zones that will be crossed by tunnels or shafts, and 3) grouting of deposition holes for limiting water inflow in the phase when canister-embedding clay and canisters are emplaced.

CUT-OFF OF THE “DISTURBED ZONE” BY GROUTING (CASE 1)

Figure 143 illustrates a KBS3 tunnel located in rock characterized by relatively conductive 3rd order discontinuities with a spacing of 50 m, one of them appearing at the end of the tunnel and the issue is to find out if grouting can reduce the axial flow through the “disturbed zone” significantly. The difference in water head over the 50 m distance between the zones is assumed to be 1 m, yielding the hydraulic gradient 2×10^{-2} , which may be the case under real circumstances in the first few thousand years. Both the inner 3rd order fracture zone and the excavation-disturbed zone are taken to have an initial hydraulic conductivity of 10^{-7} m/s. The conductivity of the 15 m diameter wide part of the fracture zone, which serves as the driving force for water flow in the local area, is assumed to be 10^{-10} m/s after grouting, which is expected to be achieved without difficulties by utilizing the rock support for grouting before the drift is fully excavated. The backfill in the tunnel is bentonite/sand with an initial conductivity of 10^{-10} m/s. The surrounding virgin rock is assumed to have a conductivity of 3×10^{-11} m/s.

The flow through the “disturbed zone” along the tunnel backfill as calculated by FEM using the element net in Figure 144, will be 990 liters per year before and 38 l/y after grouting, i.e. a significant reduction. The regional hydraulic gradient is expected to drop to 10^{-3} after a few thousand years, which brings down the annual flow through the disturbed zone to a couple of liters.

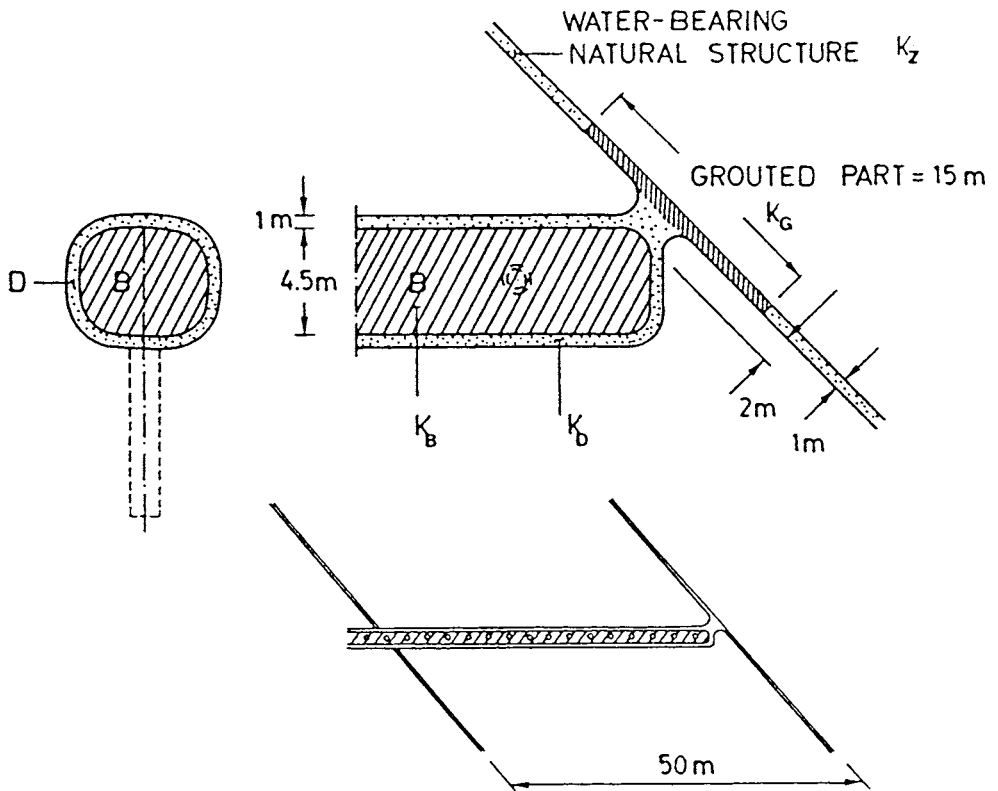


Figure 143 Example of KBS3 tunnel case used for estimating the change in axial flow through the disturbed zone D by grouting the inner 3rd order zone (Case 1)

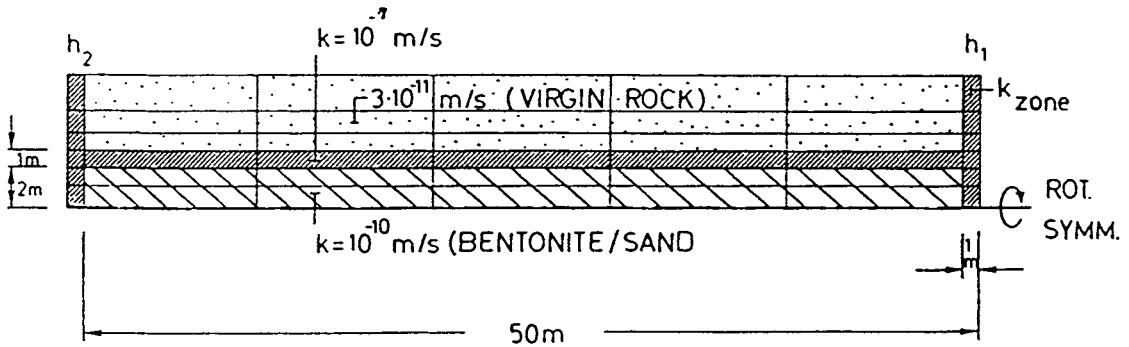


Figure 144 FEM element net used for the flow calculation in Case 1

CUT-OFF OF THE “DISTURBED ZONE” BY SLOT WITH HIGHLY COMPACTED BENTONITE (CASE 2)

Figure 145 illustrates a case with 100 m spacing of intersected 3rd order zones but otherwise the same geometries, conductivities and hydraulic gradient as in Case 1. The larger spacing of the zones represents a slightly more conservative case and the issue is to find out to what extent the axial flow through the blast-disturbed zone can be reduced by constructing 3 m long plugs of highly compacted bentonite extending 1 m into slots cut through the disturbed zone. Such an arrangement may be equivalent to concrete plugs with “O-ring”-type seals of

bentonite depending on how the chemical interaction of cement/clay affects the net hydraulic conductivity.

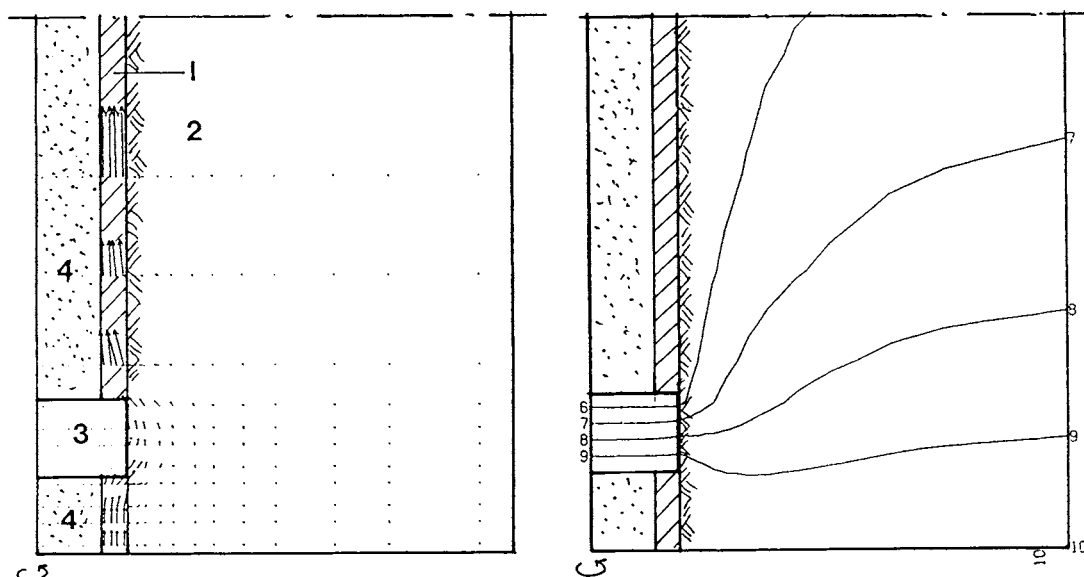


Figure 145 Example of KBS3 tunnel case used for estimating the change in axial flow through the disturbed zone D by applying a plug of highly compacted bentonite in the tunnel and in a peripheral slot (Case 2). 1) Disturbed zone, 2) Host rock, 3) Plug, 4) Tunnel backfill. Left: Redirection of flow. Right: Isobar pattern

The calculated flux through the blast-disturbed zone applying FEM is found to be 1100 l/y before any sealing is made, i.e. about the same as in Case 1, while it will be about 9 l/y after applying the plugs. This way of cutting off groundwater flow in the disturbed zone is hence concluded to be very effective. However, it remains to find out how the slot cutting can and

should be made for avoiding a second “disturbed zone” by the slot cutting. Also, parameter studies of the influence of the length of the plug should be performed before designing it. Preliminary estimates suggest that the optimum design principle from technical and economic points of view is to use two or more relatively short plugs in series, with very dense backfill in between, located where the surrounding rock is very tight. The plug construction should be adapted to the local rock structure.

SEALING OF DEPOSITION HOLES (CASE 3)

It is concluded from the preceding examination of how optimum grouting can be made in repositories that sealing by cement grouting of the uppermost part of deposition holes for minimizing water inflow at the application of waste and canisters is suitable and probably necessary. Grouting of fractures that intersect deposition holes deeper down may not yield effective or long-lasting sealing effects, but may be required for reducing water inflow at the application of canisters and bentonite in the construction phase, especially if the holes are going to host two or more canisters, because they will then be long enough to be intersected by a flatlying 3rd order discontinuities, which is expected to require sealing. The example given here refers to this latter application as well as to the general case of sealing the uppermost part of deposition holes.

Figure 146 shows a deposition hole intersected by a major 4th order fracture or a thin 3rd order zone grouted so that a disc-shaped annulus of sealed rock is formed around the hole. Taking the hydraulic conductivity to be 3×10^{-11} m/s of the virgin rock, i.e. that of the virgin Stripa rock, and to be 10^{-7} m/s of the 0.1 m wide fracture zone before and 5×10^{-10} m/s after grouting - which is very conservative - one finds, by applying FEM, that the water inflow into the hole is 2.2 l/h if the grout extends $a=0.3$ m from the periphery and 1.3 l/h if the extension is 1.0 m. If no grouting is made, the inflow is 9.4 l/h, which may be unacceptable from a practical point of view. More effective sealing can be obtained using high injection pressures but the earlier mentioned fact that sealing causes build-up of higher water pressure behind the sealed zone reduces its effectiveness in the period when the hole is open, which is amply demonstrated by the sealing-induced pressure increase around the deposition hole in our example (Figure 147).

Naturally, sealing must be performed in a rational and cost-effective fashion, which requires that standard procedures are applied. Thus, once the location of the deposition holes has been decided, which should be based on simple testing of pilot holes and on mapping of major fractures that intersect the holes, a plan for routine sealing should be worked out.

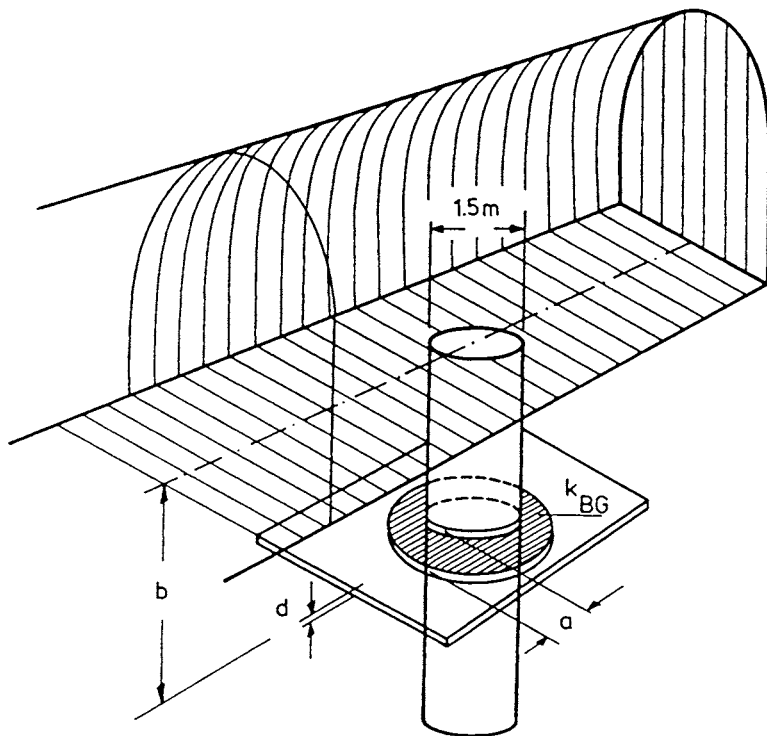


Figure 146 Schematic picture of deposition hole intersected by a flatlying fracture zone with a width d at a distance b from the tunnel floor (Case 3)

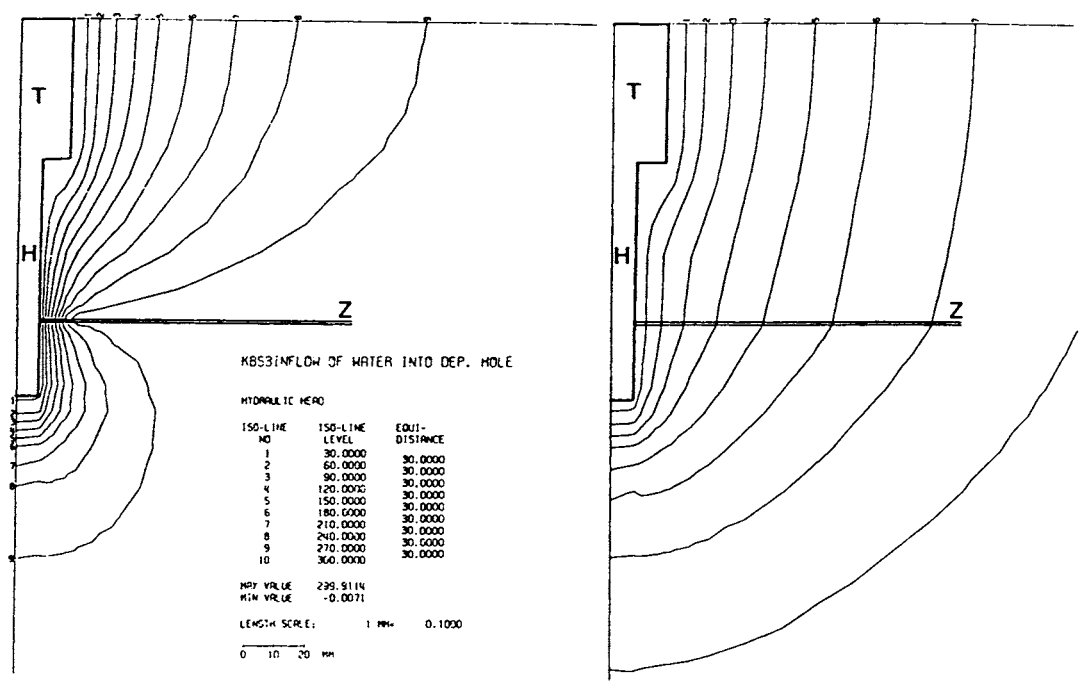


Figure 147 Isobars before (right) and after sealing by grouting. T) tunnel, H) deposition hole, Z) pervious zone with 1 m penetration depth of the grout

3-7.6 Complete system of seals in a repository

ROCK STRUCTURE MODEL

We will take the rock structure model in Figure 48 and the repository model in Figure 49 as a basis for illustrating how one can estimate the location, type and amount of seals that may be required in KBS3-type repositories, assuming that the outline of the repository in the latter figure is at optimum with respect to the orientation and frequency of major sets of discontinuities, as well as to the required distance to these discontinuities, and to the prevailing rock stresses. In principle, it implies that the deposition tunnels are oriented W/E and the main drifts oriented N/S. The schematic repository plan in Figure 49 represents about one third of a complete 6000 canister KBS3 repository. The amount of seals given here refers to a complete repository of this sort disregarding shallow seals in access ramps and all sorts of seals in ventilation and elevator shafts.

Considering in the present example only steeply oriented rock structures and taking the structural model to be a relatively conservative example of the frequency of low-order zones, which are the ones that require seals in the first place, one finds that the access tunnel or ramp leading down to the repository level passes through one 1st order discontinuity at this level, and that the main drifts, from which the deposition tunnels extend, make 13 intersections with 2nd order zones and about 100 intersections with 3rd order zones. All the intersections with 2nd order zones and presumably 30 % of the intersections with 3rd order zones require grouting, bolting and possibly concrete lining and shotcreting for stabilizing the rock and for reducing water inflow in the construction period. These operations can be made by applying ordinary construction techniques.

The deposition tunnels will interfere with 3rd order zones and, of course, with 4th order discontinuities. Assuming 50 m spacing of the steeply oriented 3rd order zones one finds that there will be 3 intersections with such zones per tunnel as an average, i.e. about 500-1000 intersections in a 6000 canister repository. For the less conservative approach with 100 m spacing of the 3rd order zones, the total number of intersections may be on the order of 500.

SEALING OF THE “DISTURBED ZONE” - OPTIONS

A major conclusion from performance analyses of major repository concepts, which will be examined in Chapter 5, is that the axial flow through the “disturbed zone” of blasted deposition tunnels of a KBS3 repository should be significantly lower than 1000 l/y in order to pre-

serve the bentonite component of 10/90 bentonite/sand backfills. This implies effective cut-off of the flow through the disturbed zone by use of either of the two methods described earlier in this chapter, i.e. grouting the zones or constructing plugs and cutting slots around the periphery for filling them with highly compacted bentonite. A further issue that must be considered is the need for applying plugs at the outer ends of the deposition tunnels. If these plugs are designed in the fashion described, i.e. by cutting slots that are filled with compacted bentonite, many of them can serve also as cut-offs of the flow in the excavation-disturbed zone required where tunnels are crossed by one steep 3rd order zone. An illustration of what this may look like is given in Figure 148. In practice, two plugs - one on each side of the fracture zone may be suitable or even necessary.

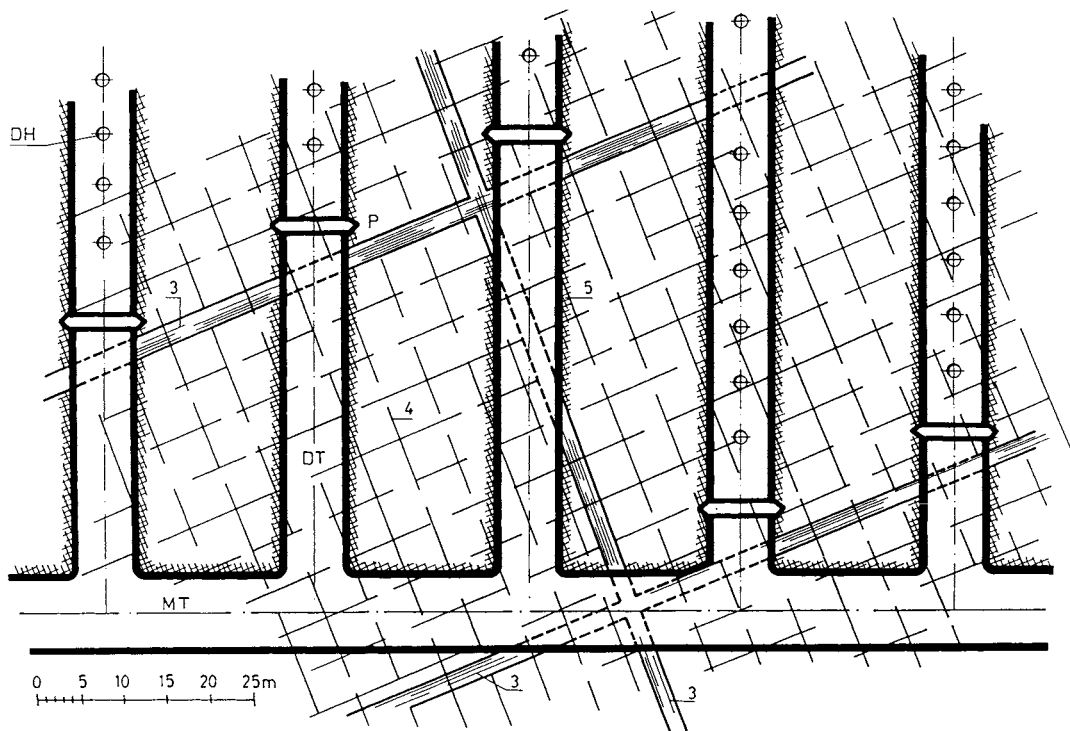


Figure 148 Plan view of part of KBS3 repository. MT is main drift, DT deposition tunnel with vertical holes for canisters. Possible sites for plugs in the tunnels are indicated. Figures denote discontinuities of respective order

SEALING OF DEPOSITION HOLES

The relatively low frequency of steeply oriented 3rd order zones that intersect the deposition tunnels according to the applied rock structure model suggests that only a small fraction of the tunnel length has to be sacrificed if the distance between the center of such zones and the nearest deposition hole can be taken as 5 m. However, an additional fraction of the tunnel length will have to be given up for the construction of plugs adjacent to intersecting fracture zones and the net fraction that can be used for locating deposition holes with 6 m spacing can therefore be estimated at 70-90 %.

It is self-evident and shown explicitly in Figure 149 that all deposition holes will be intersected by 4th order discontinuities, i.e. water-bearing rather long-extending fractures which, together with the excavation-disturbed, very shallow zone around the deposition holes are responsible for the groundwater percolation of the nearfield of the holes and thereby for the migration of radionuclides and elements that cause degradation of the canister-embedding clay (K^+). Critical stress conditions may activate a few 5th order breaks and a realistic 3D picture of the actual sets of water-bearing fractures may hence be as indicated in Figure 149, which also illustrates probable passages for hydrogen gas emanating from radiolysis and corrosion of steel-containing canisters. As demonstrated earlier in this chapter and in the preceding one, 4th order fractures exposed in large-diameter holes can be effectively sealed by grouting using megapacker technique, while injecting holes drilled around and parallel to them is not effective because of the small chance of hitting the water-bearing channels. The total number of megapacker injections is estimated to range between 2000 and 10 000 for a complete KBS3 repository, assuming about 8 m deep holes.

Adding up the number of grouting events required for effective sealing in a KBS3 repository, including grouting of some 2nd order fracture zones and a number of 3rd order zones and strongly water-bearing 4th order fractures, one arrives at the approximate figures given in Table 10. They refer to the considered rock structure model and only concern steeply oriented 2nd and 3rd order zones. The right column of the table gives an indication of the longevity of the seals with respect both to chemically and mechanically induced changes. These matters will be further considered in Chapter 5.

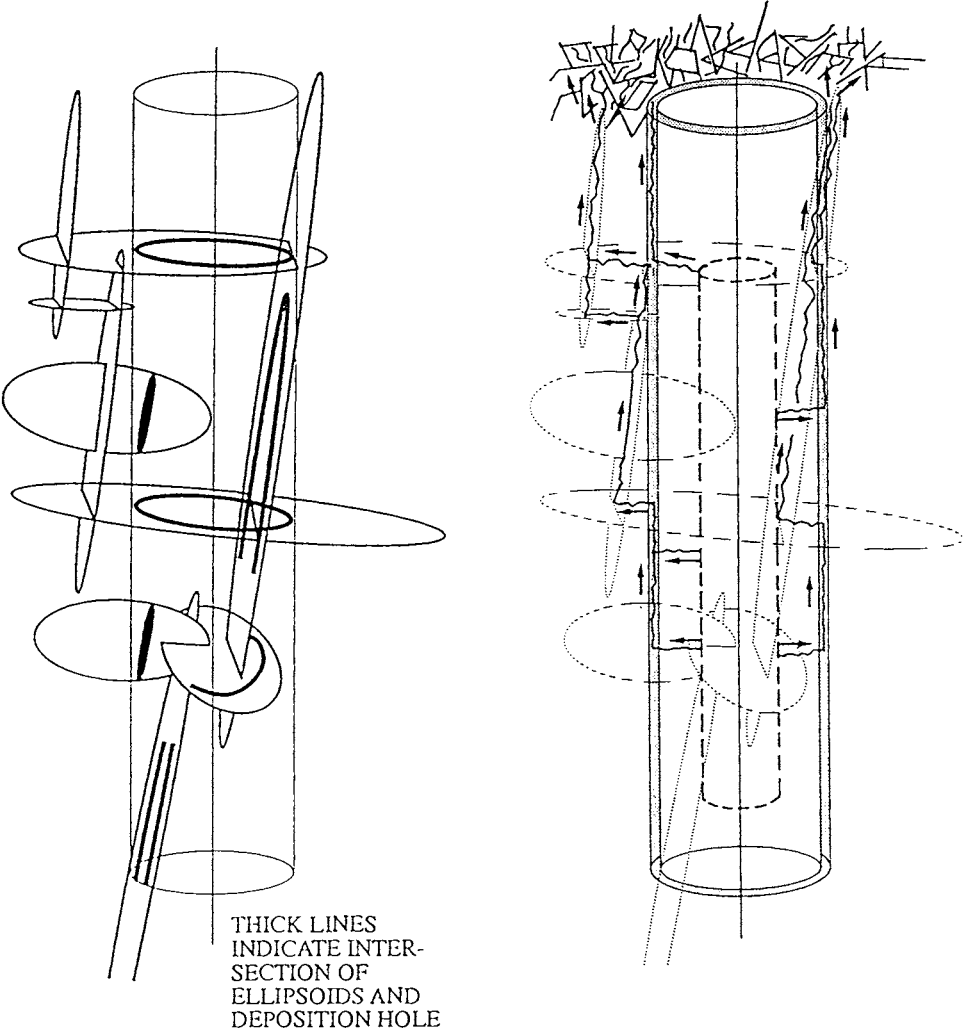


Figure 149 Schematic picture of KBS3 deposition hole. Left: Generalized rock structure. Right: Channel-type passages for water and gas

Table 10 Types and amounts of seals in 6000 canister KBS3 repository

Seal type	Construction period	Long-term	Performance
Grout seals in tunnels	40-60	-	Short
Grout seals in deposition holes	2000-10 000	-	Short to intermediate
Tunnel plugs with “O-ring” bentonite seal extending into rock slot	-	1000-2000	Long

Confining ourselves to consider the parts of a repository where deposition of canisters will take place, i.e. the deposition tunnels, it is clear from Table 10 that the number of seals is large and that it is required to make a detailed analysis of the actual need for sealing, and of the sealing efficiency, as well as of finding an optimum design principle of the plugs.

3-7.7 Design before construction or “as you go”?

GENERAL

Even very detailed rock investigations will reveal only a fraction of the rock structural features that are of importance for the selection of proper location, orientation and design of repository rooms and for sealing activities. This raises the question how detailed the rock investigations and design work should actually be and to what extent critical conditions may prevail due to structural features and stress conditions that escape identification, which naturally requires sufficient safety factors for the isolating function ascribed to the rock. Considering that even the moderate strain caused by existing regional and local stress fields may change the properties of a rock mass significantly in a long time perspective and that excavation-induced alteration of stresses and heat effects in HLW repositories cause significant changes in bulk rock properties, which is further enhanced where tectonics and glaciations

take place, one realizes that the behavior of the host rock of a repository is difficult to foresee. Very detailed room design and planning of sophisticated seals based on rock structure models derived from comprehensive preinvestigations are hence questionable. As pointed out already in the introductory chapter, this suggests that the rock mass should be considered as a mechanical protection of the “chemical apparatus”, i.e. the nearfield, rather than as a tight isolation. Applying this philosophy, the part of the design work that concerns the rock should not be overdone and, to a large extent, performed “as you go”.

DESIGN OF ROOMS

General repository plans like the one in Figure 49 for preliminary location and design of disposal rooms and for rough estimation of where and how seals should be arranged can be worked out on the basis of the rock investigations mentioned in Chapter 2. Naturally, it is of great practical importance is also to identify where difficulties can be expected, i.e. where construction may be delayed or require special techniques, as where clay- and strongly water-bearing 1st and 2nd order discontinuities have to be crossed, and to adapt the plan so that the number of such crossings is at minimum and so that the rooms become properly oriented with respect to the rock structure and stress situation.

The vast experience from underground construction in crystalline rock all over the world makes it highly probable that excavation of ramps and main drifts as well as of large disposal rooms can actually be made according to the planning, but adjustments may be necessary or preferable if structural features are met with that cause difficulties, like flatlying zones that have escaped attention in the rock characterization phase. Rock investigations continue in conjunction with the excavation work in the form of core drilling of pilot holes in which rock stress measurements, hydraulic testing and radar measurements are performed. By this, the main drifts can be suitably shaped for minimizing excavation-induced disturbance and for improving their stability, and a basis is obtained for designing also blasted deposition rooms, to which we will return in the subsequent chapter. The successively improved understanding of the large-scale rock structure, especially with respect to the occurrence of 3rd order zones, which may be difficult to identify by use of remote techniques and logging in single boreholes before excavation has started, makes it possible to work out improved plans for location of the deposition tunnels but they remain preliminary until detailed investigations have been performed as a preparation of the excavation of the individual room. Such complementary investigations preferably comprise core and percussion drilling along the central axis of the tunnels and along the periphery of the planned deposition tunnels for core mapping, hydraulic testing and rock stress measurements. The aim is naturally to obtain a picture of the rock struc-

ture that is sufficiently extensive and detailed to make a relevant performance analysis for evaluation of the isolation potential of the individual barriers and of the integrated system of barriers. By not asking too much from the rock mass, the comprehension of the rock investigations can be kept reasonably extensive and more focussed on the stability conditions in the construction and waste application phases than on the detailed hydraulic performance at distance from the canister holes.

A relatively important matter in the design is to choose a minimum distance between tunnels and deposition holes in order to avoid too much stress and heat interaction. This is achieved by applying basic rock mechanics with special respect to the rock structure, which typically yields a minimum spacing of blasted 5 m diameter tunnels of 20-30 meters, while overlap of temperature fields in HLW repositories is calculated by applying analytical or numerical methods as exemplified in the chapter on repository function. As indicated earlier in this chapter, the latter effect, which is important both for the rock strain and the longevity of the clay-based canister embedment and tunnel backfills, depends very much on the age and amount of HLW and on the spacing of the canisters. A great deal of the detailed final decisions concerning the design of the rooms has to be made rather late and in conjunction with the construction work, i.e. "as you go".

DESIGN OF DRILLED DEPOSITION HOLES

Selection of the size of deposition holes for hosting canisters with very hazardous waste has very little to do with the constitution and behavior of the host rock except for very deeply located repositories like the VDH (Figure 55). For more shallow repositories the size of the holes depends only on the size of the canister and on the required thickness of the canister-protecting embedment, as well as on the temperature, which is determined by the heat production and the heat conductivities of the embedment and rock. The heat conductivity of the clay embedment is commonly considerably lower than that of granitic rock, and the embedment therefore usually serves as insulation that raises the temperature close to the canisters. Hence, a considerable part of a thick clay embedment will be exposed to high temperatures and degrade, while a thin embedment will be less heated and degraded. Ongoing R&D work in Sweden has demonstrated that it is possible to produce very dense Na bentonite blocks with a high degree of water saturation and graphite additive that bring up the heat conductivity to nearly the same level as that of moderately quartz-rich crystalline rock. The presently considered KBS3 canister embedment of bentonite is about 0.4 m thick.

Short deposition holes like the about 8 m long and 1.6 m wide ones in a KBS3 repository can

be more suitably located than longer holes (VLH, cf. Figure 55) since rather cheap and comprehensive pre-investigations can be made to adapt the siting of short holes to the rock structure. A suitable procedure is to drill 10-15 m long slim holes vertically from the floor along the central axis of the deposition tunnel with a spacing of half the intended distance between the big holes, which is 6 m for KBS3. Simple hydraulic measurements and identification of water-bearing fractures are performed in all the holes and the most suitable sites are then selected, centering the big holes around the pilot holes that show the best rock conditions. Naturally, the exposure of the rock structure in the tunnel is of great help in the deduction of a local rock structure model as a basis of the final location of individual deposition holes.

DESIGN OF CLAY-BASED BARRIERS

The selection of suitable clay barriers depends on the rock conditions. Thus, for deep holes like VDH, drilling and “deployment” muds need to be composed to yield stabilization of the borehole walls in the drilling phase and support of the applied canisters thereafter. For concepts that make use of highly compacted bentonite as canister embedment, the density at complete water saturation should be in the interval 1.9-2.2 g/cm³ depending on the demand with respect to water tightness, anion diffusivity and risk of transferring rock shear strain to the canisters, which is controlled by the rock structure and stress conditions. For KBS3-type repositories with backfilled tunnels the composition of the backfill has to be decided on the basis of the required long-term performance of the clay component - which is a matter of groundwater chemistry and percolation rate - and of the required ability to support the tunnel roof and walls. Although optimum performance would imply different backfill composition and choice of density etc of the canister-embedment within individual rooms, a standard design with only one or a few different types of clay buffers and backfills should be applied for practical reasons and for simplifying testing for quality assurance.

SEALS

The location and design of seals of all sorts have to be decided very late and on the basis of relatively simple estimates of their performance because there will be limited time for performing comprehensive analyses of their sealing function. Thus, in the construction period the primary goal is rather to make a quick and strong effort to stop inflow of water when crossing difficult fracture zones than to spend time on planning and preparing ideal seals and crossings. We will consider methods for solving problems of this sort in Chapter 4. Design of seals, except for shallow plugs and for selection of major principles of how plugs and grou-

ing should be made, may have to be decided applying the principle “design as you go”.

3-8 References

- 1 Pusch,R. Rock mechanics on a geological base. Elsevier Publ.Co. (In press)
- 2 SKB. SKB 91 Final disposal of spent nuclear fuel. Importance of the bedrock for safety. SKB Technical Report TR 92-20, SKB, Stockholm, 1992
- 3 Forslind, E. and Jacobsson,A. Clay-water systems. Water a Comprehensive Treatise, Vol.5. Plenum Press, New York and London, 1975
- 4 Bennet,R.H. and Hulbert,M.H. Clay microstructure. Int. Human Res. Devel. Corp. Boston/Houston/London, ISBN 0-88746-065-8, 1986
- 5 Pusch,R., Karnland,O. and Hökmark,H. GMM - A general microstructural model for qualitative and quantitative studies of smectite clays. SKB Technical Report TR 90-43, SKB, Stockholm, 1990
- 6 Börjesson,L. Laboratory testing and computer simulation of clay barrier behavior. Proc. 9th Int. Clay Conf., Vol.III, No.87, 1989 (pp.117-126)
- 7 Pusch,R., Karnland,O. and Muurinen,A. Transport and microstructural phenomena in bentonite clay with respect to the behavior and influence of Na, Cu, and U. SKB Technical Report TR 89-34, SKB, Stockholm, 1989
- 8 Brandberg,F. and Skagius,K. Porosity, sorption and diffusivity data compiled for the SKB91 study. SKB Technical Report TR 91-16, SKB, Stockholm, 1991
- 9 Singh,A. and Mitchell,J.K. General stress-strain-time function for soils. Amer. Soc. Civ. Engrs., Proc. Vol.94, No SM1, 1968
- 10 Karnland,O. and Pusch,R. Development of clay characterization methods for use in repository design with application to a natural Ca bentonite clay containing a redox front. SKB Technical Report TR 90-42, SKB, Stockholm, 1990

- 11 Pusch,R. Alteration of the hydraulic conductivity of rock by tunnel excavation. Rock Mech. and Mining Sciences, Vol.26, No.1 (pp.71-83)
- 12 Hökmark,H. Numerical analyses of the nearfield rock in VLH and KBS3 repositories applying a general rock structure model. SKB Arbetsrapport AR 92-72, 1992
- 13 Pusch,R. and Börgesson,L. Performance assessment of bentonite clay barrier in three repository concepts: VDH, KBS3 and VLH. PASS-project on Alternative Systems Study. SKB Technical Report TR 92-, SKB, Stockholm, 1992
- 14 Hökmark,H. Distinct element method modeling of fracture behavior in near-field rock. Stripa Project Technical Report TR 91-01, SKB, Stockholm, 1991
- 15 Pusch,R. and Svemar,Ch. Influence on rock properties on selection of design for a spent nuclear fuel repository. Tunnelling and Underground Space Technology, Vol.8, No.3 (pp.345-356)
- 16 Börgesson,L. Pusch,R. Fredriksson,A., Hökmark,H. Karnland,O. and Sandén,T. Final Report of the Rock Sealing Project - Identification of zones disturbed by blasting and stress release. Stripa Project, Technical Report TR 92-08, 1992
- 17 Börgesson,L., Pusch,R., Fredriksson,A., Hökmark,H., Karnland,O. and Sanden,T. Final report of the Rock Sealing Project - Sealing of the near-field rock around deposition holes by use of bentonite grouts. Stripa Project Technical Report TR 91-34, SKB, Stockholm, 1991
- 18 Pusch,R. and Stanfors,C. Disturbance of rock around blasted tunnels. Proc. 4th Int. Symp. on Rock Fragmentation by Blasting, - FRAGBLAST-4, Vienna, Austria 5-8 July, 1993, Balkema, Rotterdam/Brookfield, 1993
- 19 Romero,L., Moreno,L. and Neretnieks,I. Release calculations in a repository of the type VLH. SKB Arbetsrapport AR 92-42, SKB, Stockholm, 1992
- 20 Kozlovsky,YE.A. The world's deepest well. Scientific American, Vol.251, No.6, Dec, 1984 (pp.106-112)
- 21 Johansson,E., Hakala,M. and Lorig,J.L. Rock mechanical, thermomechanical and hydraulic behavior of the near field of spent fuel. Report YJT-91-21. Nuclear Waste Commission of Finnish Power Companies, 1991
- 22 Pusch,R. Mechanisms and consequences of creep in crystalline rock. Comprehensive Rock Engineering, Rock mass and site characterization, Vol.1. Pergamon Press, 1992

- 23 Pusch,R. and Hökmark,H. Mechanisms and consequences of creep in the nearfield of KBS3 tunnels and deposition holes in granitic rock. SKB Technical Report TR 92-10, 1992
- 24 Marsh,G.P., Taylor,K.J. and Harker,A.H. The kinetics of pitting corrosion of carbon steel applied to evaluating containers for nuclear waste disposal. SKB Technical Report TR 91-62, SKB, Stockholm, 1991
- 25 Hellmuth,K-H. Natural analogues of bitumen and bituminized radioactive waste. STUK-B-VALO 58, Säteilyturvakeskus, Finnish Centre for Radiation and Nuclear Safety, Helsinki, Finland, 1989
- 26 Pusch,R. Executive summary and general conclusions of the Rock Sealing Project. Stripa Project, Technical Report TR 92-27, SKB, Stockholm, 1992
- 27 SKB, State-of-the-Art Report on potentially useful materials for sealing nuclear waste repositories. Ed. W.Coons. Stripa Project, Technical Report TR 87-12, SKB, Stockholm, 1987
- 28 Börgesson,L. and Pusch,R. Rock sealing in radwaste repositories using modern grouting methods and smectite clay. Proc. Int. Congr. Rock mechanics, Aachen, 1991
- 29 Pusch,R. Karnland,O., Hökmark,H., Sanden,T. and Börgesson,L. Final report of the Rock Sealing Project - Sealing properties and longevity of smectitic clay grouts. Stripa Project, Technical Report TR 91-30, SKB, Stockholm, 1991
- 30 Onofrei,M., Gray,M., and Roe,L. Cement based grouts - Longevity laboratory studies: Leaching Behavior. Stripa Project Technical Report TR 91-33, SKB, Stockholm, 1991
- 31 Alcorn,S.R., Coons,W.E., Christian-Frear,T.L. and Wallace,M.G. Theoretical investigations of grout seal longevity. Stripa Project Technical Report TR 91-24, SKB, Stockholm, 1991
- 32 Pusch,R. Workshop on sealing techniques tested in the Stripa Project and being of general potential use for rock sealing. Stripa Project, Technical Report TR 87-05, 1987
- 33 Börgesson,L. Pusch,R., Fredriksson,A., Hökmark,H., Karnland,O. and Sandén,T. Final report of the Rock Sealing Project. - Sealing of zones disturbed by blasting and stress release. Stripa Project, Technical Report 92-21, SKB, Stockholm, 1992

34 Pusch,R., Börgesson,L., Karnland,O. and Hökmark,H. Final report on Test 4 - Sealing of natural fine-fracture zone. Stripa Project, Technical Report TR 91-26, SKB, Stockholm, 1991

Chapter

4 *Construction*

4-1 Introduction

Construction of repositories includes a large number of activities, of which the major ones are the excavation of the rooms for waste disposal and the application and embedment of the waste. The first step comprises preparation of the construction site by geodetical measurements and establishment of utilities for electric power, ventilation, compressed air, water, sewage, and also the first phase of rock examination for the construction work, which naturally is preceded by the comprehensive geophysical, geochemical and rock structural investigations that have led to the selection of a suitable site for the entire repository and its major components, i.e. tunnels, shafts and caverns. A major issue is to arrange a central pumping station at depth, to which water drained from the repository in the construction and waste application phases will be directed and discharged to the ground surface. In this respect there are considerable advantages in using deep mines where such facilities and lifts are at hand and where prospection through geophysics and drillings has given detailed information on the rock structure and hydrology. The Stripa mine is a good example of a plant that could have been used for storing very toxic waste both in rooms from where ore had been removed and in tunnels and holes excavated in the granite mass adjacent to the mined ore bodies.

Excavation of repository tunnels, shafts and disposal rooms can be made in the same way as in any other large-scale underground project with the important exceptions that minimum disturbance should be aimed at and that a considerable flexibility in location and orientation of the rooms is required for adapting them to the rock structure, applying to a certain extent the philosophy “design as you go”. Subsequent and parallel to the excavation work, ventilation, illumination and power supply are installed and sealing and plugging performed, after which waste application and backfilling is made. At least for moderately hazardous waste it may well be possible to conduct excavation, waste application and backfilling at the same time but in different parts of a repository.

We will confine ourselves here to consider four major activities, namely excavation by drilling and blasting, application of clay buffers and backfills, sealing and plugging, and application of waste containers. Focus will be on repositories consisting of tunnels with and without

deposition holes of the KBS3 type, but very deep holes - represented by the VDH concept (SKB) - will be discussed since various versions of this concept may be of interest for disposal of radioactive or strongly toxic waste of other kinds.

4-2 Rock excavation techniques and their disturbing effect on the rock

This chapter will not include any detailed description of the excavation methodologies, which represent technical disciplines of their own and are dealt with in a vast amount of literature. Instead, the effects of excavation on the structure and physical properties of the remaining rock will be considered. The interested reader is referred to rock mechanical literature for further information on stress/strain issues [1].

4-2.1 Blasting

TUNNELS

The principle of tunnel blasting and the general impact of blasting techniques and shape of the tunnel on the disturbance of the rock are illustrated in Figure 150 [2]. The picture illustrates the wellknown fact that traditional “crude” blasting applied for quick and economic excavation causes considerable disturbance of the remaining rock. As outlined in the preceding chapter on design of repositories, particularly strong disturbance is caused if the rock structure is not taken into consideration in the planning of the repository.

For practical reasons the blast-holes are drilled in sets with a limited length in order to avoid significant deviation from the intended direction. Each set of boreholes is commonly 3-5 m long with the peripheral so-called contour holes oriented slightly outwards, which gives the blasted sections a conical shape. In recent years technical development has made it possible to make the entire work with orientation and direction as well as drilling of all the holes computer-aided and performed by use of advanced drill rigs, which significantly reduces cost and provides higher precision in the drilling/blasting operations. Still, a major reason for the often observed and unwanted local widening of the blast-disturbed zone is deviation of contour

holes from the intended direction.

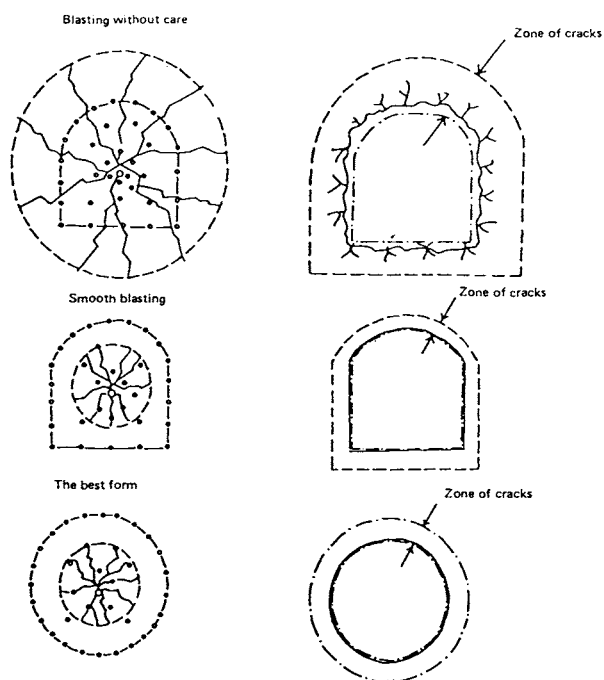


Figure 150 Impact of blasting techniques and shape on the disturbance of the rock [2]

Figure 151 shows examples of drilling and charging. The principle is that one or a few central, larger holes that are left open allow inward radial movement and disintegration of the blasted mass while the periphery is formed by the contour holes, which are commonly closely spaced and less charged than the rest of the holes. The distribution of charge and ignition should be such that fracturing outside the periphery is almost entirely caused by the detona-

tion of the explosives in the contour holes and not by that in the inner rows. This is the best way of minimizing disturbance of the remaining rock.

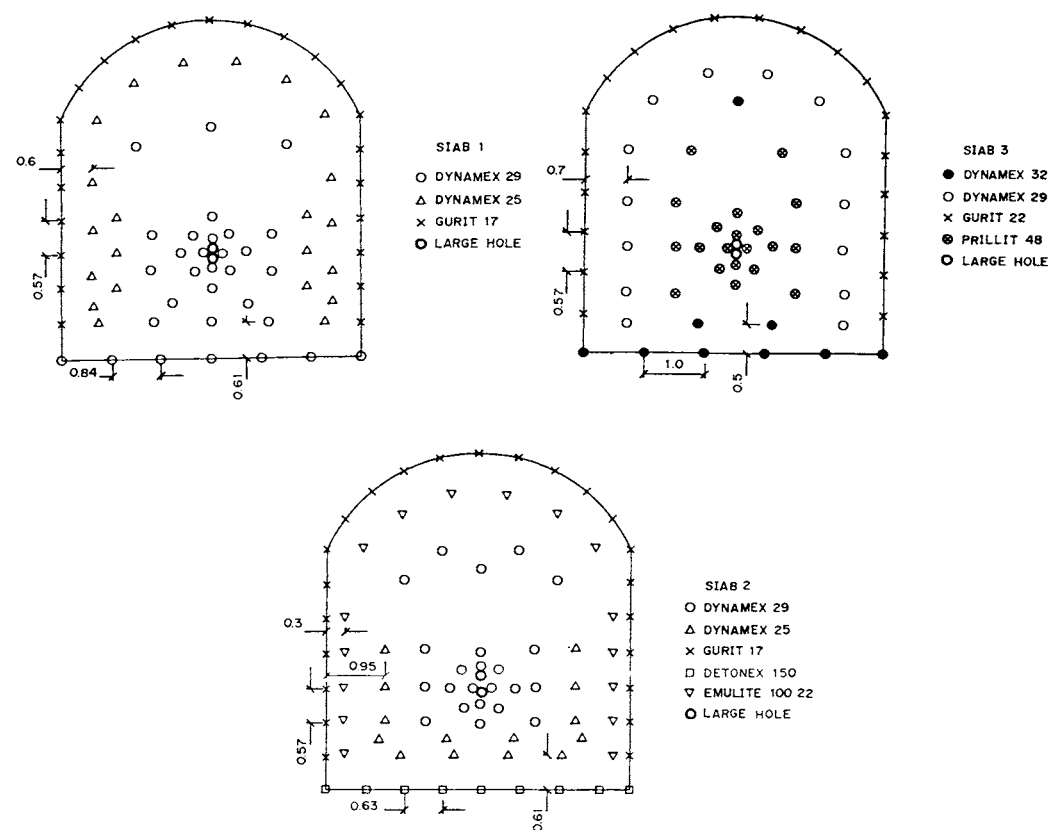


Figure 151 Blast-hole pattern and charge distribution tested at Äspö, Sweden [2]. SIAB 3 represents “normal blasting” (NB), SIAB 1 “careful blasting” (CB) and SIAB 2 “very careful blasting” (VCB)

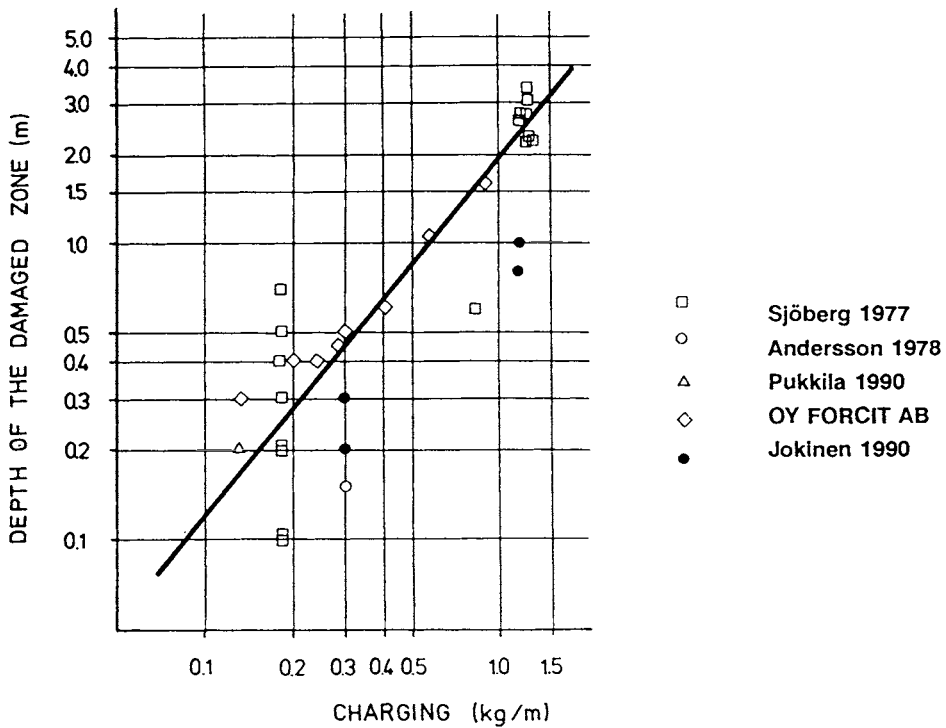


Figure 152 Compilation of empirical data on the influence of charge on the depth of the blasting-disturbed zone [3]

Figure 153 is a generalized picture of the major types of new fractures formed by ordinary blasting, i.e. with contour holes drilled at a slight angle with respect to the tunnel axis and with extra charge at the tip. We see that the radial, plane blast-induced fractures in Zones 1a - marked as rectangles - extend by around 0.3 m into the rock and that there is more intenseley disturbed zone 1b at the tips. This latter zone is more or less continuous around the periphery when the contour holes have a spacing of around 0.5 m. The problem in trying to minimize the disturbance is that the amount of charge that is required to cause sufficient disintegration to make excavation possible must not be too small and there are examples where repeated drilling and blasted were required to break up the mass sufficiently much to make it extracta-

ble. Thus, the VCB method shown in Figure 152 turned out to be too ineffective for practical application.

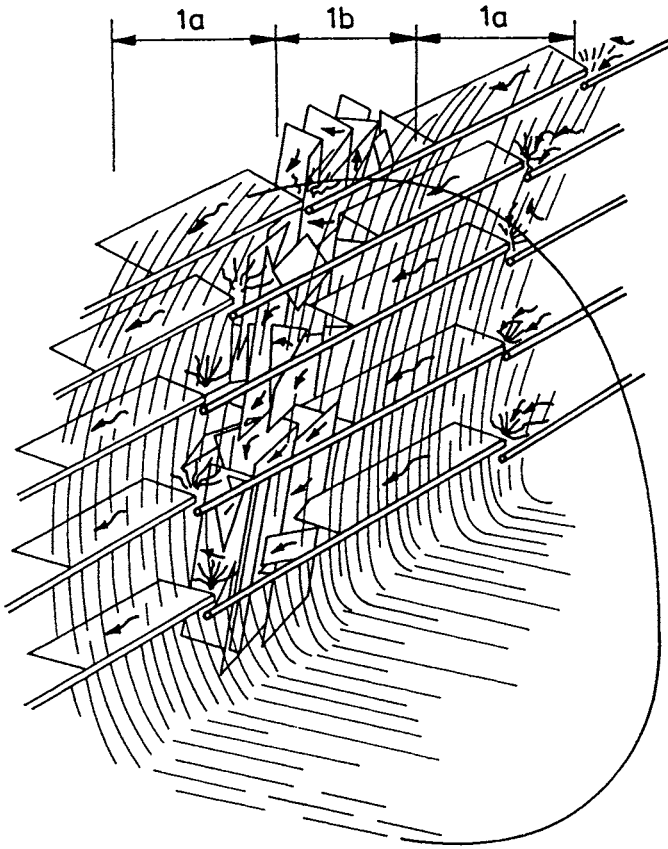


Figure 153 Major types of damage by tunnel blasting. 1a-zones are characterized by regular sets of plane fractures extending radially from the central parts of the contour holes. 1b-zones represent strongly fractured parts at the tip of the blast-holes

SHAFTS

Shafts can be excavated by bench blasting or pilot hole blasting (Figure 155). Examples of fairly quickly excavated, large and deep shafts are known from various parts of the world. Thus, both in South Africa and Canada, shafts with a diameter of up to 9 m have been excavated by bench-blasting to more than 2200 m depth at a rate of about 100 m per month [4].

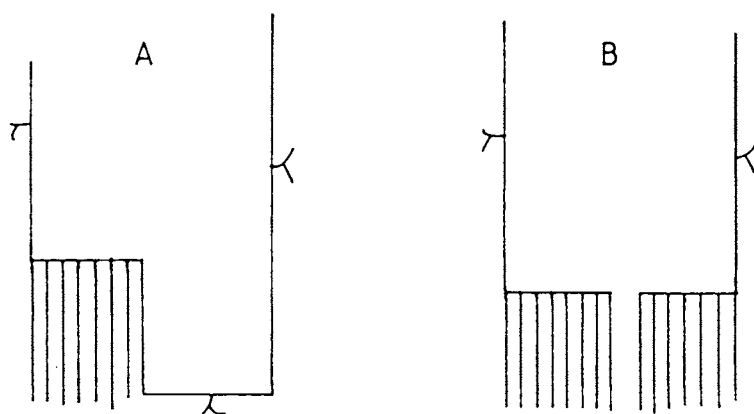


Figure 154 Shaft sinking by drilling and blasting. A) Bench blasting. B) Pilot hole blasting [4]

EXAMPLE OF THE EFFECT OF BLASTING OF TUNNELS AND SHAFTS WITH VARYING ORIENTATION WITH RESPECT TO MAJOR FRACTURE SETS

In the preceding chapters it was pointed how important it is to orient repository tunnels at a sufficiently large angle from major fracture sets. In practice, there may be significant difficulties in achieving this because of the winding nature of rock structures. Such structural variations are very common and mean that unsuitable orientation of certain parts of tunnels and

shafts cannot be avoided. The strong influence of tunnel orientation on the rock is demonstrated by the structural pattern induced in the walls of differently oriented tunnels in granite at Stripa as shown in Figures 155 and 156. Figure 155 demonstrates the very marked schistosity in a tunnel wall that was nearly parallel to the orientation of a major fracture set, while Figure 157 indicates that this effect and the associated increase in axial conductivity almost vanish when the tunnel is turned by about 15-20°.

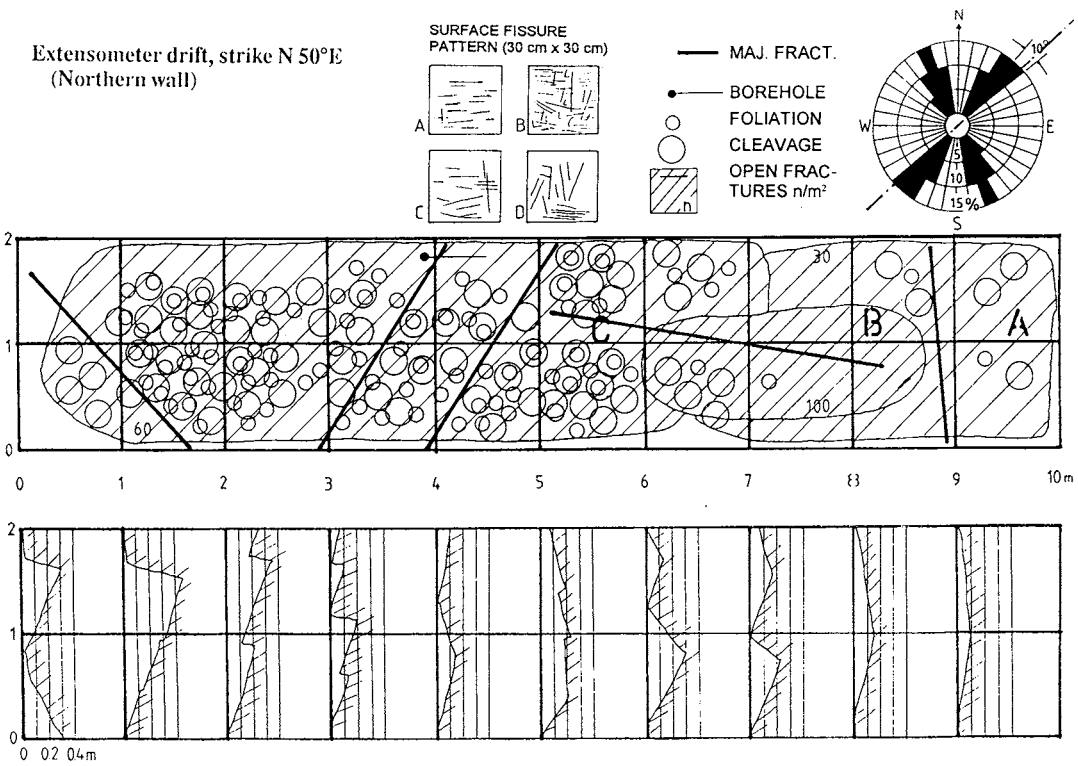


Figure 155 Example of schistosity. The rosette diagram shows the alignment of tunnel and a major fracture set. The lower diagram shows the wall profile

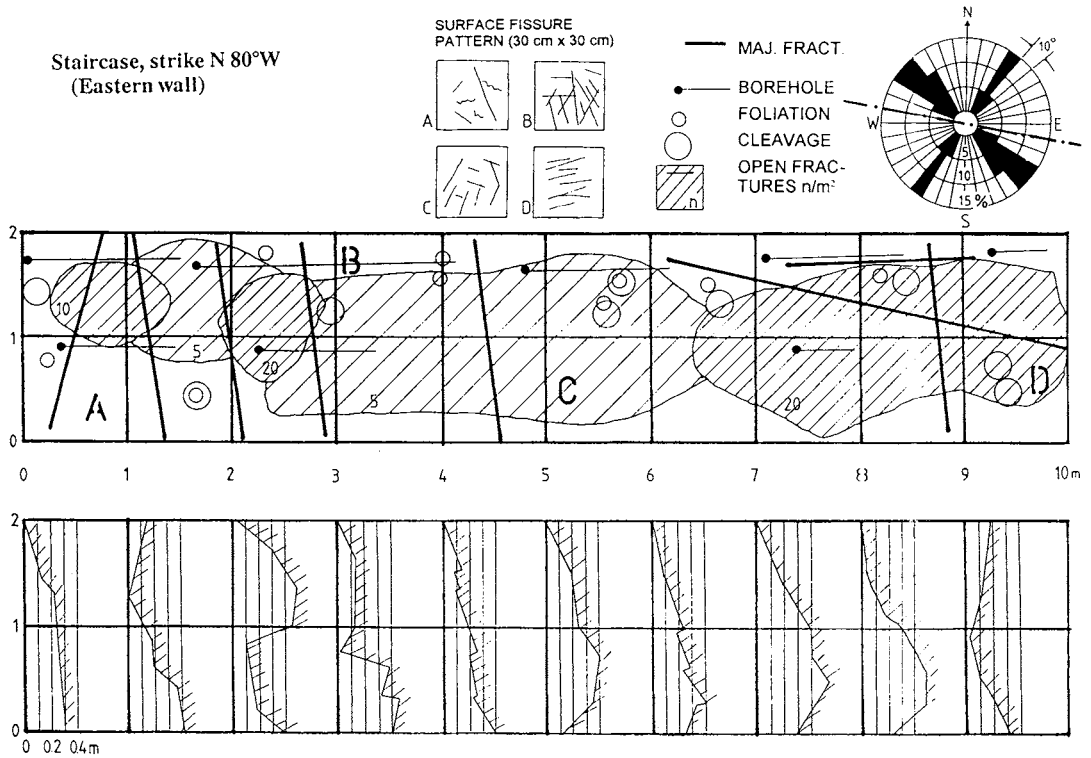


Figure 156 Appearance of tunnel wall forming 15-20° angle with the major fracture set

The combined effect of blasting, excavation-induced stress changes and orientation of an excavated room is manifested by the strongly enhanced frequency of fractures close to the periphery in Figure 107. This is compatible with the theoretical model of generation of new fractures and activation of 5th and 6th order breaks shown in Figure 76 and explains why one can consider the nearfield of normally blasted tunnels as a “porous medium” with respect to its hydraulic behavior.

4-2.2 Drilling

CORE DRILLING

Holes for prospection and logging purposes can be drilled by using coring techniques, which gives minimum disturbance and provides the investigator with samples of the rock material for characterization and testing. Such holes are particularly suitable for hydraulic measurements because the insignificant disturbance gives a smooth wall surface with no leakage along the rock/packer contact. Any diameter can be obtained but standard equipment is available for diameters in the range of about 20 to 400 mm and for drilling to depths of several kilometers. At Stripa, about 3 m deep holes were core-drilled with a hole diameter of 0.76 m.

PERCUSSION DRILLING

Percussion drilling is the only practical method for producing blast-holes, and it is also commonly applied for cheap production of holes with a maximum length of about one hundred meters for logging purposes. A further application is to produce large diameter holes by slot drilling.

Percussion drilling causes disintegration of the rock, giving fragments that are collected at the rock surface and used for current examination and characterization with respect to the mineral content, including clay material. This provides information on the degree of weathering, while recording of the rate of penetration gives an approximate picture of the fracture frequency. This requires that the drill bits are not worn, that the air pressure is constant and high, and that correction is made of the friction resistance in long holes.

Percussion drilling has three major effects that need to be considered:

1. The borehole walls are not as smooth as those in core-drilled holes and may yield leakage along rock/packer contacts at hydraulic measurements
2. The hammering produces very high stresses, which cause breakage of the grain bonds and fissuring of the rock also at some distance from the holes. This may block narrow fractures and reduce the possibility to inject grouts, while at the same time increasing the porosity and the hydraulic conductivity of the crystal matrix
3. The stress waves produce tension, which can lead to discing and softening of the rock adjacent to the holes.

Figures 157 and 158 illustrate disturbing effects of percussion drilling, which cannot be regarded as critical for most purposes, but make such holes less useful for certain applications, like tracer experiments and precision measurement of the hydraulic conductivity.

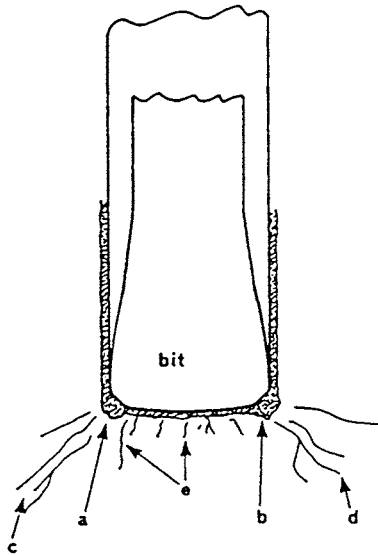


Figure 157 Indentation damage. a & b) crushed material, c & d) cracks, e) tension cracks
(After Wijk)

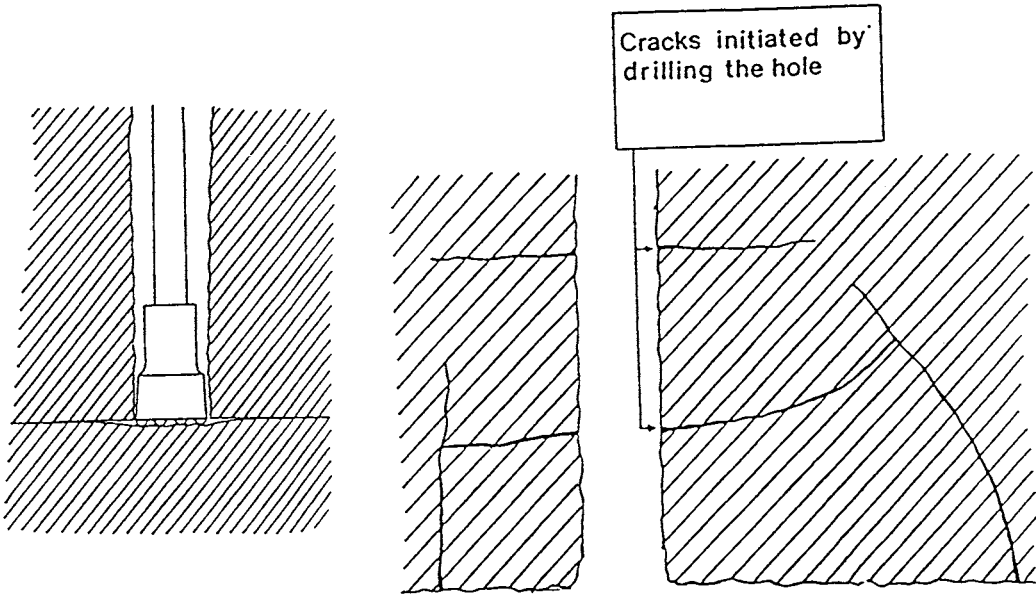


Figure 158 Discing in borehole walls (After Wijk)

LARGE HOLES, TUNNELS AND SHAFTS

There are three methods available for producing large-diameter holes in addition to core drilling and percussion drilling with rotating heads:

1. Full-face drilling with tunnel boring (pushing), oil-drilling (pushing), and raise boring (pulling) as wellknown varieties
2. Slot-drilling, i.e. drilling of overlapping holes
3. Water-jet cutting

Core drilling of the 3 m deep 0.76 m diameter BMT holes at Stripa showed that this technique is feasible but relatively slow and therefore expensive. In recent years, drilling of 1.5 m diameter holes to about 8 m depth using this technique has been performed in Spain (ENRESA).

Slot-drilling by use of percussion hammering can be made in several ways, either by overlapping the holes or by using rotating heads with one or several hammering tools. It has been successfully applied to depths of more than 10 m but deviation of the individual boreholes gives the large hole a relatively irregular cross section shape already at a few meters depth as demonstrated by Figure 159 [5]. The maximum length of such holes is probably limited to about 20 m if a reasonably regular shape is required. Water jet cutting has been applied in Canada by AECL with some success for producing several meters deep holes with 1.5 m diameter of KBS3-type and further technical development may make this technique even more competitive. The wall surfaces of the holes are very rugged. Water jet drilling seems to be very useful for cutting shallow recesses and slots as described later in this chapter.

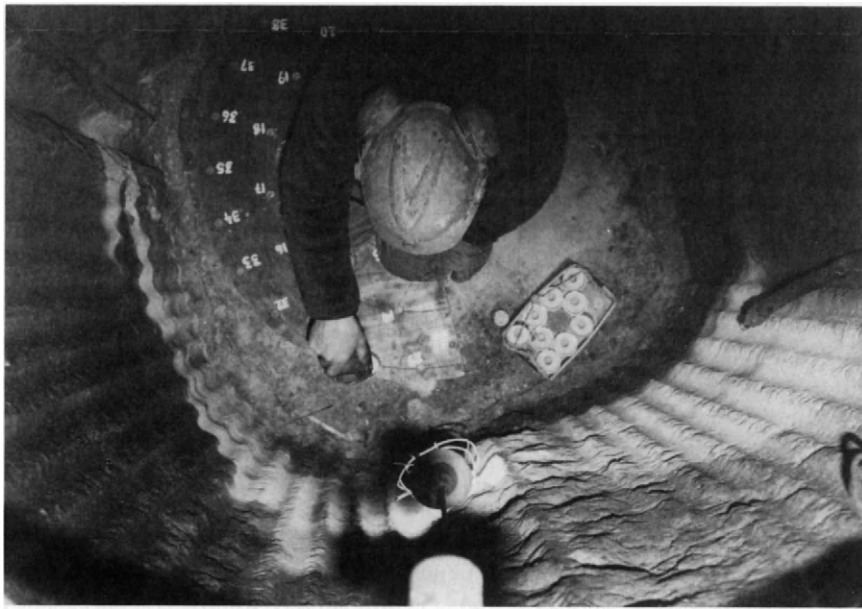


Figure 159 The 14 m deep, partly slot-drilled shaft where the Stripa shaft plugging test was conducted. Notice the rather strong deviation from circular symmetry

We will confine ourselves here to discuss the full-face boring techniques, focusing on the tunnel boring (TBM) technique, which makes it possible to produce even large-diameter tunnels quicker than by blasting and at approximately the same cost provided that the length of the tunnel exceeds a minimum value. Today, this length is estimated to be more than 10 km. It needs to be mentioned that TBM technique involves considerable risks when the hole is inclined downwards since crossing of strongly water-bearing fracture zones can cause flooding that may lead to casualties and machine breakdown with very high costs as a result. Still, beyond doubt, this sort of excavation and the related, recently introduced milling cutter technique will become dominant in the future for excavating tunnels and large-diameter holes. The cutter technique, which makes use of the same type of cutting head as TBM but with pivot-mounting that makes it possible to move and turn the head so that the shape of the cross section of the tunnel can be varied to yield stability and fit the rock structure. In this chapter oil-drilling technique adapted to crystalline rock will be referred to as well since it offers a possibility to produce very deep holes with a fairly large diameter.

TBM drilling implies that discs or bits are pressed against and moved over the face of the excavation, by which the rock is exposed to high shear stresses which break it up. The shearing naturally also affects the rock that forms the walls of the excavation and there are in fact two major factors and mechanisms that affect the remaining rock. One is that the high stress concentrations at the edges of the cutting head make 6th order discontinuities propagate and grow from Griffith voids (7th order discontinuities), and the other is that the shear stresses induced in the rock walls by the strong attack of discs and bits in the front cause growth of Griffiths voids to 6th order fissures, propagation of 6th order breaks, activation of 5th order discontinuities and propagation and shearing of 4th order fractures. These mechanisms cause some disturbance of the rock but significantly less than blasting.

Tunnel boring machines are designed to accommodate an arrangement of cutting tools supplied by the necessary energy and force (Figure 160) and there is vast experience from TBM excavation both in shallow rock and at large depth. At present there are hardly any commercial machines available for drilling holes with smaller diameter than about 2 m, while equipments with a diameter of up to around 10 m are in current use for tunnel boring.

The way the cutters attack rock depends on their function, which, for the common disc-cutters often used in medium-strong crystalline rock, is illustrated by Figure 161. Rock mechanics provides information of the failure mechanisms involved in the fragmentation process, which leads to disturbance of the rock in the walls as indicated in Figure 162 and specified in the preceding chapter [1].

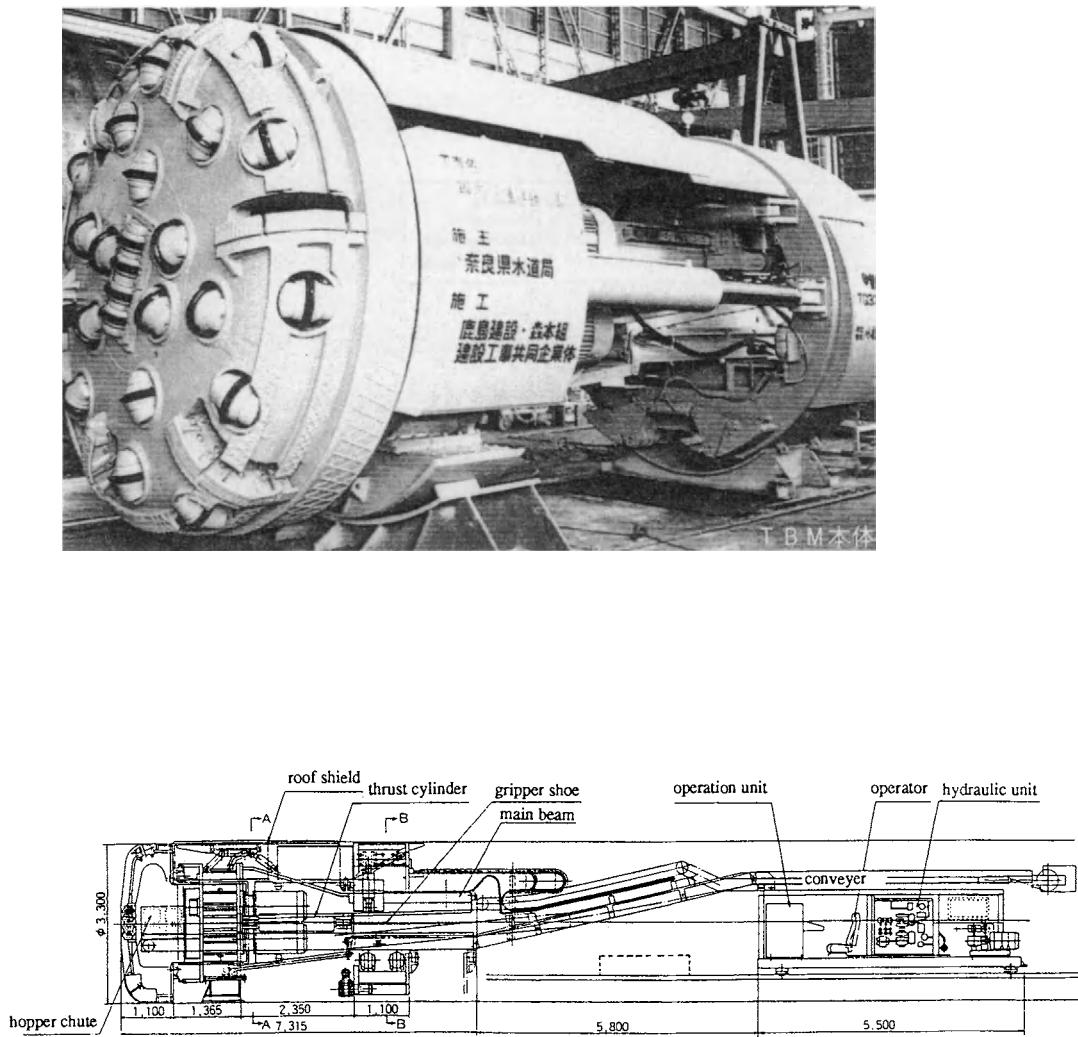


Figure 160 Schematic views of tunnel boring machine (Kajima Co, Japan)

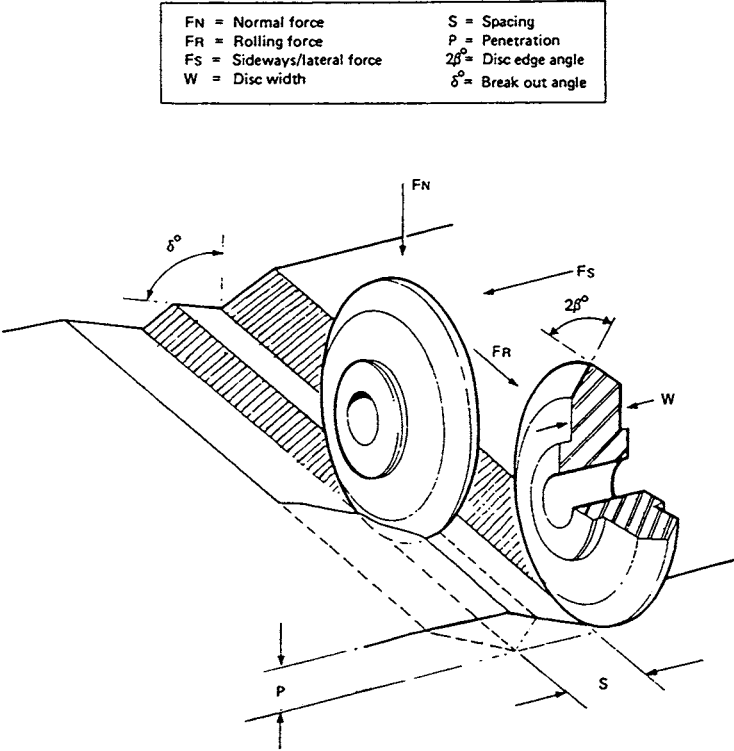


Figure 161 Terminology and geometry of disc cutting (After Hignett)

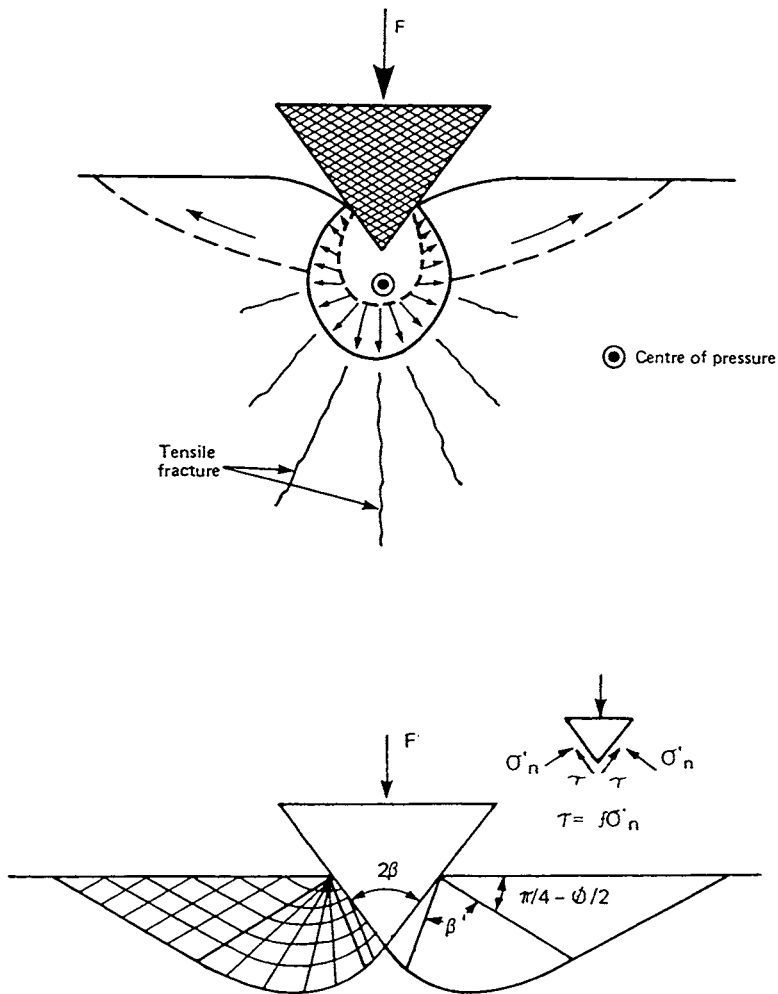


Figure 162 Fragmentation by indentation of disc cutter. Upper: Brittle chip formation at indentation of disc cutter (After Korbin). Lower: Plastic failure of Prandtl type representative of soils and sedimentary rock

Oil-drilling technique has been used for making holes with fairly large diameters down to more than 12 km depth in Russia (Kola) and to about 7 km depth at Siljan in Sweden, the lat-

ter for gas prospection. It is illustrated in Figure 164 and provides holes of possible use for the VDH concept for HLW that we will consider later in this chapter.

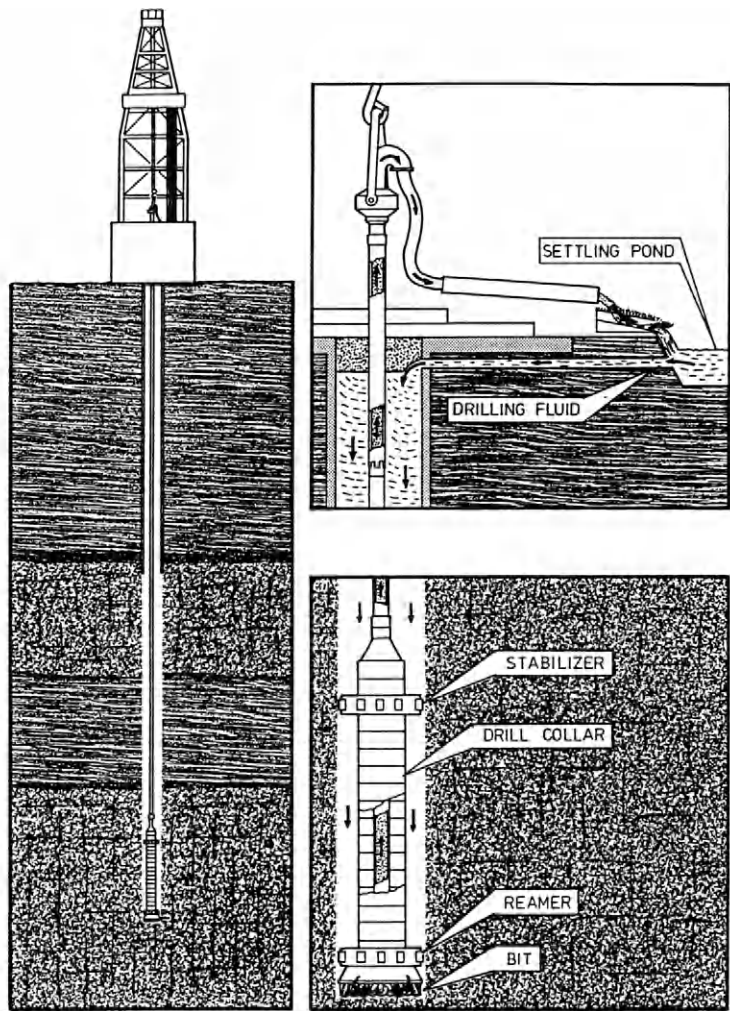


Figure 163 Schematic diagram of oil-drilling technique for use in crystalline rock (Beswick, Kenting Drilling Services, Ltd, England)

4-2.3 Special importance of the rock structure in the construction phase

GENERAL

The general impact on the hydraulic properties of excavation can be predicted and accounted for by use of the various numerical methods described in the preceding chapter. They require that a basic rock structure model is derived as a basis but there will naturally be deviations from the predictions because of deviations from this model. Changes in the design to fit the rock conditions may therefore be necessary and it will also be required that the exact location plugs and grout seals are decided in the course of the construction work.

The most important changes in design that may be required are those related to unexpected behavior of the rock, primarily overstressing and lack of stability and strong water inflow. Spalling phenomena may require changes in the shape of the cross section of blasted rooms and stabilization may be necessary, while unexpectedly strong inflow of water from intersected fracture zones or discrete fractures may call for reorientation and change of the location of deposition tunnels. Pilot drilling before excavation should reveal water-bearing fracture zones and make it possible to avoid critical sites but where they have to be crossed effective sealing operations must be planned early so that the construction work is not delayed. Naturally, seals applied for making construction possible do not have to last for a long time, while the ones applied for redirecting groundwater flow in a long-term perspective need to be long-lived. It is obvious that while underground repositories are excavated in virgin rock, one will experience more unexpected behavior of the rock than if an existing mine is used for disposal. We will confine ourselves here to discuss application of stabilization activities where they have to be planned and performed in conjunction with excavation work. Construction of seals will be discussed later in this chapter.

STABILIZATION TECHNIQUES

The following methods are commonly used for supporting rock that yields or tends to become unstable in underground excavation of all sorts:

1. Bolting - rockbolts and cable bolts
2. Lining - shotcrete
3. Construction supports - arches, buttresses

4. Backfilling of crushed rock or cement-stabilized fill.

Although repositories should naturally be planned so that dramatic events in the construction phase are avoided, examples being rock fall from high walls in big rooms or spalling in heavily stressed tunnel roofs, a number of difficulties with unstable rock have to be expected. For simple and quick stabilization, bolting and buttresses - including shotcreting - are particularly suitable and will be considered here.

Rock bolting

Stabilization can be made by systematic bolting and by securing unstable blocks by local bolting. Figure 164 illustrates systematic bolting for supporting roofs and stabilization of rock wedges by strategic application of relatively few bolts. These cases of unsufficient stability, which all contribute to the enhanced axial hydraulic conductivity of the nearfield, are related or identical to those discussed in the preceding chapter.

Two major types of bolts can be used, namely prestressed or tensioned bolts, which are exposed to a tension load and then anchored in the rock by filling the space between the bolt and the rock in the hole with cement or plastic, and untensioned bolts, which are simply driven into cement-filled holes. Tensioned bolts carry the rock load from start and tend to force the various rock blocks together by which the bulk strength of the rock is considerably increased. The anchor and embedment undergo creep deformation, which means that the tension stress drops with time and by this also the strength and stability of the bolted rock. Untensioned bolts undergo strain when the rock load is transferred to them after the hardening of the embedment and since this is associated with some widening of the aperture of the fracture, the bolts become exposed to flowing water and start corroding. Such bolts are in common use for stabilizing rock and providing safe conditions for the workmen but the rather rapid corrosion means that they cannot be relied on for more than a few tens of years. It is possible that tensioned bolts that are completely and tightly embedded may still have some stabilizing effect after a few hundred years but in practice they cannot be relied on for much longer than untensioned bolts, which is still sufficient since 25-50 years is probably the total time required for repository construction and waste application.

After backfilling of repository rooms with material that supports the rock, the bolts are of course not required any more.

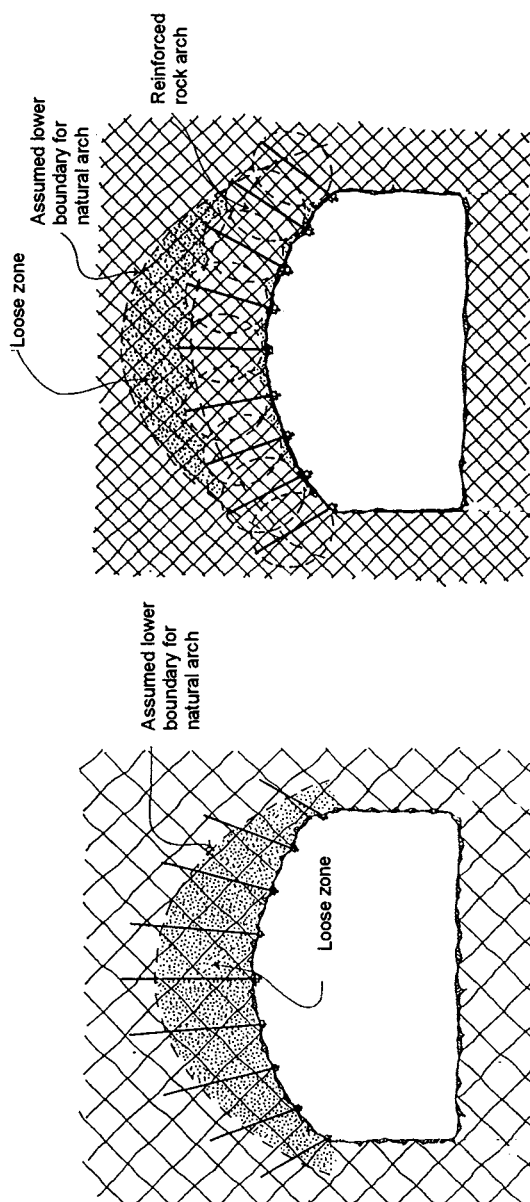


Figure 164 Bolt stabilization. Upper: Systematic bolting for supporting roofs using untensioned bolts (left) and tensioned, i.e. prestressed bolts (right). Lower: Bolt-anchored wedges (After Stillborg)

Concrete buttresses and shotcrete

Concrete supports are required where excavation is made in unstable parts of 1st and 2nd order discontinuities, and they are also major components of plug seals. They can have quite different forms depending on the required function and behave in principle as untensioned bolts, i.e. they undergo slight deformation when the rock load is transferred to them. A common form of supporting unstable rock is to put in steel arches and reinforcement nets in conjunction with the excavation and to stabilize the system of steel supports and rock by blowing cement mortar on the walls and roof, i.e. shotcreting them. Where heavy water inflow takes place, temporary drainage may be required for avoiding too quick build-up of very high water pressure on the hardening support. A number of such techniques are used in ordinary underground construction and they can be applied also in repositories in order to make it possible to cross low-order discontinuities by adits and main transport tunnels. Naturally, the rooms for waste disposal should not be intersected by such rock structures.

Where it is considered that groundwater flow along tunnels or big holes has to be cut off, which is the purpose of constructing plug seals, they need to be equipped with bentonite “O-ring”-type seals that provide tight plug/rock contact and exert pressure on the rock in order to prevent fracture apertures to increase. Such buttresses will be further discussed in conjunction with seals later in this chapter.

Backfilling

Backfilling of tunnels, shafts and other rooms so that the applied fills are tighter than the rock mass and do not serve as conductors, and so that the rock is supported is a standard procedure in repositories. The composition of the fills has to be decided on the basis of what is required from the viewpoints of hydraulic conductivity and stress/strain properties and also how the application can be made in each individual case. This will be discussed in this chapter, referring to some of the Stripa tests that gave valuable experience also in these respects.

4-3 Buffers and backfills

4-3.1 Embedment of waste containers - buffers

MATERIALS

The excellent sealing and expansion properties of dense smectite clays has made them primary candidate materials for embedment of HLW canisters in several countries as well as for plug materials and grouts. Commercially available monmorillonitic bentonites can be used and both natural Na bentonites like the Wyoming bentonites and Ca bentonites converted to Na form by treatment with sodium carbonate can be used. Suitable materials emanating from bentonite layers in North and Central America, Europe, North Africa and the Far East, are available from a number of mineral companies. The smectite content of first class material is typically in the interval 75-90 % with feldspars, quartz, pyrite, calcite and kaolinite as common accessory mineral components, which play a more or less important role for the long-term function of the smectite. Typical chemical compositions of three suitable bentonites in Na form expressed in terms of oxides are given in Table 11.

Table 11 Typical range of chemical composition of good commercial Na bentonites

Clay	SiO ₂	Al ₂ O ₃	Fe ₂ O ₃	CaO	MgO	Na ₂ O	K ₂ O	SO ₂
A	63	21	3.5	1.3	2.5	2.1	0.5	0.5
B	64	20	5	3	3	3	1	0
C	55	18	6	4	4	3	0.5	1

Bentonite material can be obtained commercially in coarsely granulated form as well as fine-grained granulate. Very fine powder material is required for preparing clay-poor mixtures while normal grading, i.e. a maximum aggregate size of 2 mm, is suitable for preparing compacted blocks. The water content of the material, which depends on the humidity of the environment where the material is stockpiled at the plants and on the transport conditions, is normally about 8-14 % and compacted blocks will have a degree of water saturation that is in

the interval 30-60 % for dry densities of 1.5-2.0 g/cm³. The compaction pressure that is needed to obtain these densities is 50-150 MPa. Very high compaction pressures and the use of somewhat wetter powder can yield material with a density of about 2 g/cm³ and a degree of water saturation of more than 90 %. This gives several advantages, like a significantly increased thermal conductivity, as explained in the subsequent chapter on function of repositories.

PREPARATION

Blocks can be prepared by uniaxial or three-dimensional compression. The lastmentioned technique, using the ABB Quintus press, was applied for the first large-scale production of highly compacted bentonite blocks, i.a. for the Stripa Project [6]. This equipment made it possible to produce uniformly dense columns with a height of 1.5 m and a diameter of 0.42 m and a dry density of about 1.8 g/cm³, applying pressures up to 150 MPa. Smaller blocks were prepared by dividing the columns using sawing, which has the advantage that any block shape can be obtained but this technique is expensive and not very practical. Uniaxial compression can be made with simpler tools yielding exactly the desired block size and shape, although there is a risk of heterogeneity because of friction effects at the compression of larger blocks by improper selection of pressure, water content and size and shape of the blocks. Also, there may be some microstructural anisotropy by uniaxial compression but various investigations of the physical properties of compacted blocks have not indicated significant differences in hydraulic conductivity and swelling potential in different directions irrespective how the compression was performed. Pilot tests using uniaxial compression technique have shown that blocks with a weight of 30-50 kg, i.e. close to what can be handled by one man, can be produced without difficulties. Larger blocks for handling by use of cranes and fork trucks can very probably be prepared but their mechanical strength in the handling and transportation stages may be questionable except if special techniques are applied.

Blocks prepared by applying high pressures on bentonite powder with a water content exceeding about 6-7 % remain physically stable if the relative humidity in the space where the blocks are stored, handled and transported does not exceed about 75 %. Since transport and intermediate storage of blocks will be made down in the repository where the humidity is commonly high, they need to be wrapped in tightly fitting plastic applied by use of vacuum technique. The blocks may then be stored for years down in the repository (Figure 165).

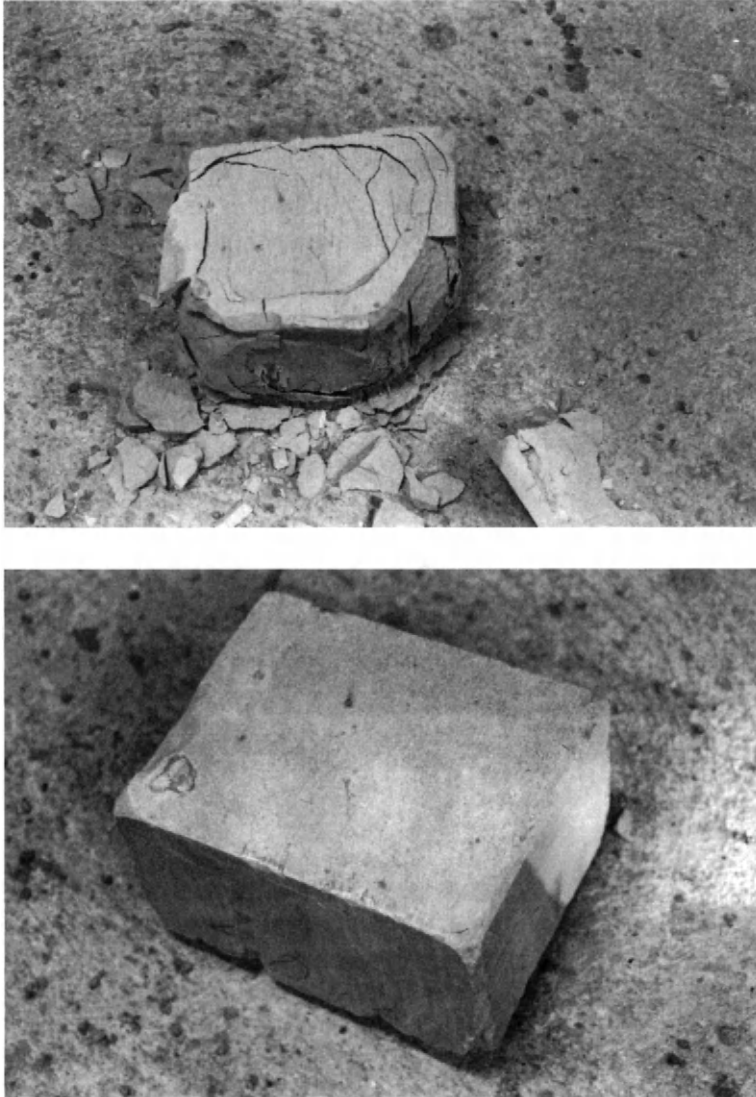


Figure 165 Appearance of blocks of highly compacted bentonite. Upper: Block exposed to very humid air for several months in the Stripa mine. Lower: Block kept in normal office atmosphere for several years

APPLICATION

There are two major options for application of dense blocks in repositories, i.e. putting them on site as individual objects, piece by piece, or applying them as units of composite systems of canisters and bentonite blocks or, in plug seals of the masonry type, as sets of blocks. The simplest procedure, intended for the KBS3 concept, is to bring down the blocks individually in the deposition holes, leaving the necessary space to get the canisters in with only minimum clearance, then checking the space with a dummy canister, and finally emplacing the canisters. This method is illustrated in Figure 166.

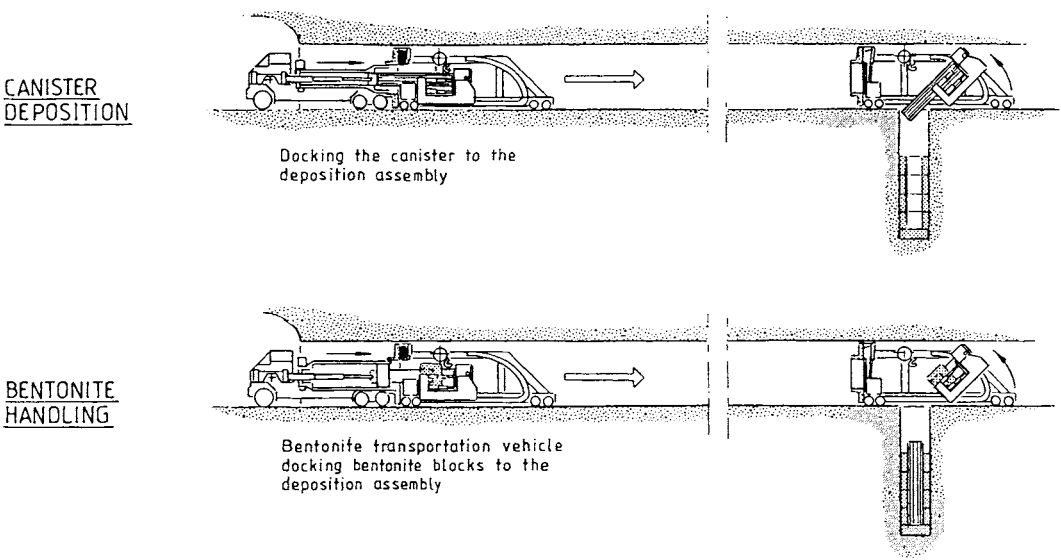


Figure 166 Emplacement of bentonite blocks and subsequent deposition of canister

The problem with highly radioactive waste is that emplacement of canisters needs to be made by remote handling using TV-aided robot techniques. Particular difficulties will be caused if breakage of bentonite blocks takes place or if canisters get stuck when fitting them in. Such problems can probably be minimized if composite systems of canisters and surrounding blocks are prepared and applied in one operation. An example of this is shown in Figure 167, which was taken in conjunction with the application of the 3 t sets of bentonite-embedded heaters simulating radioactive canisters in the Stripa BMT experiment [6]. Such techniques are particularly suitable for the much more difficult horizontal emplacement in deposition tunnels and in inclined holes as realized by considering the large number of operations involved in emplacement of canisters and individual bentonite blocks in Figure 168 [7].

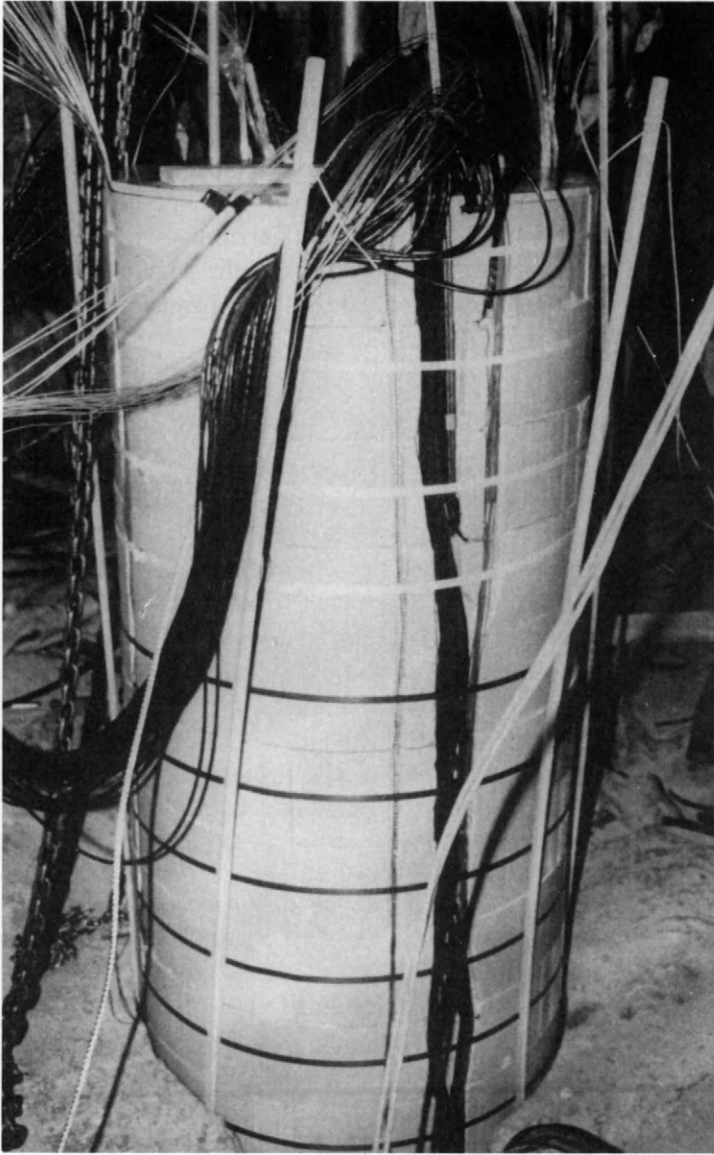


Figure 167 Emplacement of heavily instrumented bentonite/heater unit in the Stripa BMT experiment, in which the heaters represented HLW canisters. The ribbons are for keeping the cables tight to the unit

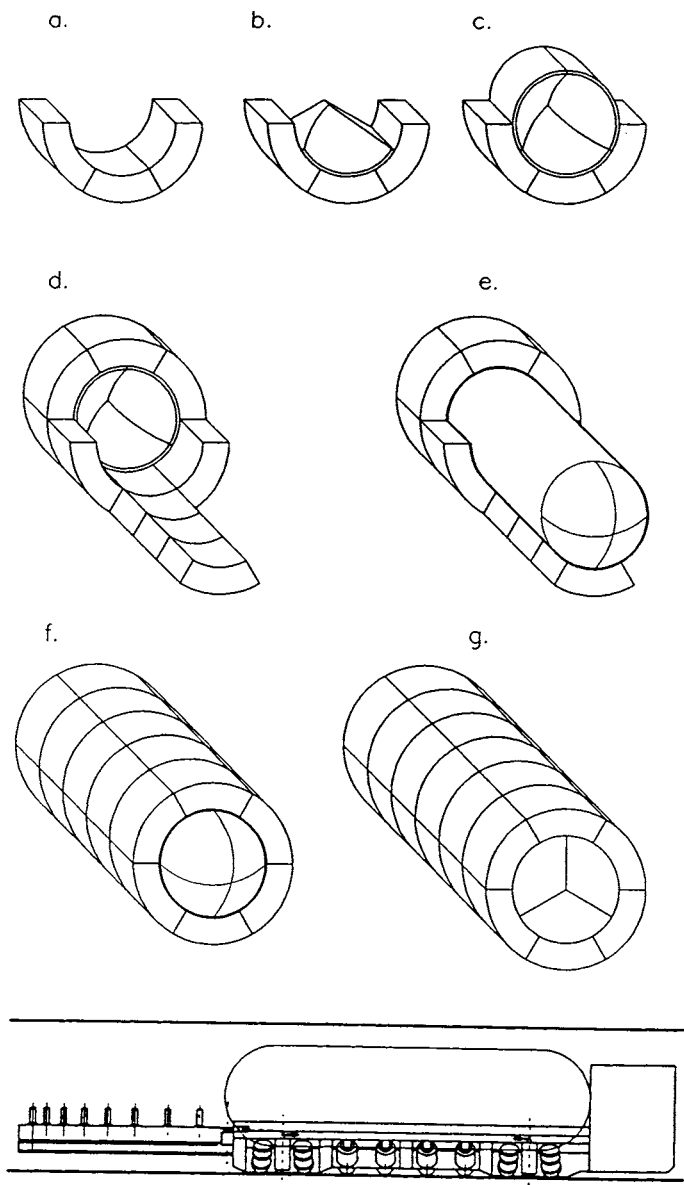


Figure 168 Phases in emplacement of big bentonite blocks and HLW canisters in VLH [7]

4-3.2 Backfilling of tunnels and shafts with no waste

PRACTICAL ASPECTS

The commonly applied principle that all types of buffers and backfills in repositories should be less conductive than the host rock requires special attention in the filling of tunnels and shafts by use of bentonite-poor materials. Thus, the conductivity criterion implies that the backfill must not only be sufficiently tight enough, as manifested by testing samples in the laboratory, but also that the entire mass must be very homogeneous, which requires great care in the preparation phase and continuous quality checking also of the mixing and application if the material is prepared in the form of a soil mixture that is applied and compacted layerwise. The homogeneity problem is largely avoided by using natural clay materials with relatively low smectite content of which there are several types available in most countries at very moderate cost. A second problem is that the rather slow procedure of application will yield inflow of water from the rock and cause local strong wetting in the course of this work, which may require comprehensive temporary drainage and locally also excavation and replacement of softened parts by material of original composition. A third and major problem, which is known to be particularly important in the case of tunnels, is that conventional layerwise application and compaction of earthen material of common types, i.e. bentonite/ballast mixtures, cannot be used in the uppermost 1.5 m for space reasons. This makes it difficult to reach the same tightness of the upper and lower parts of the backfills but there are several ways of solving this problem as will be indicated here.

MATERIALS

The composition of the backfills depends on the required function. For tunnel backfills there are requirements with respect to the hydraulic conductivity, which implies a certain minimum content of bentonite. On the other hand, certain applications require that the smectite content does not exceed a maximum value as in the case of constructing tight foundations of heavy silos of the Forsmark type, for which it must be limited in order to minimize settlement under full load and upheaval before any load is applied. The bentonite material for preparing mixtures is preferably the same as the one used for compacting blocks, but the grain size distribution must be suitable for obtaining homogeneous mixtures with the ballast.

As to the ballast material, the grain size composition should be as indicated in the design chapter and the mineral composition such that it minimizes degradation of the bentonite component, which implies that the content of potassium-bearing minerals and carbonates should

be at minimum. The ballast can be prepared by mixing different fractions of natural soil materials like glacial deposits or by crushing, grinding and sieving rock material. Naturally, the rock obtained at the excavation of the repository, properly graded in an underground crushing, grinding and sieving plant, would be suitable if its mineral composition is acceptable and the grain shape acceptable. This must be investigated by conducting a study of the compaction and conductivity properties.

LARGE-SCALE PREPARATION OF BACKFILLS

The amount of solid mineral material for backfilling a big underground repository, like a 6000 canister KBS3 disposal, may be on the order of 2-3 million tons and it must be realized that preparation of such a huge mass with very well defined composition naturally requires that there is really access to the required components. This can be ascertained by selecting materials that are known to be available in large quantities, like bentonite, or that can be produced with available technology, as the ballast (aggregates) since it can easily be produced with required granulometry by crushing and sieving rock of suitable type.

A second requirement is that the mixtures of bentonite/ballast, which can be in proportions 1:10 to 1:1 for most backfilling purposes, can be mixed so as to form homogeneous materials. This is actually a matter of how the composition should be in order to obtain maximum density, which is of fundamental importance for dam and road construction and which is basically a soil mechanical issue. This well established discipline specifies that maximum density of a soil with varying particle size is obtained by preparing it at "optimum water content" for reducing interparticle friction without creating porewater overpressure at the compaction. Figure 169 illustrates the typical effect of the water content on the dry density, which, for bentonite/ballast mixtures shows that the optimum water content is in the range of 12-16 %. At least at low clay contents it implies that water must be added and that the preparation in fact has to be made in three steps, starting with the bentonite powder and the dry ballast, and finally adding water. The opposite order makes the bentonite form a thin coating of the ballast grains with a risk of insufficient filling of the voids between these grains.

In the course of the Stripa Project it was found that compaction of mixtures of air-dry bentonite and suitably graded ballast gives approximately the same density as mixtures prepared and compacted at optimum water content, at least at low bentonite contents. The principle of dry mixing and compaction of only bentonite and sand, which can be made by use of large concrete mixers, is naturally simpler and cheaper than introducing also water, and can be recommended for practical application. The bottom bed of the Forsmark silo was prepared in this fashion as will be described in this chapter.

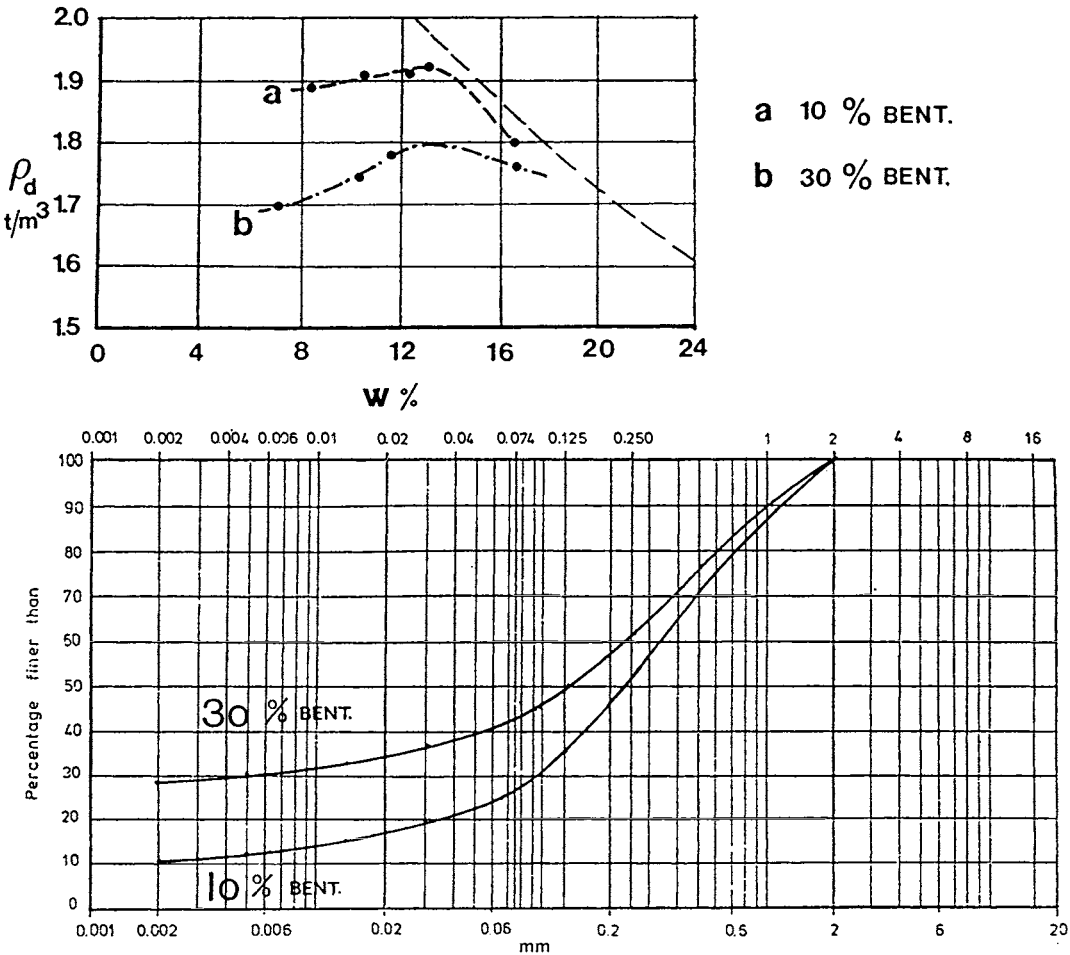


Figure 169 Dry density of mixtures of finely ground Na bentonite and suitably graded ballast material. Modified Proctor compaction technique

APPLICATION AND COMPACTION

Tunnels can be backfilled by using conventional layer-wise application and compaction techniques. The problem is that the uppermost part must be filled by use of some other technique and this has led to alternative ways of backfilling, namely those termed B and C below. Thus,

in addition to the method (A) of layer-wise application and compaction, using special methods for filling the top part, the techniques termed B and C below have been proposed for obtaining homogeneous, dense backfills.

A. Layer-wise application and compaction of bentonite/ballast materials and filling the uppermost part of the tunnel by special techniques, like blowing ("shotcreting")

B. Applying and compacting the backfill laterally

C. Emplacing blocks of compacted backfill material to form masonries

We will examine these three methods in some detail because of their general applicability in all sorts of repositories.

Method A

The lower part of tunnels and big rooms can be backfilled so that the density is high enough to exclude compression under the own weight of the overlying mass and to yield a hydraulic conductivity that is lower than that of the surrounding, virgin rock. This requires heavy compaction and the use of bentonite as a component of the backfill. In principle, layer-wise application and compaction of bentonite/ballast mixtures can be made by using conventional techniques that are common in constructing road embankments and earth dams. Such projects often represent work in large areas with easy access, which makes it possible to use rational methods for application and compaction, while underground construction means that mass transportation and access to machines is difficult except in the case of large rooms like the ones that remain open in certain types of mines. Thus, dynamic rollers with a weight of 5 t and more are often used in shallow construction and they can of course also be used in underground construction. Since they have a compaction effect on the fill to a depth of at least one meter, the layers can be applied with a thickness of at least 0.5 m. For compaction in narrow tunnels and shafts lighter compaction machines have to be used for space reasons and it is estimated that vibratory rollers with a weight of up to 3 t and vibratory plates weighing less than 500 kg are most practical. Their compaction power is considerably smaller than that of the bigger machines, which requires that the applied layers must be thinner, in practice about

0.2-0.4 m. Following normal field construction practice, compaction is suitably made by 10 runs. Close to the irregular walls of blasted tunnels compaction has to be made by use of manually operated pneumatically driven compaction tools, which are less powerful than the rollers and plates and here the material must be applied in even thinner layers, or, alternatively, the rim zone can be composed of a more bentonite-rich mixture. In fact, a possible and suitable way may be to apply a “liner” of highly compacted blocks of pure bentonite or 50/50 bentonite/ballast mixture. The cost is naturally higher but the advantages great: The contact backfill/rock becomes very tight and the dense bentonite-rich rim zone exerts a significant stabilizing pressure on the shallow rock.

The uppermost about 1.5 m high part of the rooms can be filled in two ways. One is to fill the space by blowing in the backfill pneumatically and the other is to emplace blocks of a highly compacted bentonite-rich material. The firstmentioned technique was applied in the Stripa BMT project [6], in which a mixture of sand and bentonite was blown in by using shotcreting technique (Figure 170).

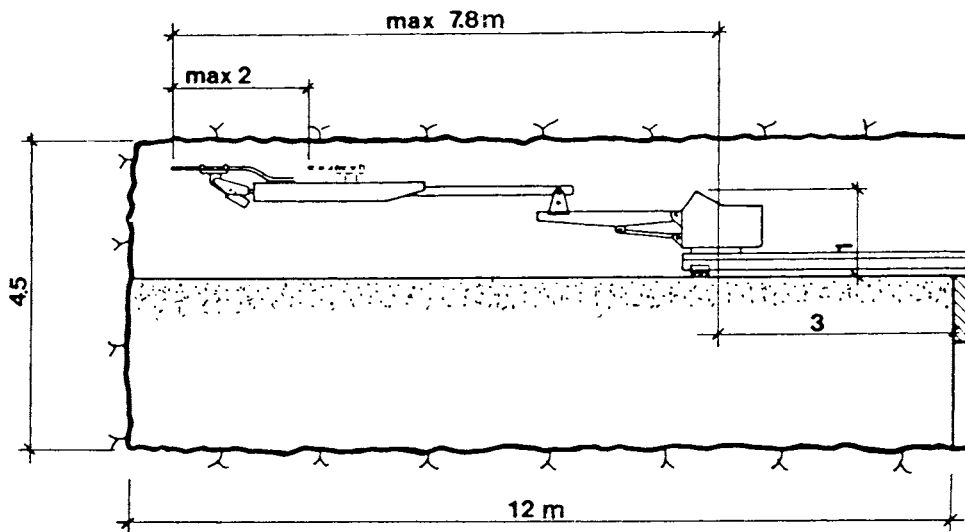


Figure 170 Principle of filling the uppermost part of tunnels with mixtures of bentonite and sand using shotcreting applied in the Stripa BMT experiment

Since the lower density of the upper shotcreted part was expected to yield a significantly higher conductivity than of the lower part, the bentonite content of the blown-in material was increased from 10 % by weight of the dry mass compacted on site to 20 % of the shotcreted material (Figure 171).

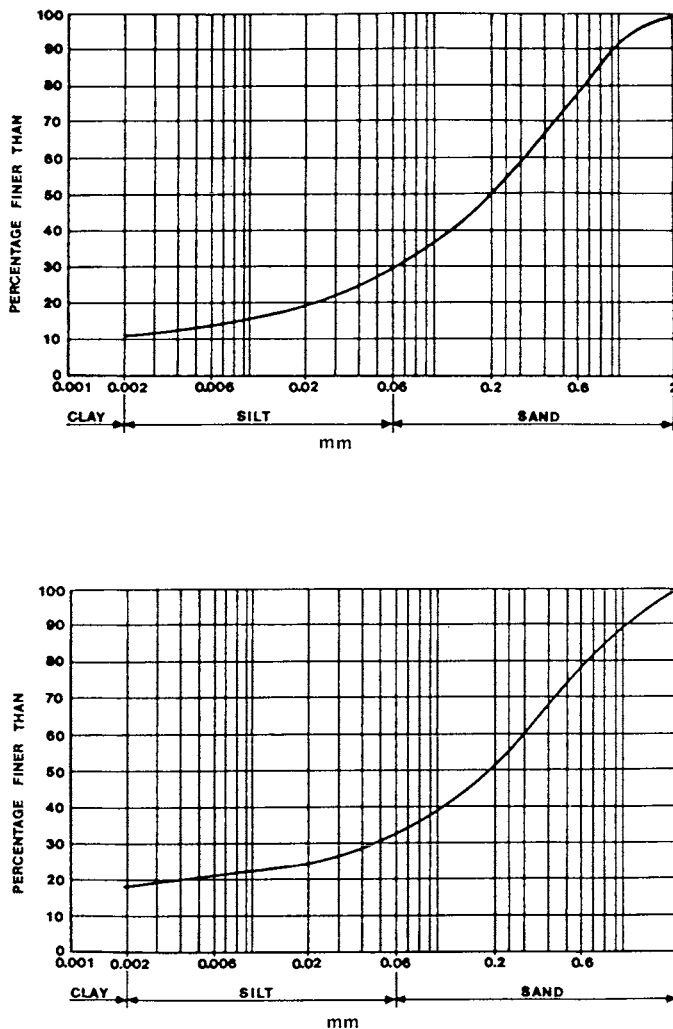


Figure 171 Grain size distribution of the BMT backfills. Upper: 10/90 bentonite/ballast. Lower: 20/80 bentonite/ballast used for shotcreting

Pilot shotcreting tests indicated that it should be possible to obtain a dry density of about 0.95 g/cm^3 , i.e. a bulk density of about 1.5 g/cm^3 after complete water saturation, but it turned out that while the average dry density was about 0.70 g/cm^3 , the variations were considerable and the lowest recorded value was only about 0.22 g/cm^3 . These tests showed that the uppermost part of the backfill would serve as a very effective conductor if it had been applied in a deposition tunnel, and that the earlier discussed phenomenon of time-dependent disintegration of the tunnel roof would take place because of the insufficient supporting power of the backfill. Actually, very salt groundwater or moderately salt groundwater with Ca as major cation could yield consolidation and settlement of the top part, leaving an open space between the backfill and the roof.

In order to make the construction of the lower part of the tunnel backfill rational, it should be applied and compacted layerwise in one sequence over the entire length of the tunnel. However, top filling by use of shotcreting is not very practical in long tunnels with a small free space and section-wise application of the lower backfill is hence preferred. In turn, this makes the application of temporary seals necessary for protecting the exposed backfill from softening due to water uptake, a matter that we will consider in Chapter 5. Top filling by employing compacted bentonitic blocks may well be performed in the small space left after application of the lower backfill over the entire tunnel length.

Method B

This technique, which has the advantage of yielding practically the same density of the entire backfill, involves application of the backfill by layerwise application by blowing in the material, and compaction using dynamic compaction units. For KBS3-type concepts this technique has the advantage that short sections can be prepared at a time, which means that the application of canisters can be made parallel to the backfilling. The remotely operated machine is equipped with nozzles for application and with compaction tools mounted on a drilling rig. It should be suitable not only for effective backfilling of tunnels and shafts with no waste in but probably also for backfilling tunnels with waste in strong canisters. No such equipment has yet been manufactured.

Method C

This method is the most rational and quickest one because sets of prefabricated blocks are transported and put on site at a higher rate than the backfill can be put on site by methods A

and B. This method has the same advantage as Method B with respect to the possibility of parallel application of canisters and backfill in HLW repositories of KBS3 type. It seems probable that this method is the most cost-effective one. The optimum block size depends on their composition (with or without ballast material), shape and density as well as on the method of application. It has to be determined for each individual case.

LOW-PERMEABLE FOUNDATIONS OF HEAVY OBJECTS LIKE THE FORSMARK SILO

The construction of the foundation of the heavy Forsmark silo containing LLW and MLW is an example of how application and compaction can be made of bentonitic backfills in horizontal or slightly inclined layers. The criteria for the construction and performance were the following:

1. Operational lifetime with largely unaltered properties 300 years
2. Maximum hydraulic conductivity lower than that of the ambient rock, i.e. 10^{-9} m/s
3. Maximum settlement of the silo filled with waste

The material components were Sardinian bentonite converted from the original Ca state to Na form, and natural granitic ballast material of glacial origin ("b" in Figure 73). The selection of the bentonite material was based on the requirements that the smectite content should be at least 70 %, and the sulphur content less than 0.2 %, and that the water content should be in the interval 10-14 %. The ballast material, which had a maximum water content of about 4 %, was the same as used for the construction of the big silo, excepting certain size fractions. Expressed in weight percentage, the fraction 0-3 mm represented 10 %, the 0-8 mm fraction 60 %, and the 8-16 mm 30 % of the ballast material.

The mixing of the air-dry ballast material and the fine-grained reddish bentonite powder was performed in big concrete mixers yielding amounts of about 500 l, which were transported on trucks, applied in 30 cm thick layers and compacted by 10 runs of a 3.5 t vibration roller. This device could compact the fill very close to the concrete wall that had been cast in contact with the rock for serving as lateral confinement of the 30 m diameter foundation. The density of each layer was determined by several methods, the most reliable one being the conventional water volumeter, which is of wide use in geotechnical engineering. Laboratory tests had

shown that both the conductivity and compression criteria would be fulfilled if a dry density of about 2.1 g/cm^3 could be reached and considering the expected statistical variation, the minimum value 2.05 g/cm^3 was selected as lower limit. The outcome of the density measurements was that the dry density, after some complementary compaction of certain layers, was in the interval $2.10\text{--}2.29 \text{ g/cm}^3$, the average value for the respective layer being 2.22, 2.17, 2.21, 2.23, 2.18 and 2.15 g/cm^3 .

Plate loading tests on the completed upper surface of the 1.5 m thick bed gave an E-modulus of 150 MPa and a friction angle of 45° . FEM analyses were made in order to predict the settlement of the silo and to estimate the risk of plastization. The settlement calculation indicated that the movement of the silo would be in the required interval, and calculation of the shear stress distribution showed that plastization would be confined to a small part of the bed assuming no vertical load on the bed that extends outside the silo bottom (Figure 174). In practice, full silo load will not be developed until long after the slot filling exerts a sufficiently high vertical load on this part of the bed, which - in practice - eliminates plastization or makes it insignificant.

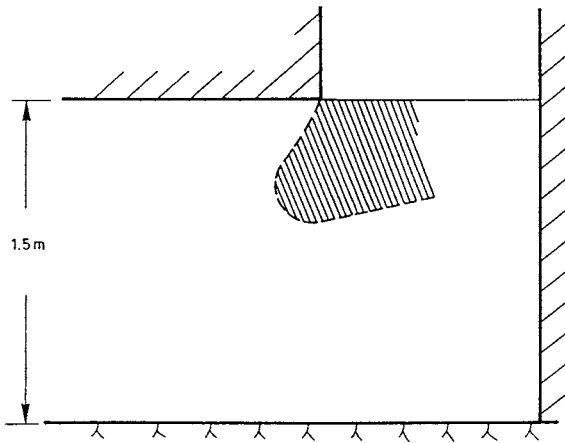


Figure 172 Plotting of the extension of plastization of the bottom bed calculated by FEM

The silo is being filled with waste at a very slow rate and annual measurements of the settlement are made by precision levelling. The settlement due to compression of the bed is about 6 mm after 6 years as illustrated by Figure 14 in Chapter 1.

4-4 Disposal in deep shafts

In principle it is possible to construct big shafts to large depths and if this is made at sea in a region where tectonic activities are low and can be expected to remain low like in certain Swedish coastal areas, one would create possibilities for safe disposal of very hazardous waste, including LLW and MLW and even possibly HLW. Such a concept, which was proposed and patented a number of years ago by the British company C.E.T. for hosting various sorts of British radioactive waste in the North Sea, can have the principal features indicated in Figure 173. The cylindrical shaft, which may well be many hundred meters deep and have a diameter that the rock structure allows for - 15-25 m would be no difficulty - has to be lined with concrete in the upper part but not necessarily deeper down. It has no access through ramps etc but only from the ground surface, which can be an artificial, temporary island.

The construction has to be completed before waste application takes place, which is made in the simplest possible fashion, i.e. by layerwise application and compaction of bentonite-rich layers interchanged with application of sets of mechanically stable waste containers embedded in on-site compacted bentonite-rich backfill or surrounded by blocks of highly compacted bentonite. Larger compartments of radioactive objects from decommissioning of nuclear plants, even complete reactor tanks from i.a. submarines, can also be applied at suitable levels. Rather comprehensive sealing may be required, except if freezing the rock is applied for tightening and stabilization, which is suitable and probably necessary in sedimentary rock. Suitable location of such shafts is expected to minimize inflow in the construction period and to reduce percolation by groundwater driven by regional hydraulic gradients to practically none at all after sealing the repository. The concept may be particularly suitable for repositories located in permafrost. Since the bentonite components maintain their ability to hold water and serve as effective seals at temperatures well below zero, the entire waste application and backfilling operation can be made at such low temperatures, which are required in order to prevent the permafrost to thaw.

The total volume available for waste containers can be estimated at 100 000-200 000 m³, which makes the concept very cost-effective since the rock construction is simple and rapid. The major advantage is naturally that the hydraulic gradients are insignificant and, hence, that

there is no driving force for percolation of the repository as long as thermal gradients are absent and the entire repository remains below the sea.

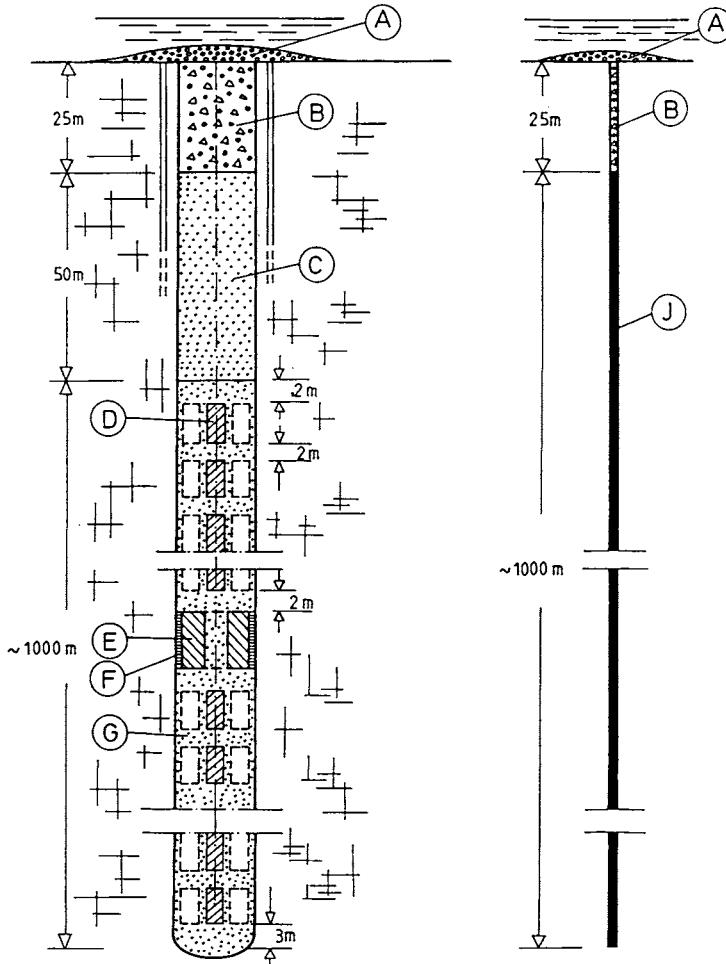


Figure 173 Example of deep shaft with 15-18 m diameter and 1 km depth after removing the temporary island filled up for the construction. A) Bottom fill of erosion-resistant block fill, B) Concrete, C) Bentonite-rich backfill, D) Waste containers, E) Large container or big subject, F) Blocks of highly compacted bentonite, G) On-site compacted bentonite-rich backfill

4-5 Disposal in very deep boreholes - The VDH concept

4-5.1 General aspects

Disposal of highly radioactive waste in deep drilled holes has been examined in a comprehensive SKB-study and found to be technically feasible [8]. The maximum depth of the considered holes was 4 km in the study and a number of interesting conclusions could be drawn both with respect to the stability of deep boreholes with a diameter of several decimeters and to the possibility to put waste in them and provide effective isolation. Recent cost analyses, to which we will return in Chapter 9, show that the concept is not very attractive in comparison with KBS3 and other solutions, but less deep holes may be competitive and justify presentation of the major features and construction activities of the VDH concept .

4-5.2 Main features

Disposal in deep holes in crystalline rock is attractive because the waste is located in rock that has an average hydraulic conductivity that is orders of magnitude lower than that of rock at a few hundred meters depth. The major features of the concept of the 4 km deep version VDH that was examined by SKB are indicated in Figure 55 in the design chapter. The lower 2 km “deployment” part, drilled with 800 mm diameter, contains sets of canisters separated by blocks of highly compacted bentonite that serve as frequent local seals, while the upper 2 km “plugged” part is drilled with 1300-1400 mm diameter from 500 to 2000 meters and excavated by shaft sinking technique from the ground surface to 500 m depth. The shaft part contains an upper part of rock fill covering concrete that is cast over a thick asphalt layer. From 500 to 2000 m depth the plugged hole contains highly compacted bentonite blocks that must be brought down in the hole. This is one of a number of practical problems that have to be solved in constructing the holes and applying the various components:

1. The stability of deep holes must be guaranteed in the construction and waste application phases
2. The hydraulic conductivity of the canister embedment should not be higher than that of the virgin host rock and that of the clay in the plugged part must be lower than the conductivity

of the surrounding rock

3. The bearing capacity of the bentonite components in the deployment part must be sufficient to prevent significant settlement of the canisters
4. The clay in all parts of the hole must create a tight contact with the rock so that leakage along the clay/rock interface does not take place
5. The sets of canisters with their separating bentonite blocks must be brought down in a controlled fashion

ROCK STABILITY

The rock stability criterion suggests that thixotropic drilling muds are used and it has been concluded that a Na bentonite mud with a density of 1.15 g/cm^3 , which has an ability to enter fractures wider than around $100 \text{ }\mu\text{m}$, is suitable. This is very advantageous for sealing of intersected fractures of no importance for the rock stability, but it may contribute to the formation of rock fall by creating unstable rock wedges. In the preliminary study of the VDH concept such rock fall, associated with further disintegration beyond the wedges due to altered stress conditions, was expected to yield a roughly elliptic cross section of the hole, with a large and small diameter of 1500 and 1300 mm, respectively, in the upper part, and 1200 and 800 mm, in the lower part. Delayed rock fall that may take place in the course of the application of canisters and bentonite blocks has to be counteracted by installing a coarse-perforated “cage” liner, which also serves to guide the waste packs. The liner, which should be made of the same kind of metal as the canisters for the sake of chemical stability of both, occupies part of the volume and reduces the effective space for blocks of highly compacted bentonite. For VDH the free inner diameter of the liner in the plugging part is 1000 mm, while it is 600 mm in the deployment part. The maximum diameter of the bentonite plugs and canister/bentonite units is estimated at 900 and 500 mm in the respective parts, which strongly reduces the net density of the bentonite clay formed from the expanded blocks.

In order to keep the density as high as possible the drilling mud is intended to be replaced by a thicker “deployment” mud and it is estimated that this can be made by extruding it stepwise from containers submerged in the drilling mud [9]. Keeping in mind that rather high salt contents with calcium as major cation are expected at depth, a suitable mud of this sort is obtained by mixing bentonite clay with 10 % CaCl_2 solution to a bulk density of 1.45 g/cm^3 , i.e. 1.5 times the liquid limit. Other candidate muds may be the one obtained by mixing Na bentonite with 10 % NaCl solution to a bulk density of 1.5 g/cm^3 , and the one consisting of 30

% and 70 % silt-sized quartz filler mixed with NaCl solution to a bulk density of 1.6 g/cm^3 .

In order to apply the sets of blocks of bentonite and the sets of canisters and bentonite blocks in a controlled fashion, they must be enclosed in metal containers submerged and moved down in the mud in metal cages (Figure 174). The cages should have a large mesh aperture, suitably at least 100 mm, for allowing clay to migrate through the cage and the outer metal liner, which serves as a protection against rock fall and for guiding the canister sets in the application phase. The liner should have a somewhat smaller mesh aperture for preventing rock fragments to enter the hole.

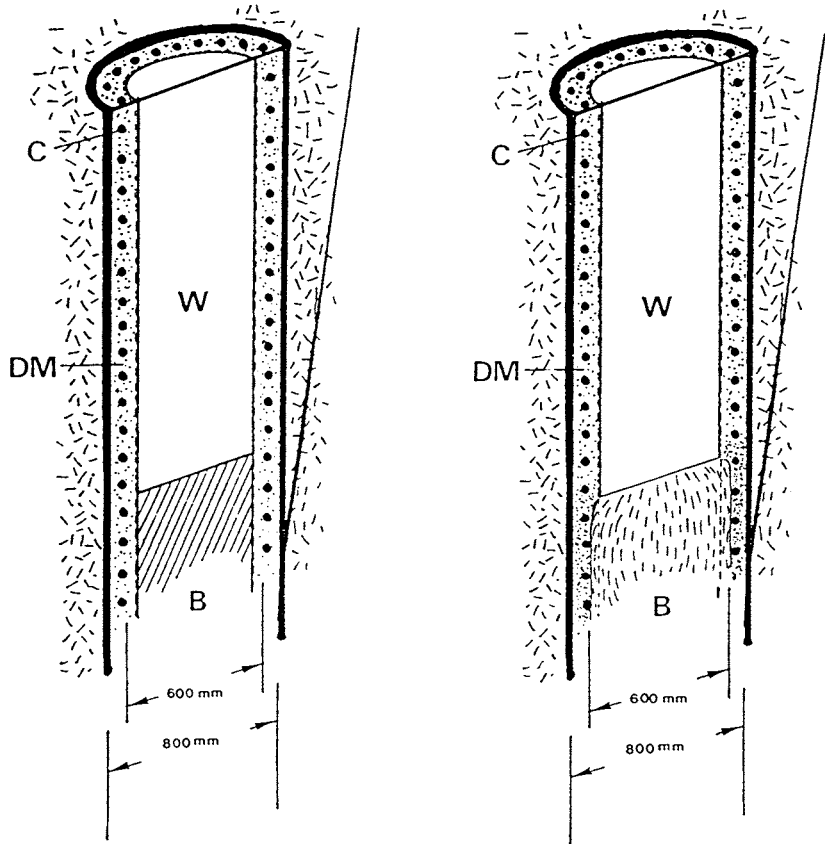


Figure 174 Canister/block set in the deployment zone. Left: Initial state of waste canister (W) and cylinder of highly compacted Na bentonite (B) submerged in deployment mud (DM). Right: State after consolidation of the mud and swelling of the bentonite core [8]

MATURATION OF THE CLAY - HYDRAULIC CONDUCTIVITY AND BEARING CAPACITY

The highly compacted bentonite blocks absorb water from the surrounding deployment mud, which provides water for the bentonite block expansion, and which consolidates under the effective pressure produced by the expanding compacted bentonite blocks. If the blocks have a bulk dry density of 2.1 g/cm^3 the net dry density is expected to be $1.4\text{-}1.5 \text{ g/cm}^3$ corresponding to a bulk density of $1.89\text{-}1.95 \text{ g/cm}^3$, which gives a hydraulic conductivity of less than about 10^{-11} m/s for temperatures below $110\text{-}130^\circ\text{C}$. This is on the same order of magnitude or somewhat less than the bulk conductivity of the host rock at depths smaller than about 2 km.

Assuming that the canisters are of a type that SKB considered in the VDH study and which is illustrated in Figure 57, the vertical pressure on the bentonite blocks will roughly correspond to the swelling pressure of the bentonite separating the canisters, and the normal pressure against the wall will be sufficient to produce a wall friction that carries the canisters [9]. The function is in fact very complex and the major question concerning the maturation phase is how quickly the bentonite around the canisters homogenizes. Preliminary estimates indicate that the application of canister/bentonite blocks in the deployment zone needs to take several months in order to yield sufficient maturation of the clay and to avoid large canister movements. In this respect, the use of deep shafts with dense embedment of the waste containers offers great advantages.

TECHNICAL DEVELOPMENT

A number of special features and ways of improving the bearing capacity and speeding up the maturation rate can be imagined and it is estimated that the VDH concept - preferably with less deep holes - represents a serious alternative for disposal of HLW. In comparing different concepts it is important to realize that the general philosophy of VDH-type repositories is that a rather poor isolating property of the embedment of canisters in the deployment part can be accepted if the plugged part serves as a very effective seal.

RETRIEVABILITY

Authorities responsible for legislation and licensing in some countries require that radioactive

waste should be retrievable. For VDH repositories retrieval of canisters is probably simpler than for various other concepts. Thus, oil well drilling expertise claims that redrilling and picking up even heavy equipment from deep holes is feasible. Still, considering the fact that the canisters may be rather quickly corroded, extraction and further handling is expected to be very hazardous and difficult.

4-6 Special techniques for use in mines

4-6.1 Conditions

Disposal of hazardous chemical waste may well be done in deep mines. There are a number of restrictions and difficulties, however, namely:

- * The waste should be in solid form, requiring solidification in a form that is compatible with both the containers and their embedment
- * pH of the groundwater should be low in order to avoid degradation of bentonite embedments and it may be lower where sulphide ore has been mined
- * The rock stability must be sufficiently high to allow for safe waste application and backfilling and this may not be the case in many mines.
- * The hydraulic conductivity and groundwater percolation of the rock mass should be low

4-6.2 Types of waste and their containment

Solidification of liquid waste makes it handable and put it in a form that releases hazardous elements at a rate that is controlled by its solubility. For many waste types, including heavy metals, Portland cement and concrete with such cement are suitable for solidification and containment since pH is enhanced and the solubility reduced. Typical dangerous wastes that can and should be emplaced in solid form are inorganic substances that contain cadmium, mercury, lead, copper, chromium, nickel, vanadium and zinc, and organics like cyanides, PCB and pesticides.

Most wastes, like hydroxides of heavy metals and slags and filter cakes rich in heavy metals from waste processing, as well as fine particulate material from scrubbers and electrofilters - suitably coarsened by cement stabilization - contain relatively moderate amounts of hazardous elements but some, like cadmium batteries and mercury from thermometers, represent very toxic substances, for which a number of deep mines would serve well as repositories.

4-6.3 Disposal in mines

Figure 175 illustrates common features of deeply located ore bodies. Excavation yields very big empty rooms if backfilling has not taken place in conjunction with the excavation, and such rooms are naturally suitable for hosting hazardous waste since they can host large quantities and make rational application possible. The problem is that such rooms, which may be more than 50 m wide and high, are usually not sufficiently stable to allow for safe operations of any kind and require expensive stabilization. Temporary shielding in the form of roof constructions and rock support consisting of concrete buttresses and comprehensive bolting may be required. The basic requirement that the groundwater movement should be limited in the rock mass may be hard to fulfil since the disturbance caused by the excavation may be considerable around big rooms. Usually, the rock immediately surrounding sulphide ore bodies have a lower strength than the surrounding host rock, which further enhances the increase in hydraulic conductivity of the nearfield of big rooms.

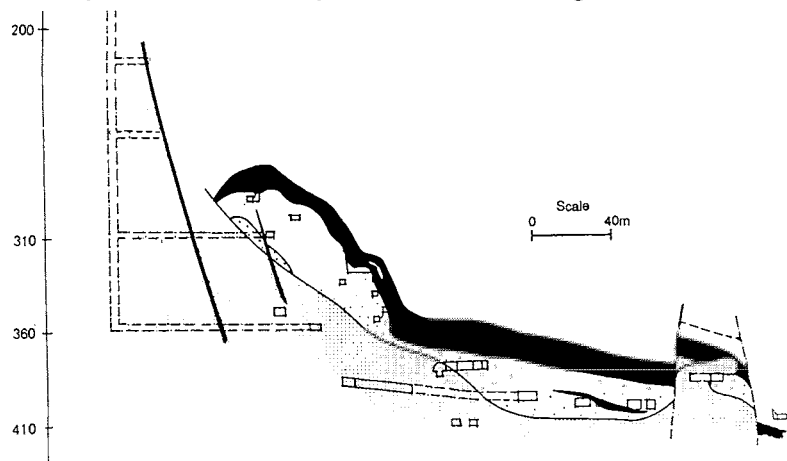


Figure 175 Ore bodies (black) and rooms at Stripa. The larger part of the ore has been mined leaving large open rooms and a number of smaller rooms and drifts

This suggests that wastes representing different risk levels should be placed in different parts of a mine; less hazardous waste in big rooms, and the most toxic waste in smaller rooms like tunnels and drifts outside the excavation-induced disturbance around the big rooms. Both types of waste should be isolated from the rock by a zone of bentonite-containing material for minimizing percolation of the waste and for maintaining a tight contact with the rock in order to avoid groundwater flow along the backfill and the rock and also for supporting the rock. Figure 176 shows how this principle can be applied in a mine, the example being from the Stripa mine. Here, hematite ore was mined, but otherwise the conditions are similar to those in many mines in sulphide ore regions.

Chapter 4 - Construction

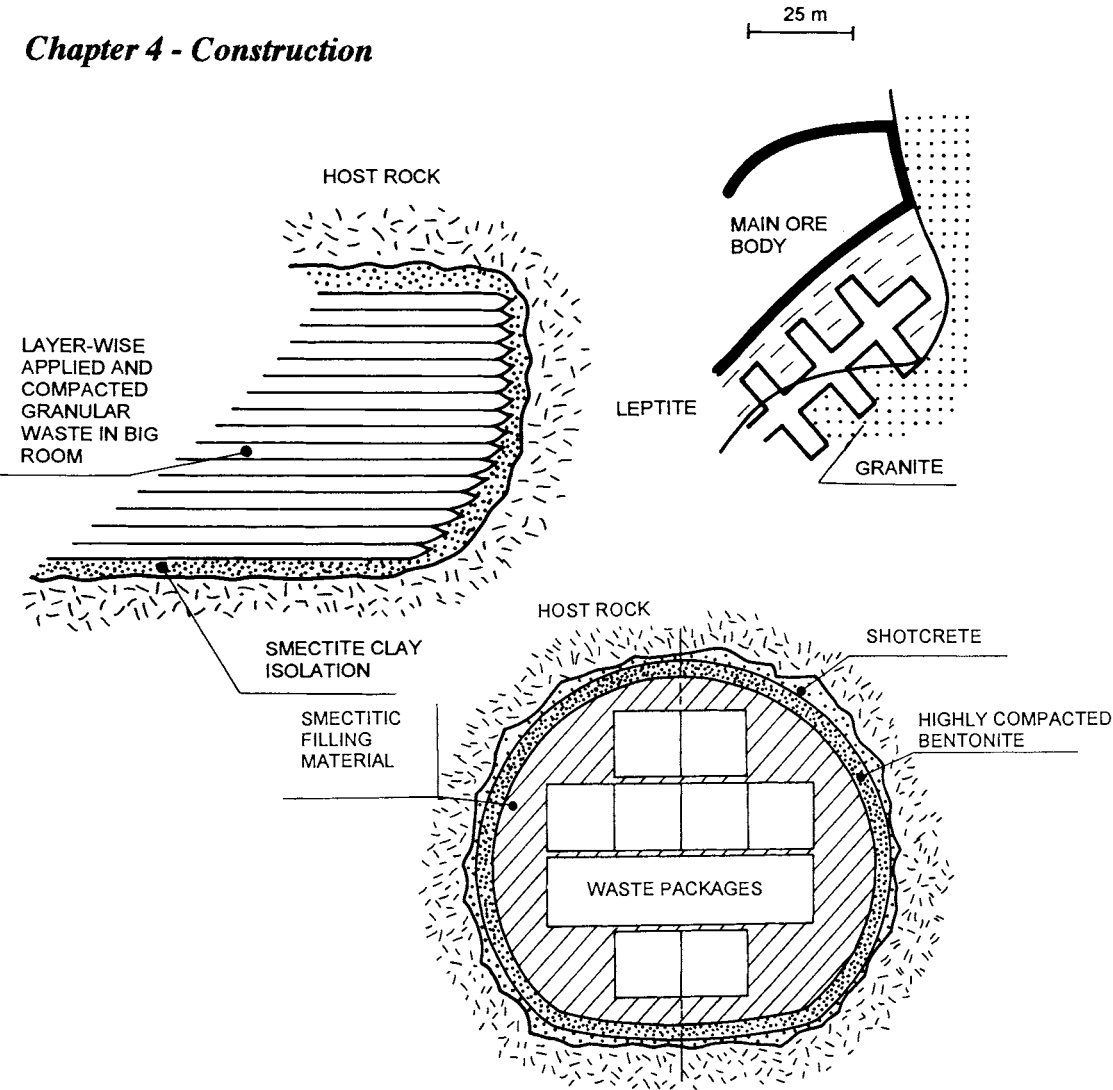


Figure 176 Possible use of mine for disposal of toxic chemical waste (Stripa). Upper: Plan drawing. Central: Moderately hazardous waste in granulated form, applied in heavily compacted layers and isolated from the rock by bentonite clay. Lower: High-risk waste cast in concrete that are separated from the rock by highly compacted bentonite and on-site compacted backfill

4-7 Seals

4-7.1 General

The sealing effect of plugs and groutings, which can be very significant as demonstrated by the examples in the chapter of design of repositories, naturally depends on how well the seals can be constructed. In turn, this is a function of how practical the design can be made and of the quality assurance.

4-7.2 Slot cutting

SLOT DRILLING

A common way of cutting recesses in rock is to bore overlapping holes by core or percussion drilling. A number of such cuttings have been made in the Stripa mine, as illustrated by Figure 160, and in various other underground construction projects. The experience is that core drilling is superior to percussion drilling in producing regularly shaped slots since orientation of the individual holes can be made with higher accuracy and because the deviation is very much smaller, but the cost is naturally much higher. 76 mm core drilling seems to represent an optimum with respect to the rate of drilling and cost.

SAWING

Stone-cutting plants make use of large stationary diamond saws but for underground application the maximum disc radius and thus the depth of the slots cut by sawing can hardly exceed 0.5-0.75 m (Figure 177). Keeping in mind that the most intensely disturbed zone around blasted tunnels is usually less than 0.5 m, except in the floor, this technique may still be used for slot cutting of recesses around tunnels for applying blocks of bentonite blocks. Stepwise excavation for reaching deeper into the rock can in fact be made so that the root of the disturbed zone in the floor is reached. As described in the chapter on design, cutting of slots by sawing has been successfully applied in the shaft sealing experiment at Stripa. The technique is time-consuming and expensive.

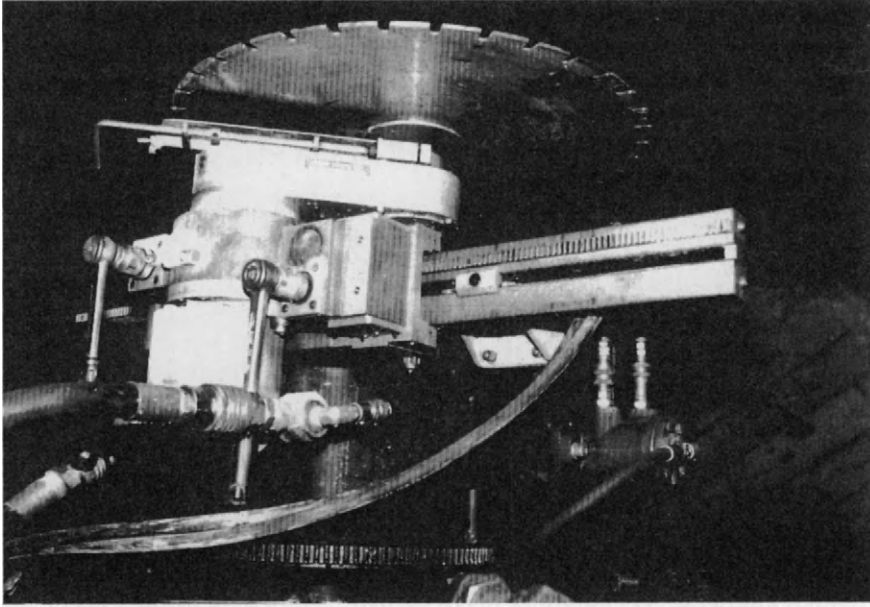


Figure 177 Equipment used for cutting 25 cm deep slots by use of diamond saw

WATER JET CUTTING

Cutting of steel, concrete and rock can be made effectively by use of water jet cutting with or without adding abrasives like metal or garnet powder. The aforementioned holes drilled in

Canada with 1.5 m diameter and several meters depth, serve as an example of the possibility to use water jet cutting in practical rock construction. Still, cutting very deep down in rock seems to be much more time-consuming than shallow penetration and the technique seems to be particularly suitable for cutting slots only to a depth of 1 to 2 meters. A particularly attractive feature is that the nozzle can be turned and adjusted to yield a more complex design and adapt to winding rock structure. Figure 178 shows the equipment for rock cutting developed by the Japanese company Kajima, and Figure 179 shows a V-shaped slot produced by a rotating twin nozzle developed by this company. This technique seems to offer the quickest and cheapest way of cutting slots.

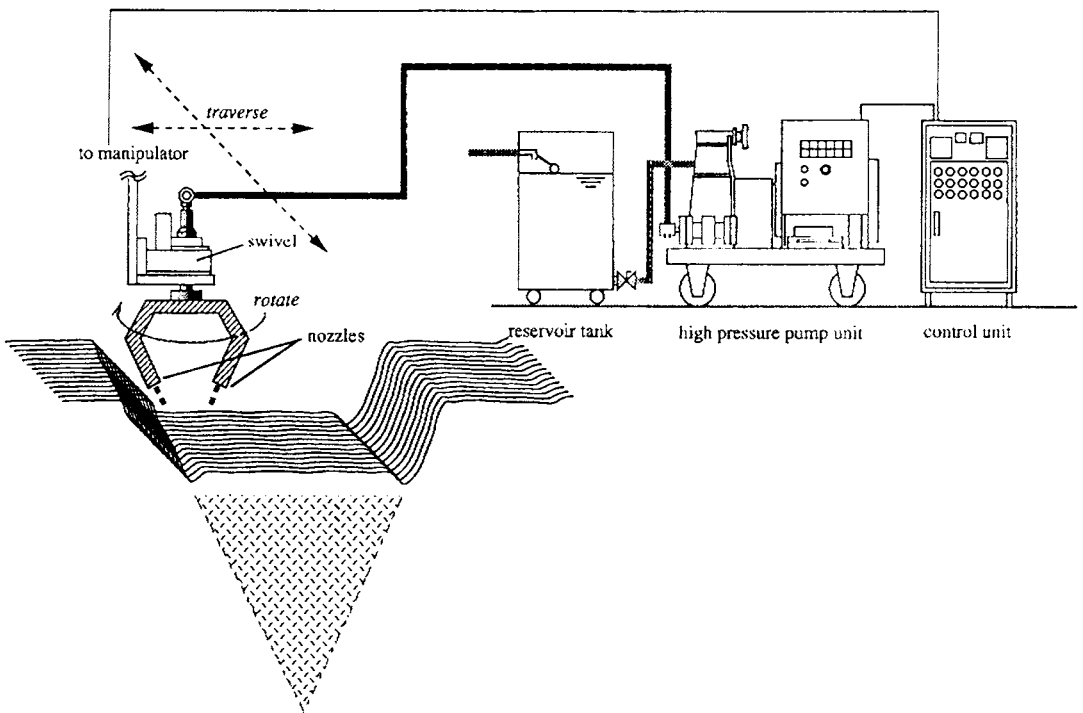


Figure 178 Schematic picture of the water jet cutting equipment developed by the Japanese company Kajima

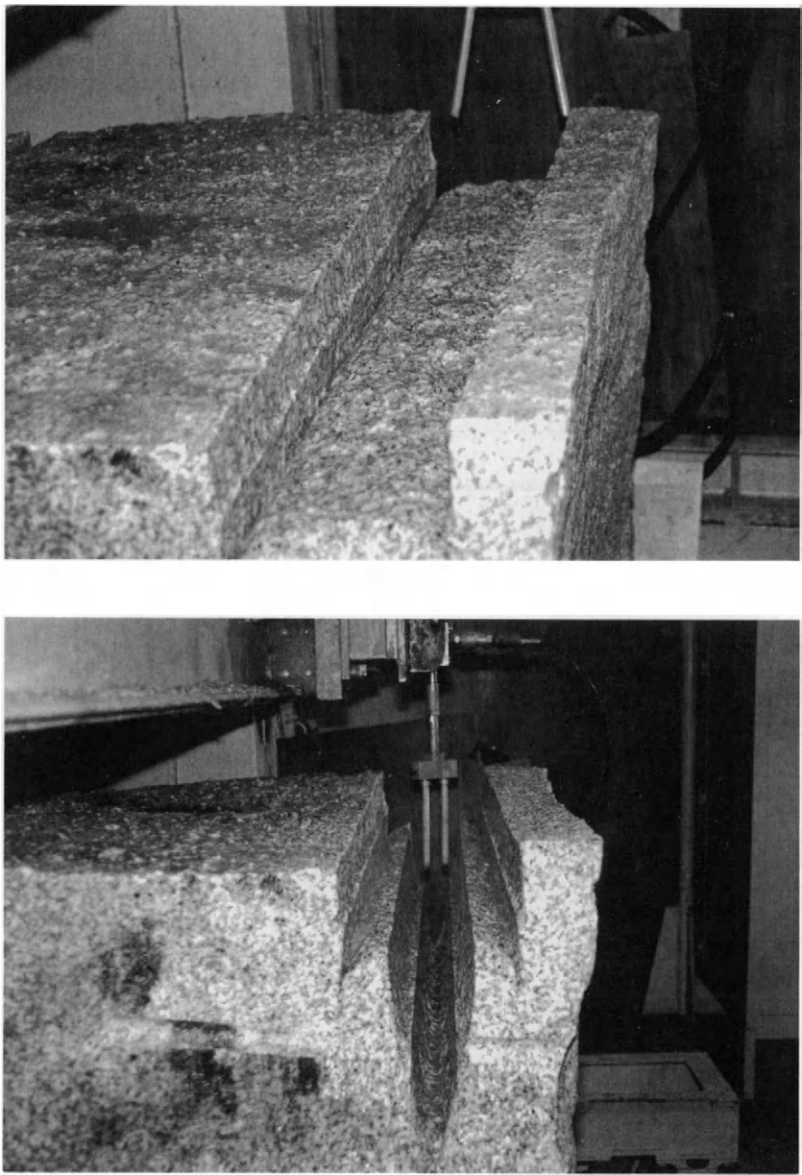


Figure 179 Successive steps in water jet cutting of V-shaped slot in granite (Kajima)

4-7.3 Plugging

CONCRETE BULWARKS WITH “O-RING” BENTONITE BLOCK SEALS

Construction of bulwarks of the type described in preceding chapters, i.e. concrete plugs with “O-ring”-type bentonite seals, requires that a number of issues be considered:

1. Shrinkage of the concrete will take place unless expansive cement is used, yielding poor contact between concrete and rock
2. The irregular shape of blasted tunnels cause difficult, tedious and expensive form work (Figure 180)

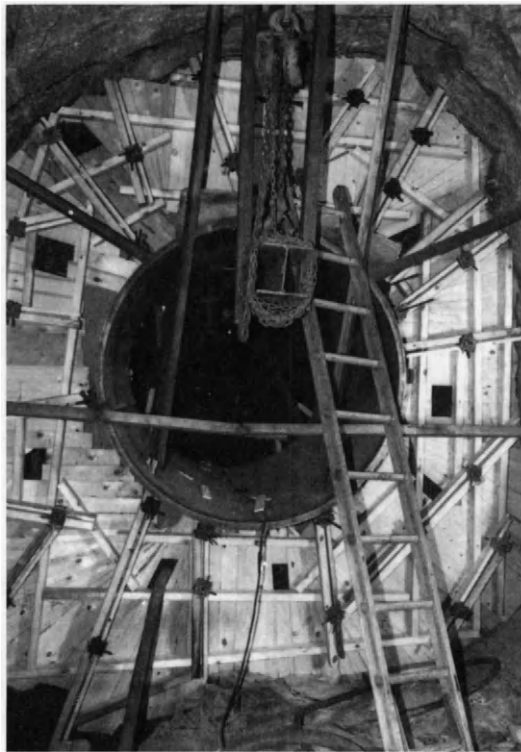


Figure 180 Complicated form work in blasted tunnel with central steel tube

3. Casting of the uppermost part must be made so that the concrete fills the space up to the irregular rock surface of blasted tunnels

4. Long-term stability.

Shrinkage of concrete plugs in the course of the hydration can be predicted using empirical rules specified in various handbooks and manuals for estimating the aperture of the resulting opening between the plug and the tunnel roof. The best method to obtain a tight contact is to leave a space of a few centimeters when casting the plug and to prestress the rock by inserting hydraulic flat-jacks that are injected with cement grout under high pressure. The remaining space is then filled with expansive cement. This procedure has the beneficial effect of compressing the “disturbed zone” before the open space is filled. Highly compacted bentonite blocks, which form the “O-ring”-type sealing, and which become exposed in the space need to be protected by cement-poor mortar and a suitable finegrained filter during the several months long period that must pass before the remaining backfilling takes place.

The matter of long-term stability is not fully cleared out. As mentioned in chapters 3-7.1 and 3-7.3 it is estimated that complete disintegration of the concrete due to dissolution of a large part of the cement may take many thousand years and even tens to hundreds of thousands of years depending on the groundwater flow and composition. However, there are reasons to believe that Portland cement and concrete with such cement do not remain intact for more than a few thousand years. Slag cement, on the other hand, may be more long-lived, although this remains to be certified. A number of steps in the design and construction phases can be taken to extend the operative lifetime of concrete plugs, like adding a proper amount and type of silica fume to the cement, using low-electrolyte water and first-class granitic ballast (aggregate) material for the preparation of the concrete.

BENTONITE BLOCK MASONRIES

Construction of block masonries is preferably made in the fashion described as Method C for tunnel backfilling in the preceding chapter. Both for backfills of this sort and for plugs consisting of bentonite blocks as major sealing component, it may be required to apply temporary seals in the course of the construction in order to avoid water uptake from the rock, which can transform the outer blocks to slurry in one or a few weeks depending on the access to water. Such temporary seals are most easily produced by applying cement coatings with a few centimeters thickness by shotcreting. For TBM-drilled tunnels large inflatable packers would offer the simplest solution.

BOREHOLE PLUGGING

One of the most important sealing activities in repositories is to plug boreholes made for geophysical and other investigations. Holes that extend from the ground surface down into the repository area would otherwise transmit radionuclides to the biosphere. A practical problem is that such holes may be more than one kilometer long and that they must be effectively sealed at least down to 500 m depth, which requires reliable application methods and sealing materials with sufficient longevity. The matter has been investigated in detail both in SKB research projects and in the international Stripa Project and plugs of the sort described here have been applied both at sea from drilling platforms (Forsmark repository) and on land for sealing prospecting drill holes in uranium shale (Ranstad, southwestern Sweden).

The excellent tightness and self-healing ability of dense bentonite makes this material very suitable for borehole plugging and a new technique using such material was developed and applied by the author in the early eighties [10]. The problem of applying bentonite blocks into long holes in a controlled fashion, i.e. so that no unfilled parts are left in the holes, was solved by using richly perforated pipes to insert the compacted bentonite. The perforation lets the clay expand through the holes, embedding the pipes and ultimately forming an almost completely homogeneous plug of bentonite. The pipes can be made of copper or bronze, which are chemically very stable and cause only little change in a long-term perspective, i.e. only cation exchange from sodium to copper. The bentonite adheres to the borehole walls and the pipes and seals off the boreholes as effectively as determined by its density, which is a function of that of the blocks and of the free space in the boreholes with the pipes that the clay will occupy. The pipes, which preferably have a thickness of 2-4 mm, need to be 2-3 mm smaller in diameter than the borehole, and using blocks with a dry density of around 2.0 g/cm^3 , the net bulk density of matured plugs is in the interval of $1.7\text{--}1.9 \text{ g/cm}^3$. This yields a hydraulic conductivity of 2×10^{-13} to $5 \times 10^{-11} \text{ m/s}$ depending on the porewater chemistry. Figure 181 shows the technical system and Figure 182 the swelling process, which leads to substantial filling of the space between the perforated pipe and the borehole wall in a few hours. After several weeks the clay embedding the pipes is largely homogeneous.

The use of stiff perforated pipes makes it possible to plug steeply inclined hole from below, which has been made without difficulty in 70 m long 76 mm diameter holes, and 100 m long subhorizontal holes with 56 mm diameter (Figure 183) have also been successfully plugged [11]. The latter application involved measurement of the maturation rate by applying water overpressure in built-in filters and recording the critical pressure for piping in the maturing clay at different times after inserting the plug, which would ultimately reach a clay bulk density of 1.9 g/cm^3 (Figure 184). It was found that it could resist a hydraulic gradient of around 60 after about 1 day, and 200 after 4 weeks. Up to 1 km long subhorizontal holes and holes

extending downwards to more than 1 km can probably be sealed in this fashion. However, since holes of this length will intersect 2nd or even 1st order discontinuities, parts of the boreholes will be unstable, which can jeopardize the sealing operation. The problem can be solved by grouting these parts using cement injection under high pressure, and redrilling after hardening of the cement.

“Sandwich”-type plugs with bentonite and long-lived cement applied interchangeably may be an optimum solution in rock with frequent break-outs and risk of creep-induced failure. In short vertical holes plugged from above, the pipes can be replaced by simple nets of copper or other suitable metals for quicker maturation (NAGRA), but their mechanical weakness limits the depth to a few tens of meters (Figure 184).

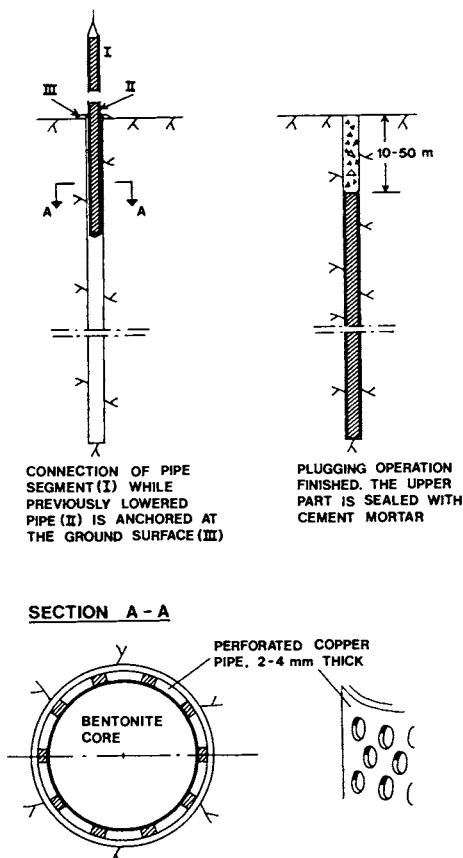
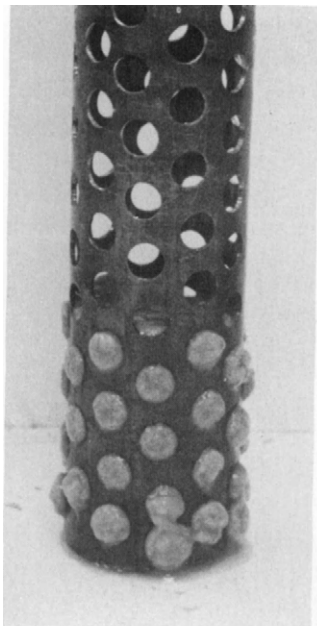
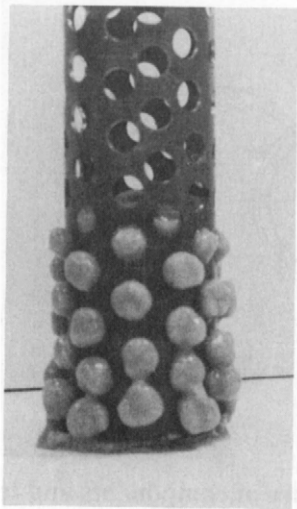


Figure 181 Schematic picture of components and technique for bentonite plugging of deep holes



1 h



8 h

Figure 182 Expansion of Na bentonite through the perforation of plug pipe

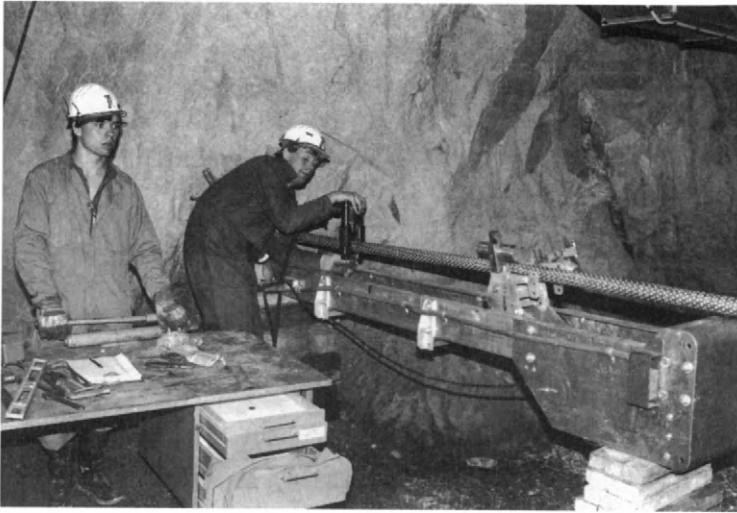


Figure 183 Upper: Insertion of 100 m long perforated pipe with highly compacted Na bentonite using hydraulic jack . Lower: Light but weak net-confined bentonite plug (NAGRA)

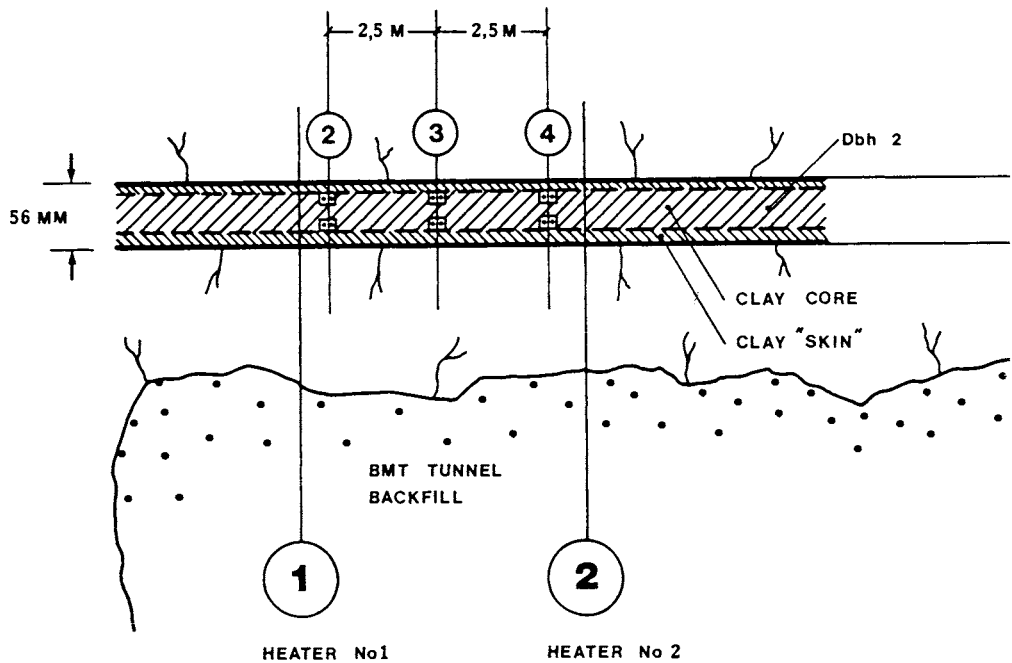


Figure 184 Test arrangement for recording the maturation rate of bentonite plug by pressurizing one built-in filter (2) or (4) and keeping the central filter (3) drained

4-7.4 Grouting

CONVENTIONAL GROUTING

The traditional way of fracture sealing is to inject grout under high constant pressure in boreholes using a packer that is expanded mechanically, hydraulically or pneumatically (Figure

185). The pressure is produced by a pump that is used both for the injection and for preparation of the grout as indicated in Figure 186. The preparation involves mixing of water, grout material - in practice cement - and possible other additives like superplastizicer and silica fume in a colloidal mixer, and effective mechanical agitation in an agitator tank. The procedure is simple and straight forward but the selection of a suitable sequence in injecting arrays of holes requires considerable understanding of the rock structure and experience, which is often interpreted as "witchcraft".

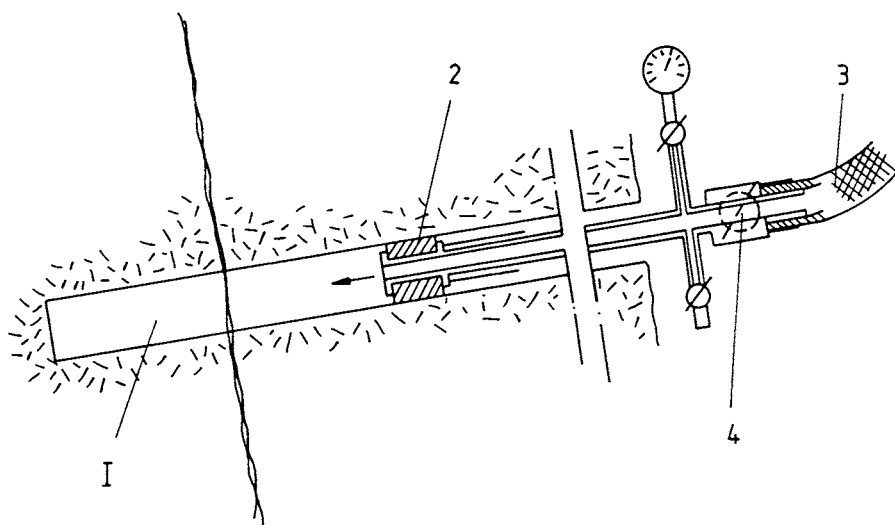


Figure 185 Grout injection in borehole (1) using single, "mechanical" packer (2). The procedure is the following: The hole is first filled with grout by use of the packer tube. The flexible tube from the pump cylinder is then attached to the packer tube and the required pressure applied

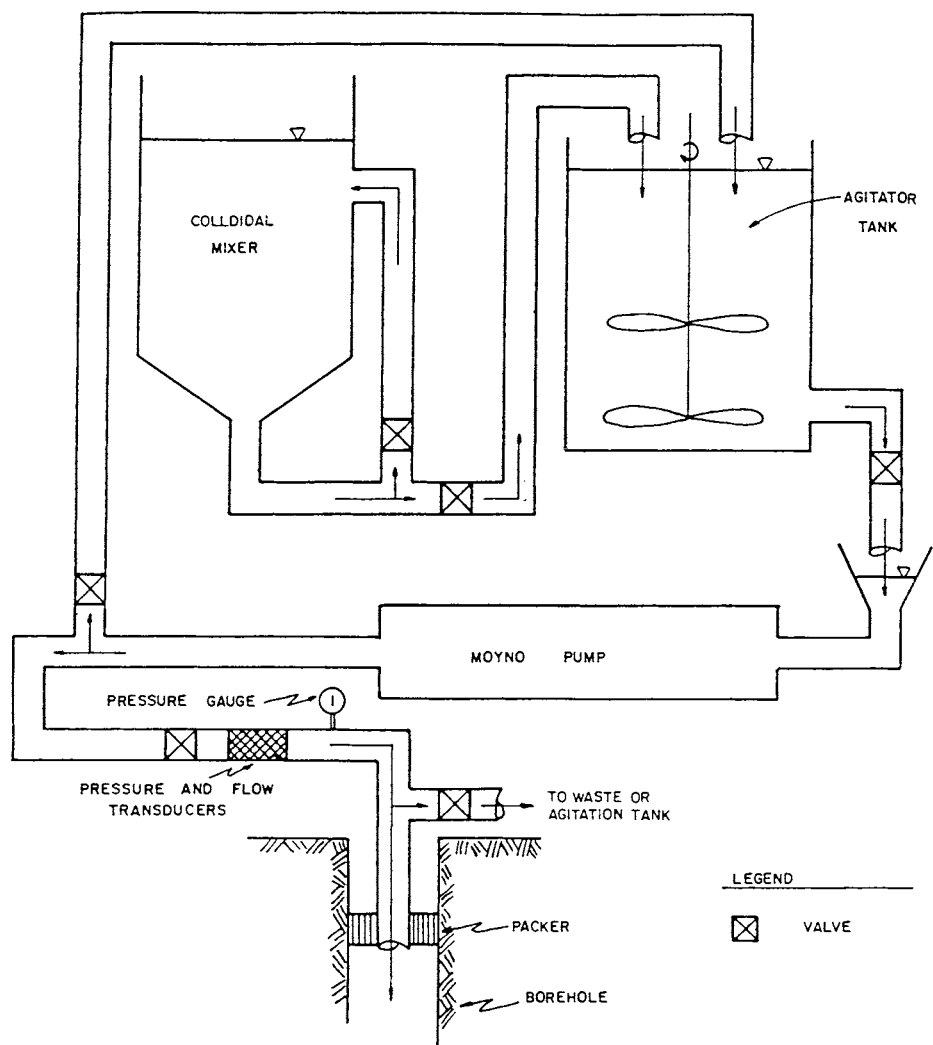


Figure 186 Schematic picture of conventional cement grouting plant

There are a number of practical rules that are helpful in predicting the effect of cement grouting and in planning such work. Major points are:

1. Fractures with smaller hydraulic aperture than 300 μm are usually considered to be too narrow to be injected
2. Finely ground cement is required for successful grouting
3. w/c should be less than 0.7 for avoiding bleeding, i.e. separation of the solid and liquid phases. In order to obtain sufficient fluidity of the grout, superplasticizer can be added up to 1.5 percent by weight of the water
4. Injection should be made not later than 30 minutes after preparation of the grout
5. Fractures corresponding to 4th and higher order discontinuities are hardly groutable
6. 3rd order fracture zones are groutable but because of the few and usually rather poorly interacting fractures the sealing effect is not always very good. The spacing of the grouting holes should not exceed 0.5 to 0.7 m for successful sealing
7. 1st and 2nd order fracture zones are effectively sealed by grouting but clay gouge may prevent effective grout penetration. The borehole spacing should not exceed 0.7-1.0 m for effective sealing because gouge may be disintegrated and moved to block fractures

For predicting penetration of the grout, its rheological properties must be known and for achieving effective sealing they must be in a certain interval, the key parameter being the m -value as described in the chapter on design. It can be determined by use of rotational viscometers like the Bohlin VOR rheometer or the Brookfield RVT-D viscometer [12], (Figure 187).

DYNAMIC INJECTION

While conventional grouting is sufficiently efficient to seal fracture-rich very permeable zones of 1st and 2nd order, 3rd order zones and discrete fractures of 4th order can hardly be sealed. If the fluidity of the grout can be decreased, for which dynamic pulse-type injection can be used, finer fracture openings can be penetrated than by using conventional, static pressure injection. . Dynamic injection involves superposition of an oscillatory pressure over a static pressure. The latter is commonly 1-2 MPa where the water pressure is low, while the oscillatory pressure has the form of high-pressure spikes of very short duration (Figure 188). The oscillatory pressurizing is particularly effective when using smectite grouts because

of their thixotropic nature, but it has some effect on cement grout too

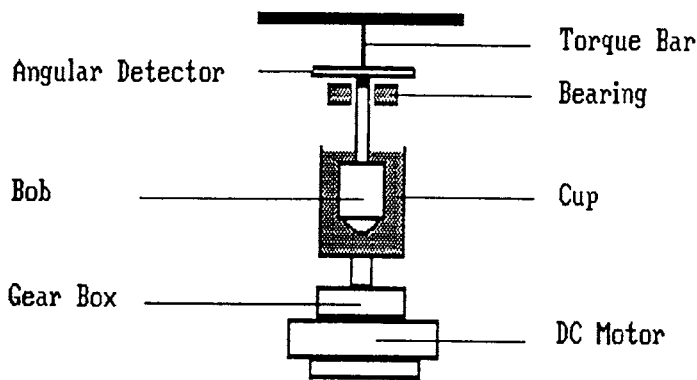


Figure 187 Schematic picture of rotational viscometer

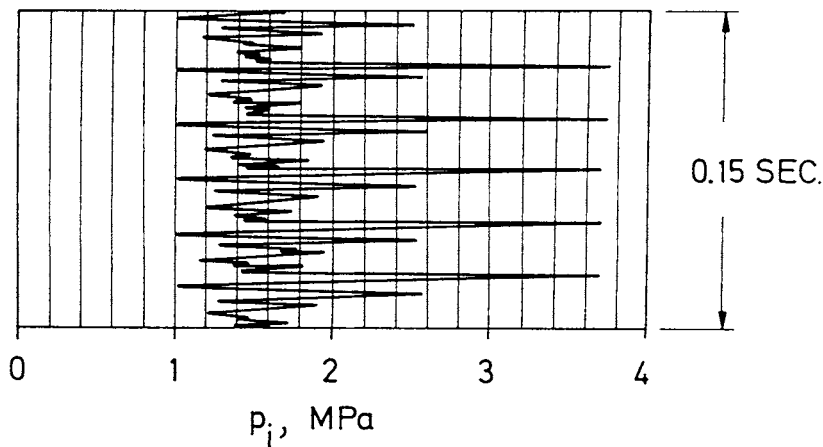


Figure 188 Example of recorded pressure spectrum at dynamic injection

The preparation of grout for effective penetration of fine fractures requires more attention than in ordinary injection, the major point being that the cement or clay material must be very fine-grained, homogeneous and freshly prepared. In practice, the grain size must be very small, i.e. significantly less than the fracture apertures that one wants to seal, and no aggregation due to chemical reactions must take place in the preparation phase. This requires that the agitation must be very effective and, in the case of cement, that the material must be delivered and stored in tight containers so that hydration is hindered. The plant comprises a very effective colloidal mixer and a screw pump for supplying the pulse-producing injection machine with very well homogenized slurry via a de-airing valve (Figure 189). In its simplest form the injection machine can be a high-frequency hammering piston operated by compressed air, on which the static back pressure is applied, but more effective equipments are under development.

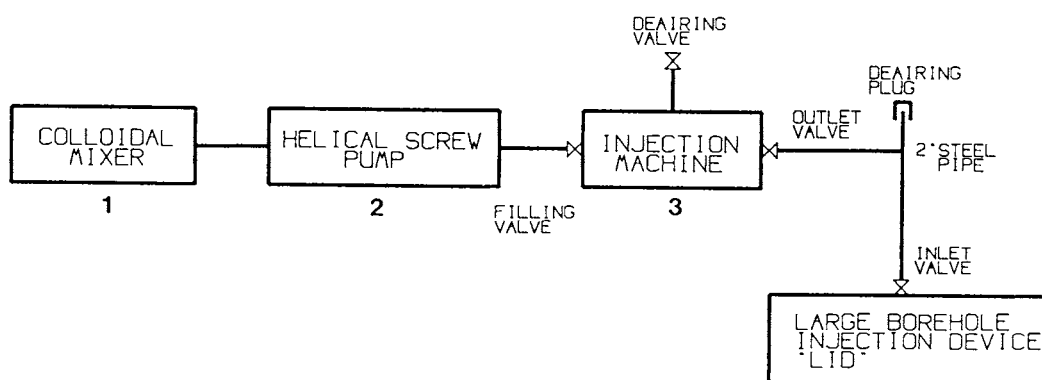


Figure 189 Schematic picture of grouting plant for dynamic injection

Figure 189 illustrates the special case when the injection machine is connected to a device “LID” for injection of large diameter boreholes, a possible application of dynamic injection as reported in Chapter 3 [12]. This apparatus, which is shown in Figure 190, has an outer diameter of the outer steel tube that is somewhat less than one centimeter smaller than the borehole diameter and its upper and lower thirds are coated by rubber membranes can be expanded by a hydraulic pressure of several MPa for preventing grout that is injected in the

along the packer units. The trumpet-like nozzle that leads grout from the pump has the important function to maintain a constant cross section through which the grout moves in order to preserve the energy and nature of pressure pulses induced by the injection machine. Figure 190 shows the machine connected to an installed megapacker for grouting in the BMT area at Stripa.

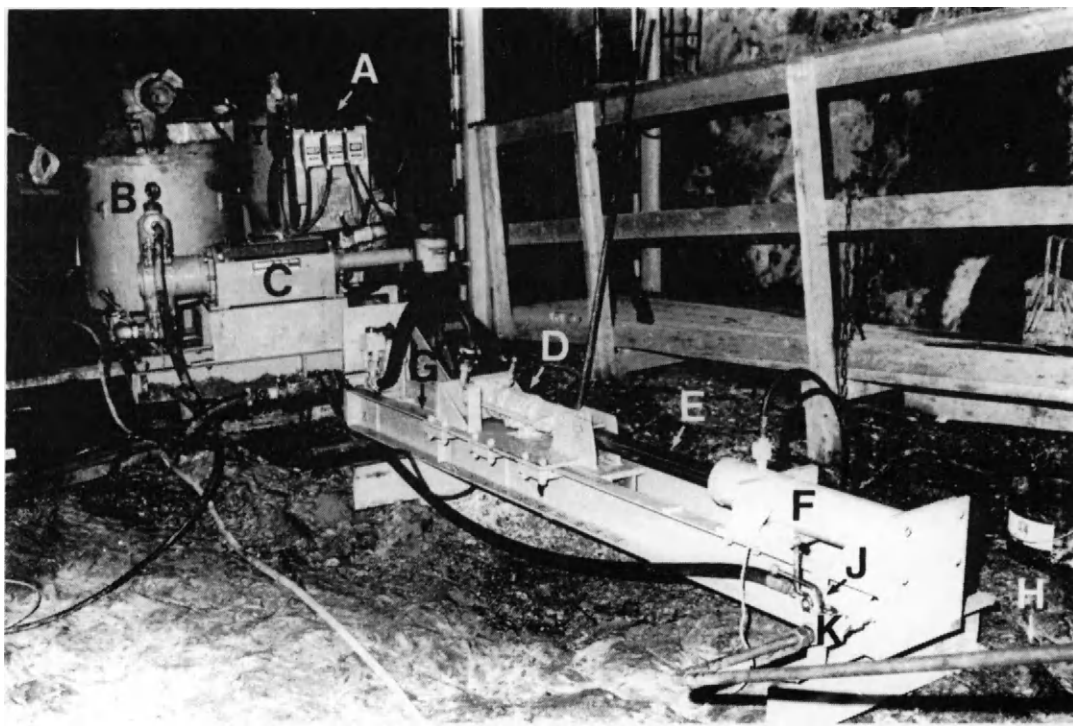


Figure 190 Prototype machine for injection of large boreholes at Stripa [12]. A) Colloidal mixer, B) Stirrer, C) Plunger pump, D) Oscillatory pressuring device, E) Piston acting on the grout in cylinder F, J) and K) are valves

4-8 References

- 1 Pusch,R. Rock mechanics on a geological base. Elsevier Publ. Co. (In press)
- 2 Andersson,B. and Halén,P.-A. Mining methods used in the underground tunnels and test rooms at Stripa. Technical Project Report No 8, Swedish-American Cooperative Program on Radioactive Waste Storage in Mined Caverns in Crystalline Rock. LBL-7081/SAC-08/UC-70, SKB/Lawrence Berkeley Laboratory, 1978
- 3 Pusch,R. and Stanfors,R. Disturbance of rock around blasted tunnels. Int. J. Rock Mech. Min. Sci. & Geomech. Abstr. Vol.29, No.5, 1992 (pp. 447-456)
- 4 Sandstedt,H., Wichmann,C., Pusch,R., Börgesson,L. and Lönnerberg,B. Storage of nuclear waste in long boreholes. SKB Technical Report TR 91-35, 1991
- 5 Pusch,R. Final report of the borehole, shaft, and tunnel sealing test - Volume II: Shaft Plugging. Stripa Project TR 87-02, SKB, Stockholm, 1987
- 6 Pusch,R., Börgesson,L. and Nilsson,J. Buffer Mass Test - buffer materials. Stripa Project, Technical Report TR 82-06, SKB, Stockholm, 1982
- 7 Henttonen,V. and Suikki,M. Equipment for deployment of canisters with spent nuclear fuel and bentonite buffer in horizontal holes. SKB Technical Report TR 92-16, 1992
- 8 Juhlin,C. and Sandstedt,H. Storage of nuclear waste in very deep boreholes. SKB Technical Report TR 89-34, SKB, Stockholm, 1989
- 9 Pusch,R. and Börgesson,L. PASS - Project on alternative systems study. Performance assessment of bentonite clay barrier in three repository concepts: VDH, KBS3 and VLH. SKB Technical Report TR 92-40, SKB,Stockholm, 1992
- 10 Pusch,R. Borehole sealing for underground waste storage. ASCE Proc. J. Geotechnical Engineering, Vol.109, No.1, 1983 (pp. 113-119)
- 11 Pusch,R., Börgesson,L. and Ramqvist,G. Final report of the borehole, shaft, and tunnel sealing test - Volume I: Borehole Plugging, Stripa Project TR 87-01, SKB, Stockholm, 1987
- 12 Börgesson,L., Pusch,R., Fredriksson,A., Hökmark,H., Karnland,O. and Sandén,T. Final report of the rock sealing roject - Sealing of the Near-field Rock around Deposition Holes by

Use of Bentonite Grouts. Stripa Project, Technical Report TR 91-34, SKB, Stockholm, 1991

Chapter

5 *Performance assessment*

5-1 Introduction

Performance assessment can be made of repository concepts that are located in well characterized rock and with defined design, using available physical models and referring to the experience from extensive field tests like those conducted in the Stripa Project. This chapter will deal with such assessment from the viewpoint of technical function only while the matter of safety analysis will not be discussed explicitly since it depends on the type and concentration of waste.

We will distinguish between “normal” and “exceptional” conditions, taking the first mentioned to represent ordinary, relatively conservative assumptions regarding the geological and geophysical properties of the host rock and the last mentioned to account for more severe conditions.

5-2 Normal conditions

5-2.1 Introduction

In this chapter the performance of the bentonite barrier and the nearfield rock will be examined in a long-term perspective and for making the description a bit quantitative we will concentrate on the nearfield rock and clay buffer materials of the aforementioned concepts VDH, KBS3, and VLH for final deposition of HLW. In particular, we will consider the isolating and transport conditions of the canister/clay/rock system with respect to possible degradation processes for outlining a general basis of performance assessment.

For illustrating and explaining the various processes that affect the transport capacity of the nearfield of repository concepts, and for comparing them, the general rock structure model outlined and defined in earlier chapters will be used. An important point is of course to realize that the present conditions concerning conditions of major significance like rock stress fields, climate and groundwater chemistry, will not persist for very long periods of time and that significant changes leading to rather severe conditions have to be considered. This calls for examining both "Normal" and "Exceptional" cases with respect to these factors, the firstmentioned ones representing average present conditions with some modifications called for because of probable exogenic processes like tectonics and glaciation, and the latter representing severely altered conditions.

We will distinguish between four different phases of function of the nearfield in the operative lifetime of a HLW repository, namely the application stage, the maturation stage, the heating stage, and the post-heating stage. Naturally, only the two first are relevant to disposal of toxic waste that does not produce heat.

5-2.2 Waste application stage

ROCK BEHAVIOR

Hydraulic conductivity of the nearfield rock

While the hydraulic conductivity of the nearfield of very deep holes is of no particular concern in the waste application stage, it is of great practical importance for the KBS3 and VLH concepts. This is because too strong inflow causes flooding and difficulties in emplacing bentonite blocks and canisters and requires sealing by grouting as discussed in Chapter 4.

One recognizes from the discussion in Chapter 4 that boring of big holes and excavation of tunnels causes a rather significantly enhanced axial hydraulic conductivity within a few meters from the periphery for all three concepts. Radial inflow, on the other hand, is in general somewhat smaller than the average flux in virgin rock because of the fracture-closing effect of the hoop stresses of blasted tunnels and bored large-diameter holes at a few hundred meters depth. The hourly rate may be as low as 0.001 l/m^2 , although typical values are in the interval $0.01\text{-}0.1 \text{ l/m}^2, \text{h}$.

The practical importance of the water inflow in the phase of application of canisters and bentonite blocks is illustrated by some simple estimates for the KBS3 concept. The earliest version of this concept implied that the slot between the clay buffer blocks and the rock should be 5 cm and filled with bentonite powder. This would allow application of large units of canisters or compartments surrounded by bentonite blocks in holes from which breakouts have taken place or which are not perfectly straight, the idea of filling the slot with bentonite being to keep the net clay density sufficiently high. The finding that the rate of wetting of the bentonite should be as high as possible and that electrolyte-poor water should be used for the saturation in order to avoid salt accumulation close to the canister, suggests that the slot should be as narrow as possible and filled with fresh water. A 5 cm slot may turn out to be too wide to yield a sufficiently high net density of the clay, while 1-2 cm aperture, which appears to be more suitable, may present difficulties at the emplacement of large canister/buffer units if the hole is not straight and vertical. For the most simple mode of application, i.e. manual emplacement of bentonite blocks, leaving a central space for the canister to be lowered afterwards, the inflow conditions determine if water will flow from the slot over already emplaced blocks into the space reserved for the canister. This is illustrated by Table 12, which shows the importance of the slot aperture for the rate of water rise (H) in the slot at different inflow rates.

Table 12 Height of water-filled part of the slot between bentonite and rock in 1.6 m diameter KBS3 holes at different slot width in cm. H2 is height in cm after 2 hours etc.

Slot width, cm	Inflow rate, l/h	H2	H5	H10	H20	H40
5	1	1	2	4	8	16
5	3	2	6	12	25	50
3	1	1	3	7	15	27
3	3	4	10	20	40	80
3	5	5	13	35	70	140
2	1	2	5	10	20	40
2	3	6	15	30	60	120
2	5	10	25	50	100	200

Provided that the blocks are applied in a hole in 5-10 hours, one finds that an inflow of as much as 5 liters per hour will cause no trouble as long as the slot is at least 2 cm wide. However, if the application of blocks is delayed by several days because of some unforeseen difficulties, or if the canister will not be inserted until after one to two weeks, overflow may take place if the slot width is smaller than 3 cm and the inflow higher than 3 liters per hour.

As discussed in preceding chapters, it is technically feasible to seal off deposition holes such that the inflow becomes less than 1 liter per hour in any type of rock.

Rock stability

The present primary stress fields, which are expected to remain unchanged in the construction and waste application phases, vary with respect to orientation, anisotropy and magnitude as manifested by many measurements described in rock mechanical literature [1] and illustrated in Chapter 2 (Figure 45). In order to quantify the differences in rock behavior that possible future changes in regional stress fields may cause, we first need to define the present ones, for which one can use generalized expressions like the following empirical rules for the primary horizontal and vertical stresses as a function of depth (Rummel):

$$\sigma_H/\sigma_v = (250/z) + 0.98 \text{ MPa}$$

$$\sigma_h/\sigma_v = (150/z) + 0.65 \text{ MPa}$$

where σ_H and σ_h are the major and minor stresses in the horizontal plane and σ_v is the vertical stress, which can be taken as $\sigma_v = 0.027z$, where z is the depth in meters.

Applying these expressions we find the primary stress conditions for the three concepts that are compiled in Table 13 [2]. They are taken to represent principal stresses.

Table 13 Theoretical primary stresses, MPa

Concept	Depth, km	Max horiz.	Min horiz.	Vertical
VDH	0.5-1.0	21-33	13-22	14-27
VDH	1.0-2.0	33-60	22-39	27-54
VDH	2.0-3.0	60-86	39-57	54-81
VDH	3.0-4.0	86-113	57-74	81-108
KBS3	0.5	21	13	14
KBS3	1.0	33	22	27
VLH	0.5	21	13	14
VLH	1.0	33	22	27
VLH	1.5	46	30	40

In general, these stress states imply that the compressive strength is not exceeded by the hoop stress and critical conditions in the form of spalling or fine-fracturing are hence not expected even at the lower end of the very deep holes. However, as illustrated by the potentially unstable large wedges in the walls of the big Forsmark silo room (Figure 7), unstable conditions in the form of rock fall caused by critically located and oriented discontinuities of 3rd to 4th order will take place frequently below about 1.5 km depth irrespective of the rock stresses. Also, stability problems are abundant in tunnels and shafts that intersect very fracture-rich low-order discontinuities, especially where they contain clay gouge, but the stabilization that has to be made in the course of the construction work will usually be sufficient also for the waste application stage. The only concept that may yield stability problems at this stage is VDH, where creep enhanced by the rather high temperature in the lower part of the holes may yield delayed rock fall, although the cage system is supposed to minimize the problem.

A major question is whether arrays of deposition tunnels and deposition holes produces potential weaknesses along which the rock mass will break under the influence of the prevailing or future regional stress fields. This matter needs to be investigated for each

individual case by use of rock mechanical analyses, which usually show that the large-scale stability is not jeopardized, while local reduction in stability may be caused where critically oriented and located weaknesses become activated by the excavation.

BEHAVIOR OF BUFFERS AND BACKFILLS

Physical stability

The high humidity that usually prevails in underground repositories means that blocks of highly compacted bentonite that are not wrapped in plastic until shortly before they are applied, will become hydrated and undergo shallow softening (Figure 165). Blocks of moderate size and weighing a few tens of kilograms have a strength that makes them robust and stable in the application work while significantly larger blocks can have some structural heterogeneity and may break when lifted and put on site. This may cause severe problems since fractured blocks may become stuck before they are on site and their removal can be tedious and cause delay in the application work, especially when remote handling is required because of the nearness of HLW canisters. When blocks of any size become exposed to the load of a canister in a deposition hole they may fracture because of high stress concentrations and imperfect fitting of the blocks, but this will escape attention. In fact, such delayed fracturing has no practical consequences since the subsequent water uptake will yield swelling and homogenization.

Local softening of tunnel backfills caused by water flowing from strongly water-bearing fractures in the course of the application and compaction is the most obvious practical problem in the backfilling process. Reasonably comprehensive and effective sealing of rock fractures by grouting or plugging minimizes this problem. Still, as long as high hydraulic gradients prevail there is a risk of erosion and piping, especially when the density is low. We will come back to this problem in examining the performance of grouts later in this chapter.

5-2.3 Maturation stage

HEAT EVOLUTION

Before going into the detailed processes in rock and clay buffers and backfills we need to have a general picture of the temperature conditions, which play a significant role in any repository containing heat-producing waste, as illustrated by the three HLW repository concepts that we are focusing on.

Ambient temperature

The ambient temperature at 500 m depth is commonly in the interval 10-15 °C, while it is considerably higher deeper down. Hence, while VLH and KBS3 repositories will be located in rock with a low initial temperature, the deployment part of VDH will be exposed to high temperatures. The natural temperature gradient in continental crystalline rock away from hydrothermally active large zones is in the range of 1.3 to 1.6°C per hundred meters, which means that the ambient temperature at the lower end of the deployment part, 4 km below the ground surface, may range between 65 and 80 °C, while it may be in the interval 40 and 55° C at the upper end of this part, i.e. around 2 km below the surface [2,3].

Maximum temperature

The heat cycle will be somewhat different in the various concepts depending on the amount of heat-producing, i.e. radioactive material. In the KBS3 concept the canisters are emplaced close enough to yield overlapping of the temperature fields around the deposition holes, while the canisters in VLH and VDH form long “linear” heat sources will negligible overlap of the temperature fields of neighboring holes. In a single storey repository of KBS3 type with 30 m tunnel distance and 6.2 m spacing of the canister holes, the maximum temperature (ambient + rise) at the canister/clay interface will be about 66 °C and this will occur after 12 years [2]. The heat generation is initially about 200 W per meter canister length and it drops by about 50 % after 100 years and by 90 % after 1000 years.

In VLH repositories hosting canisters that initially generate about 500 W/m, the temperature increase at various distances from the canister surface is given by Figure 191 for the special case with initially water saturated bentonite, which can be manufactured although at higher

cost than for ordinary blocks obtained by compacting air-dry bentonite powder. The heat generation drops by about 50 % after somewhat less than 90 years and the maximum temperature increase at this contact will be slightly less than 90°C after 10 years, which yields a maximum net temperature of about 105 °C [2]. It will be significantly higher for the ordinary type of blocks with only about 50 % degree of saturation. The marks in Figure 191 were derived by assuming the heat conductivity of the bentonite to be 1.5 W/m,K.

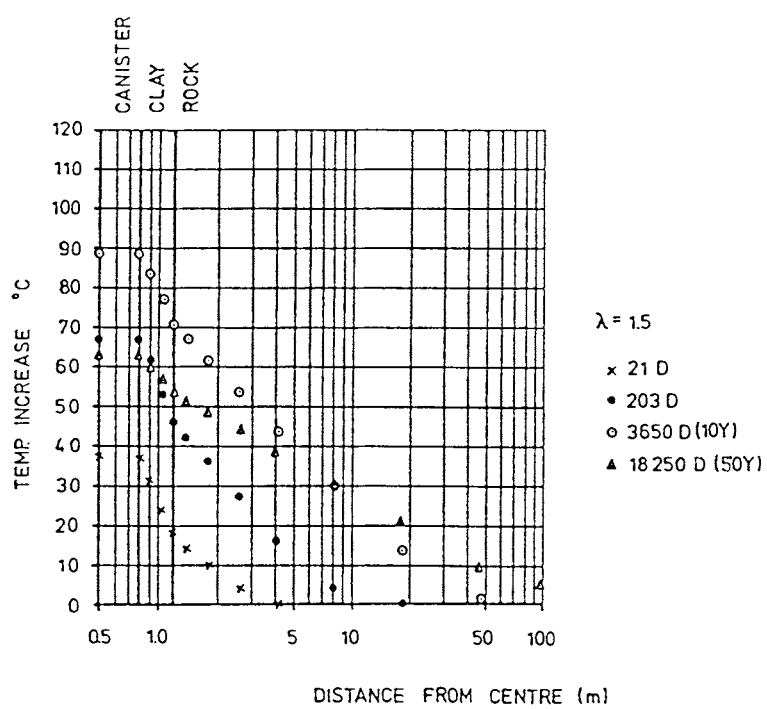


Figure 191 Temperature increase from canister center in VLH as a function of time for initially fully water saturated clay buffer [2]. D denotes elapsed time in days

In VDH the temperature increase will be considerably less than in the other concepts while the ambient and therefore also the net temperature become higher. Thus, Figure 192 shows that the temperature increase will be about 17°C at the canister/clay interface after about 6 years for an initial heat generation of 58 W per meter canister length, meaning that the net temperature at the bottom end of the deployment zone may reach a temperature of slightly less

than 100°C. At the upper end of this zone the net temperature is expected to be 55-75°C. The decay in heat generation is relatively fast and the power will drop to 30 W/m after 60 years and about 5 W/m after about 1000 years. This gives a temperature drop by 5°C at the canister/clay interface in 100 years and by 10°C after about 430 years. At the latter time the surrounding rock will have undergone heating by 1°C at a distance of 100 meters from a single hole.

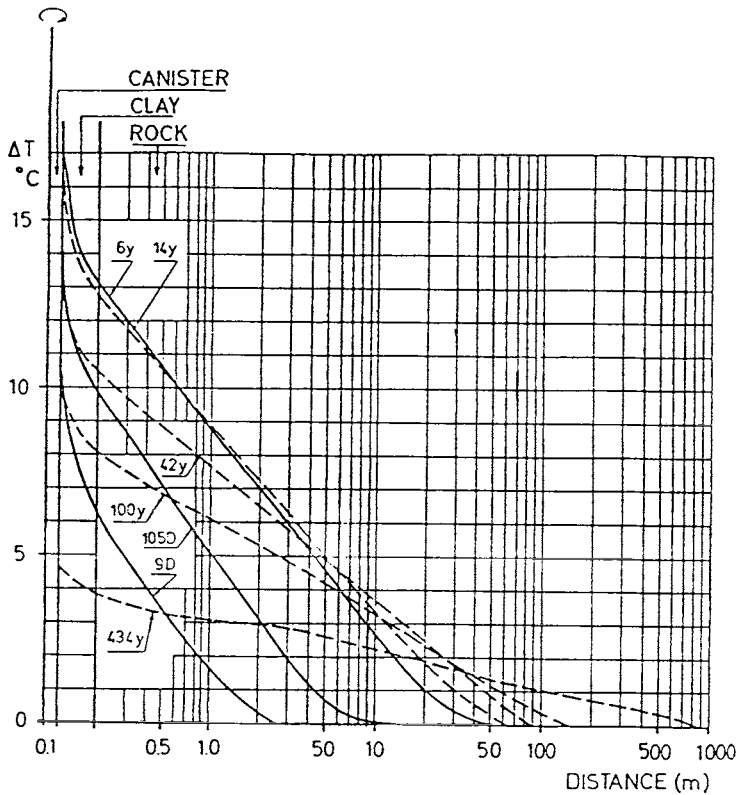


Figure 192 Temperature increase from the canister/clay interface in VDH as a function of time [2]

ROCK BEHAVIOR

General

Heating caused by the radioactive decay has an impact not only on the canister-embedding smectite clay, and on the chemical interaction of the canisters and clay, but also on the physical properties of the surrounding rock.

A major heat effect is that fractures in the nearfield will be exposed to tension or compression and shear depending on their location and orientation. These effects will be reduced in the course of the heat cycle but some permanent net change in fracture aperture will remain when cooling to the original temperatures has taken place.

Hydraulic conductivity of the nearfield rock

The access to water determines the rate at which the clay buffers and backfills of KBS3-type repositories become water saturated and homogeneous, i.e. undergo maturation, and it is controlled by the ability of the rock to give off water. Hence, the water saturation rate is determined by the hydraulic conductivity of the rock and by the piezometric pressures in the rock. The distribution of water inflow into blasted tunnels is determined by the extent to which the rock structure is disturbed by the excavation, while the influx is controlled by the bulk conductivity of the surrounding, undisturbed rock. The same applies to boreholes, which also have an excavation-induced shallow zone of enhanced hydraulic conductivity that tends to yield uniform access to water for clay buffer emplaced in them. As indicated in the preceding text on the waste application stage, the influx into empty holes varies very much and one can get the impression that certain deposition holes with 1-2 m diameter and 3-10 m depth are virtually “dry”, while other holes are very “wet”. Groundwater enters all voids at depth and there is no risk that the clay buffer will not be completely water saturated. However, this state, which implies that entrapped air is compressed and dissolved in the porewater, is approached at largely different rates: extremely slowly where no 4th and lower-order discontinuities are intersected, and very rapidly where many 4th order breaks are truncated or where the excavation is located in fracture zones of 1st to 3rd order.

The longevity of bentonite-based seals in repositories is partly determined by the access to potassium and hence by the composition of the groundwater, as well as by the rate at which it passes along the seals. The flow rate is controlled by the “axial” hydraulic conductivity of the nearfield rock as discussed in Chapters 3 and 4. It is anticipated that the axial flux along bored holes in which bentonite-embedded canisters are emplaced is not very different in the various

concepts, while the dramatic increase in conductivity of the blast-induced peripheral zone of KBS3 tunnels implies that much more groundwater will be driven along these rooms and hence also rather close to the canisters than in the VDH and VLH cases, at least in the period of maturation.

Rock stability

Since the maturation stage hardly extends over more than a few decades, the same large-scale rock stability conditions will prevail as in the waste application stage. For tunnels and deposition holes the backfill and the evolution of a swelling pressure naturally improve the stability conditions. As outlined in Chapter 3, even high swelling pressures will not cause overloading and rock failure or even significant compression of rock fractures. Heating may trigger rock block displacements where the stress conditions are critical.

Influence of heating in the maturation phase on the physical state of the nearfield rock

The rock structure, particularly the frequency, interconnectivity and orientation of water-bearing features, and the primary rock stress conditions, determine the extension of the heat-induced changes of the nearfield, and thereby of the groundwater flux along the buffers and backfills. The temperature rise in the maturation phase causes permanent changes of the rock structure by shearing, expansion or compression of fractures of 4th order type, and hydraulic activation of 5th order discontinuities. Such changes affect the hydraulic conductivity due to alteration of the aperture of certain fractures, or rather fracture channels, due to small irrecoverable block movements. It has been found that the hoop stress will rise by more than 100 % for common rock structures and primary stresses and that this will tend to close previously open fractures in the nearfield [3]. Certain critically located and oriented fractures will undergo widening and numerical calculations based on the codes UDEC and 3DEC show that the residual aperture increase may be large enough to yield an increase in axial conductivity along deposition holes by one order of magnitude.

However, there are reasons to believe that the excavation-induced increase in axial hydraulic conductivity along tunnels and large holes is reduced with time by self-sealing of fractures although this does not seem to have been generally recognized. The phenomenon has been noticed in rock grouting experiments where sticky silt/clay gouge was found to block many of the natural discontinuities [2]. It is in line with the common idea that the clay gouge in low-

order discontinuities is at least partly produced by the mechanical agitation caused by tectonically induced shearing at moderate temperatures, and it is also supported by the experimental finding that the vast number of basal crystal planes exposed in sheared chlorite fracture fillings not only become hydrated but also serve as substrate for neof ormation of clay minerals like smectites in salt groundwater at enhanced temperature [4]. The process, which is expected to yield rather effective self-healing, has been investigated by performing hydrothermal tests at 100-200° C and 2 MPa pressure of chlorite powder saturated with artificial seawater with Na, Ca, Mg as cations [5]. This study showed that smectite, primarily montmorillonite, was formed in one month, appearing as a clay gel that grew on the basal surfaces of all the chlorite particles (Figure 193). The rate of growth was significantly higher at 200°C than at 100°C but the same process was identified at both temperatures. It is expected that similar mechanisms produce crystalline or amorphous aluminosilicates of smectite type also in other types of natural fracture fillings, such as micaceous minerals.

Groundwater chemistry

The total electrolyte content and the dominant cation are determinants of the physical behavior of smectite buffers and backfills. Using Swedish data it is concluded that saline groundwater conditions with 0.4-0.8 % salinity (3000 to 6000 ppm chlorine) prevail at 200-600 m depth over relatively large areas, but less salt water is present in many regions. Deeper than 600 m the salinity is often significant and it increases with depth, but salt contents approaching or exceeding those of sea water are usually not found at less than a few thousand meters depth. In recent years the picture of how the salinity varies has become rather clear and it appears that groundwater in crystalline rock commonly has a high electrolyte content at larger depth than about 1500 m. Hence, the deployment zone of a VDH repository would probably be located in rock with a salt content that is at least on the same order of magnitude as that of sea water. Also, various studies in western countries, including the ongoing measurements in the rock laboratory at Äspö [6], show that calcium is commonly the major cation at depths larger than about 500-1000 m (Figure 194) and Russian investigations in deep boreholes tend to show the same. They indicate that salt water is met with at around 1-2 km depth and that calcium is the dominant cation down to 4-5 km. However, at even larger depths there are examples of sodium and calcium being more or less equally represented [7]. The performance analysis will be based on the data given in Table 14 for normal conditions. Much more severe conditions, primarily in the form of considerably higher salt contents for the KBS3 and VLH concepts, are valid under "exceptional" conditions, which are discussed later in this chapter.

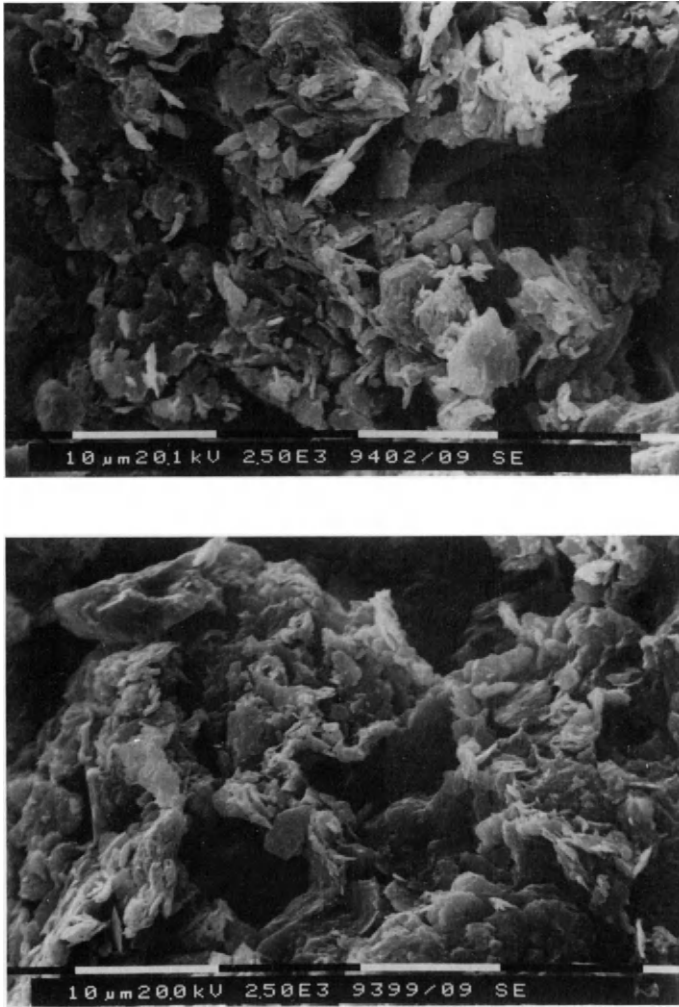


Figure 193 Mineral alteration of fine-grained chlorite. Upper: Scanning micrograph of reference material at 20°C. Lower: Smectite clay gel growing on chlorite basal planes in one month at 100°C. Hydrothermal experiment with salt water with no potassium. Scale is 10 µm

Heat-induced convection will not drive salt water up along VDHs to more than around 100 m from the upper boundary of the salt regime in a 1000 year perspective. It is also estimated that convection-induced upward transportation of salt water will be very small in a KBS3 repository during the heating period. The short heating period and the heat and water flow conditions for VLHs imply that salt groundwater conditions do not have to be considered for this concept either [2].

Low pH groundwater can be expected at smaller depths than some tens to hundreds of meters in areas where large swamps cover the ground, and such conditions may also prevail in old mines located in or close to sulphide ore bodies. At larger depths in granitic rock the chemical buffering capacity of the rock commonly brings about neutrality. Hence, pH of the groundwater is usually in the interval 6-8 in crystalline rock at 500 m depth and deeper down. Large quantities of concrete in the repository for stabilization or backfilling may affect the groundwater within the repository area and yield $pH \gg 7$, which may cause degradation of smectite clay barriers.

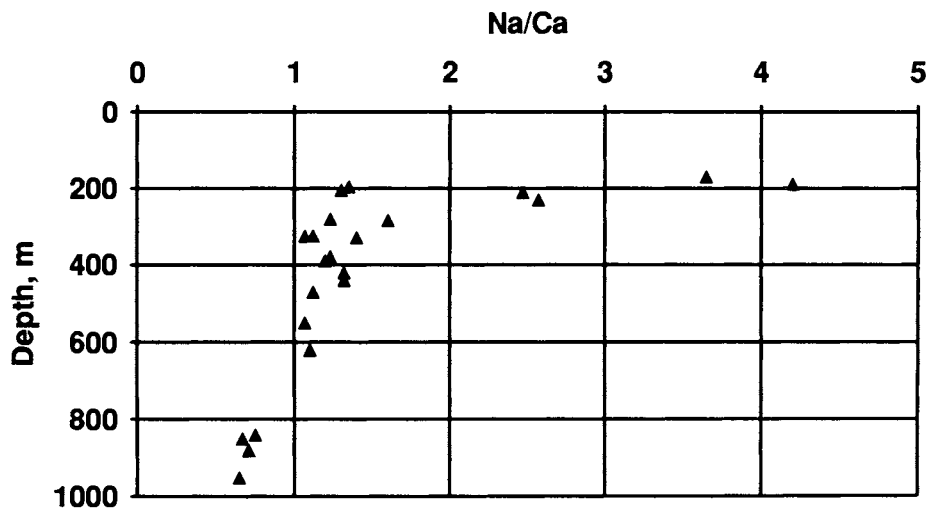


Figure 194 Na/Ca ratio as a function of depth at Äspö [6]

Table 14 Assumed groundwater composition in the functional analysis (normal conditions). Ca is taken as dominant cation

Concept	Depth, km	Total electrolyte content, ppm
VDH	<2	35 000
VDH	2-4	100 000
KBS3	0.5	5 000
VLH	0.5-1	5 000

BEHAVIOR OF BUFFERS AND BACKFILLS

Microstructural evolution

Maturation has been used earlier in the book as a general term for establishment of ultimate conditions of buffers and backfills, and proceeding deeper into the matter we will extend the use of the term to cover all the processes that ultimately lead to a state of equilibrium with respect to the physical constitution, i.e. expansion or compression implying redistribution of both water and solid clay, time-dependent shear strain, and microstructural homogenization. In this chapter we will primarily focus on the maturation of the canister-embedding clay buffers, which is particularly complex since it involves not only uptake and redistribution of water but also migration and precipitation of dissolved substances. We will start by analyzing the moistening since it is the most important process that takes place in the transformation of the incompletely water saturated, apparently solid clay that is applied in block form around canisters, to the effectively isolating, plastic substance that ultimately surrounds them.

Before the canister-embedding, dense bentonite clay reaches the ultimate state of complete water saturation, several processes take place that have an impact on the physical state and performance of the clay. The clay blocks have an initial degree of saturation of around 50 % if air-dry bentonite powder is used for the production, the unfilled parts being the voids between the powder grains. When exposing this material to water, hydration takes place by

capillary suction of the system of continuous voids, which become largely filled with water with very small air bubbles distributed in it. The dense powder grains have the highest suction potential and extract water from the voids. After complete water saturation and sufficient time for redistribution of water and solids to reach microstructural equilibrium, which involves expansion of the dense powder grains and release of thin stacks of flakes to the successively decreasing voids, a rather homogeneous microstructure is formed in which more or less cardhouse-like clay gels with low porosity link expanded but still dense grains together (Figure 195). Heating causes thermal stresses which break up the expanded grains and produce a more homogeneous microstructure, a mechanism that is of great importance for the bulk hydraulic conductivity and ion diffusion properties and also for the swelling potential.

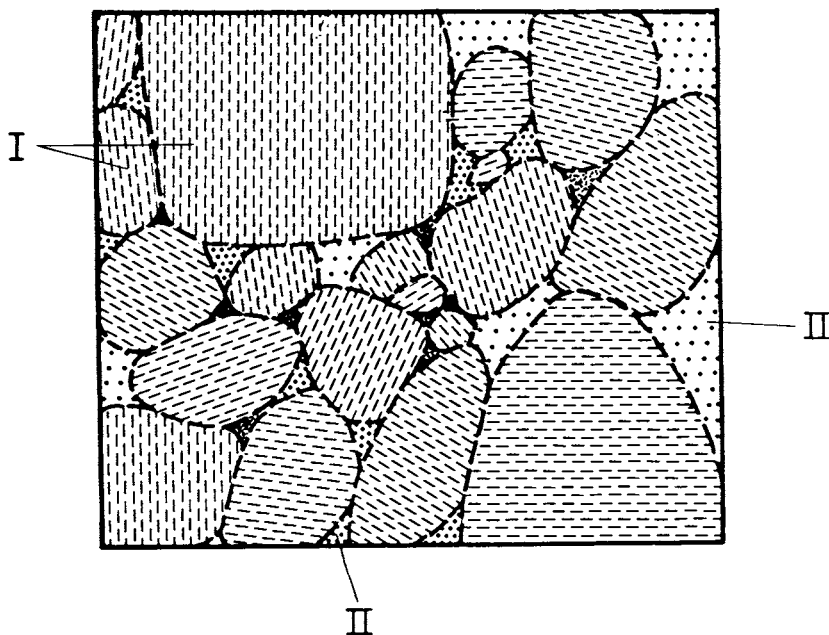


Figure 195 Schematic picture of the matured microstructure of compacted bentonite powder. I) Dense expanded powder grain, II) Clay gel formed in the voids between the grains

Heat-induced redistribution of initial porewater content of canister-embedding bentonite before wetting starts

Data from the Stripa tests with simulated HLW canisters, in which highly compacted bentonite with a dry density of 1.8 g/cm^3 and an initial water content of 9 % was exposed to a radial temperature gradient of around 2°C per centimeter, serve to illustrate the heat-induced distribution of porewater in canister-embedding bentonite as demonstrated by Table 15.

Table 15 Recorded water content in the highly compacted Na bentonite in the simulated canister holes at Stripa. Values refer to tests lasting for 3-6 months

Hot boundary	Half distance between boundaries	Cold boundary
T=70-80°C w=2-5 %	T=50-55°C w=9-11 %	T=30-40°C w=18-20 %
T=100-120°C w=0-3 %	T=70-90°C w=3-5 %	T=55-65°C w=22-26 %

Applying the microstructural data given in Chapter 3 it is estimated that 95% of the porewater is in interlamellar ("internal") positions, forming 1 to 2 hydrate layers in completely water saturated Na and Ca montmorillonite clay with a dry density of 1.8 g/cm^3 . When the total water content is 5 % and lower, as at the hot boundary, almost all the water is in interlamellar positions, forming 1 complete or incomplete hydrate layer. At water contents of 10-15%, as at half distance between the hot and cold boundaries, it can be assumed that 2-5 % of the total water content is "external", forming a very thin partly continuous film around the stacks of flakes. One concludes from this that dissolution and transport of dissolved components like Si and Al are very limited when the water content is lower than 5-10%. At higher water contents than about 15 %, "external" water forms up to 10% of the total water content, by which dissolution and ion transport are facilitated.

The matter of transient heat and mass transfer, leading to water redistribution in soils under thermal gradients, has been extensively treated in agriculture and several attempts have been made, i.a. in conjunction with the Stripa BMT study, to predict such redistribution in the highly compacted bentonite surrounding hot canisters. For this purpose a simple version of the "film" theory ("Knudsen flow") outlined by Winterkorn and others in the fifties [8,9] has been

adopted and found to yield values in reasonable agreement with measured moisture profiles in short term field experiments, like the one shown in Figure 196. Much research is going on in several countries for developing accurate physical and mathematical models for the heat-induced redistribution and subsequent wetting of canister-embedding bentonite.

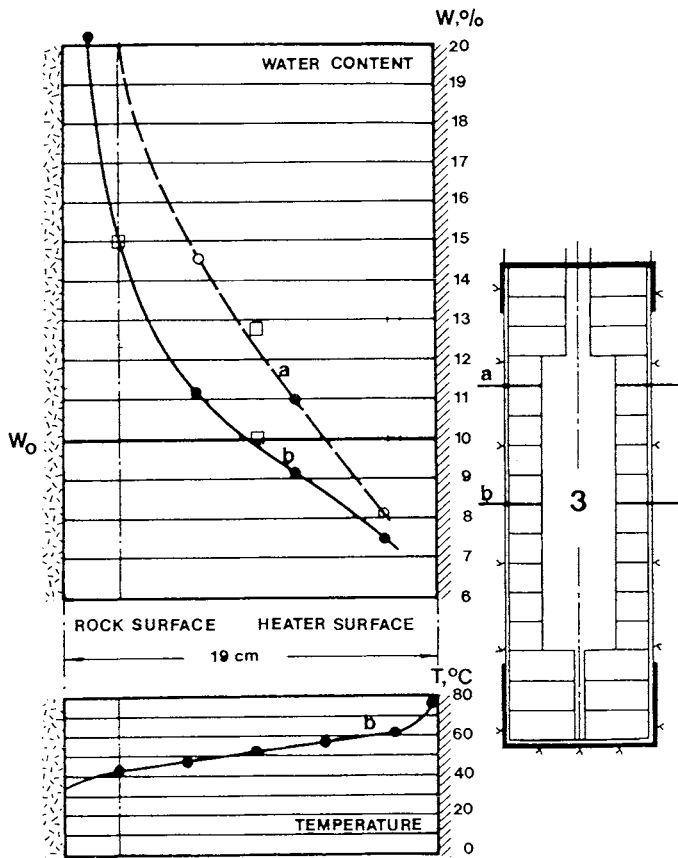


Figure 196 Example of moisture distribution at two levels in dense bentonite embedding a heater in the BMT test series after 4 months. w_0 was the initial water content of the bentonite. At the rock contact the clay was almost saturated ($w=20\%$), while the water content had been reduced from half-distance between heater and rock

The drying causes macro- and microscopic cracking, which reduces the heat conductivity and increases the temperature in the hot part. This problem can be minimized by using blocks with an initial degree of water saturation of about 90 %, which brings up the heat conductivity to at least 1 W/m.K. Current research shows that blocks prepared from mixtures of moist bentonite powder and suitable graphite additive can have a heat conductivity as high as about 3 W/m,°C, i.e. on the same order of magnitude as that of granite.

The wetting process

The combined effect of outward water migration caused by the temperature gradient, and inflow of groundwater caused by the water pressure in the surrounding rock, leads to a steep moisture gradient and a relatively distinct boundary between an outer, largely saturated and an inner rather dry zone. In the course of the water saturation process the boundary moves towards the hot canister at a rate that is determined by the suction power of the clay and by the water pressure and the hydraulic conductivity of the nearfield rock and bentonite. Under the common condition that the conductivity of the nearfield rock is higher than that of the clay and that the water pressure is sufficiently high to provide sufficient amounts of water at the rock/clay boundary, the rate of wetting can be simulated as a diffusion process, using an average value of $3 \times 10^{-10} \text{ m}^2/\text{s}$ of the diffusion coefficient for Na bentonite [10]. This simulation appears to be approximately valid also when a counteracting temperature gradient exists, provided that it is relatively low, i.e. less than about 1-2°C per centimeter [8]. The actual wetting process is very complex and involves another mechanism that must be considered, namely accumulation of salt at the inward moving wetting front. It is discussed below.

In practice, the wetting rate is controlled by the ability of the surrounding rock to give off water to the clay, and this brings us back to the discussion of the hydraulic conductivity of the rock at depth. It follows from the strategy of selecting suitable sites of deposition holes of a KBS3 repository that much less water will enter some holes than the bentonite can absorb and this will naturally retard saturation. As mentioned earlier, the stress-induced disturbance caused by boring the holes will activate a number of 5th order discontinuities, which means that even if the holes are intersected by only a few naturally water-bearing fractures, water will enter the hole from a large number of discrete breaks. It is also estimated that the very narrow and shallow “fragmentation” zone along such holes caused by the drill bits has a somewhat higher hydraulic conductivity than the compacted bentonite, which means that water entering from coarser fractures will be distributed uniformly over the periphery of the holes. This zone is connected to the pervious tunnel floor of blasted KBS3 tunnels by which the zone is

effectively supplied with water when the piezometric pressure is built up after backfilling the tunnels. Strategically placed bentonite-filled slots for cutting off the axial drainage along the tunnels help to speed up the pressure rise.

The time to reach saturation of the tunnel backfill depends on the initial degree of saturation of the mass as well as on the hydraulic conductivity of the rock and the prevailing piezometric conditions. If the average dry density of the backfill is 2.0 t/m^3 , the void ratio is 0.35 and the total amount of water in the saturated material about 4 m^3 per meter tunnel length. If the average radial hydraulic conductivity of the surrounding rock is $k=10^{-12} \text{ m/s}$ it will take about 1.5 years to saturate the backfill, while at $k=10^{-11} \text{ m/s}$, 15 years are required. However, air is entrapped in the voids and it must be compressed in order to make room for the water and this will slow down the rate of saturation. Before high water pressures have been built up there will be 50-100 liters of compressed air left per meter tunnel in the central part of the backfill. With time the air will be dissolved and move out of the backfill into the rock by diffusion.

Using the more expensive and time-consuming wet compaction technique, which also yields somewhat lower density, very little air will be left in the voids since the initial degree of saturation can be as high as 90 %.

It is estimated that 10 years are required to yield a high degree of water saturation of KBS3 canister-embedding clay produced by compacted blocks of air-dry bentonite powder even at unlimited access to water. Even longer time is required for VLH buffers, while VDH clay will get saturated much sooner. This suggests that degrading processes that depend on unsaturated conditions will go on for at least a decade except in VDH.

Special processes in the wetting clay - “evaporation/condensation”

In the successively narrowing “dry” zone close to the hot canister surface, water evaporates and moves in vapor form through continuous voids and fractures towards the cold and wet side where condensation takes place. This process is repeated in a continuous cyclic fashion since water moves in liquid form towards the hot side driven by osmosis and by the ability of clay surfaces to hydrate. The water vapor formed in this cyclic evaporation/condensation process may attack the clay and cause dissolution/precipitation and mineral alteration, which reduces the barrier capacity of the bentonite [11]. Since the degradation is at least to some degree time-dependent it is clear that a high initial degree of saturation, or a high saturation rate is beneficial. The latter case requires a quickly raised water pressure around the deposition holes.

Homogenization and development of swelling pressures

Wetting of the dense canister-embedding bentonite generates expansion and build-up of a swelling pressure as illustrated by the diagram in Figure 197, which refers to one of the Stripa experiments [8]. The maximum swelling pressure of the bentonite in the wettest hole was predicted to be 10 MPa and the required time to develop was expected to be about 3 years applying the diffusion model. This pressure was also the highest recorded one as shown by the diagram, which also confirms that the predicted rate of pressure increase was on the right order of magnitude.

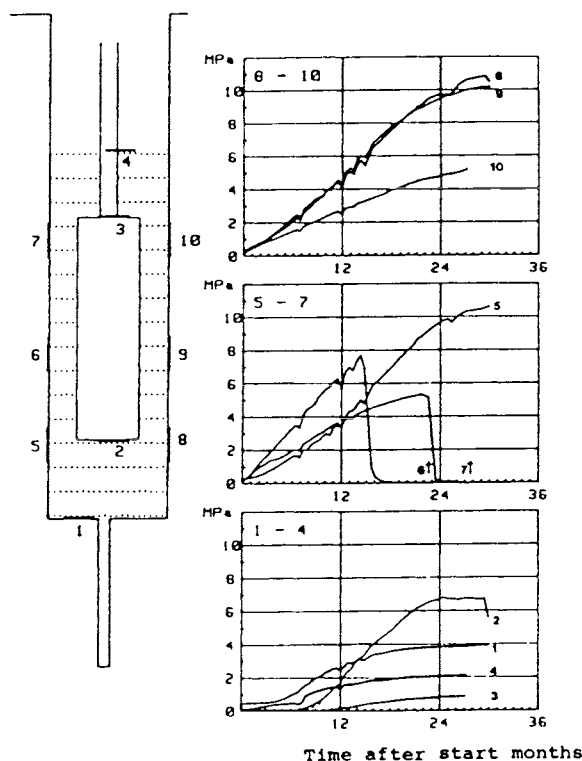


Figure 197 Build-up of swelling pressure in the wettest hole in the Stripa experiment with simulated HLW canister surrounded by highly compacted Na bentonite [8]

The slow wetting rate in very fracture-poor rock with low piezometric pressure is exemplified by one of the Stripa tests that was performed in a hole into which the natural inflow before the application of the bentonite and heater was about 0.02 l/h [8]. Despite the slow wetting rate, swelling pressures were recorded very early in the test, mainly because of the heat-induced redistribution of the porewater, which caused quick wetting of the clay contacting the rock where the pressure cells were located (Figure 198).

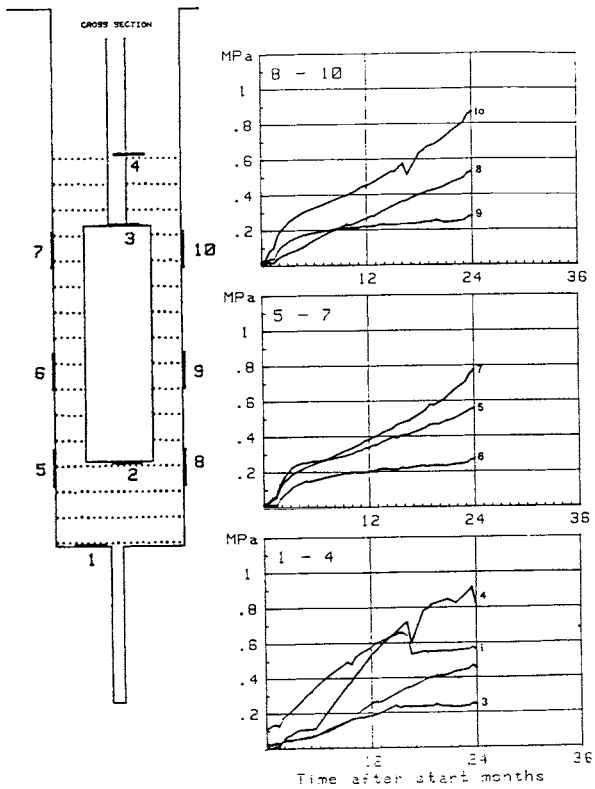


Figure 198 Swelling pressure recorded in the “driest” hole in the Stripa experiment [8]

It is important to realize that the pressure was considerably lower in the upper part of the holes in the Stripa experiments. This phenomenon was caused by upward expansion of the dense bentonite, which exerted a high swelling pressure on the compressible, rather soft overlying sand/bentonite mixture. The same thing will happen in a KBS3 repository even if the top filling of the holes and the tunnel backfill will be significantly denser and less compressible. For predicting the extent to which the expansion and associated softening of the highly compacted bentonite buffer will take place one can apply numerical methods using an axisymmetric element mesh of the hole, canister and tunnel, and assuming the rock to be an infinitely rigid medium, using also an appropriate material model for the buffer and backfill [2]. Such a model should be based on effective stress theory with plastic failure according to the Drucker-Prager theory and elastic swelling according to the Porous Elasticity Theory as indicated in Chapter 3.

The results of an analysis of this sort, assuming rather soft tunnel backfill and applying the finite element code ABAQUS, are illustrated in Figure 199, which shows the deformed element structure after about 3 and 13 years. The figure shows that two gaps will theoretically be formed: one between the floor and the backfill close to the deposition hole, and one in the bentonite at the top of the canister. As indicated by the diagram representing the state after 13 years the latter gap will only be temporary if it is formed at all. The gap at the floor, which is caused by upward displacement of the tunnel backfill may not be formed in practice but a zone of low density will definitely evolve. The swelling will make the buffer and backfill quite inhomogeneous, which is shown in Figure 200. For a suitable density of the applied clay buffer the void ratio after 3 years will vary from 0.6 in the lower part to more than 1.5 close to the buffer/backfill interface, while it will be 0.7 in the backfill close to that interface.

Theoretically, these heterogeneities are permanent and represent local, permeable passages for groundwater flow and diffusion of corrodants and radionuclides but in practice they will be sealed by expansion of nearby bentonite, although not exactly to the original density. Since the phenomenon is caused by the compressibility of the tunnel backfill it should be minimized by compacting it to a high density and its bentonite content should be sufficiently high to yield a significant swelling pressure.

A most interesting fact that is obvious from examining Figure 199, and that has been documented by a 6 years long half-scale field test at Stripa [12], is that the canister will initially be lifted by the upward expanding bentonite. The firm grip on it lower down limits the uplift to 10-20 mm but this causes very high axial tensile stresses in the canister. Creep may reduce the friction and adhesion but this has not yet been introduced in the model.

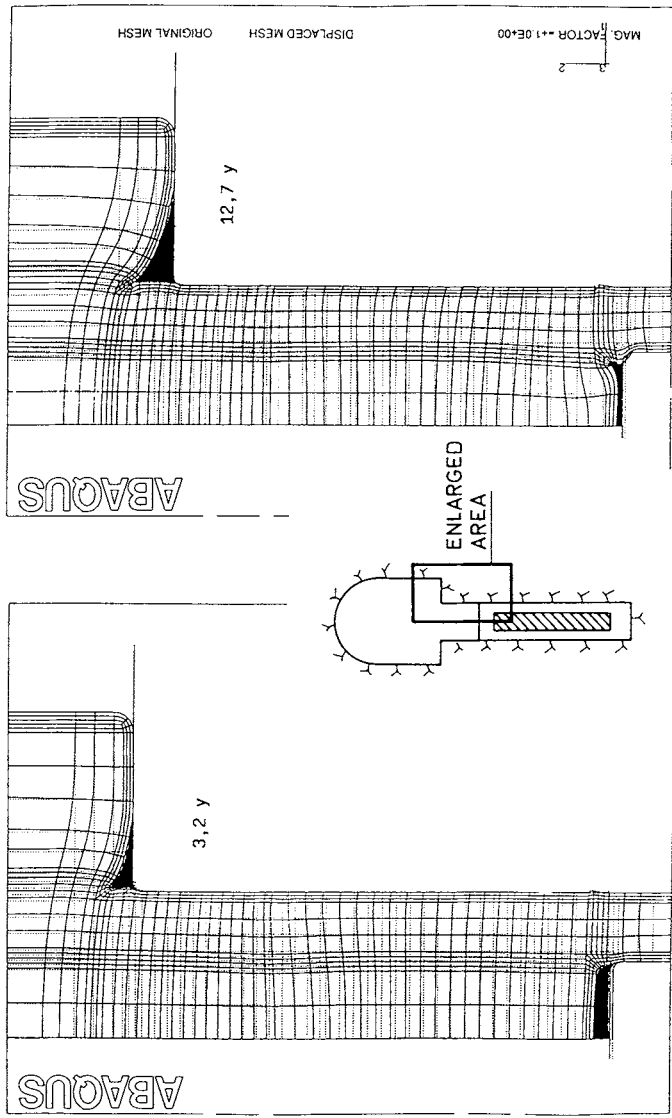


Figure 199 Deformed structure close to the tunnel floor after about 3 and 13 years. The black areas are gaps formed by swelling of the dense bentonite buffer [2]

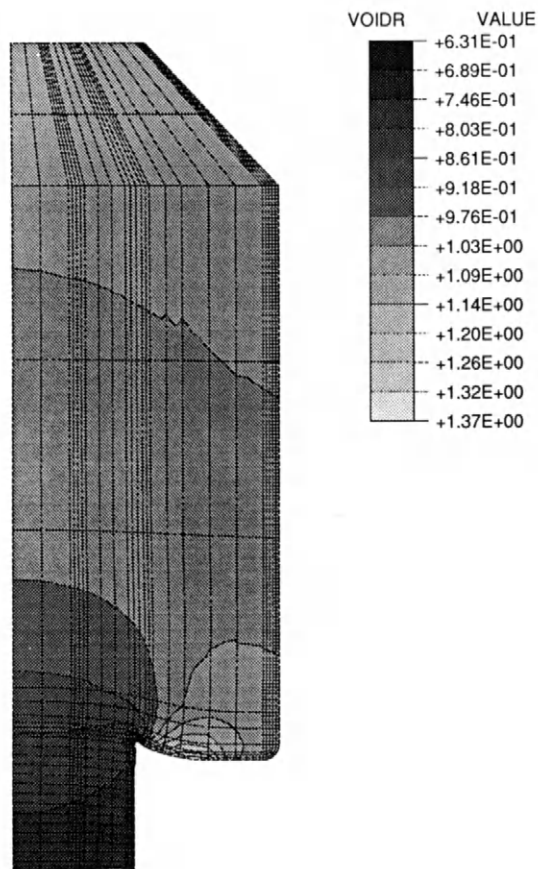


Figure 200 Perspective diagram of void ratio in the clay buffer in the upper part of a KBS3 hole and in the tunnel backfill after about 3 years [2]

Porewater pressure

Considering first the VDH concept with deployment mud surrounding the canisters, the heat

production caused by the radioactive decay raises the porewater pressure very much since the drainage required for dissipation takes a very long time. This may accerelate saturation of the large blocks of initially only partly water saturated, dense bentonite, but there is in fact a risk that the deployment mud may reach an unstable state and undergo piping because the effective stress concept implies that the high porewater pressures yields a very low effective stress and shear strength.

For the KBS3 and VLH concepts the porewater pressure will be negative in the canister-embedding dense clay in the maturation period if it consists of only partly water saturated bantonite. However, if completely water saturated bentonite blocks are used and water is filled in the voids remaining after the blocks have been emplaced, the heat-induced expansion of the pore water in the dense clay may generate very high pressures on the canisters and on the rock. Still, since it is difficult to reach more than 90-95 % degree of water saturation of the system, there is hardly any risk that critical conditions may be reached. Figure 201 shows the build-up of swelling, i.e. effective pressures in VLH with a bentonite density of 2.12 t/m^3 and water filled slots.

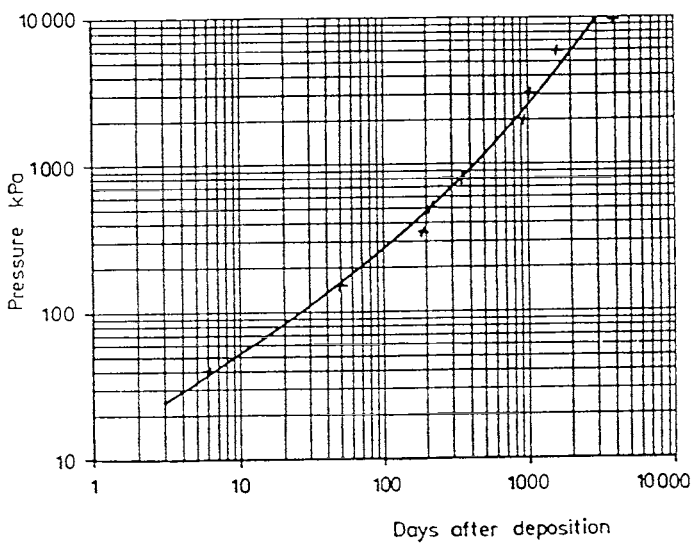


Figure 201 Calculated development of the swelling pressure exerted on the rock by initially almost fully water saturated Na benonite in VLH [2]

Chemical processes

The development of a temperature gradient in the maturation phase will induce three major types of chemical processes in the inward-moving transition zone between the outer (colder), largely water saturated clay and the innermost zone which may have a water content of 2-5%:

1. Dissolution of smectite crystals with concomitant diffusion of released elements, primarily silicon, into the colder part, where precipitation takes place in the form of amorphous silica, cristobalite or quartz. This may yield cementation of smectite stacks resulting in brittleness and reduced expandability
2. Dissolution of accessory, sulphur-bearing minerals and carbonates in the clay and migration in ionic form of sulphur, calcium and magnesium or even iron towards the hot part where precipitation takes place, yielding i.a. anhydrite. This mechanism may also yield cementation
3. Dissolved elements in the groundwater and clay porewater, moving in with the water that is taken up by the clay in the water saturation process and in the evaporation/ condensation process, will precipitate and accumulate in the incompletely water saturated transition zone. Cementation is expected as in the other cases.

The first and second processes yield attack on minerals contained in the clay. The influence on the smectite is caused by hot vapor attack in the drier part of the transition zone and by hot water in the wetter part. It is insignificant at temperatures below 80-90°C but hydrothermal tests in which such clay was exposed to vapor in a heating/cooling sequence reaching higher temperatures than 100°C have shown that a significant part of the swelling potential may be lost [11]. Less strong influence is caused in the wet part of the transition zone in the maturation period, while it becomes important in the subsequent heating period. Dissolution of sulphur-bearing minerals and carbonates takes place both in clay that is initially completely water saturated and in clay that is only partly water saturated. At temperatures well below 100°C the net effect of dissolution and loss of Si (and Al) from the smectite minerals in the “dry” transition zone is less rapid and comprehensive than in the subsequent period of complete water saturation and it is hard to distinguish from that of accumulation and precipitation of salt from electrolytes brought to the transition zone by the evaporation/condensation process, which is the dominant salt-enrichment factor in the maturation period.

This third process affects the larger part of the clay since the transition zone moves all the way

through the clay in the course of the water saturation. The elements that form precipitates emanate from the surrounding groundwater and clay porewater, and they are brought to the transition zone by the concentration gradient that is created when precipitation takes place. Naturally, the precipitates are compounds that have a lower solubility at higher than at lower temperatures and the elements that can accumulate in the clay are primarily the cations Na, Ca and Mg, and the anions Cl and SO_4 , yielding crystallites of sodium or calcium chloride, and of sodium, calcium and magnesium sulphates. Such precipitates will most certainly serve as cement, giving the clay brittle properties with a strongly reduced swelling ability but also with a reduced hydraulic conductivity. Enrichment of sulphate minerals in the maturation period with enhanced temperature may threaten the canisters by causing corrosion when the temperature eventually drops since such minerals will then become dissolved. The effect is naturally much stronger if the groundwater has a high electrolyte concentration than in the case of groundwater poor in salt.

The controlling parameters of the salt accumulation process are the thermal gradient, groundwater composition, rate of groundwater flow along the canister holes, and diffusion rate in both groundwater and clay porewater. The rate and extension of salt accumulation are indicated by the results from laboratory experiments in which cylindrical Na bentonite clay samples with a dry density of 1.27 g/cm^3 and a degree of water saturation of 24 % were exposed to a temperature gradient of 14°C/cm , the cold end being contacted with 3.5 % NaCl solution through a filter stone while keeping the hot end (steel plate at 100°C) closed in most of the experiments [2]. Figure 202 illustrates the redistribution of salt and porewater in a one month long test with the water pressurized to 50 kPa, which is significantly less than in the deposition holes of any of the HLW concepts, except, possibly, for KBS3 holes in very tight rock. A1, A2 etc denote sliced 7 mm thick elements numbered from the hot, closed end.

The diagram illustrates the enrichment of salt in the dry/wet transition zone at the end of the test period, with both chlorides and sulphates represented by "NaCl". Such enrichment was also noticed in a test with almost 100 % initial degree of water saturation (Figure 203), in which there was also a clear drop in water content at the hot end (C1) from initially about 50 %. Part of this drop was interpreted as replacement of water by precipitated salt, while part was concluded to be due to actual drying or to hydrogen gas formation from the corroding, hot steel plate. These tests showed that the rate of salt accumulation was higher than the ability of dissolved species to migrate through the outer, colder part of the sample, which therefore became exhausted in Na and Cl.

The net effect on the physical properties by cementation is expected to be relatively insignificant when the temperature gradients are low, the absolute temperatures low, and the

groundwater poor in electrolytes. If the opposite conditions prevail, very comprehensive stiffening and loss of the self-sealing properties of the buffer clay may take place in a long-term perspective. The practical importance must be judged in each particular case.

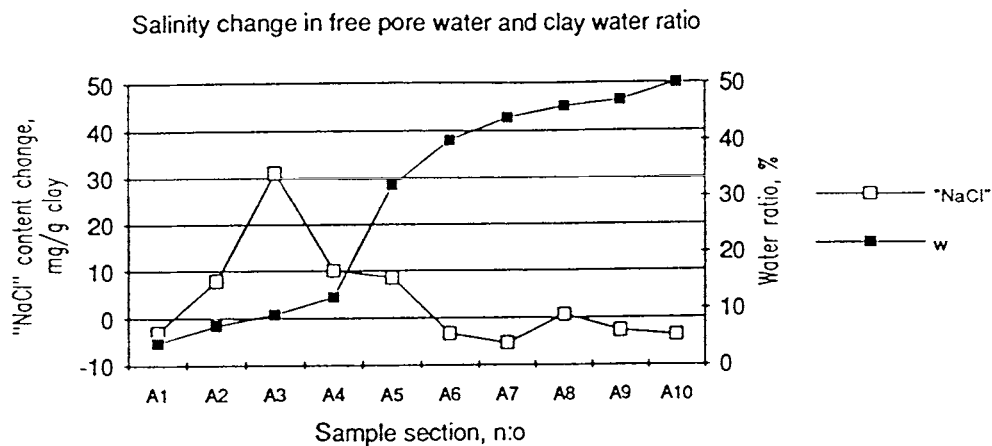


Figure 202 Change in "NaCl" content from the concentration at uniform temperature (22.4 mg/gram of solid clay). The water content is shown as well [2]

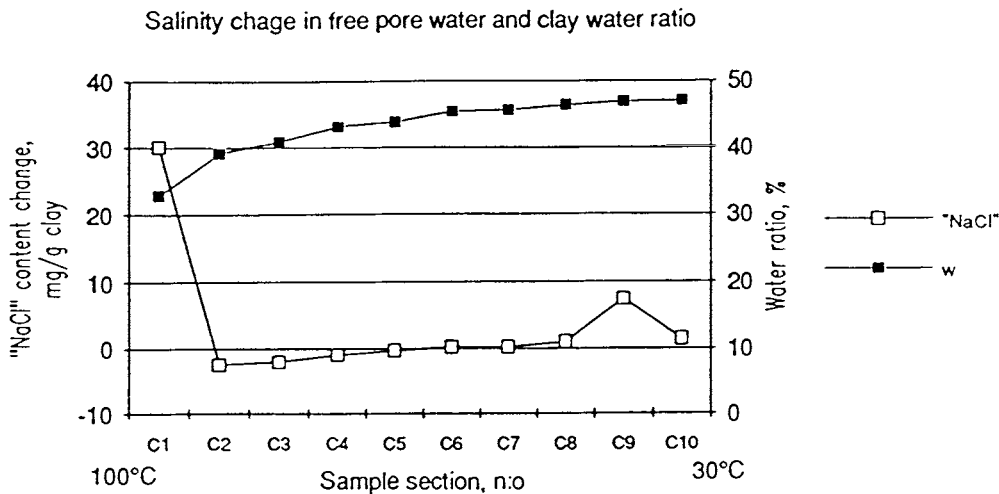


Figure 203 Change in electrolyte content in the porewater in mg salt per gram of solid clay of initially almost fully water saturated sample [2]

Figure 204, demonstrates - when compared to Figure 202 - another important effect of electrolyte concentration, i.e. the fact that the hydraulic conductivity of soft and moderately dense smectite clay increases significantly when the electrolyte content increases, and that the wetting rate is controlled by the external water pressure if it is sufficiently high. This effect, which is particularly obvious when Ca is the dominant cation, is expected to have an important effect on the saturation rate of the canister-embedding clay in the VDH concept [2].

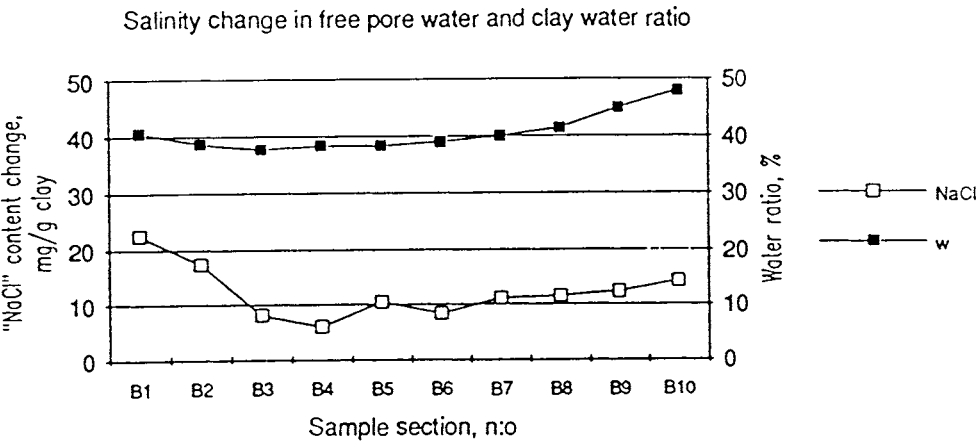


Figure 204 Example of quick saturation when the solution had a high salt concentration (10 % NaCl) [2]

The sealing power of buffers and backfills

In the maturation period no sealing effect is actually required from the buffers and backfills except that they should not let water through at a rate that causes them to disintegrate by piping or erosion, which is achieved by applying the techniques described in Chapter 4. However, their sealing efficiency in the heating period and thereafter is controlled by several processes in the maturation phase. Such a process is the cementation just described, and a second one is cation exchange from the initially adsorbed sodium to calcium as implied by the assumed, common chemical composition of the groundwater (Table 13).

Such exchange in bentonite-based buffers and backfills will take place even if the calcium concentration is significantly lower than that of sodium. The replacement of sodium by calcium, which is the only cation exchange mechanism of importance in the maturation process, has a negligible effect on the physical properties of smectite buffers of high density as described in the chapter on design. However, it causes a reduction in swelling and self-healing ability and an increase in hydraulic conductivity that can be significant for the rather soft VDH buffer and for KBS3 backfills in which the bentonite component contained in ballast voids has a density that will not exceed about 1.5 g/cm^3 at complete water saturation even when the average bulk density is as high as 2.2 g/cm^3 [2].

From the point of mineral stability, uptake of calcium is considered to have a beneficial effect, while enrichment in potassium content of the groundwater jeopardizes the chemical stability of smectite barriers in a long-term perspective [2]. These issues will be discussed below.

5-2.4 Heating stage

GENERAL

Temperature conditions

The heating stage, i.e. the period in which the temperature of the system remains higher than before the emplacement of waste, naturally involves successive heating of the rock mass hosting the repository but the essential processes are that the temperature gradients in the rock and clay buffer that developed in the maturation phase are evened out and that the absolute temperature drops. Since there is practically no overlap of temperature fields of individual

deposition holes in VLH and VDH repositories, the drop in temperature is faster than in a KBS3 repository as indicated earlier in this chapter. The temperature gradient over the buffer mass will initially be $4^{\circ}\text{C}/\text{cm}$ in VDH and $2^{\circ}\text{C}/\text{cm}$ in VLH while it will be less than $1^{\circ}\text{C}/\text{cm}$ in KBS3 holes. It will be negligible after about 100 years in all three concepts.

Large-scale thermal effects

Large-scale thermal effects are of importance only for concepts with the waste uniformly distributed over a relatively large area as in the KBS3 case. The effects on a rock mass that hosts such a repository has been investigated in a pilot study using the UDEC code and considering a rock structure dominated by a rhombohedral pattern of 2nd order discontinuities [2]. The E-modulus was taken at 39.6 GPa and Poisson's ratio as 0.2, while the linear thermal expansion coefficient was $8.3 \times 10^{-6} \text{ K}^{-1}$, the thermal conductivity $3.0 \text{ W/m}\cdot\text{K}$, and the specific heat $0.8 \text{ kJ/kg}\cdot\text{K}$. The friction and dilation angles of the large discontinuities were 21.8° and 2.9° , respectively, and the normal and shear stiffnesses 300 GPa/m and 10 GPa/m , respectively. The heat production was assumed to be uniformly distributed within a $1000 \text{ m} \times 1000 \text{ m} \times 30 \text{ m}$ repository zone, the total residual power being taken as 5400 kW. For a vertical 2D section through the repository the initial specific power was hence 0.18 W/m^2 . The outcome of the study was that the accumulated rock displacements were considerable in the rock mass overlying the repository, producing i.a. a vertical heave of somewhat less than a decimeter at the center of the repository and upward and outward movements of its edges after about 1000 years and to a couple of decimeters after about 1600 years (Figure 2).

ROCK BEHAVIOR

Major processes

The geological conditions influence the nearfield function of the respective concepts in three major fashions in the heating phase:

1. The heating/cooling cycle alters the rock structure and hydraulic conductivity
2. Creep effects influence the structure and hydraulic conductivity of the nearfield rock
3. Large-scale tectonics will cause displacement along major fracture zones and this will in

turn generate shear along higher-order discontinuities, which may have an impact on the stress conditions in the canisters with an associated risk of mechanical breakage.

Effect of heating/cooling cycle

The hydrothermal conditions that prevail in the major part of the heating period mean that the self-sealing of fractures with infillings of chlorite and micaceous minerals that is initiated in the maturation period proceeds in the nearfield rock. Silicons given off from the smectitic clay buffer may contribute to the self-sealing by forming silicious precipitates in fractures intersecting the buffer-containing deposition holes and it is expected that the bulk hydraulic conductivity of the nearfield drops successively as a result. These effects should be at maximum for the VDH concept because of the high temperature and more electrolyte-rich groundwater but it may be significant also for the other concepts.

The opposite effect, i.e. a thermally induced increase in axial conductivity by expansion of critically located and oriented fractures, is initiated in the maturation period and enhanced by rock displacements induced by the subsequent cooling. Since the rate of temperature changes is very low, creep effects and associated stress relaxation will take place simultaneously so that there may be no net thermo-mechanical effect on the hydraulic conductivity, except where stresses are very high. Disregarding heating effects by hydrothermal processes, the period of enhanced temperature is expected to have the following impact on the nearfield rock of the three concepts VDH, KBS3 and VLH.

VDH

As inferred from the description of the maturation stage, the maximum temperature increase by about 17°C in the nearfield rock is not sufficient to produce any significant change in aperture of the discontinuities or to cause shear displacements along them. However, since the hoop stress due to excavation is very high, heating may possibly enhance creep strain and trigger failure.

KBS3

In KBS3 repositories the heat-induced change in fracture aperture is limited to the vicinity of

the deposition holes, except in the upper part near the tunnel floor where changes due to block displacements will appear also at some distance from the holes as illustrated in Chapter 3 (Figures 88 and 89). With the heat production rate and geometry of KBS3 repositories, the tunnel floor will undergo heave by about 1 millimeter after around 1000 years [2]. Part of this heave persists when cooling to ambient temperature has taken place.

Numerical calculations using 2D as well as 3D codes illustrate that the heating tends to close most fractures, flatlying as well as steeply oriented, while cooling produces significant expansion [2]. As a general rule one can assume that the permanent change in rock structure yields a net increase in bulk hydraulic conductivity that is included in the conductivity-enhancing effect of the excavation, which is estimated to be 10-100 times the virgin conductivity for axial flow in the disturbed zones along tunnels and deposition holes as discussed in Chapter 3.

VLH

As compared to KBS3 repositories the effect of a temperature pulse has a significantly smaller effect on the fracture apertures in the nearfield of VLH repositories due to absence of a nearby tunnel and to the "linear" heat source, i.e. the almost continuous array of heat-producing canisters. UDEC and 3DEC calculations have shown that a temperature increase will tend to close the fractures around VLH, while the subsequent temperature decrease will bring them back to approximately the same width as before the heat pulse, with only very slight, permanent change. This is explained by the fact that the closing of the fractures on heating as well as the opening on cooling are elastic and not associated with plastic deformations. The reason for the purely elastic behavior is the high compression stress conditions caused by the circular geometry of the excavation.

In conclusion, it is estimated that the heating has only a very small effect on the fracture aperture and physical properties of the nearfield rock of VLH and VDH, while it is more obvious for KBS3 repositories. Still, the net change in hydraulic conductivity of the rock surrounding the larger part of the KBS3 deposition holes is small if one disregards from the influence of heat-affected creep and stress relaxation of the rock, as illustrated by the subsequent paragraph.

Effect of creep

Chapter 3 gave examples of ways of predicting the stress-induced increase in axial hydraulic conductivity along holes and tunnels caused by excavation, and it also showed practical examples of actually recorded enhanced conductivity, leading to the conclusion that the phenomenon is primarily caused by flatlying fractures located above the tunnel roof and below the tunnel floor, and by steeply oriented fractures near the walls, which will all undergo time-dependent change in aperture. It was also indicated that there may be time-dependent shear strain due to high hoop stresses at the periphery of tunnels and large-diameter holes and that such creep effects may yield inadequate long-term stability and a substantial time-dependent increase in axial conductivity. Returning to this matter, on which recent research has shed further light, it appears that long-term strain is strongly dependent on the presumptions made in the predictions, like application of empirical creep laws disregarding from the existence of discrete discontinuities [13,14], i.e. neglecting the actual structure of rock, and application of rate-process theory considering the structural nature of rock [15,16]. A Finnish approach of the first-mentioned type [13], based on microcrack-driven creep, which is only applicable to quartz-rich crystal matrices and not to typical discontinuities, has led to the conclusion that radial displacement by 10 mm of the periphery of KBS3-type tunnels and deposition holes may require thousands to millions of years when "good quality rock" (joint spacing 1-3 m) is at hand, while such strain may take place in tens of years in "poor rock" and high primary stresses (50 and 22 MPa horizontally and 12 MPa vertically).

An approach of the last-mentioned type [16], based on the criterion that 5×10^{-3} linear strain implies a drop in strength by 50 % and on the commonly applicable log time creep law, led to the conclusion that critical conditions will not appear in KBS3 deposition holes, but that critical strain will be developed in a few hundred years in the roof of KBS3 tunnels at the very low supporting pressures (50-100 kPa) provided by blown-in ballast-poor backfills.

Although the Finnish study did not specify the consequences of a 10 mm downward displacement of the roof and floor of KBS3-type tunnels considered in the study, it implies that part of this movement, presumably at least 25 %, has the form of expansion and propagation of natural discrete flatlying fractures above the roof and below the floor if they conform to such discontinuities, and that the movement also involves shearing and hydraulic activation of previously inactive 5th order discontinuities. Referring to the FLAC study described in Chapter 3 and illustrated in Figure 117, and assuming that the increase in axial conductivity induced by expansion and activation of 4th and 5th order discontinuities within 2-3 m distance from the roof and floor, one finds that six such breaks would each be expanded over 30-50 % of their width by about 400 μm or that three of them expand by 800 μm . In a long-term

perspective this would naturally cause an even higher axial conductivity than the one emerging from the elastostoplastic FLAC case but, as discussed in earlier chapters, the effect over longer distances than a few meters is controlled by 3D effects, especially by the orientation of the fractures and of their degree of interconnectivity. Further reduction of the net conductivity is expected by the aforementioned hydrothermal effects but a conservative estimate is that the roof and floor regions will undergo substantial increase in hydraulic conductivity in a few thousand years. This will be counteracted - probably very effectively - by self-sealing of many fractures through hydrothermal processes.

Impact of tectonics and glaciations on the nearfield rock

The risk of critical changes in primary rock stresses due to tectonics and glaciation can be neglected for the short heating period of the VDH and VLH concepts, while it needs to be considered for KBS3 repositories because of the long heating period. For all the concepts the secondary stress conditions and the nearfield rock structure will be changed by creep and relaxation processes as well as by temperature effects associated with the glaciation-induced cooling. They affect the hydraulic conductivity of the nearfield yielding both an increase and a reduction in the fashions described below.

An important question is of course whether future changes in the primary stress fields will alter the conductivity of the nearfield rock, and a first issue is how large such changes can be and how soon they may appear. There is no doubt that very large changes have taken place in magnitude and orientation of the regional stress fields in the past as documented by the formation of differently organized, superimposed structural patterns, the most important stress alterations in the latest hundred thousand years in northern hemisphere being due to glaciations and deglaciations. Several approaches have been made to deal with this problem, one being to assume more extreme stress conditions than in Table 12 by applying simple analytical stress theory assuming rotation and strongly increased anisotropy of present stress fields, and another to use numerical methods for calculating the influence on the secondary stresses in a KBS3 repository by future glaciation. We will consider these issues starting with the effect of tectonically induced shear.

It is easily demonstrated by applying simple strength analyses that tectonically induced shear will take place along preexisting weak zones of long extension, provided that their strength is considerably lower than that of the rock matrix. In later years this has been nicely documented by Slunga [17] who tentatively concluded that earthquake-related movements have the character of stick-slip sliding, triggered at asperities of steeply oriented faults where stress

concentrations are built up in the course of lateral creep motion of non-seismic type. The latter, slow motion seems to be on the order of 1 mm per year, while the peak slips that take place along the faults are typically 0.3-10 mm at earthquakes with a magnitude of about 1-3. Such faults can be identified as discontinuities of 1st and 2nd orders. Information supplied by NEDRA on Russian investigations has yielded creep rates of 2-5 mm/year along regional discontinuities of 1st order [7]. Slunga concluded that the earth crust in northern Europe undergoes lateral compression in approximately NW/SE direction, while the direction of sliding is determined by the orientation of the faults.

There are indications that vertical and horizontal slip are on the same order of magnitude, meaning that vertical movement along steeply oriented fault zones may also be about 1 mm/year, with "momentaneous" earthquake-related peak slips of at least 30 mm. This is in reasonable agreement with recorded shear displacements of 50-100 mm in 4 km deep South African mines associated with earthquakes of magnitudes 2-3 (M 2-3), cf [18].

Much larger displacements have been reported for stronger earthquakes like the "one event" slip of 20 m along the rather steep fault at Landsjärv in Sweden (M 6.5-7), a 1.4 m tunnel shear at the 1906 San Francisco event (M 8.3), and a 200 mm displacement at the Skövde event in Sweden (M 4.5). The type of damage caused by relatively strong earthquakes, i.e. with magnitudes of around 5-6, is concluded to be both very quick shearing along the fault, activation of previously healed fractures, and creation of new ones. It appears reasonable to assume that stronger earthquakes are primarily related to displacements along steep 1st and 2nd order structures and taking earthquakes of magnitude 4-5 as a basis of the functional analyses of the "normal case" one can assume that tectonically induced stress field changes are caused by instantaneous shear displacements of 200 mm along 2nd order structures. Since such movements are associated with angular distortion of the entire system of large blocks separated by low-order discontinuities, they imply shearing also along 3rd order discontinuities, and in turn along 4th order breaks. Simple proportionality would give instantaneous shear displacement of around 20 mm along 3rd order discontinuities and of a few millimeters along 4th order discontinuities, but the matter is much more complicated since the shear strength is higher of higher-order discontinuities and less displacement of 4th order breaks are in fact expected. Shearing along flatlying structures must be assumed to take place to at least the same extension as along the steep ones.

A more accurate approach for examining the matter of tectonically induced shear can be made by stress/strain analyses applying Mohr/Coulomb failure modes and the "basic rock structure" model consisting of low- and high-order discontinuities. Simple 2D estimates of the distribution of rock strain can be made by applying analytical and numerical methods. One

example of rather general applicability is the case in which a stress field with the principal stresses 30 and 10 MPa is rotated by 45° , assuming the version of the basic rock structure model shown in Figure 205 and using the Young modulus 40 GPa and Poisson's ratio 0.24. The joint normal stiffness can be taken as 10 GPa/m, the shear stiffness as 10 GPa/m and the joint friction angle as 17° . Figure 206 is a compilation of the results of analytical calculations showing that the shear displacements along the various discontinuities range between 0.1 mm for 4th order fractures ("fracture half width" about 2 m) to around 200 mm for 2nd order zones ("fracture half width" about 600 m). The reason why only 2nd to 4th order discontinuities are considered is because repositories are naturally located so that they do not interfere with the huge 1st order fracture zones, while discontinuities of higher order than 4 can be left out because of their high shear strength. One finds that the shear induced along 2nd order discontinuities by the stress field rotation is in agreement with the aforementioned strain assumed to be associated with an earthquake of magnitude 5, while the shearing of 4th order breaks of up to 10 m width is 0.5 mm at maximum, i.e. substantially less than the figure estimated on the basis of simple proportionality.

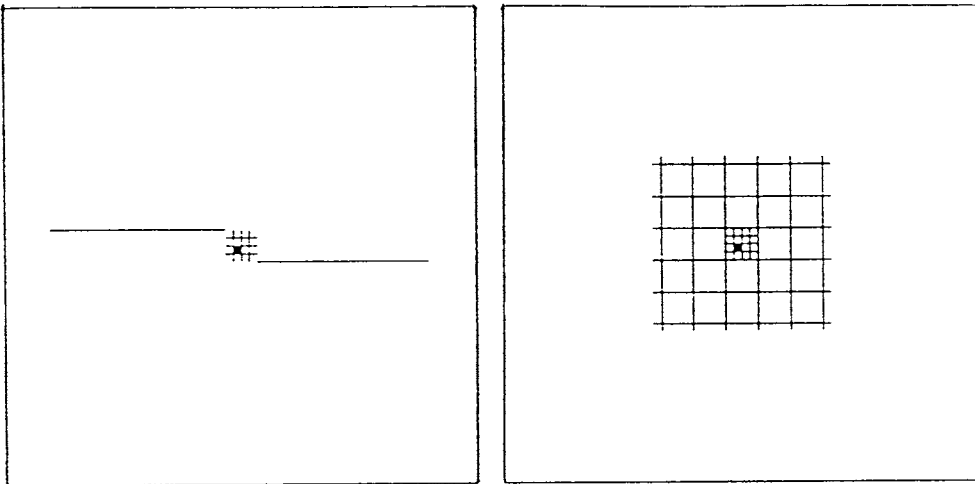


Figure 205 Geometries of sheared discontinuities [2]. The left picture shows en-echelon type 2nd order discontinuities with grid of 3rd order discontinuities, the dark square representing the system in the right picture, i.e. a grid of 4th order fractures with 5th order discontinuities in one square [2]

The impact of stress field changes on the nearfield of excavations in rock with 3rd to 5th order discontinuities can be estimated by similar analyses as illustrated by a number of UDEC calculations using $400 \times 400 \text{ m}^2$ rock model sections with the sets of orthogonally organized discontinuities given in Table 16 (cf. Figure 207). For practical reasons the higher-order discontinuities are modeled in a $30 \times 30 \text{ m}^2$ region in the central part of the large section. Figure 208 shows the central part of the fracture system and the location of the considered KBS3 tunnel and two VLH locations. The three cases are termed #1, #2 and #3 below.

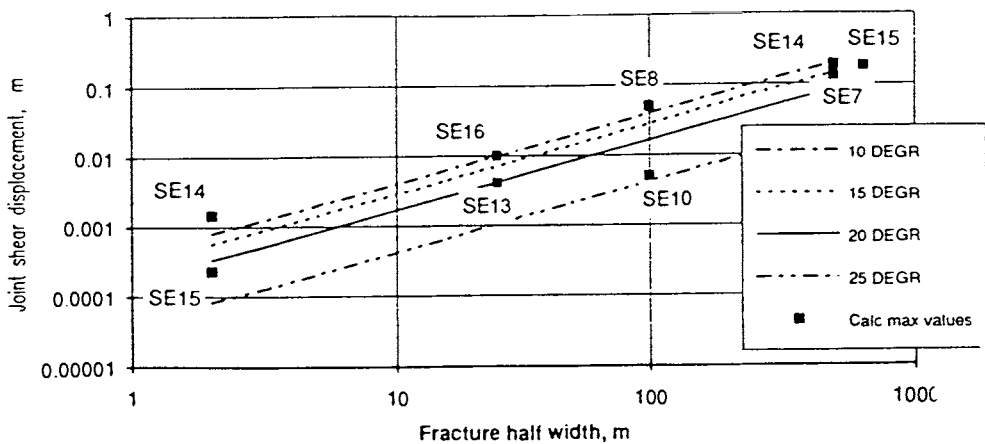


Figure 206 Maximum shear displacements produced by 45° stress field rotation. Straight lines represent values obtained by use of analytical expressions for different friction angles, while discrete plot symbols denote results from the numerical calculations using UDEC [2]

Table 16 Rock structure used for estimating the shear strain along 3rd to 5th order discontinuities caused by change of stress field

Order of discontinuities	Extension	Spacing
3rd	120 m	120 m
4th	5-30 m	5 m
5th	0.5-1 m	0,5 m

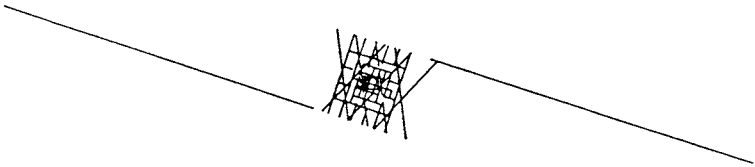


Figure 207 3rd order discontinuities and systems of 4th order fractures of rock structure model for UDEC calculation of the behavior of the nearfield of KBS3 tunnels and VLH [2]

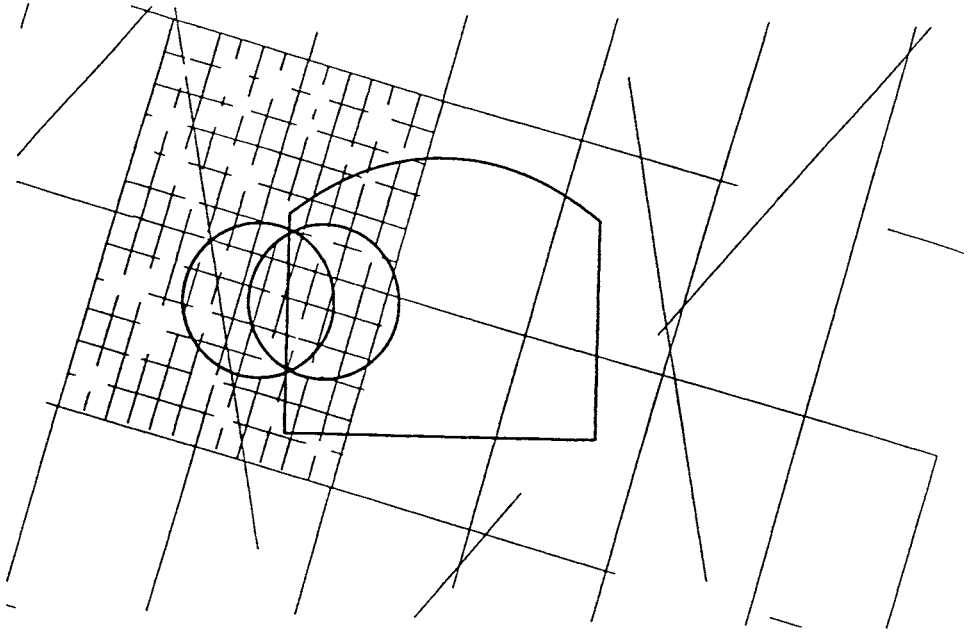


Figure 208 KBS3 tunnel (#1) and, from left to right, of two VLH cases (#2 and #3) [2]

The 3rd order discontinuities can be described by a material model with linear stress-closure behavior and a Mohr/Coulomb failure criterion for shear displacements. Dilation angle, cohesion and tensile strength can be set at zero for these fracture zones while the friction angle can be taken to be in the interval $10\text{--}20^\circ$, the lower value being suitable for making conservative estimates. The constitutive model for 4th and 5th order fractures should include a non-linear stress dependent joint normal stiffness and, for shear displacements, peak shear strengths related to the roughness of the joint surfaces. Suitable input parameters correspond to the residual friction angle 25 and 30° for 4th and 5th order discontinuities, respectively, while the friction angles at peak strength should be around 30° for 4th order fractures and 45° for 5th order fractures. The data for the higher-order discontinuities are also somewhat on the conservative side.

We will consider the impact on the nearfield for the cases #1, #2 and #3 by the following events: A) Tunnel excavation, B) Glaciation, and C) Increase in stress level and in stress anisotropy by stress field rotation [2].

The internal block stresses at the 500m level are set at 14 MPa (σ_v) and 18 MPa (σ_h). Vertical gradients, set to balance the effects of gravitational acceleration, are specified for both stresses, with a constant 4 MPa excess in horizontal stress. This means 23 MPa (σ_h) and 19 MPa (σ_v) at the bottom boundary (700 m level), and 13 MPa (σ_h) and 9 MPa (σ_v) at the top boundary (300 m level). The lower boundary is fixed, while stress conditions corresponding to the internal block stresses are specified for the other boundaries.

The calculation sequence is the following:

A) - excavation simulated as an instantaneous removal of all material within the excavation periphery

B) - glaciation simulated by increasing the boundary stresses by 30 MPa vertically and 7.5 MPa horizontally. This corresponds to the load of a 3 km thick ice sheet if the extension of the ice sheet is infinite, meaning that any increase in horizontal stresses associated with bending of the earth crust below an ice sheet of finite extension is neglected. The increase in boundary stresses is performed in steps, the final stresses at the excavation level being 44 MPa (σ_v) and 25.5 MPa (σ_h).

C) - increase of stress level and anisotropy in the tunnel region simulated by adding a 10 MPa shear component to the boundary stresses applied in B) and by reducing the friction angle of the 3rd order fractures to 6°. At the tunnel level the new boundary conditions mean that the stress field is rotated by 23° (counter clockwise) and that the principal stresses are changed to 50 MPa and 20 MPa from initially 44 and 25.5 MPa, while the average stress remains unchanged. In the tunnel region stresses are further increased as a result of slip along the 3rd order discontinuities. Figure 209 shows contours of maximum compressive stresses at the end of the C state.

C is performed in order to create conditions in the tunnel region which may initiate shear failure in that region at larger distances from the tunnel than in more normal cases. The means of creating these conditions, i.e. location of tunnel between tips of large, low strength fractures and a minor change in farfield stresses, were not related to any specific site or to any specific geological process.

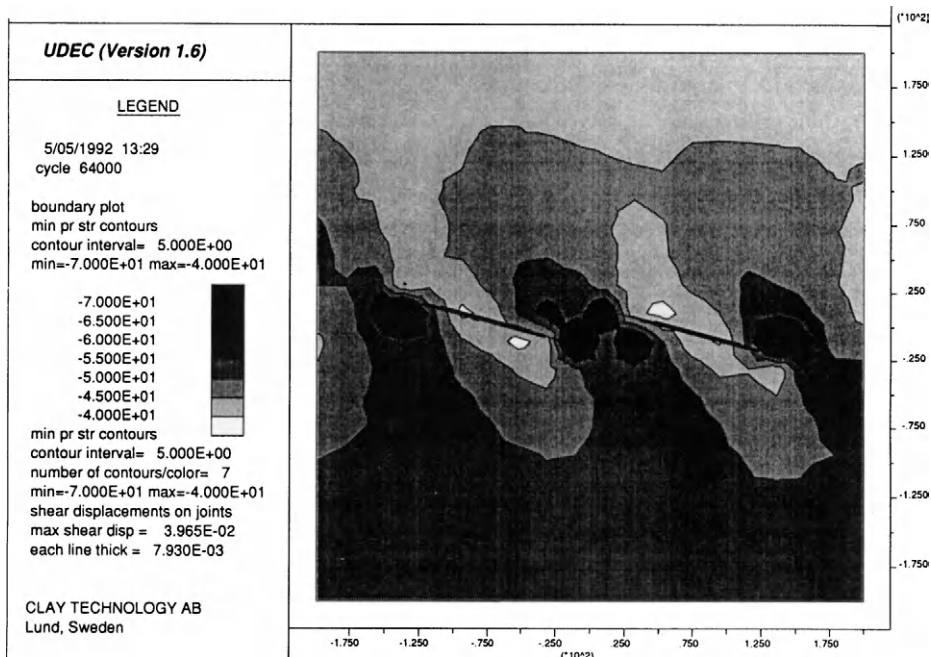


Figure 209 Maximum compressive stress contours in the C state [2]. Darkest areas represent stresses higher than 70 MPa, lightest grey represents stresses in the interval 40 to 45 MPa. In white areas the stresses are lower than 40 MPa

The outcome of the study is shown in Figures 210-213, of which the two first show joint separations larger than $5 \mu\text{m}$ in the vicinity of the VLH tunnel (#2) at stages A) and C). The maximum fracture aperture is increased from $150 \mu\text{m}$ to $240 \mu\text{m}$ as a result of the changed stress conditions in states B) and C) and the region of influence around the tunnel is increased. Both diagrams show how apertures vary along the tracks of individual fractures as a result of the interaction with intersecting, shearing fractures.

The fracture separations result in changes in hydraulic conductivity as demonstrated by Figures 212 and 213, which show the axial conductivity as a function of the distance from the excavation periphery for states A) and C) as evaluated by applying the cubic flow law. The initial apertures were set at $5 \mu\text{m}$ and $2 \mu\text{m}$ for 4th and 5th order fractures, respectively, which gives initial conductivities of about 10^{-10} m/s , i.e. the average conductivity of rock between 3rd order discontinuities at 500 m depth as discussed in Chapters 2 and 3.

Putting together the results of the numerical calculations it is concluded that the effect of excavation of normally structured, virgin crystalline rock with a virgin bulk conductivity of 10^{-10} m/s (A-stage) - excluding the influence of blasting - by far gives the strongest effect, yielding an axial conductivity of 10^{-7} to 10^{-6} m/s within about 1 m distance from the periphery of KBS3 tunnels and 10^{-9} to 10^{-7} m/s from 1-2 m distance, and 10^{-10} to 10^{-6} m/s within about 0.8 m distance from VLH. Glaciation and further stress changes leading to a more anisotropic stress state is expected to yield a net increase in axial conductivity by about 10 times, the effect being negligible beyond 1 m distance from VLH and presumably also from KBS3 deposition holes but significant at more than 2 m distance from KBS3 tunnels. Again, 2D analyses strongly exaggerate axial conductivities and 3D effects will in practice strongly reduce the effect of excavation and glaciation as well as tectonically induced strain.

The effect of glaciation and tectonic impact of the magnitude represented by states B and C under "normal conditions" are concluded to alter the axial hydraulic conductivity of the nearfield to an extent that agrees, in principle, with the generalized data specified in Table 8 in the chapter on design (Chapter 3). Under "exceptional conditions" the effect of such events is more important as we will see later.

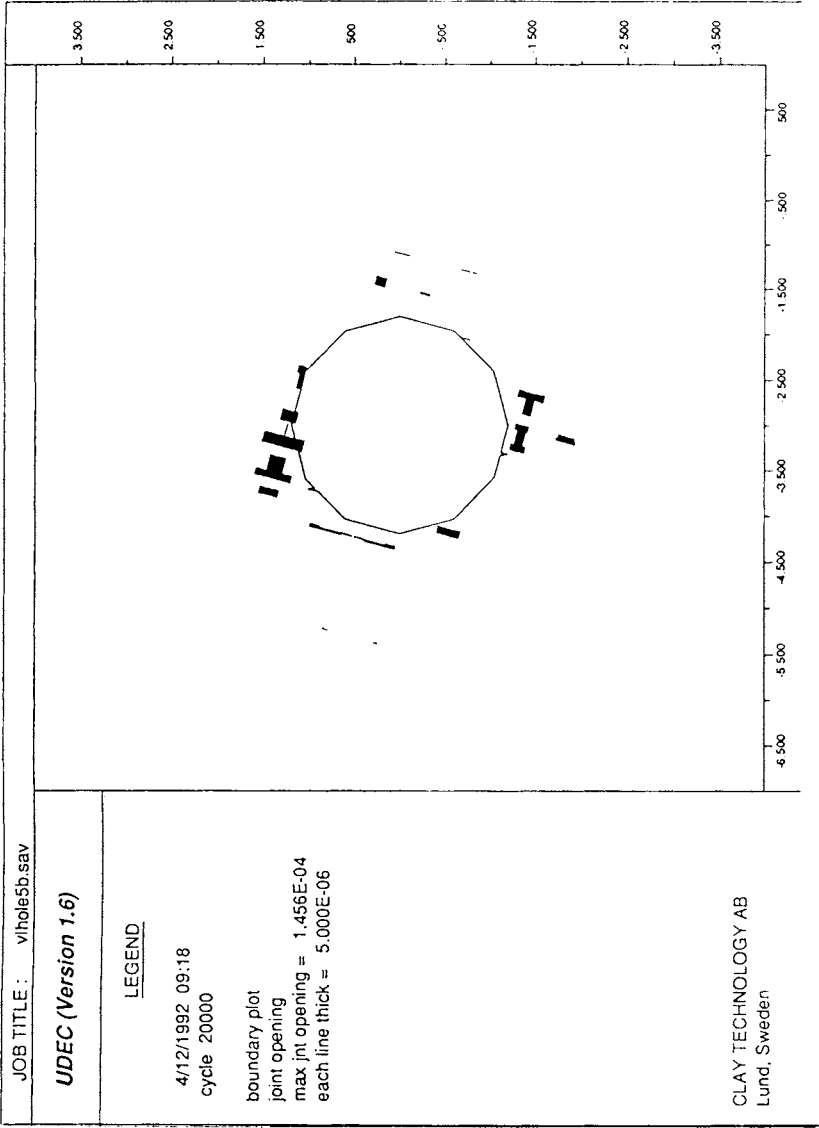


Figure 210 Fracture expansion in the excavation state (A) [2]

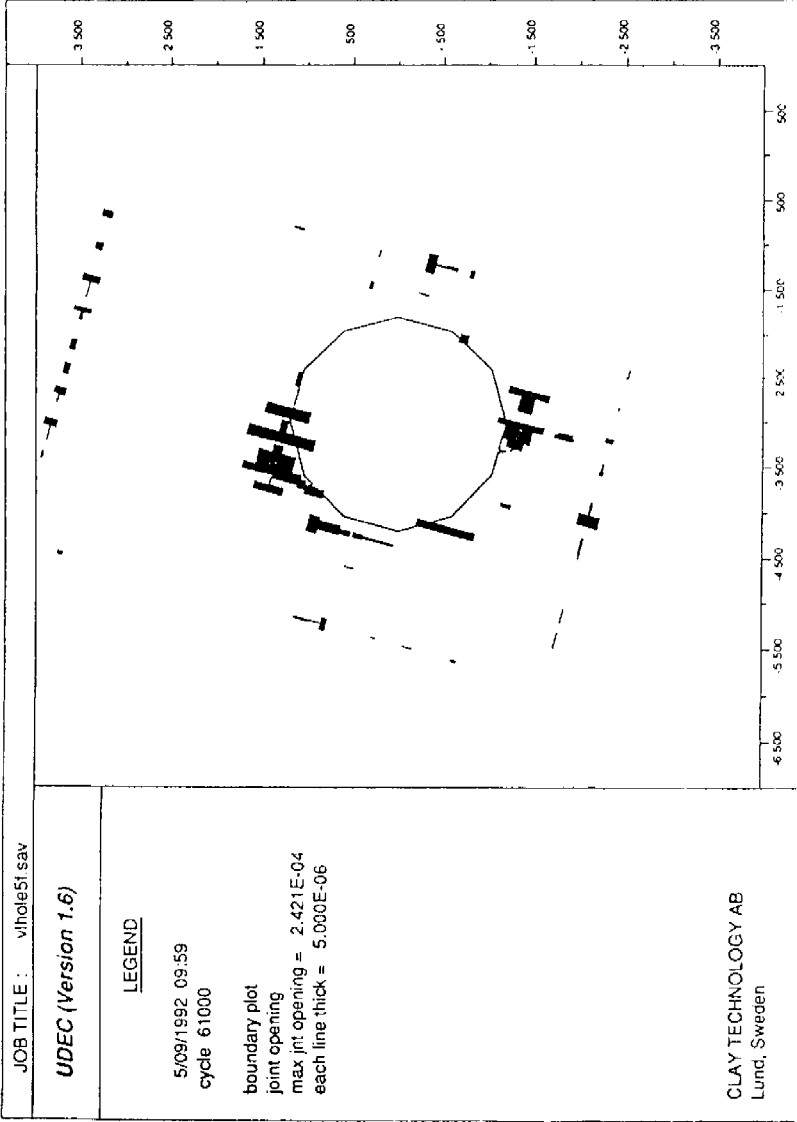


Figure 211 Fracture expansion in the “tectonic” state (C) [2]

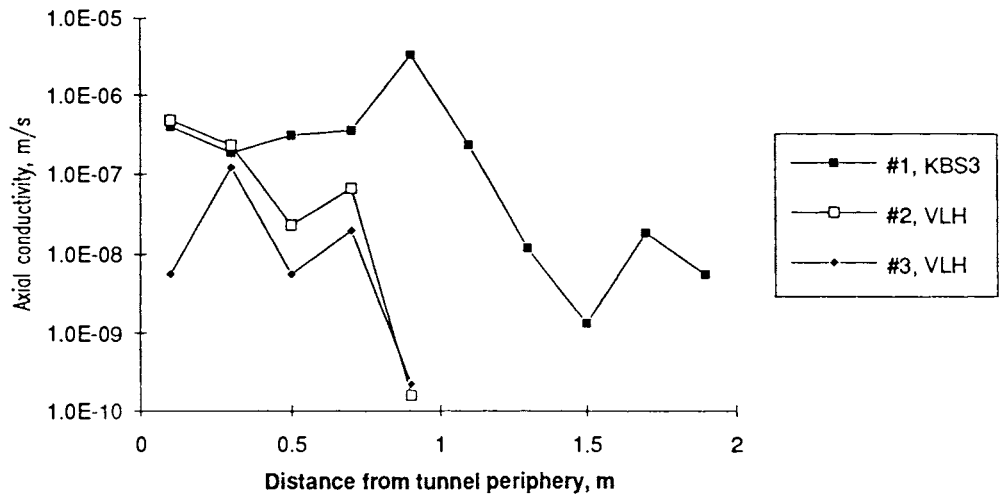


Figure 212 Axial conductivities of the nearfield rock around KBS3 tunnels and the two VLH cases (excavation state A) [2]

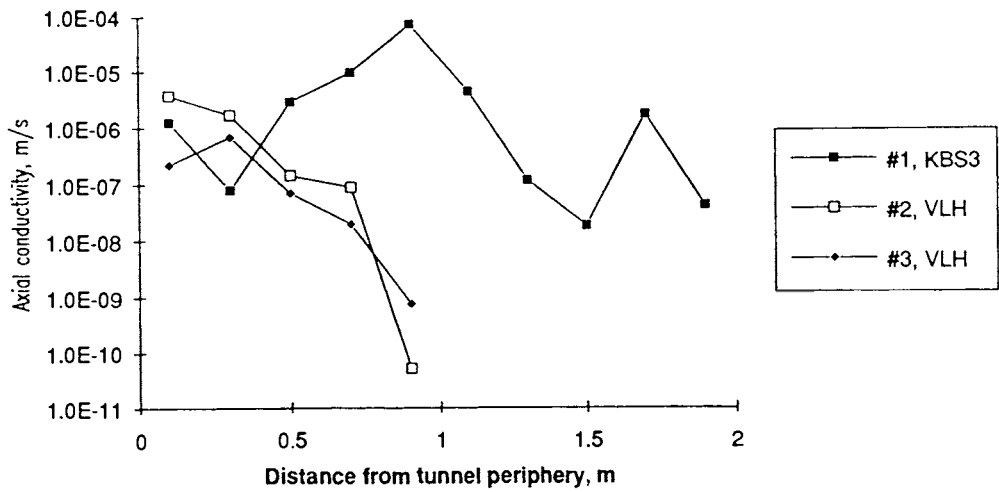


Figure 213 Axial conductivities of the nearfield rock around KBS3 tunnels and the two VLH cases ("tectonic" state C) [2]

BEHAVIOR OF BUFFERS AND BACKFILLS

Mechanisms of degradation of smectite clay in bentonitic material

As indicated in the presentation of buffers and backfills in the design chapter, the matter of chemical long-term stability of smectite clay, which is the sealing component of bentonite clay, is of great practical importance. Since temperature is the main threat to its sealing function we need to consider the longevity in detail in the performance analysis of the heating period. The discussion will be confined to the behavior of montmorillonite, which is the most common smectite mineral; we will see that other representatives of this group of clay minerals are more or less stable under repository conditions.

The long-term chemical stability of montmorillonite depends on temperature and groundwater composition in a very complex way but under commonly prevailing pH conditions the most probable alteration of smectite (S) is conversion to non-expanding hydrous mica ("illite", I), which has a crystal structure that is similar to that of montmorillonite but with a higher lattice charge due to partial replacement of tetrahedral silica by aluminum, and with the interlamellar space - defined in Figure 58 and visualized in Figure 64 - collapsed through replacement of the hydrated cations by non-hydrated potassium. Such conversion is assumed to take place in two ways: 1) replacement of tetrahedral silica by aluminum and uptake of external potassium, leading to mixed-layer (I/S) minerals with successively dominating I, and 2) neoformation of hydrous mica in the voids of the smectite clay that supplies silica and aluminum or magnesium, while potassium enters from outside and triggers crystallization of hydrous mica as indicated in Figure 214 [19]. The I/S conversion, which is commonly assumed to take place stepwise yielding irregular or regular stratification, is believed to reach a final state with around 80-90 % I and 10-20 % S, as concluded from comprehensive field investigations particularly in the Mexican Gulf area. Neoformation of illite is expected to take place at suitable concentration of silica (H_4SiO_4), aluminum and potassium, yielding crystal nuclei in the form of laths. When precipitation takes place the potassium concentration drops locally and the concentration gradient thus formed brings in more potassium by which the process continues. Geochemical codes tend to indicate that illite should be formed from smectites in a certain "window" of phase diagrams of silica, aluminum and potassium [20], but they do not seem to be able to indicate whether the conversion takes place via mixed-layer mineral stages or by dissolution/neoformation.

There is in fact a second conversion mechanism involved in the degradation of smectite, namely formation of chlorite [21,22]. However, the similar behavior of illite and chlorite and the smaller amount of chlorite allows us to disregard from the latter mineral in this context.

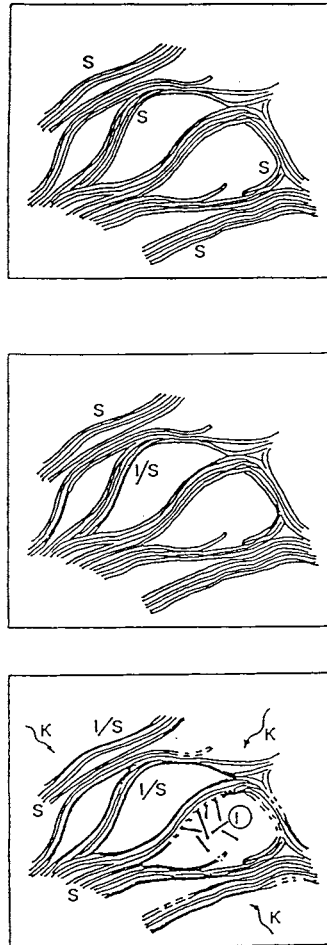


Figure 214 Schematic picture of conversion of smectite to illite via mixed-layer mineral formation or dissolution/neof ormation [19]

The smectite mineral formed by Si-to-Al substitution in tetrahedral positions is termed beidellite and it is the dominant mineral in certain natural smectite deposits, like in Spain. It is not suitable for use in repositories intended for long-term performance since the only requirement for conversion to illite is uptake of potassium, provided that the mixed-layer conversion model applies.

While neoformation of illite is an intelligible process that has also been documented in hydrothermal experiments [21], mixed-layer formation is not an easily imagined process because the smectite-to-illite conversion involves collapse of the stacks of flakes that requires either a high effective pressure and a temperature exceeding about 60°C, or drying. When heating only partly saturated clay, capillary forces may cause stack collapse and experience tells that cyclic wetting/drying yields permanent collapse and conversion of montmorillonite to non-expandable 10 Å minerals which appear as illite but are not true minerals of hydrous mica type. While interlamellar dehydration of fully water saturated montmorillonite with calcium or potassium as exchangeable cations can be imagined as a successive loss of hydrates of these cations, the mechanism may be different in lithium and sodium montmorillonite. Thus, assuming that the hydrated montmorillonite crystal lattice is of the Edelman/Favejee type one would expect that heating to a critically high temperature would invert the protruding tetrahedrons to the state they have in the Hofmann/Endell/Wilm structure (Figure 58 in Chapter 3). The interesting thing is that such inversion would be associated with an unstable state of the silica contained in the altered tetrahedrons, i.e. roughly 1/4 of the total number of silicons, which could imply release of them and conversion to beidellite provided that aluminum enters the reformed tetrahedrons [22]. The released silica is expected to be precipitated at the periphery of the stacks forming cementing bonds since the porewater will already be largely saturated with silica.

There is, however, another factor that makes the mixed-layer conversion somewhat dubious and that is the required replacement of the initially present interlamellar cations by potassium. The fact is that the affinity for potassium is not much higher than that for sodium, which is present at much higher concentration than potassium in most groundwaters, and that the affinity for calcium is significantly higher than for potassium. Thus, it is hard to believe how potassium can enter and replace initially present interlamellar cations except, possibly, when potassium is present at much higher concentration in the porewater than sodium and calcium in electrolyte-rich groundwaters. This seems to be a very rare condition.

Provided that transformation from montmorillonite to beidellite is related to a critical temperature it is expected that Ca-montmorillonite is more stable than Na-montmorillonite

when this temperature is reached and this also seems to be the case [22]. This would naturally offer a possibility to accept temperatures of 150-200°C as would also the use of certain other smectite minerals like the magnesium-rich saponite and the iron-rich version nontronite, for which no heat-related transformation between different crystal forms has been proposed, but the risk of complete dehydration, especially in the maturation stage, still suggests that the maximum temperature be kept below 100-110°C. The major reason for this recommendation is, however, the risk of cementation that may arise from the temperature gradient that prevails in deposition holes and tunnels. Thus, dissolution of the smectite minerals will yield more silicon and aluminum in the hot zone near the canister and less of these elements at the colder clay/rock contact, and the concentration gradient is expected to yield precipitation of cementing silica and aluminum compounds throughout the clay profile. Such effects have been noticed in field experiments with hot boundary temperatures of around 170°C and temperature gradients of about 10°C/cm, while they seem to be very moderate at temperatures below 130°C and gradients lower than 1-2°C/cm [23].

The lack of quantitative data for the cementation process calls for appropriate chemical modeling, which is underway in various countries. At present one can only make simple estimates, for which a general model for conversion of smectite to illite proposed by Pytte can be of some help as discussed below [23].

Longevity of montmorillonite-based buffers and backfills

The two major threats to the excellent barrier functions of smectite of any sort are ¹⁾ conversion to non-expanding 10 Å minerals, and ²⁾ cementation by precipitation of Si/Al compounds.

The firstmentioned type of alteration can take place in two major ways, i.e. by dehydration, which may produce collapsed smectite stacks with potassium - i.e. conversion of smectite to illite - or with sodium or calcium ions in interlamellar positions. Dehydration and permanent collapse, yielding illite or minerals of paragonite-type, may occur in the maturation period but hardly in the heating phase, while illitization and cementation resulting from dissolution/precipitation of smectite and accessory minerals, primarily feldspars and carbonates, can go on throughout the period of enhanced temperature.

The rate of conversion of montmorillonite to hydrous mica in the heating period is assumed to be controlled by the access to potassium irrespective of the mechanism of conversion provided

that the temperature is high enough to provide the clay-water system with silica and aluminum at a sufficiently high rate. Assuming that smectite-to-illite conversion takes place through reorganization of the smectite crystal lattice, this rate is determined by the required activation energy, which is on the order of 20-30 kcal/mole, and applying a model proposed by Pytte for such conversion, the rate of illitization can be estimated for any given K^+/Na^+ [24]. An example referring to a relatively high potassium concentration in the porewater and the activation energy 27 kcal/mole is illustrated by the diagram in Figure 215. The model suggests that insignificant alteration and release of silica will take place in a 2000 years long period with temperatures of up to 90°C, while a 1000 year period with heating at 150°C will convert 50 % of the smectite to illite and release significant amounts of cementing silica.

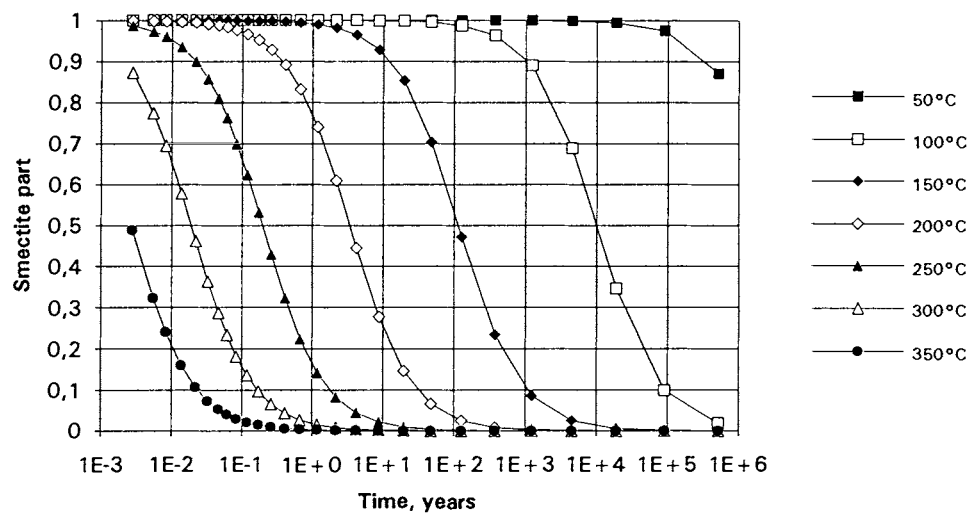


Figure 215 Rate of conversion of smectite to illite using Pytte’s model applying an activation energy of lattice reorganization of 27 kcal/mole and appropriate literature-derived constants [cf. 24]. The initial content of smectite is assumed to be 100 % (smectite part=1), and it drops to 0 depending on temperature and time

Nature provides several geological examples of smectite-to-illite conversion that are in reasonable agreement with this model but there are indications that the conversion is considerably slower in certain cases. This can be explained by limited access to potassium, which successively becomes the rate-controlling factor when the temperatures increases beyond about 60°C as mentioned above. The matter of potassium supply is thus of primary importance and needs to be investigated for predicting the performance of smectite-based buffers and backfills.

A classic approach is to regard accessory potassium-bearing minerals in the smectite clay and also such minerals in the rock hosting the clay as the primary source of potassium for conversion of smectite but this does not seem to be entirely true. Instead, the potassium content of the groundwater may be the major supply of this element, at least at temperatures below 100°C at which potassium-bearing minerals like feldspars and micas are relatively stable. This would imply that the groundwater motion along deposition holes in repositories is of major importance. Thus, under stagnant conditions, migration of potassium takes place by diffusion, which delays the conversion very much, while moving groundwater will bring in potassium at a rate that may keep up the concentration at a level that produces quick conversion. Hence, in addition to the K^+ -content of the groundwater, the hydraulic conductivity and gradients are determinants of the conversion rate in practice.

Turning now to the three repository concepts VDH, KBS3 and VLH we can make the following rough estimates of the rate of conversion and cementation of the montmorillonite-based buffers and backfills [2].

VDH

Using the flow data in Table 8 in Chapter 3 and assuming a hydraulic gradient of 10^{-2} , which is reasonable for the larger part of the period of enhanced temperature, one finds that around 3 liters per year pass along the deployment part of the deep holes. Applying the figure 50 ppm K^+ -concentration of the assumed 100 000 ppm total electrolyte content (Table 14) one finds that about 0.2 g of potassium may be available per year for conversion of the montmorillonite in the deployment zone. A rough estimate is that all montmorillonite has been converted when potassium makes up 5-10 % of the total solid mass, from which one finds that less than 1/1000 of the montmorillonite content may be converted to hydrous mica in the heating period. A conservative estimate is that complete conversion is therefore that it will take at least about 20 000-30 000 years. The rather low temperature gradient that prevails in the larger part of the heating period is expected to make cementation less extensive than in the other concepts but

since the density of the clay is low the physical properties may be rather significantly changed; in particular the deformation moduli will be increased.

Under stagnant groundwater conditions conversion to illite will take place by uptake of potassium that migrates by diffusion through and from the surrounding rock, which yields even slower conversion.

As to the plugging zone, of which at least 1 km will not be exposed to higher temperatures than about 30°C, degradation will be considerably slower than in the deployment zone. Using Pytte's model, it is expected that it will take hundreds of thousands of years before significant mineral alteration has taken place in the larger part of this zone.

KBS3

Considering first the tunnel backfill its temperature is estimated to be in the interval 45-55°C after about 100 years and it will remain approximately at this level for one to two thousand years. Applying the same simple model for conversion as in the VDH case one finds that the degradation of montmorillonite-poor backfill may be rather quick because of the high groundwater flow through the excavation-disturbed zone around the tunnels. Thus, reconsidering the case of KBS3 tunnels intersected by 3rd order fracture zones with an average spacing of 50-100 m that was discussed in Chapter 3 and described in Figures 143-145, one finds that around 1000 liters of groundwater pass along the rock/backfill interface per year, which makes about 40 g of potassium available for transformation of backfill montmorillonite to illite per year. With a good commercial bentonite a 10/90 mixture contains around 7 % of montmorillonite by weight and a total amount of montmorillonite of around 25 000 kg over the 50 m long distance, and applying the rule that conversion of montmorillonite requires an amount of potassium that corresponds to around 5-10 % of the montmorillonite mass, one finds that 4-8 % of the smectite will undergo transformation in the heating period.

Although this may seem to be of little concern it has a significant effect on the conductivity and rock-supporting ability of the backfill. Thus, the conductivity of the peripheral part of the backfill will increase by 1000 to 10 000 times and this will increase the groundwater flow through the backfill and accelerate the conversion to illite. Also, the conversion of even a small part of the montmorillonite content means that the swelling power, and thereby the rock-supporting ability, will be lost. In turn, this means that the aforementioned disintegration of the roof and upper parts of the walls of the tunnels takes place and that the nearfield also

becomes more permeable, which causes further acceleration of the degradation of the tunnel backfill.

The beneficial effect of properly designed and located seals for cutting off axial groundwater flow in the disturbed zone is particularly obvious in this context. Thus, as demonstrated in Chapter 3, plugging by use of highly compacted bentonite can reduce the axial flow by about 99 % (cf. Figure 145), which means that a practically stagnant groundwater regime is created. Potassium will then migrate to the backfill by diffusion but at a rate that makes conversion of the montmorillonite to illite by uptake of potassium negligible in the heating period.

Considering also the supply of potassium by degradation of K-bearing minerals of ballast minerals, one finds that if material rich in the feldspars microcline and orthoclase are used, potassium may be released to an extent that yields complete conversion of the montmorillonite content in the heating period. Also, it can be expected that the associated precipitation of released amorphous silica/aluminum complexes, which emanate from all the silicates in the backfill, produces cementation by which it will lose practically all of its rock-supporting and self-sealing ability in this period. If the ballast consists of minerals that are poor in potassium, such as crushed, feldspar-poor crystalline rock, and - ideally - quartz sand, the conditions will be much less severe both with respect to the degradation of the montmorillonite and to cementation effects. Thus, the aforementioned scenario with potassium being supplied only by groundwater flowing in the nearfield is most probable if the amount of K-bearing minerals is less than 1-2 % by weight. The cementation effects are then estimated to be rather insignificant, i.e. comparable to those in lower parts of ordinary podsol profiles in the northern hemisphere. Naturally, an increase of the bentonite content of the backfill by 2 to 3 times greatly improves its performance throughout the heating period.

Turning now to the KBS3 deposition holes we find, by using the hydraulic data given in Table 8 and taking the hydraulic gradient as 2×10^{-2} , i.e. the same as for the tunnel backfill, that around 10-1000 liters pass along the central and lower parts of a deposition hole per year, which may make 0.4 to 40 g of potassium available for conversion to illite per year. Applying the same crude criterion concerning the required amount of potassium for complete transformation from montmorillonite to hydrous mica as in the previous cases, i.e. that potassium must make up 5-10 % of the solid mass, it is clear that complete alteration of the 15-20 t of montmorillonite in each hole will take hundreds of thousands of years. Insignificant changes in physical behavior are expected in the heating period.

In the period when temperature gradients prevail in the buffers and backfills, silica will also

migrate from the hot part of the clay to colder parts where it is expected to precipitate in the form of cristobalite or amorphous silica, causing cementation. There is no physico/chemical model that describes this process but a rough estimate can be made by application of Pytte's model of smectite-to-illite conversion. This model suggests that 10 % of the montmorillonite mass is converted in 100 000 years at 70°C, while less than 1 % will convert in the heating period. Since 100 % conversion will cause dissolution and release of 10 % of this mass, assuming the alteration to take place only through beidellitization, the ultimate amount of silicious cementing precipitates will not exceed 1 % of the bentonite clay mass in the deposition holes, which is totally negligible in the few thousand years long heating period. However, this is under isothermal conditions and since the temperature gradient that prevails in the first few hundred years cause migration of released silica and aluminum from the hot zone near the canisters to the colder clay/rock boundary, some additional cementation is expected. Also, as described earlier in this chapter, enrichment of cementing substances of low solubility at higher temperatures, like sulphates, will take place in the hot zone as long as temperature gradients prevail.

The practical importance of cementing processes of the described types is not well known but it can be estimated by considering the physical state of natural bentonite beds that have been heated to at least 100°C and exposed to temperature gradients of up to about 1-2°C/cm. Such an example is represented by the Ordovician Kinnekulle "metabentonite", that was exposed to 110-160°C for 1000-2000 years by intrusion of magma at a distance of slightly less than 100 m, creating an estimated temperature gradient of the order mentioned [25]. The amount of cementing material has been estimated at 5-10 % by weight [26] and samples taken for creep testing demonstrate that it certainly affects the physical behavior but that the typical ductile and time-dependent stress/strain behavior of unheated montmorillonite illustrated in Figure 70 is largely preserved as shown by the diagrams in Figures 216 and 217. Figure 216 also exhibits a diagram of more strongly heat-induced cementation of bentonite from Sardinia. The major differences when compared to unheated montmorillonite clay are the jerky strain fashion at higher shear stresses that is associated with breakage of strong bonds in the cemented clay (Figure 216), and the less quick retardation of the strain of the cemented clay than of unheated clay as indicated by the flatter slope of the creep curve in Figure 217. The latter phenomenon can be explained by the shift in shape and composition of the energy barrier spectrum caused by the cementation process [27].

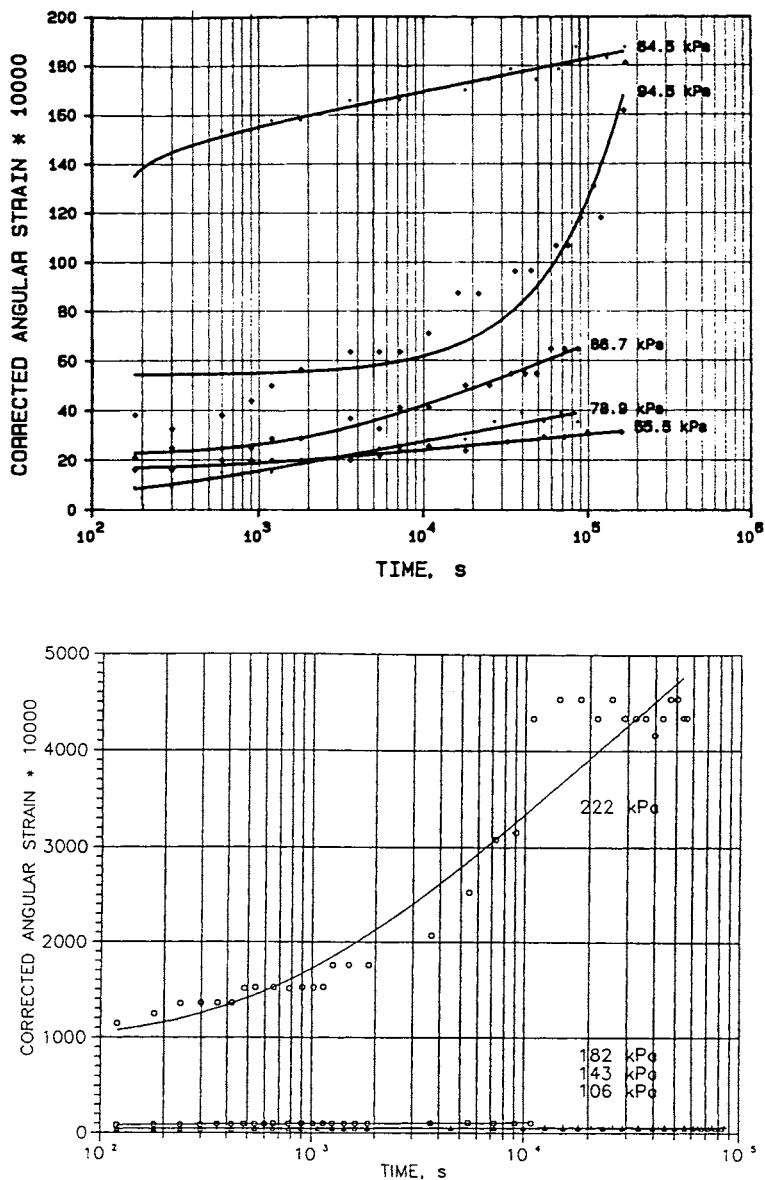


Figure 216 Creep strain of cemented smectite clay. Upper: Slightly cemented Kinnekulle "metabentonite" clay [27]. Lower: Strongly cemented Sardinian bentonite. Notice the insignificant strain until a critically high stress is applied

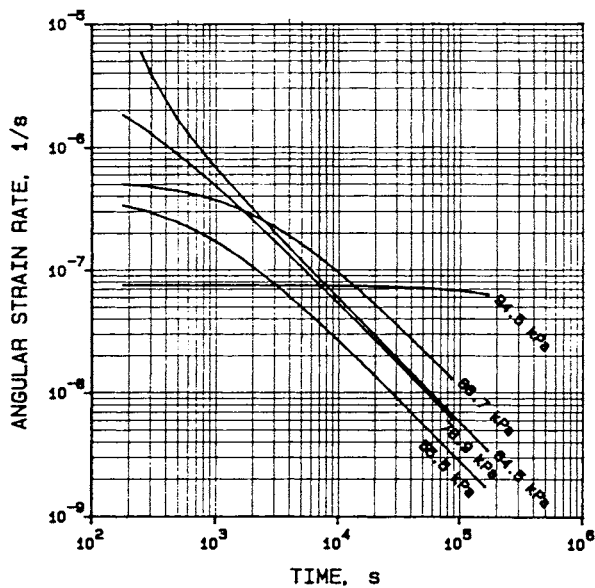


Figure 217 Creep strain rate of Kinnekulle clay versus time for different shear stresses (cf. Figure 70) [27]

VLH

The temperature level, i.e. about 100°C for less than 100 years, is sufficiently high to make the rate of conversion of the montmorillonite in the canister-embedding buffer depend on the access to dissolved potassium. Also, cementation will be of some importance because of the relatively high temperature.

Applying, as for the KBS3 and VDH concepts, the hydraulic data in Table 8 and assuming that the hydraulic gradient is 2×10^{-2} as for the nearfield of KBS3 holes, one finds that around 10 liters of groundwater per year will pass along VLHs in the heating period. This will make around 0.2 g of potassium available for illitization per year and meter length of the buffer material in the large holes, which means that the conversion will be even slower than for KBS3, and that the montmorillonite content of the dense bentonite will be largely preserved in the heating period. However, cementation may be somewhat more extensive than in the

KBS3 case.

BEHAVIOR OF SEALS

Seals will behave differently depending on the temperature and rock movements that they are exposed to. Thus, plugs of highly compacted bentonite that are located in shafts and tunnels of KBS3 and VLH repositories will be very moderately heated and retain their properties throughout the heating period like the dense bentonite in the plugged part of VDH.

Cement and clay grouts in narrow fractures in the nearfield of KBS3 canister holes and VLH may undergo significant degradation due to dissolution and mechanical strain caused by rock movements. They are not expected to serve as effective seals when the heating period is over, while grouts injected in wider fractures in low-order zones may have a considerable part of their sealing ability preserved, provided that the grout density is high.

INTERACTION OF BUFFERS AND CANISTERS

Shearing of canisters

The potential of canisters to isolate waste is naturally controlled by their tightness, which is threatened by corrosion and tectonically induced shearing as indicated in Chapter 1 (Figure 3). We will consider both effects here, starting with the influence of tectonics, which may become important in a few thousand years perspective [2].

The analyses presented earlier in this chapter indicate that even very severe earthquakes, yielding quick shearing of 2nd order discontinuities by 200 mm will not generate shearing by more than a few tenths of a millimeter along 4th order breaks, i.e. the ones that may interfere with canisters. This amount of instantaneous strain is certainly too small to harm canisters of the type illustrated in Figure 57 but accumulation of creep-induced shear strain and of repeated tectonic events over long periods of time may yield practically important deformation.

Still, the fact that shear strain will not be uniformly distributed among high-order discontinuities when a low-order zone is activated implies that 4th order discontinuities may undergo more strain when they are located closer to the major shear planes, i.e. within 5-10 m distance from 3rd order zones and presumably within 25 m from 2nd order discontinuities. We will

therefore consider larger shearing of 4th order breaks by which also accumulated strain caused by creep in the rock and by repeated tectonic events will be accounted for. A rough estimate is that accumulation of 100 shear events in a 100 000 year perspective may yield a total shear strain along 4th order breaks by 100 mm.

Considering the three concepts VDH, KBS3 and VLH, one finds that VDH represents more hazardous conditions because of the difficulty of identifying and paying attention to all important discontinuities. Thus, since the deployment parts of VDHs are expected to be intersected by almost 150 more or less flatlying 3rd order discontinuities and by 10 similarly oriented 2nd order zones, as well as by 1 st order zone, at least 25 % of the canisters may be exposed to instantaneous transverse shear by more than 1 mm, and 10 % of them may be exposed to considerably more transverse strain. 20 canisters may well be exposed to transverse shear by as much as 200 mm.

The shearing of deposition holes of the types represented by concepts like KBS3 and VLH can be investigated by applying numerical methods and a recently performed analysis, using the material models of the rheological behavior of montmorillonite clay referred to in Chapter 3, has shown that the shear resistance of the clay is the major parameter in assessing the performance of HLW canisters [2]. A general conclusion is that bulk clay densities below 1.9 g/cm^3 do not cause critical stress and strain conditions for most types of thick-walled canisters, while higher clay densities, which are beneficial because they yield an extremely low hydraulic conductivity and very low anion diffusion capacity, may cause mechanical failure and thereby exposure of the interior of the canisters to groundwater. However, even at a bulk density of the clay of 2.05 g/cm^3 at water saturation, a hollow 83 cm diameter canister with 6 cm copper surrounding the inner 5.5 cm thick steel tube will not undergo more plastic strain than 4 % at quick rock shearing of 100 mm as indicated by the ABAQUS calculation illustrated in Figure 218. This strain, caused by a single tectonic event, is not critical and if it results from repeated events, the harm will be even less because stress relaxation and some homogenization of the clay will take place between the shearings. Considering that single events are not expected to generate more strain along fractures intersecting deposition holes than a millimeter, higher bulk densities implying a higher shear resistance, may be used but the risk of additional strength increase by cementation effects must then be kept in mind.

The use of low-density clay buffer will of course eliminate the risk of critical stress/strain conditions in the canisters but rock shearing will instead tend to produce an open space between the canister and the clay as illustrated by the small-scale experiment with an X-rayed deposition hole shown in Figure 219. Since lower densities also imply less effective homogenization and self-healing and also settlement of the canisters, it is wise to use higher densities than 1.9 g/cm^3 rather than lower ones.

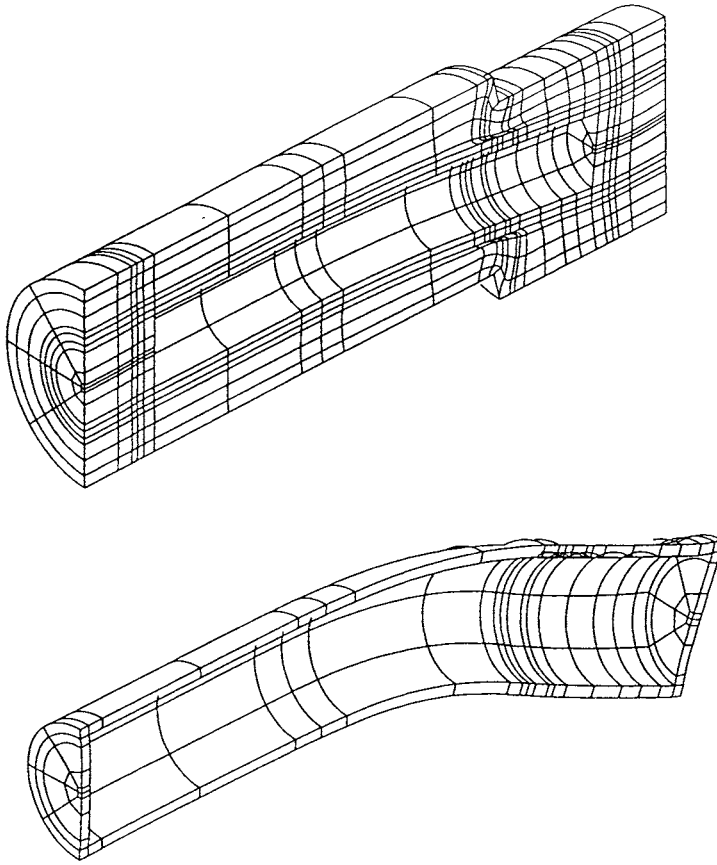


Figure 218 Deformed clay/canister system at 100 mm rock displacement occurring across a 4.5 m long hollow KBS3 canister at a distance from its end of 1.2 m. Upper: Entire system. The canister, which is located in the central open space, has only undergone continuous slight deformation, while the clay boundary is discontinuous (Strain magnified by 2.5 times). Lower: Deformed copper (Strain magnified by 10 times) [2]

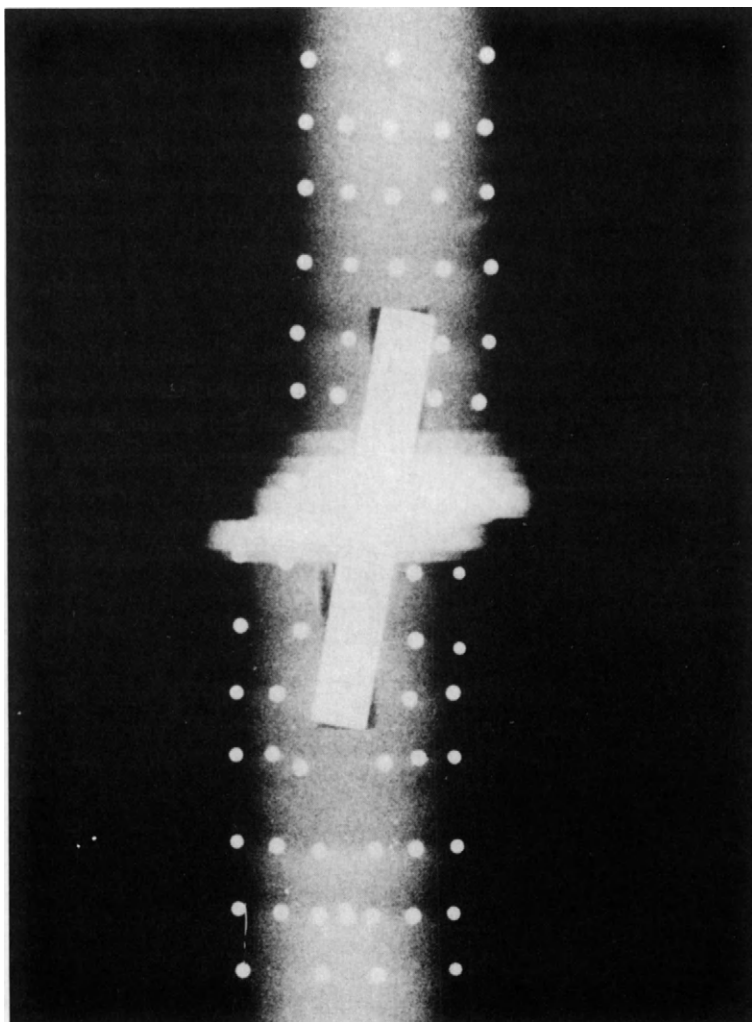


Figure 219 X-ray picture of small scale experiment with sheared deposition hole hosting canister in relatively soft bentonite clay. The canister remained straight and produced open space (black) at the clay/canister interface. White dots are lead shots for evaluating the strain; the white part in the center belong the shear box arrangement

Chemical interaction of the clay buffer and the canister metal

For canisters consisting of copper the influence on the clay is limited to quick release of copper in ionic form in the oxidation phase, i.e. when there is still air contained in the incompletely water-filled voids in the clay, and initiation of cation exchange from Na to Cu when the clay has been wetted all the way to the clay/metal contact, which happens early in the heating phase. Cu ions will be given off from the copper at a rate that is determined by the solubility of copper, which can be taken as 1 ppm in the heating period. In a 2000 year perspective this may bring about complete copper saturation and ion exchange from sodium to copper in a few millimeter thick annulus, and partial saturation within 1-2 centimeters distance from the canister surface. This process, which is expected to have a similar influence on the clay as saturation with calcium, will not cause any significant changes in physical behavior of the canister-embedding clay in KBS3 and VLH because of the high bulk density. For VDH, on the other hand, the significantly lower bulk density of the clay will cause significant increase in hydraulic conductivity and loss in swelling power of the few millimeter thick annulus of clay at the canister contact if the clay is not initially saturated with calcium. Although such changes may not be very critical to the overall function of the clay, it further reduces its rather poor performance in VDH.

Steel canisters will corrode when wetting all the way to the clay/canister contact has taken place and iron hydroxide, and magnetite and various oxy/hydroxides will be formed. They are both expected to be accompanied by hydrogen gas production, yielding free Fe^{3+} under the high pH conditions of low-saline water, and presumably Fe^{2+} in salt water. Iron in ionic form will migrate very slowly from the clay canister interface, probably at a rate that is comparable to that of copper ions, causing ion exchange but only insignificant change of the physical properties of the clay, except if copper is used instead of titanium in VDH canisters.

However, iron in ionic form (Fe^{2+} or Fe^{3+}) may become precipitated as $\text{Fe}^{2+}\text{Fe}^{3+}$ hydroxy compounds in the clay. Goethite may be formed from small soluble entities like $[\text{Fe}(\text{OH})_2]^+$ which feed the growing FeOOH crystals, and it may even precipitate directly from the porewater solution. A number of such compounds can be formed, cementing the smectite stacks together, and when they precipitate, a concentration gradient is created that brings more iron from the canister into the clay. The precipitates are expected to form coatings that prevent the stacks from expanding and the clay may ultimately undergo complete cementation and turn into claystone. The concentration gradient will keep the migration rate rather high and it is estimated that extensive cementation may take place in a few hundred or thousand years. The hydrogen gas that is most probably formed irrespective of the corrosion mechanism, is anticipated to follow a few major continuous passages through the clay when the pressure

equals the sum of the prevailing piezometric head and the swelling pressure, and the migration pattern is expected to be finger-like and only affect a small part of the clay buffer. Continuous or intermittent gas passage may, over a long period of time, create microstructural changes and there may be chemical reactions between the clay and the hydrogen gas as indicated by pilot tests.

5-2.5 Post-heating stage

GENERAL

The length of the post-heating period that one needs to consider has to be defined and a conservative but practical rule for radioactive waste repositories can be defined as the time at which the radioactivity of the waste has dropped to the level that is representative of the virgin host rock. A conservative assumption for HLW repositories in crystalline rock is that the period extends to at least 100 000 years, which will be taken here as a limit. In this period significant climatic changes are expected yielding conversion of presently desert-type areas to humid land or sea, and of present estuaries and shallow sea to dry land. Significant upheaval of salt-domes and certain mountain ridges, and descent of large areas will take place in northwestern Europe. Tectonic events of higher magnitude than in the heating period are expected and future Europe and North America will probably face extensive glaciation (Figure 220).

While the physical state and isolating properties of the host rock may undergo practically important changes, the clay buffers and backfills will be very much changed in the post-heating period.

ROCK BEHAVIOR

The regional stress conditions may undergo considerable changes in a 100 000 year perspective due to more intense tectonics and more extensive glaciation in the post-heating period than at the preceeding stages. A simple way of estimating the influence on the nearfield rock by stronger tectonic events is to apply the same type of numerical analyses that were used for the heating period but assuming larger instantaneous strain along low-order discontinuities. We will use this approach here and again refer to the three HLW concepts VDH, KBS3 and VLH.

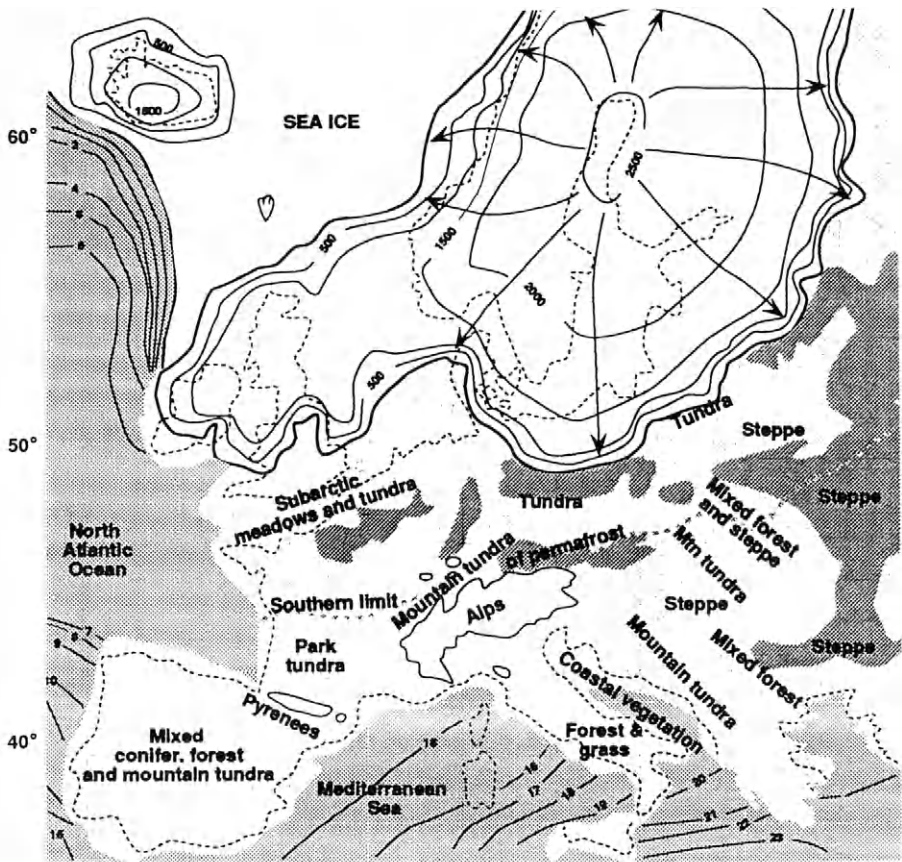


Figure 220 Reconstruction of the conditions in Europe at the latest glacial maximum 18000 years ago. Thick solid line represent the ice contour and figures 500 , 1000 etc the topographic height of the ice. Light-grey areas show water and figures 2 to 23 sea-surface temperature in August. Dark-grey areas represent steppe with loess deposition [28]

Earthquakes of magnitude 8 or higher can be expected, yielding rather quick shearing of 2nd order discontinuities by several meters, possibly by as much as 20 m, which may induce quick shearing of 3rd order zones by several decimeters and instantaneous shearing of 4th order discontinuities by several millimeters. Applying this to VDH with frequent low-order discontinuities intersecting the deployment part of the holes, the shearing of 4th order breaks in the rim zones may be much larger than in the heating period and up to 50 % of the canisters may be exposed to larger transversal shear strain than 10-20 mm. KBS3 and VLH canisters may be exposed to transverse shear by a few centimeters. However, the practical consequences of the shear strain is in fact very small for all three concepts. Thus, for VDH, the softness of the deployment mud means that the induced strain in the canisters will not be sufficient to cause plastization, and the preceding analysis of the shearing of KBS3 canisters at 100 mm rock shear shows that they will also remain unharmed.

BEHAVIOR OF BUFFERS AND BACKFILLS

The same basic mechanism of smectite conversion to illite proceeds in the post-heating period as in the preceding phase but at a strongly retarded rate because of the low temperature in the KBS3 and VLH cases. However, the high ambient temperature in the VDH case makes the degradation go on at a high rate. The fact that there are no temperature gradients in the nearfield means that cementation by salt enrichment or silica precipitation is not expected in any of the concepts.

As in the heating period the potassium content in the groundwater and the flow conditions in the nearfield are essential parameters for the performance of the barriers. While the amount of potassium in the natural groundwater and the contribution by dissolution of K-bearing minerals in the clay and the surrounding rock will be sufficient to keep up the conversion to illite, the conditions will be different in a long-term perspective. This is because the regional hydraulic gradients are expected to drop and the conversion will then depend on how effectively potassium is provided by diffusion. Thus, under stagnant groundwater conditions the K^+ -concentration in the porewater of the dense canister-embedding clay is reduced at a successively increased distance from the buffer and backfill. The driving force is that the formation of illite creates a sink that causes a concentration gradient in potassium that drives K^+ -ions to the reaction zone by diffusion.

Uptake of potassium from the surroundings to yield conversion of montmorillonite to illite may be a major mechanism in nature and it seems to apply in several practical cases, like the aforementioned Kinnekulle “metabentonite” and a 0.3 m thick bentonite bed at Hamra on the island Gotland in the Baltic Sea [29]. The latter bentonite was exposed to a temperature of 100-

120°C for millions of years and is still plastic due to a preserved montmorillonite content of about 30 %, which is also the figure arrived at by assuming that the rate of conversion to illite is controlled solely by potassium diffusion from the surroundings. This example, which is represented by the theoretical K-exhaustion profile in Figure 221, indicates that in the special case of very potassium-poor, stagnant groundwater in the host rock of a repository, the clay buffer will be largely preserved in its original form even after many millions of years.

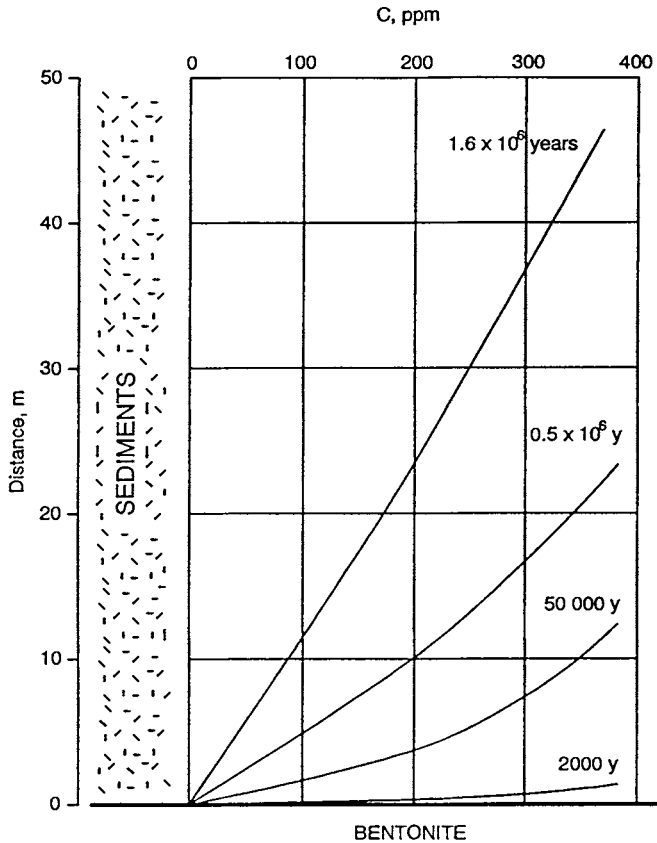


Figure 221 Theoretical example of exhaustion in potassium in a marine sediment profile overlying a 0.3 m thick bentonite bed. The initial potassium concentration in the porewater of the sediment is 400 ppm, corresponding to seawater [29]

Since there will be some groundwater movement along the canister-embedding clay in all the concepts, potassium will be provided both by flowing groundwater, although at a lower rate than in the heating phase, and by diffusion. Conservative quantitative estimates of the clay degradation can be made by applying the same hydraulic conductivity data and gradients as in the preceding analysis of the heating period and assuming that potassium is brought to the clay/rock interface by flowing groundwater.

In contrast to KBS3 and VLH, the high ambient rock temperature in the deployment zone of VDH keeps up the dissolution rate of the smectite so that the rate of potassium uptake will control the conversion to illite also in the post-heating period. Complete conversion of the smectite component in the deployment zone is estimated to require at least 15 000 years. In the larger part of the plugging zone the conversion rate will be much slower than in the deployment zone primarily because of the lower temperature, and down to about 1 km depth the smectite clay will actually not be significantly degraded even after hundreds of thousands of years.

The temperature will only be 10-15°C in KBS3 and VLH repositories in the post-heating period, which implies that the conversion of the smectite component will not be controlled by the access to potassium but by the rate of dissolution of the smectite component according to the simple degradation model. This means that the conversion rate will be very much lower than in the heating period and one finds that complete alteration of the smectite component of bentonite-poor KBS3 tunnel backfills will require more than 25 000-50 000 years and much more than that if axial groundwater flow along the tunnels is cut off by effective seals. The smectite contained in the central part of the backfill will not be very much changed in hundreds of thousands of years. Complete conversion of the 15-20 tons of montmorillonite in each deposition hole in a KBS3 repository is not expected until after hundreds of thousands of years and a correspondingly slow degradation is expected for the VLH clay buffer.

The interaction between the canister-embedding clay and the canister metal will be a slow process in the post-heating period. Considering first copper canisters, the solubility of copper at 10-15°C is only a fraction of 1 ppm, meaning that further release and migration of copper after the heating period is very much retarded, except in VDH where the process may go on at a constant rate and yield complete exchange of adsorbed cations after some thousand or tens of thousands of years. For the KBS3 and VLH concepts a rough estimate would be that complete saturation of the canister-embedding clay with copper would take hundreds of thousands, or even millions of years. In contrast to the rather soft VDH clay, which undergoes significant microstructural reorganization by exchange of initially adsorbed sodium to copper if the canisters are copper-shielded, the physical properties of the dense canister-embedding clay

buffers of KBS3 and VLH will be insignificantly changed. As to steel canisters, it is expected that corrosion yielding iron in ionic form will continue to cause very slow but finally complete exchange of the adsorbed cations by iron. As in the case of copper, the cation exchange will not alter the physical properties of the dense KBS3 and VLH canister embedments significantly. However, the precipitation of hydrated iron complexes that most certainly is initiated in the heating period, is expected to continue and alter the smectite clay to claystone in a few thousand years. The hydraulic conductivity of the clay may be reduced by this process but the swelling and self-sealing ability will disappear completely because the stacks of montmorillonite will be cemented together. Tectonically induced shear may produce fractures in the claystone and openings along the canisters, by which the tightness of the clay buffer will deteriorate significantly. It is anticipated that the production of hydrogen gas that is expected to be initiated in the heating period will continue. The extent to which the "finger-like" capillary channel system may develop is not known and requires attention.

BEHAVIOR OF SEALS

Plugs of dense bentonite will stay largely intact in hundreds of thousands of years and grouts that have survived the heating/cooling cycle may also have part of their sealing ability preserved.

5-3 Exceptional conditions

5-3.1 General aspects

The choice of unsuitable repository sites or unexpected events may cause significant deviation from the "normal" conditions with respect both to rock structural features, tectonics, and groundwater composition [2]. The major general difference between the "normal" and "exceptional" cases is that the latter are expected to represent more intense tectonics induced by glaciation/deglaciation and large-scale faulting. This will be focused on here but significant changes in ambient temperature and groundwater chemistry will also be considered.

5-3.2 Rock structure

LOW-ORDER DISCONTINUITIES

Unsuitable location of repositories may imply interaction with many more low-order discontinuities than in the “normal case”. Also, one has to realize the possibility that discontinuities of 1st to 3rd order may be more frequent because future tectonic events may make the present discontinuities of 2nd to 4th order develop to become zones of lower orders and we will therefore apply the following version of the structural model:

- * 1st order structures, 1 km spacing
- * 2nd order structures, 200 m spacing
- * 3rd order structures, 25 m spacing

The denser spacing of low-order discontinuities implies more frequent unexpected interaction with deposition holes for VDH and VLH but hardly for KBS3 although the fraction of the tunnel length that can be effectively utilized for waste disposal in the lastmentioned concept may drop from about 80-90 % for “normal conditions” to 60-80 % for “exceptional” conditions. For VDH and VLH the corresponding fraction may be even less as discussed later in this chapter [2].

HIGH-ORDER DISCONTINUITIES

Exceptional conditions with respect to rock structure represent the two extremes “obelisque”-type rock, i.e. extremely fracture-poor rock with a spacing of 4th order discontinuities of much more than the common interval 5-10 m, or very richly fractured rock. The first-mentioned type of rock would imply a very high bulk strength and an ability to sustain considerably increased stresses, while tectonically induced shear may cause large changes in aperture of the few water-bearing fractures. The small average spacing of the discontinuities in richly

fractured rock, on the other hand, would cause less change per structure unit and is therefore less critical (Figure 222).

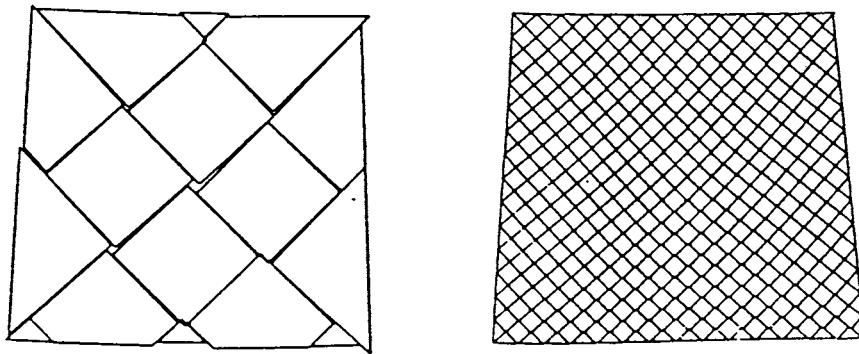


Figure 222 Fracture response to stress changes. Left: Richly fractured rock. Right: "obelisque"-type rock according to Figure 47 (After Stephansson)

Since "obelisque"-type rock implies that most KBS3 deposition holes would not be intersected by any water-bearing fractures at all, application of the general rock structure scheme in Table 3 with more frequent high-order discontinuities is more conservative and therefore applied also when dealing with "exceptional" conditions.

5-3.3 Rock stress conditions

PRIMARY ROCK STRESSES

General

The rock stress conditions in certain areas of the world, particularly concerning the horizontal primary stresses, are more severe than those assumed to be valid under "normal" conditions.

This is the case in parts of the Caledonian ridge and in certain areas in Switzerland as well as in Canada, as indicated by the comprehensive rock stress measurements in the AECL underground rock laboratory in Canada [30]. The recorded stresses at that site may be taken as a basis for defining “exceptional” primary rock stress conditions (Table 17).

Table 17 Primary rock stresses in MPa under “exceptional” conditions [2]

Concept	Depth, km	Maximum horizontal	Minimum horizontal	Vertical
VDH	0.5-1.0	35-45	15-20	12-25
VDH	1.0-2.0	45-75	20-35	25-57
VDH	2.0-3.0	75-100	35-60	57-80
VDH	3.0-4.0	100-125	60-85	80-108
KBS3	0.5	35	15	12
VLH	0.5	35	15	12

Glaciation/deglaciation

The stress evolution in a complete glaciation/deglaciation scenario may be very complex and more critical than under “normal” conditions. Disregarding from temperature effects it is probable that the rock stresses are altered by the following mechanisms:

1. Due to the build-up of glaciers the ground surface will be exposed to a steadily growing vertical pressure of up to 30 MPa, which creates high lateral stresses that are largely preserved after the retreat of the glaciers. Such stresses may have been the main cause of the commonly observed sets of long-extending flatlying major fractures in shallow rock. Thus, they may have originated from pre-existing natural 4th order discontinuities that grew in the almost uniaxial field of high lateral, more or less horizontal stresses that prevailed at the end of the glaciation period

2. The flow motion of glaciers produces tangential forces in the rock, especially where the top surface is strongly inclined. The surface topography of the ice mass will vary and the pressure that the ice exerts on the ground surface will hence not be uniformly distributed. This induces

shear stresses in the rock mass as well

3. At rapid ice front retreat the glacier shape may imply that high "artesian" pressures exist in flatlying structures, by which fractures in such structures may be expanded and filled with soil material like silt and sand [31].

The firstmentioned process, i.e. the loading of the rock mass by the glacier build-up, affects the rock at larger depth than the other two phenomena and it certainly needs to be considered. The stress conditions below a large glaciated area with an ice cap of 3 km thickness, like in the major Pleistocene glaciation stage, can be estimated by numerical calculations, from which it can be found that a horizontal pressure increment of 7-30 MPa may be generated depending on the extension of the glaciated area [32]. The higher figure evolves from calculations using ordinary rock moduli and a reasonably curved top surface of the ice mass but it also represents the case of complete dissipation of deviatoric stresses below the center of the ice cap by long-term creep. This represents the condition of "earth pressure at rest" with $K_0=1$ (Heim's rule) and yields the primary stresses in Table 18 for the maximum glaciation stage [1]. At rapid glacier retreat, as in Scandinavia some 10 000 years ago, the vertical rock stresses drop parallel to the reduction in vertical load, while the horizontal stresses may remain almost constant for a considerable periods of time, yielding the postglacial stress conditions that can be recorded today.

Table 18 Approximate "exceptional" primary rock stresses in MPa at glaciation/deglaciation. The maximum pressures include the effect of a 3 km ice load

Depth km	Max glaciation pressures, MPa		Postglacial pressures, MPa	
	Horizontal	Vertical	Horizontal	Vertical
0.1	35	35	35	5
0.5	45	45	45	15
1.0	60	60	60	25
2.0	85	85	85	55
3.0	110	110	110	80
4.0	140	140	140	110

Naturally, the assumption that the horizontal stresses are preserved during deglaciation cannot be perfectly true since stress relaxation will take place due to creep and to the aforementioned formation of subhorizontal long-extending fractures. Still, the fact that basal tills often exhibit a stress condition representing $K_0=1$ conditions means that the same stress state may prevail also down in the rock mass and the present rock stresses may therefore not be very different from the ones termed "postglacial" in Table 18. This would suggest that a larger part of the very high lateral stresses recorded in Scandinavia and Canada may be relicts from Quaternary glaciations.

Applying the data in Table 18 one finds that the maximum principal stress ratio after deglaciation should be at least 0.7, i.e. not far from isotropy at more than 2 km depth, while it may be considerably lower, i.e. about 0.4 at 1 km depth, and 0.3 at 500 m depth. At 100 m depth the ratio may be only slightly higher than 0.1, representing an almost uniaxial stress field. One immediately finds that the tangential stresses at the periphery of horizontal tunnels of KBS3 and VLH types located at 500 m may yield unstable conditions with spalling in the roof and expansion of flatlying fractures at midheight of the walls.

INFLUENCE OF EXCAVATION- AND HEAT-INDUCED DISTURBANCE OF THE NEAR-FIELD ROCK

Mechanical damage

In principle, the damage caused by fragmentation, i.e. drilling and blasting, is estimated to be the same as under "normal" conditions. However, unforeseen difficulties with respect to drilling of deposition holes may create stronger disturbance and it cannot be excluded that the average hydraulic conductivity of the rock within 10 cm distance from the periphery may be up to 10 times higher than assumed for "normal" conditions, thus becoming 10^{-8} m/s for the deposition holes of KBS3 and VLH types and 10^{-7} m/s for those of VDH, irrespective of the type and conductivity of the virgin crystalline rock.

As to the influence of blasting of KBS3 tunnels, it is estimated that the disturbance of the nearfield may be stronger than under "normal" conditions, i.e. because of technical difficulties with orientation of the blast-holes. This can result in an average hydraulic conductivity of 10^{-7} m/s within 1 m distance from the periphery.

Stress redistribution

The higher primary stresses assumed for "exceptional" conditions have several important effects on the rock stability in the construction period. Hence, using the data in Table 17, the horizontal (lateral) primary stresses may be up to 35 MPa at 0.5 km depth, while the vertical pressure may be only around 12 MPa, which creates tangential stresses at the periphery of VLH that varies between about 93 MPa and almost zero along the periphery (cf. Table 19).

Table 19 Tangential stresses at the periphery of the deposition holes in the three concepts VDH, KBS3 and VLH

Concept	Depth, km	Max. stress, MPa	Min. stress, MPa
VDH	0.5	90	10
VDH	1.0	115	15
VDH	2.0	190	30
VDH	4.0	290	130
KBS3	0.5	90	10
VLH	0.5	93	1

For VDH the extreme stress conditions imply that the density of the drilling mud has to be higher than under "normal" conditions in order to prevent spalling [1], and since this is not believed to be possible from practical points of view this concept can hardly be considered as feasible for "exceptional" conditions. Possibly, special types of muds that do not enter fractures can be considered but at present there is neither any design or thoroughly examined technology available for safe replacement of the drilling mud by deployment mud.

The stress conditions in KBS3 deposition holes are different at the upper end of the holes, where the secondary stress regime is caused by the nearness of the tunnel, and deeper down where they may be as indicated in Table 19. The hoop stresses at the peripheries of the holes of KBS3 and VLH type are considerably lower than the compressive strength of granite core

samples, which is commonly in the interval 200-350 MPa, but critical conditions, yielding spalling and local rock fall, may still occur close to unfavorably oriented 3rd and 4th order discontinuities as concluded from the analysis of the "normal" conditions. Also, discing in the upper parts of KBS3 holes may take place.

The strongly anisotropic primary stress field and high stress level under "exceptional" conditions cause significant damage in the form of shear strain and expansion of certain critically oriented discontinuities in the nearfield of VLH, and - although to a smaller extent - in the surroundings of KBS3 deposition holes. Also, there will be more creep strain in the rock and an increased risk of delayed failure. The net effect will be an enhanced axial hydraulic conductivity along holes and tunnels, particularly where the rock structure implies formation of inter-connected wedges that become unstable at the excavation or later by heat-influenced creep. Since 3rd order discontinuities intersecting KBS3 tunnels and VLHs are supposed to have a smaller spacing than under "normal" conditions, a more conductive system will be created. 3D effects and hydrothermally induced self-sealing of sheared fractures reduce the axial conductivity except in the most shallow, "overstressed" nearfield zone.

An attractive property of the KBS3 concept is that the shape of the tunnel section can be selected so as to fit even very anisotropic primary stress fields better than the circular shape of VLHs [1]. An example of such adaption is offered by the "elliptic" so-called SCV drift at Stripa (Figure 22), which was produced by very careful blasting that gave only very moderate disturbance of the rock as indicated by hydraulic measurements. Figure 223, which illustrates a 2D numerical stress/strain analysis of this drift, shows that the hoop stress should be rather constant over the periphery, preventing expansion of water-bearing fractures at the periphery and associated increase in axial conductivity, thereby [33]. For construction of such tunnel cross sections freely movable cutting heads should be suitable (Chapter 4-2.2).

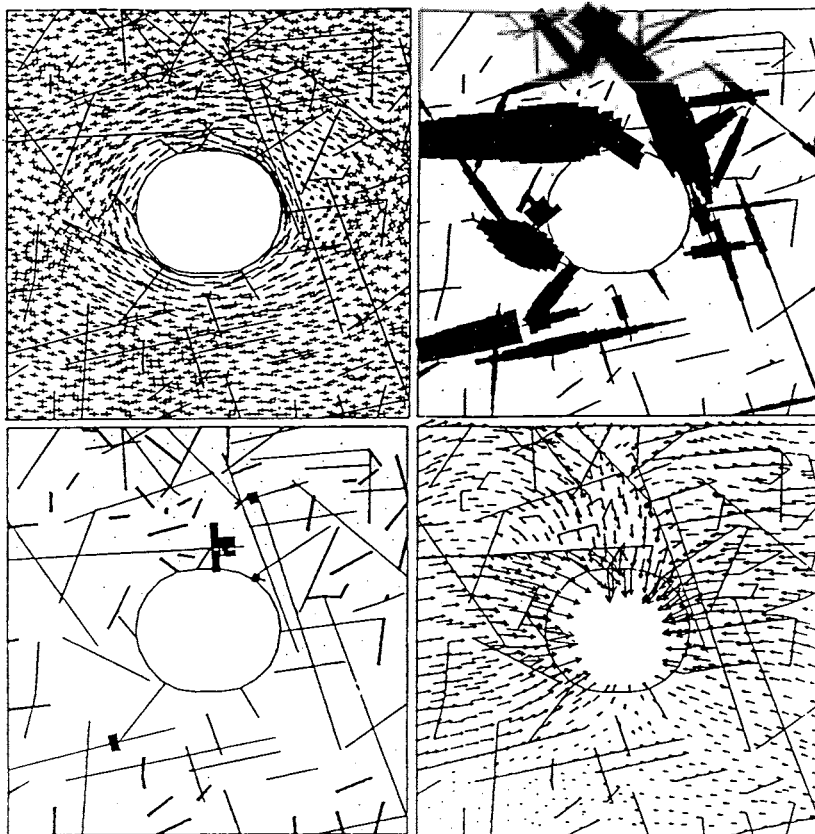


Figure 223 Example of adaption of tunnel shape to the primary rock stress conditions. Results of 2D (UDEC) calculation showing - in clockwise order - principal stresses in the upper left diagram (max. 62 MPa), joint shearing (max. 0.8 mm), inward movement of the periphery (max. 1.32 mm), and apertures of major conducting discontinuities [33]

Basic structural and hydraulic models of the nearfield

Adaption of the cross section shape to the primary stress field and rock structure minimizes the excavation-induced increase in axial hydraulic conductivity and the difference between “normal” and “exceptional” conditions are then not very significant. Still, it is expected that tectonic events associated with glaciation and very large changes in the regional stress fields will result in a higher axial conductivity along the holes and tunnels than in the “normal” case but the general shape and size of the zones of disturbance illustrated in Figures 109 and 110 can still be taken to be of the sort assumed for the latter conditions.

Assuming that the mechanical damage due to blasting and drilling operations cause a ten times higher increase in hydraulic conductivity in the most shallow rock than under “normal” conditions, and estimating the increase in axial conductivity caused by stress release in the surrounding rock to be one to two orders of magnitude higher than under “normal” conditions, one arrives at the hydraulic data in Table 20.

Table 20 Hydraulic data for “exceptional conditions” [2]

Rock zone	Concept	Hydraulic conductivity, m/s
Virgin rock (isotropic)	All	3×10^{-10}
Mechanically disturbed zone by drilling (10 cm)	VDH	10^{-7}
Mechanically disturbed zone by drilling (10 cm)	KBS3	10^{-8}
Mechanically disturbed zone by drilling (10 cm)	VLH	10^{-7}
Blast-disturbed zone (1 m)	KBS3	10^{-7}
Stress-disturbed zone	VDH	10^{-8}
Stress-disturbed zone	KBS3 holes (upper part)	2×10^{-6}
Stress-disturbed zone	KBS3 holes (central part)	2×10^{-7}
Stress-disturbed zone	KBS3 holes (lower part)	3×10^{-9}
Stress-disturbed zone	VLH	10^{-7}

INFLUENCE OF GLACIATION AND TECTONICS

One finds from Tables 17-19 that the primary stress conditions at 0.5 km depth at glaciation of the Pleistocene type yield a uniform hoop stress of 90 MPa, which is on the same order of magnitude as the maximum hoop stress in the construction period. Since the isotropic secondary stress field produces less shear strain than in this earlier period and in the heating and post-heating periods before glaciation takes place, the glaciation case implying $K_0 < 1$ considered for the “normal” conditions is more critical.

However, deglaciation under “exceptional” conditions turns out to be the most critical state as indicated by the strongly anisotropic primary stress field that is manifested by the figures 45 and 15 MPa for the postglacial state in Table 18. For VLH one finds that the hoop stress at the top and floor will be 120 MPa, while the hoop stress at mid-height of the walls will be zero, and like in the construction and preglacial operation periods this will yield expansion of flat-lying 4th order discontinuities that intersect the walls and also activate and propagate similarly oriented 5th order breaks in the walls. In the roof and floor spalling may take place to a somewhat larger extent than at the preglaciation stage. The strongly anisotropic stress field is expected to cause more shear strain and fracture expansion within a larger distance from the periphery, yielding a higher axial groundwater flux.

The effect of tectonic events of any origin, including deglaciation, can be visualized by considering the scale-dependence of the strength of the discontinuities [2,34]. Using the basic rock structure model and the friction coefficients in Table 5 and common data of the elastic properties of the bulk rock, and applying analytical solutions of the stress equations, the maximum total inelastic shear displacement of the discontinuities in a given stress field can be obtained as for the “normal” conditions. Figure 224 shows the magnitude of inelastic relative block displacements along discontinuities of 1st to 5th orders that would occur if they were subjected to anisotropic stress fields oriented with their maximum shear-to-normal stress ratios in the planes of the discontinuities, assuming the shear modulus of the rock to be 25 GPa and Poisson's ratio to be 0.24. One finds that the stronger anisotropy of the stress field under “exceptional” conditions yields significantly larger strain than under “normal” conditions. The diagram gives two sets of curves, one representing the principal stresses 10 and 30 MPa (thick lines, “a”) and the other the principal stresses 5 and 60 MPa (thin lines, “b”). Displacements are given for a number of assumptions regarding the joint friction angle, the case with friction angles exceeding 30° (line 4, i.e. the thick line in the lower right corner) giving no inelastic displacements at all. For 15° friction angle, which is representative of 1st order discontinuities, the firstmentioned stress field case gives a shear displacement of about 0.5 m (I,

line 2). The more anisotropic stress field gives no inelastic displacements for friction angles exceeding 57° (line 11, i.e. bottom thin line), while discontinuities of 1st order (15°) will undergo shear displacement by about 2 m (II, line 6). For 35° friction angle - representing 4th order discontinuities - the shear displacement would be about 0.8 mm (III, line 8) assuming the breaks to be a few meters long. Since it is realized that the second case of regional stress field is really extreme and probably representing states at which large tectonic events are triggered, one concludes that even very significant instantaneous shear strain along low-order discontinuities is not expected to produce critical displacements along high-order breaks intersecting deposition holes or KBS3 and VLH repositories. This also suggests that the hydraulic conductivity of the nearfield rock around such holes will not be significantly altered.

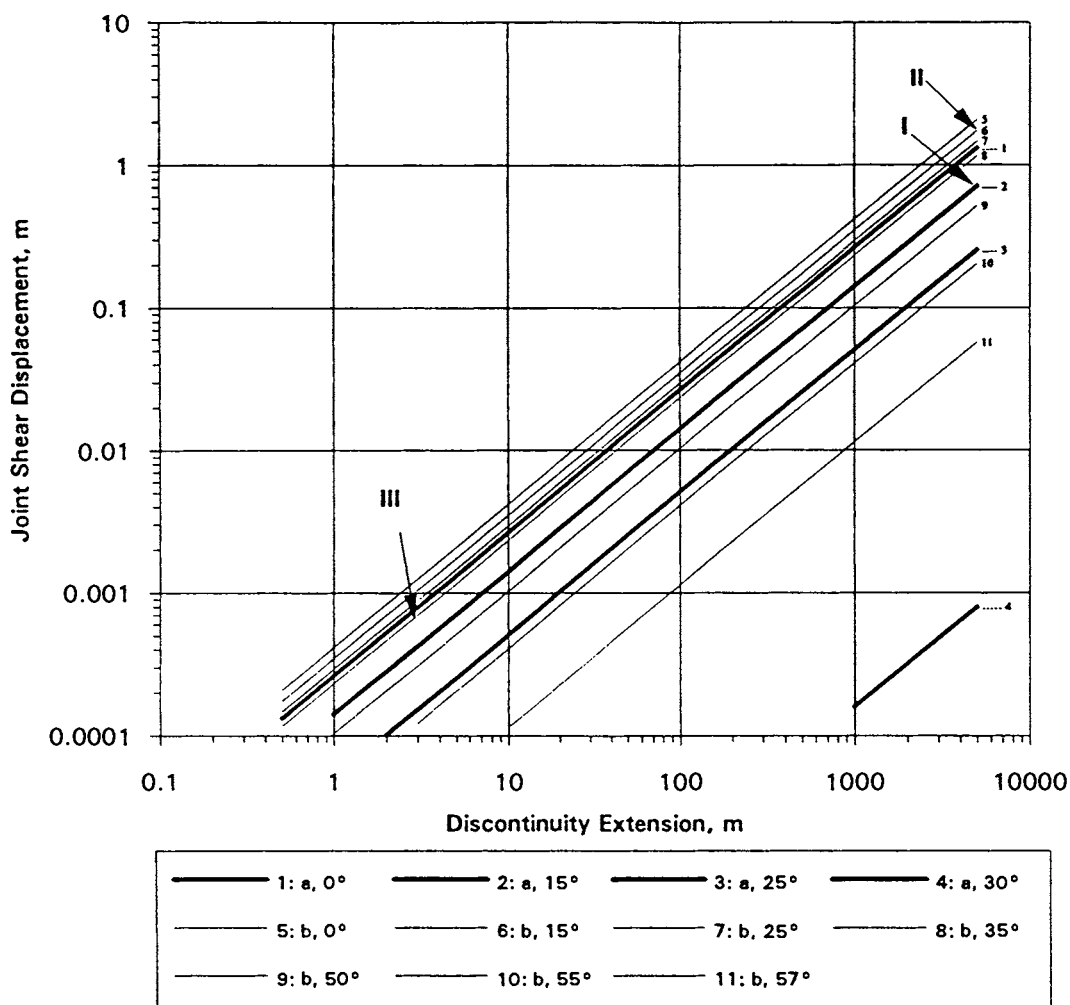


Figure 224 Analytically derived maximum shear displacements along discontinuities with different friction angles as a function of their extension [2]

NET EFFECT ON THE GROUNDWATER FLUX ALONG DEPOSITION HOLES

It is estimated that the net effect of possible glaciation and tectonic events on the hydraulic properties of the nearfield of deeply located repositories in a 100 000 years perspective is rather insignificant and that it is considered in the specification of the hydraulic data in Table 20. Thus, the around 10-100 times higher hydraulic conductivity figures for “exceptional”

conditions than for “normal” conditions yield the average axial flux values of the nearfield of the respective concepts in Table 21.

Table 21 Groundwater flux along deposition holes under “exceptional conditions” [2]

Concept	Flux q, m ³ /s	Remark
VDH	10 ⁻⁷	About 100 x "normal case"
KBS3 holes (upper part)	5x10 ⁻⁶	100 x “normal case”, tangential flow
KBS3 holes (central part)	2x10 ⁻⁷	10 x “normal case”, tangential and axial flow
KBS3 holes (lower part)	3x10 ⁻⁹	10 x “normal case”, tangential and axial flow
VLH	5x10 ⁻⁶	About 100 x “normal case”, axial flow

GROUNDWATER COMPOSITION

The chemical composition of the groundwater assumed for “normal” conditions and specified in Table 14 may not be conservative in a long-term perspective and significantly higher salt contents should be assumed for “exceptional” conditions. The potassium content in the water should also be taken higher than in the earlier analysis of smectite degradation. Table 22 is proposed to represent possible, severe conditions with respect to the impact of groundwater chemistry on clay buffers backfills in crystalline rock at depth. As to the VDH concept no change in total electrolyte content from the earlier assumptions is required while, for KBS3 and VLH, the earlier total concentration is increased to correspond to that of seawater, except for the potassium concentration, for which experience shows that the figures in the table represent extreme cases.

Table 22 Groundwater composition under “exceptional conditions”

Concept	Depth, km	Total electrolyte content, ppm	Potassium concentration, ppm
VDH	<2	35 000	50
VDH	2-4	100 000	100
KBS3	0.5	35 000	70
VLH	0.5	35 000	40

5-3.4 Application stage

GENERAL

As for “normal” conditions performance assessment should cover the entire evolution that a repository undergoes in a 100 000 years period of time, i.e. the application stage, the maturation of buffers and backfills, as well as the heating and the post-heating stages. We will consider them all in this chapter, pointing out the differences between the “normal” and “exceptional” conditions.

VDH

The major difference between “normal” and “exceptional” conditions is that the higher primary rock stresses under the latter conditions yield much higher hoop stresses with the following consequences:

* Greater risk of break-outs and outflow of deployment mud into the rock in the course of application of canister sets. This process may be severely disturbed or even impossible and only partly filled holes may have to be abandoned and plugged, causing low efficiency and

requiring new holes and hence high cost

- * Greater risk of unstable rock conditions over the entire hole length, with more extensive rock fall resulting in less dense and much more heterogeneous canister-embedding clay after consolidation of the deployment mud

- * Greater risk of unstable rock that may both damage the outer cage and make the nearfield rock very pervious.

The most severe event is of the firstmentioned type, i.e. sudden rock failure under ongoing waste application, since it may lead to uncontrolled movement, breakage and eccentric location of canisters in the holes, as well as to large heterogeneity and density variations in the deployment mud. If rock fall takes place in the deeper part of the plugging holes or high up in the deployment holes when only a few sets of canisters have been emplaced, a large part of the holes may have to be deserted with no or only few canisters in them.

Stable walls require drilling and deployment muds of higher density than assumed for “normal” conditions, but this is hardly feasible with a maintained high content of smectite clay. The effect on the isolating properties of the deployment mud by the larger cross section that results from extensive rock fall may be very significant. Thus, a drop in dry density by 30 %, which may well take place locally, will make the clay microstructure unstable and apt to consolidate under its own weight. It is expected that the matured clay will have a hydraulic conductivity of at least one order of magnitude higher than of the clay under “normal” conditions over a significant part of the hole length. Since the density under the lastmentioned conditions is already low it is estimated that the concept will not work in an acceptable fashion with the present design if exceptional conditions prevail. Cement filling and redrilling has to be applied but the holes may still not have an adequate cross section or stability.

KBS3

Rock behavior

The most critical issue is that the rock in the floor and roof of the tunnels will be less stable than under “normal” conditions and that substantial spalling and rock fall may take place both in the construction and waste application phases. It is estimated that the construction work needs much more temporary and permanent support in the form of bolting and also that

the design must be made very carefully with respect to the cross section shape, which should be adapted to the prevailing primary rock stresses and to the rock structure. No significant stability problems are foreseen except where 3rd and 2nd order discontinuities are intersected. Here, shotcreting and casting of buttresses may be required and if the spacing of such low-order discontinuities is small, the amount of cement in the repository is estimated to be sufficiently high to make the matter of chemical stability of interacting clay/cement an important issue.

Under the assumed high-stress conditions, creep effects are expected to cause significant time-dependent propagation of natural and blast-induced fractures, by which the hydraulic conductivity of the nearfield rock and the risk of rock fall increase. This calls for early closure of the repository as well as for the use of backfills with a strong supporting ability like dense, bentonite-rich material.

Behavior of buffers and backfills

The high horizontal primary rock stresses and the high primary stress ratio under "exceptional" conditions make the nearfield more conductive as shown in this chapter, and this may imply a higher inflow of water into the deposition holes in the waste application phase than under "normal" conditions. In turn, this may mean that a larger number of potential sites for the holes have to be abandoned and that there will be more need for sealing by "megapacker" grouting. The particularly intense rock disturbance that is expected in the floor by the combined effect of blast-damage and high horizontal stresses can be partly counteracted by giving the tunnel section a suitable shape through which discing can be minimized. Still, a great advantage may be to extend the length of the deposition holes by at least about 3 m. The fraction of the tunnel length that can be used for drilling deposition holes with no interaction with low-order structures will probably drop from around 90% under "normal" conditions to 60-70%.

As to backfilling of the tunnels, the expected higher inflow of water in the application phase probably requires extensive grouting of intersected low-order discontinuities in order to prevent substantial piping and erosion. If the sealing is sufficiently effective, the same backfilling technique can be used as under "normal" conditions but it is felt that the technique to apply sets of precompacted blocks of bentonite or bentonite mixtures and applying shotcrete at regular intervals is advantageous.

VLH

Rock behavior

As in KBS3 tunnels the high tangential stresses in the roof and floor may cause spalling and unstable wedges and cause safety problems. However, the risk is much higher in VLH, especially since the hoop stresses at the periphery of the bored holes are much higher than of blasted KBS3 tunnels. Thus, creep-induced failure that takes place in the course of transportation and application of bentonite blocks and canisters may cause very critical conditions.

The higher frequency of low-order discontinuities and more complex rock structure assumed for "exceptional" than under "normal" conditions makes it more difficult to adapt VLH to the rock structural framework and unexpected interaction of the large holes with low-order structures that have escaped identification is probable. Hence, it can be assumed that at least 2-3 fracture zones of 1st order and 10-20 zones of 2nd order will be intersected by a 4-5 km long VLH. There will be very frequent interaction with 3rd order zones and several zones of this order as well as of low orders will be intersected at a small angle, which may cause considerable rock fall. This means that the fraction of the hole that can be used for locating canisters may be reduced from 70-80 % for "normal" conditions to less than 50 % for "exceptional" conditions.

Behavior of buffers

The larger number of strongly water-bearing discontinuities under "exceptional" than under "normal" conditions means that drainage problems will appear unless very effective grouting has been made. As demonstrated in Chapter 3 and illustrated by Figure 147, the net effect on the inflow of water into grouted tunnels and holes is still far from eliminated because effective sealing means that the water pressure will increase as a result of the tightening. The major beneficial effect is that water will be redistributed from low-order zones to 4th and activated 5th order discontinuities under the higher piezometric conditions that are created. The following difficulties may arise if sealing is not applied or if it is insufficient:

* Even after comprehensive grouting water may enter the space between the canister-embedding clay and the rock at a rate that causes softening in the course of the block application, which may become very difficult

* After application of a canister/clay set, water entering from the rock builds up high water pressures and causes piping and erosion. If the inflow is high, a slurry of clay and water may thereby flow along the bentonite blocks to the front of the set that is being applied, making the whole operation difficult or impossible

5-3.5 Maturation stage

GENERAL

As to the water saturation and homogenization of buffers and backfills, “exceptional” conditions mean that the maturation scenario under “normal” conditions may not be valid because the hydraulic properties of the rock and the groundwater composition may change the performance of the clay materials substantially and, in fact, provide improvements.

BEHAVIOR OF VDH, KBS3 AND VLH

VDH

Even if the canisters and clay can be acceptably located and embedded in the application phase, the heterogeneity and locally very low density of the clay barrier will persist. Despite the possibility one has to fill the holes with cement and redrill where break-outs have occurred, the concept in its present form can hardly yield acceptable conditions for effective support and isolation of the canisters. Still, the plugged part of the holes will perform in a similar way as the KBS3 and VLH, which is acceptable as we will see below.

KBS3

The various processes in the maturation phase are the same as under “normal” conditions but some of them may actually improve the performance of the clay buffer. Thus, the water saturation process will be quicker due to the higher average hydraulic conductivity of the rock mass and the quicker build-up of high piezometric pressures, as well as to the significantly higher electrolyte content as outlined in Chapter 3. With the assumed higher salinity of the

groundwater under "exceptional" conditions, the water saturation rate is expected to be significantly higher than under "normal conditions" as illustrated by Figure 203 earlier in this chapter. Quicker saturation means that salt accumulation will probably be less extensive and that the heat conductivity increases faster than under "normal" conditions.

VLH

The bentonite blocks have to be largely water saturated at the application as under "normal" conditions, which means that there will hardly be any significant difference between the two conditions, except that the higher inflow from the rock under "exceptional" conditions means that the joints between the blocks are quickly filled with water and that no artificial water injection is required in order to bring up the heat conductivity of the buffer. This is of course an advantage.

5-3.6 Heating stage

GENERAL

The main difference between the "normal" and "exceptional" conditions at the heating stage is that groundwater is expected to flow along the deposition holes and tunnels at a higher rate in the latter case, which will cause quicker degradation of the smectites in the buffers. The influence of tectonics, yielding shear that may influence the properties of nearfield rock and affect canisters is expected to be less important than in the long post-heating phase and these processes will therefore be treated in the chapter dealing with this later stage.

BEHAVIOR OF BUFFERS AND BACKFILLS OF VDH, KBS3 AND VLH

VDH

Using the flux data in Table 21 and applying the same hydraulic gradient as for the "normal conditions", i.e. 10^{-2} , one finds that around 100 liters per year pass along the deployment part of the holes. Applying the figure 100 ppm for the potassium concentration in Table 22, one

finds that the larger part of the smectite content may become converted into illite in the heating period. Thereby, shrinkage of the clay will take place due to an almost complete loss in swelling capacity and water may flow freely along the interface between rock and clay. The canister sets will settle in an uncontrolled fashion unless they are self-supporting.

Degradation of the clay in the plugged part of the holes will proceed much slower. Since convection will not bring up very salt water to more than 50-100 m over the boundary between the deployment and plugged parts [35], the smectite is expected to behave as under "normal" conditions and hence be largely intact for hundreds of thousands of years. The risk of significant downward movement of canisters and clay in the deployment zone suggests that a concrete plug should be cast at the lower end of the plugged parts of the holes so that they can maintain their physical and physico/chemical constitutions irrespective of the processes deeper down. This requires that the influence of chemical interaction of the clay and concrete be considered, a matter that is not yet fully understood.

It is clear that the quick degradation of the smectite buffer in the deployment zone underlines the earlier conclusion that VDH will not perform acceptably under "exceptional" conditions. Still, if the sealing function of the plugged zones is considered to be sufficiently good, the quicker clay degradation is of less importance to the overall performance.

KBS3

Considering first the backfilled, blasted tunnels, and assuming that the disturbed zone around their peripheries is characterized by the hydraulic conductivity 10^{-7} m/s, and that the potassium concentration is 70 ppm, one finds that a hydraulic gradient of 10^{-2} may cause conversion of the major part of the montmorillonite component of the backfill to illite in the heating period. This will increase the hydraulic conductivity of a 10/90 bentonite/ballast backfill to around 10^{-7} to 10^{-6} m/s, which makes it the dominant water conductor in a KBS3 repository.

This problem can be reduced by increasing the bentonite content somewhat as illustrated by the fact that, with the described conservative scenario of the smectite degradation rate, a bentonite/ballast ratio of 1/3 will leave at least 50 % of the smectite intact after 2000 years [2]. The net hydraulic conductivity of the backfill at the assumed high electrolyte conductivity of the groundwater will probably not exceed 10^{-10} m/s, which is acceptable. However, the swelling potential will be very strongly reduced at that time and thereby the major part of the rock-supporting ability. It can be maintained only if the bentonite content is increased beyond 30 % and the density increased significantly, which suggests use of highly compacted blocks of bentonite/ballast mixtures provided that the ballast is rather poor in potassium-bearing

minerals. Since the temperature may in fact not be sufficiently high to make the access to potassium a determinant of the conversion process, the degradation may actually be significantly slower in practice.

Considering now the central and lower parts of the KBS3 deposition holes, one finds, by using the flux data in Table 21 and applying the hydraulic gradient 10^{-2} and the potassium concentration 70 ppm, that less than 10% of the montmorillonite content will be converted to illite in the heating phase. In contrast, the larger part of the bentonite in the upper third of the holes, which are assumed to be located in the very pervious tunnel floor, may have degraded to non-expandable minerals. Since the density of the highly compacted bentonite will remain at least at 1.9 g/cm^3 if this is the initial bulk density at complete saturation, the hydraulic conductivity will still be on the order of 10^{-11} m/s , while the swelling potential and self-sealing ability may be strongly reduced. It is estimated that the effect of cementation will be small; no more than 1 % of the total mineral mass may appear in the form of cementing substances and this will not affect the physical properties significantly.

A simple way of compensating for the smectite degradation is to deepen the holes by 3-4 m because this will result in the same insignificant conversion of the buffer from the base of the holes to well over the top of the canisters.

The estimate that the conversion of the smectite in the buffer may be comprehensive in the heating stage is in fact very conservative since its solubility rather than the access to potassium may be a determinant at the relatively low temperature level. A significant part of the smectite content of the bentonite may therefore still be intact in the upper part of the holes at the end of the heating period.

VLH

Applying, as for the other concepts, the hydraulic data in Table 21 and taking the hydraulic gradient as 10^{-2} , one finds that around 500 liters will pass along each hole per year in the heating period, making around 10 000 g of potassium available for illite formation in this period. Assuming the same conservative flow conditions in the nearfield, one finds that about 5 % of the smectite will be converted to illite in the heating period, which means that VLH will serve almost as well as under "normal" conditions with respect to the longevity of the smectite component and to the sealing potential of the buffer in this period.

BEHAVIOR OF SEALS

The large smectite mass with strong self-sealing ability of plugs of dense bentonite means that they will perform well in the larger part of the plugged zone of VDH and in KBS3 and VLH. In contrast, the more intense rock movements and the higher potassium content than under "normal" conditions may cause complete destruction of grouts in the heating period, except for dense grouts in wide fractures.

5-3.7 Post-heating stage

GENERAL

The major difference between "normal" and "exceptional" conditions in a long-term perspective is that tectonics may be much more important under the latter conditions and that the different geochemical conditions will lead to quicker degradation of the clay buffers. As indicated in the discussion of rock stresses under "exceptional" conditions earlier in this chapter, even rather extreme tectonic events are not expected to generate instantaneous shearing of fractures intersecting KBS3 by more than about one millimeter, which is not critical to the mechanical stability of ordinary HLW canisters (Chapter 5-1.4). The present discussion will therefore be confined to the long-term function of the buffers and backfills.

VDH

Almost complete conversion to cemented hydrous mica clay is expected in the deployment zone already in the heating phase. In a longer time perspective, the altered clay will probably remain stable with respect to the mineralogy, as indicated by a number of geological examples [36].

Since the rock stresses are very high and the clay offers practically no support to the rock, large time-dependent deformations may take place by rock moving into the hole and compressing the clay. The fact that its density is low initially in the post-heating stage and its porosity consequently high, suggests that precipitation of various components, brought to the clay by diffusion or flow, will take place. This is expected to cause stiffening and transformation to claystone and probably also tightening and although the brittleness of such material

causes fracturing by tectonics it may perform better as a seal in the long run than in the first few thousand years. In summary, rather little change or possibly even improvement of the physical properties of VDH clay buffers will take place in the post-heating period.

KBS3

A considerable part of the smectite component of 10/90 bentonite/ballast tunnel backfills may be converted to illite in the heating period, but further degradation will be slowed down very much. Hence, significant conversion of the smectite content in a backfill poor in potassium-holding ballast grains is not expected to be completely converted until after 10 000 to 20 000 years.

If a very dense mixture with more bentonite is used for backfilling, like the one considered earlier in this chapter, conversion of the smectite that remains after the heating period, i.e. at least about 50 % of the original amount, will stay virtually intact for several tens of thousands of years and it will perform acceptably - also after significant conversion to illite - for hundreds of thousands of years.

In the deposition holes further degradation beyond the one taking place in the heating period will proceed at a strongly retarded rate. Thus, the rate of dissolution of the remaining smectite is expected to be a determinant of the conversion to illite and of the cementation and it is estimated that the larger part will remain intact for hundreds of thousands of years as under "normal" conditions. The reason for this is that the temperature, which is taken as a determinant of the degradation, is similar in both cases, and that tectonically induced shearing will be insignificant even under "exceptional" conditions, provided that only 4th and higher order discontinuities of moderate extension intersect the holes.

VLH

Since the temperature will be low and of similar magnitude for the KBS3 and VLH concepts, and the potassium content of percolating groundwater is expected to be somewhat lower for VLH, further smectite conversion and cementation in the post-heating stage is expected to be slower in VLH than in the KBS3 deposition holes. Hence, it is estimated that the buffer of VLH will stay largely intact for hundreds of thousands of years.

5-4 Conclusions concerning performance assessment

5-4.1 What can be assessed and how accurately?

The question of how reliably one can assess the performance of repositories naturally depends on how accurately the behavior of the host rock and the engineered barriers can be predicted. It goes without saying that the actual variation in rock structure and rock stress conditions make rock mechanical calculations rather hypothetical. Still, the fairly good agreement between the theoretical exercises using UDEC and 3DEC, and the actually recorded mechanical and hydraulic behavior of the nearfield of a KBS3-type tunnel with simulated canister holes in the Stripa mine, indicates that at least the rock behavior at the application, maturation and heating stages can be foreseen. Prediction of the performance of the host rock in the subsequent very long post-heating period is much more uncertain, especially where glaciation can be expected.

In contrast, the performance of engineered barriers, i.e. clay buffers and waste containers, can be more safely assessed, primarily because the scale-dependence of the rheological properties is much smaller than that of rock, and because nature provides us with several examples of smectitic clays that have sustained more severe conditions than in repositories of the types KBS3 and VLH.

5-4.2 Are there repository concepts that perform acceptably in a 100 000 years long perspective?

GENERAL

The performance analysis of the VDH, KBS3 and VLH concepts shows that the nearfield rock, buffers and backfills behave in different ways in the concepts both in short- and long-term perspectives. Although this may not be of importance for their overall performance, we need to reconsider the criteria on which the design principles were founded before the performance of the respective concepts can be assessed and comparison of them be made.

The main requirement of an underground HLW repository is to retard and minimize release of radionuclides from the nearfield as much as possible and the basic criterion is that the canisters remain virtually tight over a sufficiently long period and that the surrounding barriers, i.e. the clay embedment and the nearfield rock, provide sufficient confinement of possibly escaping radionuclides in the first 100 000 years. Since it is concluded that tectonic events are not critical to the mechanical stability of commonly proposed canisters of concepts like KBS3 and VLH, the entire problem of isolating the waste would be solved by preparing containers that do not corrode in this period, which is in thought to be certified by using the HLW canisters proposed by SKB and various other organizations. However, it is also required that the canisters do not leak through openings originating from the manufacturing processes, primarily welding, and this can not be guaranteed. Hence, the clay embedment of the canisters plays an important role and its barrier function has to be reasonably well preserved in the first 100 000 years. A rough estimate is that at least 50 % of the smectite content must remain intact throughout this period and that cementation must not be excessive, and one concludes that this can be achieved by applying the KBS3 and VLH concepts. These requirements are not fulfilled by the VDH concept but it may still perform acceptably, provided that the plugged part is considered to be the essential sealing component, and that it is accepted that the deployment zone does not retard release of radionuclides at all.

COMPARISON OF THE CONCEPTS VDH, KBS3 AND VLH

Basis of comparison

The ambition to maintain the physical and chemical properties of the rock, buffers and backfills as long as possible, implies that the design and construction techniques should be such that the nearfield rock, the clay buffers and the waste containers undergo as little change as possible in 100 000 years.

From an economic point of view it is valuable if the rock volume hosting the repository can be used as effectively as possible. This can be expressed in terms of what can be called the utilization factor, which is the percentage of the length of depositions holes - or for KBS3 - of the tunnel length, that can be used for locating canisters. This factor depends on the frequency of discontinuities of 1st to 3rd order and strongly water-bearing breaks of 4th order, as well as on the possibility of adapting the deposition holes to the rock structure for minimizing interaction with these types of discontinuities.

We will examine the repository concepts VDH, KBS3 and VLH with respect to the rock conditions, including the utilization factor, and to the buffer longevity and canister tightness.

Rock conditions

The VDH concept implies that both the deployment and plugged holes may interact with long-extending low order discontinuities much more frequently than in the deposition holes of the other concepts. The utilization factor may not be higher than 50 % and there may still be a risk that a number of canisters become located in a critical fashion with respect to discontinuities that may undergo significant shearing.

The KBS3 concept offers a very good possibility of eliminating the risk of interaction of the deposition holes with low-order discontinuities. In fact, the intended position of each individual hole can be investigated so that the holes can be suitably located and given an optimum depth for avoiding intersection of strongly water-bearing fractures over the part where the canister will be located. This can be made with a rather high efficiency as manifested by a utilization factor of 60-70 % even for “exceptional” conditions.

VLH is intermediate to VDH and KBS3 since a significant number of potential shear planes represented by 3rd and lower order discontinuities will be intersected. In contrast with VDH some adaption to the rock structure can be made in the course of the drilling and since detailed mapping of the drilled holes can be made and geophysical methods applied for characterizing the nature and extension of intersected major breaks, the canisters can be located so that the risk of tectonic shearing can almost be eliminated. However, this results in a lower efficiency than what is offered by KBS3. It may be lower than 50 % for “exceptional” conditions.

Groundwater flux along deposition holes

The combination of mechanical damage and disturbance induced by stress release, as well as special effects like wedge-formation results in an axial flux along the deposition holes that is a determinant both of the degradation rate of the canister-embedding clay and of the radionuclide transport capacity of the nearfield rock.

Although VDH offers good net waste isolation properties because of the deep plugged zone, the nearfield rock in the lower part of this zone and in the entire deployment zone may be very permeable due to delayed rock breakage. The axial flux along the deployment zone and the lower 500 m of the plugged zone is expected to be high even under “normal” conditions.

KBS3 yields a very small flux along the major part of the deposition holes under "normal" conditions. Deepening of the holes by a few meters should improve the tightness and create excellent conditions with respect to groundwater flow along the deposition holes even under "exceptional" conditions.

VLH exhibits flow properties of the nearfield rock that are similar to those of KBS3, but the very limited possibility of adapting the TBM-drilled holes to the rock structure means that the risk of formation of interacting sets of rock wedges may yield a somewhat higher axial flux than in the nearfield of KBS3 holes, especially in the strongly anisotropic primary stress field under "exceptional" conditions. The risk of rock fall in the waste application phase is much higher than for KBS3, which makes the VLH concept less attractive.

Groundwater chemistry, temperature

The potassium content of the groundwater and the temperature are the key parameters for clay degradation. They are highest for VDH while KBS3, which represents the lowest temperature level of all the concepts, is assumed to be exposed to the second highest potassium content in the groundwater.

VLH groundwater is expected to have the lowest potassium content but the temperature will be slightly higher than 100°C, i.e. intermediate to that of VDH and KBS3.

Buffers

The required high density of the canister-embedding clay can be obtained for KBS3 and VLH, while the net density of both the deployment zone and the plugged zone of VDH will be lower and hence result in a significantly higher hydraulic conductivity of the canister embedment than for KBS3 and VLH. The risk of widening of the holes by rock fall may result in an even stronger reduction of the clay density for VDH. This may require comprehensive cement-filling and redrilling.

The rate of degradation of the canister-embedding clay is high for VDH due to the high ambient temperature and access to much potassium. A considerable part of the smectite may be converted to illite in the heating period and the associated shrinkage may cause a very significant loss in sealing power of the clay in the deployment zone.

The degradation rate of the canister-embedding clay of KBS3 is sufficiently low to leave the

majority of the the smectite intact for several hundreds of thousands of years or probably more than that even under "exceptional" conditions. The ultimate reaction product is believed to consist of illite (and some chlorite), which serves as a relatively low-permeable seal although with low swelling and sorption potentials, and with a higher ion diffusion transport capacity than the virgin, smectite-rich clay. Cementation effects will further reduce the self-sealing ability.

The canister-embedding clay of VLH is expected to be intact for a longer period of time than for the other concepts because of the slower transformation to non-expanding minerals. However, the somewhat higher temperature than in KBS3 may cause some more cementation.

Canister tightness

From a chemical point of view the canister-embedding smectite clay provides similar conditions for all the concepts. However, they will be different with respect to the accumulation of salt corrodants at the canister surface, which takes place when temperature gradients prevail and the groundwater is salt and the clay only partly water saturated. Since the temperature gradient is highest in VDH and lowest in KBS3, the latter concept is advantageous. The initial high degree of water saturation of the VLH clay implies minimum salt accumulation and this concept hence offers even better properties from this point of view.

From a mechanical point of view the rheological properties of the canister-embedding clay are of major importance for the canister integrity at tectonically induced shearing. VDH does not offer the required properties since the clay may be displaced and yield locally higher and lower density than average. This may lead to load transfer to the canisters and uncontrolled displacement and pressurizing of the canisters. The risk of tectonically induced shearing of canisters is high.

KBS3 canisters can be located so that the risk of rock shearing is practically eliminated but the concept has the disadvantage of upward movement of the upper part of the dense clay in the deposition holes. This generates tension stresses in the canisters, which are firmly held by the clay in the lower part of the holes. This effect can be practically eliminated by deepening the holes by a few meters and compacting the tunnel backfill more effectively than the presently intended method of layerwise compaction and blowing in soft backfill. Depending on the density of the buffer and backfills, the canisters may be displaced upwards by a few millimeters early after application, while there may be some minor settlement in a very long time perspective.

VLH implies a somewhat greater risk of tectonically induced canister shearing than KBS3 but there will not be any relative movement of canisters and embedding clay that can induce critical stresses in the canisters.

Seals

Plugs of dense bentonite will perform well in repositories of the three concepts even under “exceptional” conditions. Grouts will behave similarly but KBS3 with its lower temperatures may provide better conditions for survival than VLH.

Evaluation

Focusing on the long-term canister integrity and long-term performance of the canister-embedding clay as being the two most important functions, one concludes that the KBS3 and VLH concepts are almost equivalent while VDH will not perform acceptably. Still, the very effective sealing function of the plugged zone makes this concept a possible candidate.

Considering the practicality of the waste application procedure and the utilization factor, the picture is somewhat different. The major differences of practical importance concern the need for drainage in the application phase and the handling of the canisters and clay materials as well as the preparation of the latter:

VDH implies remote handling of materials at very large depths for which no technical solution is at hand. The concept has the advantage of not requiring preparation of very large clay blocks or blocks with a high initial degree of water saturation. The utilization factor is low.

KBS3 requires that some and possibly most of the deposition holes be sealed by grouting their uppermost parts. This concept does not require very advanced technology for application of clay blocks and canisters, or for preparing large blocks. The utilization factor is high.

VLH requires advanced technique for transporting clay blocks and canisters over long distances in the rather narrow tunnel. The risk of getting stuck is almost as great as in the VDH concept. There is also a need for preparation of blocks with a high initial degree of water saturation, for which special technique is required. The practical difficulties can possibly be reduced by using small blocks and insertion of prefabricated units of clay/canisters confined

by perforated metal containers but this requires further examination and technical development. The utilization factor is intermediate to that of VDH and KBS3.

Taking both the long-term performance and the conditions at waste application into consideration it appears that KBS3 should be ranked number one of the three investigated concepts. Naturally, other solutions that make use of suitable canisters and clay buffers may serve equally well or even better for safe isolation of HLW. Attractive concepts that need special consideration are VLH versions with a few hundred meters long horizontal or vertical raise-bored deposition holes extending between blasted or TBM-drilled tunnels (cf. Figures 54 and 55).

5-4.3 Aspects on the performance of repositories for hazardous waste other than radioactive material

TIME PERSPECTIVE TO BE CONSIDERED

While contamination of the biosphere with radioactive matter from repositories can be practically eliminated during the limited period in which they represent risks, release of toxic substances from disposed hazardous waste of other sorts will ultimately take place since such waste retains its toxicity over any period of time. As pointed out in the introductory part of this book the principle of “absolute confinement” has to be given up for this reason and also for economical reasons, and a proper design basis should instead be to isolate such waste in a fashion that limits the release to yield concentrations of toxic elements that are below prescribed levels. The design work of chemical waste repositories must naturally comprise the same performance analyses as repositories for radioactive products but since groundwater contamination has to be and should be accepted, even greater emphasis has to be put on geohydrological analyses than in the case of repositories for HLW. This makes it necessary to consider topographic features in greater detail and for the northern hemisphere it implies that the issue of future glaciations should be more thoroughly investigated. Probable and possible climatic changes, implying very high annual precipitation or extreme draught, need to be taken into account.

The hydraulic gradients in a repository are controlled by the regional and local topographies and by the hydraulic conductivity of the structural units that make up the regional and local parts of the earth crust, as well as by the precipitation and the groundwater density. They can all be considered in performing flow calculations for the present conditions using available porous medium and discrete fracture flow models, which are all estimated to yield reasonably reliable results for areas where stable conditions with respect to rock structure, topography and climate are expected. Still, for Northern Europe, Asia and America, future glaciations, which are expected to begin within a few thousand years from now and which may have the moderate impact on the technical performance of deeply located repositories described earlier in this chapter, are expected to have a very strong effect on the regional and local flow patterns because of dramatic changes in topography and consequently in regional hydraulic gradients. Naturally, inhabitants will leave the area already at the stage when permafrost appears and no settlers will be around until after very long periods of time: major glaciations are estimated to last for about 100 000 years and since effective confinement of HLW will not be required after this period of time, the regional and local groundwater flow conditions after deglaciation are of almost no concern. This is not the case for areas with repositories hosting high-risk toxic waste because this sort of waste retains its toxicity. While it is required, primarily for psychological reasons, that HLW repositories are located at a considerable depth, one could in fact imagine location of repositories for highly toxic waste at shallow depth since advancing glaciers will disintegrate the waste and lead to dispersion over large areas at deglaciation and thereby to very low concentrations in the recipients. However, the uncertainty whether glaciation will take place at all and to what extension, both geographically and with respect to time, calls for deeply located repositories for all sorts of very hazardous waste.

DESIGN PRINCIPLES

Naturally, repositories of the types considered in this chapter will, in principle, perform in the same fashion irrespective of the waste composition and one may well consider application of any of the concepts also for disposal of very hazardous chemical or biological waste products. Since such sorts of waste do not usually produce heat, the problem of safe long-term isolation from the biosphere is a simpler issue and it would be natural to consider less sophisticated repository concepts with clay-embedded waste canisters in large tunnels or rooms in abandoned parts of mines or extending from such mines. Also, the tightness of the containers may well be much lower than in the case of radioactive waste and sufficient only to keep the waste confined in the transport and application phases. Still, the same principle of using low-permeable waste canister embedment is required and this has the following important implications:

- * Low temperatures mean that the dissolution of smectites and conversion to non-expanding minerals is insignificant provided that pH is in the interval 7-10 [37]. This means that relatively smectite-poor backfills, like low-quality commercial bentonites or smectitic soils available in the construction area, can be used
- * If the containment leaks, water enters and the waste dissolves and migrates in ionic form into the backfill and further into the surrounding rock. Many chemical wastes are much more easily dissolved than nuclear fuel or reprocessed reactor wastes and if the leakage is comprehensive due to poor containment the concentration of toxic elements in the porewater may become very high soon after the waste emplacement. If the smectite component is initially saturated with sodium, which is preferable from various points of view, and its density low, microstructural rearrangement will take place if the toxic substance consists of cadmium, mercury, arsenic or copper because of cation exchange, and this may lead to a strong increase in hydraulic conductivity and an almost complete loss in swelling and self-sealing ability and hence a significant loss in waste-isolating capacity
- * As in the case of repositories for radioactive waste, a significant increase in hydraulic conductivity of smectite-poor backfills and a reduction in swelling and self-sealing capacity may take place by ion exchange from sodium to calcium and magnesium if the groundwater is rich in these element and the density low. Such increase also takes place if the groundwater has a high electrolyte content irrespective of the ionic composition except at high densities.

Since the change in physical properties due to ion-exchange may imply that smectite-poor backfills of low density may not be able to swell and self-seal it is necessary to prepare and apply them such that the homogeneity is high and the filling complete. From a practical point of view it is preferable to use a fairly high smectite content and to compact the backfill to a high density. In turn, this requires that the waste confinement is sufficiently strong and in practice it is naturally a matter of optimizing the composition of the various components.

The production, accumulation and migration of gas caused by corrosion of waste embedment of steel or emanating from organic material needs to be considered since it may affect both waste containers and clay-based embedments. The matter is of particular importance in repositories for radioactive waste. We will touch on the subject in Chapter 6.

5-4.4 Safety assessment

RELEASE AND TRANSPORT OF HAZARDEOUS SUBSTANCES

As in the case of repository performance in the waste application and clay barrier maturation phases, as well as in the post-heating period, the matter of release and transport of hazardous elements emanating from deeply buried waste has been studied almost exclusively in the comprehensive R&D activities for safe disposal of radioactive products. They have indicated various different ways of predicting the migration of long-lived radionuclides that can also be applied to disposal of hazardous chemical waste. We will not go deep into this matter but indicate possible methods for safety assessment.

METHODOLOGY

With smectite clay embedding waste containers, the output of released hazardous elements to the geosphere is limited by the very low hydraulic conductivity of the clay. Solute transport will occur predominantly by diffusion, and sorption yields very low diffusivities of many species. We have seen in Chapter 3 how water flowing along the rock/clay interface picks up elements released from the waste container, assuming that the concentration at its periphery is known. Naturally, this concentration is in fact controlled by the solubility of the waste, i.e. for HLW, by the solubility of glass of vitrified waste or - in countries like Sweden - of the uranium rods of burnt-out fuel. For hazardous chemical waste the same principle is naturally valid, which means that the groundwater chemistry - particularly pH - is the controlling parameter for both types.

TRANSPORT

The migration of hazardous elements released from the dissolving waste and transported through the nearfield naturally depends on the character of the host rock. For modelling purposes one can divide its porosity into one part where flow takes place with advection and hydrodynamic dispersion, and another part termed matrix porosity with diffusion only. The firstmentioned is related to discontinuities of 1st to 4th order, while the second concerns rock with only higher order discontinuities. Hence, adequate modelling requires specification of the rock structure.

There are two approaches to assessing element transport through the farfield, i.e. steady-state analytical solution and numerical analyses using codes of various types. The first mentioned can be used for assessing the function of the geosphere for the condition of constant output concentration, while numerical analyses give a more detailed picture of the function and includes - for radioactive waste - the decay in radioactivity [38]. Several of the numerical codes used for the groundwater flow calculations have been applied and tested in international projects.

MODELLING FOR SAFETY ASSESSMENT

For multibarrier concepts with the waste matrix, waste containers, clay embedments, and host rock operating as barriers, there are various codes in use, which allow for variation of the characteristic parameters and which yields the concentration of hazardous elements emanating from the waste and having passed through the barriers and reached the biosphere. More or less comprehensive codes are in use for various purposes like the one applied to SFR and mentioned in Chapter 1.

The Japanese code GSRW serves as an example of tools that incorporate all major transport and retardation mechanisms in a repository and it is expected to be applicable also to toxic chemical waste of any type [39]. It is composed of three interlinked models, a source term, a geosphere or rock model, and a biosphere model. The source term describes the concentration of hazardous elements as a function of the solubility of its specific chemical form at the interface of the waste and clay barrier. The geosphere model is based on analytical or numerical solutions of a mass transport equation involving advection, dispersion, sorption and decay of radioactivity. The biosphere model assesses the transport of the elements in the biosphere and the resulting consequences to man.

5-5 References

- 1 Pusch,R. Rock mechanics on a geological base. Elsevier Publ. Co. (In press)
- 2 Pusch,R. and Börgesson,L. Performance assessment of bentonite clay barrier in three repository concepts: VDH, KBS3 and VLH. PASS project on Alternative Systems Study. SKB

Technical Report TR 92-40, SKB, Stockholm, 1992

3 Pusch,R. and Hökmark,H. Characterization of nearfield rock - A basis for comparison of repository concepts. SKB Technical Report TR 92-06, SKB, Stockholm, 1992

4 Kühnel,R.A. and Van der Gaast,S.J. Formation of clay minerals by mechanochemical reaction during grinding of basalt under water. *Applied Clay Science*, Vol.4, 1989 (pp.295-305)

5 Pusch,R. and Karnland,O. Physical and mineralogical changes in mechanically disintegrated chlorite. SKB Arbetsrapport AR 92-70, SKB, Stockholm, 1992

6 Landström,O. and Tullborg,E.L. Results from a geochemical study of Zone NE-1, based on samples from the Äspö tunnel and drillcore KAS 16 (395 to 451 m). Äspölaboratoriet, Progress Report 25-93-01. SKB, Stockholm, 1993

7 NEDRA. Characterization of crystalline rocks. SKB Technical Report TR 92-39, SKB, Stockholm, 1992

8 Pusch,R., Börgesson,L. and Ramqvist,G. Final Report of the Buffer Mass Test - Volume II: test results. Stripa Project, Technical Report TR 85-12, SKB, Stockholm, 1985

9 Winterkorn,H.F. Mass transport phenomenon in moist porous systems as viewed from thermodynamics of irreversible processes. Water and its conduction in soils. Highw. Res. Board, Spec. Report 40, Nat. Acad. of Sciences, Washington D.C., 1958

10 Börgesson,L. Water flow and swelling pressure in non-saturated bentonite-based clay barriers. *Engineering Geology*, Vol.21, 1985 (pp.229-237)

11 Couture,R.A. Steam rapidly reduces the swelling capacity of bentonite. *Nature*, Vol. 318, No.6041, 1985 (pp.50-52)

12 Börgesson,L. Final Report on the Pilot Settlement Test in Stripa. SKB Arbetsrapport AR 92-73, SKB, Stockholm, 1992

13 Eloranta,P., Sinonen,A. and Johansson,E. Creep in crystalline rock with application to high level nuclear waste repository. Report YJT-92-13, Nuclear Waste Commission of Finnish Power Companies, 1992

14 Carter,N.L. and Gnirk,P.F. Immobilized Fuel and Reprocessing Waste Values: Long-term creep rupture - Review and Assessment, TR-56, Scientific Doc. Distr. Office, AECL, 1980

15 Pusch,R. and Hökmark,H. Mechanisms and Consequences of creep in the nearfield of

- KBS3 tunnels and canister holes in granitic rock. SKB Technical Report TR 92-10, SKB, Stockholm, 1992
- 16 Pusch,R. Mechanisms and consequences of creep in crystalline rock. *Comprehensive Rock Engineering*, Vol.1, Pergamon Press, 1992
- 17 Slunga,R. Earthquake mechanisms in northern Sweden Oct. 1987-Apr.1988. SKB Technical Report TR 89-28, SKB, Stockholm, 1989
- 18 Röshoff,K. Characterization of the morphology, basement rock and tectonics in Sweden. SKB Technical Report TR 89-03, SKB, Stockholm, 1989
- 19 Pusch,R. and Karnland,O. Hydrothermal effects on montmorillonite, A preliminary study. SKB Technical Report TR 88-15, SKB, Stockholm, 1988
- 20 Fritz,B. Etude thermodynamique et modélisation des réactions hydrothermales et diagénétiques. *Sciences Géologiques*, Mem. No.65, Université Louis Pasteur de Strasbourg. ISSN 0302-2684, 1981
- 21 Pusch,R. and Güven,N. Electron microscopic examination of hydrothermally treated bentonite clay. *Artificial Clay Barriers for High Level Radioactive Waste Repositories. Engineering Geology*, Volume 28, Nos. 3-4, Special Issue, Edit. R.Pusch, 1990 (pp.303-314)
- 22 Pusch,R., Karnland,O., Hökmark,H., Sandén,T. and Börgesson,L. Final report of the Rock Sealing Project - Sealing properties and longevity of smectitic clay grouts. Stripa Project, Technical Report TR 91-30, SKB, Stockholm, 1991
- 23 Pusch,R., Karnland,O., Lajudie,A. and Decarreau,A. MX 80 clay exposed to high temperatures and gamma radiation. SKB Technical Report TR 93-03, SKB, Stockholm, 1993
- 24 Pytte,A.M. The kinetics of the smectite to illite reaction in contact metamorphic shales. M.A. Thesis, Dartmouth College, Hanover, N.H., 1982
- 25 Pusch,R. Stability of deep-sited smectite minerals in crystalline rock - chemical aspects. SKBF/KBS Technical Report TR 83-16, SKB, Stockholm, 1983
- 26 Müller-Vonmoos,M., Kahr,G., Bucher,F. and Madsen,F.T. Investigations of the metabentonites aimed at assessing the long-term stability of bentonites under repository conditions. *Artificial Clay Barriers for High Level Radioactive Waste Repositories. Engineering Geology*, Vol.28, Nos.3-4, Special Issue, Edit. R.Pusch, 1990 (pp.269-280)

- 27 Pusch,R., Börjesson,L. and Erlström,M. Alteration of isolating properties of dense smectite clay in repository environments as exemplified by seven pre-Quaternary clays. SKB Technical Report TR 87-29, SKB, Stockholm, 1987
- 28 Skinner,B.J. and Porter,S.C. Physical Geology. J.Wiley and Sons, 1987 (750 pp)
- 29 Pusch,R. and Karnland,O. Geological evidence of smectite longevity. The Sardinian and Gotland cases. SKB Technical Report TR 88-26, 1988
- 30 Martin,C.D. and Simmons,G.R. The underground research laboratory. News Journal, Int. Soc. Rock Mech., Vol.1, No.1, 1992
- 31 Pusch,R., Börjesson,L. and Knutsson,S. Origin of silty fracture fillings in crystalline bedrock. Geol. Fören. Sthlm. Förh., Vol.112, Pt.3, 1990 (pp. 209-213)
- 32 Shen,B. and Stephansson,O. 3DEC mechanical and thermo-mechanical analysis of glaciation and thermal loading of a waste repository. SKI Technical Report TR 90:3, SKI, Stockholm, 1990
- 33 Vik,G. and Barton,N. Stage I Joint characterization and Stage II Preliminary prediction using small core samples. Stripa Project, Technical Report TR 88-08, SKB, Stockholm, 1988
- 34 Hökmark,H. Numerical analysis of the nearfield rock in VLH and KBS repositories applying a general rock structure model. SKB Arbetsrapport AR 92-72, SKB, Stockholm, 1992
- 35 Claesson,J. Buoyancy flow in fractured rock with a salt gradient in the groundwater - A second study. SKB Technical Report TR 92-41, SKB, Stockholm, 1992
- 36 Pusch,R. Investigations of a clay profile on southern Gotland of presumed value for documentation of smectite/illite conversion. SKB Arbetsrapport AR 92-74, SKB, Stockholm, 1992
- 37 Correns,C.W. Einführung in die Mineralogie. Springer Verlag, Berlin, 1949
- 38 Zuidema,P., McKinley,I.G., Smith,P.A., Curti,E., Klos,R., Hugi,M. and Niemeyer,M. Kristalline-I performance assessment: First Results. Proc. Int. Conf. Nucl. Waste Management and Environmental Remediation, Vol 1, Amer. Soc. Mech. Eng., Prague, Sept.5-11, 1993
- 39 Kimura,H. and Takahashi,T. A generic safety assessment code for geologic disposal of radioactive waste: GSRW computer code user's manual, JA ER1-N92-161. Japan Atomic

Energy Research Institute, 1992

Chapter

6 *Disposal of radioactive waste*

6-1 Introduction

The main reason for referring to highly radioactive products in the preceding chapters and for taking repositories for disposal of such wastes as examples throughout this book is that they represent high-risk chemical products that can dissolve and release dangerous species and that high-level waste represents heat-producing material of any sort. In doing so, we have, however, not considered an additional unique property of radioactive waste that causes problems, namely the effects of radiation, and this requires some further consideration. Thus, one difficulty is that HLW waste produces γ radiation to an extent that requires special shielding and remote handling of the canisters in the transportation and application phases, and another one is the influence of α and γ radiation on canister-embedding clay. This latter issue, which brings up the question of gas transport through the clay and further through the rock, will be touched on in this chapter.

6-2 Influence of γ radiation on canister-embedding clay buffers

6-2.1 General

A number of laboratory experiments have indicated that γ radiation has two major effects, i.e. radiolysis of the porewater, by which the radical OH and various other products like negatively charged O_2^- are produced, and breakdown of the crystal lattice of clay minerals. The first process yields decomposition of the porewater that can result in gas accumulation at the surface of HLW canisters, while the second mechanism yields mechanical disintegration of the

crystallites by which the average particle size is reduced and the crystal lattice fragmented. The impact of strong radiation does not necessarily cause a dramatic loss in sealing power of the clay buffer but it has to be considered since the physical properties like expandability and self-healing may be significantly changed by radiation emanating from HLW. In practice, the issue of gas formation is controlled by the dose rate rather than the total dose and if the latter is sufficiently low, the various dissolved decomposition products will diffuse through the clay without producing any gas. This can be obtained by keeping the amount of HLW per canister relatively low as for the KBS3 concept, according to which there are 12 BWR elements of burnt-out fuel each with 180 kg uranium in the 60-100 fuel rods (Figure 225). Intermediate storage for 40 years will lead to reduction of the initial activity by 90 %.

Applying this principle, gas production will be insignificant and only caused by steel corrosion, and we will therefore confine the description of gas formation to the production of hydrogen in gaseous form from corroding steel canisters and from leaking canisters of copper-shielded steel.

6-2.2 Effects of gas formation and migration through smectite clay

GENERAL

The production of hydrogen in gaseous form is initiated early after application of the waste canisters and it may retard the moistening of clay buffer that is not water saturated from start. If the rate of gas formation is low and the porewater pressure high due to quick build-up of high piezometric pressures in the surrounding rock, hydrogen gas may dissolve and migrate through the clay in ionic or molecular form, having practically no impact on the microstructure of the clay and the physical properties. However, it is anticipated that gas will be formed close to the canisters, particularly those made of steel, and that this may yield pressurized gas bubbles from which protuberances grow when the gas pressure has become sufficiently high. It has been feared that such finger-like migration of pressurized gas may cause permanent microstructural changes in the form of passages which allow for two-phase flow - gas out and water in - and we will examine this matter in this chapter. Another risk is that gas migration may cause displacement of contaminated water all the way to the biosphere.

THE CONCEPT OF CRITICAL GAS PRESSURE

Laboratory experiments with hydrogen and nitrogen gas have demonstrated that gas penetra-

tes smectite clay buffers and backfills when a certain critical gas pressure has developed [1,2]. This pressure, which can be understood as capillary pressure, is related to the swelling pressure, which means that it is on the order of 10-20 MPa for montmorillonite-rich clay with a bulk density of $2.1\text{--}2.3\text{ g/cm}^3$ at complete water saturation, and only a few hundred kPa when the bulk density is below $1.6\text{--}1.8\text{ g/cm}^3$, and even lower for backfills with low contents of smectite clay.

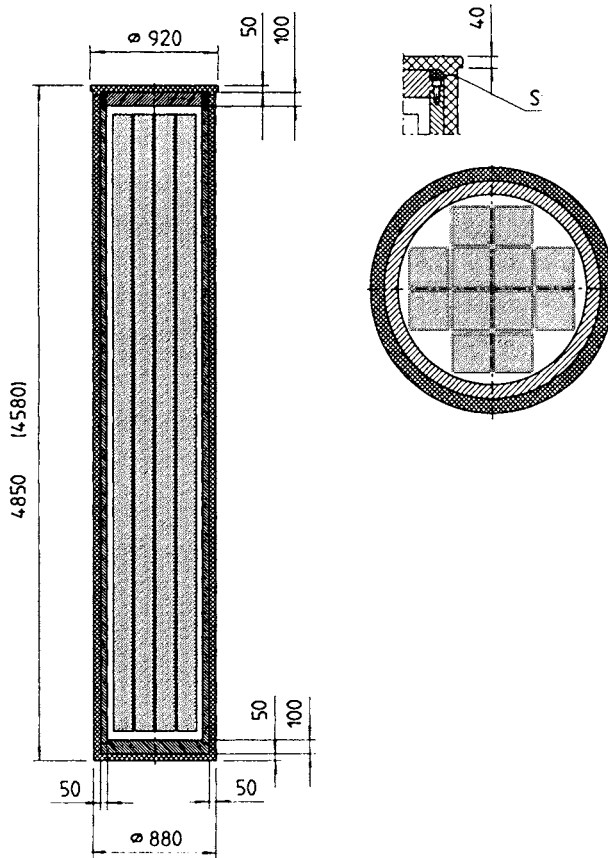


Figure 225 Example of HLW canister intended for KBS3 repositories (SKB). The canister is of hollow type with an inner steel tube surrounded by copper. Dimensions are in millimeters. S denotes welding

The porewater pressure is of great importance as demonstrated by the effect of applying backpressures in the experiments referred to. Thus, gas makes its way through the clay when the gas pressure is equal to the sum of the critical pressure and the porewater pressure, which is equal to the prevailing piezometric pressure when complete restoration of the hydraulic regime has ultimately been reached after repository closure.

MECHANISMS INVOLVED IN GAS MIGRATION

Careful determination of the degree of water saturation and direct observation of the distribution of gas breakthrough spots in clay samples of different size, and application of microscopy have shown that pressurized gas does not penetrate uniformly and “front-wise” through clays, but that it makes its way through a very small number of passages and continues to do so if the pressure is maintained. This means that a very small part of the porewater is displaced to yield breakthrough and that very little contaminated water will leave the clay buffer, leaving gas channels of finger-like type in it. It is not known if widening of the passages and emptying of adjacent voids is caused if continuous gas percolation persists, but this would require both that the gas conductivity of the surrounding rock is significantly higher than that of the clay and that the gas pressure is maintained.

The first condition is certainly valid for the KBS3 repository concept with blasted tunnels with their highly permeable floors and with the high probability of intersection of tunnels and low-order fracture zones, and it is assumed to be valid also for the VLH concept. The matter of a constant high gas pressure has to do with the gas production rate. In practice, it is anticipated that it will be irregular and retarded in many cases, which means that gas will probably penetrate in the form of intermittently moving trains of gas bubbles that tends to stagnate with time. Subsequent dissolution leads to a decrease in size of the bubbles, by which the clay microstructure is restored if the density is not very low, i.e. less than about $1.2\text{--}1.4\text{ g/cm}^3$, and migration by diffusion of the dissolved gas then proceeds at least at large depths. Higher up in the rock mass where the piezometric pressures are lower, dissolved hydrogen will again be transformed to gaseous form and form bubbles in rock fractures.

The heterogeneous gas penetration pattern in the dense canister-embedding clay buffer can be visualized by applying the clay microstructural models referred to in the discussion of the hydraulic conductivity in Chapter 3 [3]. Thus, the distribution of continuous voids of larger width in smectite clay buffers of various densities shown in Figures 226 and 227 is in reasonable agreement with the recorded displacement of porewater at breakthrough, and with the observation that only a few passages, i.e. the largest ones in the respective model, let gas

through. The structural heterogeneity of backfills consisting of mixtures of ballast material and relatively little clay, which is caused by the preparation and compaction processes, results in a stronger scale-dependence of the microstructural features. Thus, a number of even wider voids appear in larger cross section areas, yielding critical gas pressures of only some ten kilopascals in 10/90 bentonite/sand mixtures.

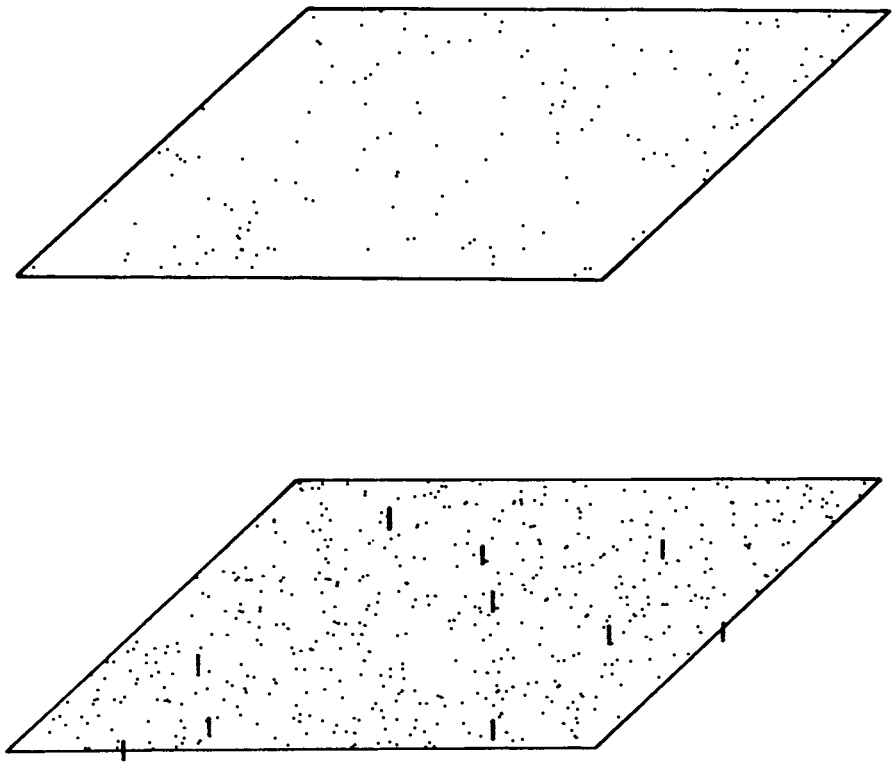


Figure 226 Theoretical distribution of continuous voids of different size over a 250x250 μm cross section in Na bentonite clay. Upper: Bulk density 2.13 g/cm^3 . Lower: Bulk density 1.85 g/cm^3 . Dots represent 1-5 μm wide and short bars 5-20 μm wide voids filled with soft clay gel [3]

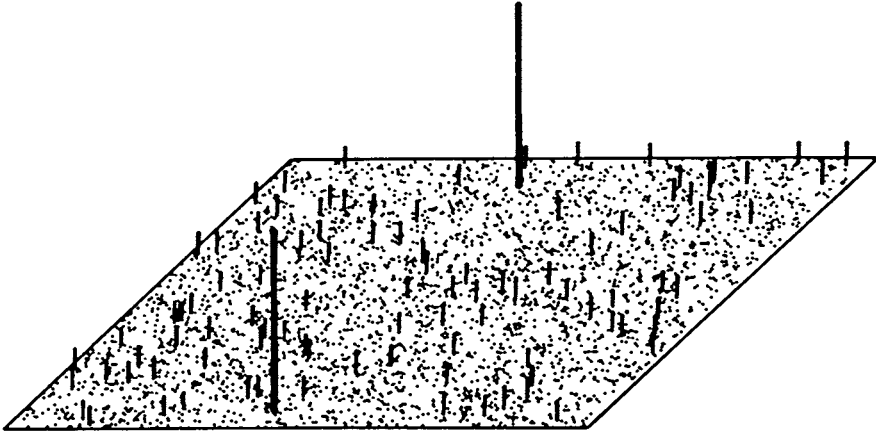


Figure 227 Theoretical distribution of continuous voids of different size over a 250x250 μm cross section in Na bentonite clay with a bulk density of 1.57 g/cm^3 . Dots and short bars are defined in Figure 227, long bars represent 20-50 μm wide voids filled with soft clay gel [3]

6-2.3 Degradation of minerals

Early estimates have indicated that strong γ radiation has a degrading effect on clay minerals [4] but only recently the type of influence and net effect on the physical properties of smectite clays has been more thoroughly investigated. A recent study which gave much information on this issue was performed in a joint venture of SKB and CEA and we will refer to it here as

the SKB/CEA project in summarizing the major outcome of it.

THE SKB/CEA PROJECT

The aim of the study was to investigate the effect of γ radiation on the constitution and physical properties of montmorillonite-rich bentonite [5]. It comprised an experiment in which a clay sample with a density of 2.05 g/cm^3 after complete saturation with weakly brackish "Allard" water (dry density of 1.65 g/cm^3), was exposed to γ radiation over 1 year, corresponding to a total dose of slightly more than $3 \times 10^7 \text{ Gy}$. The test arrangement, which is illustrated in Figure 228, was of "open hydrothermal" type with an applied piezometric pressure of 1.5 MPa and with the sample confined in a cylindrical steel tube that was closed at one end and equipped with a porous steel filter at the other. The closed end consisted of a steel plate, which was exposed to radiation from the outside by a ^{60}Co radiation source and held at 130°C throughout the test. The filter end was maintained at 90°C and the experiment - termed IR below - carried out such that the temperature gradient remained constant at slightly less than 6°C/cm over the 7 cm long sample. For distinguishing between the heat and radiation effects, a second equally long experiment was conducted without radiation (NON-IR) and a third one was also made with neither radiation or heating (REF).

"Allard" water is an artificial reference groundwater with sodium as major cation, prepared to represent rock groundwater at a depth down to a few hundred meters. The clay was a commercial Wyoming bentonite with a smectite content of 70 % or slightly higher and with sodium as major adsorbed cation in the natural condition. The adsorbed dose rate was 3972 Gy/h at the clay/steel interface, around 700 Gy/h at mid-length and 456 Gy/h at the clay/filter interface of outer end.

The evaluation of the experiments comprised mineralogical analyses using X-ray diffraction (XRD) and electron microscopy for morphological investigations and for semi-quantitative element analysis (EDX), chemical analyses primarily by use of atomic absorption spectroscopy (AAS) and infrared spectrometry (IR), determination of the cation exchange capacity, and physical testing for determination of the hydraulic conductivity, i.e. the most essential parameter, and of the rheological properties as represented by the swelling pressure and the creep behavior. As described in Chapters 3 and 5 the swelling pressure is a measure of the smectite content and the degree of cementation, while the creep behavior is a practical measure of how extensive the cementation is.

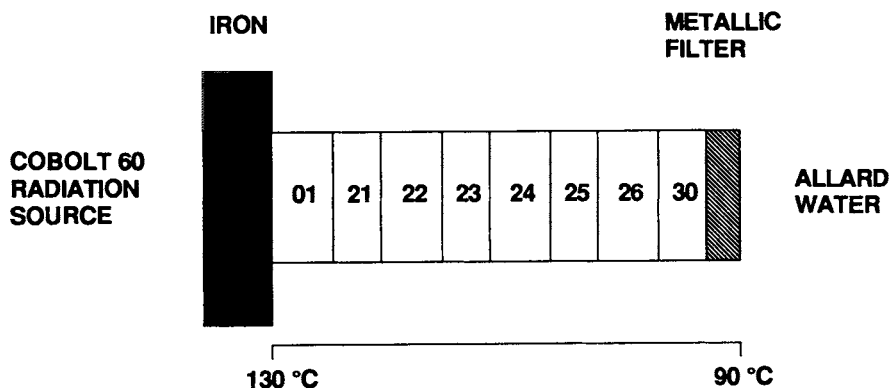


Figure 228 Schematic test arrangement of the IR experiment [5]. The figures 01, 21 etc denote samples cut for the various laboratory tests

INFLUENCE OF HEATING AND RADIATION ON THE MINERALOGY

The reference sample, which had not been exposed to heating or radiation, had retained its greyish color except at the contacts with the steel components where it had changed to orange/yellow within about 1 mm distance from the contacts. The same changes had occurred also in the NON-IR sample. XRD data revealed that the virgin clay consisted of the dioctahedral smectite species montmorillonite, being the dominant mineral, quartz, Na-Ca feldspars, calcite, iron sulphide and oxide, and the amorphous silica mineral opal.

The sample that had been exposed to both radiation and heating (IR) and the one exposed only to heating (NON-IR) both had the large majority of their smectite contents preserved. The major changes from the original composition were that calcite had disappeared and that a large part of the feldspars had been lost, while calcium sulphate (anhydrite) and magnesium sulphate (hexahydrate) had formed close to the hottest end of the samples. The amount of quartz had also increased at high temperatures while there was insignificant conversion to illite, which can be explained by the low concentration of potassium in the solution (7 ppm).

A change of the biggest montmorillonite XRD peak was interpreted as formation of chlorite-type minerals, possibly in the form of interlamellar establishment of iron hydroxide in the smectite stacks. Figure 229 illustrates the major differences between the REF and IR spectra, while Figure 230 shows the distribution of the changes along the sample.

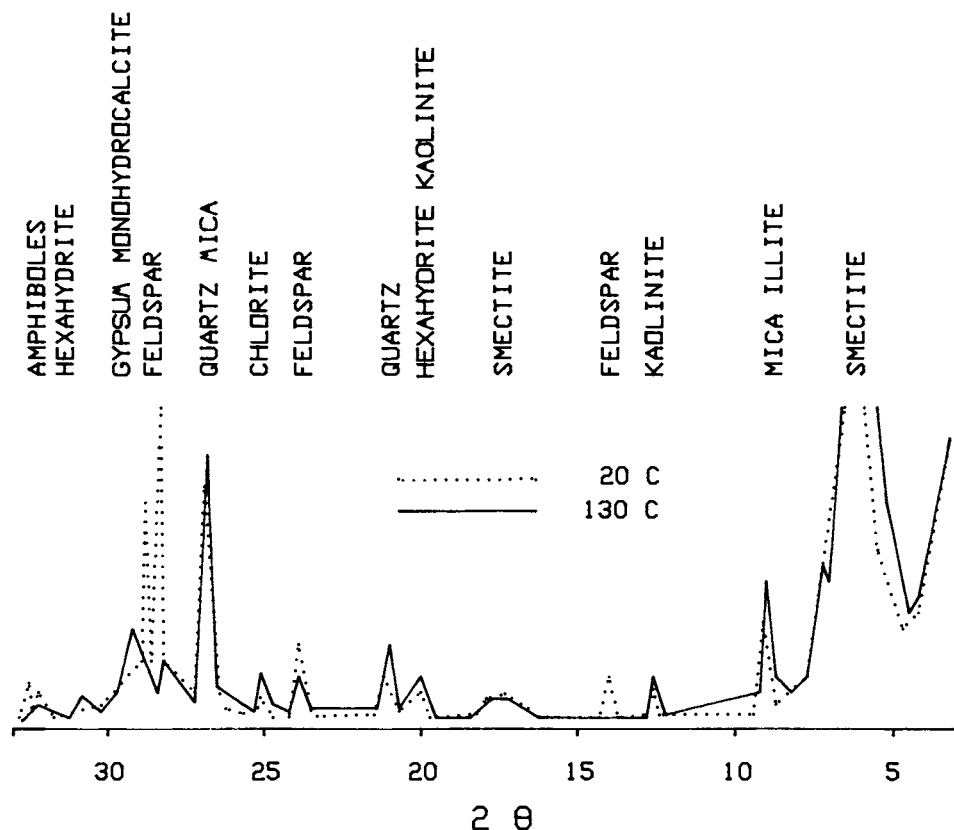


Figure 229 Schematic diffractograms of the REF specimen 00 (20°C) and the most heated IR specimen 01 (130°C) [5]

The major interpreted changes from the XRD analyses are summarized in Table 23. The results of the chemical analyses were in complete agreement with the data in this table and they also showed that the amount of Fe_2O_3 had increased strongly close to the hot steel in the NON-IR sample and that it had increased throughout the IR sample. This indicates that the

irradiation speeded up the clay/steel reaction but that it had no particular degrading effect. An important finding was that the cation exchange capacity, which was 99 meq/100 g of the reference material, remained almost constant throughout the irradiated sample. The value recorded for specimen 01 (130°C) was 93 meq/100 g.

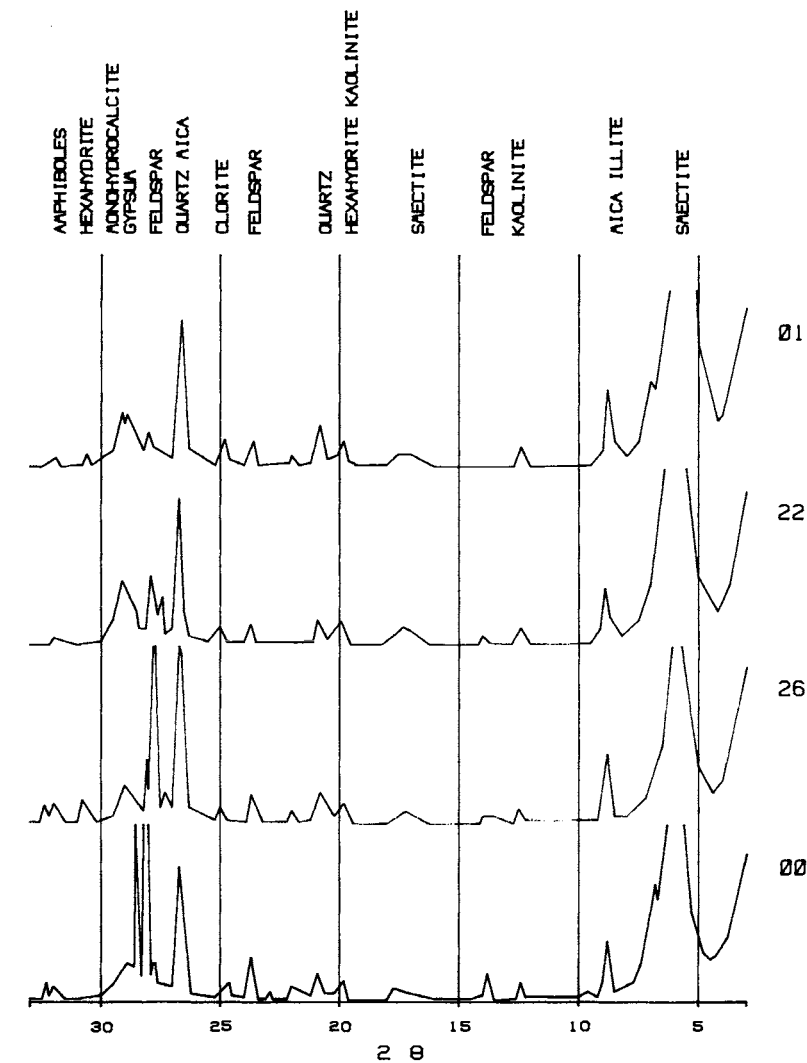


Figure 230 Diffractograms of all IR samples [5]

Table 23 Major changes mineralogical changes of IR samples as evaluated from XRD spectra. Specimen numbers are those in Figure 228 [5]

Specimen No	Reduction	Increase	Degree of change
01 (130°C)	Feldspars		Strong
01		Chlorite-type	Medium
01		10 Å minerals	Weak
01		Anhydrite (+ gypsum)	Strong
01		Hexahydrate	Medium
22 (115°C)	Feldspars		Strong
22		Chlorite-type	Weak
22		10 Å minerals	Weak
22		Anhydrite (+ gypsum)	Strong
22		Quartz	Weak
26 (95°C)	Feldspars		Medium
26		Anhydrite	Weak
26		Quartz	Weak

IR and NON-IR samples showed the same major changes, which demonstrates that the radiation did not have any significant effect on the thermodynamic processes. The observed accumulation of sulphates at the hottest end of the samples, which results from the reduced solubility of these minerals at increased temperature, is in agreement with the general alteration model described in Chapters 3 and 5.

The electron microscopy demonstrated that the typical microstructural features of dense smectite clay, i.e. stacks of flakes separated by voids occupied by softer clay gels, were preserved and the homogenization of the microstructure that is known to result from hydrother-

mal treatment under fully water saturated conditions at temperatures below 150°C of highly compacted smectite-rich clay was also identified.

The main conclusion from the mineralogical and chemical analyses was that the combination of strong γ radiation and heating up to 130°C under repository-like conditions with electrolyte-poor groundwater only caused insignificant alteration of the smectite.

INFLUENCE OF HEATING AND RADIATION ON THE PHYSICAL PROPERTIES

The hydraulic conductivity remained almost unchanged as shown by Table 24, which is in agreement with the observation that the microstructure remained largely unchanged by the irradiation and heating. A small change in swelling ability was noticed as demonstrated by the diagram in Figure 231, which shows the expansion of bulk samples by reducing the confining pressure from 6 MPa, i.e. the swelling pressure of the REF sample at 2.05 g/cm³ bulk density, to 5 MPa. However, the differences are more due to the influence of friction resistance and the relatively low accuracy in recording changes in height of thin samples than to actual changes in expandability.

The creep tests were made by using shear boxes and evaluation of the material properties by use of a FEM-derived stress/strain model [6]. As indicated by the diagrams in Figure 232 the creep curves were smooth with no sign of significant cementation. The only clear difference was a somewhat smaller creep strain of the IR sample 01 (130°C) than of the REF sample, which could be interpreted as slight strengthening of the irradiated and heated sample by comparing the evaluated creep parameter values. It is probable that iron stemming from the irradiated steel plate at the hot end contributed to the strengthening by replacing some of the initially adsorbed sodium by iron and it is also possible that some slight cementation took place by formation of iron and silicious compounds.

In summary, it is clear that the results of the physical testing reconfirm the conclusion from the mineralogical and chemical analyses, namely that the clay underwent insignificant changes in the 1 year long experiment. Considering that the radiation dose rate to which the canister-embedding clay is exposed in repositories of KBS3-type is not too different from what it was in the tests, it is expected that the clay will not be significantly harmed by γ radiation. The long duration of the heating period in a real repository of this type may lead to more cementation although the temperature gradient will be much lower than in the SKB/CEA study.

Table 24 Hydraulic conductivity of IR samples [5]

Specimen No	Temp. °C	Distance from irradiated, hot iron plate, cm	Hydraulic conductivity, m/s
00	20	0	1.7×10^{-13}
01	130	0.5	2.9×10^{-13}
22	115	2.5	1.1×10^{-13}
26	95	5.7	2.6×10^{-13}

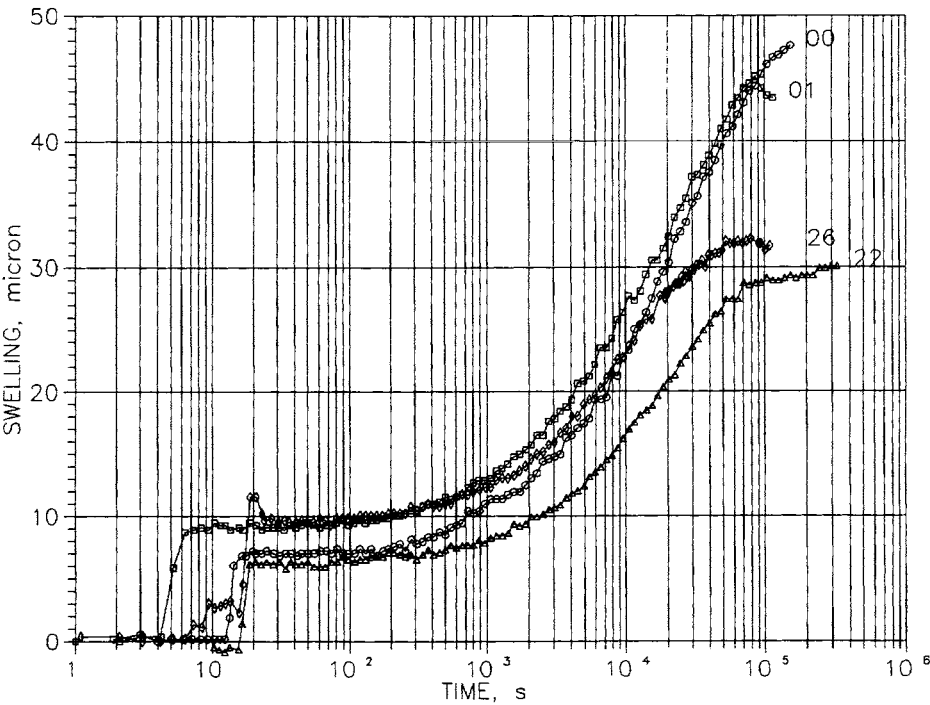


Figure 231 Swelling behavior of the IR samples as recorded by reducing the confining pressure from 6 to 5 MPa [5]

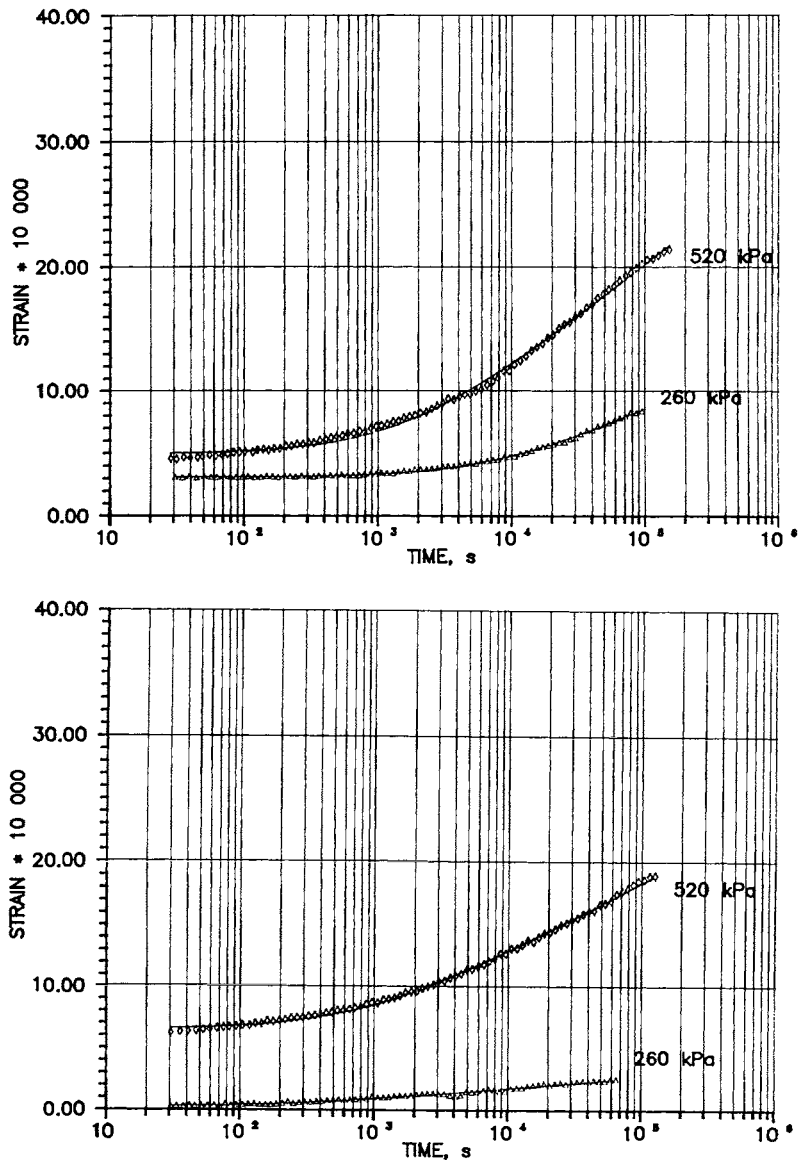


Figure 232 Creep curves. Upper: REF sample (20°C). Lower: Sample 01 (130°C) [5]

6-3 Influence of α radiation on canister-embedding clay buffer

Porewater from the canister-embedding smectite clay will enter leaking canisters and cause dissolution of radioactive waste and released radionuclides will diffuse through the water into the clay. Positively charged elements will migrate into the clay by cation exchange, which means that they get adsorbed and expose the crystal lattice to α radiation [7]. Plutonium and americium are radionuclides of major concern and laboratory tests have shown that montmorillonite that has been saturated with either of these elements, yielding around 5×10^{18} alpha doses per gram of clay, is completely destroyed and converted to an amorphous, silicious mass. Using a relevant value of the number of alphas per mass unit of waste and considering a single hole representing a manufacturing defect or resulting from “pitting” corrosion of a KBS3-type canister, one finds that such degradation may take place in a cone-shaped zone all the way through the clay to the rock in about 1000 years, i.e. in the midst of the heating period.

While formation of passages through the copper of a KBS3 canister by corrosion is estimated to require at least 100 000 years, manufacturing defects in the form of continuous pores in weldings may well exist by which α radiation may become practically important rather early. However, it is expected that only microscopic voids escape the rigorous testing and significant degradation of embedding clay by α radiation is therefore assumed to require tens of thousands of years. If canisters can be prepared in the form of an extruded or cast tube there will only be one or two welded joints, which means that damage will be confined to a relatively small part of the clay buffer. More weldings naturally mean a significantly increased risk of leaking defects.

6-4 Performance

Putting together the net effect of γ radiation it is clear that there are limitations with respect to the amount of HLW that can suitably be contained in canisters. Thus, the high temperature that is caused by much waste per canister has the earlier described negative effects on the nearfield rock structure and on the performance of the canister-embedding clay and for each individual application one therefore needs to carry out a complete analysis of the net effect of the isolation properties of the multibarrier system in order to determine the maximum allowed content of HLW. Equally severe, or even more critical, may be the leakage of radionucli-

des, yielding mineral degradation by α radiation. However, the use of tight canisters, which resist corrosion for at least 100 000 years and which contain moderate amounts of HLW, is expected to yield excellent isolation of such radioactive waste. It must be underlined that as long as the canisters are tight no radionuclides will be released at all.

As to the much less troublesome LLW and MLW, the mode of disposal represented by the Swedish Forsmark repository described in Chapter 1 can be regarded as extremely safe. Less sophisticated concepts, implying disposal on or near the ground surface, have been accepted in several other countries, like France, Japan and Spain.

6-5 References

- 1 Pusch,R., Ranhagen,L. and Nilsson,K. Gas migration through MX-80 bentonite, Final Report. Technical Report 85-36, NAGRA, 1985
- 2 Pusch,R., Hökmark,H. and Börgesson,L. Outline of models of water and gas flow through smectite clay buffers. SKB Technical Report TR 87-10, SKB, Stockholm, 1987
- 3 Pusch,R., Karnland,O. and Hökmark,H. GMM - A general microstructural model for qualitative and quantitative studies of smectite clays. SKB Technical Report TR 90-43, SKB, Stockholm, 1990
- 4 Ewing,R.C., Haaker,R.F., Headly,T.J. and Hlava,P.F. Scientific basis for nuclear waste management. Ed. S.V.Topp. Elsevier Publ. Co., New York, 1982
- 5 Pusch,R., Karnland,O., Lajudie,A. and Decarreau,A. MX 80 clay exposed to high temperatures and gamma radiation. SKB Technical Report TR 93-03, SKB, Stockholm, 1993
- 6 Pusch,R. & Börgesson,L. and Erlström,M. Alteration of isolating properties of dense smectite clay in repository environment as exemplified by seven pre-Quaternary clays. SKB Technical Report TR 87-29, SKB, Stockholm, 1987
- 7 Beall,G.W. The implications of alpha radiation damage for bentonites utilized in high-level waste disposal. Smetictie Alteration, SKB Technical Report TR 84-11, 1984

7 *Quality Assurance*

7-1 What needs to be tested and which are the requirements?

Naturally, performance assessment is relevant only if the various components of the multibarrier system of a repository are really characterized by the physical data ascribed to them. Their properties must hence be determined using representative materials and applying tests techniques with a certain required accuracy, which offers considerable difficulties for some of the barrier components. Thus, applying the principle that the rock, the embedment of the waste containers, and the containers themselves, constitute the barriers, all three should be checked and one realizes that while manufactured engineered barriers can be tested in detail, the properties of the rock can only be roughly estimated because of the large natural variations in structure, implying that all the physical properties are strongly scale-dependent. This is also the case for the buffers and backfills although to a smaller extent. In fact, even the apparently simple issue to determine the properties of the most well-defined barrier, the waste containers, offers difficulties since the manufacturing may produce a number of critical conditions that are hard to identify, like leaking weldings and critical stress concentrations in the canister metal. The practical problems and the very high cost of performing relevant large-scale tests of the rock mass and its relatively unimportant contribution to the overall isolating power of the multibarrier system, mean that quality assurance should primarily concern the more important barrier components, i.e. the canisters and their embedment, which are also more easily tested.

We have seen in this book that the tightness of the containers is most essential in the case of highly radioactive waste because leakage of radionuclides may cause comprehensive degradation of the next barrier, i.e. the smectitic canister embedment. This suggests that the most careful checking for quality assurance should be made of the canisters for which there is huge experience in the discipline of metal material testing. For the isolation of less harmful substances, like shortlived radioactive material and many solid hazardous chemical waste types, the waste containers are not so important since one can often rely on the isolating ability of a sufficiently dense and tight embedment by smectitic clay.

We will confine ourselves here to examine the smectitic engineered barriers, i.e. the buffers and backfills, but before doing this we will see to what extent one can and should test the natural barrier, i.e. the rock.

7-2 The host rock

7-2.1 Rock structure

Quality assurance of rock has to do both with its natural constitution and with the effect of excavation. Considering the structural variations of rock one realizes the impossible task of characterizing a large rock mass in detail and the difficulty in describing it even in very general terms. True quality assurance in the sense of certifying that the rock has a certain constitution, conductivity and stress conditions cannot be provided and only very general criteria should be formulated for accepting a certain rock mass as repository host rock as discussed in Chapter 3. As to the rock structure it should simply be required to make sure that only predicted, very large fractures zones of 1st and 2nd orders, to which the waste containers should have a reasonable distance, are actually present. Once the repository is being constructed and the more detailed structural features of the rock mass are revealed, it is a matter of adapting the repository rooms to practically important 3rd and 4th order discontinuities, applying - more or less - the philosophy of “design as you go”.

7-2.2 Disturbance by excavation

One of the parameters that is expected to be considered in the performance assessment and safety analysis of HLW repositories is the hydraulic conductivity of the excavation-disturbed rock. Naturally, it can not be determined by use of any form of routine testing procedure, but field tests of the sort applied in Stripa and described in Chapter 3 can be made for checking the influence of the applied blasting and boring technique on the conductivity of the nearfield of tunnels and large holes. The high costs and need of experienced personnel make it necessary to reduce the number of such tests very much and in practice designers have to apply generalized conductivity values like the ones proposed in Chapter 3.

For blasted tunnels the deviation of contour holes from the planned direction is a major source of disturbance and increased hydraulic conductivity. Checking of the deviation of the blast-holes from their intended directions, which should be defined and specified in the construction plans and documents, is therefore a form of quality assurance. As mentioned in the construction chapter, modern robot drilling technique with computerized directing of the drilling rods naturally minimizes the deviation but it may still be significant and local rock disturbance and enhanced hydraulic conductivity of the nearfield rock around blasted tunnels is therefore a factor that should be considered, particularly in the location of HLW canister holes.

7-2.3 Stress conditions and groundwater chemistry

As indicated in the chapters on location and design of repositories, the rock stresses and groundwater chemistry are essential for the planning and the performance assessment and basic data of these parameters have to be at hand early for the preliminary design. This requires recording and logging in a number of deep boreholes in conjunction with the prospection work for characterizing the structural features of the rock mass. These data form the basis of the definition of the stress fields and chemical conditions and of maximum acceptable deviation from average values. Complementary stress measurements and groundwater analyses made in the course of the construction will show the actual spectrum of rock stresses and groundwater chemistry and serve as checking of the initially defined ranges and thereby as quality assurance. If the accepted span of stresses and chemical composition is exceeded, changes in design and construction may be required. Thus, once the decision has been taken to construct the repository at a certain site and in a certain fashion, the issue should be to adapt the geometry and adjust the design to fit the variations in rock structure, stress fields and groundwater chemistry rather than to desert the site.

7-3 Buffers and backfills

7-3.1 General

The composition and application of the various clay-based materials specified in the design phase of HLW repositories must be documented in the construction phase and the same goes

for repositories containing MLW, LLW and hazardous chemical waste although the requirements may not be equally demanding. The types and properties of buffers and backfills and the techniques for application of these barriers must be well defined and maximum acceptable deviation from the required data must be specified as well. This requires that methods for characterization have been defined, of which we will give a number of examples.

A most important matter is what smectite species should be used. For the most qualified practical cases, montmorillonite, which is the most common smectite constituent in bentonite, is suitable because of its excellent swelling properties, but for clay buffers exposed to significantly higher temperatures than 100-130°C, saponite and nontronite may be preferable while beidellite should be avoided as discussed in Chapters 3 and 5. Of equal importance for best possible performance in particularly demanding cases, represented by HLW repositories, is the content of accessory minerals since sulphates, calcite and K-bearing feldspars will influence the isolating potential of canister embedment. A third issue of fundamental importance for all types of clay-based waste isolation is the mode of application on site. We will touch on all three matters, referring back to the text in preceding chapters for getting the background.

7-3.2 Clay buffers

MATERIAL COMPOSITION

The buffers and backfills originate from natural rock and soil deposits, which are always characterized by a certain degree of variation both with respect to the mineral composition and to the grain size distribution. Smectite is often the major mineral constituent of bentonite beds, but since they were commonly formed by sedimentation with frequent changes in temperature and flow conditions and also in source material, there may be a very significant difference in smectite content and composition in different parts of the beds. Smectite-weathered rock, of which rhyolite is a rather common type in countries like Japan and Italy (Sardinia), is usually more homogeneous and forms much thicker deposits than ordinary bentonites of sedimentary origin. The thickness of the latter rarely exceeds one to two meters.

The manufacturer must be able to show that the requested brand has been used and that the delivered material, i.e. in practice compacted bentonite blocks or granulated bentonite powder, have the specified content and required type of this mineral. This requires XRD analysis and determination of CEC, and analysis of the chemical composition of the clay fraction, i.e. the part of the material that has a particle size smaller than 2 µm, as well as of the total mineral material. The content of accessory minerals, especially carbonates and sulphur- and potas-

sium-bearing minerals, as well as of organic substances must be determined and quantified. Checking at delivery to the construction site should naturally be made, but it requires access to advanced laboratory facilities and a skilled staff and the problem is in practice that mineral and chemical analyses are very time-consuming and expensive. For this reason simple methods for checking the smectite content have been introduced, primarily for use at the bentonite processing plants, common tests being based on the use of methylene blue or other organic dyes as reactants, and determination of the capillary suction power [1].

A very practical, simple way of estimating the smectite content is to determine the Atterberg liquid limit, which is a measure of the hydration potential of soil materials and represents a specific water content [2]. It requires that the major adsorbed cation is known and that the evaluation refers to the clay fraction, typical data being those given in Table 25. The method has been in wide use in the various sealing projects at Stripa and it was applied for checking the delivery of 7000 tons of bentonite to the Forsmark repository described in Chapter 1. For this project samples were taken from each fiftieths big-bag delivered to the construction site. The bentonite had calcium as major adsorbed cation in the natural state and had been converted to sodium form by soda treatment at the deliverer's processing plant in the usual way. The required minimum smectite content had been set at 60 % and the liquid at 325 % using the Casagrande equipment as concluded from comprehensive chemical and mineralogical as well as rheological tests [2]. The simpler cone test for determination of the liquid limit gave consistently lower values and $w_L=250$ % was accepted as minimum value applying this method. Figure 233 shows the variation in water content and in liquid limit, which had the average value 272 %, and it is a good example of the expected variation in composition of large amounts of commercially available smectitic clays.

MATERIAL FORM

There is a good deal of experience in proper processing and preparation of blocks of highly compacted, smectite-rich bentonite, especially with montmorillonite as major component. As discussed in Chapters 3 and 6 the bulk density controls the hydraulic and gas conductivities and the ion diffusion capacity as well as the swelling potential, and the water content - or rather the degree of water saturation - determines the thermal conductivity and a number of physico/chemical processes in the maturation phase. The density and water content of delivered blocks therefore need to be determined as part of the quality assurance and it is easily made by checking at the delivery to the construction site or material storage. The manufacturer should be able to guarantee that the dry bulk density does not deviate from the required value by more than ± 2 % and that the water content is within ± 3 percent units from the

required value. As to deliveries of granulated bentonite for mixing with ballast material on the construction site or for preparation of clay grouts for fracture sealing, the requirements are discussed later in this chapter.

Table 25 Typical liquid limit data of commercial bentonites

Major adsorbed cation	Clay content	Liquid limit, w_L %	Smectite content, weight percent of total clay mass
Li	85-95	550	75-85
Na	85-95	400-500	75-85
Na	70-80	300-400	60-70
Ca	85-95	100-150	75-85

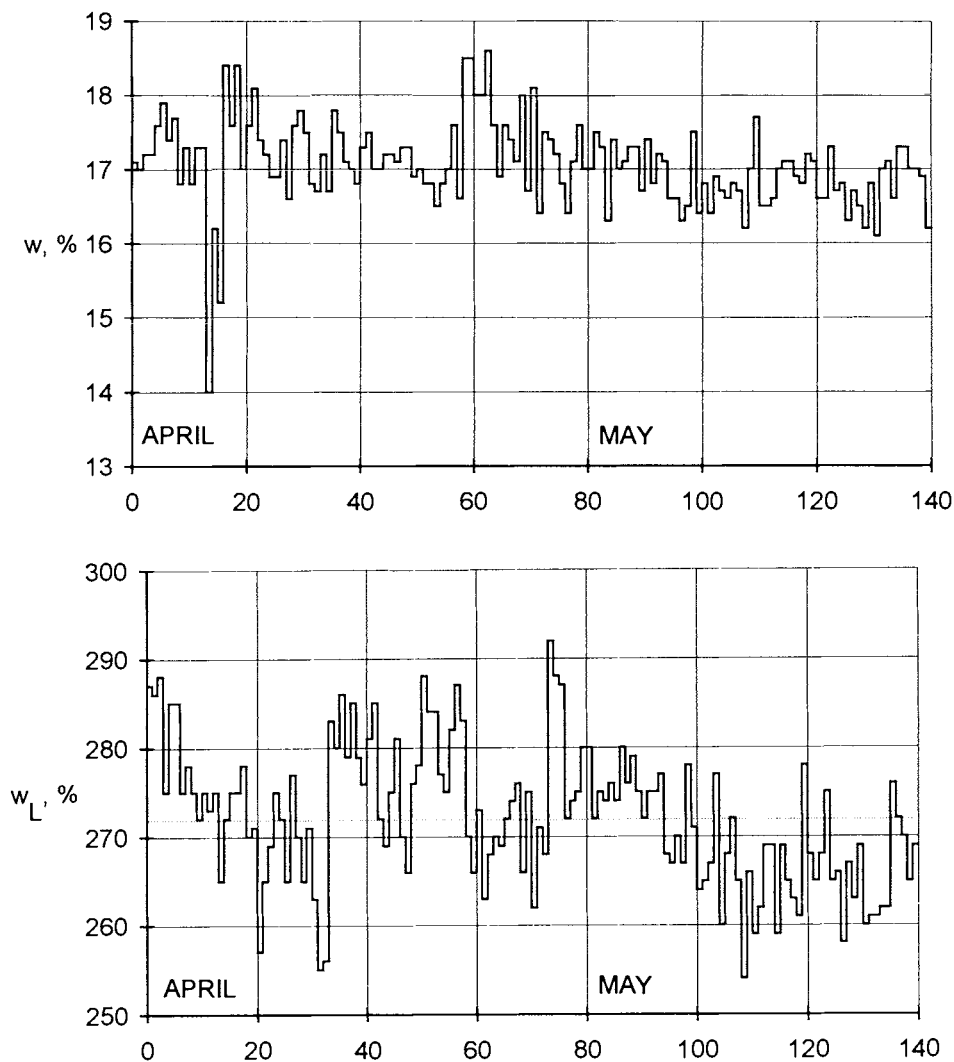


Figure 233 Recorded material properties of 7000 tons of Na bentonite delivered to the Forsmark LLW/MLW repository in Sweden. Upper: Water content of delivered material. Notice the smaller interval from early May, partly because of lower humidity at the stockpile. Lower: Laboratory-determined liquid limit with the average value given by the broken line. The variation is large and the tendency towards lower values in the later part of the delivery significant

MATERIAL PROPERTIES

The large amount of laboratory tests that has been made of bentonite materials for use in repositories has given detailed information of the relationship between smectite content, density and physical properties as well as physico/chemical behavior as described in Chapters 3 and 5. Comprehensive testing of the hydraulic conductivity, swelling potential and ion diffusion properties or of the chemical stability is therefore usually not needed but a certain number of representative samples should be taken for determination of these properties. For clay grouts there are additional requirements, particularly respecting the grain size distribution. Thus, the material must not contain particles larger than about 1/3 of the estimated geometric aperture of the fractures to be sealed, a requirement that in practice means that all particles belong to the clay fraction, which, in turn, means that the content of smectite is not far from 100 %. All testings must be made by a qualified laboratory using standardized methods [2].

APPLICATION

The strong influence of the density on the physical properties of smectite buffers makes it necessary to certify that the space in which the material is applied is not larger than assumed and specified in the design work. For block filling it is hence important that the total volume of the space to be filled, such as canister deposition holes or slots cuts for “O-ring”-type sealing around tunnels, is measured and that the mass of solid clay required to yield the specified net density after maturation is applied. The bulk density and the porosity of the blocks are the parameters for this exercise. For canister deposition holes where rock fall from the walls has taken place, the cavities is suitably filled with clay buffer material with approximately the same density as the material in the holes. Problems of this sort are expected in repositories of the VDH and VLH types as discussed in Chapter 3, but they may appear also in KBS3-type deposition holes. A general requirement is that the blocks of buffer clay should be reasonably well fitted together although very careful emplacement is not at all needed. It is important, however, that any deviation from the design criteria is evaluated in terms of the performance of the buffer and that required adjustments with respect to the density and geometry of all the clay barriers are made in the construction phase.

7-3.3 Backfills

COMPOSITION

Clay component

The same aspects apply to clay/ballast mixtures as to buffer materials. However, for mixtures the smectite content is of vital importance, especially when the ratio of clay/ballast is low in order to yield low compressibility while it is still required that the material must also have low hydraulic conductivity, as in the case of the bottom bed of the Forsmark silo. For such purposes, careful and detailed checking of the type and amount of smectite and accessory minerals needs to be made and it is also required that the grain size distribution of the clay powder - which should be very fine-grained - is also determined. For many other less qualified applications, natural smectitic soil material of sedimentary origin or originating from smectite-weathered rock can be considered. One must, however, make sure what the variation in mineral composition and grain size distribution really are since they may be considerable and yield very significant variations in tightness and compactability, leading to a markedly heterogeneous mixture if a standard application and compaction technique is used. Comprehensive field investigations are required before naturally occurring soil material can be accepted and detailed checking of the smectite content and the granulometry is required at the construction site. In practice, this is an issue of great economical importance to which we will return in a later chapter.

Ballast (“aggregate”) material

The ballast material used in the preparation of clay/ballast mixtures for backfilling purposes should not only be to provide a mineral component that - together with the clay - offers the desired physical properties, like a low hydraulic conductivity and suitable rheological behavior, but it must also be able to coexist with the smectite component and the rock without undergoing or causing significant chemical alteration. This is most easily achieved by using crushed and ground rock material from the excavation of the repository. The amount of potassium-bearing minerals should naturally be small.

It was pointed out in Chapter 3 that the granulometry should be of a certain type for obtaining a high density and low compressibility, which means that the gradation curve should be within a certain zone in the sieve diagram. The bottom bed of the Forsmark silo had 10 % bentonite content and laboratory testing using both ordinary 50 mm oedometers and

“megapermeameters” with about 15 times larger diameter, demonstrated that a suitable gradation curve should be in the range indicated in Figure 234 for optimum performance. It was hence decided to require that all sieve curves should be within this zone at the testing of ballast material delivered to the construction site. Samples for sieving were taken from each delivery of 50 tons, and we see from the figure that the variation was not large.

A third criterion is that the water content of the ballast material must be within a specified interval, i.e. lower than a few percent units for preparation of “dry” mixtures of ballast and smectite clay, and within a certain interval for preparation of mixtures at “optimum” water content [3]. The samples taken for sieving tests can also be used for determination of the water content.

MATERIAL PROPERTIES

Naturally, the distribution of the clay component and the bulk density determine the physical behavior of the compacted backfills. The firstmentioned can be currently checked in the course of the preparation while the density has to be determined in the course of and after the application. In practice, only a limited number of freshly prepared samples from the mixing process need to be tested with respect to the hydraulic conductivity and compressibility and expandability, primarily for validating the laboratory data determined in the design phase. Instead, great effort should be made to record the clay content in the preparation of the backfills, for which the procedure mentioned later in this chapter can be applied. It is estimated that the clay content should be tested for each ton of mixed material while laboratory testing of the conductivity and rheological behavior of compacted backfill does not have to be more frequent than one test per 500-1000 tons of prepared material for a repository with 1000 000 to 2000 000 tons of bentonite/ballast backfills. More detailed checking of the applied backfill is needed, however, and this is preferably made by determining the bulk density, the clay content and the liquid limit, since, in combination, they control the physical behavior of the compacted mixture.

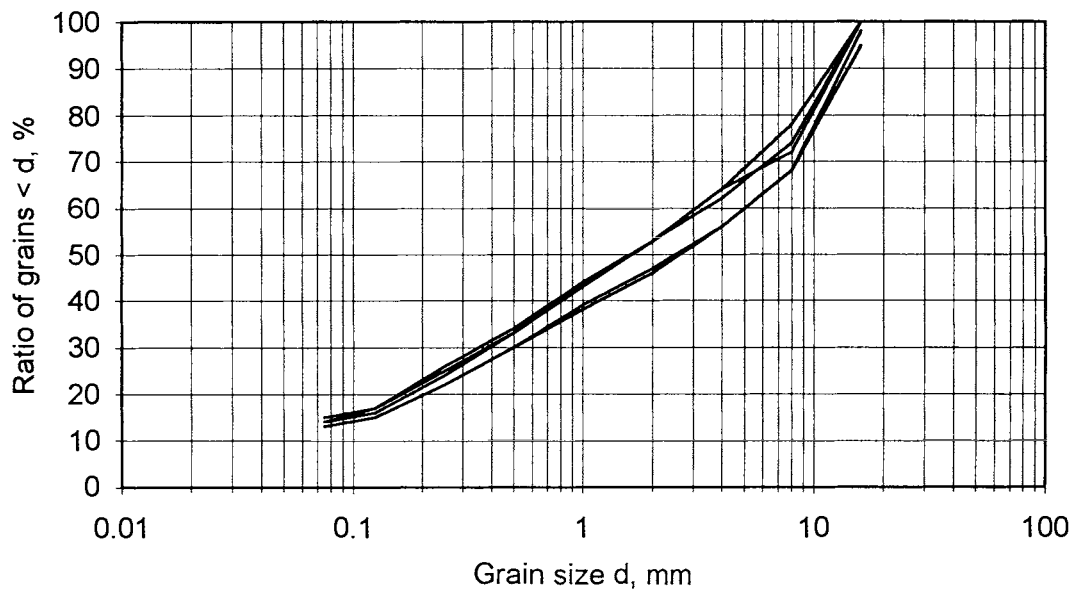


Figure 234 Example of range of ballast grain size distribution accepted for the bottom bed of the Forsmark silo

PROPERTIES OF COMPACTED BACKFILLS

Density

The most easily determined property that needs checking for quality assurance is the bulk density. It can be made by applying various methods developed and frequently applied in road and earth dam construction, such as densitometer techniques using “water balloon volumeters”, which involves excavation of a small semi-spherical volume of the compacted mate-

rial and weighing it, and measuring this volume carefully by filling a tightly fitting rubber bladder with water (Figure 235) [3] . More advanced equipments like the compaction meter, isotope methods and gamma ray backscattering [3,4] have been applied with some success, but the simple water balloon technique seems to be most accurate as concluded from the testing of the Forsmark silo bed. For this project, water balloon testing was finally selected with a frequency of about 12 determinations per 0.3 m layer with a total area of 700 m². It also comprised plate loading tests from the E-modulus was evaluated [5].

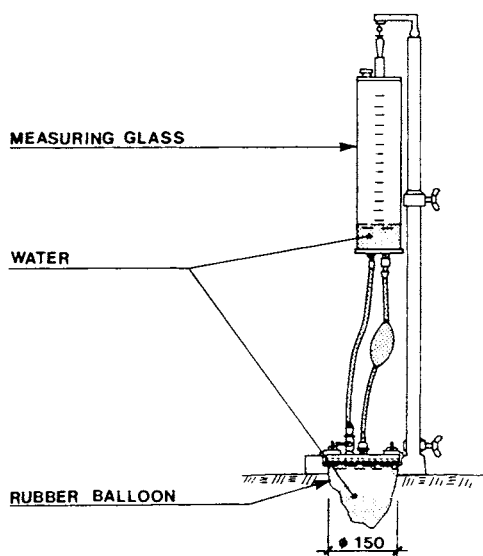


Figure 235 Determination of the volume of excavated sample using water densitometer technique

Clay content

The clay content is determined by mechanical disintegration of the samples and dispersing them in water for determination of the grain size distribution by sieving and sedimentation analysis according to well established techniques in soil mechanics and soil physics, to which the interested reader is referred. Recently developed semi-automatic methods for quick and

accurate evaluation of the grain size distribution, including particles of colloidal size, make it possible to rationalize the testing. These methods employ laser beams for determining the density of the suspension, from which the equivalent grain size is determined by use of Stoke's law or other relationships between the grain size and shape, and the settling rate.

Liquid limit

The Atterberg liquid limit, which is basically a measure of the hydration potential of clay soils, can be determined by use of Casagrande's apparatus or by cone penetration tests. Both are described in soil mechanical textbooks.

7-3.4 Seals

Quality assurance of the most important material properties of seals is possible by applying the various testing procedures mentioned earlier in the chapter. For bentonite plugs this can have the form of certifying that the density of plugs is as required by applying the method described in Chapter 7-3.2 (Application). Field recording of their sealing effect requires test arrangement of the sort used at Stripa and described in Chapter 3, which is naturally very expensive and time-consuming.

The performance of grouts can only be determined by measuring the inflow of water into the space, i.e. boreholes or tunnels, before and after grouting but the aforementioned effects, i.e. increase in water head behind the sealed section, the redistribution of water flow make the interpretation difficult. Furthermore, such measurements do not give any information on whether the grout has entered deeply into fractures or just sealed off the outermost part. There are three possible ways of investigating this. One is to record the amount of injected grout and compare this volume to the fracture space evaluated from preceding hydraulic testing [6,7], while the other is to drill holes in the grouted rock mass and perform hydraulic testing. The latter method requires a considerable number of holes for yielding statistically safe results. The third method applies to rock that is rich in fractures with appreciable apertures, where core drilling for direct inspection of the location and nature of the grout is possible.

If the degree of fracture-filling is high it is reasonable to believe that the sealing effect will be preserved at least in a short-term perspective (cf. Chapter 3).

7-4 References

- 1 Pusch,R. Use of clays as buffers in radioactive repositories. SKBF/KBS Technical Report TR 83-46, SKB, Stockholm, 1983
- 2 Karnland,O. and Pusch,R. Development of clay characterization methods for use in repository design with application to a natural Ca bentonite clay containing a redox front. SKB Technical Report TR 90-42, SKB, Stockholm, 1990
- 3 Forssblad,L. Vibratory soil and rock fill compaction. Dynapac Maskin AB, Solna, Sweden, 1981
- 4 Proc. Colloque International sur le Compactage. Volume II, Editions Anciens ENPC, Paris, 1980, ISBN 2-85978-019-X
- 5 Bowles,J.E. Foundation analysis and design. 3rd Ed. McGraw-Hill Int. Book Co. ISBN 0-07-085192-8, 1982
- 6 Börgesson,L., Pusch,R., Fredriksson,A., Hökmark,H., Karnland,O. and Sandén,T. Final report of the rock sealing project - sealing of zones disturbed by blasting and stress release. Stripa Project Technical Report TR 92-21, SKB, Stockholm, 1992
- 7 Pusch,R., Börgesson,L., Fredriksson,A., Markström,I., Erlström,M., Ramqvist,G., Gray,M. and Coons,W. Rock sealing - interim report on the Rock Sealing Project (Stage I). Stripa Report TR 88-11, SKB, Stockholm, 1988

Chapter

8 *Instrumentation and Recording*

8-1 General

Ideally, no recordings or measurements should be required after closing a waste repository, since the designers or the licensing authorities should be convinced of the isolating ability of repository concept in general and of the barrier system in particular. Still, there are circumstances that legitimate instrumentation and monitoring of various functions, as in the case when new techniques are employed and when technical and economical optimization is aimed at when constructing a repository in steps. An example is the LLW and MLW repository at Forsmark where a number of instruments were applied in the room with the big silo for recording the silo and rock movements and the build-up of swelling pressures and water heads around the silo (cf. Chapter 1). Comprehensive sampling for identifying changes in groundwater composition is currently made and there is a significant number of piezometers installed for measuring changes in groundwater pressure.

There may be a need for other monitoring as well, and a complete list may be the following:

- * Rock deformation and pressure
- * Stress and strain of buffers and backfills - evolution of swelling pressure
- * Movement of waste containers
- * Changes in groundwater pressure and chemistry
- * Change in groundwater flow
- * Temperature changes
- * Recording of seismic events

We will focus here on recording of temperature, swelling pressures in buffers and backfills and of groundwater pressure and we will also consider ways of recording displacements, confining ourselves to describe the techniques used for recording the vertical movement of the big Forsmark silo and displacements in heated rock. The lastmentioned issue is considered first.

8-2 Rock displacements

GENERAL

Rock stress and strain recording is made worldwide using techniques, which are well established and which have an accuracy that is adapted to the respective purpose [1]. Most of the strain recording events do not require an accuracy better than a few hundred micrometers, which is provided by various sorts of extensometers, but for certain purposes, like in pretesting the behavior of the nearfield rock of heated HLW canister holes, precision methods that yield very accurate strain data are required. The technique used at Stripa, the “sliding micrometer”, had a high accuracy and served well and therefore deserves to be described here.

THE SLIDING MICROMETER

The principle of recording rock strain, primarily widening of discrete discontinuities and shear strain along them, by the sliding micrometer (ISETH) is to apply fixed reference marks at 0.5-1.0 m distance in a borehole by grouting, and to connect them by axially deformable and movable short tubes. These are also grouted in the hole and serve to guide the measuring rod, which is inserted at each recording event so that it slips in between two marks (Figure 236). The distance between neighboring marks is determined by adjusting the length of the temperature-compensated rod to make it fit between them. With this method changes in aperture of fractures intersecting the hole can be recorded with an accuracy of $\pm 10 \mu\text{m}$ or possibly somewhat better than that, provided that the hole is oriented perpendicularly to the fracture [2]. Shear displacements can be recorded by orienting the hole at a small angle to the fracture. Several readings should be made at each recording event and the mean value used for evaluation of the rock displacements. The technique was applied in the Stripa BMT experiments, using 86 mm boreholes, and it turned out to give valuable information on the displa-

cements in heated rock [3]. A practical observation of great importance from this study was that it is essential to clean the marks regularly so that debris emanating from fracture coatings does not accumulate on them.

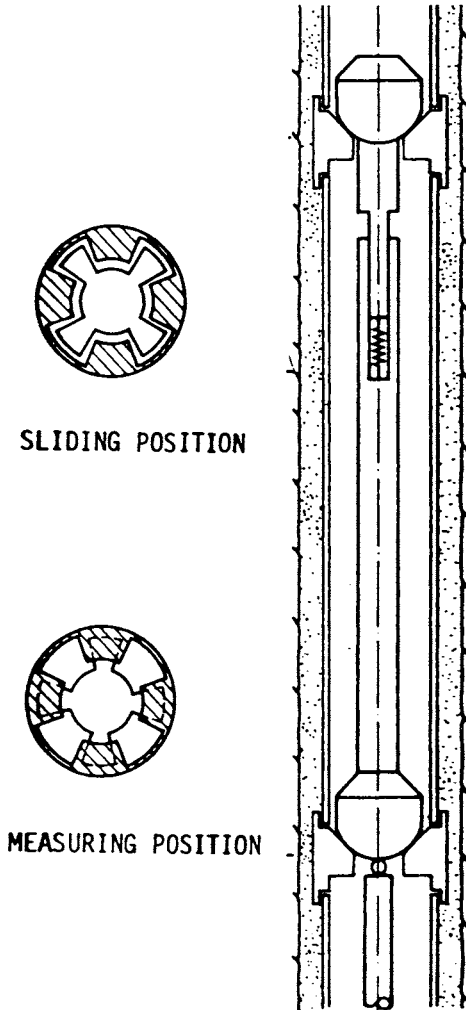


Figure 236 Main features of the sliding micrometer ISETH (Kovari)

8-3 Temperature recording

Temperatures can be measured without great difficulties in rock and buffers and backfills. It is required, however, that the gauges are mechanically stable and that they do not corrode in the period over which they are required to yield reliable heat data. Temperature recording in the Stripa BMT project, where steel-sheathed copper/constantan thermocouples with MgO insulation were used for recording temperatures of up to 200°C, gave important information on these issues [2]. Preceding experiments in the Stripa mine had demonstrated that corrosion had caused degradation of steel-sheathed thermal elements despite the low electrolyte content of the groundwater (chloride content lower than 85 ppm) and a steel quality of low-corrosion type was therefore employed. The accuracy, which is a function of the integrated measuring and recording systems, was estimated at $\pm 0.5^\circ\text{C}$ even up to the highest temperatures.

The thermocouples can be inserted in holes drilled in compacted blocks and backfills. Rock temperatures are suitably measured by use of thermocouples embedded in quartz sand in boreholes. The thermocouple wires can be bent to a radius of down to about 2 cm.

Recording is made by PC-based data logging systems. In the BMT project, where the total number of thermocouples was about 1200 with reading intervals of down to a few minutes, a high capacity data acquisition system was required. Separate tests with only about 25 thermocouples, but operating in principle as the BMT experiment, were made using the system shown in Figure 237.

8-4 Pressure recording

Figure 238 illustrates the instrumentation of the Forsmark silo. P denotes pressure gauges for recording the total pressure, i.e. the sum of the effective (swelling) pressure and the porewater pressure at the bentonite/rock interface, while U refers to piezometers located in short boreholes in the rock close to this interface.

Both types of gauges operate as “active” pressure cells, i.e. the soil or water pressure acts on a membrane on which backpressure is applied and measured (Figure 239). When equilibrium is reached, which is indicated by quick flow of the oil fluid used for pressurizing, the pressure is measured by use of a precision manometer or a transducer for digital reading or recording by use of printing facilities. The activation only produces a deflection of the cell by a few micrometers, which means that “arching” effects are insignificant and the accuracy therefore

rather good. Pressure cells and piezometers of this sort are not as sensitive as cells equipped with transducers or other electronic components for direct recording of soil or water pressure

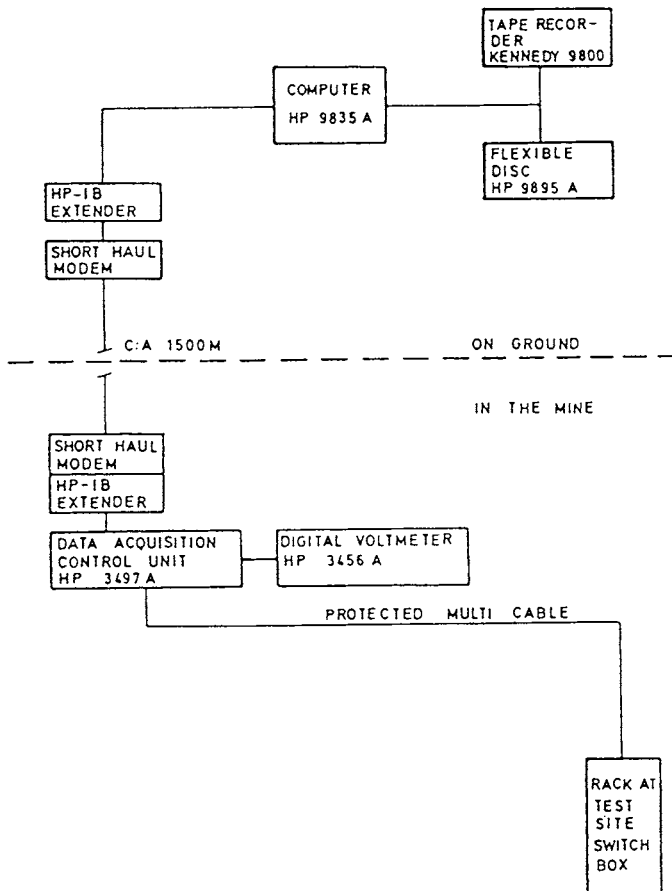


Figure 237 Layout of data acquisition system used for recording temperatures with a small number of thermocouples [5]

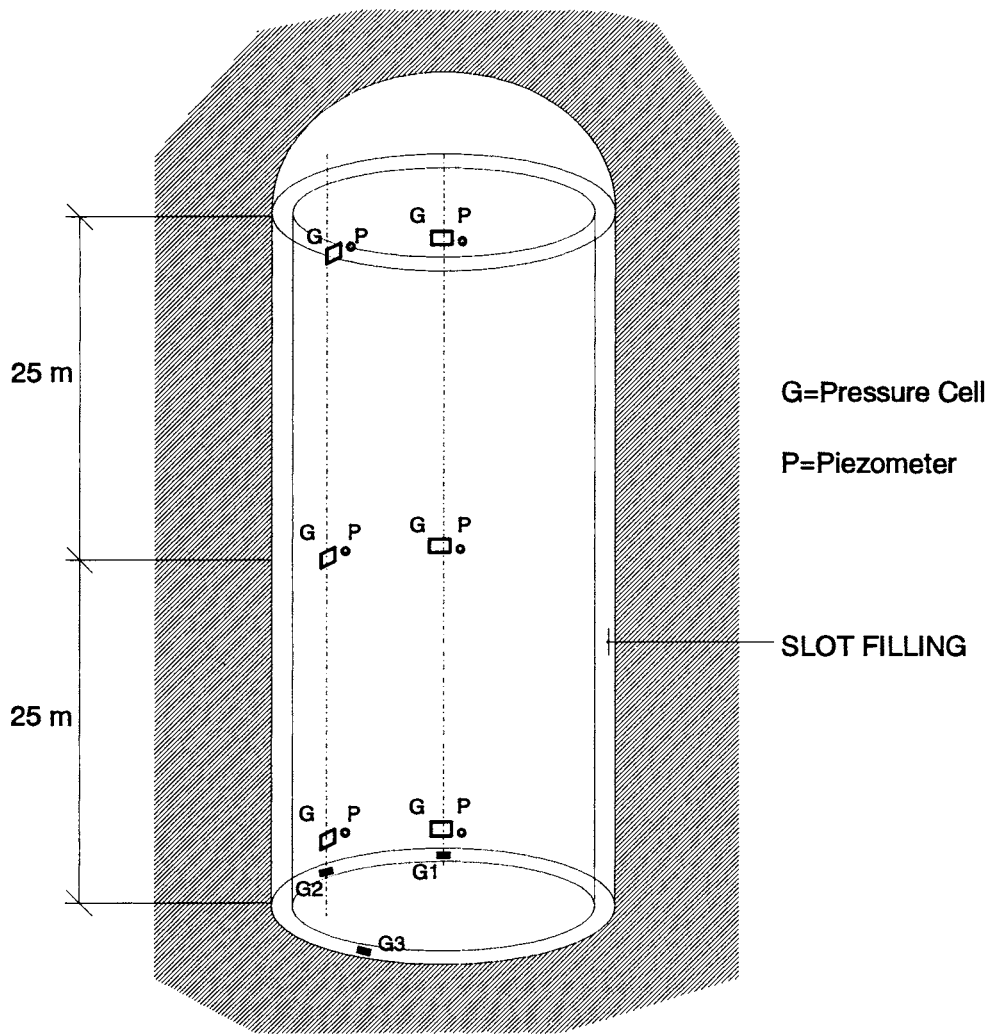


Figure 238 Location of pressure gauges in the silo room at Forsmark. G stands for total-pressure cells located at the interface of the bentonite slot fill and the shot-creted rock. P denotes piezometers in short boreholes

but they are very reliable and have a lifetime of several decades or even more. The accuracy, which depends on the measuring range, is a few kilopascals at constant low temperature. At higher temperature inadequate data are obtained if the heat-induced volume change of the liquid in the cell, usually mercury, is not compensated for. In the Stripa BMT project, where several cells were applied in the heater holes for recording the build-up of swelling pressures the net accuracy was estimated at $\pm 10\%$ at 70°C (Figure 240).

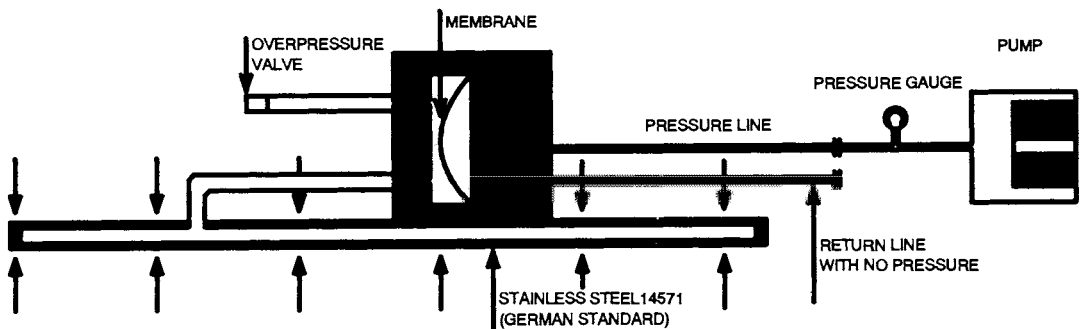
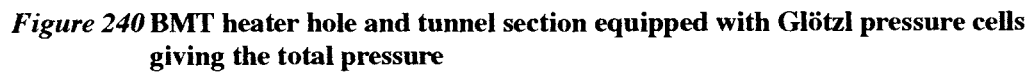


Figure 239 Schematic picture of “active” pressure cell (Glötzl)

The recording procedure is that the backpressure is increased slowly until a steady, maximum value is obtained. In its simplest form the pressure increase is produced by use of a simple hand-operated hydraulic pump connected to one of the tubings leading to the cell, a technique that is employed in the Forsmark repository. Fully automatic pressurizing of a number of

cells, one at a time, can be used for remote recording as in the Stripa BMT project, where 128 cells had been installed. A complete recording cycle took about five hours. Figure 241 illustrates schematically the BMT data acquisition system with one underground instrumentation room in which the tubings from the cells were connected to the recording unit with backpressure pumps, and a data acquisition center at the ground surface. This center was in turn connected, through modems for automatic data transfer, to the center where data processing was made.



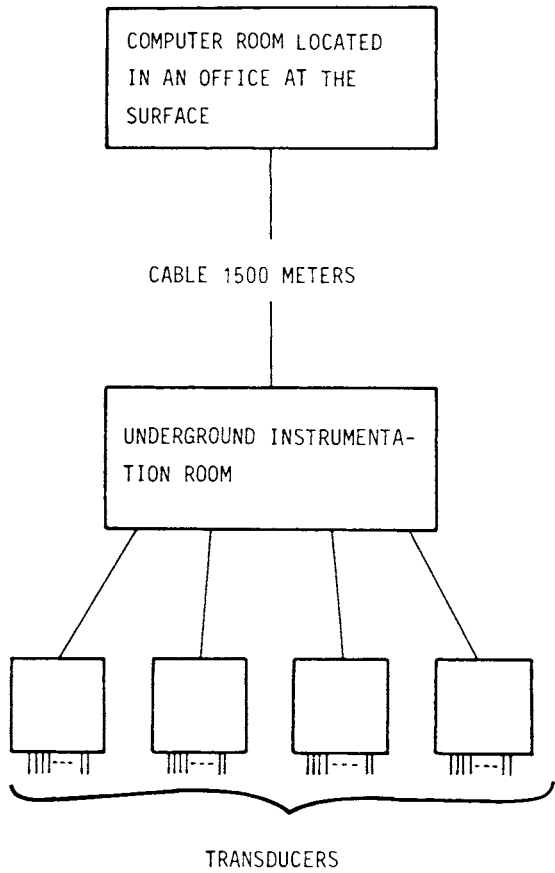


Figure 241 The Stripa BMT acquisition system

In a repository for radioactive waste no tubings or pipes should extend to the ground surface for eliminating the risk of radionuclide migration to the biosphere. At the final repository sealing, recording therefore has to be terminated and the stainless steel tubings sealed with epoxy. Neither this substance nor the tubings are expected to be intact for longer periods of time.

DISPLACEMENT OF WASTE CONTAINMENT

Experiments with recording of vertical movements of a heater simulating a buffer-embedded HLW canister have been performed in the Stripa mine by use of dial gauges with an estimated net accuracy of the readings of around $\pm 10 \mu\text{m}$ [5]. Such experiments are difficult because reference bolts anchored in the rock do not represent fixed points due to rock block movements caused by stress and temperature, and because recording has to be made by use of a shaft extending from the heater through the clay embedment and upper seal, which causes friction and locking.

An example of techniques for recording vertical movements of a large waste container is offered by the settlement recording of the big silo at Forsmark. It is made by use of precision levelling of a number of measuring bolts anchored in the uppermost part of the silo and an equal number of reference bolts anchored in the rock at a few meters distance from the measuring bolts. The measurements are estimated to yield values with an accuracy of $\pm 10 \mu\text{m}$, and the mean value of three individual readings are used for the recording (cf. Figure 14).

DISPLACEMENTS OF ROCK

Movements inside a rock mass is commonly recorded in many contexts, particularly in mines where continuous stability checking is required because of the low factor of safety that is associated with the extraction of large amounts of rock. No such measurements should be required in repositories excavated in virgin crystalline rock of reasonable quality but they may be asked for in mines intended for disposal of chemical waste since the rooms may be very large and the stability poor. The interested reader is referred to rock mechanical and mining literature for details.

8-5 References

- 1 Pusch, R. Rock mechanics on a geological base. Elsevier Publ. Co., (In press)
- 2 Pusch, R., Nilsson, J. and Ramqvist, G. Final report of the Buffer Mass Test - Volume I: scope, preparative field work and test arrangement. Stripa Project Technical Report TR 85-

11, SKB, Stockholm, 1985

3 Pusch,R., Börgesson,L. and Ramqvist,G. Final report of the Buffer Mass Test - Volume II: test results. Stripa Project Technical Report TR 85-12, SKB, Stockholm, 1985

4 Pusch,R., Karnland,O., Lajudie,A., Lechelle,J. and Bouchet,A. Hydrothermal field tests with French candidate clay embedding steel heater in the Stripa mine. SKB Technical Report 93-02, SKB, Stockholm, 1992

5 Börgesson,L. and Pusch,R. Interim report on the settlement test in Stripa. SKB Technical Report 89-29, SKB, Stockholm, 1989

Chapter

9 *Economy*

9-1 Factors

The total cost for disposal of hazardous waste in deeply located repositories naturally depends on the type of waste and whether the repositories are constructed for the purpose or if mines or other underground excavations can be used. We will confine ourselves here to estimate the cost of repositories for radioactive HLW, constructed in crystalline rock at 500 m depth, and of adapting available rooms in mines for hosting hazardous chemical waste. The cost for a LLW/MLW repository of the Forsmark type was indicated in Chapter 1.

9-2 HLW repositories

9-2.1 General

The cost of constructing underground repositories for HLW represents a rather small fraction of the total expense for disposal, which is in fact a comprehensive and very advanced industrial process. Thus, plants are required for encapsulation of the highly radioactive waste from nuclear reactors, which can be burnt-out fuel from nuclear reactors or products from reprocessing of such fuel, and special facilities are required for preparation and storage of clay buffers and backfills. Roads and railways have to be constructed and a number of buildings are required on the ground surface for various activities and service functions, like offices, factories, garages. We will consider only the cost of construction or adaption of underground rooms including estimated costs for prospection and geological, geophysical and geochemical characterization of the site, as well as the cost for preliminary design.

9-2.2 KBS3 repository

FEATURES

We will take as an example a KBS3 repository with about 6 000 HLW canisters as outlined by SKB [1]. It consists of deposition tunnels with a total length of 30 km and a spacing of 40 m, each about 250 m long. Access to the 1 km² underground repository area can be either through a ramp (Figure 243), which offers the safest transportation conditions, or through elevator shafts. The idea is to construct it in two parts so that one can be used for waste application while the other one is being prepared for such work. While the most cost-effective way would be to prepare the entire repository in one sequence, the plans are to conduct the work with tunnel excavation more or less parallel to the waste application and tunnel backfilling. This has the advantage that the piezometric pressures are maintained high in the vicinity of the tunnels and deposition holes, which leads to quick water saturation of the buffers and backfills. Tunnel backfilling very soon after application of the canisters minimizes the problem with softening of the clay buffer in the deposition holes.

The total excavated rock volume in the ramp version is estimated at 950 000 m³, of which the deposition tunnels and holes represent 550 000 m³, which can host up to 7000 canisters with a total amount of HLW in the form of burnt-out fuel of about 15 000 tons. The tunnel excavation rate is determined by the rate of waste production and application and it is slow. Thus, it is estimated to be 4 km in the first phase for 3 years waste application, and then continues intermittently.

COSTS OF AN UNDERGROUND REPOSITORY

SKB utilizes a computerized system BECOST for cost calculation, which makes continuous updating possible in the forthcoming very long construction and operation periods [1]. One uncertainty that affects the cost is the time for operation of the Swedish nuclear reactors and different scenarios have been assumed by SKB for estimating the importance of this factor. The current plan, which is based on a referendum back in 1976, implies that all the 12 reactors will be operated to the year 2010, yielding a total amount of energy of about 2 000 TWh.

The cost for construction and preliminary design, backfilling and sealing of a KBS3 repository with 6 000 canisters containing 15 000 tons of burnt-out fuel is as estimated by SKB to be about 6 000 MSEK, including underground installations like elevators and ventilation and costs for site investigations and design, referring to the Swedish price level in January 1993

[1]. One finds that this cost represents about 0.003 SEK per kWh, or roughly 0.03 US\$ per kWh, which is about 15-20 % of the total cost of taking care of the radioactive waste products from the nuclear energy production in Sweden to the year 2010. The figure 0.003 SEK/kWh is about 0.5 % of the present cost for household consumers of electric energy in Sweden.

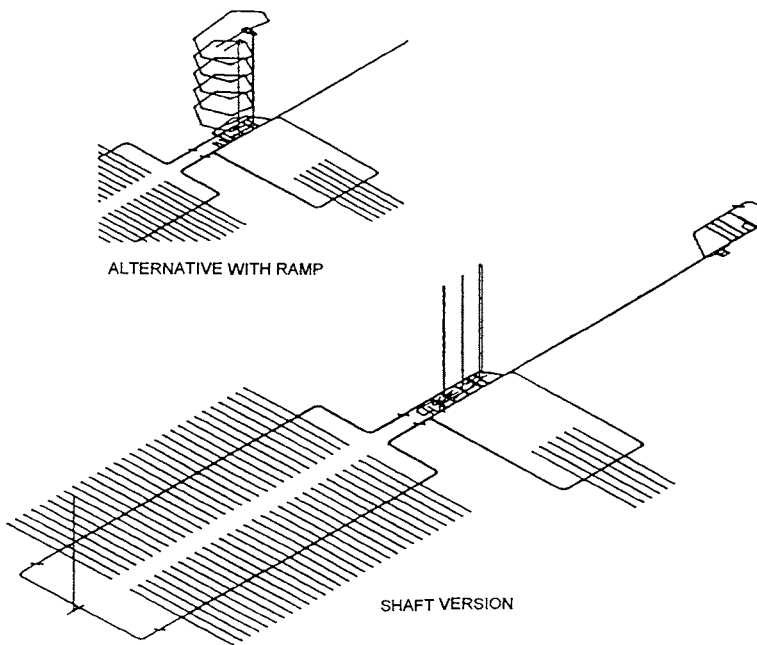


Figure 242 Generalized KBS3 repository with access through ramp or shafts [1]

The relatively small fraction of the total cost that will be spent for constructing a KBS3 repository suggests that there should not be a strong demand of cutting costs by significant reduction in quality or geometrical dimensions of the engineered barriers, or by applying simpler and less safe concepts. Thus, there are very good reasons for HLW being disposed of in suitably located and carefully constructed repositories especially prepared for this type of waste. Cost cutting should instead take place, as in all large-scale projects, by performing the construction operations in a continuous fashion, and by appointing an effectively operating staff organization and naturally by utilizing experienced consultants, constructing companies and manufacturers. The importance of employing a simple, straightforward concept with well tested barrier materials and sealing techniques and commonly applied excavation and construction methods must be underlined in this context.

For the present purpose it is interesting to compare the estimated cost for the competing HLW candidate concepts referred to earlier in the book, i.e. the very deep boreholes (VDH) and the very long boreholes (VLH), which are more or less equivalent with KBS3 from the viewpoint of safety. SKB's calculations showed that VDH would give an underground repository cost that is almost five times higher than that of KBS3, while VLH would cost about 70 % of the sum estimated for KBS3 [2]. The considerably higher cost for VDH is naturally discouraging and makes this concept unattractive. It should be mentioned also that the underground repository cost of the concept termed ENRESA and illustrated in Figure 55, is intermediate to that of KBS3 and VLH and may represent an optimum solution both technically and economically.

COSTS FOR SITE INVESTIGATIONS AND DESIGN

So far no radioactive repository project has been pursued in a purely commercial fashion and it is therefore difficult to assess the true cost for carrying out and interpreting site investigations, and for the design work. The geophysical and geological investigations are always carried out in steps parallel to preliminary design work for current safety assessment, and it is difficult to distinguish between these activities. Still, a rough picture of the costs can be obtained by examining the various expenses for the LLW/MLW disposal at Forsmark described in Chapter 1-5.7. This project, which involved comprehensive geophysical and geohydrological investigations of an approximately 10^8 m^3 big rock volume, and excavation of $430\,000 \text{ m}^3$ of rock down to about 100 m depth, as well as construction of the big silo, caused construction costs of about 280 MSEK and expenses for site investigation and design of about 230 MSEK, referring to the 1987 price level. A considerable part of this latter cost referred to administration and other staff costs and it is reasonable to believe that the true cost for making site

investigations and evaluating them for finding a suitable position of the silo and caverns was about 50 MSEK, and that the cost of the design work was on the same order of magnitude. If this is taken as representative of repositories in general, it would suggest that the cost of site investigations, excluding preceding pilot investigations and overviews, and of final, complete design, may each represent about one fifth of the construction cost. This is naturally much more than for ordinary underground constructions.

A second hint of the expected cost of site investigations is offered by the geophysical and geohydrological investigations in the Stripa mine for characterizing a rock volume of somewhat less size than that hosting the Forsmark repository. Here, several consecutive studies were made in a number of deep drillings for hydrological, petrological and chemical characterization, and structural modelling based on such investigations and comprehensive radar measurements was also applied to an extent similar to what can be asked for in the survey for a new repository. The total cost for those studies that were not of purely scientific art or solely for development of new techniques, is estimated at 25-50 MSEK, i.e. on the same order of magnitude as for the Forsmark investigations.

It is reasonable to believe that the experience from Forsmark and Stripa and the improved understanding of the constitution of rock at larger depth that is presently evolving, makes it possible to do more rational site investigations for a future KBS3 repository, and that this reduces the ratio of the costs of site investigations and construction to 1:10 rather than 1:5. If so, the total cost of site investigation and rock characterization for a KBS3 repository including preliminary design will be around 600 MSEK.

9-3 Repositories for hazardous chemical waste

GENERAL

It goes without saying that while radioactive waste from nuclear reactors can be stored at large depths at costs that can well be taken because of the competitiveness of this energy production technique, the cost for disposal of chemical waste has to be kept at absolute minimum. This raises a number of questions concerning future environmental policy but we will refrain from entering this debate and confine ourselves to conclude that modern society will always produce a certain amount of very toxic substances that have to be safely stored. For this purpose, suitable techniques are required of which a number of the engineered barriers and sealing techniques described in this book are applicable.

The most attractive proposal for disposal of hazardous chemical waste is to bring it down in deep mines that are about to be abandoned or where suitable rooms are available in parts where mining operations have been finished. Preferably mines should be used where the chemical conditions are akin to the waste. Thus, arsenic and mercury products are suitably stored where ore dominated by the respective element was once extracted.

Like in the case of radioactive repositories the release of hazardous chemical substances must be kept acceptably low, which requires tight containers embedded by a suitable medium that can be smectite clay or cementitious material for the most dangerous materials, and embedment of simple containers by natural smectitic soil for somewhat less but still toxic and dangerous substances.

COST ESTIMATES

Individual solutions are required depending on the sort and toxicity of the waste and the design may be quite different because of differences in geometry and rock stability in old mines. The need for rock excavation is naturally largely eliminated and so is the cost of elevators, ventilation and electric power systems if the mine is in operation or recently deserted. While the construction cost is therefore limited to the preparation and application of embedment of the waste containers and to effective sealing by plugging and grouting, rock characterization and stabilization work need much attention and may represent rather high costs. However, one of the advantages in using mines is that the prospection work and the experience from the mining operations with respect to rock stability and conductivity is of great help in assessing the performance of the rock mass.

In principle, the following steps have to be taken in characterizing and describing the mine as a basis of the required reconstruction and of the safety assessment:

- * Documentation and validation of mine data respecting all rooms and drillings that have been made; determination of available space for waste emplacement and of space that can not be utilized but requires sealing
- * Assessment of the stability of the rock and planning of stabilization work
- * Evaluation of the rock strain induced in the mining period and of its effect on the rock mass with respect to the gross hydraulic conductivity

* Evaluation of the groundwater flow regime

For well maintained and operated mines these activities do not not require very much work, except for the lastmentioned issue concerning the groundwater, which may cost a few MSEK. The subsequent preliminary design work comprises selection of a principle for distribution of the waste in existing rooms and an outline of required rock stabilization and waste isolation, as well as estimation of the groundwater flow pattern in the repository and a general risk analysis based on prediction of the dissolution and release of hazardous substances. After safety assessment and request for licensing a detailed design is worked out. All these activities are estimated to be relatively expensive; it is probably a matter of some tens of millions of SEK.

Finally, with licensing arranged, selection is made of suitable materials for the engineered barriers and of techniques for their application. The required amount of barrier material, forming embedment of waste containers or layers in a sandwich construction of granular solid waste, is about $1\text{--}10\text{ m}^3$ per m^3 of dense waste and the cost of the backfilling can be fairly safely estimated. Thus, a carefully prepared backfill of fairly smectite-rich backfill will represent a cost in the range of 500–1000 SEK per m^3 , from which one finds that the cost of backfilling is about 500–10 000 SEK per m^3 of waste. An amount of 10 000 m^3 of qualified chemical waste stored in a repository of this type hence needs embedment that costs at least 5 MSEK and possibly up to 100 MSEK. To this comes the backfilling of rooms that can not be used for waste storage, rock stabilization and the construction of plugs down in the former mine and in shafts and ramps. These operations are estimated to cost 10–100 MSEK depending on the actual geometry and size of the mine.

Although these estimates are very rough we see that disposal of chemical waste is expensive and the example indicates that the cost of site investigations, design and construction will be in the range of 5 000 to 20 000 SEK per m^3 of solid waste. Although this is less than 1 % of the corresponding cost for HLW disposal it still means that only very toxic waste can be considered for disposal in deep mines. It seems realistic to select a few suitable mines for disposal of such waste in each country.

9-4 References

1 SKB. Kostnader för kärnkraftens radioaktiva restprodukter, Bilagor. Kärnkraftens Slutsteg, Plan 93. SKB, Stockholm, Juni 1993

2 Ageskog, L. and Högbom, T. Project on alternative systems study - PASS. Cost comparison of repository systems. SKB Technical Report TR 92-44, SKB, Stockholm, 1992

Symbols

- "film" theory 319
- "obelisque"-type rock 372
- "Allard" water 417
- "apparent" diffusion 109
- "axial" hydraulic conductivity 312
- "curtain" grouting 207
- "deployment" muds 230
- "disturbed" zones 179
- "effective" diffusion 109
- "hedgehog" grouting 207, 208
- "latent" discontinuities 124
- "O-ring" seals 177
- "O-ring"-type bentonite seals 176, 218, 192, 434
- "pitting" corrosion 425
- "skin" zone 65
- "source" term 23

- α radiation 425
- γ radiation 411, 422

Numerics

- 2D 139
- 3D, 3D effects 139, 225, 338, 346, 378
- 3DEC 65, 138, 313, 336, 395
- ^{60}Co radiation source 417

- 1st order discontinuities 36, 57, 59, 67, 381
- 2nd order discontinuities 36, 37, 62, 67, 69, 80, 174, 223, 361, 368
- 3rd order discontinuities 36, 37, 44, 59, 63, 67, 68, 80, 143, 149, 174, 180, 184, 185, 204, 215, 216, 218, 220, 223, 225, 228, 343, 344, 351, 356, 378, 388

- 4th order discontinuities 36, 41, 42, 52, 53, 68, 79, 123, 143, 144, 149, 157, 169, 174, 179, 198, 204, 205, 210, 220, 223, 225, 312, 337, 339, 343, 361, 368, 372, 374, 381, 382,

- 394, 428
- 5th order discontinuities 36, 40, 53, 68, 123, 144, 148, 149, 153, 157, 179, 198, 204, 210, 313, 321
- 6th order discontinuities 37, 38, 68, 123, 126, 137, 165, 167
- 7th order discontinuities 37, 38, 68, 126, 165, 167
- 7 order general rock structure scheme 62, 174

A

- AAS 417
- ABAQUS 325, 362
- AECL 247, 374
- ALARA principle 7, 90
- Alofix cement 208

- absolute confinement 401
- accessory minerals 99, 430
- acoustic logging 152
- aquifers 174
- activation energy 354
- activity 7, 25, 412
- adhesion 325
- adits 17
- adsorbed cation 431
- advection 404
- aggregate 117
- air 365
- alteration 422
- ambient temperature 309
- americium 425
- amorphous silica 418
- anhydrite 329
- anion diffusion 105, 230
- anisotropic stress state 346, 378, 381, 382
- anisotropy 338, 381
- annual precipitation 401
- application phases 179, 229, 400, 430

arching 253, 444
arsenic 6, 32, 403, 458
artesian 375
asphalt 95, 173
Äspö Hard Rock Laboratory 52, 314
atomic absorption spectroscopy 417
Atterberg liquid limit 431, 439
axial hydraulic conductivity 138, 144, 156, 157, 165, 167, 169, 171, 175, 179, 187, 203, 242, 313, 335, 337, 346, 378, 380
axial flow, flux 65, 160, 203, 218, 336, 370, 397

B

Baltic Sea 82
BMT, Buffer Mass Test 142, 143, 149, 153, 187, 197, 204, 247, 261, 268, 319, 442, 444, 448
BWR elements 412

back pressure 299
backfill 27, 171, 172, 175, 176, 204, 216, 224, 229, 230, 254, 256, 264, 266, 270, 308, 313, 317, 322, 325, 333, 350, 355, 356, 357, 384, 387, 394, 395, 396, 399, 413, 415, 427, 428, 430, 441, 453
backfilling 117, 254, 256, 387, 435, 454, 459
backpressure 213, 444, 447
ballast 117, 118, 120, 264, 271, 333, 435
barium 6
barriers 25, 90, 322
basalt 82
batteries 32
bearing capacity 67, 105, 276
beidellite 352
beidellitization 358
bench-blasting 241
bentonite 16, 20, 83, 91, 98, 107, 117, 120, 121, 161, 204, 224, 257, 264, 265, 271, 317, 323, 350, 358, 403, 417, 430, 434, 444
bentonite bed 117, 358, 430
bentonite blocks 192, 275, 277, 278, 283, 288, 304, 305, 388, 389, 390, 400
bentonite content 121, 391

- bentonite granulate 21
- bentonite grout 200
- bentonite block masonry 200, 201, 288, 434
- bentonite mixtures 110, 118, 264, 265, 387, 415, 435, 436
- bentonite plugs 204, 276, 434
- bentonite powder 271, 310, 317
- bentonite processing 431
- bentonite seals 287
- bentonite slurry 146
- bentonite-embedded canisters 312
- bentonite-filled slots 203, 216, 322
- beta/gamma-activity 7
- big holes 304
- big-bag 431
- biosphere 2, 23, 78, 402
- biosphere modelling 405
- bladder 145
- blast-disturbed zone 122, 148, 149, 155, 164, 187, 197, 205, 210, 387
- blasted tunnel 18, 304, 156
- blast-generated fractures 144, 153, 157, 387
- blast-holes 376
- blasting 19, 123, 164, 165, 169, 175, 210, 236, 376, 380, 428
- block displacements 336
- blowing 399
- bolting 223, 253, 254, 451
- borehole inspection 77
- borehole plugging 289
- boreholes 14, 78
- boring 428
- boundary stresses 344
- break-outs 385, 389
- breakthrough 414
- brittleness 82, 329, 393
- buffer 264, 312, 317, 322, 333, 335, 350, 355, 362, 366, 370, 384, 389, 390, 391, 392, 395, 396, 412, 414, 427, 430, 434, 441, 453, 454
- bulk compression modulus 130
- bulk density 270, 362, 365, 392, 413, 431
- bulk strength 372

bulwarks 176, 195
burnt-out fuel 412
buttresses 204, 253, 280, 387

C

Caledonian ridge 165, 374
Cam-clay 113
Ca-montmorillonite 352
Canada 241, 374
Casagrande 431
Casagrande's apparatus 431, 439
CEA 416, 430

cadmium 6, 32, 279, 403
cage 386
calcite 418, 430
calcium 329
canister 223, 265, 306
canister defects 95, 425
canister embedment (clay) 13, 174, 179, 216, 229, 312, 328, 368, 370, 388, 396, 397, 398, 402, 411, 414, 422, 425, 430
canister holes 91, 127, 160, 229, 434
canister metal 370, 412
canister tightness 396
canister transport 163
canisters 9, 13, 91, 174, 225, 276, 278, 304, 308, 362, 385, 388, 389, 393, 396, 400, 411
capillary forces 352
capillary pressure 413
capillary suction 318, 431
carbonate rock 32
carcinogenic 5
cation diffusion 105
cation exchange 105, 333, 365, 403, 417
caverns 71, 78, 89
cement 175, 179, 188, 190, 214, 361, 386
cement grout 183, 191, 298

- cement mortar 256
- cement paste 173
- cement shotcrete 176
- cement stabilization 280
- cementation 188, 329, 330, 333, 353, 355, 358, 360, 365, 368, 394, 396, 399, 417, 422
- cement-filling 398
- cementing bonds 352, 358
- cesium 26, 162
- change in fracture aperture 131, 210, 172, 312
- channels 147, 157, 174, 185, 210, 212, 214, 215, 225, 371
- charging 237
- chemical alteration 435
- chemical analyses 417
- chemical attack 96, 172
- chemical compatibility 176
- chemical environment 13, 429
- chemical stability 333, 387, 434
- chemical waste 33, 279, 403, 458
- chloride 330
- chlorite 335, 350, 399
- chromium 6, 279
- clay 9, 12, 13, 27, 214, 389
- clay content 36, 436, 438
- clay density 305
- clay fraction 434
- clay gouge 44, 123, 307, 313
- clay grout 188, 361, 432
- clay matrix 121
- clay microstructure 414
- clay-based materials 429
- claystone 371, 393
- climate 304
- climatic changes 366, 401
- coagulation 121
- cobalt 26
- cohesion 67, 68, 124, 343
- colloidal mixer 299
- compaction 258, 267, 415, 430

- compaction meter 438
- compatibility of rock and waste 32
- compressibility 117, 119, 436
- compression 28, 312, 313, 317, 336
- compression modulus 123
- compressive strength 75, 80, 133, 307, 377
- concentration gradient 353, 365, 368
- concrete 9, 27, 200, 256, 316
- concrete bulwarks, buttresses 175, 253, 190
- concrete plugs 176, 200, 203, 287
- conductor 167, 270
- cone penetration 431, 439
- cone test 431
- confining pressure 186
- confining rock 18
- consolidation 176, 386
- construction 235, 271, 386, 429, 454
- construction cost 457
- construction site 431
- containers 235, 273, 427, 458
- contaminated water 96, 414
- continuous slot 144
- contour holes 239, 429
- convection 316
- conversion 353, 356, 360, 370, 392, 393, 394
- copper 6, 13, 95, 279, 365, 403, 425
- copper canisters 370
- copper saturation 365
- copper/steel composite 95
- core discing 167
- core drilling 14, 15, 77, 126, 246
- corrosion 13, 95, 115, 173, 225, 325, 361, 365, 371, 403
- cost 29, 31, 33, 70, 98, 192, 220, 264, 428, 453, 455, 458, 459
- cracking 321
- creep 10, 28, 69, 136, 169, 172, 254, 307, 325, 334, 336, 337, 339, 358, 375, 378, 387, 417
- creep laws 114, 337, 422
- creep strain 335, 361, 422
- creep tests 422

creep-induced failure 290, 388
 critical gas pressure 413
 critical strain 169, 337
 cross section shape 380, 387, 415
 crushed rock 208, 265
 crystal lattice 411
 crystalline rock 33, 63, 309, 384
 cubic flow law 345
 cutting head 248
 cyanides 6, 279
 cyclic load 155

D

Donnan exclusion 105
 Drucker-Prager 113, 114, 325

damage 378, 380
 data acquisition 448
 data processing 448
 debris 123, 187
 decay rate 25, 405
 decomposition 411
 deep drilling 61
 deglaciation 374, 376, 381
 degradation 172, 179, 356, 390, 392, 393, 397
 degree of water saturation 192, 322
 dehydration 111
 delayed failure 378
 densitometer techniques 437
 density 119, 189, 333, 399, 417, 436, 439
 deployment 92, 275, 362
 deployment mud 368, 385, 386
 deployment zone 310, 314, 355, 356, 370, 391, 397, 398
 deposition holes 133, 167, 169, 174, 215, 216, 220, 225, 229, 306, 321, 335, 336, 355, 357,
 376, 377, 378, 382, 387, 390, 392, 394, 398

- deposition tunnels 79, 223, 227, 230, 253
- design 9, 13, 20, 91, 429, 457
- design "as you go" 231, 235
- deviator stresses 165
- diamond saws 283
- dickite 104
- diffusion 26, 105, 109, 161, 180, 318, 322, 323, 355, 356, 368, 370, 393, 399, 404
- diffusion coefficient 161, 321
- diffusion process 321
- dilatancy 67, 334, 343
- dioctahedral smectite 418
- dip 71
- discing 167
- discontinuities 35, 79, 127, 131, 137
- discrete fractures 179, 197, 200
- disposal 89
- dissolution 319, 329, 368, 403, 414
- dissolution/neoformation 322, 350
- distilled water 121
- disturbance 122, 163, 236, 238, 376, 380
- disturbed zone 63, 80, 146, 152, 160, 167, 200, 203, 204, 207, 208, 216, 219, 220, 223, 239, 357, 391
- dose 25, 26
- dose rate 412, 417, 422
- drainage 400
- draught 401
- drilling 380
- drilling and blasting 235, 236
- drilling mud 276, 377
- drilling phase 230
- drinking water 5
- dry density 192, 200, 272, 278, 386, 417, 431
- drying 330
- ductility 215
- dynamic (oscillatory) injection 182, 190, 200, 205, 208, 297

E

Edelman/Favejee 352
EDX 417
E-modulus 154, 334, 438
ENRESA 247, 456
Europe 366
European communities 5

earth crust 344, 402
earth dam construction 267, 437
earth dams 267
earth pressure at rest 375
earthquakes 69, 70, 338, 339, 368
effective pressure 105, 328, 352
elastostoplastic 338
elastic behavior 336
electrical double-layers 100, 109
electrolyte concentration 332
electrolyte content 121, 314, 335, 389, 403
electron microscopy 417, 421
element net 216
elliptical 167
embryotic breaks 38
emplacement 434
encapsulation 95, 453
engineered barriers 91, 96, 395, 457
epoxy 175
erosion 187, 188, 191, 308, 389
evaporation/condensation 322
excavation 165, 213, 235, 253, 304, 335, 337, 344, 346, 458
excavation-induced disturbance 197, 216, 228
excavation-induced increase in aperture 140
excavation-induced stress changes 131, 137
exchange sites 99
expandability 215, 329
expansion 140, 167, 186, 187, 313, 317, 325, 336
expansive cement 200

explosives 4, 238
extensometers 442

F

FEM 147, 148, 197, 216, 219, 220, 272, 422
Fick's law 105, 109
Finland 9
FLAC 171, 185, 337, 338
Forsmark repository 9, 13, 175, 431
Forsmark silo 113, 435, 438
France 426
Fuller's curve 118

farfield 172
faults 10, 339
feldspars 357, 418
field surveying 77
fine-grained cement 183
fissures 34, 126
floor 175, 388
flow, model, pattern 25, 148, 157, 181, 216, 197, 312, 393
flow vectors 147
fluoride 6
flux 25, 147, 161, 390, 392
foliation 167
foundation 271
fractal 50, 59, 84
fracture aperture 335, 336
fracture fillings 67, 314
fracture frequency 36
fracture mapping 127
fracture topography 67
fracture zones 15, 17, 175, 179, 334
fragmentation 248, 321, 376
freezing 174
friction 67, 124, 325, 334

friction angle 42, 67, 68
friction coefficients 381
fuel rods 412
full-face 126
full-face drilling 126, 246

G

Gefügekunde 38
Gloetzl pressure cells 200
Gotland 82
Griffith 248
Griffith cracks 37
GWHRT 24

gamma radiation 411, 416, 417, 422, 425
gabbro 82
gamma ray backscattering 438
gas 21, 95, 124, 403
gas breakthrough 414
gas bubbles 414
gas conductivity 414
gas formation 412
gas pressure 18, 123, 167, 414, 415
gas transport 411
gelation 98
geophysical investigations 14, 15, 77, 152
geosphere 2, 23, 405
glacial deposits 265
glaciation 6, 62, 63, 227, 271, 304, 338, 344, 346, 366, 374, 380, 383, 395, 401, 402
glaciers 374, 402
glass matrix 95
gneiss 81
goethite 365
grain size distribution, granulometry 181, 265, 435, 438
granite 52, 81, 126, 133, 143, 165, 321
granulated bentonite 107, 430, 432

granules 108
graphite 115
groundwater chemistry 173, 191, 304, 314, 441
groundwater contamination 32
groundwater density 402
groundwater flow 24, 63, 398, 441
groundwater pressure 441
groundwater regimes 179
grouts 104, 179, 180, 181, 188, 189, 191, 244, 295, 308, 393, 400, 439
grout penetration depth 181, 208
grout strength 215
grouting 70, 173, 174, 176, 179, 181, 187, 189, 192, 196, 200, 205, 210, 212, 215, 220, 223, 225, 230, 283, 290, 297, 304, 387, 388, 400, 439

H

HLW (High-level Radioactive Waste) 7, 9, 10, 13, 78, 82, 95, 127, 136, 165, 169, 176, 227, 229, 252, 271, 273, 304, 308, 309, 319, 330, 362, 366, 393, 402, 411, 412, 425, 426, 428, 442, 453, 456
Hofmann/Endell/Wilm 352

hammering 244
hardening rate 213, 214
hazardous chemical waste 1, 175, 402, 430, 453
healed fractures 69, 339
heat capacity 121
heat conductivity 115, 121, 321, 390
heat cycle 309
heat effects 227
heat production 7, 310, 334, 336
heat pulse 205
heat source 336
heat-induced strain 136
heating 205, 215, 318, 335, 336
heating period 353, 370, 392
heating/cooling cycle 136, 334
heave 334

heavy metals 280
hematite ore 281
high-order discontinuities 50, 67, 335, 343
highly compacted bentonite 167, 171, 200, 203, 204, 218, 224, 308, 319, 357, 361, 392
highly compacted bentonite/ballast 391
highly radioactive waste 31, 173, 411
high-risk chemical and industrial waste products 91, 411
homogenization 362, 389
hoop stress 304, 335, 337, 377, 378, 381, 388
hopper 21
host rock 395
humidity 257, 308
hydrate layers 319
hydration potential 431
hydraulic activation 313
hydraulic conductivity 3, 14, 20, 21, 36, 38, 57, 65, 71, 91, 107, 120, 121, 147, 148, 149, 182, 185, 192, 203, 204, 205, 210, 212, 213, 214, 216, 264, 271, 279, 312, 321, 322, 332, 335, 336, 338, 371, 383, 386, 392, 402, 403, 414, 417, 422, 434, 436, 458
hydraulic gradient 8, 25, 83, 91, 160, 187, 216, 218, 273, 355, 391, 392, 402
hydraulic packer testing 48
hydrodynamic dispersion 404
hydrogen gas 173, 225, 330, 365, 366, 412
hydrothermal 82, 335, 338, 417, 421
hydrous mica 104, 188, 189, 353
hydroxyls 98

I

ICRP 7
International Atomic Energy Agency 7
IR 417
I/S conversion 350
Italy 430

ice cap 375
ice front 375
ice sheet 344

ignition 237
illite 104, 188, 350, 353, 357, 392, 394, 398, 399
illitization 353, 354
inelastic displacements 381
inflow of water 305, 387, 388, 389, 439
inflow tests 77
infrared spectrometry 417
injection pressure (grouts) 184, 185, 187, 190, 213, 215, 297
instrumentation 14, 441
interlamellar positions, space 98, 99, 100, 105, 109, 319, 350, 353, 419
intermediate storage 412
ion diffusion properties 107, 434
ion exchange 403
ion transport 319
ionic strength 189
iron 365
iron hydroxide 365, 419
iron sulphide 418
irradiation 420
isotope methods 438

J

GSRW 405
Japan 426, 430

joint cohesion 128
joint dilation angle 128
joint friction 128, 381
joint friction angle 340
joint normal stiffness 127, 340
joint shear stiffness 128
joint tensile strength 127
joints 127, 136, 137, 192, 390

K

KBS3 78, 91, 127, 157, 160, 162, 165, 167, 169, 180, 191, 223, 225, 229, 230, 236, 247, 260, 270, 271, 275, 303, 309, 312, 314, 321, 322, 328, 330, 333, 334, 335, 338, 341, 346, 355, 357, 360, 361, 362, 368, 370, 372, 377, 382, 391, 392, 393, 394, 395, 396, 397, 398, 399, 400, 412, 414, 425, 434, 454, 456

KBS3 tunnels 175, 313, 321, 388

Kola 165

K-bearing feldspars 430

kandites 104

kaolinite 104

L

Li-bentonite 200

LID 204

LLW (Low-level Radioactive Waste) 7, 9, 13, 16, 95, 175, 273, 426

laboratory facilities 431

lamellae 98

land rise 25

large clay blocks 400

large-diameter holes 167, 225, 299, 304

latent 157

latent breaks 125, 157

lattice contraction 111

layerwise compaction 399

lead 6, 279

leakage 173, 195, 203, 425, 427

leptite 143

lifting power 167

lining 223, 253

location of repositories 13, 429

logging 244, 429, 444

longevity, long-term stability 9, 12, 175, 176, 179, 225, 288, 312, 350, 392, 396

long-term performance 200, 215

low-density grouts 191
low order discontinuities 96, 397
low-order discontinuities 44, 57, 67, 89, 96, 191, 215, 223, 307, 313, 372, 382, 387, 388, 397, 414

M

Macro Flow Test 208
Mexican Gulf area 350
MLW (Medium-level Radioactive Waste) 7, 13, 16, 91, 95, 175, 273, 426
Mohr/Coulomb 56, 57, 67, 339, 343

magnesium 329
magnetite 365
major primary stress 167
major principal stress 167
manometer 444
manufacturing 396
masonries of bentonite blocks 176, 200, 260
maturation 313, 317, 328, 329, 333, 353
maximum shear stress 129
mechanical damage 397
mechanical support 172
megapacker 149, 176, 204, 225, 300, 387
megapermeameters 436
mercury 6, 32, 279, 403, 447, 458
metabentonite 358, 368
metal canisters 173
metalloids (waste) 5
metals (waste) 5
methylene blue 431
micaceous minerals 335
microscopy 414
microstructure 21, 100, 102, 109, 318, 412, 421, 422
migration rate 161
mineral stability 9, 12, 175, 176, 179, 225, 288, 312, 333, 350, 392, 396, 426
mines 32, 89, 143, 402, 458, 459

modems 448
monitoring 14, 441
montmorillonite 98, 105, 350, 353, 355, 357, 360, 391, 392, 413, 417, 418, 425, 430, 431
movable cutting heads 378
movement of waste containers 441
muds 377
multibarrier 3, 18, 405, 425, 427
mutagenic 5

N

Na bentonite 20, 121, 229, 321
Na-montmorillonite 352
NEDRA 339
North America 366

nearfield 19, 82, 90, 133, 144, 149, 156, 160, 162, 172, 173, 228, 313, 321, 334, 335, 338, 341, 383, 392, 395, 396, 404, 442
nearfield rock 2, 163, 165, 204, 335, 336, 338, 382, 386, 396, 397, 398
neoformation of illite 350, 352
nickel 279
nitrate 6
non-expanding 10 Å minerals 353
non-linear elastic 113
nontronite 353, 430
normal and shear stiffnesses 334
normal stress 129
nozzle 270, 285
nuclear energy 164
nuclear fuel 403
numerical calculations 70, 138, 325, 362, 375

O

Ordovician 83, 358

oedometer 107
oil-drilling 251
onion-type fractures 65
operative lifetime 12, 172
ore 235, 280
organic colloids 190
organic material 403, 431
organohalogen compounds 4
organophosphorous compounds 4
orthogonal 42, 44, 60, 84, 157
oscillatory 297
osmotic pressure 111
overstressing 163, 164
oxidation 365
oxy/hydroxides 365
oxydizing 4
oxygen 173

P

PCB 279
Pleistocene 381
Poisson's ratio 334
Porous Elasticity Theory 325
Portland cement 32, 279, 288
Pytte's model 356, 358

packer 244, 187, 244, 288, 300
paragonite 353
particle size 430
peak strength 343
percolation 160, 279
percussion drilling 144, 208, 244, 246, 283
perforated metal containers 401
performance assessment 303
permafrost 273, 402
permeability 14

- pesticides 6, 279
- pH 95, 175, 279, 316, 365, 403, 404
- phenol 6
- piezometers 145, 147, 444
- piezometric pressure, conditions 27, 28, 185, 312, 322, 366, 388, 389, 414
- pilot drilling 220, 230, 241, 253
- pipng and erosion 182, 187, 188, 191, 214, 308, 328, 389
- plastic 113, 155, 317
- plastization 272
- plate loading 272
- plug construction 220
- plug material 179
- plugging 70, 172, 187, 220, 235, 357, 370, 386
- plugs 12, 173, 179, 175, 179, 192, 208, 215, 216, 218, 219, 227, 230, 256, 283, 361, 400, 439, 459
- plutonium 26, 162, 425
- podsol profiles 357
- polycyclic aromatic hydrocarbons 6
- porewater 330, 411, 414
- porewater pressure 328, 412, 414
- porosity 105, 119, 155, 161, 404
- porous medium 14, 147, 197, 200, 203, 243
- porous steel filter 417
- postglacial 381
- post-heating period 366, 390, 395
- potassium 333, 352, 357, 370, 398, 418
- potassium concentration, content 354, 368, 384, 390, 391, 392, 393, 398
- potassium-bearing minerals 355, 435
- powder 102, 317, 318
- practicality 400
- precipitated silica 188
- precipitation 329, 330, 402
- precision levelling 451
- prefabricated blocks 270, 400, 431
- preglaciation stage 381
- preliminary design 454
- preparation 415
- pressure cells 324, 444

pressurized gas 412
primary stress ratio 387
primary rock stresses 63, 80, 124, 130, 165, 169, 306, 313, 318, 338, 374, 377, 378, 381, 387
principal stress ratio 376
principal stresses 75, 80, 306, 340, 344, 381
profile 144
prospection 244
protuberances 412

Q

Quaternary glaciations 376

quality assurance 427
quartz 115, 418
quartz sand 357

R

radar measurements 77
radial conductivity 156
radiation 411, 412, 417, 418, 421
radiotoxicity 7
radioactivity 4, 7, 28, 164, 261, 427
radiolysis 225
radionuclide transport 397
radionuclides 82, 90, 179, 190, 225, 325, 396, 397
radwaste 10
raise boring 246
ramp 174, 176, 273, 454
rate of gas formation 412
rate-process theory 169, 337
recess 200, 247
recording 429
redirection of flowing groundwater 210
redrilling 398

- regional fracture zones 35
- regional hydraulic gradients 91
- regional stress fields 70, 338
- reinforcement bars 26
- release of radionuclides 162
- release of silica 352, 354
- relic 27
- remote handling 400
- repositories 411
- repository concepts 157, 411
- reprocessed reactor wastes 403
- residence time 161
- residual friction angle 343
- retardation mechanisms 405
- retrievability 279
- rheological properties 107, 113, 115, 362, 399
- rhombohedral 44, 60, 83
- rhyolite 98
- rim zones 59
- risk 7
- robot drilling 429
- rock burst 80
- rock classification 34
- rock failure 163, 164, 386
- rock fall 307, 378, 398
- rock mechanics 2, 8, 28
- rock shearing 362, 399
- rock stability 279, 313, 377
- rock stabilization 459
- rock stress measurement 77,78
- rock stresses 20, 71, 75, 79, 223, 376, 395, 429
- rock structure 14, 34, 91, 137, 163, 204, 220, 223, 225, 228, 230, 253, 313, 387, 388, 395, 397, 402
- rock structure models 49
- rockfill 173
- roof 19, 171, 270, 388

S

- Sardinia 430
- Scandinavia 8, 165, 375
- Silurian 83
- SKB 78
- South Africa 241
- South Dakota 99
- Soviet Union 2
- Spain 426
- Stoke's law 439
- Sweden 9, 29

- safety analysis 23
- safety assessment 24, 404
- safety problems 388
- salinity 314
- salt 89, 321, 399
- salt accumulation 329, 330, 368
- salt water 314, 316, 365, 391
- sandstone 84
- saponite 353, 430
- saturation 310
- scale-dependence 381, 395, 415
- scanning 144
- schistosity 165, 242
- sea water 314
- sealed fractures 41
- sealing 12, 17, 160, 172, 175, 179, 208, 210, 220, 235, 304, 388, 454, 457, 458
- sealing ability, potential 13, 227, 361, 392, 398, 400
- sealing effect 197, 212, 215, 333, 400
- sealing materials 172
- seals 14, 163, 172, 174, 175, 223, 228, 230, 273, 361, 370, 439
- sector-wise grouting 174
- sedimentation analysis 438
- seismic events 70, 154, 441
- selenium 6
- self-healing 181, 182, 190, 203, 313, 335, 338, 362, 378, 392, 399, 403

- self-repeating patterns 49
- sets of canisters 386
- settlement 271, 273, 362, 391, 399
- shafts 223, 273, 275
- shallow repositories 31
- shallow sealing 173
- shear stress/strain 69, 70, 129, 130, 181, 230, 312, 317, 340, 343, 381, 382
- shear box 422
- shear failure 344
- shear modulus 130
- shear rate 181
- shear strength 105
- shearing of deposition holes 362
- shotcrete 223, 267, 269, 270, 387
- shrinkage 176, 287, 391, 398
- sieving 265, 438
- silica fume 295
- silica precipitation 368
- silicious compounds 422
- silo 15, 16, 18, 20, 21, 24, 25, 174, 265, 271, 272, 307
- site investigations 456
- slabbing 167
- slag cement 288
- sliding micrometer 442
- slim holes 230
- slip 339, 344
- slot cutting 220, 246, 305
- slots 21, 176, 203, 220, 224, 246, 285, 305, 434
- smectite 98, 100, 105, 175, 179, 188, 189, 190, 200, 257, 314, 350, 352, 353, 390, 395, 391, 399, 404, 418, 430, 458
- Smectite grouts 187, 297
- smectite content 391, 392, 431, 434, 435
- smectite conversion to illite 353, 354, 356, 358, 360, 368, 370, 384, 391, 392, 393, 394
- smectite-poor backfills 403
- smectite-rich backfill 459
- smectitic soil material 403, 435
- solidification 191, 279
- solubility 404

- sorption 3, 109, 399, 404
- source material 430
- source term 405
- spalling 80, 164, 167, 376, 377, 378, 381, 388
- specific heat 334
- specific power 334
- s-planes 38
- stacks of flakes 108, 421
- stagnant groundwater 188, 190, 356, 357, 368
- static injection 208
- steel 95
- steel canisters 371, 412
- steel drums 26, 95
- steel reinforcement 173
- stereo net 72
- stereographic projection 72
- stick-slip 69
- stochastic 50
- storage 14, 258
- strain 337, 339, 441, 442
- strategic sealing 192, 205
- strengthening 422
- stress concentration 133, 427
- stress conditions, fields 8, 59, 63, 91, 127, 227, 228, 230, 313, 336, 338, 375, 378, 429, 442
- stress ellipsoid 75
- stress relaxation 105, 336
- stress release 210, 380
- stress tensor 78
- stress waves 124
- stress-disturbed zone 149, 203
- strike 65, 71
- Stripa, Stripa Project 33, 89, 127, 141, 146, 148, 178, 180, 182, 184, 187, 190, 192, 197, 200, 208, 215, 244, 247, 256, 258, 261, 265, 283, 303, 319, 324, 325, 395, 428, 431, 439, 442, 444, 448, 451
- structural modelling 70, 304, 457
- structural pattern 63, 70, 304, 338, 402, 427
- submicroscopic defects 38
- substitution 352

sulphates 6, 358, 421, 430
sulphide ore 281, 316
sulphur 329
superplasticizer 181, 183, 295
supporting pressures 337
swelling 325, 328, 399
swelling ability, potential 107, 110, 204, 329, 330, 356, 365, 392, 422, 434
swelling pressure 21, 105, 107, 109, 110, 111, 121, 172, 192, 200, 203, 313, 323, 324, 325, 366, 417, 422, 441, 442, 447
syneresis 107

T

TBM 126, 248, 398

tangential (hoop) stress 133, 164, 165, 374, 377, 388
tectonic events 4, 10, 62, 215, 227, 304, 334, 338, 366, 381, 383, 390, 393, 396
tectonic shearing, impact 96, 338, 346, 361, 397, 399, 400
temperature 309, 355, 370, 392, 394, 441
temperature fields 333
temperature gradient 136, 321, 329, 330, 353, 355, 357, 399, 422
temperature pulse 336
temperature recording 444
temporary seals 176
tensile strength 343
tension 312
tension fractures 123
tension stresses 399
tensioned bolts 254
teratogenic 5
thermal conductivity 258, 334
thermal elements 444
thermal expansion coefficient 334
thermal gradient 274, 330
thermal loads 136
thermal properties 107, 115, 117, 121
thermal stresses 318

thermocouples 444
thermodynamic processes 421
thermo-mechanical effect 335
thixotropy 98, 187, 188, 191, 276, 298
three-dimensional compression 258
tidal phenomena 10
time-dependent strain 172
titanium 95, 365
tolerable concentration 5
tortuosity 109
total dose 412
total pressure 444
toxic elements 4, 5, 401
toxic waste 4, 31, 304, 402
toxicity 31, 401
tracer tests 213, 245
transducer 444, 445
transient heat and mass transfer 319
transition zone 329, 330
transmissivity 14
triaxial cell 107, 114
tunnel backfilling 91
tunnel boring 126, 164
tunnel excavation 57, 174, 175, 190, 454
tunnel floor 336, 337
tunnel roof 171, 337
twisting 52

U

UDEC 65, 131, 313, 334, 341, 395

ultrasonic 154
unconfined 102
unconfined compressive strength 165
undulation 52, 63
uniaxial stress field 376

unsaturated conditions 322
unstable rock conditions 386
untensioned bolts 254
uranium 32, 412
utilization factor 92, 396, 397, 400

V

VDH 91, 157, 160, 165, 230, 236, 252, 275, 303, 307, 309, 310, 314, 322, 332, 333, 334, 335, 338, 355, 356, 360, 361, 362, 365, 368, 370, 372, 385, 394, 396, 397, 399, 400, 434, 456

VLH 91, 126, 157, 160, 162, 165, 230, 303, 309, 313, 314, 322, 328, 334, 335, 336, 338, 341, 346, 355, 361, 362, 368, 370, 377, 382, 388, 394, 396, 397, 398, 399, 400, 414, 434, 456

vanadium 279
vault 16, 24, 71, 78, 89
vibrating rollers 20, 267
vibration testing 152
vibratory plates 267
virgin rock 148, 149, 216
viscometer 297
viscosity 181, 190
void ratio 105
volcanic ash 98

W

Wyoming bentonite 99, 417

wall friction 278
waste application 304, 386
waste composition 402
waste containers 3, 395, 404
waste containment 90
water balloon volumeters 271, 437

water content 200, 257, 265, 436
water head 439
water inflow 179, 220, 305, 312
water jet cutting 246, 284
water pressure 322, 332, 388, 439
water saturation 230, 257, 321, 330, 389, 390, 400, 431
water uptake 270
water/cement ratio 181
water-bearing discontinuities 4, 149, 157, 166, 204, 225, 378
wave propagation rate 154
wedges 18, 169, 307, 388, 397, 398
welding 396, 427
wet compaction technique 322
wetting process 321
wetting/drying 352

X

X-ray diffraction, XRD 417, 419

Y

Young modulus 340

yield curve 114

Z

zink 6, 279

zonal enrichment of minerals 50

The cross-scientific nature of the matters discussed in this book means that many terms are used in the literature for expressing or denoting the same or practically the same process or object. The following list serves to indicate major synonyms used in the book.

canister holes, canister deposition holes, deposition holes
compression strength, compressive strength
(waste) containers, canisters (the latter is commonly reserved for HLW)
disturbance, damage
electrolytes, salt
flow, flux (distinguished by dimensions)
hazardeous, high-risk, toxic (waste)
heat, thermal (effects)
illite, hydrous mica, hydromica, non-expanding 10 Å minerals (hydrous mica and hydromica have a wider meaning than illite)
longevity, long-term stability, chemical stability
radioactive waste, radwaste
rock burst, spalling
saline, salt-water, marine, ocean (conditions)
salinity, salt concentration, salt content, electrolyte content, electrolyte concentration
salt enrichment, accumulation
sealing ability, capacity, potential, power
smectite flakes, lamellae, layers, sheets
strain, displacement, movement (distinguished by dimensions)
swelling ability, capacity, potential, power
tectonics, seismic events, earthquakes
water pressure, water head, piezometric head, piezometric pressure
water, groundwater